Oxidative Medicine and Cellular Longevity

Oxidative Stress and Trauma Repair

Lead Guest Editor: Yanqing Wu
Guest Editors: Rui Li, Xu Ke, and Zonghao Tang

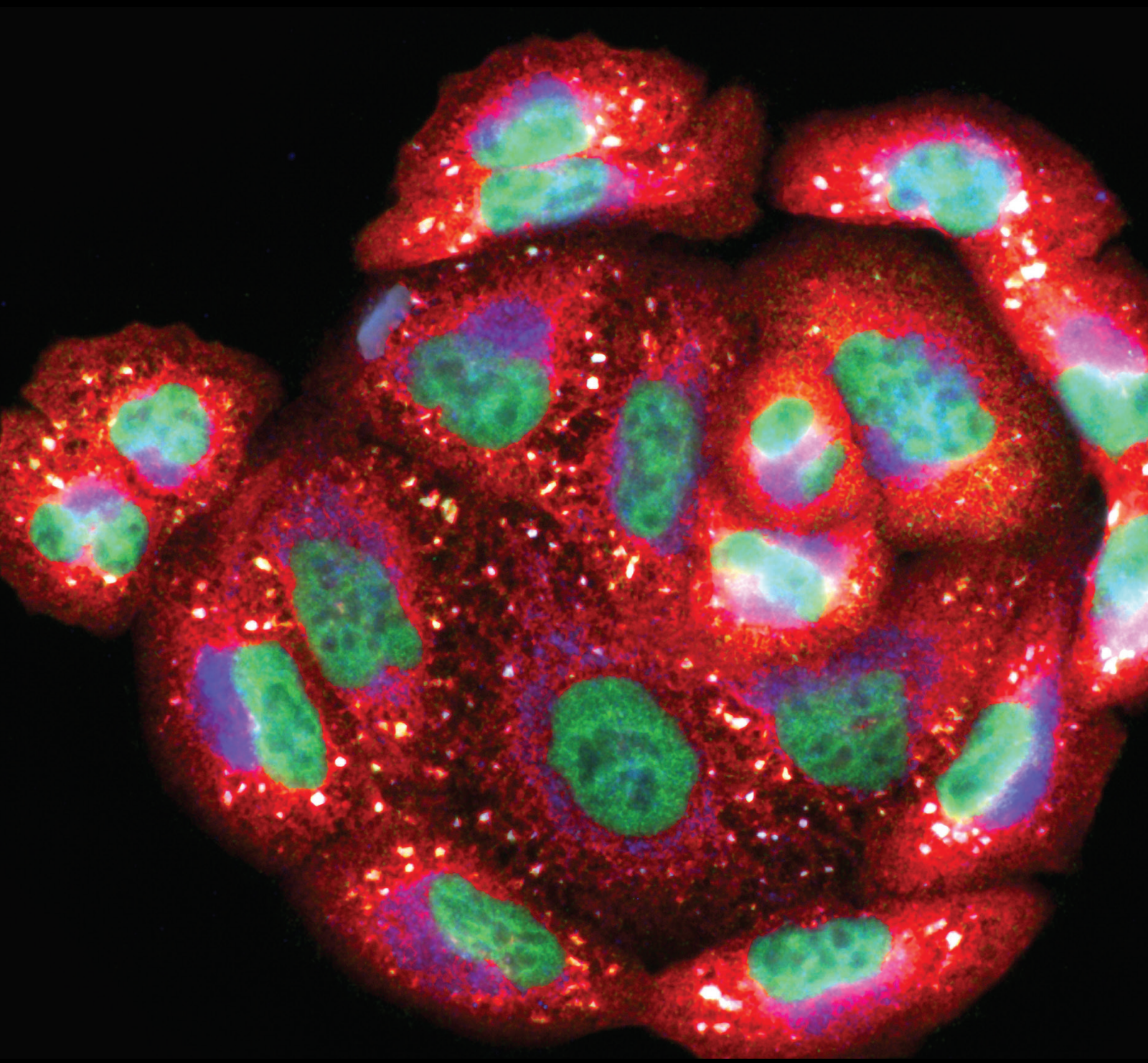

Oxidative Stress and Trauma Repair

Oxidative Medicine and Cellular Longevity

Oxidative Stress and Trauma Repair

Lead Guest Editor: Yanqing Wu
Guest Editors: Rui Li, Xu Ke, and Zonghao Tang

Contents

Hindawi
Oxidative Medicine and Cellular Longevity
Volume 2022, Article ID 2076680, 12 pages
https://doi.org/10.1155/2022/2076680

Review Article

Silk Fibroin Hydrogels Could Be Therapeutic Biomaterials for Neurological Diseases

Chun Yang[1], **Sunao Li**[1], **Xinqi Huang**[1], **Xueshi Chen**[1], **Haiyan Shan**[2], **Xiping Chen**[1], **Luyang Tao**[1], **and Mingyang Zhang**[1]

[1]*Institute of Forensic Sciences, School of Basic Medicine and Biological Sciences, Soochow University, Suzhou, China*
[2]*Department of Obstetrics and Gynecology, The Affiliated Suzhou Hospital of Nanjing Medical University, Suzhou, China*

Correspondence should be addressed to Haiyan Shan; ghostqth@163.com, Luyang Tao; taoluyang@suda.edu.cn, and Mingyang Zhang; ghost8469@163.com

Received 24 September 2021; Accepted 18 April 2022; Published 2 May 2022

Academic Editor: Rui Li

Silk fibroin, a natural macromolecular protein without physiological activity, has been widely used in different fields, such as the regeneration of bones, cartilage, nerves, and other tissues. Due to irrevocable neuronal injury, the treatment and prognosis of neurological diseases need to be investigated. Despite attempts to propel neuroprotective therapeutic approaches, numerous attempts to translate effective therapies for brain disease have been largely unsuccessful. As a good candidate for biomedical applications, hydrogels based on silk fibroin effectively amplify their advantages. The ability of nerve tissue regeneration, inflammation regulation, the slow release of drugs, antioxidative stress, regulation of cell death, and hemostasis could lead to a new approach to treating neurological disorders. In this review, we introduced the preparation of SF hydrogels and then delineated the probable mechanism of silk fibroin in the treatment of neurological diseases. Finally, we showed the application of silk fibroin in neurological diseases.

1. Introduction

Silks, popularly known for their flexibility and degradability, have been used as suture materials, and silk fibroin (SF) is a natural nonphysiological macromolecular protein extracted from boiling silk cocoons in an alkaline solution. SF is made up of a light chain (25 kDa) and a heavy chain (391 kDa). The heavy chain is the dominant component of 5263 amino acid residues, most of which are glycine (G, 45.9%), alanine (A, 30.3%), and serine (S, 12.1%). Because hydrophobic regions of short side chain acids dominate in the primary sequence, silk usually consists of β-sheet structures, which allow for tight packing of stacked slices of hydrogen-bonded antiparallel chains of the protein [1]. Based on these structures, SF has impressive mechanical properties to assist the development of functional tissues, especially SF from silkworms and orb-weaving spiders. Excellent biocompatibility is the premise of its application as a biomaterial. Most biomaterials should be degraded at a rate that matches the formation of the new tissue to facilitate the deposition of extracellular matrix and tissue regeneration. In addition, silk fibroin can be modified with amino acid side chain chemistry to alter surface properties and impact cell proliferation. It is also noteworthy that SF has versatility options for sterilization compared with other fibrous proteins [2]. Under high-temperature environmental conditions, it can maintain its original form and structure [3]. In summary, SF is a representative structural protein due to its features that suit a wide range of biomedical applications.

Hydrogels are a sort of polymer material with a three-dimensional (3D) network structure, which is formed by chemical or physical cross-linking of hydrophilic polymer chains in an aqueous solution [4]. It absorbs large amounts of water molecules and swells but does not dissolve. Owing to their excellent water solubility, biocompatibility, ductility, and deformability, hydrogels are advanced material platforms in biomedical therapies [5]. However, the single cross-linking method and the lack of an effective energy

dissipation mechanism make the mechanical properties of traditional hydrogels poor, which limits their large-scale applications. The structure and conformation of SF strongly affect its mechanical properties, and the formation of β-sheets in the structure of SF enhances its mechanical properties [6, 7]. Based on the adjustability of SF structure by physical or chemical treatment and cross-linking strategies of SF hydrogels with other biological materials, not only did SF hydrogels solve this problem but also the application value of SF hydrogels in tissue regeneration and treatment of tumors was found.

Neurological diseases are caused by a variety of factors that lead to organic or functional disorders of the brain and spinal cord. Because of the irreversibility of neurons, the treatment and prognosis of related diseases are not satisfactory. Despite attempts to propel neuroprotective therapeutic approaches, effective advances in neuroregeneration have still not been reached. It has been suggested that silk fibroin can promote neuroregeneration, and the development of silk fibroin-based biomaterials indicates a new frontier to apply in neuroregenerative therapies. This review is aimed at introducing advances in SF hydrogels. Pathophysiological mechanisms and applications of SF in neurological disorders will also be examined.

2. Preparation of SF Hydrogels

Silk fibroin can be processed in versatile patterns, specifically aqueous-based platforms, and hydrogels are examples. When subjected to controllable physical factors such as temperature, solution concentration, shear force, and ions, SF can spontaneously aggregate or self-assemble into hydrogels [8]. Chemical cross-linking can also accelerate the gel by adding functional groups to form covalent bonds. There are sundry methods to fabricate SF hydrogels, and these techniques are important factors affecting their properties.

2.1. Physical Methods

2.1.1. Temperature. It has been shown that temperature plays a critical role in influencing protein aggregation, which depends to a large extent on the hydration of the system [9]. Increasing temperature can increase the average kinetic energy of the particles in the system and then increase the opportunity for effective collision, which is beneficial to the assembly of macromolecules. On the one hand, the dense accumulation of water around the protein encourages an increase in dehydration in the hydrophobic region and enhances hydrophobic interactions and cross-linking. On the other hand, it can perturb the free energy state of macromolecules and promote protein unfolding and hydrophobic region exposure [10]. These events work together to assemble and aggregate proteins.

2.1.2. Shear Forces. Shear force is applied to silk protein solution to cause fluid rotation and stretching, which changes the macromolecule orientation and polymer chain stretching [11]. It impacted the end-to-end distance and arrangement of the polymer chain, propelling the fluctuation of concentration and the intermolecular force [12]. The extended vortex-induced method is an easy way to make SF hydrogels with appropriate mechanical properties [13]. With increasing vortex time, the molecular conformation and intermolecular self-assembly changed with increasing protein β-sheet content, which may reflect the viscoelasticity of SF hydrogels.

2.1.3. Ultrasound. Ultrasound can affect other physical stimuli, such as local temperature raising, shear force extension, and changes in gas-liquid interface equilibrium, to promote SF rapid gelation [14, 15]. Von et al. reported that ultrasonication is a more effective way to produce hydrogel composite systems that are stable, homogenous, and well blended without phase separation [16]. Noticeably, although the gel time is controllable and it did not introduce other immunogenic substances, it requires high preparation conditions and has poor reproducibility.

2.1.4. Electric Field. Several studies are prospective on how to apply an electric field to prepare electroactive SF hydrogels. The extra electric field can indirectly affect the local pH by increasing the proton concentration in the positive electrode, thereby regulating the aggregation of silk proteins [13]. Leisk et al. [17] discovered that in 8.4% SF solution, 25 V direct current was inserted into the gel on the positive electrode of platinum, and the gel had excellent adhesion. This study also demonstrates that the self-assembly of SF hydrogels is reversible. When the electrode is exchanged, the SF hydrogel reaggregates on the new positive electrode.

2.2. Chemical Methods

2.2.1. Organic Solvent Induction. At present, classical precipitators mainly include salt, organic solvents, and surfactants. Adding salt to SF aqueous solution can increase the ionic strength of the solvent and enhance the ability to combine with water, thus changing the interaction between the protein molecules to promote the internal binding of the protein [18]. Numerous studies have confirmed that the formation of SF hydrogels can be regulated by organic solvents. First, the addition of an organic solvent can alter the dielectric properties of the solvent and reduce the solubility of water, thus promoting supersaturation of the solution [18, 19]. Simultaneously, organic solvents generally with strong polarity destroy the intermolecular hydrogen bonds and electrostatic bonding, increasing molecular chain unfolding and β-sheet generation, and then the chain segments rearrange and self-assemble [20]. Among those organic solvents, alcohol is the most common [21, 22]. Besides, glycerol [23] and ethylene glycol diglycidyl ether (EGDE) [24] are can be used as well. Surface agents refer to making the interface state of the solution change dramatically, such as poloxamer 407 [25] and sodium dodecyl sulfate (SDS) [26].

2.2.2. pH. pH is one of the crucial parameters to readjust SF hydrogels. It can convert the ionization state of the amino acid residues on the gel surface and can promote gel formation when the pH is on the brink of the isoelectric point (pI). In a study, it was impressive to note that adjusting the pH allows the solution to transform between gel and sol, but

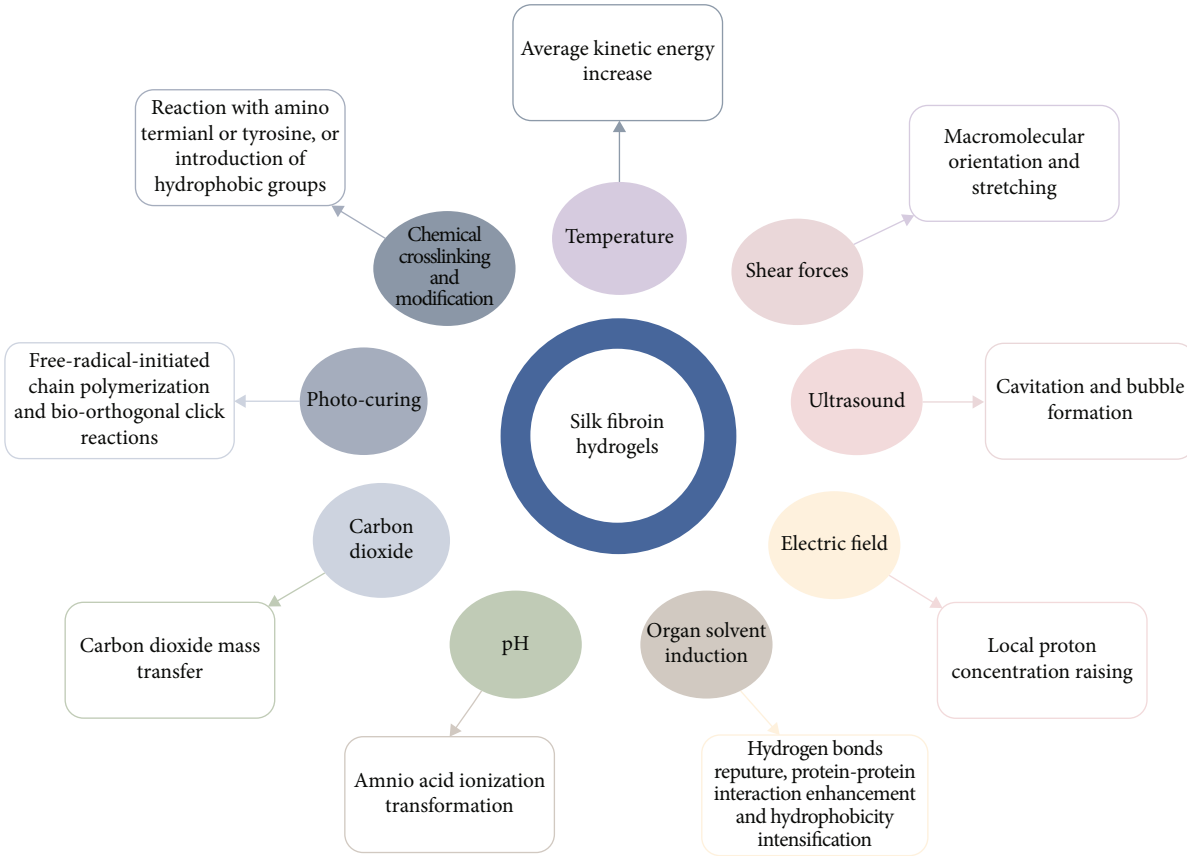

Figure 1: The preparation of SF hydrogels.

only under transient exposure conditions [27]. Mechanistically lowering the pH inhibits the ionization of the acidic amino acid so that the balance between repulsion and attraction is crippled and the hydrophobic interaction is strengthened, resulting in a weaker bond [27]. Nevertheless, under acidic conditions for long periods, the denaturation of SF and extended intramolecular and intermolecular hydrogen bonds promote the formation of large amounts of β-sheets, forming stable gels [27, 28].

2.2.3. Carbon Dioxide. Carbon dioxide (CO_2), as a volatile acid, can be a novel way to prepare SF hydrogels without surfactants or chemical cross-linking agents. Floren et al. [29] obtained stable hydrogels under high-pressure CO_2 treatment for less than 2 hours with tremendous physical properties such as porosity, sample homogeneity, swelling behavior, and compressive features. However, whether high pressure has a promoting effect on gel formation is still complex and worth exploring. Another study experimented with low-pressure CO_2, in which gel time was briefly within ten minutes because of very small gas bubble-to-liquid path lengths, significantly shorter than the high-pressure condition (120 minutes) [30]. Therefore, high pressure does not seem to necessarily reduce the gel time.

2.2.4. Photocuring. Photocuring is a method of preparing hydrogels by chemical cross-linking. The presence of light energy, including ultraviolet (200-400 nm) and visible light (400-800 nm), provides photons to photoinitiators, and then they absorb the energy of the photons to split into free radical molecules. These molecules react with the vinyl bonds in the prepolymer, resulting in chemical cross-linking of the polymer chain, namely, free radical-initiated chain polymerization [31, 32]. Photooxidation is advantageous in maintaining the protein structure and eliminating the need for chemical modification. In contrast, methacrylate is better in terms of photo-cross-linking efficiency by organic solvents, such as acetone and ethanol [33].

2.2.5. Chemical Cross-Linking and Modification. Chemical cross-linking agents, including glutaraldehyde, genipin, diepoxide, and horseradish peroxidase (HRP) enzyme plus hydrogen peroxide (H_2O_2), have been used in practice [8, 34–36]. Chemical cross-linking and modification are fabricated to prepare hydrogels by forming covalent bonds according to the molecular structure of SF. Most of them are located in the amino group of SF. Chemical modification can involve the chemical properties of SF to achieve SF hydrogel functionalization. Modifications such as sulfation of tyrosine, azo-modified tyrosine, and arginine masking provide sites for growth factors, cell-binding domains, and other polymers to attach to SF, expanding the range of biomaterial applications [37]. Herein, regulatory factors of SF hydrogels are diverse, which interact with each other (Figure 1).

Silk fibroin hydrogels can be processed in versatile patterns. The methods to fabricate SF hydrogels, including

physical and chemical methods, are important factors affecting the properties of SF. SF hydrogels exhibited networks morphology with β-sheet structure through the mutual influence of each regulatory factor.

2.3. Blend Hydrogels. Poor elasticity, low water retention ability, and lack of a cell attachment sequence limit the usage of SF. As long as the materials have no vital negative biological impact, both natural and synthetic polymers can be utilized to fabricate hydrogels, which result in rapid gelation and high biological activity. Natural polymers have higher biocompatibility, excellent biodegradability, and no toxicity. So far, collagen, chitosan, gelatin, silk fibroin, alginate, cellulose, hyaluronic acid (HA), and starch, alone or in combination, have been widely used in tissue engineering. Polymerization with gelatin can improve biological activity, such as cell attachment, diffusion, and proliferation [38]. In recent years, tyramine modification catalysis by enzymes has gradually become the emerging trend of HA involvement in SF hydrogels. HA content can affect the extracellular matrix and upregulate matrix protein expression, and HA-Tyr-SF is suitable for tissue engineering and drug delivery as an injectable biomaterial [39]. Apart from the abovementioned polymers, the combination of SF with cellulose, alginate, and chitosan has exceptional ability in tissue regeneration engineering, drug delivery, wound healing, and other fields [40–42]. SF can be mixed also with synthetic polymers. Silk fibroin-based mixtures with poly (ethylene glycol), poly (vinyl alcohol), polyacrylamide, polycaprolactone, poly (lactic-co-glycolic acid), polyurethane, and polylactide have been reported [43]. Adjusting the properties of macromolecular polymers, such as molecular weight transitions or chemical modifications, directly urges the mechanical, degradability, and physical capabilities of synthetic polymers, all of which afford functionality and task-specific biomaterial traits in tissue regeneration and wound healing [44]. Designing SF hydrogels with controllable mechanical properties, degradation rate, and biocompatibility per regenerated tissue is key to regenerative therapies to better achieve individualized therapeutic goals.

3. Pathophysiological Mechanisms of SF Hydrogels

3.1. Neuroregeneration. Regeneration and repair of nerve tissue after brain injury are difficulty in the treatment and improvement of neurological diseases. Regenerative therapies based on active biomaterials and encapsulated therapeutic stem cells have profound therapeutic potential. As a naturally energetic material, SF has nerve biocompatibility and can support cell adhesion, proliferation, and neural differentiation. Hydrogels can modulate the mechanical stiffness of brain tissue and replace the damaging environment, acting as cell carriers or growth factor delivery vehicles. Seed cells, such as embryonic stem cells, neural stem cells, and mesenchymal stem cells, completed cell adhesion, cell proliferation, and cell differentiation in the ECM microenvironment mimicked by SF hydrogels and achieved tissue regeneration under the interaction of growth factors and nutrients [45–47]. The biochemical factors fixed on the ECM regulate local concentrations and influence cell proliferation and differentiation. Although SF hydrogel scaffolds can mimic the 3D microenvironment of natural ECM to facilitate nutrient exchange and provide mechanical protection, the effects of the secretive activity of encapsulated stem cells remain to be seen. Martín-Martín et al. demonstrated that MSCs encapsulated in SF hydrogels may induce the secretion of several neurogenic and angiogenic factors more than the nonencapsulated group, such as brain-derived neurotrophic factor (BDNF), vascular endothelial growth factor (VEGF), and SDF-1 protein [48]. Biomaterial surfaces can present nanoscale topographical cues which influence neuronal differentiation and process outgrowth. Bai et al. designed SF nanofiber hydrogels and complex three-dimensional (3D) porous structures to mimic the elastic modulus and topography by altering the annealing process [46]. They demonstrated that 50% methanol promoted the differentiation of NSCs into astrocytes, while 80% methanol inhibited this phenomenon, and the number of caspase 3^+ cells in the treatment groups was decreased, suggesting that the topography and mechanical evaluation brought by annealing treatments prevented or delayed NSC apoptosis [46]. In this context, we briefly summarize that SF hydrogels may play a 3D microenvironment akin to natural ECM, facilitating mechanical protection and nutrient exchange (Figure 2).

Recognition between the arginine sequence in SF and integrin on the cell membrane mediates cell adhesion to the ECM and then affects cytoskeletal motion. On the other hand, growth factors, such as PDGF and FGF, combined with receptors, induce cell proliferation through the MAPK signaling pathway. In parallel, they also induce the differentiation of encapsulated stem cells into the neuronal cells, which then secrete related growth factors and nutritional factors to accelerate nerve tissue regeneration and improve tissue repair.

3.2. Regulating Inflammation. Active inflammatory activity after brain injury causes irreversible damage to the brain, which is not conducive to the treatment and postoperative recovery of patients. SF hydrogels play an anti-inflammatory role because they are regarded as mechanical barriers to block the negative regulation of inflammatory factors (such as TNF-α) interacting with anti-inflammatory factors and neurotrophic factors. More importantly, it upregulates the expression of the anti-inflammatory factor TGF-β, which in turn allows microglia to differentiate into an anti-inflammatory phenotype and repair brain damage [48]. This may be linked to cytoskeletal abnormalities, oxidative stress responses, and hypoxic microenvironments [48]. Some researchers have combined anti-inflammatory active substances or drugs with SF hydrogels to exert anti-inflammatory effects. After introducing biliverdin, a precursor of bilirubin, into the SF hydrogel systems for incubation, the expression of the inflammatory factors TNF-α and interleukin-1 (IL-1) was significantly downregulated at 7 and 14 days [49]. In another study, betamethasone was loaded into tyramine-modified gellan gum with silk fibroin (Ty-GG/SF), hydrogel and the concentration of TNF-α was

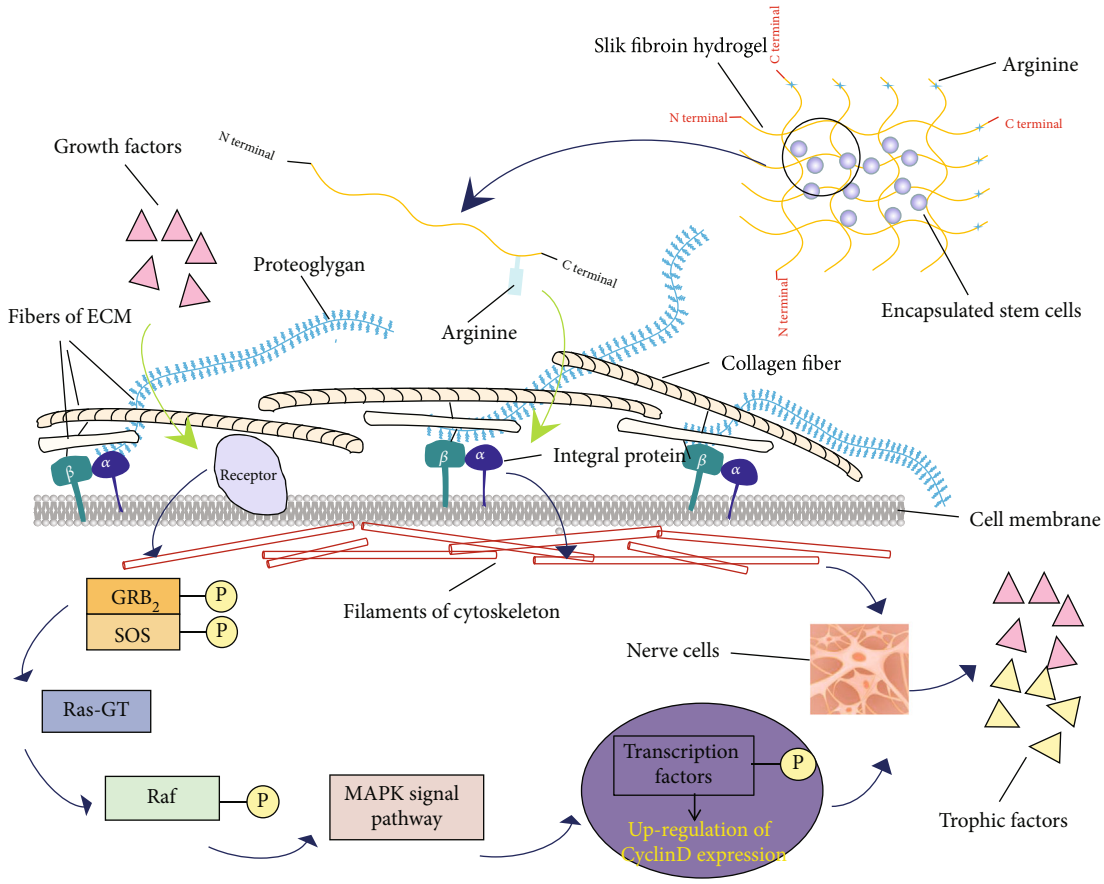

Figure 2: SF hydrogels play a 3D microenvironment akin to natural ECM.

undoubtedly decreased [50]. In contrast to traditional drug administration, this method can enhance the local concentration of drugs in the inflammatory environment to exert its efficacy, preventing normal tissues from the toxic effect of drugs on cells and tissues.

3.3. Sustained Drug Release. Owing to its unique material properties, stabilization effects, and tight controllability, silk fibroin hydrogel represents a promising, controlled, sustained drug release from fully degrading implants. Betamethasone has a short half-life, meaning that it needs to inject with repeated doses to maintain the active drug concentration. Oliveira et al. designed composite Ty-GG/SF hydrogels that have more β-sheet structures, better mechanical properties, and more resistance to enzymatic degradation than pure SF hydrogels [50]. Thus, it can improve the pharmacokinetic characteristics of the controlled release of betamethasone over time, prolong the duration of treatment, reduce the frequency of administration, and decrease the toxicity of drugs. As a drug-loading platform, SF hydrogels have the problem of initial drug release. However, this does not necessarily lead to bad results. Some scholars have concluded that the addition of SF can enable the rapid release of hydrophobic drugs, providing a new technical means for the rapid increase in local drug concentration in some diseases [51]. Other studies have shown that adjusting SF and other drugs/polymers ratios can lead to sustained-release capabilities of risperidone. At ratios of 1 : 3 and 1 : 6, SF/methanol hydrogels contained risperidone, which could be made public for 25 days, but the former had better structural stability [52]. In conclusion, SF-based platforms that permit both sustained and local release of factors represent an attractive approach for efficient delivery of the factor to the brain. Therefore, emphasis should be placed on the combination of material characteristics, drug effects, clinical therapeutic purposes, and expected efficacy, and appropriate SF hydrogels should be selected as drug-loading vehicles.

3.4. Antioxidative Stress. Oxidative-antioxidant dynamic balance in the central nervous system (CNS) affects normal brain function. Excessive production of endogenous or exogenous oxides and/or inadequate function of the antioxidant response system will lead to the accumulation of adverse reactive oxygen species (ROS), leading to oxidative stress response and making brain tissue overly susceptible to damage [53]. Oxidative stress is the main cause of neurodegenerative diseases due to the oxidation of DNA, lipids, and proteins, thereby inducing a secondary cellular response. Antioxidants can be used to scavenge free radicals, and SF biomaterials can be regarded as good carriers of antioxidants. In a study, SF nanoparticles (SFSNPs), which were infiltrated into the antioxidant sulforaphane, effectively reduced the increase of ROS levels caused by hydrogen peroxide- (H_2O_2-) mediated oxidative stress [54]. Based on the

excellent mechanical properties and biocompatibility of SF hydrogels, we speculated that SF hydrogels could form a physical barrier to protect antioxidants from removal, prolong the preservation time, and exert a lasting antioxidant stress effect. On the other hand, SF hydrogels equipped with stem cells or growth factors and other active substances can be developed to provide a living space for antioxidant enzymes and simulate the physiological antioxidant system.

3.5. Regulating Cell Death. Cell death is important in both physiological and pathological conditions. Cell death in the brain contains the following characteristics: (1) neurons are permanent cells with limited regenerative capacity; (2) because of the various types of ion channels in nerve cells, damage to them may result in various death patterns; and (3) the high consumption of ATP in brain tissue and the modest turnover of ATP may induce the death of ischemic hypoxia stimulation [55]. Currently, cell death can be divided into programmed and nonprogrammed cell death. In general, except necrosis, apoptosis, autophagic cell death, ferroptosis, and pyroptosis constitute programmed cell death. The control and regulation of the apoptotic events that occur through SF have been reported recently. Anticancer activity of SF peptides (SFPs) has been proven to be associated with the inhibition of tumor cell proliferation, induction of apoptosis, and cell cycle arrest [56]. NSCs encapsulated by SF nanofiber hydrogels exhibited a reduced number of caspase 3^+ cells, suggesting that SF prevented or delayed NSCs from undergoing apoptosis [46]. Our team is currently investigating other cell death pathways. Overall, we are positive about the SF prospect of regulating cell death, including pyroptosis and ferroptosis.

3.6. Hemostasis. Bleeding is a common clinical symptom caused by acute trauma. The amount of blood loss, timing, and timely intervention are closely related to the patient's prognosis. Effective hemostasis and hemostatic materials play an important role in controlling blood loss. Current medical hemostatic materials have side effects, such as wound infection, inflammatory injury, and body allergies caused by gelatin [57]. Studies have begun to consider SF an alternative material with good biocompatibility and hemostatic properties. Visceral injury is very common in trauma and is easily accompanied by blood loss. A team constructed an animal model of liver injury (wound size: 1.5 cm × 1.0 cm × 0.2 cm) to evaluate the hemostasis of SF by hemostasis time and blood loss. The results showed that the addition of SF, as part of the material composition, improved hemostatic performance and was superior to the gelatin group and the blank group [58]. SF can rapidly gel to block the bleeding site as a physical barrier and induce platelet adhesion and aggregation and enhance platelet and fibrinogen interactions while maintaining platelet activity [58]. This performance is similar to that of the endogenous platelet agonist ADP, which induces blood coagulation and has a hemostatic effect. Research on the hemostatic performance of SF is just beginning, and the specific mechanism of SF on physiological hemostasis, such as the mechanism affecting the release of coagulation factors, still needs more research explanation. The role of silk fibroin hydrogels in brain hemostasis can be studied in the future.

4. Potential Roles of SF Hydrogels in Neurological Diseases

Laboratory applications of SF cover a wide range of fields, with outstanding performance in vivo and/or in vitro experiments (Table 1). Clinical trials have been carried out in some areas dabbling in neurological diseases, but the results are less satisfactory than had been anticipated (Table 2). The potential value of SF hydrogels in neurological diseases is systematically described in Table 1.

4.1. Cerebral Stroke. Acute cerebral strokes, also known as cerebrovascular accidents, are broadly classified as either ischemic or hemorrhagic. The time window of treatment is narrow after the onset of stroke, accompanied by severe complications such as angioedema, intracranial hemorrhage, or systemic massive hemorrhage, which is a leading cause of serious long-term disability [73]. Therefore, early identification and intervention affect the clinical evolution of stroke. The safety of silk fibroin in the brain has been investigated. Fernandez-Garcia et al. reported that the striatal injection of SF hydrogel was reasonably well tolerated by the animals because the survival rate exceeded 90% and was similar to that of the saline group [74]. The authors also demonstrated that SF hydrogel encapsulated stem cells reduced the damaged cortical infected area and exerted progressive neuroprotective effects in ischemic stroke [75]. Another study explained the excellent spatial consistency of SF hydrogels in filling the stroke cavity and provided a reliable matrix for regeneration without significant inflammation mediated by microglia/macrophage activation [76]. Lim et al. developed an injectable gelatin hydrogel containing epidermal growth factor (Gtn-ECF), which can effectively repair the defective tissue and restore nerve function after intracerebral hemorrhage (ICH) [77]. However, the application of SF hydrogel in hemorrhagic stroke is still in the theoretical stage, and the role of SF hydrogel in ICH needs to be investigated.

4.2. Traumatic Brain Injury. Traumatic brain injury (TBI), also known as an intracranial injury, causes functional impairment of key brain areas under the action of strong external forces, which has brought a huge burden to families and society and has become a major problem endangering public health security [78]. After TBI, the microenvironment of ischemia and hypoxia caused by glial hyperplasia, inflammation, and lack of neurotrophic factors inhibits the regeneration and repair of brain tissue. The development of SF hydrogel either alone or in combination with other therapies will be a reasonable and innovative choice in the field of TBI treatment. Moisenovich et al. reported that transplantation of silk fibroin microparticles into the injury locus of the brain resulted in a decrease in damage volume, as well as the restoration of sensorimotor functions [79]. Tang-Schomer et al. showed that silk fibroin films can be utilized to evaluate drug actions in both in vitro and in vivo studies

Table 1: List of the applications of SF or SF blends.

Application	Materials	In vitro	In vivo	Cite
Cartilage tissue engineering	GMA/SF	Human chondrocytes	Female athymic mice, rabbits	[59]
Bone defect repair	n-HA-GO/SF	Rabbit bone marrow mesenchymal stem cells (BMSCs)	Male mice critical-sized bone defect models	[60]
Ligament reconstruction	SF/HA-SF	Rat BMSCs	Rabbit models of ACLR	[61]
Wound healing	CF@GO/SF	Human fibroblast (L929) cells	Rat models of wound	[62]
Reconstitution of cardiac function	SF	Rat quiescent ventricular cardiomyocytes	Left ventricles of rats	[63]
Vascular remolding	SF/GT	Mouse BMSCs	/	[64]
Trachea reconstruction	SF/CVM	Human-induced pluripotent stem cells (hiPSCs)	Porcine tracheal defect models	[65]
Artificial cornea engineering	PVA/SF/n-HA/GP	Human corneal fibroblasts (HCFs)	/	[66]
Enamel regeneration	SF/HA	/	/	[67]
Hepatic tissue engineering	SF	Stem cells from human exfoliated deciduous teeth (SHED)	/	[68]
Bladder reconstruction	SF	Adipose-derived stem cells (ASCs)	Rat bladder augmentation models	[69]
Nucleus pulposus replacement	SF/PU	/	Rabbits	[70]
Nerve regeneration	Collagen/SF	Human umbilical cord mesenchymal stem cells (hUC-MSCs)	Rat models of SCI	[71]
Tumor therapy	Biliverdin/SF	/	Mice tumor models	[49]
Drug delivery	DEX/CSNPs/SF	L929 fibroblast cell line	/	[72]

GMA: glycidyl methacrylate; n-HA: nanohydroxyapatite; GO: graphene oxide; ACLR: anterior cruciate ligament reconstruction; CF: ciprofloxacin; GT: gelatin-tyramine; CVM: collagen vitrigel membrane; GP: genipin; PU: polyurethane; SCI: spinal cord injury; DEX: dexamethasone; CSNPs: chitosan nanoparticles.

of brain injury with greater efficiency than existing approaches [80]. Silk film-delivered necrostatin reduced cell necrosis in the TBI model, which is consistent with intracerebroventricular delivery of necrostatin in reducing histopathology and improving functional outcomes [81]. A combination of SF/collagen/human umbilical cord mesenchymal cells (hUMSCs) coculture (CB group) has been implanted into TBI canine models, showing great potential for treating TBI. Compared with the stem cells group (SC group) and the collagen/SF group (CS group), the CB group displayed a significant anti-inflammation effect and repair of cerebral cortical motility after TBI [82]. Although the study confirmed the potential of SF hydrogels and stem cells regeneration therapies for clinical applications, questions remain to be considered. For example, the regulation of stem cells survival and targeted differentiation, the specific mechanism of injury repair, and the optimal time window for implantation necessitated further exploration and discussion [83].

4.3. Brain Tumors. Glioblastoma (GBM) is the most frequent tumor in the central nervous system and has highly diffuse malignant infiltration behavior. Chemotherapy, a routine operation for the clinical treatment of GBM, lacks the specificity of systemic administration, and side effects that occur during chemotherapy treatment seriously affect the homeostasis of the body in patients, which are not conducive to treatment and recovery [84]. Moreover, hydrophobic chemotherapeutic drugs account for a large proportion of chemotherapeutic drugs, and their solubility in water medium is scant. SF contains more hydrophobic areas, and cross-linking between SF and hydrogels can enhance hydrophobicity to directly transport hydrophobic drugs to the tumor site. Xu et al. constructed indocyanine green-SF nanoparticles (ICG-SFNPs) for photothermal therapy of glioblastoma, which can form local high temperatures and cause a large area of tumor necrosis [85]. Recently, Ribeiro et al. reported that the crystalline SF hydrogels converted into β-sheet structure induced the formation of TUNEL-positive apoptosis in a human neuronal glioblastoma cell line (U251) [86]. Wang et al. showed that a silk fibroin microneedle (SMN) patch loaded with chemotherapeutic agents (thrombin and temozolomide) and targeted drug (bevacizumab) induces rapid drug delivery and results in decreased tumor volume and increased survival rate in GBM mice [87]. From the foregoing description, we boldly assume that SF hydrogels can act as a physical barrier to resist the degradation of encapsulated drugs. In parallel, enhancement of hydrophobicity is beneficial for SF hydrogels as drug delivery systems for the targeted therapy of GBM.

4.4. Neurodegenerative Diseases. Neurodegenerative diseases are characterized by progressive loss of vulnerable populations of neurons and histopathological findings of abnormal conformational change of self-proteins, including amyloidosis, tau protein, alpha-synuclein, and transactivation response DNA binding protein 43 (TDP-43) [88]. The highly repetitive GAGAGS in SF can be analogous in structure to VGGVV in amyloidosis β42 peptide and VGGAVV

Table 2: List of the published clinical trials that highlight the application of silk-based materials.

No.	Intervention/treatment	Condition/disease	Number of participants	Compete date	Clinical trial identifier
1	Device: The SF patch or paper patch	Diseases of the ear and mastoid process	60	June 2012	KCT0000305
2	Device: HQ® matrix medical wound dressing Device: Sidaiyi® wound dressing	Donor site wound	71	September 2014	NCT01993030
3	Device: silk fibroin with bioactive coating layer dressing	Late complication from skin graft; infection of skin donor site; impaired wound healing; pain, intractable	29	May 2015	NCT02091076
4	Bilayer scaffold composed of amniotic membrane and silk fibroin	Diabetes mellitus; Wagner ulcer grade II	20	February 2018	IRCT2016071328903N1
5	Absorbable SF membrane	Alveolar ridge preservation after tooth extraction	65	December 2018	ChiCTR1800016759
6	Autologous chondrocytes seeded in SF scaffolds	Osteochondral defects	15	July 2019	IRCT2017062434731N1
7	SF membrane combined with xenograft	K053-chronic periodontitis	15	December 2019	CTRI/2018/12/016509
8	SeriossÂ® (SF scaffold)	Patients undergoing surgery for bone void filling	10	/	CTRI/2021/01/030589
9	Device: Silk Bridge	Peripheral nerve injury digital nerve hand	4	March 2021	NCT03673449
10	Silk sericin dressing with collagen	Wound heal; wound surgical; donor site complication	30	December 2021	NCT04743375
11	Procedure: Silk microparticle filler injection	Vocal cord paralysis unilateral; dysphonia; dysphagia, oropharyngeal	100	September 2024	NCT03790956

Source: data retrieved from International Clinical Trials Registry Platform.

AGV in alpha-synuclein [89]. Simultaneously, the silk I structure (random coil and helix-like forms) turns into silk II (beta-sheet and beta-sheet-like forms), a nucleation-dependent conformation transition principle, that bears extreme resemblance to that of neurodegenerative-related proteins [90]. The antioxidant, neuroprotective, and acetylcholinesterase inhibitory mechanisms of silk proteins could prove promising in the treatment of neurodegenerative diseases [91]. However, the application of SF hydrogel in neurodegenerative diseases is still in the theoretical stage and needs to be investigated.

4.5. Traumatic Spinal Cord Injury. Traumatic spinal cord injury (TSCI) is a devastating central nervous system disease and can be divided into primary injury (initial mechanical injury) and secondary injury, including ischemia, oxidative stress, axonal degeneration, and cell death triggered by inflammatory processes [92]. The involvement of SF in post-SCI has been demonstrated in several studies [71, 93, 94]. In vitro culture of human amniotic epithelial cells (AECs) implanted with SF scaffolds showed active proliferation and migration, which improved motor function after SCI [95]. Bone mesenchymal stem cells (BMSCs) implanted in SF scaffolds confirmed the excellent performance in axonal regeneration, myelination, and functional recovery in SCI rat models [96]. Drug-loaded injectable SF scaffolds for the treatment of SCI have also great potential for spinal cord regeneration. Han et al. reported that metformin-loaded silk fibroin microsphere could improve the growth and spreading behavior of cortical neurons after SCI [97]. Taken together, the application of SF hydrogel in TSCI is promising and worthy of further exploration.

5. Conclusion and Limitations

In summary, with in-depth research, the silk fibroin hydrogels have transformed from simple and independent structures to functionalized cross-linked forms with other polymers by physical or chemical methods. It is widely accepted that SF hydrogels loaded with cells and growth factors have great potential to address the challenge of regenerating neuronal cells. The prospects of using silk fibroin hydrogels alone and their blends are quite exciting in neurological disease due to the positive results achieved in vitro and in vivo. Despite the promising results mentioned earlier, there are still some important issues to be addressed in the future. First, the major disadvantages of silk fibroin hydrogels are their poor mechanical properties and swelling behavior, which are very important parameters in biomedical applications. To improve the properties of SF hydrogels, silk fibroin has been blended with various other polymers. Therefore, the potential long-term toxicity and the nonbiodegradability of blended SF hydrogel should be further investigated. Second, the specific effects of SF hydrogel on

cells, tissues, or organs and their metabolic pathway in vivo remain unclear and require further studies. Third, the cellular/molecular mechanisms behind the neuroprotective ability of SF hydrogel should be further investigated. It is expected that the silk fibroin hydrogels loaded with or without seed cells or drug agents may be the most effective treatment for brain disease and are subject to future clinical trials. However, at present, the functionalization of the silk fibroin hydrogels in the neurological disease is still in its infancy; thus, many aspects are still needed to be developed and improved. In summary, silk fibroin hydrogels have great prospects of expanding their niche in the field of brain tissue regeneration, repairing damaged brain tissue, and improving neurologic recovery after injury.

Conflicts of Interest

The authors declare no conflicts of interest.

Authors' Contributions

Chun Yang, Sunao Li, and Xinqi Huang Contributed equally to this work.

Acknowledgments

This work was supported by the National Natural Science Foundation of China (No. 82071382, No. 81971800, and No. 81601306), Priority Academic Program Development of Jiangsu Higher Education Institutions (PAPD), Jiangsu Maternal and Child Health Research Key Project (F202013), Jiangsu Talent Youth Medical Program (QNRC2016245), Shanghai Key Lab of Forensic Medicine (KF2102), Suzhou Science and Technology Development Project (SYS2020089), Fifth Batch of Gusu District Health Talent Training Project (GSWS2019060), and Undergraduate Training Program for Innovation and Entrepreneurship, Soochow University (202010285139Y).

References

[1] C. Vepari and D. L. Kaplan, "Silk as a biomaterial," *Progress in Polymer Science*, vol. 32, no. 8-9, pp. 991–1007, 2007.

[2] A. Sugihara, K. Sugiura, H. Morita et al., "Promotive effects of a silk film on epidermal recovery from full-thickness skin wounds," *Proceedings of the Society for Experimental Biology and Medicine*, vol. 225, no. 1, pp. 58–64, 2000.

[3] L. Meinel, S. Hofmann, V. Karageorgiou et al., "Engineering cartilage-like tissue using human mesenchymal stem cells and silk protein scaffolds," *Biotechnology and Bioengineering*, vol. 88, no. 3, pp. 379–391, 2004.

[4] J. L. Drury and D. J. Mooney, "Hydrogels for tissue engineering: scaffold design variables and applications," *Biomaterials*, vol. 24, no. 24, pp. 4337–4351, 2003.

[5] C. M. Kirschner and K. S. Anseth, "Hydrogels in healthcare: from static to dynamic material microenvironments," *Acta Materialia*, vol. 61, no. 3, pp. 931–944, 2013.

[6] Y. Lin, X. Xia, K. Shang et al., "Tuning chemical and physical cross-links in silk electrogels for morphological analysis and mechanical reinforcement," *Biomacromolecules*, vol. 14, no. 8, pp. 2629–2635, 2013.

[7] A. T. Nguyen, Q. L. Huang, Z. Yang, N. Lin, G. Xu, and X. Y. Liu, "Crystal networks in silk fibrous materials: from hierarchical structure to ultra performance," *Small*, vol. 11, no. 9-10, pp. 1039–1054, 2015.

[8] W. H. Elliott, W. Bonani, D. Maniglio, A. Motta, W. Tan, and C. Migliaresi, "Silk hydrogels of tunable structure and viscoelastic properties using different chronological orders of genipin and physical cross-linking," *ACS Applied Materials & Interfaces*, vol. 7, no. 22, pp. 12099–12108, 2015.

[9] W. Wang, S. Nema, and D. Teagarden, "Protein aggregation–pathways and influencing factors," *International Journal of Pharmaceutics*, vol. 390, no. 2, pp. 89–99, 2010.

[10] S. Nagarkar, T. Nicolai, C. Chassenieux, and A. Lele, "Structure and gelation mechanism of silk hydrogels," *Physical Chemistry Chemical Physics*, vol. 12, no. 15, pp. 3834–3844, 2010.

[11] C. Rangelnafaile, A. B. Metzner, and K. F. Wissbrun, "Analysis of stress-induced phase separations in polymer-solutions," *Macromolecules*, vol. 17, no. 6, pp. 1187–1195, 1984.

[12] H. Ji and E. Helfand, "Concentration fluctuations in sheared polymer-solutions," *Macromolecules*, vol. 28, no. 11, pp. 3869–3880, 1995.

[13] T. Yucel, P. Cebe, and D. L. Kaplan, "Vortex-induced injectable silk fibroin hydrogels," *Biophysical Journal*, vol. 97, no. 7, pp. 2044–2050, 2009.

[14] X. Wang, J. A. Kluge, G. G. Leisk, and D. L. Kaplan, "Sonication-induced gelation of silk fibroin for cell encapsulation," *Biomaterials*, vol. 29, no. 8, pp. 1054–1064, 2008.

[15] J. M. J. Paulusse and R. P. Sijbesma, "Ultrasound in polymer chemistry: revival of an established technique," *Journal of Polymer Science Part A: Polymer Chemistry*, vol. 44, no. 19, pp. 5445–5453, 2006.

[16] T. Vu, Y. Xue, T. Vuong et al., "Comparative study of ultrasonication-induced and naturally self-assembled silk fibroin-wool keratin hydrogel biomaterials," *International Journal of Molecular Sciences*, vol. 17, no. 9, p. 1497, 2016.

[17] G. G. Leisk, T. J. Lo, T. Yucel, Q. Lu, and D. L. Kaplan, "Electrogelation for protein adhesives," *Advanced Materials*, vol. 22, no. 6, pp. 711–715, 2010.

[18] A. McPherson and J. A. Gavira, "Introduction to protein crystallization," *Acta Crystallographica Section F*, vol. 70, no. 1, pp. 2–20, 2014.

[19] T. A. Duncombe, C. C. Kang, S. Maity et al., "Hydrogel pore-size modulation for enhanced single-cell Western blotting," *Advanced Materials*, vol. 28, no. 2, pp. 327–334, 2016.

[20] C. L. Stevenson, "Characterization of protein and peptide stability and solubility in non-aqueous solvents," *Current Pharmaceutical Biotechnology*, vol. 1, no. 2, pp. 165–182, 2000.

[21] Z. Gong, L. Huang, Y. Yang, X. Chen, and Z. Shao, "Two distinct β-sheet fibrils from silk protein, Chemical Communications," *Chemical Communications*, vol. 48, pp. 7506–7508, 2009.

[22] K. Numata, T. Katashima, and T. Sakai, "State of water, molecular structure, and cytotoxicity of silk hydrogels," *Biomacromolecules*, vol. 12, no. 6, pp. 2137–2144, 2011.

[23] T. Hanawa, A. Watanabe, T. Tsuchiya, R. Ikoma, M. Hidaka, and M. Sugihara, "New oral dosage form for elderly patients: preparation and characterization of silk fibroin gel," *Chemical And Pharmaceutical Bulletin*, vol. 43, no. 2, pp. 284–288, 1995.

[24] I. Karakutuk, F. Ak, and O. Okay, "Diepoxide-triggered conformational transition of silk fibroin: formation of hydrogels," *Biomacromolecules*, vol. 13, no. 4, pp. 1122–1128, 2012.

[25] M. K. Yoo, H. Y. Kweon, K. G. Lee, H. C. Lee, and C. S. Cho, "Preparation of semi-interpenetrating polymer networks composed of silk fibroin and poloxamer macromer," *International Journal of Biological Macromolecules*, vol. 34, no. 4, pp. 263–270, 2004.

[26] X. Wu, J. Hou, M. Li, J. Wang, D. L. Kaplan, and S. Lu, "Sodium dodecyl sulfate-induced rapid gelation of silk fibroin," *Acta Biomaterialia*, vol. 8, no. 6, pp. 2185–2192, 2012.

[27] A. E. Terry, D. P. Knight, D. Porter, and F. Vollrath, "pH induced changes in the rheology of silk fibroin solution from the middle division of Bombyx mori silkworm," *Biomacromolecules*, vol. 5, no. 3, pp. 768–772, 2004.

[28] A. Matsumoto, J. Chen, A. L. Collette et al., "Mechanisms of silk fibroin sol-gel transitions," *The Journal of Physical Chemistry. B*, vol. 110, no. 43, pp. 21630–21638, 2006.

[29] M. L. Floren, S. Spilimbergo, A. Motta, and C. Migliaresi, "Carbon dioxide induced silk protein gelation for biomedical applications," *Biomacromolecules*, vol. 13, no. 7, pp. 2060–2072, 2012.

[30] R. R. Mallepally, M. A. Marin, and M. A. McHugh, "CO_2-assisted synthesis of silk fibroin hydrogels and aerogels," *Acta Biomaterialia*, vol. 10, no. 10, pp. 4419–4424, 2014.

[31] C. C. Lin, C. S. Ki, and H. Shih, "Thiol-norbornene photo-click hydrogels for tissue engineering applications," *Journal of Applied Polymer Science*, vol. 132, no. 8, p. n/a, 2015.

[32] N. Annabi, A. Tamayol, J. A. Uquillas et al., "25th anniversary article: rational design and applications of hydrogels in regenerative medicine," *Advanced Materials*, vol. 26, no. 1, pp. 85–124, 2014.

[33] X. Mu, J. K. Sahoo, P. Cebe, and D. L. Kaplan, "Photo-crosslinked silk fibroin for 3D printing," *Polymers*, vol. 12, no. 12, p. 2936, 2020.

[34] T. Srisawasdi, K. Petcharoen, A. Sirivat, and A. M. Jamieson, "Electromechanical response of silk fibroin hydrogel and conductive polycarbazole/silk fibroin hydrogel composites as actuator material," *Materials Science & Engineering C-Materials for Biological Applications*, vol. 56, pp. 1–8, 2015.

[35] Z. Oztoprak and O. Okay, "Reversibility of strain stiffening in silk fibroin gels," *International Journal of Biological Macromolecules*, vol. 95, pp. 24–31, 2017.

[36] A. Sundarakrishnan, E. Herrero Acero, J. Coburn, K. Chwalek, B. Partlow, and D. L. Kaplan, "Phenol red-silk tyrosine crosslinked hydrogels," *Acta Biomaterialia*, vol. 42, pp. 102–113, 2016.

[37] A. R. Murphy and D. L. Kaplan, "Biomedical applications of chemically-modified silk fibroin," *Journal of Materials Chemistry*, vol. 19, no. 36, pp. 6443–6450, 2009.

[38] U. Hersel, C. Dahmen, and H. Kessler, "RGD modified polymers: biomaterials for stimulated cell adhesion and beyond," *Biomaterials*, vol. 24, no. 24, pp. 4385–4415, 2003.

[39] R. Ziadlou, S. Rotman, A. Teuschl et al., "Optimization of hyaluronic acid-tyramine/silk-fibroin composite hydrogels for cartilage tissue engineering and delivery of anti-inflammatory and anabolic drugs," *Materials Science & Engineering. C, Materials for Biological Applications*, vol. 120, p. 111701, 2021.

[40] P. Dorishetty, R. Balu, S. S. Athukoralalage et al., "Tunable biomimetic hydrogels from silk fibroin and nanocellulose," *ACS Sustainable Chemistry & Engineering*, vol. 8, no. 6, pp. 2375–2389, 2020.

[41] F. Rezaei, S. Damoogh, R. L. Reis, S. C. Kundu, F. Mottaghitalab, and M. Farokhi, "Dual drug delivery system based on pH-sensitive silk fibroin/alginate nanoparticles entrapped in PNIPAM hydrogel for treating severe infected burn wound," *Biofabrication*, vol. 13, no. 1, article 015005, 2020.

[42] R. Eivazzadeh-Keihan, F. Radinekiyan, H. A. M. Aliabadi et al., "Chitosan hydrogel/silk fibroin/$Mg(OH)_2$ nanobiocomposite as a novel scaffold with antimicrobial activity and improved mechanical properties," *Scientific Reports*, vol. 11, no. 1, p. 650, 2021.

[43] G. D. Mogosanu and A. M. Grumezescu, "Natural and synthetic polymers for wounds and burns dressing," *International Journal of Pharmaceutics*, vol. 463, no. 2, pp. 127–136, 2014.

[44] M. Floren, C. Migliaresi, and A. Motta, "Processing techniques and applications of silk hydrogels in bioengineering," *Journal Of Functional Biomaterials*, vol. 7, no. 3, p. 26, 2016.

[45] G. J. Wei, M. Yao, Y. S. Wang et al., "Promotion of peripheral nerve regeneration of a peptide compound hydrogel scaffold," *International Journal of Nanomedicine*, vol. 8, pp. 3217–3225, 2013.

[46] S. Bai, W. Zhang, Q. Lu, Q. Ma, D. L. Kaplan, and H. Zhu, "Silk nanofiber hydrogels with tunable modulus to regulate nerve stem cell fate," *Journal of Materials Chemistry B*, vol. 2, no. 38, pp. 6590–6600, 2014.

[47] W. Sun, T. Incitti, C. Migliaresi, A. Quattrone, S. Casarosa, and A. Motta, "Genipin-crosslinked gelatin-silk fibroin hydrogels for modulating the behaviour of pluripotent cells," *Journal of Tissue Engineering and Regenerative Medicine*, vol. 10, no. 10, pp. 876–887, 2016.

[48] Y. Martín-Martín, L. Fernández-García, M. H. Sanchez-Rebato et al., "Evaluation of neurosecretome from mesenchymal stem cells encapsulated in silk fibroin hydrogels," *Scientific Reports*, vol. 9, no. 1, p. 8801, 2019.

[49] Q. Yao, Q. H. Lan, X. Jiang et al., "Bioinspired biliverdin/silk fibroin hydrogel for antiglioma photothermal therapy and wound healing," *Theranostics*, vol. 10, no. 25, pp. 11719–11736, 2020.

[50] I. M. Oliveira, C. Gonçalves, M. E. Shin et al., "Anti-inflammatory properties of injectable betamethasone-loaded tyramine-modified gellan gum/silk fibroin hydrogels," *Biomolecules*, vol. 10, no. 10, p. 1456, 2020.

[51] J. Youn, J. H. Choi, S. Lee et al., "Pluronic F-127/silk fibroin for enhanced mechanical property and sustained release drug for tissue engineering biomaterial," *Materials*, vol. 14, no. 5, p. 1287, 2021.

[52] A. Ebrahimi, K. Sadrjavadi, M. Hajialyani, Y. Shokoohinia, and A. Fattahi, "Preparation and characterization of silk fibroin hydrogel as injectable implants for sustained release of risperidone," *Drug Development and Industrial Pharmacy*, vol. 44, no. 2, pp. 199–205, 2018.

[53] S. Salim, "Oxidative stress and the central nervous system," *The Journal of Pharmacology and Experimental Therapeutics*, vol. 360, no. 1, pp. 201–205, 2017.

[54] M. Passi, V. Kumar, and G. Packirisamy, "Theranostic nanozyme: silk fibroin based multifunctional nanocomposites to combat oxidative stress," *Materials Science & Engineering. C, Materials for Biological Applications*, vol. 107, p. 110255, 2020.

[55] M. Fricker, A. M. Tolkovsky, V. Borutaite, M. Coleman, and G. C. Brown, "Neuronal cell death," *Physiological Reviews*, vol. 98, no. 2, pp. 813–880, 2018.

[56] M. S. Wang, Y. B. Du, H. M. Huang et al., "Silk fibroin peptide suppresses proliferation and induces apoptosis and cell cycle arrest in human lung cancer cells," *Acta Pharmacologica Sinica*, vol. 40, no. 4, pp. 522–529, 2019.

[57] T. Fukui, M. Ii, T. Shoji et al., "Therapeutic effect of local administration of low-dose simvastatin-conjugated gelatin hydrogel for fracture healing," *Journal of Bone and Mineral Research*, vol. 27, no. 5, pp. 1118–1131, 2012.

[58] W. Wei, J. Liu, Z. Peng, M. Liang, Y. Wang, and X. Wang, "Gellable silk fibroin-polyethylene sponge for hemostasis," *Artificial Cells, Nanomedicine, and Biotechnology*, vol. 48, no. 1, pp. 28–36, 2020.

[59] H. Hong, Y. B. Seo, D. Y. Kim et al., "Digital light processing 3D printed silk fibroin hydrogel for cartilage tissue engineering," *Biomaterials*, vol. 232, p. 119679, 2020.

[60] B. Wang, S. Yuan, W. Xin et al., "Synergic adhesive chemistry-based fabrication of BMP-2 immobilized silk fibroin hydrogel functionalized with hybrid nanomaterial to augment osteogenic differentiation of rBMSCs for bone defect repair," *International Journal of Biological Macromolecules*, vol. 192, pp. 407–416, 2021.

[61] Z. Yan, W. Chen, W. Jin et al., "An interference screw made using a silk fibroin-based bulk material with high content of hydroxyapatite for anterior cruciate ligament reconstruction in a rabbit model," *Journal of Materials Chemistry B*, vol. 9, no. 26, pp. 5352–5364, 2021.

[62] M. Dong, Y. Mao, Z. Zhao et al., "Novel fabrication of antibiotic containing multifunctional silk fibroin injectable hydrogel dressing to enhance bactericidal action and wound healing efficiency on burn wound: in vitro and in vivo evaluations," *International Wound Journal*, vol. 19, no. 3, pp. 679–691, 2022.

[63] Y. F. Hu, A. S. Lee, S. L. Chang et al., "Biomaterial-induced conversion of quiescent cardiomyocytes into pacemaker cells in rats," *Nature Biomedical Engineering*, 2021.

[64] S. Xu, Q. Li, H. Pan et al., "Tubular silk fibroin/gelatin-tyramine hydrogel with controllable layer structure and its potential application for tissue engineering," *ACS Biomaterials Science & Engineering*, vol. 6, no. 12, pp. 6896–6905, 2020.

[65] R. Varma, A. E. Marin-Araujo, S. Rostami, T. K. Waddell, G. Karoubi, and S. Haykal, "Short-term preclinical application of functional human induced pluripotent stem cell-derived airway epithelial patches," *Advanced Healthcare Materials*, vol. 10, no. 21, article e2100957, 2021.

[66] H. Zhou, Z. Wang, H. Cao et al., "Genipin-crosslinked polyvinyl alcohol/silk fibroin/nano-hydroxyapatite hydrogel for fabrication of artificial cornea scaffolds-a novel approach to corneal tissue engineering," *Journal of Biomaterials Science. Polymer Edition*, vol. 30, no. 17, pp. 1604–1619, 2019.

[67] S. Wang, L. Zhang, W. Chen et al., "Rapid regeneration of enamel-like-oriented inorganic crystals by using rotary evaporation," *Materials Science & Engineering. C, Materials for Biological Applications*, vol. 115, p. 111141, 2020.

[68] T. Y. Huang, G. S. Wang, C. S. Ko, X. W. Chen, and W. T. Su, "A study of the differentiation of stem cells from human exfoliated deciduous teeth on 3D silk fibroin scaffolds using static and dynamic culture paradigms," *Materials Science & Engineering. C, Materials for Biological Applications*, vol. 109, p. 110563, 2020.

[69] S. Xiao, P. Wang, J. Zhao et al., "Bi-layer silk fibroin skeleton and bladder acellular matrix hydrogel encapsulating adipose-derived stem cells for bladder reconstruction," *Biomaterials Science*, vol. 9, no. 18, pp. 6169–6182, 2021.

[70] J. Hu, Y. Lu, L. Cai et al., "Functional compressive mechanics and tissue biocompatibility of an injectable SF/PU hydrogel for nucleus pulposus replacement," *Scientific Reports*, vol. 7, no. 1, p. 2347, 2017.

[71] W. S. Deng, X. Y. Liu, K. Ma et al., "Recovery of motor function in rats with complete spinal cord injury following implantation of collagen/silk fibroin scaffold combined with human umbilical cord-mesenchymal stem cells," *Revista da Associação Médica Brasileira*, vol. 67, no. 9, pp. 1342–1348, 2021.

[72] M. Akrami-Hasan-Kohal, M. Eskandari, and A. Solouk, "Silk fibroin hydrogel/dexamethasone sodium phosphate loaded chitosan nanoparticles as a potential drug delivery system," *Colloids and Surfaces. B, Biointerfaces*, vol. 205, p. 111892, 2021.

[73] C. Zerna, G. Thomalla, B. C. V. Campbell, J. H. Rha, and M. D. Hill, "Current practice and future directions in the diagnosis and acute treatment of ischaemic stroke," *Lancet*, vol. 392, no. 10154, pp. 1247–1256, 2018.

[74] L. Fernandez-Garcia, N. Mari-Buye, J. A. Barios et al., "Safety and tolerability of silk fibroin hydrogels implanted into the mouse brain," *Acta Biomaterialia*, vol. 45, pp. 262–275, 2016.

[75] L. Fernandez-Garcia, J. Perez-Rigueiro, R. Martinez-Murillo et al., "*Cortical Reshaping and Functional Recovery Induced by Silk Fibroin Hydrogels-Encapsulated Stem Cells Implanted in Stroke Animals*," *Frontiers in Cellular Neuroscience*, vol. 12, article 296, 2018.

[76] N. Gorenkova, I. Osama, F. P. Seib, and H. V. O. Carswell, "In vivo evaluation of engineered self-assembling silk fibroin hydrogels after intracerebral injection in a rat stroke model," *ACS Biomaterials Science & Engineering*, vol. 5, no. 2, pp. 859–869, 2019.

[77] T. C. Lim, E. Mandeville, D. Weng et al., "Hydrogel-based therapy for brain repair after intracerebral hemorrhage," *Translational Stroke Research*, vol. 11, no. 3, pp. 412–417, 2020.

[78] J.-Y. Jiang, G.-Y. Gao, J.-F. Feng et al., "Traumatic brain injury in China," *The Lancet Neurology*, vol. 18, no. 3, pp. 286–295, 2019.

[79] M. M. Moisenovich, E. Y. Plotnikov, A. M. Moysenovich et al., "Effect of silk fibroin on neuroregeneration after traumatic brain injury," *Neurochemical Research*, vol. 44, no. 10, pp. 2261–2272, 2019.

[80] M. D. Tang-Schomer, D. L. Kaplan, and M. J. Whalen, "Film interface for drug testing for delivery to cells in culture and in the brain," *Acta Biomaterialia*, vol. 94, pp. 306–319, 2019.

[81] Z. You, S. I. Savitz, J. Yang et al., "Necrostatin-1 reduces histopathology and improves functional outcome after controlled cortical impact in mice," *Journal of Cerebral Blood Flow and Metabolism*, vol. 28, no. 9, pp. 1564–1573, 2008.

[82] J. Jiang, C. Dai, X. Liu et al., "Implantation of regenerative complexes in traumatic brain injury canine models enhances the reconstruction of neural networks and motor function recovery," *Theranostics*, vol. 11, no. 2, pp. 768–788, 2021.

[83] M. Ganau, N. Syrmos, M. Paris et al., "Current and future applications of biomedical engineering for proteomic profiling: predictive biomarkers in neuro-traumatology," *Medicines*, vol. 5, no. 1, article 19, 2018.

[84] J. Basso, A. Miranda, S. Nunes et al., "Hydrogel-based drug delivery nanosystems for the treatment of brain tumors," *Gels*, vol. 4, no. 3, article 62, 2018.

[85] H. L. Xu, D. L. ZhuGe, P. P. Chen et al., "Silk fibroin nanoparticles dyeing indocyanine green for imaging-guided photothermal therapy of glioblastoma," *Drug Delivery*, vol. 25, no. 1, pp. 364–375, 2018.

[86] V. P. Ribeiro, J. Silva-Correia, C. Goncalves et al., "Rapidly responsive silk fibroin hydrogels as an artificial matrix for the programmed tumor cells death," *PLoS One*, vol. 13, no. 4, article e0194441, 2018.

[87] Z. Wang, Z. Yang, J. Jiang et al., "Silk microneedle patch capable of on-demand multidrug delivery to the brain for glioblastoma treatment," *Advanced Materials*, vol. 34, article e2106606, 2022.

[88] B. N. Dugger and D. W. Dickson, "Pathology of neurodegenerative diseases," *Cold Spring Harbor Perspectives in Biology*, vol. 9, no. 7, 2017.

[89] T. Lefèvre, S. Boudreault, C. Cloutier, and M. Pézolet, "Diversity of molecular transformations involved in the formation of spider silks," *Journal of Molecular Biology*, vol. 405, no. 1, pp. 238–253, 2011.

[90] L. Xu, S. Tu, C. Chen, J. Zhao, Y. Zhang, and P. Zhou, "Effect of EGCG on Fe (III)-induced conformational transition of silk fibroin, a model of protein related to neurodegenerative diseases," *Biopolymers*, vol. 105, no. 2, pp. 100–107, 2016.

[91] A. Banagozar Mohammadi, S. Sadigh-Eteghad, M. Torbati et al., "Identification and applications of neuroactive silk proteins: a narrative review," *Journal of Applied Biomedicine*, vol. 17, no. 3, pp. 147–156, 2019.

[92] R. Galeiras Vázquez, M. E. Ferreiro Velasco, M. Mourelo Fariña, A. Montoto Marqués, and S. Salvador de la Barrera, "Actualización en lesión medular aguda postraumática. Parte 1," *Medicina Intensiva*, vol. 41, no. 4, pp. 237–247, 2017.

[93] J. P. Jiang, X. Y. Liu, F. Zhao et al., "Three-dimensional bioprinting collagen/silk fibroin scaffold combined with neural stem cells promotes nerve regeneration after spinal cord injury," *Neural Regeneration Research*, vol. 15, no. 5, pp. 959–968, 2020.

[94] Y. G. Chung, K. Algarrahi, D. Franck et al., "The use of bi-layer silk fibroin scaffolds and small intestinal submucosa matrices to support bladder tissue regeneration in a rat model of spinal cord injury," *Biomaterials*, vol. 35, no. 26, pp. 7452–7459, 2014.

[95] T. G. Wang, J. Xu, A. H. Zhu et al., "Human amniotic epithelial cells combined with silk fibroin scaffold in the repair of spinal cord injury," *Neural Regeneration Research*, vol. 11, no. 10, pp. 1670–1677, 2016.

[96] K. You, H. Chang, F. Zhang et al., "Cell-seeded porous silk fibroin scaffolds promotes axonal regeneration and myelination in spinal cord injury rats," *Biochemical and Biophysical Research Communications*, vol. 514, no. 1, pp. 273–279, 2019.

[97] Q. Han, T. Zheng, L. Zhang et al., "Metformin loaded injectable silk fibroin microsphere for the treatment of spinal cord injury," *Journal of Biomaterials Science Polymer Edition*, vol. 33, no. 6, pp. 747–768, 2022.

Hindawi
Oxidative Medicine and Cellular Longevity
Volume 2022, Article ID 1015791, 24 pages
https://doi.org/10.1155/2022/1015791

Review Article

Targeting Nrf2-Mediated Oxidative Stress Response in Traumatic Brain Injury: Therapeutic Perspectives of Phytochemicals

An-Guo Wu,[1] **Yuan-Yuan Yong**,[1] **Yi-Ru Pan**,[1] **Li Zhang**,[1] **Jian-Ming Wu**,[1] **Yue Zhang**,[1] **Yong Tang**,[1,2] **Jing Wei**,[1] **Lu Yu**,[1] **Betty Yuen-Kwan Law**,[2] **Chong-Lin Yu**,[1] **Jian Liu**,[1] **Cai Lan**,[1] **Ru-Xiang Xu**,[3] **Xiao-Gang Zhou**,[1] **and Da-Lian Qin**[1]

[1]*Sichuan Key Medical Laboratory of New Drug Discovery and Drugability Evaluation, Materia Medica, Luzhou Key Laboratory of Activity Screening and Druggability Evaluation for Chinese Materia Medica, Education Ministry Key Laboratory of Medical Electrophysiology, School of Pharmacy, Southwest Medical University, Luzhou 646000, China*
[2]*State Key Laboratory of Quality Research in Chinese Medicine, Macau University of Science and Technology, Taipa, Macau SAR, 99078, China*
[3]*Department of Neurosurgery Sichuan Provincial People's Hospital, University of Electronic Science and Technology of China, Chengdu 610000, China*

Correspondence should be addressed to An-Guo Wu; wuanguo@swmu.edu.cn, Ru-Xiang Xu; zjxuruxiang@163.com, Xiao-Gang Zhou; zxg@swmu.edu.cn, and Da-Lian Qin; dalianqin@swmu.edu.cn

Received 24 September 2021; Revised 22 November 2021; Accepted 19 March 2022; Published 4 April 2022

Academic Editor: Zonghao Tang

Traumatic brain injury (TBI), known as mechanical damage to the brain, impairs the normal function of the brain seriously. Its clinical symptoms manifest as behavioral impairment, cognitive decline, communication difficulties, etc. The pathophysiological mechanisms of TBI are complex and involve inflammatory response, oxidative stress, mitochondrial dysfunction, blood-brain barrier (BBB) disruption, and so on. Among them, oxidative stress, one of the important mechanisms, occurs at the beginning and accompanies the whole process of TBI. Most importantly, excessive oxidative stress causes BBB disruption and brings injury to lipids, proteins, and DNA, leading to the generation of lipid peroxidation, damage of nuclear and mitochondrial DNA, neuronal apoptosis, and neuroinflammatory response. Transcription factor NF-E2 related factor 2 (Nrf2), a basic leucine zipper protein, plays an important role in the regulation of antioxidant proteins, such as oxygenase-1(HO-1), NAD(P)H Quinone Dehydrogenase 1 (NQO1), and glutathione peroxidase (GPx), to protect against oxidative stress, neuroinflammation, and neuronal apoptosis. Recently, emerging evidence indicated the knockout (KO) of Nrf2 aggravates the pathology of TBI, while the treatment of Nrf2 activators inhibits neuronal apoptosis and neuroinflammatory responses via reducing oxidative damage. Phytochemicals from fruits, vegetables, grains, and other medical herbs have been demonstrated to activate the Nrf2 signaling pathway and exert neuroprotective effects in TBI. In this review, we emphasized the contributive role of oxidative stress in the pathology of TBI and the protective mechanism of the Nrf2-mediated oxidative stress response for the treatment of TBI. In addition, we summarized the research advances of phytochemicals, including polyphenols, terpenoids, natural pigments, and otherwise, in the activation of Nrf2 signaling and their potential therapies for TBI. Although there is still limited clinical application evidence for these natural Nrf2 activators, we believe that the combinational use of phytochemicals such as Nrf2 activators with gene and stem cell therapy will be a promising therapeutic strategy for TBI in the future.

1. Introduction

Traumatic brain injury (TBI) refers to the damage to the brain structure and function caused by mechanical and external forces, including two stages of primary injury and secondary injury [1]. It is a global neurological disease and is the biggest cause of death and disability in the population under 40 years of age [2]. The current clinical treatments for TBI mainly include interventional treatments such as hyperventilation, hypertonic therapy, hypothermia therapy, surgical treatment, drug therapy, hyperbaric oxygen therapy, and rehabilitation therapy [3, 4]. In the past few decades, the main interventions that have had the greatest impact and can reduce the mortality rate of severe TBI by several times are immediate surgical intervention and follow-up care by specialist intensive care physicians [5]. Post-traumatic intracranial hypertension (ICH) makes patient care more complicated, but new data shows that hypertonic therapy is the use of hypertonic solutions, such as mannitol and hypertonic saline (HTS) in the early treatment of ICH after severe TBI, which can reduce the burden of ICH and improve survival and functional outcomes [6]. Hypothermia therapy can reduce the effects of TBI through a variety of possible mechanisms, including reducing intracranial pressure (ICP), reducing innate inflammation, and brain metabolic rate. However, the results of a randomized POLAR clinical trial showed that early preventive hypothermia did not improve the neurological outcome at 6 months in patients with severe TBI [7]. Therefore, the effectiveness of hypothermia for TBI remains to be discussed. Surgical treatments include decompressive craniectomy (DC), which is a method that removes most of the top of the skull to reduce ICP and the subsequent harmful sequelae. However, the treatment effects for TBI are not satisfactory [8]. Many patients have a poor prognosis and will be left with serious disabilities and require lifelong care [9]. In addition, chemicals including corticosteroids, progesterone, erythropoietin, amantadine, tranexamic acid, citicoline, and recombinant interleukin-1 receptor (IL-1R) antagonist are used for the treatment of TBI [2]. However, these drugs are less safe and cannot work well, or may lead to unfavorable physiological conditions [10]. Recently, many studies have begun to investigate the possibility of using natural compounds with high safety as therapeutic interventions after TBI [11]. The latest evidence indicates that phytochemicals, including quercetin, curcumin, formononetin, and catechin, exert neuroprotective effects in TBI and other brain diseases via attenuating oxidative stress [12]. It is known to us, transcription factor NF-E2 related factor 2 (Nrf2) plays an important role in the regulation of heme oxygenase-1 (HO-1), NAD(P)H Quinone Dehydrogenase 1 (NQO1), glutathione peroxidase (GPx), and other antioxidant proteins, which ameliorates oxidative damage in TBI [13]. In this review, we discussed the critical role of oxidative stress in the pathology of TBI and the regulation of Nrf2-mediated oxidative stress response in TBI. In addition, we summarized the study advances of phytochemicals, including polyphenols, terpenoids, natural pigments, and otherwise, in the activation of Nrf2 signaling and their potential therapies for TBI in vivo and in vitro. Finally, we hope this review sheds light on the study on the treatment of TBI using phytochemicals as Nrf2 activators. Moreover, the combinational use of phytochemicals such as Nrf2 activators with gene and stem cell therapy will be a promising strategy for the treatment of TBI.

2. TBI

TBI, also known as acquired intracranial injury, occurs in the brain. It is caused by an external force, including a blow, bump, or jolt to the head, and the sudden and serious hit of the head by an object or the deep pierce of an object into the skull through the brain tissue [14]. According to the data from the Center for Disease Control and Prevention (CDC) of Unite States (U.S.), the most common causes mainly include violence, transportation, accidents, construction, and sports. In addition, there are about 288,000 hospitalizations for TBI a year, and males hold 78.8% [15, 16]. Usually, older adults (>75 years) have the highest rates of TBI. Therefore, TBI brings serious economic and spiritual burdens to the family and society [17].

TBI is classified in various ways, including type, severity, location, mechanism of injury, and the physiological response to injury [18]. In general, the Glasgow Coma Scale (GCS) score and neurobehavioral deficits are extensively used, and TBI is classified into mild, moderate, and severe types [19]. The clinical symptoms of TBI are greatly dependent on the severity of the brain injury and mainly include perceptual loss, cognitive decline, communication difficulties, behavioral impairment, affective changes, and otherwise [20] (Figure 1). The pathophysiology of TBI includes the primary injury, which is directly caused by physical forces, and the secondary injury referring to the further damage of tissue and cells in the brain [21]. The physical forces on the brain cause both focal and diffuse injuries. Emerging evidence indicates that patients who suffer from moderate or severe TBI are found to have focal and diffuse injuries simultaneously [22]. Most seriously, secondary brain injury is followed owing to the occurrence of biochemical, cellular, and physiological events during the primary brain injury [23]. Mechanistic studies demonstrate that several factors, including inflammation, oxidative stress, mitochondrial dysfunction, BBB disruption, DNA damage, glutamate excitotoxicity, complement activation, and neurotrophic impairment, are involved in the pathology and progression of TBI [24] (Figure 1). Currently, there is a growing body of studies showing that increasingly abnormal proteins or molecules are biomarkers closely associated with TBI, which helps to better understand the mechanism of TBI [25]. For example, the level of early structural damage biomarkers, including S100B protein in cerebrospinal fluid or blood nerve glial acidic protein, ubiquitin carboxyl-terminal hydrolase L1 and Tau helps to determine whether the head scan is required after TBI [26].

At present, the therapeutic strategies for TBI include hyperbaric oxygen therapy (HBOT), hyperventilation and hypertonic therapy, noninvasive brain stimulation, drug therapy, and biological therapy [27]. Most importantly, the combinational use of novel biological reagents (genes and stem cells) and pharmacological intervention preparations can decrease the complications and mortality of TBI [28].

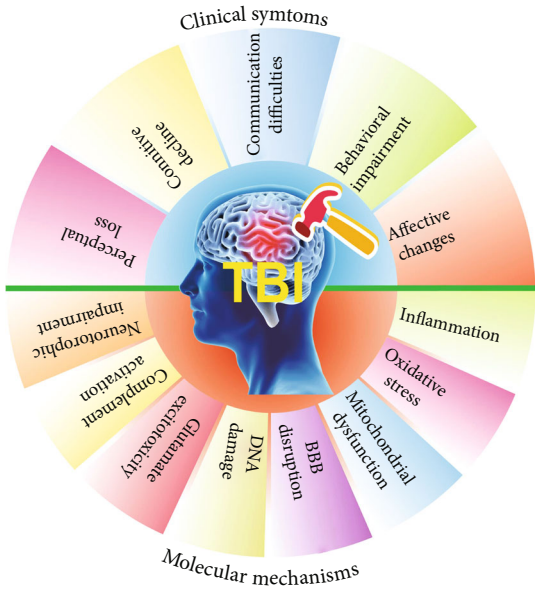

Figure 1: The clinical symptoms and molecular mechanism of TBI, an injury to the brain caused by an external force. The clinical symptoms of TBI mainly manifest as perceptual loss, cognitive decline, communication difficulties, behavioral impairment, and affective changes. The molecular mechanisms of TBI include inflammation, oxidative stress, mitochondrial dysfunction, blood-brain barrier (BBB) disruption, DNA damage, glutamate excitotoxicity, complement activation, and neurotrophic impairment.

Stem cell therapy includes stem cells regeneration transplantation and induction of endogenous stem cells activation through pharmacological or environmental stimuli. Several studies have shown that some drugs can not only improve the survival rate of stem cells but also enhance their efficacy. For example, the intravenous injection of mesenchymal stem cells (MSCs) and atorvastatin or simvastatin 24 hours after TBI could improve the recovery of modified neurological severity score (mNSS) [29]. In addition, the administration of calpain inhibitors 30 minutes after TBI followed by the transplantation of MSCs 24 hours after TBI could reduce the proinflammatory cytokines around the lesions, increase the survival rate of MSCs, and improve mNSS [30]. Moreover, the pretreatment with minocycline for 24 hours could protect transplanted stem cells from ischemia-reperfusion injury by inducing Nrf2 nuclear translocation and increasing the expression of downstream proteins [31]. Therefore, the in-deep clarification of the mechanism of TBI and adopting targeted methods for precise intervention will help the recovery of post-traumatic neurological function and further prevent the occurrence and development of complications, and ultimately open up a new way for effective treatment of TBI [32].

3. The Role of Oxidative Stress in TBI

Oxidative stress occurs owing to an imbalance of free radicals and antioxidants in the body, which lead to cell and tissue damage [32]. Therefore, oxidative stress plays a critical role in the development of diseases. As is known to us, diet, lifestyle, and environmental factors such as pollution and radiation contribute to the induction of oxidative stress, resulting in the excessive generation of free radicals [33]. In general, free radicals, including superoxide, hydroxyl radicals, and nitric oxide radicals, are molecules with one or more unpaired electrons [34]. It is well known that oxidative stress is implicated in the pathogenesis of various diseases, such as atherosclerosis, hypertension, diabetes mellitus, ischemic disease, neurodegeneration, and other central nervous system (CNS) related diseases [35, 36]. During normal metabolic processes, although many free radicals are generated, the body's cells can produce antioxidants to neutralize these free radicals and maintain a balance between antioxidants and free radicals [37]. A large body of evidence indicates that the overgenerated free radicals attack biological molecules, such as lipids, proteins, and DNA, ultimately breaking this balance and resulting in long-term oxidative stress [38]. However, oxidative stress also plays a useful role in some cases, such as physiologic adaptation and the modulation of intracellular signal transduction [39]. Thus, a more accurate definition of oxidative stress may be a state in which the oxidation system exceeds the antioxidant system owing to the occurrence of imbalance between them. At present, the biomarkers of oxidative stress, which are used to evaluate the pathological conditions of diseases and the efficacy of drugs, are becoming popular and attract increasing interest [40]. For example, lipid peroxides, 4-hydroxynonenal (4-HNE), and malondialdehyde (MDA) are the indicators of oxidative damage to lipids [41]. Thymine glycol (TG) and 8-oxoguanine (8-oxoG) are the biomarkers of oxidative damage to DNA [42]. In addition, a variety of proteins and amino acids, including carbonyl protein, dehydrovaline, nitrotyrosine, and hydroxyleucine, are oxidized and generate several products that are recognized to be biomarkers of oxidative stress. Among them, lipid peroxide as one of the most important biomarkers was determined in clinical. Furthermore, oxidative stress plays a pivotal role in the regulation of signaling transduction, including the activation of protein kinases and transcription factors, which affect many biological processes such as apoptosis, inflammatory response, and cell differentiation [43]. For example, gene transcription factors include nuclear factor κB (NF-κB) and activator protein-1 (AP-1) sense oxidative stress via oxidation and reduction cycling [44]. In addition, the generation of active oxygen species leads to the activation of NF-κB, resulting in proinflammatory responses in various diseases such as neurodegenerative diseases, spinal cord injury, and TBI [45]. Therefore, oxidative stress is one of the important mechanisms that has been implicated in the pathology of CNS-related diseases.

Although the initial brain insult of TBI is an acute and irreversible primary damage to the parenchyma, the ensuing secondary brain injury progressing slowly over months to years seriously affects the treatment and prognosis of TBI [46]. Therefore, therapeutic interventions during secondary brain injury are essential. To date, many hallmarks are exhibited during delayed secondary CNS damage, mainly including mitochondrial dysfunction, Wallerian degeneration of

axons, excitotoxicity, oxidative stress, and eventually neuronal death and overactivation of glial cells [24]. Recently, emerging evidence indicates that oxidative stress plays an important role in the development and pathogenesis of TBI [46]. In general, oxidative stress is resulted from or is accompanied by other molecular mechanisms, such as mitochondrial dysfunction, activation of neuroexcitation pathways, and activated neutrophils [47]. Kontos HA et al. first reported that superoxide radicals are immediately increased in brain microvessels after injury in a fluid percussion TBI model, while the scavengers of oxygen radicals including superoxide dismutase (SOD) and catalase significantly decrease the level of superoxide radicals and partly reverse the injury of the brain [48]. During the beginning minutes or hours after brain injury, a large number of superoxide radicals are generated owing to the enzymatic reaction or autoxidation of biogenic amine neurotransmitters, arachidonic acid cascade, damaged mitochondria, and oxidized extravasated hemoglobin [49]. Soon afterwards, the microglia are overactivated and neutrophils and macrophages are infiltrated, which also contribute to the production of superoxide radicals [50, 51]. In addition, iron overload and its resultant generation of several hydroxyl radicals and lipid peroxidation induce oxidative stress and neuronal ferroptosis, which significantly aggravate the pathogenesis of TBI from the following aspects, such as cerebral blood flow, brain plasticity, and the promotion of immunosuppression [52]. In this review, we focused on the research advance of the role of oxidative stress in TBI. At neutral pH, the iron in plasma is bound to the transferrin protein in the form of Fe^{3+}, which also can be sequestered intracellularly by ferritin, an iron storage protein. Thus, iron in the brain is maintained at a relatively low level under normal conditions. However, the value of pH is decreased in the brain of TBI, which is accompanied by the release of iron from both transferrin and ferritin. Then, the excessive levels of active iron catalyze the oxygen radical reaction and induce oxidative damage and ferroptosis [53]. Additionally, hemoglobin is the second source that catalyzes the active iron after the mechanical trauma of the brain [54]. Iron is released from hemoglobin owing to the stimulation of hydrogen peroxide (H_2O_2) or lipid hydroperoxides, and the level of iron can be further increased as the pH decreases to 6.5 or even below [55]. Therefore, targeting the inhibition of iron levels by iron chelators may be a promising strategy for the treatment of TBI. For example, deferoxamine (DFO), a potent chelator of iron, can attenuate iron-induced long-term neurotoxicity and improve the spatial learning and memory deficit of TBI rats [56]. Moreover, nitric oxide (NO) is involved in the cascade of injury triggered by TBI. The activity of nitric oxide synthase (NOS) contributing to the generation of NO is increased as the accumulation of Ca^{2+} in TBI secondary injury. Then, NO reacts with free radical superoxide to generate "reactive nitrogen species" peroxynitrite (PN) in the forms of 3-nitrotyrosine (3-NE) and 4-HNE, which are found in the ipsilateral cortex and hippocampus of TBI animal models [24]. For example, N(omega)-nitro-L-arginine methyl ester (L-NAME), a NO-synthase inhibitor, was reported to attenuate neurological impairment in TBI and reduce the formation of NE and the number of NE-positive neurons [14]. Therefore, targeting the inhibition of oxidative stress in the brain is a promising strategy for the treatment of TBI.

4. Nrf2 Signaling-Mediated Oxidative Stress Response

In 1995, Itoh, K. et al. first discovered and reported that Nrf2 was the homolog of the hematopoietic transcription factor p45 NF-E2 [57]. To date, a total of 6 members including NF-E2, Nrf1, Nrf2, Nrf3, Bach1, and Bach2 are identified from the Cap "n" Collar (CNC) family [58]. Among them, Nrf2 is a conserved basic leucine zipper (bZIP) transcription factor. The literature reports that Nrf2 possesses seven highly conserved functional domains from NRF2-ECH homology 1 (Neh1) to Neh7, which are identified in multiple species including humans, mice, and chicken (Figure 2) [59]. Of these domains, Neh2, located in the N-terminal of Nrf2, possesses seven lysine residues and ETGE and DLG motifs, which are responsible for the ubiquitin conjugation and the binding of Nrf2 to its cytosolic repressor Keap1 at the Kelch domain, then facilitating the Cullin 3 (Cul3)-dependent E3 ubiquitination and proteasome degradation [60]. Both Neh4 and Neh5 domains with a lot of acidic residues act as transactivation domains to bind to cAMP response element-binding protein (CREB), which regulates the transactivation of Nrf2. Neh7 is a domain that interacts with the retinoic X receptor (RXRα), which can inhibit CNC-bZIP factors and the transcription of genes targeting Nrf2. Neh6 has two motifs including DSGIS and DSAPGS of β-transducing repeat-containing protein (β-TrCP) functioning as a substrate receptor for the Cul3-Rbx1/Roc1 ubiquitin ligase complex [61]. DSGIS is modulated by glycogen synthase kinase-3 (GSK-3) activity and enables β-TrCP to ubiquitinate Nrf2 [62]. The Neh1 domain has a Cap "N" Collar Basic Leucine Zipper (CNC-bZIP) DNA-binding motif, which allows Nrf2 to dimerize with small Maf proteins including MAFF, MAFG, and MAFK [63]. The Neh3 domain in the C-terminal of Nrf2 protein regulates chromoATPase/helicase DNA-binding protein 6 (CHD6), which is known as the Nrf2 transcriptional co-activator [64]. In addition, Neh3 also plays a role in the regulation of Nrf2 protein stability.

Under normal conditions, Nrf2 is kept in the cytoplasm by a cluster of proteins including Keap1 and Cul3, which then undergoes degradation via the ubiquitin-proteasome system (UPS) [65]. In brief, Cul3 ubiquitinates Nrf2 and Keap1 act as a substrate adaptor to facilitate the reaction. Then, Nrf2 is transported to the proteasome for its degradation and recycling, and the half-time of Nrf2 is only 20 minutes. Under the condition of oxidative stress or the treatment of Nrf2 activators, the Keap1-Cul3 ubiquitination system is disrupted. Then, Nrf2 is translocated from the cytoplasm into the nucleus and forms a heterodimer with one of the sMAF proteins, which binds with the ARE and initiates the transcription of many antioxidative genes including HO-1, glutamate-cysteine ligase catalytic subunit (GCLC), SOD, and NQO1 (Figure 3). Emerging evidence

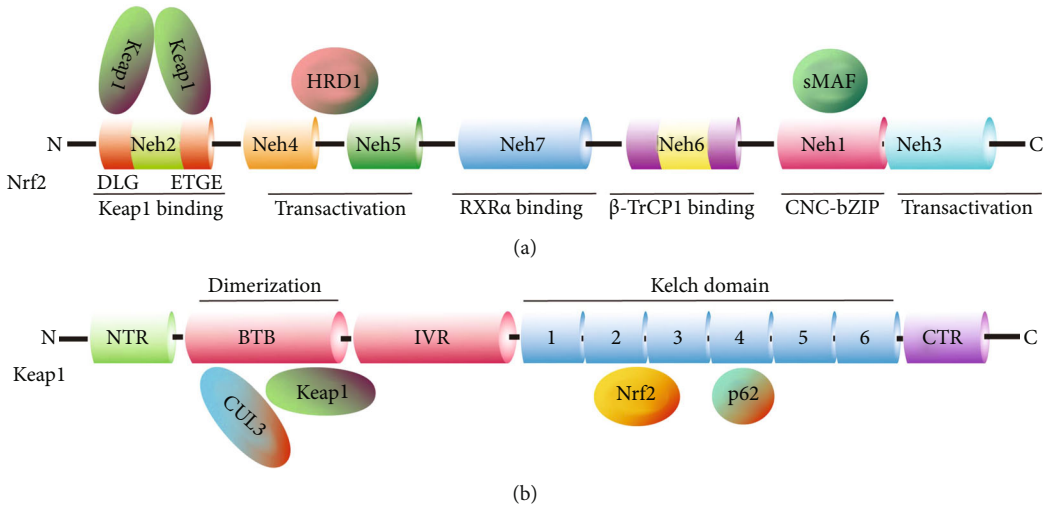

Figure 2: Structures of Nrf2 and Keap1 protein domains. (a) Nrf2 consists of 589 amino acids and has seven evolutionarily highly conserved domains (Neh1-7). Neh1 contains a bZIP motif and is responsible for DNA recognition and mediates the dimerization with the small MAF (sMAF) protein. Neh6 acts as a degron to mediate the degradation of Nrf2 in the nucleus. Neh4 and 5 are transactivation domains. Neh2 contains ETGE and DLG motifs which are required for the binding of Nrf2 to Keap1. Neh7 is a domain that interacts with RXRα to inhibit CNC-bZIP factors and the transcription of genes. Neh3 regulates CHD6. (b) Keap1 consists of 624 amino acids and has five domains. BTB domain together with the N-terminal region (NTR) of IVR to mediate the homodimerization of Keap1 and binding to Cul3. The Kelch domain and the C-terminal region (CTR) mediate the interaction with Neh2 of Nrf2 at the ETGE and DLG motifs.

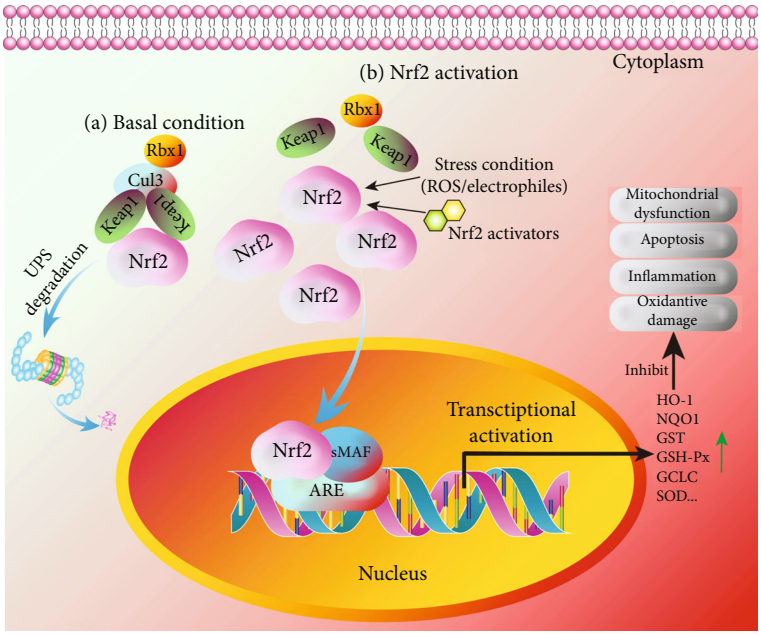

Figure 3: The regulation of the Nrf2 signaling pathway in TBI. Under basal conditions (a), Keap1 functions as a substrate adaptor protein for Cul3 to mediate the degradation of Nrf2 via the UPS pathway. Under Nrf2 activation (b), the stress condition or the treatment of Nrf2 activators induces the dissociation of Nrf2 from Keap1 and leads to the accumulation of Nrf2 in the cytoplasm and the nuclear translocation of Nrf2. Then, Nrf2 binds to sMAF and ARE to regulate the expression of its downstream transcription factors including HO-1, NQO1, GST, GSH-Px, GCLC, and SOD. Then, oxidative damage, inflammation, neuronal apoptosis, and mitochondrial dysfunction are inhibited.

indicates that Nrf2 is the most important protein that induces various gene expression to counter oxidative stress or activate the antioxidant response, which protects against cell damage, and death triggered by various stimuli including environmental factors such as pollution, lifestyle factors such as smoking or exercise, and other factors. There is a growing body of evidence showing that Nrf2 plays multiple roles in the regulation of oxidative stress, inflammation, metabolism, autophagy, mitochondrial physiology, and other biological processes [64]. It has been reported that Nrf2-KO mice are susceptible to suffering diseases, which are associated with oxidative damage [66]. Therefore, Nrf2

plays a critical role in cell defense and the regulation of cell survival in various diseases such as TBI.

5. The Potential Therapy of Phytochemicals as Nrf2 Activators in TBI

Because the primary injuries in TBI commonly result in acute physical damage and irreversible neuronal death, the therapies mainly aim at stabilizing the injury site and preventing it from secondary damage. As described above, the secondary damage of TBI is induced by various risks such as oxidative stress and develops progressively. To date, multiple therapeutic manners are developed, including the inhibition of excitotoxicity by glutamate receptor antagonists such as dexanbionol, the improvement of mitochondrial dysfunction using neuroprotective agents such as cyclosporine A, and the inhibition of axonal degeneration by calpain inhibitors such as MDL 28170 [67]. Emerging evidence indicates that oxidative stress is not only one of the pathogenesis of TBI but also the initiator and promoter of excitotoxicity, mitochondrial dysfunction, neuroinflammation, and other risks. Nrf2 plays a protective role in TBI via fighting against oxidative damage and inflammatory response in TBI [68], while the genetic deletion of Nrf2 delayed the recovery of post-TBI motor function and the cognitive function [69]. Therefore, targeting the discovery of Nrf2 activators to alleviate oxidative damage is a promising therapeutic strategy for TBI [70]. Recently, there are a lot of phytochemicals isolated from natural plants such as fruits, vegetables, grains, and other medicinal herbs and reported to activate the Nrf2 signaling pathway to exert neuroprotective effects in TBI [71]. In general, these natural phytochemicals as Nrf2 activators are used for the alleviation of the secondary damage of TBI. In this review, we summarize the research advances of phytochemicals, including polyphenols, terpenoids, natural pigments, and otherwise, in the activation of Nrf2 signaling and their potential therapies for TBI during secondary injury (Table 1).

5.1. Quercetin. Quercetin belonging to flavonoids is commonly found in dietary plants including vegetables and fruits such as onions, tomatoes, soy, and beans [72]. Emerging evidence indicates quercetin exerts a variety of pharmacological effects mainly involving antioxidation, anti-inflammation, antivirus, anticancer, neuroprotection, and cardiovascular protection [73]. It is known to us that the inflammatory response promotes oxidative damage in TBI [74]. In weight drop injury (WDI)-induced TBI mice, quercetin was reported to significantly inhibit neuroinflammation-medicated oxidative stress and histological alterations as demonstrated by the decreased lipid peroxidation and increased activities of SOD, catalase, and GPx [75]. Meanwhile, quercetin could significantly reduce the brain water content and improve the neurobehavioral status, which is closely associated with the activation of the Nrf2/HO-1 pathway [74]. The impairment of mitochondria function leads to an increase in reactive oxygen species (ROS) production and damages mitochondrial proteins, DNA, and lipids [72]. Quercetin was reported to significantly inhibit mitochondrial damage of TBI male Institute of Cancer Research (ICR) mice as evidenced by the decreased expression of Bax and increased levels of cytochrome c in mitochondria, as well as increased mitochondrial SOD and decreased mitochondrial MDA content, and the recovery of mitochondrial membrane potential (MMP) and intracellular ATP content. The mechanistic study demonstrated that quercetin promoted the translocation of Nrf2 from the cytoplasm to the nucleus, suggesting that quercetin exerts neuroprotective effects in TBI mice via maintaining mitochondrial homeostasis through the activation of Nrf2 signaling pathway [76]. In moderate TBI rats, quercetin inhibited oxidative nitrosative stress by reducing the activity of NOS including inducible nitric oxide synthase (iNOS) and constructive nitric oxide synthase (cNOS), as well as the concentration of thiobarbituric acid (TBA)-lipid peroxidation in the cerebral hemisphere and periodontal tissues [77]. Therefore, quercetin exerts neuroprotective effects in TBI via multiple biological activities, including inhibition of oxidative damage, nitrosative stress, and inflammatory response, as well as the improvement of mitochondrial dysfunction and neuronal function through the Nrf2 signaling pathway.

5.2. Curcumin. Curcumin, a polyphenol isolated from *Curcuma longa* rhizomes, has been reported to possess multiple biological activities, including antioxidative, anti-inflammatory, and anticancer effects [78]. Most importantly, curcumin is also demonstrated to cross the BBB and exert neuroprotection in various neurodegenerative diseases, such as Alzheimer's disease (AD), Parkinson's disease (PD), and amyotrophic lateral sclerosis (ALS), via the inhibition of neuronal death and neuroinflammation [79]. In addition, emerging evidence indicates that curcumin presents protective effects in TBI and activates the Nrf2 signaling pathway in vivo and in vitro [78, 80–82]. In mild fluid percussion injury (FPI)-induced TBI rats, curcumin significantly attenuated oxidative damage by decreasing the oxidized protein levels and reversing the reduction in the levels of brain-derived neurotrophic factor (DBNF), synapsin I, and cyclic AMP (cAMP)-response element-binding protein 1 (CREB) [81]. Meanwhile, curcumin improved the cognitive and behavioral function of TBI rats [81, 83–85]. In addition, the intraperitoneal administration of curcumin could improve the neurobehavioral function and decrease the brain water content in Feeney or Marmarou's weight drop-induced TBI mice. Furthermore, curcumin reduced the oxidative stress in the ipsilateral cortex by decreasing the level of MDA and increasing the levels of SOD and GPx, as well as promoted neuronal regeneration and inhibited neuronal apoptosis [80, 85]. Moreover, curcumin inhibited the neuroinflammatory response as demonstrated by the decreased number of myeloperoxidase (MPO) positive cells and increased levels of cytokines such as tumor necrosis factor-alpha (TNF-α), interleukin 6 (IL-6), and interleukin-1beta (IL-1β) [80]. The mechanistic study found that curcumin promoted the nuclear translocation of Nrf2 and increased the expression of downstream genes, including HO-1, NQO1, and GCLC, while the neuroprotective effects of curcumin including antioxidation, antiapoptosis, and anti-

Table 1: Phytochemicals from various plants possess multiple pharmacological effects via the antioxidant mechanism in various in vitro and in vivo models of TBI.

Phytochemicals	Plants	Models	Pharmacological effects	Detected markers	Antioxidant mechanism	Ref
Polyphenol						
Quercetin	Onions, tomatoes, etc.	Weight drop-induced TBI mice/rats,	Improved behavioral function, neuronal viability, and mitochondrial function; reduced brain edema and microgliosis, oxidative damage and nitrosative stress, neuronal apoptosis, inflammatory response	Motor coordination; latency period; NSS; brain water content; MDA; SOD; catalase; GPx; lipid peroxidation; neuronal morphology; cytochrome c; Bax; MMP; ATP; Iba-1; TNF-α; iNOS; cNOS; IL-1β; Nrf2; HO-1	Nrf2 pathway	[74–77]
Curcumin	*Curcuma longa*	FPI-induced TBI rats; Feeney or weight drop-induced TBI WT, Nrf2-KO or TLR4-KO mice; LPS-induced microglia or the co-culture of neuron and microglia	Improved cognitive function; reduced axonal injury, neuronal apoptosis, inflammatory response, and oxidative damage	NSS; brain water content; Tuj1; H&E; Nissl; Congo red, silver, TUNEL, MPO, and FJC staining; caspase 3; Bcl-2; NeuN/BrdU double labeling; Iba-1; GFAP; TNF-α; IL-6; IL-1β; MCP-1; RANTES; CD11B; DCX; TLR4; MyD88; NF-κB; IkB; AQP4; Nrf2; HO-1; NQO1; PERK; eIF2α; ATF4; CHOP; GSK3β; p-tau; β-APP; NF-H	Nrf2 pathway; PERK/Nrf2 pathway	[80, 81, 86–88]
Formononetin	Red clover	Weight drop-induced TBI rats	Reduced brain edema, pathological lesions, inflammatory response, and oxidative damage,	NSS; brain water content; H&E and Nissl staining; neuronal ultrastructural organization; SOD; GPx; MDA; TNF-α; IL-6; COX-2; IL-10; Nrf2	Nrf2 pathway	[91, 95]
Baicalin	*Scutellaria baicalensis*	Weight drop-induced TBI rats	Improved behavioral function and neuronal survival; reduced brain edema, oxidative damage, BBB disruption, and mitochondrial apoptosis	NSS; brain water content; EB leakage, Nissl, and TUNEL staining, grip test score; cleaved caspase 3; Bcl-2, cytochrome c, p53, SOD, MDA, GPx, NeuN, Nrf2, HO-1, NQO1, AMPK, mTOR, LC3, Beclin-1, p62	Akt/Nrf2 pathway	[96, 97]
Catechin	Cocoa, tea, grapes, etc.	CCI- or weight drop-induced TBI rats	Improved long-term neurological outcomes, neuronal survival, and white matter recovery; reduced brain edema, brain lesion volume, neurodegeneration, inflammatory response, BBB disruption, neutrophil infiltration, and oxidative damage	NSS; brain water content; brain infarct volume; forelimb score; Hindlimb score; latency; quadrant time; EB extravasation; ZO-1; Occludin; TNF-α⊠IL-1β⊠IL-6; iNOS; arginase; TUNEL, PI, FJB, Cresyl violet, and MPO staining; myelin; caspase 3; caspase 8;	Nrf2-dependent and Nrf2-independent pathways	[103, 104]

Table 1: Continued.

Phytochemicals	Plants	Models	Pharmacological effects	Detected markers	Antioxidant mechanism	Ref
Fisetin	*Cotinus coggygria*, onions, cucumbers, etc.	Weight drop-induced TBI mice	Improved neurological function; reduced cerebral edema, brain lesion, oxidative damage, and BBB disruption	Bcl-2; Bax; BDNF; ROS; MMP-2; MMP-9; Nrf2, Keap1, SOD1; HO-1; NQO1; NF-κB NSS; brain water content; grip score; EB extravasation; lesion volume; MDA; GPx Nissl and TUNEL staining; caspase 3; Bcl-2; Bax; Nrf2, HO-1; NQO1; TLR4; NF-κB; NeuN; TNF-αIL-1β IL-6; MPP-9; ZO-1; EB leakage	Nrf2-ARE signaling pathway	[109, 110]
Luteolin	Carrots, green tea, celery, etc.	Marmarou's weight drop-induced TBI mice/rats; scratch injury-induced TBI primary neurons	Improved motor performance, and learning and memory; reduced cerebral edema, apoptosis index, and oxidative damage	Latency time; brain water content; grip score; MDA; GPx; catalase; SOD; TUNEL, H&E, Cresyl violet, and TB staining; ROS; LDH release assay; Nrf2; HO-1; NQO1	Nrf2-ARE signaling pathway	[116, 117]
Isoliquiritigenin	*Sinofranchetia chinensis*, *Glycyrrhiza uralensis*, and *Dalbergia odorifera*	CCI-induced TBI mice/rats; ODG-induced SH-SY5Y cells	Improved motor performance, cognitive function, and cell viability; reduced cerebral edema, neuronal apoptosis, inflammatory response, BBB damage, and oxidative damage	Garcia neuroscore; MWM test; beam-balance latency; beam-walk latency; brain water content; contusion volume; EB extravasation; apoptosis rate; MDA; GPx; SOD; H_2O_2; H&E and Nissl staining; GFAP; NFL; AQP4; caspase 3; Bcl-2; Bcl-xL; Bax; Nrf2, HO-1; NQO1; TNF-α; INF-γ; IL-1β; IL-6; IL-10; Iba-1; CD68; AKT; GSK3β; P-120; Occludin; NF-κB; IkB; CCK-8 assay	Nrf2-ARE signaling pathway	[121–123]
Tannic acid	Green and black tea, nuts, fruits, and vegetables	CCI-induced TBI mice/rats; ODG-induced SH-SY5Y cells	Improved behavioral performance; reduced cerebral edema, neuronal apoptosis, inflammatory response, and oxidative damage	Grip test score; Rotarod test; beam balance; brain water content; GSH; LPO; GST; GPx; CAT; SOD; Nissl staining; caspase 3; Bcl-2; Bax; PARP; Nrf2; PGC-1α; Tfam; HO-1; NQO1; TNF-α; IL-1β; 4HNE; GFAP	PGC-1α/Nrf2/HO-1 pathway	[133]
Ellagic acid	Various berries, walnuts, and nuts	Experimental diffuse TBI rats; CCl4-induced brain injury rats	Improved memory, hippocampus electrophysiology and long-term potentiation deficit; reduced neuronal apoptosis, inflammatory response,	Initial latency; step through latency; EB leakage; NSS; MDA; GSH; CAT; caspase 3; Bcl-2; NF-κB; PARP; Nrf2; Cox-2, VEGF; TNF-α IL-1β; IL-6	Nrf2 signaling pathway	[134, 135]

Table 1: Continued.

Phytochemicals	Plants	Models	Pharmacological effects	Detected markers	Antioxidant mechanism	Ref
			oxidative damage, and BBB disruption			
Breviscapine	Erigeron	Weight drop- or CCI-induced TBI rats	Improved neurobehavior; reduced neuronal apoptosis, inflammatory response, and oxidative damage	NSS; TUNEL staining; MDA; GSH; CAT; caspase 3; Bcl-2; Bax; IL-6; Nrf2; HO-1; NQO1; GSK3β; SYP	Nrf2 signaling pathway	[138–140]
Terpenoids						
Asiatic acid	*Centella asiatica*	CCI-induced TBI rats	Improved neurological deficits; inhibited brain edema, neuronal apoptosis, and oxidative damage	NSS; brain water content; TUNEL staining; MDA; 4-HNE; 8-OhdG; Nrf2; HO-1	Nrf2 signaling pathway	[149]
Aucubin	*Eucommia ulmoides*	Weight drop-induced TBI mice; H_2O_2-induced primary cortical neurons	Improved neurological deficits, and cognitive function; reduced brain edema, neuronal apoptosis and loss, inflammatory response, and oxidative damage	NSS; brain water content; TUNEL and Nissl staining; MWM test; Bcl-2; Bax; CC3; MAP2; MMP-9; MDA; SOD; GSH; GPx; 8-HdG; NeuN; Iba-1; HMGB1; TLR4; MyD88; NF-κB; iNOS; COX2; IL-1β; Nrf2; HO-1; NQO1	Nrf2 signaling pathway	[155]
Ursolic acid	Apples, bilberries, lavender, hawthorn, etc.	Weight drop-induced TBI mice	Improved neurobehavioral and mitochondrial function; reduced brain edema, oxidative damage, and neuronal cytoskeletal degradation	NSS; brain water content; TUNEL and Nissl staining; MDA; SOD; GPx; AKT; 4-HNE; 3-NE; ADP rate; succinate rate; Spectrin; Nrf2; HO-1; NQO1	AKT/Nrf2 signaling pathway	[158]
Carnosic acid	*Rosmarinus officinalis* and *Salvia officinalis*.	CCI-induced acute post-TBI mice;	Improved motor and cognitive function, and neuronal viability; reduced brain edema, neuronal apoptosis and loss, inflammatory response, and oxidative damage	Duration of apnea; mitochondrial respiration; Barnes maze test; novel object recognition (NOR) task; GFAP; Iba-1; NeuN; MAP2; vGlut1; HO-1	Nrf2-ARE signaling pathway	[157–159]
Natural pigments						
Fucoxanthin	*Rosmarinus officinalis* and *Salvia officinalis*	Weight drop-induced TBI mice; scratch injury-induced TBI primary cortical neurons	Improved neurobehavioral function, and neuronal viability; reduced brain edema, neuronal apoptosis, and oxidative damage	NSS; grip test score; brain water content; lesion volume; TUNEL staining; caspase 3; PARP; cytochrome c; MDA; GPx; ROS; LC3; NeuN; p62; Nrf2; HO-1; NQO1	Nrf2-ARE and Nrf2-autophagy	[170]
β-Carotene	Fungi, plants, and fruits	Weight drop-induced TBI mice	Improved neurological function; reduced brain edema, BBB disruption, neuronal apoptosis, and oxidative damage	Neurological deficit score; wire hanging; brain water content; EB extravasation; MDA; SOD; NeuN; Nissl and TUNEL staining; caspase 3; Bcl-2; Keap1; Nrf2; HO-1; NQO1	Keap1-Nrf2 signaling pathway	[174]

Table 1: Continued.

Phytochemicals	Plants	Models	Pharmacological effects	Detected markers	Antioxidant mechanism	Ref
Astaxanthin	Salmon, rainbow trout, shrimp, and lobster	CCI- or weight drop-induced TBI mice; H_2O_2-induced primary cortical neurons	Improved neurological, motor, and cognitive function; reduced brain edema, BBB disruption, neuronal apoptosis, and oxidative damage	NSS; Rotarod test time; neurological deficit scores; rotarod performance; beam walking score; wire hanging test; MWM test; brain water content; 8-OhdG; immobility time; latency to immobility; SOD1; MDA; H_2O_2; GSH; ROS; CC3; Nissl, Cresyl violet, and TUNEL staining; Prx2; SIRT1; ASK1; p38; NeuN; Bax; Bcl-2; caspase 3; Nrf2; HO-1; NQO1	Nrf2 signaling pathway; SIRT1/Nrf2/Prx2/ASK1/p38 signaling pathway	[172, 173]
Lutein	*Calendula officinalis*, spinach, and *Brassica oleracea*	CCI-induced STBI mice; H_2O_2-induced primary cortical neurons	Improved motor and cognitive function; reduced brain edema, contusion volume, inflammatory response; and oxidative damage	Forelimb reaching test; immobility time; latency to immobility; brain water content; 8-OhdG; TNF-α; IL-1β; IL-6; MCP-1; ROS; SOD; GSH; ICAM-1; COX-2 NF-κB; ET-1; MDA; H_2O_2; CC3; Nissl, Cresyl violet, and TUNEL staining; Prx2; SIRT1; ASK1; p38; NeuN; Bax; Bcl-2; caspase 3; Nrf2; HO-1; NQO1	ICAM-1/Nrf-2 signaling pathway	[176, 177]
Others						
Sodium aescinate	*Aesculus chinensis* Bunge and chestnut	Weight drop-induced TBI mice; scratch injury-induced primary cortical neurons	Improved neurological function; reduced brain edema, inflammatory response; and oxidative damage	NSS; brain water content; lesion volume; MDA; GPx; Nissl and TUNEL staining; Bax; Bcl-2; cytochrome c; caspase 3; cell survival; ROS; Nrf2; HO-1; NQO1	Nrf2-ARE pathway	[187]
Melatonin	Plants, animals, fungus, and bacteria	Marmarou's weight drop-induced TBI mice	Reduced brain edema, neuronal degeneration and apoptosis, and oxidative damage	Brain water content; MDA; 3-NT; GPx; SOD; FJC staining; NeuN; Beclin-1; Nrf2; HO-1; NQO1	Nrf2-ARE pathway	[193]
Sinomenine	*Sinomenium acutum* (Thunb.) Rehd. Et Wils. and *Sinomenium acutum* var. cinereum Rehd. Et Wils.	Marmarou's weight drop-induced TBI mice	Improved motor performance; reduced brain edema, neuronal apoptosis, and oxidative damage	Grip test score; brain water content; NeuN and TUNEL staining; Bcl-2; caspase 3; MDA; GPx; SOD; Nrf2; HO-1; NQO1	Nrf2-ARE pathway	[196]
Sulforaphane	Vegetable, including cabbage,	CCI-induced TBI mice	Improved motor performance and cognitive function,	MWZ test; EB extravasation; brain water content;	Nrf2 signaling pathway	[158, 196–198]

Table 1: Continued.

Phytochemicals	Plants	Models	Pharmacological effects	Detected markers	Antioxidant mechanism	Ref
	broccoli, and cauliflower		reduced brain edema, BBB permeability, mitochondrial dysfunction, and oxidative damage	Occludin; Claudin-5; RECA-1; vWF; EBA; ZO-1; AQP4; GPx; GSTα3; 4-HNE; ADP rate; succinate rate; NeuN; Nrf2; HO-1; NQO1		

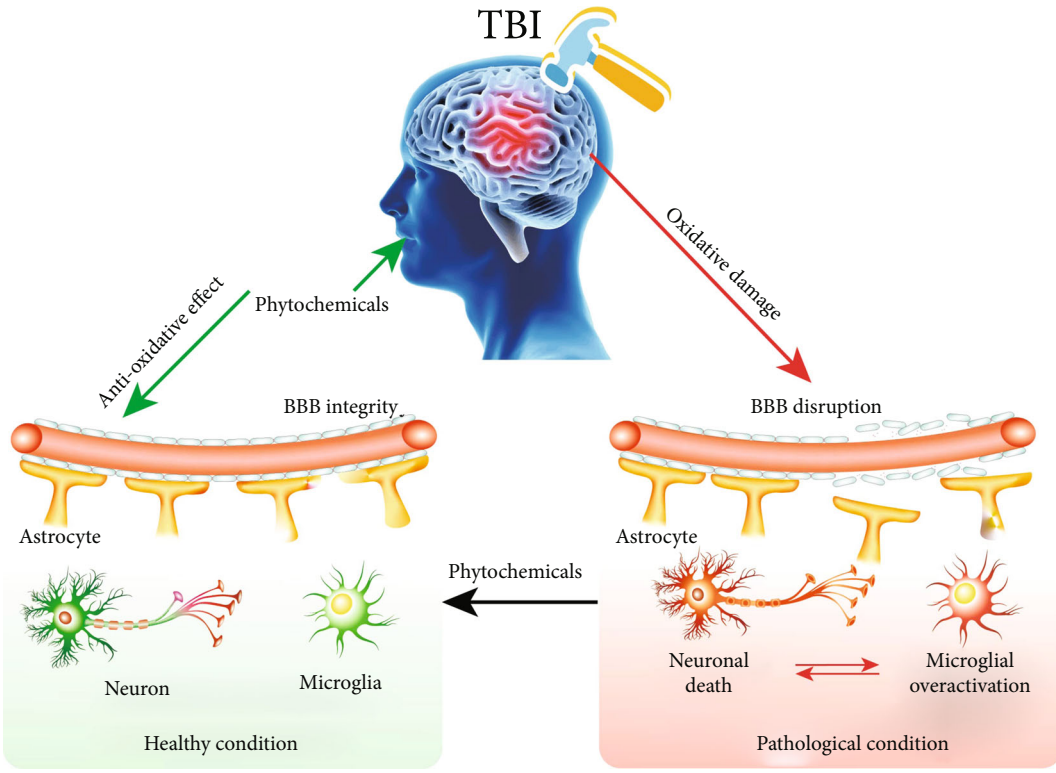

Figure 4: The potential therapy of phytochemicals for TBI. Oxidative damage in TBI plays an important role in the pathology of TBI, including BBB disruption and then neuronal death and microglial overactivation, while the treatment of phytochemicals with antioxidative properties can improve BBB integrity and then recover neuronal viability and inhibit microglial overactivation.

inflammation were attenuated in Nrf2-KO mice after TBI [80]. In addition, the anti-inflammatory effect of curcumin in TBI was also regulated by the TLR4/MyD88/NF-κB signaling pathway [86] and aquaporin-4 (AQP4) [87]. Diffuse axonal injury (DAI), a type of TBI, is recognized as an important cause that results in long-term problems in motor and cognition, while curcumin could ameliorate axonal injury and neuronal degeneration of rats after DAI. In addition, curcumin overcame endoplasmic reticulum (ER) stress via strengthening the ability of the unfolded protein response (UPR) process and reducing the levels of plasma tau, β-APP, and NF-H. The mechanistic study revealed that curcumin activated the PERK/Nrf2 signaling pathway [88]. Most importantly, the combinational use of curcumin and candesartan, an angiotensin II receptor blocker used for the treatment of hypertension, showed better antioxidative, antiapoptotic, and anti-inflammatory effects than curcumin or candesartan alone [89]. In addition, tetrahydrocurcumin, the metabolite of curcumin, could also alleviate brain edema and reduce neuronal cell apoptosis, as well as improve neurobehavioral function via the Nrf2 signaling pathway in weight drop-induced TBI mice [90]. Taken together, curcumin together with its metabolites are useful for the treatment of TBI.

5.3. Formononetin. Formononetin, an O-methylated isoflavone phytoestrogen, is commonly found in plants such as red clover [91]. Accumulating studies show that formononetin has various biological activities, including the improvement of blood microcirculation, anticancer, and antioxidative [92]. In addition, formononetin exhibits neuroprotection in AD, PD, spinal cord injury, and TBI [93, 94]. It has been reported that the administration of formononetin could decrease the neurological score and cerebral

moisture content of TBI rats [91]. In addition, the HE staining images showed that formononetin attenuated the edema and necrosis in the lesioned zones of the brain and increased the number of neural cells. At the same time, the oxidative stress was significantly reversed by formononetin as indicated by the increased enzymatic activity of SOD and GPx activity and decreased MDA content. The inflammatory cytokines including TNF-α and IL-6 as well as the mRNA level of Cyclooxygenase-2(COX-2) were also reduced by formononetin. The mechanistic study revealed that formononetin increased the protein expression of Nrf2 [95]. Furthermore, the same research team found that microRNA-155 (miR-155) is involved in the neuroprotection of formononetin in TBI. The pretreatment of formononetin significantly increased the expression of miR-155 and HO-1, which is accompanied by the downregulation of BACH1 [91]. All evidence suggests that formononetin provides neuroprotection in TBI via the Nrf2/HO-1 signaling pathway.

5.4. Baicalin. Baicalin, known as 7-D-Glucuronic acid-5,6-dihydroxyflavone, is a major flavone found in the radix of *Scutellaria baicalensis* [96]. Emerging evidence indicates that baicalin can cross the BBB and exert neuroprotective effects in various CNS-related diseases including AD, cerebral ischemia, spinal cord injury, and TBI [97]. In addition, baicalin was reported to activate the Nrf2 signaling pathway and attenuate subarachnoid hemorrhagic brain injury [98]. In weight drop-induced TBI mice, baicalin significantly reduced the neurological soft signs (NSS) score and the brain water content, and inhibited neuronal apoptosis as evidenced by the decreased terminal deoxynucleotidyl transferase dUTP nick end labeling (TUNEL)-positive neurons, Bax/Bcl-2 ratio, and the cleavage of caspase 3. Meanwhile, baicalin attenuated oxidative damage by decreasing MDA levels and increasing GPx and SOD activity and expression. The mechanistic study found that baicalin increased the expression of Nrf2 and promoted the nuclear translocation of Nrf2, meanwhile upregulated the mRNA and protein expression of HO-1 and NQO1, while the treatment of ly294002 reversed the effect of baicalin on antiapoptosis, antioxidation, and activation of the Nrf2 signaling pathway, suggesting that baicalin exerts neuroprotective effects via the Akt/Nrf2 pathway in TBI [96]. As is known to us, autophagy plays a protective mechanism in neurodegenerative diseases. Furthermore, the same research team found that baicalin induced autophagy and alleviated the BBB disruption and inhibited neuronal apoptosis of mice after TBI, while the co-treatment of 3-MA partly abolished the neuroprotective effect of baicalin. Therefore, baicalin provides a beneficial effect via the Nrf-2 regulated antioxidative pathway and autophagy induction.

5.5. Catechin. Catechin is a flavan-3-ol and belongs to a type of natural polyphenols [99]. It is a plant secondary metabolite and a potent antioxidant [100]. Structurally, it has four diastereoisomers, including two isomers with trans configuration called (+)-catechin and two isomers with cis configuration called (-)-epicatechin [101]. They are commonly found in food and fruits, such as cocoa, tea, and grapes. The pharmacological activity of catechin mainly involves antioxidative, anti-inflammatory, antifungal, antidiabetic, antibacterial, and antitumor effects [102]. In addition, catechin also exhibits neuroprotective effects in CCI-induced TBI rats by inhibiting the disruption of BBB and excessive inflammatory responses [103]. The expression of junction proteins including occludin and zonula occludens protein-1 (ZO-1) associated with BBB integrity was increased, while the levels of proinflammatory cytokines including IL-1β, iNOS, and IL-6 were decreased by catechin. At the same time, catechin significantly alleviated the brain damage as revealed by the decrease in the brain water content and brain infarction volume, as well as improved motor and cognitive deficits [103]. In addition, catechin inhibited cell apoptosis and induced neurotrophic factors in rats after TBI [104]. In CCI-induced TBI mice, the administration of epicatechin significantly attenuated the neutrophil infiltration and oxidative damage. Specifically, epicatechin could reduce lesion volume, edema, and cell death, as well as improve neurological function, cognitive performance, and depression-like behaviors. In addition, epicatechin decreased white matter injury, HO-1 expression, and the deposition of ferric iron. The mechanistic study found that epicatechin decreased the Keap1 expression while increasing the nuclear translocation of Nrf2. Meanwhile, epicatechin reduced the activity of Matrix metallopeptidase 9 (MMP9) and increased the expression of SOD1 and quinone 1 [102]. Therefore, epicatechin exerts neuroprotective effects in TBI mice via modulating Nrf2-regulated oxidative stress response and inhibiting iron deposition.

5.6. Fisetin. Fisetin, also known as 3,3′,4′,7-tetrahydroxyflavone, is a flavonol compound and was first extracted from *Cotinus coggygria* by Jacob Schmid in 1886 [105], and its structure was elucidated by Joseph Hergig in 1891. In addition, fisetin is also found in many vegetables and fruits, such as onions, cucumbers, persimmon, strawberries, and apples [106]. Emerging evidence indicates that fisetin acting as a potent antioxidant possesses multiple biological activities, including anti-inflammatory, antiviral, anticarcinogenic, and other effects [107]. Fisetin also presents neuroprotective effects via the antioxidative stress in AD, PD, etc. [108]. In addition, fisetin also showed protective effects in weight drop-induced TBI mice as shown by the decreased NSS, brain water content, Evans blue (EB) extravasation, and lesion volume of brain tissue, as well as the increased grip test score. Meanwhile, the MDA level was decreased and GPx activity was increased by fisetin, suggesting that fisetin provides a neuroprotective effect via suppressing TBI-induced oxidative stress [109]. In addition, the neuronal cell outline and structure stained by Nissl solution showed that fisetin improved neuronal viability, while neuronal apoptosis was inhibited by fisetin as demonstrated by the decreased TUNEL signals, and the reduced protein expression of Bax/Bcl-2 and cleaved caspase-3. The mechanistic study demonstrated that fisetin promoted the Nrf2 nuclear translocation and increased the expression of HO-1 and NQO1, while the KO of Nrf2 abrogated the neuroprotective effect

of fisetin including antioxidation and antiapoptosis [109]. Moreover, fisetin was reported to exert anti-inflammatory effects in TBI mice via the TLR4/NF-κB pathway, and the level of TNF-α, IL-1β, and IL-6 was significantly decreased. Meanwhile, the BBB disruption of TBI mice was attenuated by fisetin [110]. Therefore, fisetin exerts neuroprotective effects in TBI via the Nrf2-regulated oxidative stress and the NF-κB-mediated inflammatory signaling pathway.

5.7. Luteolin. Luteolin, belonging to flavonoids, is abundant in fruits and vegetables such as carrots, green tea, and celery [111]. Emerging evidence indicates luteolin has a wide variety of biological activities including antioxidative and anti-inflammatory effects [112, 113]. In addition, several studies have demonstrated the neuroprotective effect of luteolin in multiple in vivo and in vitro models [114, 115]. For example, luteolin could recover motor performance and reduce post-traumatic cerebral edema in weight drop-induced TBI mice. The oxidative damage was reduced by luteolin as demonstrated by the decrease in MDA levels and the increase in GPx activity in the ipsilateral cortex. The mechanistic study found that luteolin promoted the nuclear translocation of Nrf2 and increased the mRNA and protein expressions of HO-1 and NQO1 [116]. In addition, luteolin significantly improved TBI-induced learning and memory impairment in rats after TBI, which was closely associated with the attenuation of oxidative damage indicated by the decreased MDA level and increased SOD and CAT activity [117, 118]. Therefore, the Nrf2-regulated oxidative stress response plays an important role in luteolin against TBI.

5.8. Isoliquiritigenin. Isoliquiritigenin, a chalcone compound, is often found in plants including *Sinofranchetia chinensis*, *Glycyrrhiza uralensis*, and *Dalbergia odorifera*. [119]. Isoliquiritigenin has been reported to attenuate oxidative damage, inhibit the inflammatory response, and suppress tumor growth [120]. In addition, isoliquiritigenin activates the Nrf2 signaling pathway to exert antioxidative and anti-inflammatory effects in multiple cellular and animal models. Isoliquirtigenin also exerts a neuroprotective effect in CCI-induced TBI mice via the Nrf2-ARE signaling pathway [121]. For example, isoliquiritigenin increased the Garcia Neuro score and decreased the brain water content, as well as the expression of aquaporin 4 (AQP4) and EB leakage. The glia activation indicated by GFAP expression was inhibited and the neuron viability showed by neurofilament light (NFL) expression was increased by isoliquiritigenin. In addition, isoliquiritigenin increased the number of Nissl staining-positive neurons and inhibited neuronal apoptosis as evidenced by the decreased expression of cleaved caspase-3. Furthermore, the oxidative damage was ameliorated by isoliquiritigenin as shown by the increased GPx activity, SOD levels, and decreased H_2O_2 concentration and MDA levels. However, the KO of Nrf2 significantly attenuated the neuroprotective effect of isoliquiritigenin in mice after TBI. The mechanistic study demonstrated that isoliquiritigenin increased the nuclear translocation of Nrf2 and the protein and mRNA expression of NQO1 and HO-1. In the in vitro study, isoliquiritigenin also activated the Nrf2-ARE signaling pathway and increased the cell viability in oxygen and glucose deprivation (OGD)-induced SH-SY5Y cells. In addition, isoliquiritigenin inhibited shear stress-induced cell apoptosis in SH-SY5Y cells, as well as suppressed the inflammatory response and inhibited neuronal apoptosis in CCI-induced TBI mice or rats via the PI3K/AKT/GSK-3β/NF-κB signaling pathway [122, 123]. Moreover, isoliquiritigenin protected against BBB damage in mice after TBI via inhibiting the PI3K/AKT/GSK-3β pathway [123]. Therefore, isoliquiritigenin may be a promising agent for the treatment of TBI via the inhibition of oxidative stress, inflammatory response, and BBB disruption in TBI.

5.9. Tannic Acid. Tannic acid, a natural polyphenol, is commonly found in green and black teas as well as nuts, fruits, and vegetables [124]. Emerging evidence indicates that tannic acid possesses multiple biological activities such as antioxidative, anti-inflammatory, antiviral, and antiapoptotic effects [125–127]. In addition, tannic acid exhibits neuroprotective effects as shown by the improvement of behavioral deficits and the inhibition of neurodegeneration [128]. Recently, tannic acid has been proven to ameliorate the oxidative damage and behavioral impairments of mice after TBI [128]. For example, tannic acid significantly increased the score in the grip test and the motor coordination time as well as decreased the stay time in the balance test. In addition, tannic acid inhibited neuronal damage and reduced the brain water content of TBI mice. A further study found that tannic acid could attenuate oxidative stress as evidenced by increased glutathione (GSH) levels, 1-Chloro-2,4-dinitrobenzene (CDNB) conjunction, NADPH oxidation, and H_2O_2 consumption. In addition, apoptosis-related proteins including cleaved caspase-3 and Poly (ADP-ribose) polymerase (PARP), as well as Bax/Bcl-2, were significantly inhibited by tannic acid. Meanwhile, the inflammatory response indicated by the increased levels of TNF-α and IL-1β and GFAP immunofluorescence intensity was also suppressed. The mechanistic study demonstrated that tannic acid increased the protein expression of Nrf2, PGC-1α, Tfam, and HO-1. Therefore, tannic acid exerts a neuroprotective effect in TBI via activating the PGC-1α/Nrf2/HO-1 signaling pathway.

5.10. Ellagic Acid. Ellagic acid, an innate polyphenol, is commonly found in various berries such as blueberries, strawberries, blackberries, together with walnuts and nuts [129]. Several studies show that ellagic acid exerts multiple biological activities, including anti-inflammatory, antioxidative, antifibrosis, antidepressant, and neuroprotective effects [130]. In addition, ellagic acid also exhibits protective effects in various brain injuries such as neonatal hypoxic brain injury, cerebral ischemia/reperfusion injury, carbon tetrachloride (CCl4)-induced brain damage, and TBI [131–133]. Here, we summarize the neuroprotective effect of ellagic acid in TBI and its mechanism of action. In experimental diffuse TBI rats, the treatment of ellagic acid significantly improved memory and hippocampus electrophysiology deficits [134]. Meanwhile, the inflammatory responses indicated by the elevated TNF-α, IL-1β, and IL-6 levels were reduced by ellagic

acid [134, 135]. In addition, ellagic acid could also decrease the BBB permeability of mice after TBI [135]. In CCl4-induced brain injury rats, ellagic acid decreased MDA levels, increased GSH content, and CAT activity. The mechanistic study demonstrated that ellagic acid inhibited the protein expression of NF-κB and COX-2 while increasing the protein expression of Nrf2 [133]. Therefore, ellagic acid exerts an antioxidative effect via activating the Nrf2 pathway and exhibits anti-inflammatory effects via inhibiting the NF-κB pathway in TBI.

5.11. Breviscapine. Breviscapine is an aglycone flavonoid and is isolated from the Erigeron plant [136]. Modern pharmacological studies indicate that breviscapine can expand blood vessels to assist in microcirculation, suggesting its potential therapeutic role in cardiovascular and CNS-related diseases [137]. In addition, breviscapine, acting as a scavenger of oxygen-free radicals, is demonstrated to improve ATPase and SOD activity. Recently, breviscapine is also reported to improve neurobehavior and decrease neuronal apoptosis in TBI mice, which is closely associated with the translocation of Nrf2 from the cytoplasm into the nuclear and the subsequent upregulation of Nrf2 downstream factors such as HO-1 and NQO1 [138]. In addition, the inhibition of glycogen synthase kinase-3β (GSK-3β) and IL-6 by breviscapine is associated with its neuroprotective effect in TBI [139, 140]. Therefore, breviscapine exerts neuroprotective effects in TBI via antioxidation, antiapoptosis, and anti-inflammatory responses.

5.12. Asiatic Acid. Asiatic acid belonging to pentacyclic triterpene is isolated from natural plants such as *Centella asiatica* [141]. Studies have shown that asiatic acid exhibits potent anti-inflammatory and antioxidative properties, which contributes to its protective effects in spinal cord injury, ischemic stroke, cardiac hypertrophy, liver injury, and lung injury through multiple mechanisms [142]. For example, the administration of asiatic acid could increase Basso, Beattie, Bresnahan scores and the plane test score in spinal cord injury (SCI) rats. Meanwhile, asiatic acid inhibited the inflammatory response by reducing the levels of IL-1β, IL-18, IL-6, and TNF-α, and counteracted oxidative stress by decreasing ROS, H_2O_2, and MDA levels while increasing SOD activity and glutathione production. The underlying mechanisms include the activation of Nrf2/HO-1 and the inhibition of the NLRP3 inflammasome pathway. In addition, asiatic acid could alleviate tert-butyl hydroperoxide (tBHP)-induced oxidative stress in HepG2 cells. The researchers found that asiatic acid significantly inhibited tBHP-induced cytotoxicity, apoptosis, and the generation of ROS, which attributed to the activation of Keap1/Nrf2/ARE signaling pathway and the upregulation of transcription factors including HO-1, NQO-1, and GCLC [143]. In a CCI-induced TBI model, the administration of asiatic acid significantly improved neurological deficits and reduced brain edema. Meanwhile, asiatic acid counteracted oxidative damage as evidenced by the reduced levels of MDA, 4-HNE, and 8-hydroxy-2′-deoxyguanosine (8-OHdG). The mechanistic study further found that asiatic acid could increase the mRNA and protein expression of Nrf2 and HO-1 [144]. Taken together, asiatic acid improves neurological deficits in TBI via activating the Nrf2/HO-1 signaling pathway.

5.13. Aucubin. Aucubin, an iridoid glycoside isolated from natural plants such as *Eucommia ulmoides* [145], is reported to have several pharmacological effects including antioxidation, antifibrosis, antiageing, and anti-inflammation [145–147]. Recently, emerging evidence indicates that aucubin exerts neuroprotective effects via antioxidation and anti-inflammation [148]. In addition, aucubin also inhibited lipid accumulation and attenuated oxidative stress via activating the Nrf2/HO-1 and AMP-activated protein kinase (AMPK) signaling pathways [147]. Moreover, aucubin inhibited lipopolysaccharide (LPS)-induced acute pulmonary injury through the regulation of Nrf2 and AMPK pathways [149]. In H_2O_2-induced primary cortical neurons and weight drop-induced TBI mouse model, aucubin was found to significantly decrease the excessive generation of ROS and inhibit neuronal apoptosis. In addition, aucubin could reduce brain edema, improve cognitive function, decrease neural apoptosis and loss of neurons, attenuate oxidative stress, and suppress the inflammatory response in the cortex of TBI mice. The mechanistic study demonstrated that aucubin activated the Nrf2-ARE signaling pathway and upregulated the expression of HO-1 and NQO1, while the neuroprotective effect of aucubin in Nrf2-KO mice after TBI was reversed [150]. Therefore, aucubin provides a protective effect in TBI via activating the Nrf2 signaling pathway.

5.14. Ursolic Acid. Ursolic acid, a pentacyclic triterpenoid compound, is widely found in various fruits and vegetables such as apples, bilberries, lavender, and hawthorn. [151]. Ursolic acid has been reported to possess multiple pharmacological effects including anti-inflammatory, antioxidative, antifungal, antibacterial, and neuroprotective properties [152]. In addition, ursolic acid activates the Nrf2/ARE signaling pathway to exert a protective effect in cerebral ischemia, liver fibrosis, and TBI [153]. In weight drop-induced TBI mice, the administration of ursolic acid could improve neurobehavioral functions and reduce the cerebral edema of mice after TBI. In addition, ursolic acid inhibited neuronal apoptosis as shown by the Nissl staining images and TUNEL staining. Meanwhile, ursolic acid ameliorated oxidative stress by increasing SOD and GPx activity as well as decreasing MDA levels. The mechanistic study demonstrated that ursolic acid promoted the nuclear translocation of Nrf2 and increased the levels of transcription factors including HO-1 and NQO1, while the KO of Nrf2 could partly abolish the protective effect of ursolic acid in TBI [153]. Therefore, ursolic acid exerts a neuroprotective effect in TBI via partly activating the Nrf2 signaling pathway.

5.15. Carnosic Acid. Carnosic acid, a natural benzenediol abietane diterpene, is found in *Rosmarinus officinalis* and *Salvia officinalis* [154]. Carnosic acid and carnosol are two major antioxidants in *Rosmarinus officinalis* [155].

Emerging evidence indicates that carnosic acid is a potent activator of Nrf2 and exerts a neuroprotective effect in various neurodegenerative diseases [156]. In CCI-induced acute post-TBI mice, carnosic acid could reduce TBI-induced oxidative damage by decreasing the level of 4-HNE and 3-NE in the brain tissues. A further study demonstrated that carnosic acid maintained mitochondrial respiratory function and attenuated oxidative damage by reducing the amount of 4-HNE bound to cortical mitochondria [157, 158]. In addition, carnosic acid showed a potent neuroprotective effect in repetitive mild TBI (rmTBI) as evidenced by the significant improvement of motor and cognitive performance. Meanwhile, the expression of GFAP and Iba1 expression was inhibited, suggesting that carnosic acid inhibited the neuroinflammation in TBI [159]. Therefore, carnosic acid exerts a neuroprotective effect via inhibiting the mitochondrial oxidative damage in TBI through the Nrf2-ARE signaling pathway.

5.16. Fucoxanthin. Fucoxanthin, a carotenoid isolated from natural plants such as seaweeds and microalgae, is considered a potent antioxidant [160]. Several studies show that fucoxanthin exerts various pharmacological activities such as antioxidation, anti-inflammation, anticancer, and health protection effects [161]. In addition, fucoxanthin exerts anti-inflammatory effects in LPS-induced BV-2 microglial cells via increasing the Nrf2/HO-1 signaling pathway [162] and inhibits the overactivation of NLRP3 inflammasome via the NF-κB signaling pathway in bone marrow-derived immune cells and astrocytes [163]. In mouse hepatic BNL CL.2 cells, fucoxanthin was reported to upregulate the mRNA and protein expression of HO-1 and NQO1 via increasing the phosphorylation of ERK and p38 and activating the Nrf2/ARE pathway, which contributes to its antioxidant activity [164]. Recently, it has been reported that the neuroprotective effect of fucoxanthin in TBI mice was regulated via the Nrf2-ARE and Nrf2-autophagy pathways [165]. In this study, the researchers found that fucoxanthin alleviated neurological deficits, cerebral edema, brain lesions, and neuronal apoptosis of TBI mice. In addition, fucoxanthin significantly decreased the generation of MDA and increased the activity of GPx, suggesting its antioxidative effect in TBI. Furthermore, in vitro experiments revealed that fucoxanthin could improve neuronal survival and reduce the production of ROS in primary cultured neurons. A further mechanistic study revealed that fucoxanthin activated the Nrf2-ARE pathway and autophagy in vivo and in vitro, while fucoxanthin failed to activate autophagy and exert a neuroprotective effect in $Nrf2^{-/-}$ mice after TBI. Therefore, fucoxanthin activates the Nrf-2 signaling pathway and induces autophagy to exert a neuroprotective effect in TBI.

5.17. β-carotene. β-carotene, abundant in fungi, plants, and fruits, is a member of the carotenes and belongs to terpenoids [166]. Accumulating studies indicate that β-carotene acting as an antioxidant has potential therapeutic effects in various diseases, such as cardiovascular disease, cancer, and neurodegenerative diseases [167, 168]. Meanwhile, the neuroprotective effect of β-carotene was also reported in CCI-induced TBI mice; the administration of β-carotene significantly improved neurological function and brain edema as evidenced by the decreased neurological deficit score and brain water content and increased time of wire hanging of mice after TBI. In addition, β-carotene could maintain the BBB permeability as indicated by the EB extravasation and ameliorate oxidative stress as showed by the increased SOD level and decreased MDA levels. The mechanistic study demonstrated that β-carotene activated the Keap1-Nrf2 signaling pathway and promoted the expression of HO-1 and NQO1 [169]. Therefore, β-carotene provides a neuroprotective effect in TBI via inhibiting oxidative stress through the Nrf2 pathway.

5.18. Astaxanthin. Astaxanthin is a carotenoid and is commonly found in certain plants and animals, such as salmon, rainbow trout, shrimp, and lobster [170]. Emerging evidence indicates that astaxanthin exhibits multiple biological activities, including antiageing, anticancer, heart protection, and neuroprotection [171]. Recently, astaxanthin was reported to present neuroprotection in CCI-induced TBI mice, such as increasing NSS score and immobility time and increasing rotarod time and latency to immobility. In addition, astaxanthin increased SOD1 levels and inhibited the protein expression of cleaved caspase 3 and the number of TUNEL-positive cells, suggesting that astaxanthin exerted antioxidative and antiapoptotic effects. The mechanistic study demonstrated that astaxanthin increased the protein and mRNA expressions of Nrf2, HO-1, NQO1, and SOD1 [172]. Moreover, in weight drop-induced TBI mice, astaxanthin significantly reduced brain edema and improved behavioral functions including neurological scores, rotarod performance, beam walking performance, and falling latency during the hanging test. In addition, astaxanthin improved neuronal survival indicated by Nissl staining. Furthermore, astaxanthin exerted an antioxidative effect by increasing the SOD1 protein expression and inhibited neuronal apoptosis by reducing the level of cleaved caspase 3 and the number of TUNEL-positive cells. The mechanistic study revealed that astaxanthin promoted the activation of the Nrf2 signaling pathway as demonstrated by the increased mRNA levels and protein expressions of Nrf2, HO-1, and NQO1, while the inhibition of Prx2 or SIRT1 reversed the antioxidative and antiapoptotic effect of astaxanthin. Therefore, astaxanthin activated the SIRT1/Nrf2/Prx2/ASK1 signaling pathway in TBI. Moreover, astaxanthin also provided a neuroprotective effect in H_2O_2-induced primary cortical neurons by reducing oxidative damage and inhibiting apoptosis via the SIRT1/Nrf2/Prx2/ASK1/p38 signaling pathway [173]. Therefore, astaxanthin exerts a neuroprotective effect including antioxidation and antiapoptosis via activating the Nrf2 signaling pathway in TBI.

5.19. Lutein. Lutein, a natural carotenoid, is commonly found in a variety of flowers, vegetables, and fruits, such as *Calendula officinalis*, spinach, and *Brassica oleracea* [174]. Accumulating studies demonstrate that lutein is a potent antioxidant and exhibits benefits in various diseases,

including ischemia/reperfusion injury, diabetic retinopathy, heart disease, AD, and TBI [175]. In severe TBI rats, the administration of lutein significantly increased the inhibition of skilled motor function and reversed the increase in contusion volume of TBI rats. In addition, lutein suppressed the inflammatory response by decreasing the levels of TNF-α, IL-1β, IL-6, and Monocyte chemoattractant protein-1 (MCP-1). Meanwhile, lutein decreased ROS production and increased SOD and GSH activity, suggesting that lutein attenuated TBI-induced oxidative damage. Moreover, the mechanistic study found that lutein inhibited the protein expression of intercellular adhesion molecule-1 (ICAM-1), COX-2, and NF-κB, while increasing the protein expression of ET-1 and Nrf2. Therefore, the neuroprotective effect of lutein in TBI may be regulated via the NF-κB/ICAM-1/Nrf2 signaling pathway [176]. It is known that zeaxanthin and lutein are isomers and have identical chemical formulas. Recently, it is reported that lutein/zeaxanthin exerted a neuroprotective effect in TBI mice induced by a liquid nitrogen-cooled copper probe, and the brain infarct and brain swelling were remarkably declined by lutein/zeaxanthin. The protein expression of Growth-Associated Protein 43 (GAP43), ICAM, neural cell adhesion molecule (NCAM), brain-derived neurotrophic factor (BDNF), and Nrf2 were increased, while the protein expression of GFAP, IL-1β, IL-6, and NF-κB was inhibited by lutein/zeaxanthin [177]. Therefore, lutein/zeaxanthin presents antioxidative and anti-inflammatory effects via the Nrf2 and NF-κB signaling pathways.

5.20. Sodium Aescinate. Sodium aescinate (SA) is a mixture of triterpene saponins isolated from the seeds of *Aesculus chinensis* Bunge and chestnut [178]. Amounting studies show that SA exerts anti-inflammatory, anticancer, and antioxidative effects [179–181]. In addition, SA has been reported to exhibit neuroprotective effect in 1-methyl-4-phenyl-1,2,3,6-tetrahydropyridine (MPTP)-induced PD mice and mutant huntingtin (mHTT) overexpressing HT22 cells [182, 183]. A recent study reported that SA could attenuate brain injury in weight drop-induced TBI mice [182]. The intraperitoneal administration of SA significantly decreased NSS, brain water content, and lesion volume of mice after TBI. A further study found that SA suppressed TBI-induced oxidative stress as evidenced by the decreased MDA levels and increased GPx activity. The Nissl staining images displayed that SA increased the viability of neurons, and the TUNEL staining showed that SA inhibited neuronal apoptosis. Meanwhile, SA decreased the ratio of Bax/Bcl-2 and the cleaved form of caspase-3, while increasing the release of cytochrome c from mitochondria into the cytoplasm. The mechanistic study demonstrated that SA promoted the translocation of Nrf2 from the cytoplasm into the nuclear and subsequently increased the expression of HO-1 and NQO1. Moreover, the neuroprotective effect and mechanism of action of SA have been confirmed in scratch injury-induced TBI primary neurons and Nrf2-KO mice after TBI. Therefore, SA exerts a neuroprotective effect in TBI via activating the Nrf2 signaling pathway.

5.21. Melatonin. Melatonin, commonly found in plants, animals, fungi, and bacteria, plays an important role in the regulation of the biological clock [184]. Melatonin as a dietary supplement is widely used to treat insomnia. Emerging evidence indicates that melatonin exerts neuroprotection in various diseases including brain injury, spinal cord injury, and cerebral ischemia [185]. In addition, melatonin is demonstrated to be a potent antioxidant with the ability to reduce oxidative stress, inhibit the inflammatory response, and attenuate neuronal apoptosis [186]. In craniocerebral trauma, melatonin showed a neuroprotective effect due to its antioxidative, anti-inflammatory, and inhibitory effects on activation adhesion molecules [187]. In Marmarou's weight drop-induced TBI mice, melatonin significantly inhibited neuronal degeneration and reduced cerebral edema in the brain. Meanwhile, melatonin also attenuated the oxidative stress induced by TBI as evidenced by the decreased MDA levels and 3-NE expression, as well as increased GPx and SOD levels. The mechanistic study demonstrated that melatonin increased the nuclear translocation of Nrf2 and promoted the protein expression and mRNA levels of HO-1 and NQO1, while the KO of Nrf2 could partly reverse the neuroprotective effect of melatonin, including antioxidation, inhibition of neuronal degeneration, and alleviation of cerebral edema in mice after TBI. Therefore, melatonin provides a neuroprotective effect in TBI via the Nrf-ARE signaling pathway [188]. Due to the complex pathophysiology of TBI, the combinational use of melatonin and minocycline, a bacteriostatic agent reported to inhibit neuroinflammation, did not exhibit a better neuroprotective effect than either agent alone. The dosing and/or administration issues may attribute to this result [189]. Therefore, the optimal combination should be explored for the treatment of TBI.

5.22. Sinomenine. Sinomenine is an alkaloid compound that is isolated from the roots of climbing plants including *Sinomenium acutum* (Thunb.) Rehd. et Wils. and *Sinomenium acutum* var. cinereum Rehd. et Wils [190]. Sinomenine has been demonstrated to exhibit an antihypertensive and anti-inflammatory effect and is commonly used to treat various acute and chronic arthritis, rheumatism, and rheumatoid arthritis (RA). In addition, sinomenine provides a neuroprotective effect in Marmarou's weight drop-induced TBI mice. The administration of sinomenine significantly increased the grip test score and decreased brain water content. In addition, the neuronal viability was increased by sinomenine as shown by the increased NeuN-positive neurons and decreased TUNEL-positive neurons. Meanwhile, sinomenine increased Bcl-2 protein expression and decreased cleaved caspase-3 expression. Furthermore, sinomenine attenuated oxidative stress by decreasing MDA levels and increasing SOD and GPx activity. The mechanistic study revealed that sinomenine promoted the nuclear translocation of Nrf2 and increased the mRNA and protein expression of HO-1 and NQO1 in mice after TBI [191]. Therefore, sinomenine, acting as a potent anti-inflammatory agent, provides antiapoptotic and antioxidative effects in TBI via the Nrf2-ARE signaling pathway.

5.23. Sulforaphane. Sulforaphane, also known as isothiocyanate, is commonly found in certain kinds of vegetables, including cabbage, broccoli, and cauliflower [192]. Emerging evidence indicates that sulforaphane is widely used to treat prostate cancer, autism, asthma, and many other diseases [193–195]. In addition, sulforaphane also showed a neuroprotective effect in TBI. For example, sulforaphane decreased BBB permeability in CCI-induced TBI rats as evidenced by the decreased EB extravasation and the relative fluorescence intensity of fluorescein [196]. Meanwhile, the loss of tight junction proteins (TJs) including occluding and claudin-5 was attenuated by sulforaphane. The mechanistic study found that sulforaphane increased the mRNA level of Nrf2-driven genes including GST-alpha3(GSTα3), GPx, and HO-1, as well as enhanced the enzymatic activity of NQO1 in the brain and brain microvessels of TBI mice, suggesting that sulforaphane activated the Nrf2-ARE signaling pathway to protect BBB integrity. Furthermore, sulforaphane could reduce brain edema as evidenced by the decrease in brain water content, which was closely associated with the attenuation of AQP4 loss in the injury core and the further increase of AQP4 level in the penumbra region [197]. Moreover, the Morris water maze (MWZ) test showed that sulforaphane improved spatial memory and spatial working memory. Meanwhile, TBI-induced oxidative damage was significantly attenuated by sulforaphane as demonstrated by the reduced 4-HNE levels [198]. In addition, sulforaphane also attenuated 4-HNE induced dysfunction in isolated cortical mitochondria [158]. Taken together, sulforaphane provides a neuroprotective effect in TBI via the activation of the Nrf2-ARE signaling pathway.

6. Conclusions and Perspective

It is known to us that TBI causes irreversible primary mechanical damage, followed by secondary injury. Studies have shown that multiple mechanisms contribute to the development of TBI during secondary injury, mainly including inflammatory response, oxidative stress, mitochondrial dysfunction, BBB disruption, and otherwise. Among them, oxidative stress leads to mitochondrial dysfunction, BBB disruption, and neuroinflammation. Therefore, oxidative stress plays a central role in the pathogenesis of TBI. Nrf2 is a conserved bZIP transcription factor, and the activation of the Nrf2 signaling pathway protects against oxidative damage. Under stress conditions or the treatment of Nrf2 activators, Nrf2 is translocated from the cytoplasm into the nucleus where it protects against oxidative damage via the ARE-mediated transcriptional activation of genes, including HO-1, NQO1, and GCLC, thereby inhibiting mitochondrial dysfunction, apoptosis, inflammation, and oxidative damage. Therefore, targeting the activation of the Nrf2 signaling pathway is a promising therapeutical strategy for TBI. To date, increased Nrf2 activators were reported to exert neuroprotective effects in various neurodegenerative diseases, cerebral ischemia, cerebral hemorrhage, and TBI [199, 200]. Phytochemicals are rich and isolated from fruits, vegetables, grains, and other medicinal herbs. In this review, polyphenols, terpenoids, natural pigments, and other phytochemicals were summarized. They exhibit potent neuroprotective effects, including the improvement of BBB integrity, recovery of neuronal viability, and inhibition of microglial overactivation via the Nrf2-mediated oxidative stress response (Figure 4).

Although a large number of studies have demonstrated the neuroprotective effect of most of the phytochemicals in vivo and in vitro models of TBI, there is a lack of effective clinical application evidence. In addition, little is known about the safety and pharmacokinetics of these phytochemicals. Therefore, increasing studies are needed to be performed to accelerate the process of phytochemicals entering the clinic. In the later period of TBI recovery, the selective permeability of BBB also gradually recovered. At this time, BBB is a big obstacle, which greatly limits the neuroprotective effect of drugs, and the use of drugs based on nanomaterials effectively improves the BBB permeability of drugs, bringing new hope for these phytochemicals. In addition, the combinational use of phytochemicals targeting multi-targets such as Nrf2, NF-κB, NADPH oxidase-2 (NOX-2) with gene, and stem cell therapy will be a promising strategy for the treatment of TBI.

Data Availability

The data used to support the findings of this study are available from the corresponding author upon request.

Conflicts of Interest

All authors have disclosed that they do not have any conflicts of interest.

Authors' Contributions

An-Guo Wu, Yuan-Yuan Yong, and Yi-Ru Pan conceptualized and wrote the manuscript. An-Guo Wu, Li Zhang, Yue Zhang, and Yong Tang created the figures. Jing Wei, Lu Yu, Chong-Lin Yu, and Jian Liu contributed to the writing of the manuscript. Betty Yuen-Kwan Law, Ru-Xiang Xu, Xiao-Gang Zhou, Jian-Ming Wu, and Da-Lian Qin reviewed and modified the manuscript. All authors approved the final version of the manuscript. An-Guo Wu, Yuan-Yuan Yong, and Yi-Ru Pan contributed equally to this work.

Acknowledgments

This work was supported by Grants from the National Natural Science Foundation of China (Grant No. 81903829), Grants from the Sichuan Science and Technology Program (grant nos. 2022YFH0115 and 21RCYJ0021), The Southwest Medical University (Grant Nos. 2021ZKZD015, 2021ZKZD018, and 2021ZKMS046), The Macao Science and Technology Development Fund of Macao SAR (Project Nos. SKL-QRCM(MUST)-2020-2022 and MUST-SKL-2021-005), The Collaborative Innovation Center for Prevention and Treatment of Cardiovascular Disease of Sichuan Province Funded Project (Grant No. xtcx2019-20), The Joint Project of Luzhou Municipal People's Government and Southwest Medical University, China (Grant no. 2020LZXNYDJ37).

References

[1] W. Liu, Y. Chen, J. Meng et al., "Ablation of caspase-1 protects against TBI-induced pyroptosis in vitro and in vivo," *Journal of Neuroinflammation*, vol. 15, no. 1, p. 48, 2018.

[2] A. Khellaf, D. Z. Khan, and A. Helmy, "Recent advances in traumatic brain injury," *Journal of Neurology*, vol. 266, no. 11, pp. 2878–2889, 2019.

[3] B. Dang, W. Chen, W. He, and G. Chen, "Rehabilitation treatment and progress of traumatic brain injury dysfunction," *Neural Plasticity*, vol. 2017, Article ID 1582182, 6 pages, 2017.

[4] M. Galgano, G. Toshkezi, X. Qiu, T. Russell, L. Chin, and L. R. Zhao, "Traumatic brain injury: current treatment strategies and future endeavors," *Cell Transplantation*, vol. 26, no. 7, pp. 1118–1130, 2017.

[5] H. S. Mangat, "Hypertonic saline infusion for treating intracranial hypertension after severe traumatic brain injury," *Critical Care*, vol. 22, no. 1, p. 37, 2018.

[6] H. Chen, Z. Song, J. A. Dennis, and Cochrane Injuries Group, "Hypertonic saline versus other intracranial pressure-lowering agents for people with acute traumatic brain injury," *Cochrane Database of Systematic Reviews*, vol. 12, 2019.

[7] D. J. Cooper, A. D. Nichol, M. Bailey et al., "Effect of early sustained prophylactic hypothermia on neurologic outcomes among patients with severe traumatic brain injury: the POLAR randomized clinical trial," *JAMA*, vol. 320, no. 21, pp. 2211–2220, 2018.

[8] Y. Zhou, A. Shao, W. Xu, H. Wu, and Y. Deng, "Advance of stem cell treatment for traumatic brain injury," *Frontiers in Cellular Neuroscience*, vol. 13, p. 301, 2019.

[9] P. O. Jenkins, M. A. Mehta, and D. J. Sharp, "Catecholamines and cognition after traumatic brain injury," *Brain*, vol. 139, no. 9, pp. 2345–2371, 2016.

[10] E. Engleder, C. Honeder, J. Klobasa, M. Wirth, C. Arnoldner, and F. Gabor, "Preclinical evaluation of thermoreversible triamcinolone acetonide hydrogels for drug delivery to the inner ear," *International Journal of Pharmaceutics*, vol. 471, no. 1-2, pp. 297–302, 2014.

[11] S. W. Scheff and M. A. Ansari, "Natural compounds as a therapeutic intervention following traumatic brain injury: the role of phytochemicals," *Journal of Neurotrauma*, vol. 34, no. 8, pp. 1491–1510, 2017.

[12] H. Si and D. Liu, "Dietary antiaging phytochemicals and mechanisms associated with prolonged survival," *The Journal of Nutritional Biochemistry*, vol. 25, no. 6, pp. 581–591, 2014.

[13] C. A. Silva-Islas, M. E. Chánez-Cárdenas, D. Barrera-Oviedo, A. Ortiz-Plata, J. Pedraza-Chaverri, and P. D. Maldonado, "Diallyl trisulfide protects rat brain tissue against the damage induced by ischemia-reperfusion through the Nrf2 pathway," *Antioxidants*, vol. 8, no. 9, p. 410, 2019.

[14] L. M. Huynh, M. P. Burns, D. D. Taub, M. R. Blackman, and J. Zhou, "Chronic neurobehavioral impairments and decreased hippocampal expression of genes important for brain glucose utilization in a mouse model of mild TBI," *Frontiers in Endocrinology*, vol. 11, article 556380, 2020.

[15] F. Sivandzade, F. Alqahtani, and L. Cucullo, "Impact of chronic smoking on traumatic brain microvascular injury: an in vitro study," *Journal of Cellular and Molecular Medicine*, vol. 25, no. 15, pp. 7122–7134, 2021.

[16] B. Lee, J. Leem, H. Kim et al., "Herbal medicine for acute management and rehabilitation of traumatic brain injury: a protocol for a systematic review," *Medicine*, vol. 98, no. 3, p. e14145, 2019.

[17] B. Diaz, A. Elkbuli, R. Wobig et al., "Subarachnoid versus nonsubarachnoid traumatic brain injuries: the impact of decision-making on patient safety," *Journal of Emergencies, Trauma, and Shock*, vol. 12, no. 3, pp. 173–175, 2019.

[18] M. L. Werhane, N. D. Evangelista, A. L. Clark et al., "Pathological vascular and inflammatory biomarkers of acute- and chronic-phase traumatic brain injury," *Concussion*, vol. 2, no. 1, p. 0022, 2017.

[19] K. L. Lambertsen, C. B. Soares, D. Gaist, and H. H. Nielsen, "Neurofilaments: the C-reactive protein of neurology," *Brain Sciences*, vol. 10, no. 1, p. 56, 2020.

[20] K. O. Yeates, H. G. Taylor, J. Rusin et al., "Premorbid child and family functioning as predictors of post-concussive symptoms in children with mild traumatic brain injuries," *International Journal of Developmental Neuroscience*, vol. 30, no. 3, pp. 231–237, 2012.

[21] L. Lorente, M. M. Martín, T. Almeida et al., "Total antioxidant capacity is associated with mortality of patients with severe traumatic brain injury," *BMC Neurology*, vol. 15, no. 1, p. 115, 2015.

[22] P. E. Vos, "Biomarkers of focal and diffuse traumatic brain injury," *Critical Care*, vol. 15, no. 4, p. 183, 2011.

[23] N. Khatri, M. Thakur, V. Pareek, S. Kumar, S. Sharma, and A. K. Datusalia, "Oxidative stress: major threat in traumatic brain injury," *CNS & Neurological Disorders Drug Targets*, vol. 17, no. 9, pp. 689–695, 2018.

[24] S. Y. Ng and A. Y. W. Lee, "Traumatic brain injuries: pathophysiology and potential therapeutic targets," *Frontiers in Cellular Neuroscience*, vol. 13, p. 528, 2019.

[25] W. T. O'Brien, L. Pham, G. F. Symons, M. Monif, S. R. Shultz, and S. J. McDonald, "The NLRP3 inflammasome in traumatic brain injury: potential as a biomarker and therapeutic target," *Journal of Neuroinflammation*, vol. 17, no. 1, pp. 1–12, 2020.

[26] E. Suehiro, Y. Fujiyama, M. Kiyohira, Y. Motoki, J. Nojima, and M. Suzuki, "Probability of soluble tissue factor release lead to the elevation of D-dimer as a biomarker for traumatic brain injury," *Neurologia Medico-Chirurgica (Tokyo)*, vol. 59, no. 2, pp. 63–67, 2019.

[27] N. Parizad, K. Hajimohammadi, and R. Goli, "Surgical debridement, maggot therapy, negative pressure wound therapy, and silver foam dressing revive hope for patients with diabetic foot ulcer: a case report," *International Journal of Surgery Case Reports*, vol. 82, p. 105931, 2021.

[28] K. Zibara, N. Ballout, S. Mondello et al., "Combination of drug and stem cells neurotherapy: potential interventions in neurotrauma and traumatic brain injury," *Neuropharmacology*, vol. 145, pp. 177–198, 2019.

[29] A. Mahmood, A. Goussev, D. Lu et al., "Long-lasting benefits after treatment of traumatic brain injury (TBI) in rats with combination therapy of marrow stromal cells (MSCs) and simvastatin," *Journal of Neurotrauma*, vol. 25, no. 12, pp. 1441–1447, 2008.

[30] J. Hu, L. Chen, X. Huang et al., "Calpain inhibitor MDL28170 improves the transplantation-mediated therapeutic effect of bone marrow-derived mesenchymal stem cells following

traumatic brain injury," *Stem Cell Research & Therapy*, vol. 10, no. 1, pp. 1–3, 2019.

[31] K. M. Kanninen, Y. Pomeshchik, H. Leinonen, T. Malm, J. Koistinaho, and A. L. Levonen, "Applications of the Keap1-Nrf2 system for gene and cell therapy," *Free Radical Biology & Medicine*, vol. 88, pp. 350–361, 2015.

[32] S. Tal, A. Hadanny, E. Sasson, G. Suzin, and S. Efrati, "Hyperbaric oxygen therapy can induce angiogenesis and regeneration of nerve fibers in traumatic brain injury patients," *Frontiers in Human Neuroscience*, vol. 11, p. 508, 2017.

[33] I. M. Ayoub, M. Korinek, M. El-Shazly et al., "Anti-allergic, anti-inflammatory, and anti-hyperglycemic activity of Chasmanthe aethiopica leaf extract and its profiling using LC/MS and GLC/MS," *Plants*, vol. 10, no. 6, p. 1118, 2021.

[34] A. J. P. O. de Almeida, M. S. de Almeida Rezende, S. H. Dantas et al., "Unveiling the role of inflammation and oxidative stress on age-related cardiovascular diseases," *Oxidative Medicine and Cellular Longevity*, vol. 2020, Article ID 1954398, 20 pages, 2020.

[35] H. Suzuki, J. Matsuzaki, and T. Hibi, "Ghrelin and oxidative stress in gastrointestinal tract," *Journal of Clinical Biochemistry and Nutrition*, vol. 48, no. 2, pp. 122–125, 2011.

[36] B. Loessner, S. Bullock, and S. P. Rose, "411B: a monoclonal postsynaptic marker for modulations of synaptic connectivity in the rat brain," *Journal of Neurochemistry*, vol. 51, no. 2, pp. 385–390, 1988.

[37] G. Li, S. Xiang, Y. Pan et al., "Effects of cold-pressing and hydrodistillation on the active non-volatile components in lemon essential oil and the effects of the resulting oils on aging-related oxidative stress in mice," *Frontiers in Nutrition*, vol. 8, p. 689094, 2021.

[38] B. A. Philippe, N. Karine, A. K. Barthélemy et al., "Bio-guided isolation of antioxidant compounds from Chrysophyllum perpulchrum, a plant used in the Ivory Coast pharmacopeia," *Molecules*, vol. 15, no. 9, pp. 6386–6398, 2010.

[39] B. Mukhopadhyay, A. N. Gongopadhyay, A. Rani, R. Gavel, and S. P. Mishra, "Free radicals and antioxidants status in neonates with congenital malformation," *Journal of Indian Association of Pediatric Surgeons*, vol. 20, no. 4, pp. 179–183, 2015.

[40] S. Nishikawa, Y. Inoue, Y. Hori et al., "Anti-inflammatory activity of kurarinone involves induction of HO-1 via the KEAP1/Nrf2 pathway," *Antioxidants*, vol. 9, no. 9, p. 842, 2020.

[41] Y. H. Gu, T. Yamashita, H. Yamamoto et al., "Plant enzymes decrease prostate cancer cell numbers and increase TNF-alpha in vivo: a possible role in immunostimulatory activity," *International Journal of Food Science*, vol. 2019, Article ID 8103480, 7 pages, 2019.

[42] M. Wessels, G. Leyhausen, J. Volk, and W. Geurtsen, "Oxidative stress is responsible for genotoxicity of camphorquinone in primary human gingival fibroblasts," *Clinical Oral Investigations*, vol. 18, no. 6, pp. 1705–1710, 2014.

[43] A. S. Glotov, E. S. Tiys, E. S. Vashukova et al., "Molecular association of pathogenetic contributors to pre-eclampsia (pre-eclampsia associome)," *BMC Systems Biology*, vol. 9, no. 2, pp. 1–12, 2015.

[44] Y. Tao, Y. Wang, Z. Ma et al., "Subretinal delivery of erythropoietin alleviates the N-methyl-N-nitrosourea-induced photoreceptor degeneration and visual functional impairments: an in vivo and ex vivo study," *Drug Delivery*, vol. 24, no. 1, pp. 1273–1283, 2017.

[45] L. Cannizzaro, G. Rossoni, F. Savi et al., "Regulatory landscape of AGE-RAGE-oxidative stress axis and its modulation by PPARγ activation in high fructose diet-induced metabolic syndrome," *Nutrition & Metabolism (London)*, vol. 14, no. 1, pp. 1–13, 2017.

[46] H. M. Zhang, W. Chen, R. N. Liu, and Y. Zhao, "Notch inhibitor can attenuate apparent diffusion coefficient and improve neurological function through downregulating NOX2-ROS in severe traumatic brain injury," *Drug Design, Development and Therapy*, vol. 12, pp. 3847–3854, 2018.

[47] P. Chen, M. Totten, Z. Zhang et al., "Iron and manganese-related CNS toxicity: mechanisms, diagnosis and treatment," *Expert Review of Neurotherapeutics*, vol. 19, no. 3, pp. 243–260, 2019.

[48] H. A. Kontos and J. T. Povlishock, "Oxygen radicals in brain injury," *Central Nervous System Trauma*, vol. 3, no. 4, pp. 257–263, 1986.

[49] C. Angeloni, C. Prata, F. Vieceli Dalla Sega, R. Piperno, and S. Hrelia, "Traumatic brain injury and NADPH oxidase: a deep relationship," *Oxidative Medicine and Cellular Longevity*, vol. 2015, Article ID 370312, 10 pages, 2015.

[50] A. Jarrahi, M. Braun, M. Ahluwalia et al., "Revisiting traumatic brain injury: from molecular mechanisms to therapeutic interventions," *Biomedicine*, vol. 8, no. 10, p. 389, 2020.

[51] M. Abbasi-Kangevari, S. H. Ghamari, F. Safaeinejad, S. Bahrami, and H. Niknejad, "Potential therapeutic features of human amniotic mesenchymal stem cells in multiple sclerosis: immunomodulation, inflammation suppression, angiogenesis promotion, oxidative stress inhibition, neurogenesis induction, MMPs regulation, and remyelination stimulation," *Frontiers in Immunology*, vol. 10, p. 238, 2019.

[52] S. Tang, P. Gao, H. Chen, X. Zhou, Y. Ou, and Y. He, "The role of iron, its metabolism and ferroptosis in traumatic brain injury," *Frontiers in Cellular Neuroscience*, vol. 14, p. 590789, 2020.

[53] G. Marchi, F. Busti, A. Lira Zidanes, A. Castagna, and D. Girelli, "Aceruloplasminemia: a severe neurodegenerative disorder deserving an early diagnosis," *Frontiers in Neuroscience*, vol. 13, p. 325, 2019.

[54] G. Cossu, M. Messerer, M. Oddo, and R. T. Daniel, "To look beyond vasospasm in aneurysmal subarachnoid haemorrhage," *BioMed Research International*, vol. 2014, Article ID 628597, 14 pages, 2014.

[55] E. D. Hall, R. A. Vaishnav, and A. G. Mustafa, "Antioxidant therapies for traumatic brain injury," *Neurotherapeutics*, vol. 7, no. 1, pp. 51–61, 2010.

[56] L. Zhang, R. Hu, M. Li et al., "Deferoxamine attenuates iron-induced long-term neurotoxicity in rats with traumatic brain injury," *Neurological Sciences*, vol. 34, no. 5, pp. 639–645, 2013.

[57] D. Y. Lee, M. Y. Song, and E. H. Kim, "Role of oxidative stress and Nrf2/KEAP1 signaling in colorectal cancer: mechanisms and therapeutic perspectives with phytochemicals," *Antioxidants*, vol. 10, no. 5, p. 743, 2021.

[58] D. Li, H. Zhao, Z. K. Cui, and G. Tian, "The role of Nrf2 in hearing loss," *Frontiers in Pharmacology*, vol. 12, p. 620921, 2021.

[59] D. D. Zhu, X. M. Tan, L. Q. Lu et al., "Interplay between nuclear factor erythroid 2-related factor 2 and inflammatory

mediators in COVID-19-related liver injury," *World Journal of Gastroenterology*, vol. 27, no. 22, pp. 2944–2962, 2021.

[60] K. Smolková, E. Mikó, T. Kovács, A. Leguina-Ruzzi, A. Sipos, and P. Bai, "Nuclear factor erythroid 2-related factor 2 in regulating cancer metabolism," *Antioxidants & Redox Signaling*, vol. 33, no. 13, pp. 966–997, 2020.

[61] E. Zgorzynska, B. Dziedzic, and A. Walczewska, "An overview of the Nrf2/ARE pathway and its role in neurodegenerative diseases," *International Journal of Molecular Sciences*, vol. 22, no. 17, p. 9592, 2021.

[62] S. Ning, T. V. Sekar, J. Scicinski et al., "Nrf2 activity as a potential biomarker for the pan-epigenetic anticancer agent, RRx-001," *Oncotarget*, vol. 6, no. 25, pp. 21547–21556, 2015.

[63] J. J. Qin, X. D. Cheng, J. Zhang, and W. D. Zhang, "Dual roles and therapeutic potential of Keap1-Nrf2 pathway in pancreatic cancer: a systematic review," *Cell Communication and Signaling: CCS*, vol. 17, no. 1, pp. 1–15, 2019.

[64] C. H. Yen, C. M. Hsu, S. Y. Hsiao, and H. H. Hsiao, "Pathogenic mechanisms of myeloma bone disease and possible roles for NRF2," *International Journal of Molecular Sciences*, vol. 21, no. 18, p. 6723, 2020.

[65] D. Moretti, S. Tambone, M. Cerretani et al., "NRF2 activation by reversible KEAP1 binding induces the antioxidant response in primary neurons and astrocytes of a Huntington's disease mouse model," *Free Radical Biology & Medicine*, vol. 162, pp. 243–254, 2021.

[66] Y. Yagishita, T. N. Gatbonton-Schwager, M. L. McCallum, and T. W. Kensler, "Current landscape of NRF2 biomarkers in clinical trials," *Antioxidants*, vol. 9, no. 8, p. 716, 2020.

[67] D. P. Schafer, S. Jha, F. Liu, T. Akella, L. D. McCullough, and M. N. Rasband, "Disruption of the axon initial segment cytoskeleton is a new mechanism for neuronal injury," *The Journal of Neuroscience*, vol. 29, no. 42, pp. 13242–13254, 2009.

[68] F. Sivandzade, S. Prasad, A. Bhalerao, and L. Cucullo, "NRF2 and NF-κB interplay in cerebrovascular and neurodegenerative disorders: molecular mechanisms and possible therapeutic approaches," *Redox Biology*, vol. 21, p. 101059, 2019.

[69] R. Chandran, T. H. Kim, S. L. Mehta et al., "A combination antioxidant therapy to inhibit NOX2 and activate Nrf2 decreases secondary brain damage and improves functional recovery after traumatic brain injury," *Journal of Cerebral Blood Flow and Metabolism*, vol. 38, no. 10, pp. 1818–1827, 2018.

[70] K. F. Bell, B. al-Mubarak, M. A. Martel et al., "Neuronal development is promoted by weakened intrinsic antioxidant defences due to epigenetic repression of Nrf2," *Nature Communications*, vol. 6, no. 1, pp. 1–15, 2015.

[71] M. Ismail, A. Alsalahi, M. U. Imam et al., "Safety and neuroprotective efficacy of palm oil and tocotrienol-rich fraction from palm oil: a systematic review," *Nutrients*, vol. 12, no. 2, p. 521, 2020.

[72] X. Li, H. Wang, G. Wen et al., "Neuroprotection by quercetin via mitochondrial function adaptation in traumatic brain injury: PGC-1α pathway as a potential mechanism," *Journal of Cellular and Molecular Medicine*, vol. 22, no. 2, pp. 883–891, 2018.

[73] T. Yang, B. Kong, J. W. Gu et al., "Anti-apoptotic and anti-oxidative roles of quercetin after traumatic brain injury," *Cellular and Molecular Neurobiology*, vol. 34, no. 6, pp. 797–804, 2014.

[74] J. Song, G. du, H. Wu et al., "Protective effects of quercetin on traumatic brain injury induced inflammation and oxidative stress in cortex through activating Nrf2/HO-1 pathway," *Restorative Neurology and Neuroscience*, vol. 39, no. 1, pp. 73–84, 2021.

[75] H. H. Kom et al., "Protective effect of quercetin on weight drop injury model-induced neuroinflammation alterations in brain of mice," *Journal of Applied Pharmaceutical Science*, vol. 9, no. 4, pp. 96–103, 2019.

[76] X. Li, H. Wang, Y. Gao et al., "Protective effects of quercetin on mitochondrial biogenesis in experimental traumatic brain injury via the Nrf2 signaling pathway," *PLoS One*, vol. 11, no. 10, p. e0164237, 2016.

[77] I. V. Yavtushenko, S. M. Nazarenko, O. V. Katrushov, and V. O. Kostenko, "Quercetin limits the progression of oxidative and nitrosative stress in the rats' tissues after experimental traumatic brain injury," *Wiadomości Lekarskie*, vol. 73, no. 10, pp. 2127–2132, 2020.

[78] W. Dai, H. Wang, J. Fang et al., "Curcumin provides neuroprotection in model of traumatic brain injury via the Nrf2-ARE signaling pathway," *Brain Research Bulletin*, vol. 140, pp. 65–71, 2018.

[79] G. Sun, Z. Miao, Y. Ye et al., "Curcumin alleviates neuroinflammation, enhances hippocampal neurogenesis, and improves spatial memory after traumatic brain injury," *Brain Research Bulletin*, vol. 162, pp. 84–93, 2020.

[80] W. Dong, B. Yang, L. Wang et al., "Curcumin plays neuroprotective roles against traumatic brain injury partly via Nrf2 signaling," *Toxicology and Applied Pharmacology*, vol. 346, pp. 28–36, 2018.

[81] A. Wu, Z. Ying, and F. Gomez-Pinilla, "Dietary curcumin counteracts the outcome of traumatic brain injury on oxidative stress, synaptic plasticity, and cognition," *Experimental Neurology*, vol. 197, no. 2, pp. 309–317, 2006.

[82] T. Farkhondeh, S. Samarghandian, B. Roshanravan, and L. Peivasteh-roudsari, "Impact of curcumin on traumatic brain injury and involved molecular signaling pathways," *Recent Patents on Food, Nutrition & Agriculture*, vol. 11, no. 2, pp. 137–144, 2020.

[83] F. Samini, S. Samarghandian, A. Borji, G. Mohammadi, and M. bakaian, "Curcumin pretreatment attenuates brain lesion size and improves neurological function following traumatic brain injury in the rat," *Pharmacology, Biochemistry, and Behavior*, vol. 110, pp. 238–244, 2013.

[84] L. Liang, H. Wei, Y. Sun, and J. Tian, "Anti-oxidative stress effects of curcumin on rat models of traumatic brain injury," *Chinese Journal of Comparative Medicine*, vol. 28, no. 4, pp. 73–80, 2018.

[85] Y. Shu, T. Wang, X. Tang, and C. Pan, "The effect of curcumin on endogenous neuron regeneration in rats after TBI," *Revista Argentina de Clínica Psicológica*, vol. 29, no. 4, p. 864, 2020.

[86] H. T. Zhu, C. Bian, J. C. Yuan et al., "Curcumin attenuates acute inflammatory injury by inhibiting the TLR4/MyD88/NF-κB signaling pathway in experimental traumatic brain injury," *Journal of Neuroinflammation*, vol. 11, no. 1, p. 59, 2014.

[87] M. D. Laird, S. Sukumari-Ramesh, A. E. B. Swift, S. E. Meiler, J. R. Vender, and K. M. Dhandapani, "Curcumin attenuates cerebral edema following traumatic brain injury in mice: a possible role for aquaporin-4?," *Journal of Neurochemistry*, vol. 113, no. 3, pp. 637–648, 2010.

[88] T. Huang, J. Zhao, D. Guo, H. Pang, Y. Zhao, and J. Song, "Curcumin mitigates axonal injury and neuronal cell apoptosis through the PERK/Nrf2 signaling pathway following diffuse axonal injury," *Neuroreport*, vol. 29, no. 8, pp. 661–677, 2018.

[89] S. Baraka, "Effect of combination treatment of candesartan and curcumin on traumatic brain injury in mice," *Al-Azhar Journal of Pharmaceutical Sciences*, vol. 54, no. 1, pp. 70–85, 2016.

[90] G. Wei, B. Chen, Q. Lin et al., "Tetrahydrocurcumin provides neuroprotection in experimental traumatic brain injury and the Nrf2 signaling pathway as a potential mechanism," *Neuroimmunomodulation*, vol. 24, no. 6, pp. 348–355, 2018.

[91] Z. Li, Y. Wang, G. Zeng et al., "Increased miR-155 and heme oxygenase-1 expression is involved in the protective effects of formononetin in traumatic brain injury in rats," *American Journal of Translational Research*, vol. 9, no. 12, pp. 5653–5661, 2017.

[92] S. K. L. Ong, M. Shanmugam, L. Fan et al., "Focus on Formononetin: Anticancer Potential and Molecular Targets," *Cancers*, vol. 11, no. 5, p. 611, 2019.

[93] H. Xiao, X. Qin, J. Wan, and R. Li, "Pharmacological targets and the biological mechanisms of formononetin for Alzheimer's disease: a network analysis," *Medical Science Monitor*, vol. 25, pp. 4273–4277, 2019.

[94] A. C. P. de Vasconcelos, R. P. Morais, G. B. Novais et al., "_In situ_ photocrosslinkable formulation of nanocomposites based on multi- walled carbon nanotubes and formononetin for potential application in spinal cord injury treatment," *Nanomedicine*, vol. 29, p. 102272, 2020.

[95] Z. Li, X. Dong, J. Zhang et al., "Formononetin protects TBI rats against neurological lesions and the underlying mechanism," *Journal of the Neurological Sciences*, vol. 338, no. 1-2, pp. 112–117, 2014.

[96] J. Fang, H. Wang, J. Zhou et al., "Baicalin provides neuroprotection in traumatic brain injury mice model through Akt/Nrf2 pathway," *Drug Design, Development and Therapy*, vol. 12, pp. 2497–2508, 2018.

[97] J. Fang, Y. Zhu, H. Wang et al., "Baicalin protects mice brain from apoptosis in traumatic brain injury model through activation of autophagy," *Frontiers in Neuroscience*, vol. 12, p. 1006, 2019.

[98] X. Shi, Y. Fu, S. Zhang, H. Ding, and J. Chen, "Baicalin attenuates subarachnoid hemorrhagic brain injury by modulating blood-brain barrier disruption, inflammation, and oxidative damage in mice," *Oxidative Medicine and Cellular Longevity*, vol. 2017, Article ID 1401790, 2017.

[99] J. Bernatoniene and D. M. Kopustinskiene, "The role of catechins in cellular responses to oxidative stress," *Molecules*, vol. 23, no. 4, p. 965, 2018.

[100] E. Tsouko, M. Alexandri, K. V. Fernandes, D. M. Guimarães Freire, A. Mallouchos, and A. A. Koutinas, "Extraction of phenolic compounds from palm oil processing residues and their application as antioxidants," *Food Technology and Biotechnology*, vol. 57, no. 1, pp. 29–38, 2019.

[101] V. L. Truong and W. S. Jeong, "Cellular defensive mechanisms of tea polyphenols: structure-activity relationship," *International Journal of Molecular Sciences*, vol. 22, no. 17, p. 9109, 2021.

[102] T. Cheng, W. Wang, Q. Li et al., "Cerebroprotection of flavanol (-)-epicatechin after traumatic brain injury via Nrf2-dependent and -independent pathways," *Free Radical Biology & Medicine*, vol. 92, pp. 15–28, 2016.

[103] Z. Jiang, J. Zhang, Y. Cai, J. Huang, and L. You, "Catechin attenuates traumatic brain injury-induced blood-brain barrier damage and improves longer-term neurological outcomes in rats," *Experimental Physiology*, vol. 102, no. 10, pp. 1269–1277, 2017.

[104] R. Ratnawati, A. N. Arofah, A. Novitasari et al., "Catechins decrease neurological severity score through apoptosis and neurotropic factor pathway in rat traumatic brain injury," *Universa Medicina*, vol. 36, no. 2, pp. 110–122, 2017.

[105] D. Kashyap, V. K. Garg, H. S. Tuli et al., "Fisetin and quercetin: promising flavonoids with chemopreventive potential," *Biomolecules*, vol. 9, no. 5, p. 174, 2019.

[106] A. R. Ravula, S. B. Teegala, S. Kalakotla, J. P. Pasangulapati, V. Perumal, and H. K. Boyina, "Fisetin, potential flavonoid with multifarious targets for treating neurological disorders: an updated review," *European Journal of Pharmacology*, vol. 910, p. 174492, 2021.

[107] S. C. Kim, Y. H. Kim, S. W. Son, E. Y. Moon, S. Pyo, and S. H. Um, "Fisetin induces Sirt1 expression while inhibiting early adipogenesis in 3T3-L1 cells," *Biochemical and Biophysical Research Communications*, vol. 467, no. 4, pp. 638–644, 2015.

[108] S. Kakutani, H. Watanabe, and N. Murayama, "Green tea intake and risks for dementia, Alzheimer's disease, mild cognitive impairment, and cognitive impairment: a systematic review," *Nutrients*, vol. 11, no. 5, p. 1165, 2019.

[109] L. Zhang, H. Wang, Y. Zhou, Y. Zhu, and M. Fei, "Fisetin alleviates oxidative stress after traumatic brain injury via the Nrf2-ARE pathway," *Neurochemistry International*, vol. 118, pp. 304–313, 2018.

[110] C. Zhou, S. Nie, Z. Wang et al., *Fisetin has inhibitory effects on the TLR 4/NF-κB-mediated inflammatory pathway after traumatic brain injury in mice: A Potential Neuroprotective Role*, Research Square, 2021.

[111] H. J. Shin, K. A. Hwang, and K. C. Choi, "Antitumor effect of various phytochemicals on diverse types of thyroid cancers," *Nutrients*, vol. 11, no. 1, p. 125, 2019.

[112] F. Gendrisch, P. R. Esser, C. M. Schempp, and U. Wölfle, "Luteolin as a modulator of skin aging and inflammation," *BioFactors*, vol. 47, no. 2, pp. 170–180, 2021.

[113] Y. C. Cho, J. Park, and S. Cho, "Anti-inflammatory and anti-oxidative effects of luteolin-7-O-glucuronide in LPS-stimulated murine macrophages through TAK1 inhibition and Nrf2 activation," *International Journal of Molecular Sciences*, vol. 21, no. 6, p. 2007, 2020.

[114] S. F. Nabavi, N. Braidy, O. Gortzi et al., "Luteolin as an anti-inflammatory and neuroprotective agent: a brief review," *Brain Research Bulletin*, vol. 119, pp. 1–11, 2015.

[115] D. Kempuraj, R. Thangavel, D. D. Kempuraj et al., "Neuroprotective effects of flavone luteolin in neuroinflammation and neurotrauma," *BioFactors*, vol. 47, no. 2, pp. 190–197, 2021.

[116] J. Xu, H. Wang, K. Ding et al., "Luteolin provides neuroprotection in models of traumatic brain injury via the Nrf2-ARE pathway," *Free Radical Biology & Medicine*, vol. 71, pp. 186–195, 2014.

[117] Z. Ashaari, G. Hassanzadeh, T. Mokhtari et al., "Luteolin reduced the traumatic brain injury-induced memory impairments in rats: attenuating oxidative stress and dark neurons

of hippocampus," *Acta Medica Iranica*, vol. 56, no. 9, p. 570, 2018.

[118] R. Crupi, D. Impellizzeri, G. Bruschetta et al., "Co-ultramicronized palmitoylethanolamide/luteolin promotes neuronal regeneration after spinal cord injury," *Frontiers in Pharmacology*, vol. 7, p. 47, 2016.

[119] B. Li, B. Liu, J. Li, H. Xiao, J. Wang, and G. Liang, "Experimental and theoretical investigations on the supermolecular structure of isoliquiritigenin and 6-O-α-D-maltosyl-β-cyclodextrin inclusion complex," *International Journal of Molecular Sciences*, vol. 16, no. 8, pp. 17999–18017, 2015.

[120] X. Tan, Y. Yang, J. Xu et al., "Luteolin exerts neuroprotection via modulation of the p62/Keap1/Nrf2 pathway in intracerebral hemorrhage," *Frontiers in Pharmacology*, vol. 10, p. 1551, 2019.

[121] M. Zhang, L. L. Huang, C. H. Teng et al., "Isoliquiritigenin provides protection and attenuates oxidative stress-induced injuries via the Nrf2-ARE signaling pathway after traumatic brain injury," *Neurochemical Research*, vol. 43, no. 12, pp. 2435–2445, 2018.

[122] J. Liu, X. Xiong, and Y. Sui, "Isoliquiritigenin attenuates neuroinflammation in traumatic brain injury in young rats," *Neuroimmunomodulation*, vol. 26, no. 2, pp. 102–110, 2019.

[123] M. Zhang, Y. Wu, L. Xie et al., "Isoliquiritigenin protects against blood-brain barrier damage and inhibits the secretion of pro-inflammatory cytokines in mice after traumatic brain injury," *International Immunopharmacology*, vol. 65, pp. 64–75, 2018.

[124] K. Ganesan and B. Xu, "Telomerase inhibitors from natural products and their anticancer potential," *International Journal of Molecular Sciences*, vol. 19, no. 1, p. 13, 2018.

[125] W. Shi, Y. Kong, Y. Su et al., "Tannic acid-inspired, self-healing, and dual stimuli responsive dynamic hydrogel with potent antibacterial and anti-oxidative properties," *Journal of Materials Chemistry B*, vol. 9, no. 35, pp. 7182–7195, 2021.

[126] P. O. Perumal, P. Mhlanga, A. M. Somboro, D. G. Amoako, H. M. Khumalo, and R. M. Khan, "Cytoproliferative and anti-oxidant effects induced by tannic acid in human embryonic kidney (Hek-293) cells," *Biomolecules*, vol. 9, no. 12, p. 767, 2019.

[127] N. Braidy, B. E. Jugder, A. Poljak et al., "Molecular targets of tannic acid in Alzheimer's disease," *Current Alzheimer Research*, vol. 14, no. 8, pp. 861–869, 2017.

[128] M. Salman, H. Tabassum, and S. Parvez, "Tannic acid provides neuroprotective effects against traumatic brain injury through the PGC-1α/Nrf2/HO-1 pathway," *Molecular Neurobiology*, vol. 57, no. 6, pp. 2870–2885, 2020.

[129] K. Latoszkiewicz and J. Krasnodebski, "Necrosis of a postoperative uterine wound after cesarean section," *Przegląd Lekarski*, vol. 45, pp. 656–658, 1988.

[130] T. Nikawa, A. Ulla, and I. Sakakibara, "Polyphenols and their effects on muscle atrophy and muscle health," *Molecules*, vol. 26, no. 16, p. 4887, 2021.

[131] M. Goudarzi, S. Amiri, A. Nesari, A. Hosseinzadeh, E. Mansouri, and S. Mehrzadi, "The possible neuroprotective effect of ellagic acid on sodium arsenate-induced neurotoxicity in rats," *Life Sciences*, vol. 198, pp. 38–45, 2018.

[132] N. Li, K. Chen, J. Bai et al., "Tibetan medicine Duoxuekang ameliorates hypobaric hypoxia-induced brain injury in mice by restoration of cerebrovascular function," *Journal of Ethnopharmacology*, vol. 270, p. 113629, 2021.

[133] A. Aslan, O. Gok, S. Beyaz, E. Arslan, O. Erman, and C. A. Ağca, "The preventive effect of ellagic acid on brain damage in rats via regulating of Nrf-2, NF-kB and apoptotic pathway," *Journal of Food Biochemistry*, vol. 44, no. 6, p. e13217, 2020.

[134] S. Mashhadizadeh, Y. Farbood, M. Dianat, A. Khodadadi, and A. Sarkaki, "Therapeutic effects of ellagic acid on memory, hippocampus electrophysiology deficits, and elevated TNF-α level in brain due to experimental traumatic brain injury," *Iranian Journal of Basic Medical Sciences*, vol. 20, no. 4, pp. 399–407, 2017.

[135] Y. Farbood, A. Sarkaki, M. Dianat, A. Khodadadi, M. K. Haddad, and S. Mashhadizadeh, "Ellagic acid prevents cognitive and hippocampal long-term potentiation deficits and brain inflammation in rat with traumatic brain injury," *Life Sciences*, vol. 124, pp. 120–127, 2015.

[136] Z. Li, X. B. Zhang, J. H. Gu, Y. Q. Zeng, and J. T. Li, "Breviscapine exerts neuroprotective effects through multiple mechanisms in APP/PS1 transgenic mice," *Molecular and Cellular Biochemistry*, vol. 468, no. 1-2, pp. 1–11, 2020.

[137] J. Gao, G. Chen, H. He et al., "Therapeutic effects of breviscapine in cardiovascular diseases: a review," *Frontiers in Pharmacology*, vol. 8, p. 289, 2017.

[138] F. Li, X. Wang, Z. Zhang, P. Gao, and X. Zhang, "Breviscapine provides a neuroprotective effect after traumatic brain injury by modulating the Nrf2 signaling pathway," *Journal of Cellular Biochemistry*, vol. 120, no. 9, pp. 14899–14907, 2019.

[139] L. Jiang, Q. J. Xia, X. J. Dong et al., "Neuroprotective effect of breviscapine on traumatic brain injury in rats associated with the inhibition of GSK3β signaling pathway," *Brain Research*, vol. 1660, pp. 1–9, 2017.

[140] L. Jiang, Y. Hu, X. He, Q. Lv, T. H. Wang, and Q. J. XiaBreviscapine reduces neuronal injury caused by traumatic brain injury insult: partly associated with suppression of interleukin-6 expression," *Neural Regeneration Research*, vol. 12, no. 1, pp. 90–95, 2017.

[141] J. Lv, A. Sharma, T. Zhang, Y. Wu, and X. Ding, "Pharmacological review on asiatic acid and its derivatives: a potential compound," *SLAS TECHNOLOGY*, vol. 23, no. 2, pp. 111–127, 2018.

[142] N. N. M. Razali, C. T. Ng, and L. Y. Fong, "Cardiovascular protective effects of Centella asiatica and its triterpenes: a review," *Planta Medica*, vol. 85, no. 16, pp. 1203–1215, 2019.

[143] Z. Qi, X. Ci, J. Huang et al., "Asiatic acid enhances Nrf2 signaling to protect HepG2 cells from oxidative damage through Akt and ERK activation," *Biomedicine & Pharmacotherapy*, vol. 88, pp. 252–259, 2017.

[144] F. Han, N. Yan, J. Huo, X. Chen, Z. Fei, and X. Li, "Asiatic acid attenuates traumatic brain injury via upregulating Nrf2 and HO-1 expression," *International Journal of Clinical and Experimental Medicine*, vol. 11, no. 1, pp. 360–366, 2018.

[145] X. Zeng, F. Guo, and D. Ouyang, "A review of the pharmacology and toxicology of aucubin," *Fitoterapia*, vol. 140, p. 104443, 2020.

[146] Y. Xiao, W. Chang, Q. Q. Wu et al., "Aucubin protects against TGFβ1-Induced cardiac fibroblasts activation by mediating the AMPKα/mTOR signaling pathway," *Planta Medica*, vol. 84, no. 2, pp. 91–99, 2018.

[147] B. Shen, C. Zhao, Y. Wang et al., "Aucubin inhibited lipid accumulation and oxidative stress via Nrf2/HO-1 and AMPK

signalling pathways," *Journal of Cellular and Molecular Medicine*, vol. 23, no. 6, pp. 4063–4075, 2019.

[148] Y. C. Li, J. . Hao, B. Shang et al., "Neuroprotective effects of aucubin on hydrogen peroxide-induced toxicity in human neuroblastoma SH-SY5Y cells via the Nrf2/HO-1 pathway," *Phytomedicine*, vol. 87, p. 153577, 2021.

[149] Y. L. Qiu, X. N. Cheng, F. Bai, L. Y. Fang, H. Z. Hu, and D. Q. Sun, "Aucubin protects against lipopolysaccharide-induced acute pulmonary injury through regulating Nrf2 and AMPK pathways," *Biomedicine & Pharmacotherapy*, vol. 106, pp. 192–199, 2018.

[150] H. Wang, X. M. Zhou, L. Y. Wu et al., "Aucubin alleviates oxidative stress and inflammation via Nrf2-mediated signaling activity in experimental traumatic brain injury," *Journal of Neuroinflammation*, vol. 17, no. 1, p. 188, 2020.

[151] J. Xu, F. Chen, G. Wang, B. Liu, H. Song, and T. Ma, "The versatile functions of G. Lucidum polysaccharides and G. Lucidum triterpenes in cancer radiotherapy and chemotherapy," *Cancer Management and Research*, vol. Volume 13, pp. 6507–6516, 2021.

[152] N. H. Nguyen, Q. T. H. Ta, Q. T. Pham et al., "Anticancer activity of novel plant extracts and compounds from Adenosma bracteosum (Bonati) in human lung and liver cancer cells," *Molecules*, vol. 25, no. 12, p. 2912, 2020.

[153] H. Ding, H. Wang, L. Zhu, and W. Wei, "Ursolic acid ameliorates early brain injury after experimental traumatic brain injury in mice by activating the Nrf2 pathway," *Neurochemical Research*, vol. 42, no. 2, pp. 337–346, 2017.

[154] A. Argüelles, R. Sánchez-Fresneda, J. P. Guirao-Abad et al., "Novel bi-factorial strategy against Candida albicans viability using carnosic acid and propolis: synergistic antifungal action," *Synergistic Antifungal Action. Microorganisms*, vol. 8, no. 5, p. 749, 2020.

[155] M. H. Grace, Y. Qiang, S. Sang, and M. A. Lila, "One-step isolation of carnosic acid and carnosol from rosemary by centrifugal partition chromatography," *Journal of Separation Science*, vol. 40, no. 5, pp. 1057–1062, 2017.

[156] T. Rezaie, S. R. McKercher, K. Kosaka et al., "Protective effect of carnosic acid, a pro-electrophilic compound, in models of oxidative stress and light-induced retinal degeneration," *Investigative Ophthalmology & Visual Science*, vol. 53, no. 12, pp. 7847–7854, 2012.

[157] D. M. Miller, I. N. Singh, J. A. Wang, and E. D. Hall, "Nrf2-ARE activator carnosic acid decreases mitochondrial dysfunction, oxidative damage and neuronal cytoskeletal degradation following traumatic brain injury in mice," *Experimental Neurology*, vol. 264, pp. 103–110, 2015.

[158] D. M. Miller, I. N. Singh, J. A. Wang, and E. D. Hall, "Administration of the Nrf2-ARE activators sulforaphane and carnosic acid attenuates 4-hydroxy-2-nonenal-induced mitochondrial dysfunction ex vivo," *Free Radical Biology & Medicine*, vol. 57, pp. 1–9, 2013.

[159] M. E. Maynard, E. L. Underwood, J. B. Redell et al., "Carnosic acid improves outcome after repetitive mild traumatic brain injury," *Journal of Neurotrauma*, vol. 36, no. 13, pp. 2147–2152, 2019.

[160] M. Liu, W. Li, Y. Chen, X. Wan, and J. Wang, "Fucoxanthin: a promising compound for human inflammation-related diseases," *Life Sciences*, vol. 255, p. 117850, 2020.

[161] S. Méresse, M. Fodil, F. Fleury, and B. Chénais, "Fucoxanthin, a marine-derived carotenoid from Brown seaweeds and microalgae: a promising bioactive compound for cancer therapy," *International Journal of Molecular Sciences*, vol. 21, no. 23, p. 9273, 2020.

[162] D. Zhao, S. H. Kwon, Y. S. Chun, M. Y. Gu, and H. O. Yang, "Anti-neuroinflammatory effects of fucoxanthin via inhibition of Akt/NF-κB and MAPKs/AP-1 pathways and activation of PKA/CREB pathway in lipopolysaccharide-activated BV-2 microglial cells," *Neurochemical Research*, vol. 42, no. 2, pp. 667–677, 2017.

[163] A. H. Lee, H. Y. Shin, J. H. Park, S. Y. Koo, S. M. Kim, and S. H. Yang, "Fucoxanthin from microalgae _Phaeodactylum tricornutum_ inhibits pro- inflammatory cytokines by regulating both NF- κB and NLRP3 inflammasome activation," *Scientific Reports*, vol. 11, no. 1, pp. 1–12, 2021.

[164] C. L. Liu, Y. T. Chiu, and M. L. Hu, "Fucoxanthin enhances HO-1 and NQO1 expression in murine hepatic BNL CL.2 cells through activation of the Nrf2/ARE system partially by its pro-oxidant activity," *Journal of Agricultural and Food Chemistry*, vol. 59, no. 20, pp. 11344–11351, 2011.

[165] L. Zhang, H. Wang, Y. Fan et al., "Fucoxanthin provides neuroprotection in models of traumatic brain injury via the Nrf2-ARE and Nrf2-autophagy pathways," *Scientific Reports*, vol. 7, no. 1, p. 46763, 2017.

[166] T. Bohn, C. Desmarchelier, S. N. el et al., "β-Carotene in the human body: metabolic bioactivation pathways - from digestion to tissue distribution and excretion," *The Proceedings of the Nutrition Society*, vol. 78, no. 1, pp. 68–87, 2019.

[167] A. Bast, R. M. Van der Plas, H. Van Den Berg, and G. R. Haenen, "Beta-carotene as antioxidant," *European Journal of Clinical Nutrition*, vol. 50, pp. S54–S56, 1996.

[168] G. N. Bosio, T. Breitenbach, J. Parisi et al., "Antioxidant β-Carotene does not quench singlet oxygen in mammalian cells," *Journal of the American Chemical Society*, vol. 135, no. 1, pp. 272–279, 2013.

[169] P. Chen, L. Li, Y. Gao et al., "β-carotene provides neuro protection after experimental traumatic brain injury via the Nrf2-ARE pathway," *Journal of Integrative Neuroscience*, vol. 18, no. 2, pp. 153–161, 2019.

[170] B. Nan, X. Gu, and X. Huang, "The role of the reactive oxygen species scavenger agent, Astaxanthin, in the protection of cisplatin-treated patients against hearing loss," *Drug Design, Development and Therapy*, vol. 13, pp. 4291–4303, 2019.

[171] C. D. Fan, J. Y. Sun, X. T. Fu et al., "Astaxanthin attenuates homocysteine-induced cardiotoxicity in vitro and in vivo by inhibiting mitochondrial dysfunction and oxidative damage," *Frontiers in Physiology*, vol. 8, p. 1041, 2017.

[172] F. Gao, X. Wu, X. Mao et al., "Astaxanthin provides neuroprotection in an experimental model of traumatic brain injury via the Nrf2/HO-1 pathway," *American Journal of Translational Research*, vol. 13, no. 3, pp. 1483–1493, 2021.

[173] X. S. Zhang, Y. Lu, W. Li et al., "Astaxanthin ameliorates oxidative stress and neuronal apoptosis via SIRT1/NRF2/Prx2/ASK1/p38 after traumatic brain injury in mice," *British Journal of Pharmacology*, vol. 178, no. 5, pp. 1114–1132, 2021.

[174] B. Ouyang, Z. Li, X. Ji, J. Huang, H. Zhang, and C. Jiang, "The protective role of lutein on isoproterenol-induced cardiac failure rat model through improving cardiac morphology, antioxidant status via positively regulating Nrf2/HO-1 signalling pathway," *Pharmaceutical Biology*, vol. 57, no. 1, pp. 529–535, 2019.

[175] T. T. Woo, S. Y. Li, W. W. K. Lai, D. Wong, and A. C. Y. Lo, "Neuroprotective effects of lutein in a rat model of retinal detachment," *Graefe's Archive for Clinical and Experimental Ophthalmology*, vol. 251, no. 1, pp. 41–51, 2013.

[176] D. Tan, X. Yu, M. Chen, J. Chen, and J. Xu, "Lutein protects against severe traumatic brain injury through antiinflammation and antioxidative effects via ICAM1/Nrf2," *Molecular Medicine Reports*, vol. 16, no. 4, pp. 4235–4240, 2017.

[177] M. Y. Gunal, A. A. Sakul, A. B. Caglayan et al., "Protective effect of lutein/zeaxanthin isomers in traumatic brain injury in mice," *Neurotoxicity Research*, vol. 39, no. 5, pp. 1543–1550, 2021.

[178] X. J. Huang, D. G. Wang, L. C. Ye et al., "Sodium aescinate and its bioactive components induce degranulation via oxidative stress in RBL-2H3 mast cells," *Toxicology Research*, vol. 9, no. 4, pp. 413–424, 2020.

[179] Z. Zhang, G. Cao, L. Sha, D. Wang, and M. Liu, "The efficacy of sodium aescinate on cutaneous wound healing in diabetic rats," *Inflammation*, vol. 38, no. 5, pp. 1942–1948, 2015.

[180] Y. Du, T. Wang, N. Jiang et al., "Protective effect of sodium aescinate on lung injury induced by methyl parathion," *Human & Experimental Toxicology*, vol. 30, no. 10, pp. 1584–1591, 2011.

[181] R. Cauchois, M. Koubi, D. Delarbre et al., "Early IL-1 receptor blockade in severe inflammatory respiratory failure complicating COVID-19," *Proceedings of the National Academy of Sciences of the United States of America*, vol. 117, no. 32, pp. 18951–18953, 2020.

[182] L. Zhang, M. Fei, H. Wang, and Y. Zhu, "Sodium aescinate provides neuroprotection in experimental traumatic brain injury via the Nrf2-ARE pathway," *Brain Research Bulletin*, vol. 157, pp. 26–36, 2020.

[183] P. Cheng, F. Kuang, and G. Ju, "Aescin reduces oxidative stress and provides neuroprotection in experimental traumatic spinal cord injury," *Free Radical Biology & Medicine*, vol. 99, pp. 405–417, 2016.

[184] P. Jalmi, P. Bodke, S. Wahidullah, and S. Raghukumar, "The fungus Gliocephalotrichum simplex as a source of abundant, extracellular melanin for biotechnological applications," *World Journal of Microbiology and Biotechnology*, vol. 28, no. 2, pp. 505–512, 2012.

[185] Z. Li, X. Li, M. T. V. Chan, W. K. K. Wu, D. X. Tan, and J. Shen, "Melatonin antagonizes interleukin-18-mediated inhibition on neural stem cell proliferation and differentiation," *Journal of Cellular and Molecular Medicine*, vol. 21, no. 9, pp. 2163–2171, 2017.

[186] M. Ghareghani, L. Scavo, Y. Jand et al., "Melatonin therapy modulates cerebral metabolism and enhances remyelination by increasing PDK4 in a mouse model of multiple sclerosis," *Frontiers in Pharmacology*, vol. 10, p. 147, 2019.

[187] M. D. Maldonado, F. Murillo-Cabezas, M. P. Terron et al., "The potential of melatonin in reducing morbidity–mortality after craniocerebral trauma," *Journal of Pineal Research*, vol. 42, no. 1, pp. 1–11, 2007.

[188] K. Ding, H. Wang, J. Xu et al., "Melatonin stimulates antioxidant enzymes and reduces oxidative stress in experimental traumatic brain injury: the Nrf2-ARE signaling pathway as a potential mechanism," *Free Radical Biology & Medicine*, vol. 73, pp. 1–11, 2014.

[189] M. L. Kelso, N. N. Scheff, S. W. Scheff, and J. R. Pauly, "Melatonin and minocycline for combinatorial therapy to improve functional and histopathological deficits following traumatic brain injury," *Neuroscience Letters*, vol. 488, no. 1, pp. 60–64, 2011.

[190] T. H. Tsai and J. W. Wu, "Regulation of hepatobiliary excretion of sinomenine by P-glycoprotein in Sprague-Dawley rats," *Life Sciences*, vol. 72, no. 21, pp. 2413–2426, 2003.

[191] Y. Yang, H. Wang, L. Li et al., "Sinomenine provides neuroprotection in model of traumatic brain injury via the Nrf2-ARE pathway," *Frontiers in Neuroscience*, vol. 10, p. 580, 2016.

[192] M. Russo, C. Spagnuolo, G. L. Russo et al., "Nrf2 targeting by sulforaphane: a potential therapy for cancer treatment," *Critical Reviews in Food Science and Nutrition*, vol. 58, no. 8, pp. 1391–1405, 2018.

[193] M. H. Traka, A. Melchini, J. Coode-Bate et al., "Transcriptional changes in prostate of men on active surveillance after a 12-mo glucoraphanin-rich broccoli intervention-results from the Effect of Sulforaphane on prostate CAncer PrEvention (ESCAPE) randomized controlled trial," *The American Journal of Clinical Nutrition*, vol. 109, no. 4, pp. 1133–1144, 2019.

[194] K. Singh, S. L. Connors, E. A. Macklin et al., "Sulforaphane treatment of autism spectrum disorder (ASD)," *Proceedings of the National Academy of Sciences of the United States of America*, vol. 111, no. 43, pp. 15550–15555, 2014.

[195] N. O. Al-Harbi, A. Nadeem, S. F. Ahmad et al., "Sulforaphane treatment reverses corticosteroid resistance in a mixed granulocytic mouse model of asthma by upregulation of antioxidants and attenuation of Th17 immune responses in the airways," *European Journal of Pharmacology*, vol. 855, pp. 276–284, 2019.

[196] J. Zhao, A. N. Moore, J. B. Redell, and P. K. Dash, "Enhancing expression of Nrf2-driven genes protects the blood brain barrier after brain injury," *The Journal of Neuroscience*, vol. 27, no. 38, pp. 10240–10248, 2007.

[197] J. Zhao, A. N. Moore, G. L. Clifton, and P. K. Dash, "Sulforaphane enhances aquaporin-4 expression and decreases cerebral edema following traumatic brain injury," *Journal of Neuroscience Research*, vol. 82, no. 4, pp. 499–506, 2005.

[198] P. K. Dash, J. Zhao, S. A. Orsi, M. Zhang, and A. N. Moore, "Sulforaphane improves cognitive function administered following traumatic brain injury," *Neuroscience Letters*, vol. 460, no. 2, pp. 103–107, 2009.

[199] M. J. Calkins, R. J. Jakel, D. A. Johnson, K. Chan, Y. W. Kan, and J. A. Johnson, "Protection from mitochondrial complex II inhibition in vitro and in vivo by Nrf2-mediated transcription," *Proceedings of the National Academy of Sciences of the United States of America*, vol. 102, no. 1, pp. 244–249, 2005.

[200] X. Zhao, G. Sun, J. Zhang et al., "Transcription factor Nrf2 protects the brain from damage produced by intracerebral hemorrhage," *Stroke*, vol. 38, no. 12, pp. 3280–3286, 2007.

Hindawi
Oxidative Medicine and Cellular Longevity
Volume 2022, Article ID 1623181, 15 pages
https://doi.org/10.1155/2022/1623181

Review Article

Microtubule Organization Is Essential for Maintaining Cellular Morphology and Function

Lijiang Huang,[1] **Yan Peng**,[2] **Xuetao Tao**,[3] **Xiaoxiao Ding**,[4] **Rui Li**,[1,5] **Yongsheng Jiang**,[1] **and Wei Zuo**[1]

[1]*The Affiliated Xiangshan Hospital of Wenzhou Medical University, No. 291 Donggu Road, Xiangshan County, Zhejiang 315000, China*
[2]*Hangzhou Institute for Food and Drug Control, Hangzhou, Zhejiang, China*
[3]*The Second Affiliated Hospital, Zhejiang University School of Medicine, Hangzhou, Zhejiang 310009, China*
[4]*Department of Pharmacy, The People's Hospital of Beilun District, Ningbo, Zhejiang 315807, China*
[5]*PCFM Lab, GD HPPC Lab, School of Chemistry, Sun Yat-sen University, Guangzhou 510275, China*

Correspondence should be addressed to Rui Li; xiaoerrui1989@163.com, Yongsheng Jiang; shenren34127@163.com, and Wei Zuo; zuowei196412@163.com

Received 5 August 2021; Revised 10 January 2022; Accepted 26 February 2022; Published 7 March 2022

Academic Editor: Amadou Camara

Microtubules (MTs) are highly dynamic polymers essential for a wide range of cellular physiologies, such as acting as directional railways for intracellular transport and position, guiding chromosome segregation during cell division, and controlling cell polarity and morphogenesis. Evidence has established that maintaining microtubule (MT) stability in neurons is vital for fundamental cellular and developmental processes, such as neurodevelopment, degeneration, and regeneration. To fulfill these diverse functions, the nervous system employs an arsenal of microtubule-associated proteins (MAPs) to control MT organization and function. Subsequent studies have identified that the disruption of MT function in neurons is one of the most prevalent and important pathological features of traumatic nerve damage and neurodegenerative diseases and that this disruption manifests as a reduction in MT polymerization and concomitant deregulation of the MT cytoskeleton, as well as downregulation of microtubule-associated protein (MAP) expression. A variety of MT-targeting agents that reverse this pathological condition, which is regarded as a therapeutic opportunity to intervene the onset and development of these nervous system abnormalities, is currently under development. Here, we provide an overview of the MT-intrinsic organization process and how MAPs interact with the MT cytoskeleton to promote MT polymerization, stabilization, and bundling. We also highlight recent advances in MT-targeting therapeutic agents applied to various neurological disorders. Together, these findings increase our current understanding of the function and regulation of MT organization in nerve growth and regeneration.

1. Introduction

A multitude of cellular processes rely on the cytoskeleton, a filamentous scaffold of proteins that is essential for cell morphogenesis and division and intracellular transport. In eukaryotic cells, the cytoskeleton consists of three types of polymers: microtubules (MTs), actin filaments, and intermediate filaments. All three polymers provide a complex internal structure that maintains cellular homeostasis and fulfills different physiological functions. In general, actin filaments and MTs exhibit structural and regulatory interactions and such cytoskeletal crosstalk allows rapid intracellular reorganization, shape maintenance, and intracellular organelle movement [1, 2]. Additionally, all three polymers undergo dynamic assembly and disassembly through whole cellular processes [3]. This dynamic instability generates forces that drive changes in cell shape and motility [4].

In many cells, MTs are created through the spontaneous assembly of alpha/beta-tubulin dimers into polarized filaments, which allows them to act as structural scaffolds and signaling platforms for cellular behavior. During nervous system development, MTs are abundant in axons and dendrites

and have a nearly uniform polarity orientation [5]. This oriented array allows the directional transport of cargoes to be properly orchestrated. Given the distinct polarity, organization, and posttranslational modifications, it is not surprising that microtubule (MT) organization and orientation are one of the most essential and earliest developmental differences between axons and dendrites [6]. In axons, MTs are uniformly orientated with their plus-ends towards the axon tip, whereas in dendrites, MTs are either oriented in the same manner or the opposite manner, depending on neuronal type and organism [7, 8]. Proper MT function as well as proper functioning of their assortment of interacting and regulatory proteins and regulatory pathways is particularly important in neurons. Abnormalities of the MT system in axons and dendrites, i.e., MT depolymerization, loss, or dysfunction or disorganized MT arrays, are a common insult during the pathogenesis of nerve traumatic disorders [9, 10].

Here, we summarize our current understanding of the basic biological features of MT organization within the cell, focusing on MT self-assembly and the direct participation of microtubule-associated proteins (MAPs) in MT nucleation, stabilization, and postmodification. We also discuss the current state of microtubule-stabilizing agents (MSAs), a new pharmacological intervention for treating central nervous system disorders, and address several microtubule-destabilizing agents (MDAs) as therapeutic strategies for suppressing cancer activity and vasculogenesis. Such diversified MT functions may provide us with new insights into MT-targeting therapies that mitigate structural and functional alterations linked to nervous system disorders.

2. MT Organization and Dynamic Regulation in Eukaryotic Cells

MTs are hollow cylindrical tubes consisting of repeating α-tubulin and β-tubulin heterodimers that play central roles in cellular morphogenesis, division, and development. The α-tubulin subunit is the minus-end in MT networks and exhibits slow growth rates and fast dissociation rates. The β-tubulin subunit is the plus-end and exhibits opposite growth and dissociation rates relative to the α-tubulin subunit. Within eukaryotic cells, tubulin dimers can form heterogeneous and dynamic protofilaments by aligning head to tail; approximately 13 protofilaments of MT are needed to form a hollow tube. During the process of MT polymerization, it usually exhibits dynamic instability, i.e., assembly and disassembly occur simultaneously, which is essential for normal functioning of the MT cytoskeleton [11]. The mechanism of such behavior is governed by the presence of two distinct states of GTP-GDP shafts at the β-tubulin end [12]. When tubulin dimers are free in solution, MT at the β-tubulin end is under the GTP-bound state and can be exchanged [13]. After incorporation of the tubulin dimers into the MT, β-tubulin hydrolyzes the GTP to GDP [14]. Thus, as long as subunits of GTP-bound β-tubulin form a GTP-tubulin cap at the plus-end [15], MTs can grow, but when GTP at the exchangeable site (E-site, located at the α/β-tubulin dimer of the plus-end) becomes hydrolyzed to GDP due to the GTPase activity of β-tubulin, the MT enters a state of shortening. With the help of the GTP-tubulin cap and E-site, MT polymerization and depolymerization occur primarily at the plus-ends.

During the initial stage of MT formation (also termed MT nucleation, Figure 1), α/β-tubulin dimers need a template to guide assembly and elongation. This template is named the gamma-tubulin ring complex (γ-TuRC), which consists of numerous γ-tubulin molecules with various types of gamma-tubulin complex proteins (GCPs) [3]. GCPs at the N-terminal regions can interact directly with mitotic spindle organizing protein 1 (MZT1), a key regulator of the centromere structure [16]. The MZT1 protein is capable of binding to the N-terminal centrosomin motif 1 (CM1) domain of CDK5RAP2, a tethering protein that can recruit and bind γ-TuRC to diverse microtubule organizing centers (MTOCs), including the centrosome, Golgi apparatus, or mitotic chromatin [17, 18]. After forming the γ-TuRC ring structure, γ-tubulin molecules can anchor the minus-end of α/β-tubulin dimers to support a lateral association between α/β-tubulin dimers and polymerize into MTs with parallel orientations [19]. Thus, MT nucleation plays a crucial role in regulating MT self-assembly in various eukaryotic cells.

3. Types of MT Regulatory Proteins

MT stability, predominantly its mass and conformation, is controlled by the activities of several MAPs. They participate in a plethora of cellular processes, including cellular division, polarization, and intracellular transport, and can be categorized into MT-stabilizing proteins and MT-destabilizing proteins. The former group including MAP2, Tau, and Doublecortin (DCX), can interact with different MT-binding domains to bundle neighboring MTs [20]. MT-destabilizing proteins, on the other hand, perturb specific interaction nodes within the MT minus-end by accelerating the frequency of MT depolymerization. Different MAPs may regulate the stability and dynamics of MTs by creating different assembly patterns, either by altering the stability of lateral bonding tip extensions or altering the delivery of tubulin subunits to the tip [21, 22]. This regulation creates spatial and temporal patterns in the MT network within cells that are particularly important for cell morphogenesis, division, and physiology [23]. Although some MAPs remain poorly understood due to their high degree of homology, a huge number of mammalian MAPs have been characterized using proteomics and the construction of transgenic animal models [24, 25]. Here, we highlight some typical MAPs involved in their features and physiological functions as well as in the molecular mechanisms of stabilizing MTs.

MAP2, a microtubule-associated protein (MAP) family member, produces four different isoforms (MAP2A-D) according to alternative splicing of the same transcript. Generally, these four isoforms are highly expressed in differentiated neuronal dendrites, resulting in their utilization for labeling mature neurons. In addition, MAP2C and MAP2D are also widely distributed in glial cells. During the stages of neuronal development, MAP2 modulates MT-mediated cellular transport to participate in nucleation and stabilize MTs and bundling [26]. In particular, MAP2 is expressed in

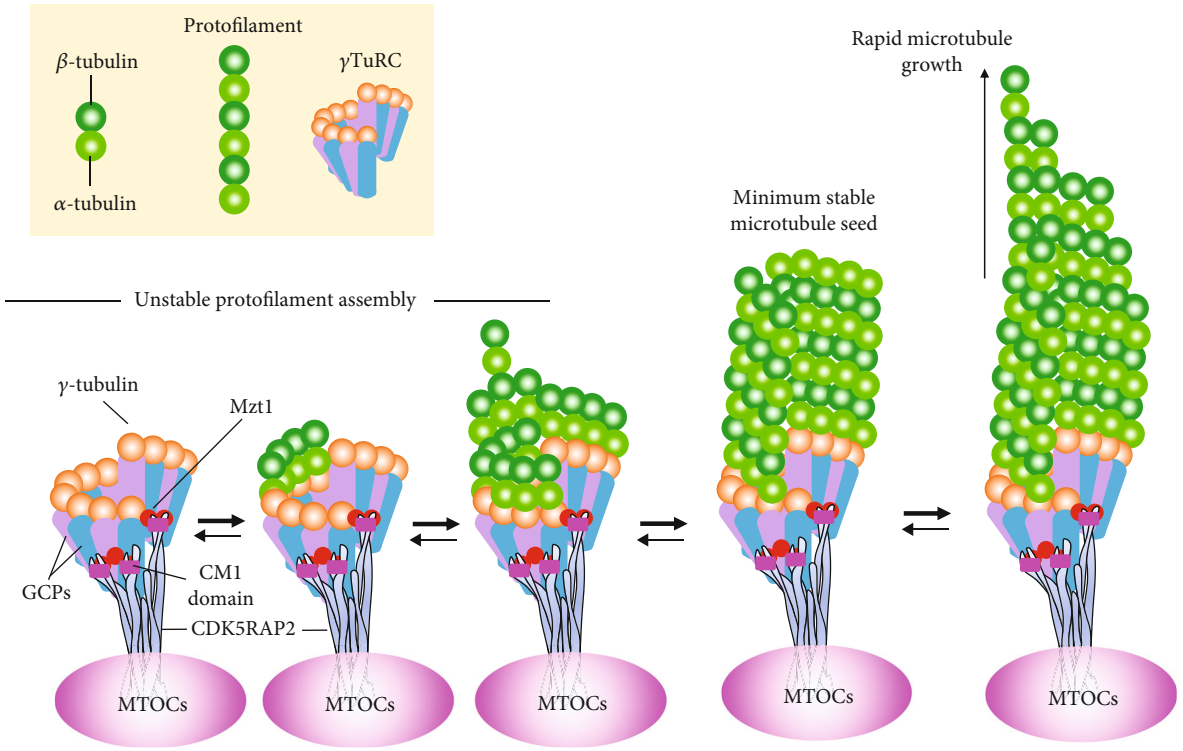

FIGURE 1: The process of γ-TuRC-mediated MT nucleation. The formation of the γ-TuRC ring structure and its interaction with α/β-tubulin dimers are described above. Briefly, the γ-TuRC complex can be recruited to various MTOCs via linking other accessory proteins to form a ring-like structure. Such structure allows the rapid growth of complex MT networks via γ-tubulin molecules interacting longitudinally with the MT minus-ends. It should be noted that MTs have the characteristic of dynamic instability, which allows MTs to spontaneously switch between assembly and disassembly phases. If there are sufficient tubulin dimers, MT polymerization can progress rapidly.

mature dendrites and is critically essential for protein synthesis and organelle biogenesis, as it controls cargo sorting at the predendritic filtering zone [27, 28].

Another MAP, Tau, also supports the stability and dynamics of the cytoskeleton but is mainly enriched in axons [29, 30]. While MTs and Tau share a conserved carboxy-terminal domain that can specifically interact under physiological conditions, the amino-terminal non-MT-binding domain, another region of the Tau protein, provides a large area for interacting with other cellular components, such as actin, kinesin, and dynein, thus ensuring the movement of cargo packages from the cytoplasm to the distal end of the axon [31, 32]. Over the last several years, a larger number of studies have revealed that the Tau protein is encoded by the MAPT gene and can interact with MTs in a "kiss-and-hop" fashion, namely, temporarily dwelling on a single MT before hopping to the adjacent MT, regulating MT dynamics [33, 34]. This dynamic MT Tau interaction is maintained mainly through electrostatic interactions between the positively charged MT-binding region and the negatively charged acidic glutamate-rich C-terminal regions of the tubulin surface [35, 36]. In addition to these electrostatic interactions, posttranslational modifications of Tau, mainly phosphorylation and acetylation, strongly affect MT-Tau binding and thereby have the potential to modulate the organization of MTs [37, 38].

DCX is a unique MAP that has been shown to be involved in MT assembly, turnover, and posttranslational modification of α- and β-tubulin proteins [39]. Binding of DCX to tubulin increases MT homeostasis in neurons, which can be disturbed via knockout of the DCX gene sequence using an inducible transgenic mouse approach [40]. Additionally, DCX is expressed in various regions of the developing nervous system and is regarded as a gold standard biomarker for identifying neuronal precursors and migration during adult neurogenesis [41, 42].

In addition, fibroblast growth factor 13 (FGF13) acts as an intracellular MAP that promotes axonal development, neuronal polarization and migration, and brain development [43]. It is rich in the central nervous system, especially for the developing brain. The regulatory mechanism by which FGF13 induces MT polymerization and stabilization is through binding to a tubulin-binding domain to directly interact with tubulin and colocalize with MTs in the growth cone [44]. Accumulating evidence suggests that overexpression of FGF13 enhances axonal regeneration and functional recovery by maintaining MT stabilization following spinal cord injury (SCI) and FGF13 deficiency causes cognitive impairment due to delayed neuron migration in both the cortex and hippocampus [44, 45]. Overall, these MT-stabilizing proteins are essential for cytoskeletal reorganization, growth orientation, and intracellular organization.

Several regulatory proteins can interact with dynamic MT minus-ends to catalyze the removal of tubulin subunits. These MT-destabilizing proteins are mainly MT depolymerases or the members of the calmodulin-regulated

spectrin-associated protein (CAMSAP) family. MT depolymerases, also known as kinesin family proteins, have been reported to break the lateral links of protofilaments and tear off the tubulin monomer from the spindle by attaching to the minus-end of MT [46]. Currently, over 40 known kinesins have been identified in mammalian cells and are constitutively expressed in neurons [47]. Kinesins are known to modulate various cellular functions, including energy transport, spindle elongation during cell division, and alteration of the MT dynamics [48]. Some studies have indicated that kinesins that regulate neuronal behavior and function are closely associated with the MAPK cascade. For instance, kinesin-8 connects and interacts with the MAPK pathway to induce neuronal migration and differentiation [49]. Meanwhile, kinesin-5-induced MAPK signaling activation regulates myelination of the nervous system and promotes neuronal polarization and morphogenesis in cortical pyramidal neurons [50, 51]. Similar to the functions of the kinesin family, the CAMSAP family also binds to free minus-ends of MTs to slow tubulin addition, leading to the arrest of their growth at minus-ends [52]. This family of proteins, including CAMSAP1-3, contains an amino-terminal CH domain. In worms and mammals, CAMSAPs are localized to the outermost tips of the minus-ends, which play a crucial role in transporting new MTs into an axon or a dendrite in neuron differentiated from neural stem cells (NSCs) [53, 54]. A study by Cao et al. recently proposed that CAMSAP2 was capable of slowing minus-end polymerization and facilitating polarized cargo trafficking, which strengthened MT organization [55]. Additionally, Pongrakhananon et al. revealed that CAMSAP3 was required to retain a dynamic pool of MTs as it prevented αTAT1-mediated acetylation and thus maintained neuronal polarity [56]. Depletion of neuronal CAMSAP3 reduced dynamic MTs, resulting in supernumerary axon formation [56].

4. MT Organization in Neurons

A vertebrate neuron is an exquisitely polarized cell whose structure is composed of a cell body, a single elongated axon, and several dendrites [57]. In neuronal networks, axons play the major role in transmitting information and transporting macromolecules, while dendrites form numerous spine apparatuses for receiving information [58, 59]. During neuronal development, the cell body initially produces several short motile lamellipodia (stages 1-2); one of these lamellipodia rapidly becomes the axon (stage 3), while the remaining neurites transform into dendrites and gradually mature to build neural networks (stages 4–5) [60]. At stages 1-2, a fan-shaped structure is found at the tip of the growing axon; this growth cone can perceive the surrounding environment changes and regulates the rate and direction of axon extension, guiding axons over long distances to connect their specific targets [61]. If axons fail to grow due to a hostile local environment (e.g., hemorrhages, ischemia, the accumulation of inflammatory factors, myelin debris, or axonal inhibitory molecules), the tips of growing neurites form retraction bulbs. According to the cytoskeletal organization, the growth cone can be separated into three regions: peripheral (P-) and central (C-) regions as well as the transitional zone (T-zone). The P-region contains actin-rich lamellar protrusions, and its surface stretches out many lamellipodia and filopodia, which are pivotal to control the extension and retraction of the growth cone [62]. The C-region, located at the base of the growth cone, is the MT-rich region contiguous with the axonal shaft that shapes the morphology of the growth cone and orchestrates cytoskeletal remodeling. The T-zone is located between the P- and C-regions. Such domain encompasses actin arcs, a dense meshwork of actin filaments that creates a barrier to hinder MT forward from the C-region to the P-region [63, 64]. For the growth cone to advance, a dense MT array from the C-region must penetrate the T-zone to reach the P-region, preferentially polymerizing after incorporation of GTP to the β-tubulin subunit [65]. Axonal protrusion, retraction, and turning in response to signaling cascades require the coordination of the neuronal MT network and the actin cytoskeleton within the growth cone [66]. Specifically, recent studies have shown that growth cone steering and advancement in response to environmental cues depend on MT assembly and dynamics [67, 68]. Thus, understanding the intrinsic regulatory mechanisms of MT dynamics and function within the growth cone may provide therapeutic targets for interventions that improve axon growth and guidance during neurodevelopment and neuroregeneration following injury.

Neuronal MTs are arranged in a specific orientation [9, 69]. In axons, MTs have an almost exclusive plus-end-out orientation, whereas in dendrites, MTs have an antiparallel organization with equal proportions of plus-end and minus-end towards the soma [70]. This distinct orientation is partially regulated by kinesin and dynein, two molecular motor proteins that cooperate with protofilaments to drive MT elongation from the C-region to the P-region [71, 72]. Moreover, these proteins also act as vectors for transporting organelles and other cargo towards axons or dendrites [73]. Kinesins have been determined to move cargo to axon terminals, whereas MTs of mixed polarity allow dynein motors to drive cargoes, such as that from the Golgi apparatus and ribosomes, specifically into dendrites [74]. Such distinct MT polarity patterns and cargo sorting are essential for distinguishing neurons into axons or dendrites (Figure 2).

The overall appearance and arrangement of the MT network within neurons are variable and depend on their maturation stage [75, 76]. At the early stages of initial neurite outgrowth, MTs are of mixed polarity as short mobile polymers are rapidly released to be used by other MTs for their elongation. However, at the later stages of development, i.e., adult neurons, MTs have minus-end-out orientation with hundreds of micrometers in length and act as major long-distance railways for organelle transport. During development, MT orientation according to a network of feedback loops is essential for maintaining proper neuronal shape and inducing neuronal polarization [77, 78]. Upon neuronal polarization, posttranslational modifications of MTs in the nascent axon provide selective transport routes that increase the neurite length-dependent feedback and anterograde transport [79, 80]. The establishment of a normal feedback loop network is required for the activation of various

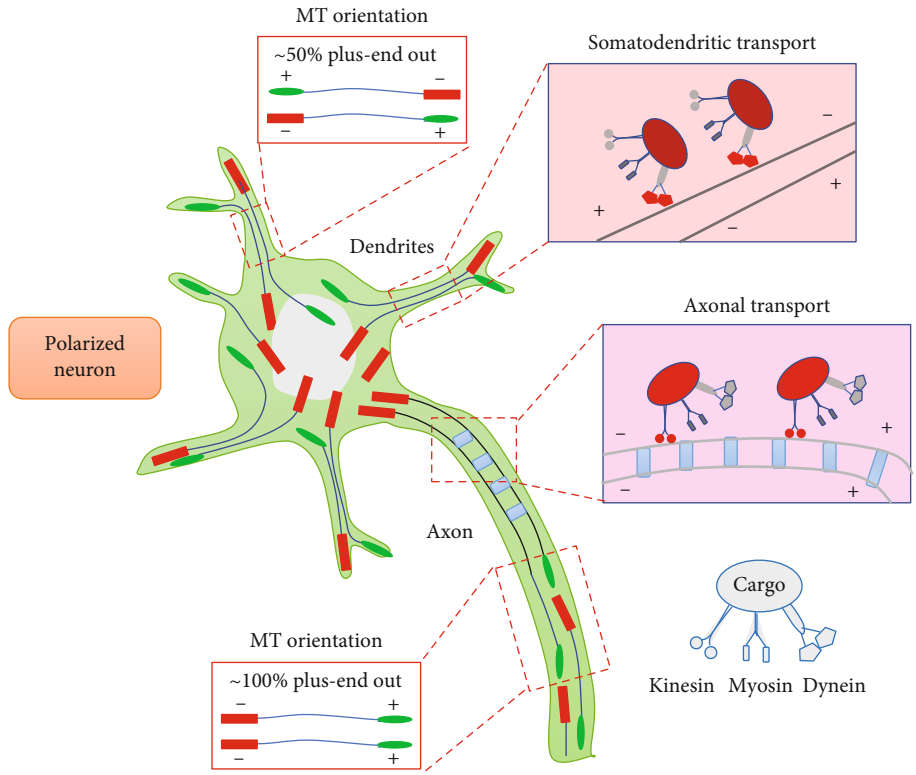

Figure 2: Basic mechanisms of MT organization during the differentiation of neurons into axons or dendrites. In axons, MTs display uniform polarity orientation with their plus-ends out. This array is essential to drive cargo transport through the proximal-end to the distal-end by kinesins, whereas in dendrites, MTs are mixed polarity with half of their minus-ends pointing to the soma, which allows dynein motors to selectively transport cargoes across this mixed MT arrays.

signaling cascades and for modulation by several molecules [81, 82]. For instance, Shootin1 is a brain-specific cytoplasmic molecule that can be detected in the MT-associated protein fraction [83]. It is highly expressed in axonal growth cones and plays the central role for promoting neuronal polarity and axon outgrowth through a self-promoting feedback loop involving the Rac1/Pak1 signaling cascade [84, 85]. This facilitatory effect provides the driving force to induce one neurite under the growing state, while the remaining neurites are still in a pause state, ultimately driving neuron-autonomous neuronal polarization to generate a long signal-sending axon and several shorter signal-receiving dendrites.

5. MT Modifications in Nervous System Injury

Injury to the central nervous system (CNS) induces severe neurological complications for individuals with traumatic brain injury (TBI) or SCI because various inhibitory factors secreted by oligodendrocytes and scar-forming cells and the poor intrinsic growth ability upon neuronal maturation hamper axon regeneration and functional recovery [86, 87]. A growing number of studies have recently identified MTs as promising targets for coaxing regeneration of injured adult axons [88, 89]. The functions of MTs include (1) providing a structural backbone to maintain axon-specialized morphologies [57], (2) acting as the major long-distance railways for substrate transport in both directions [90], (3) ensuring the growth and steering of developing axons [91], and (4) regulating the extent of regeneration in injured axons [9]. Accordingly, moderate stabilization of MTs by Taxol enables MT polymerization and cytoskeleton organization, which transform the nongrowing retraction bulbs into growing axons [92]. Conversely, adding the MT-depolymerizing drug nocodazole to cultured dorsal root ganglia (DRG) neurons disturbs cytoskeleton organization and dynamics and increases the number of retraction bulbs [93].

TBI involves trauma to the CNS with characteristics of hypotension, hypoxia, and behavioral/cognitive abnormalities [94]. A common characteristic of TBI is loss of axonal integrity and cytoskeletal derangement, which are intrinsically associated with MT deficits and axonal dysfunction. Recently, MT disruption and loss, manifesting as MT depolymerization and the decrease of related proteins, such as Tau, p-Tau, and acetublin, were found to be key ultrastructural hallmarks of brain damage [95]. Thus, inducing MT stabilization is a novel therapeutic strategy to protect the damaged brain from high intracranial pressure and ischemia. A previous study reported that maintaining MT stabilization by local administration of FGF13 promoted neuronal migration and axon formation; in contrast, suppression of FGF13 expression delayed neuron migration and brain development [44]. Further studies revealed that administration of an MT-stabilizing drug, epothilone D, altered synaptic plasticity and dampened detrimental neuroglial responses

after mild TBI of mice for 1 week [96]. However, intraperitoneal injections of low doses of exogenous nocodazole after TBI destroyed MT assembly and triggered a degenerative response characterized by loss of synapses and abnormal cytoskeletal rearrangement, as well as impairments in learning and memory [97]. While stabilizing the MT cytoskeleton is vital for ameliorating damage from TBI, there is still much to learn about the potential mechanisms involved in controlling this process.

SCI induces severe neurological deficits causing MT disorganization and deregulation of the MT cytoskeleton. Accumulating evidence has demonstrated that MT formation and stabilization are important for maintaining cytoskeletal integrity and axonal transport, as well as preventing detrimental gliotic responses [98]. Remodeling axonal MTs through genetic intervention or pharmacological treatment significantly enhanced axon regrowth and extension and reduced scar formation in an *in vivo* model of traumatic SCI, whereas the inhibition of MT stabilization by nocodazole weakens this beneficial effect [99]. Duan et al. demonstrated that systemic administration of epothilone B, an MT-stabilizing agent, reconstructed neovascularization by facilitating apoptosis and the migration of endothelial cells and pericytes and promoting their proliferation after SCI [100]. Moreover, regulation of MT dynamics by upregulating FGF13 expression is essential for promoting growth cone initiation, neuronal polarization, and regeneration of damaged axons following SCI [45]. Further studies found that MSAs also prevented fibroblast migration and prolonged the retention of MAPs, reducing inhibitory fibrotic scarring and improving intrinsic growth capacity, ultimately improving spinal cord restoration after injury [101–103]. In addition, recent studies on the relationship between autophagy and MT dynamics revealed that autophagy activation increased the expression of acetylated MT, a key modification for controlling MT stability and growth, thus attenuating axonal retraction and consequently enhancing locomotor recovery after SCI [104, 105]. Overall, stabilizing MTs in damaged neuron plays a pivotal role in determining their regenerative capacity after SCI.

6. MT-Targeting Agent

MT-targeting agents can be classified into two main categories: MSAs and MDAs. The former, including paclitaxel, docetaxel, epothilones, and laulimalide, can bind to the tubulin heterodimer at the plus-end to promote the polymerization of tubulin to MTs. The latter induces MT dysfunction at the end of the mitotic spindle by preventing tubulin polymerization on both plus- and minus-ends of MT, leading to the arrest of mitosis. Representative examples of MDAs include vincristine, vinblastine, colchicine, and combretastatin. The regulatory mechanism by which MT-targeting agents influence MT dynamics depends on which MT domain they bind to [106] (Figure 3). According to their binding affinities to tubulin, these binding domains can be categorized as Taxol-binding domain, colchicine-binding domain, and vinca-binding domain [107]. MSAs are able to target the cytoskeleton and inhibit cell division by binding to β-tubulin of inner surface of MT lumen, which is generally described as the Taxol-binding domain [108]. Taxol-binding drugs, such as laulimalide, are shown to increase MT polymerization and assembly by allosterically stabilizing the Taxol-site M-loop [109]. MDAs depolymerize MTs by interacting with the vinca-binding domain or colchicine binding domain. Vincristine and vinblastine are two typical vinca-binding analogues. They induce mitotic arrest and block cell division by blocking tubulin polymerization at the interdimer interface, which is named the vinca-binding domain [110]. Colchicine and combretastatin are colchicine-binding analogues. They bind to the Cys241 residue of β-tubulin (termed colchicine-binding domain) via hydrogen bonding to induce mitotic arrest and chromosome missegregation [111].

MT-targeting agents were traditionally used as anticancer agents for the treatment of various solid tumors [112]. To date, some of these agents are commonly approved for clinical anticancer chemotherapy for many types of solid tumors. However, recent work has shed light on their potential for treating traumatic nerve damage and neurodegenerative diseases, including Alzheimer's disease (AD), Parkinson's disease (PD), amyotrophic lateral sclerosis (ALS), and SCI (Table 1). This dual treatment ability aroused our curiosity. MTs are found in all characterized eukaryotic organisms, but exert diverse cellular functions in different cell types [113]. In cancer cells, MTs are one of the important components of the mitotic spindle and are capable of pulling sister chromatids towards opposite poles [114]. Thus, MT assembly and disassembly are critical for determining the proliferative capability of cancer cells. As mentioned in the previous passage, MT-targeting agents can interfere with the corresponding binding domains of tubulin to block their polymerization. This event impairs the ability of spindle MTs to capture chromosomes and interferes with the G2/M phase of the cell division, leading to mitotic arrest and even death in cancer cells [115]. In neurons, MTs, as one of the major longitudinal cytoskeletal filaments, are abundant in axons and dendrites [116]. Additionally, adult neurons or permanent differentiated neurons lack high proliferative capacity, resulting in few concerns and studies that are focused on MT-regulating neuronal division after damage or degeneration. Based on this fact, current studies are concentrated on the role of MT stability in regulating axon growth and steering as well as the intracellular trafficking of cargos during neuronal development [9, 116]. Following neuronal injury or neurodegenerative diseases, MTs become disassembled and gradually lose mass, leading to axonal atrophy and degeneration [117]. MSAs, such as Taxol and epothilones, promote the polymerization of tubulin to MTs during disease and/or injury [106, 118]. Thus, MSAs are regarded as potential candidates for treating neuronal disorders. However, the precise mechanism of MSAs for treating cancer and neuronal diseases needs to be explored in future research. In this section, we will introduce some background information on these therapeutic compounds and elucidate their application.

MSAs have been used as cancer therapeutic drugs for more than 20 years [130]. They were originally derived from

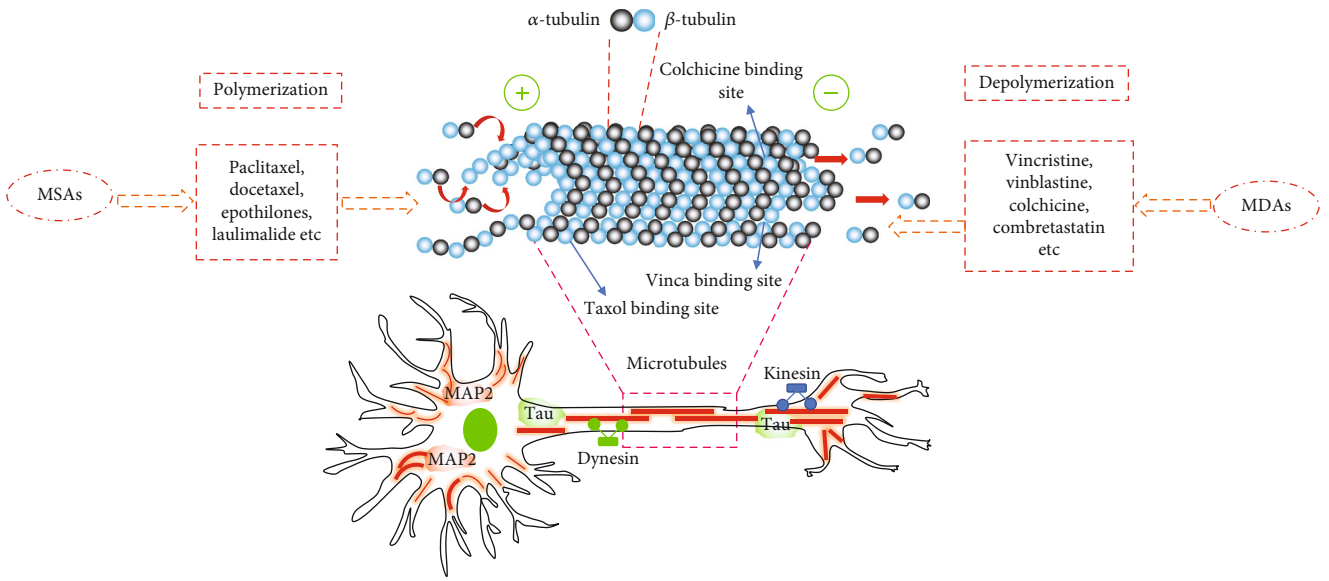

Figure 3: Diagram of MAPs, MSAs, and MDAs involved in the regulation of MT dynamics within neurons. MT organization and dynamics are regulated by MT proteins, MSAs and MDAs. MT-targeting agents can interfere with the dynamic equilibrium of MT polymerization and depolymerization. According to their mechanisms of action, MT-targeting agents can be divided into two groups: MSAs and MDAs. The former includes paclitaxel, docetaxel, epothilones, and laulimalide. They exert bind and interfere with the Taxol-binding domain and nontaxane sites. MDAs include vincristine, vinblastine, colchicine, and combretastatin. They depolymerize MTs by targeting the vinca-binding domain and colchicine-binding domain. These MT-targeting agents influence the polymerization and depolymerization of MTs and are patterned by a variety of MAPs, including MAP2, Tau, dynein, and kinesin. These MAPs play the critical roles in mediating a plethora of cellular processes such as cell division and motility, intracellular transport, axonal specification, and neuronal development.

Table 1: Summary of various MT-targeting agents applied to protect the nervous system.

Classification	Compound	Pathological model	Outcome	Ref.
MSAs	Paclitaxel (Taxol)	SCI	Enhancement of nerve regeneration and functional recovery	[119, 120]
		Retinal nerve injury	Increased MT numbers and stabilization to restore axonal transport	[121]
		AD	Improvements in axonal transport, tissue, and motor function	[122]
	Epothilones	SCI	Decreased scarring, increased axon regeneration, and improved motor function	[102, 103]
		PD	Rescued MT defects and attenuated nigrostriatal degeneration	[123]
		AD	Reduced axonal dystrophy, increased axonal MT density, improved speed of axonal transport, and improved cognitive performance	[124, 125]
	Davunetide (NAP)	AD, ALS	Prevented axonal transport disruption, synaptic defects, and behavioral impairments	[126, 127]
MDAs	Vincristine	iPSC-derived neurons from HSP patients	Ameliorated axonal swelling	[128]
	Okadaic acid	Hyperphosphorylated Tau to model AD	Reduced the growth of the rat cortical neuron axons	[129]

natural resources. For instance, paclitaxel (Taxol®) was the first MSA to be isolated (derived from the Pacific yew tree in 1971) and approved by the FDA for the treatment of breast cancer, with an optimal therapeutic concentration of 260 mg/m^2 [131]. This is decomposed into 6α-hydroxy-paclitaxel by activating CYP2C8 enzyme in human liver microsomes [132]. Due to the difficulty of obtaining paclitaxel from the plant, various analogues, such as docetaxel, cabazitaxel, larotaxel, and TPI-287, have been synthesized through modification of its side chains and have exhibited encouraging clinical efficacy for treating breast cancer [133, 134]. Recent studies have shown that paclitaxel can maintain specialized neuronal morphology and support axonal and dendritic transport by resisting MT dynamic instability. For instance, Hellal et al. found that stabilizing the MT network with Taxol hindered the formation of scarring and prevented axonal retraction and swelling after SCI in rodents [119]. In another work, paclitaxel encapsulated in a collagen microchannel was shown to enhance neuronal differentiation of NSCs *in vitro* and improve axonal transport and

axonal functional recovery in a complete spinal transsection injured models of rats [135].

Epothilones are another class of MSAs that include a 16-membered macrocyclic lipid compound [136]. To date, six natural epothilone variants, i.e., epothilones A-F, can be easily obtained at a large scale by isolation from soil bacteria or by chemical synthesis [137]. Compared with paclitaxel, epothilones are more soluble in water and have better tumor resistance, which make them a viable alternative to paclitaxel in facilitating antitumor activity [138]. Data from phase III clinical trials revealed that ixabepilone, a semisynthetic analogue of epothilone B, effectively improved the survival rate of patients with metastatic breast cancer to 70% with an intravenous infusion dose of $30\,mg/m^2$ every 3 weeks [139]. In addition to treating cancer, a series of studies have shown that epothilones possess therapeutic potential for repairing neurological disorders. For instance, in a Tau transgenic mouse model of tauopathies characteristic of AD, intraperitoneal injections of $3\,mg\,kg^{-1}$ epothilone D once weekly for a 3-month period were demonstrated to support MT assembly and axon extension as well as reduce brain cognitive deficits [140]. In addition, this compound also exhibited beneficial effects on neuronal differentiation of cultured NSCs *in vitro* and improved axonal sprouting and functional recovery *in vivo* following SCI [103, 141]. Additionally, epothilones are easier to administer than paclitaxel due to their higher water solubility, which endows epothilones with the capability to cross the blood-brain barrier [138]. In short, compared to paclitaxel, epothilones show several physicochemical advantages including (1) increased water solubility for direct delivery without solvent, (2) a lack of intracellular toxicity and strong antineoplastic activity, and (3) the capacity of easily crossing the blood-brain barrier. In addition, the chemical structure of epothilones exhibits 16-membered macrocyclic lactones, which can produce synthetic analogues during clinical drug design [142]. It has been shown that systemic administration of epothilone B moderates MT stabilization to reduce fibrotic scarring and increase axon growth after SCI [102]. Additionally, epothilones augmented axonal growth and improved skilled limb function after cortical stroke in the brain [143]. Thus, both paclitaxel and epothilones are regarded as attractive therapeutic compounds for promoting the functional and structural recovery from neurodegenerative diseases and disorders.

MDAs, also called polymerizing inhibitors, possess the ability to promote the depolymerization of MTs by interfering with the colchicine-binding domain and vinca-binding domain to block cell division and interfere with the formation of a normal mitotic spindle. Thus, they have shown a strong antiangiogenic and antivascular activity and offer a pharmaceutical opportunity for treating different tumor types, including breast, lung, ovarian, and hematologic tumors [144]. According to their tubulin-binding domains, MDAs can be further divided into two groups: vinca-binding analogues and colchicine-binding analogues [145]. The representative example in the former is vinca alkaloid (VA), a natural chemotherapy agent obtained from the Madagascar periwinkle plant in 1950. It was first approved by the FDA for the clinical treatment of lung cancer and breast cancer, but provoked severe neurotoxicity [146]. To overcome this defect, other VA analogues, including natural (vinblastine and vincristine) and semisynthetic (vinorelbine, vindesine, and vinflunine) analogues, have gained attracted attention in cancer treatment [147]. Data on clinical pharmacokinetics revealed that the terminal half-lives of VA and its derivatives range from 18 to 85 h [148]. Furthermore, they were found to be first metabolized within the liver through the action of cytochrome P450 CYP3A4 and then subjected to biliary elimination and finally excreted into the feces [148, 149]. It should be addressed that VA and its derivatives can rapidly enter the peripheral tissues, including the peripheral nervous system; thus, administration of these antimitotic agents probably causes characteristic peripheral neurotoxicity [150]. To overcome this defect, researchers have identified three beneficial strategies to reduce these adverse effects, i.e., combination with other drugs, investigation of novel drug delivery platforms, and the synthesis of new VA analogues [147].

Colchicine, an alkaloid derived from the meadow saffron plant, belongs to the group of colchicine-binding analogues and is used as a therapeutic drug for anticancer treatment, such as lung, breast, and gynecological cancers [151]. Similar to VA metabolism, colchicine is broken down by the CYP3A4 enzyme within liver microsomes [152]. However, colchicine may cause toxicity in normal cell proliferation. A phase II clinical trial established that the safe dose of colchicine was $0.015\,mg\,kg^{-1}$, a higher dose of $0.1\,mg\,kg^{-1}$ resulted in intoxication, and the maximum fatal dose was $0.8\,mg\,kg^{-1}$ [153–155]. Due to colchicine's low therapeutic index and severe cytotoxicity, various colchicine analogues have been synthesized by modifying the tricyclic-membered rings. Urbaniak et al. synthesized 16 novel colchicine derivatives, namely, double- (4-7) or triple-modified (17-28) urethanes, and found that these novel colchicine derivatives (IC_{50} range of 1.1-6.4 nM) had higher antiproliferative activity than colchicine (IC_{50} = 8.6 nM) by testing the viability of primary breast cancer cells [156]. Recently, the colchicine analogue combretastatin was found to promote anticancer activity by inhibiting the elongation of MTs [157]. Moreover, its synthetic derivatives show strong antioxidant activity and anti-inflammatory activity. For instance, Huang et al. demonstrated that the combretastatin derivatives NTU-228 and HK-72 exhibited significant leukocyte inflammatory responses by quantifying N-formyl-Met-Leu-Phe- (fMLF-) induced reactive oxygen species production in human leukocytes [158]. Evidence from antioxidant studies in a subcutaneous dorsal CaNT tumor model revealed that combretastatin A-4, a combretastatin analogue, had strong protective effects against hydroxyl radicals and radical-based DNA damage [159].

7. Concluding Remarks and Future Perspectives

As briefly summarized here, MTs are dynamic cytoskeletal filaments that carry out the distinct functions of cellular physiology, such as cell division and motility, organelle positioning, and intracellular transport. Generally, MTs exhibit

extensive dynamic instability, i.e., constant transition between phases of growing and shrinking. This allows them to enhance tubulin–tubulin interactions, create pushing and pulling forces, and direct cell locomotion via crosstalk with the actin cytoskeleton [160]. *In vitro*, the dynamic state of MTs can be recorded by measuring their rate of growth and shrinkage or by quantifying their mass [161]. The most common and reliable way to track MT dynamics is using high-resolution imaging methods, including fluorescent speckle microscopy and cryo-electron microscopy [162]. Additionally, MT acetylation is a common posttranslational modification that can protect MTs against mechanical stresses by polarizing the centrosome or the mitotic spindle within the cell [163]. Eliminating MT acetylation by reducing the activity of α-tubulin acetyltransferase 1 enzyme does not impair protofilament organization but does cause a reduction in MT dynamics [164]. In brief, understanding the role of MT dynamics in cargo transportation and cytoskeletal reorganization has provided further insights into the biophysics and biochemistry of MT function involved in neuronal development, disease, and injury.

Given the importance of MT dynamics in cytoskeleton reconstruction, designing novel compounds that facilitate MT polymerization or upregulate MT acetylation has received increasing attention, due to the applications for different neurotraumatic diseases [57]. Encouragingly, some works have achieved positive therapeutic effects in cellular and animal models. For instance, systematic administration of epothilone B, a kind of MT-stabilizing agent, not only facilitated the growth of both sensory and motor axons in an unfavorable environment *in vitro* but also demonstrated dual effects on improving intrinsic neuron growth and reducing fibrotic scar in an *in vivo* SCI model [101, 102, 165]. While some natural MSAs can cause significant adverse side effects, including neutropenia, chemotherapy-induced peripheral neuropathy, and alopecia when used in cancer treatment at a high concentration [106, 166], researchers have proposed alternative and beneficial strategies, including synthesis of new MSA analogues, design of novel drug delivery platforms, and combinations with other drugs, to reduce these adverse effects [147]. Additionally, application of these therapeutic strategies can reduce the dosage of MSAs and their analogues; thus, administration at low concentrations can significantly enhance axonal regeneration and functional recovery in neuronal injury models. Further studies addressing the mechanisms that regulate the dynamic remodeling of MT networks will greatly increase our understanding of the intricacies of MT organization in various cell types.

Abbreviations

MT: Microtubule
MTs: Microtubules
MAPs: Microtubule-associated proteins
MTAs: Microtubule-targeting agents
γ-TuRC: The gamma-tubulin ring complex
GCPs: Gamma-tubulin complex proteins
MZT1: Mitotic spindle organizing protein 1
CM1: N-terminal centrosomin motif 1
MTOCs: Microtubule organizing centers
MAP: Microtubule-associated protein
DCX: Doublecortin
FGF13: Fibroblast growth factor 13
SCI: Spinal cord injury
CAMSAP: The calmodulin-regulated spectrin-associated protein
MSAs: Microtubule-stabilizing agents
MDAs: Microtubule-destabilizing agents
NSCs: Neural stem cells
CNS: The central nervous system
TBI: Traumatic brain injury
DRG: Dorsal root ganglia
AD: Alzheimer's disease
PD: Parkinson's disease
ALS: Amyotrophic lateral sclerosis
VA: Vinca alkaloid.

Data Availability

No new data are generated in this study.

Conflicts of Interest

The authors declare that they have no conflict of interest.

Authors' Contributions

H.L., T.X., and D.X. contributed in the validation, investigation, and data curation as well as in writing the manuscript. P.Y., L.R., J.Y., and Z.W. contributed in reviewing and editing the manuscript. All the authors read and approved the final manuscript.

Acknowledgments

This study was supported by a research grant from Medical and Health Science and Technology Project of Zhejiang Province (2019KY646 and 2020KY908), Science and Technology Project of Zhejiang Health Committee (2021KY1075), and the National Natural Science Funding of China (81802238).

References

[1] O. C. Rodriguez, A. W. Schaefer, C. A. Mandato, P. Forscher, W. M. Bement, and C. M. Waterman-Storer, "Conserved microtubule–actin interactions in cell movement and morphogenesis," *Nature Cell Biology*, vol. 5, no. 7, pp. 599–609, 2003.

[2] K. R. Navarrete and V. A. Jimenez, "Interdimeric Curvature in Tubulin–Tubulin Complexes Delineates the Microtubule-Destabilizing Properties of Plocabulin," *Journal of Chemical Information and Modeling*, vol. 60, no. 8, pp. 4076–4084, 2020.

[3] J. Roostalu and T. Surrey, "Microtubule nucleation: beyond the template," *Nature Reviews. Molecular Cell Biology*, vol. 18, no. 11, pp. 702–710, 2017.

[4] S. S. Parker, J. Krantz, E. A. Kwak et al., "Insulin induces microtubule stabilization and regulates the microtubule plus-end tracking protein network in adipocytes∗[S]," *Molecular & cellular proteomics : MCP*, vol. 18, no. 7, pp. 1363–1381, 2019.

[5] M. Vleugel, M. Kok, and M. Dogterom, "Understanding force-generating microtubule systems throughin vitroreconstitution," *Cell Adhesion & Migration*, vol. 10, no. 5, pp. 475–494, 2016.

[6] P. Guedes-Dias and E. L. F. Holzbaur, "Axonal transport: driving synaptic function," *Science*, vol. 366, no. 6462, article eaaw9997, 2019.

[7] A. Valenzuela, L. Meservey, H. Nguyen, and M. M. Fu, "Golgi outposts nucleate microtubules in cells with specialized shapes," *Trends in Cell Biology*, vol. 30, no. 10, pp. 792–804, 2020.

[8] R. P. Tas, A. Chazeau, B. M. C. Cloin, M. L. A. Lambers, C. C. Hoogenraad, and L. C. Kapitein, "Differentiation between oppositely oriented microtubules controls polarized neuronal transport," *Neuron*, vol. 96, no. 6, article e1265, pp. 1264–1271, 2017.

[9] M. M. Rolls, P. Thyagarajan, and C. Feng, "Microtubule dynamics in healthy and injured neurons," *Developmental Neurobiology*, vol. 81, no. 3, pp. 321–332, 2021.

[10] F. Marchisella, E. T. Coffey, and P. Hollos, "Microtubule and microtubule associated protein anomalies in psychiatric disease," *Cytoskeleton*, vol. 73, no. 10, pp. 596–611, 2016.

[11] A. Desai and T. J. Mitchison, "Microtubule polymerization dynamics," *Annual Review of Cell and Developmental Biology*, vol. 13, no. 1, pp. 83–117, 1997.

[12] T. Horio and T. Murata, "The role of dynamic instability in microtubule organization," *Frontiers in Plant Science*, vol. 5, article 511, 2014.

[13] L. Penazzi, L. Bakota, and R. Brandt, "Microtubule dynamics in neuronal development, plasticity, and neurodegeneration," *International Review of Cell and Molecular Biology*, vol. 321, pp. 89–169, 2016.

[14] E. W. Dent, "Of microtubules and memory: implications for microtubule dynamics in dendrites and spines," *Molecular Biology of the Cell*, vol. 28, no. 1, pp. 1–8, 2017.

[15] R. Heald and E. Nogales, "Microtubule dynamics," *Journal of Cell Science*, vol. 115, no. 1, pp. 3-4, 2002.

[16] A. C. Schmit, E. Herzog, and M. E. Chaboute, "GIP/MZT1 proteins: key players in centromere regulation," *Cell Cycle*, vol. 14, no. 23, pp. 3665-3666, 2015.

[17] C. A. Tovey and P. T. Conduit, "Microtubule nucleation by γ-tubulin complexes and beyond," *Essays in Biochemistry*, vol. 62, no. 6, pp. 765–780, 2018.

[18] P. Liu, M. Wurtz, E. Zupa, S. Pfeffer, and E. Schiebel, "Microtubule nucleation: The waltz between γ-tubulin ring complex and associated proteins," *Current Opinion in Cell Biology*, vol. 68, pp. 124–131, 2021.

[19] S. L. Leong, E. M. Lynch, J. Zou et al., "Reconstitution of microtubule nucleation in vitro reveals novel roles for Mzt1," *Current Biology*, vol. 29, no. 13, article e2110, pp. 2199–2207, 2019.

[20] H. V. Goodson and E. M. Jonasson, "Microtubules and microtubule-associated proteins," *Cold Spring Harbor perspectives in biology*, vol. 10, no. 6, article a022608, 2018.

[21] K. K. Gupta, C. Li, A. Duan et al., "Mechanism for the catastrophe-promoting activity of the microtubule destabilizer Op18/stathmin," *Proceedings of the National Academy of Sciences of the United States of America*, vol. 110, no. 51, pp. 20449–20454, 2013.

[22] P. Ayaz, S. Munyoki, E. A. Geyer et al., "A tethered delivery mechanism explains the catalytic action of a microtubule polymerase," *Elife*, vol. 3, article e03069, 2014.

[23] J. Olah, A. Lehotzky, S. Szunyogh, T. Szenasi, F. Orosz, and J. Ovadi, "Microtubule-associated proteins with regulatory functions by day and pathological potency at night," *Cells*, vol. 9, no. 2, article 357, 2020.

[24] Y. Ruan, L. S. Halat, D. Khan et al., "The microtubule-associated protein CLASP sustains cell proliferation through a brassinosteroid signaling negative feedback loop," *Current Biology*, vol. 28, no. 17, article e2715, pp. 2718–2729, 2018.

[25] Y. Fan, G. M. Burkart, and R. Dixit, "The arabidopsis SPIRAL2 protein targets and stabilizes microtubule minus ends," *Current Biology*, vol. 28, no. 6, article e983, pp. 987–994, 2018.

[26] L. Dehmelt and S. Halpain, "The MAP2/Tau family of microtubule-associated proteins," *Genome Biology*, vol. 6, no. 1, article 204, 2005.

[27] J. Zhang, R. W. M. Min, K. Le et al., "The role of MAP2 kinases and p38 kinase in acute murine liver injury models," *Cell Death & Disease*, vol. 8, no. 6, article e2903, 2017.

[28] L. F. Gumy, E. A. Katrukha, I. Grigoriev et al., "MAP2 defines a pre-axonal filtering zone to regulate KIF1- versus KIF5-dependent cargo transport in sensory neurons," *Neuron*, vol. 94, no. 2, article e347, pp. 347–362, 2017.

[29] K. Melkova, V. Zapletal, S. Narasimhan et al., "Structure and functions of microtubule associated proteins Tau and MAP2c: similarities and differences," *Biomolecules*, vol. 9, no. 3, article 105, 2019.

[30] R. Brandt, N. I. Trushina, and L. Bakota, "Much more than a sytoskeletal protein: physiological and pathological functions of the non-microtubule binding region of Tau," *Frontiers in Neurology*, vol. 11, article 12691269, 2020.

[31] R. L. Mueller, B. Combs, M. M. Alhadidy, S. T. Brady, G. A. Morfini, and N. M. Kanaan, "Tau: a signaling hub protein," *Frontiers in Molecular Neuroscience*, vol. 14, article 647054, 2021.

[32] B. Caballero, M. Bourdenx, E. Luengo et al., "Acetylated tau inhibits chaperone-mediated autophagy and promotes tau pathology propagation in mice," *Nature Communications*, vol. \, no. 1, article 2238, 2021.

[33] D. Janning, M. Igaev, F. Sundermann et al., "Single-molecule tracking of tau reveals fast kiss-and-hop interaction with microtubules in living neurons," *Molecular Biology of the Cell*, vol. 25, no. 22, pp. 3541–3551, 2014.

[34] N. I. Trushina, L. Bakota, A. Y. Mulkidjanian, and R. Brandt, "The evolution of Tau phosphorylation and interactions," *Frontiers in aging Neuroscience*, vol. 11, article 256, 2019.

[35] H. Kadavath, R. V. Hofele, J. Biernat et al., "Tau stabilizes microtubules by binding at the interface between tubulin heterodimers," *Proceedings of the National Academy of Sciences of the United States of America*, vol. 112, no. 24, pp. 7501–7506, 2015.

[36] Y. Okada and N. Hirokawa, "Mechanism of the single-headed processivity: diffusional anchoring between the K-loop of kinesin and the C terminus of tubulin," *Proceedings of the National Academy of Sciences of the United States of America*, vol. 97, no. 2, pp. 640–645, 2000.

[37] S. Wegmann, J. Biernat, and E. Mandelkow, "A current view on Tau protein phosphorylation in Alzheimer's disease," *Current Opinion in Neurobiology*, vol. 69, pp. 131–138, 2021.

[38] L. Wang, F. X. Shi, N. Li et al., "AMPK ameliorates tau acetylation and memory impairment through Sirt1," *Molecular Neurobiology*, vol. 57, no. 12, pp. 5011–5025, 2020.

[39] B. Klein, H. Mrowetz, C. Kreutzer et al., "DCX(+) neuronal progenitors contribute to new oligodendrocytes during remyelination in the hippocampus," *Scientific Reports*, vol. 10, no. 1, article 20095, 2020.

[40] J. Dhaliwal, Y. Xi, E. Bruel-Jungerman, J. Germain, F. Francis, and D. C. Lagace, "Doublecortin (DCX) is not essential for survival and differentiation of newborn neurons in the adult mouse dentate gyrus," *Frontiers in Neuroscience*, vol. 9, article 494, 2015.

[41] C. J. Bott, L. P. McMahon, J. M. Keil, C. C. Yap, K. Y. Kwan, and B. Winckler, "Nestin selectively facilitates the phosphorylation of the lissencephaly-linked protein doublecortin (DCX) by cdk5/p35 to regulate growth cone morphology and Sema3a sensitivity in developing neurons," *The Journal of neuroscience : the official journal of the Society for Neuroscience*, vol. 40, no. 19, pp. 3720–3740, 2020.

[42] T. Pramparo, Y. H. Youn, J. Yingling, S. Hirotsune, and A. Wynshaw-Boris, "Novel embryonic neuronal migration and proliferation defects in Dcx mutant mice are exacerbated by Lis1 reduction," *The Journal of neuroscience : the official journal of the Society for Neuroscience*, vol. 30, no. 8, pp. 3002–3012, 2010.

[43] E. Q. Wei, D. S. Sinden, L. Mao, H. Zhang, C. Wang, and G. S. Pitt, "Inducible Fgf13 ablation enhances caveolae-mediated cardioprotection during cardiac pressure overload," *Proceedings of the National Academy of Sciences of the United States of America*, vol. 114, no. 20, pp. E4010–E4019, 2017.

[44] Q. F. Wu, L. Yang, S. Li et al., "Fibroblast growth factor 13 is a microtubule-stabilizing protein regulating neuronal polarization and migration," *Cell*, vol. 149, no. 7, pp. 1549–1564, 2012.

[45] J. Li, Q. Wang, H. Wang et al., "Lentivirus mediating FGF13 enhances axon regeneration after spinal cord injury by stabilizing microtubule and improving mitochondrial function," *Journal of Neurotrauma*, vol. 35, no. 3, pp. 548–559, 2018.

[46] J. Atherton, Y. Luo, S. Xiang et al., "Structural determinants of microtubule minus end preference in CAMSAP CKK domains," *Nature Communications*, vol. 10, no. 1, article 5236, 2019.

[47] K. Vukusic, I. Ponjavic, R. Buda, P. Risteski, and I. M. Tolic, "Microtubule-sliding modules based on kinesins EG5 and PRC1-dependent KIF4A drive human spindle elongation," *Developmental Cell*, vol. 56, no. 9, article e1210, pp. 1253–1267, 2021.

[48] M. K. Gardner, M. Zanic, C. Gell, V. Bormuth, and J. Howard, "Depolymerizing kinesins Kip3 and MCAK shape cellular microtubule architecture by differential control of catastrophe," *Cell*, vol. 147, no. 5, pp. 1092–1103, 2011.

[49] A. Mitra, F. Ruhnow, S. Girardo, and S. Diez, "Directionally biased sidestepping of Kip3/kinesin-8 is regulated by ATP waiting time and motor–microtubule interaction strength," *Proceedings of the National Academy of Sciences of the United States of America*, vol. 115, no. 34, pp. E7950–E7959, 2018.

[50] Y. J. Liang and W. X. Yang, "Kinesins in MAPK cascade: how kinesin motors are involved in the MAPK pathway?," *Gene*, vol. 684, pp. 1–9, 2019.

[51] K. C. McNeely, T. D. Cupp, J. N. Little, K. M. Janisch, A. Shrestha, and N. D. Dwyer, "Mutation of kinesin-6 Kif20b causes defects in cortical neuron polarization and morphogenesis," *Neural Development*, vol. 12, no. 1, article 684, pp. 1–9, 2017.

[52] A. Akhmanova and M. O. Steinmetz, "Microtubule minus-end regulation at a glance," *Journal of Cell Science*, vol. 132, no. 11, article jcs227850, 2019.

[53] M. C. Hendershott and R. D. Vale, "Regulation of microtubule minus-end dynamics by CAMSAPs and Patronin," *Proceedings of the National Academy of Sciences of the United States of America*, vol. 111, no. 16, pp. 5860–5865, 2014.

[54] A. Akhmanova and C. C. Hoogenraad, "Microtubule minus-end-targeting proteins," *Current Biology : CB*, vol. 25, no. 4, pp. R162–R171, 2015.

[55] Y. Cao, J. Lipka, R. Stucchi et al., "Microtubule minus-end binding protein CAMSAP2 and kinesin-14 motor KIFC3 control dendritic microtubule organization," *Current Biology*, vol. 30, no. 5, article e896, pp. 899–908, 2020.

[56] V. Pongrakhananon, H. Saito, S. Hiver et al., "CAMSAP3 maintains neuronal polarity through regulation of microtubule stability," *Proceedings of the National Academy of Sciences of the United States of America*, vol. 115, no. 39, pp. 9750–9755, 2018.

[57] P. W. Baas, A. N. Rao, A. J. Matamoros, and L. Leo, "Stability properties of neuronal microtubules," *Cytoskeleton*, vol. 73, no. 9, pp. 442–460, 2016.

[58] P. Kratsios and O. Hobert, "Nervous system development: flies and worms converging on neuron identity control," *Current biology : CB*, vol. 28, no. 19, pp. R1154–R1157, 2018.

[59] M. Schelski and F. Bradke, "Neuronal polarization: from spatiotemporal signaling to cytoskeletal dynamics," *Molecular and Cellular Neurosciences*, vol. 84, pp. 11–28, 2017.

[60] C. G. Dotti, C. A. Sullivan, and G. A. Banker, "The establishment of polarity by hippocampal neurons in culture," *The Journal of neuroscience : the official journal of the Society for Neuroscience*, vol. 8, no. 4, pp. 1454–1468, 1988.

[61] X. Liang, M. Kokes, R. D. Fetter et al., "Growth cone-localized microtubule organizing center establishes microtubule orientation in dendrites," *Elife*, vol. 9, article e56547, 2020.

[62] P. R. Gordon-Weeks, "Microtubules and growth cone function," *Journal of Neurobiology*, vol. 58, no. 1, pp. 70–83, 2004.

[63] O. F. Omotade, S. L. Pollitt, and J. Q. Zheng, "Actin-based growth cone motility and guidance," *Molecular and Cellular Neurosciences*, vol. 84, pp. 4–10, 2017.

[64] T. D. Pollard, "New Light on Growth Cone Navigation," *Developmental Cell*, vol. 35, no. 6, pp. 672-673, 2015.

[65] Y. Zou, "Breaking symmetry - cell polarity signaling pathways in growth cone guidance and synapse formation," *Current Opinion in Neurobiology*, vol. 63, pp. 77–86, 2020.

[66] E. S. Chhabra and H. N. Higgs, "The many faces of actin: matching assembly factors with cellular structures," *Nature Cell Biology*, vol. 9, no. 10, pp. 1110–1121, 2007.

[67] S. Geraldo and P. R. Gordon-Weeks, "Cytoskeletal dynamics in growth-cone steering," *Journal of Cell Science*, vol. 122, no. 20, pp. 3595–3604, 2009.

[68] J. Round and E. Stein, "Netrin signaling leading to directed growth cone steering," *Current Opinion in Neurobiology*, vol. 17, no. 1, pp. 15–21, 2007.

[69] M. T. Kelliher, H. A. Saunders, and J. Wildonger, "Microtubule control of functional architecture in neurons," *Current Opinion in Neurobiology*, vol. 57, pp. 39–45, 2019.

[70] E. M. Craig, H. T. Yeung, A. N. Rao, and P. W. Baas, "Polarity sorting of axonal microtubules: a computational study," *Molecular Biology of the Cell*, vol. 28, no. 23, pp. 3271–3285, 2017.

[71] W. Lu and V. I. Gelfand, "Moonlighting motors: kinesin, dynein, and cell polarity," *Trends in Cell Biology*, vol. 27, no. 7, pp. 505–514, 2017.

[72] G. Bhabha, G. T. Johnson, C. M. Schroeder, and R. D. Vale, "How dynein moves along microtubules," *Trends in Biochemical Sciences*, vol. 41, no. 1, pp. 94–105, 2016.

[73] N. Hirokawa, S. Niwa, and Y. Tanaka, "Molecular motors in neurons: transport mechanisms and roles in brain function, development, and disease," *Neuron*, vol. 68, no. 4, pp. 610–638, 2010.

[74] S. F. van Beuningen and C. C. Hoogenraad, "Neuronal polarity: remodeling microtubule organization," *Current Opinion in Neurobiology*, vol. 39, pp. 1–7, 2016.

[75] O. R. Wilkes and A. W. Moore, "Distinct microtubule organizing center mechanisms combine to generate neuron polarity and arbor complexity," *Frontiers in Cellular Neuroscience*, vol. 14, article 594199, 2020.

[76] T. Y. Eom, A. Stanco, J. Guo et al., "Differential regulation of microtubule severing by APC underlies distinct patterns of projection neuron and interneuron migration," *Developmental Cell*, vol. 31, no. 6, pp. 677–689, 2014.

[77] X. Xie, S. Wang, M. Li et al., "alpha-TubK40me3 is required for neuronal polarization and migration by promoting microtubule formation," *Nature Communications*, vol. 12, no. 1, article 4113, 2021.

[78] D. Seetapun and D. J. Odde, "Cell-length-dependent microtubule accumulation during polarization," *Current biology : CB*, vol. 20, no. 11, pp. 979–988, 2010.

[79] T. Namba, Y. Funahashi, S. Nakamuta, C. Xu, T. Takano, and K. Kaibuchi, "Extracellular and intracellular signaling for neuronal polarity," *Physiological Reviews*, vol. 95, no. 3, pp. 995–1024, 2015.

[80] H. Witte and F. Bradke, "The role of the cytoskeleton during neuronal polarization," *Current Opinion in Neurobiology*, vol. 18, no. 5, pp. 479–487, 2008.

[81] S. M. Hapak, S. Ghosh, and C. V. Rothlin, "Axon regeneration: antagonistic signaling pairs in neuronal polarization," *Trends in Molecular Medicine*, vol. 24, no. 7, pp. 615–629, 2018.

[82] S. Gomis-Ruth, C. J. Wierenga, and F. Bradke, "Plasticity of polarization: changing dendrites into axons in neurons integrated in neuronal circuits," *Current biology : CB*, vol. 18, no. 13, pp. 992–1000, 2008.

[83] M. Toriyama, S. Kozawa, Y. Sakumura, and N. Inagaki, "Conversion of a signal into forces for axon outgrowth through Pak1-mediated shootin1 phosphorylation," *Current biology : CB*, vol. 23, no. 6, pp. 529–534, 2013.

[84] T. Sapir, T. Levy, A. Sakakibara, A. Rabinkov, T. Miyata, and O. Reiner, "Shootin1 acts in concert with KIF20B to promote polarization of migrating neurons," *The Journal of neuroscience : the official journal of the Society for Neuroscience*, vol. 33, no. 29, pp. 11932–11948, 2013.

[85] Y. Kubo, K. Baba, M. Toriyama et al., "Shootin1–cortactin interaction mediates signal–force transduction for axon outgrowth," *The Journal of Cell Biology*, vol. 210, no. 4, pp. 663–676, 2015.

[86] A. Capizzi, J. Woo, and M. Verduzco-Gutierrez, "Traumatic brain injury: an overview of epidemiology, pathophysiology, and medical management," *The Medical Clinics of North America*, vol. 104, no. 2, pp. 213–238, 2020.

[87] B. Fan, Z. Wei, X. Yao et al., "Microenvironment imbalance of spinal cord injury," *Cell Transplantation*, vol. 27, no. 6, pp. 853–866, 2018.

[88] G. Liu and T. Dwyer, "Microtubule dynamics in axon guidance," *Neuroscience Bulletin*, vol. 30, no. 4, pp. 569–583, 2014.

[89] I. Hahn, A. Voelzmann, Y. T. Liew, B. Costa-Gomes, and A. Prokop, "The model of local axon homeostasis - explaining the role and regulation of microtubule bundles in axon maintenance and pathology," *Neural Development*, vol. 14, no. 1, pp. 1–28, 2019.

[90] O. Blanquie and F. Bradke, "Cytoskeleton dynamics in axon regeneration," *Current Opinion in Neurobiology*, vol. 51, pp. 60–69, 2018.

[91] A. Kumari and D. Panda, "Regulation of microtubule stability by centrosomal proteins," *IUBMB Life*, vol. 70, no. 7, pp. 602–611, 2018.

[92] A. Erturk, F. Hellal, J. Enes, and F. Bradke, "Disorganized microtubules underlie the formation of retraction bulbs and the failure of axonal regeneration," *The Journal of neuroscience : the official journal of the Society for Neuroscience*, vol. 27, no. 34, pp. 9169–9180, 2007.

[93] Z. Xu, L. Schaedel, D. Portran et al., "Microtubules acquire resistance from mechanical breakage through intralumenal acetylation," *Science*, vol. 356, no. 6335, pp. 328–332, 2017.

[94] D. Najem, K. Rennie, M. Ribecco-Lutkiewicz et al., "Traumatic brain injury: classification, models, and markers," *Biochemistry and Cell Biology = Biochimie et biologie cellulaire*, vol. 96, no. 4, pp. 391–406, 2018.

[95] R. Rubenstein, B. Chang, J. K. Yue et al., "Comparing plasma phospho tau, total tau, and phospho tau-total tau ratio as acute and chronic traumatic brain injury biomarkers," *JAMA Neurology*, vol. 74, no. 9, pp. 1063–1072, 2017.

[96] J. A. Chuckowree, Z. Zhu, M. Brizuela, K. M. Lee, C. A. Blizzard, and T. C. Dickson, "The microtubule-modulating drug epothilone D alters dendritic spine morphology in a mouse model of mild traumatic brain injury," *Frontiers in Cellular Neuroscience*, vol. 12, article 223, 2018.

[97] Y. C. Yap, A. E. King, R. M. Guijt et al., "Mild and repetitive very mild axonal stretch injury triggers cytoskeletal mislocalization and growth cone collapse," *PloS One*, vol. 12, no. 5, article e0176997, 2017.

[98] J. M. Griffin and F. Bradke, "Therapeutic repair for spinal cord injury: combinatory approaches to address a multifaceted problem," *EMBO Molecular Medicine*, vol. 12, no. 3, article e11505, 2020.

[99] H. de Forges, A. Bouissou, and F. Perez, "Interplay between microtubule dynamics and intracellular organization," *The International Journal of Biochemistry & Cell Biology*, vol. 44, no. 2, pp. 266–274, 2012.

[100] Y. Y. Duan, Y. Chai, N. L. Zhang, D. M. Zhao, and C. Yang, "Microtubule stabilization promotes microcirculation reconstruction after spinal cord injury," *Journal of molecular neuroscience : MN*, vol. 71, no. 3, pp. 583–595, 2021.

[101] J. Ruschel and F. Bradke, "Systemic administration of epothilone D improves functional recovery of walking after rat

spinal cord contusion injury," *Experimental Neurology*, vol. 306, pp. 243–249, 2018.

[102] J. Ruschel, F. Hellal, K. C. Flynn et al., "Systemic administration of epothilone B promotes axon regeneration after spinal cord injury," *Science*, vol. 348, no. 6232, pp. 347–352, 2015.

[103] B. Sandner, R. Puttagunta, M. Motsch et al., "Systemic epothilone D improves hindlimb function after spinal cord contusion injury in rats," *Experimental Neurology*, vol. 306, pp. 250–259, 2018.

[104] M. He, Y. Ding, C. Chu, J. Tang, Q. Xiao, and Z. G. Luo, "Autophagy induction stabilizes microtubules and promotes axon regeneration after spinal cord injury," *Proceedings of the National Academy of Sciences of the United States of America*, vol. 113, no. 40, pp. 11324–11329, 2016.

[105] Y. Rong, W. Liu, J. Wang et al., "Neural stem cell-derived small extracellular vesicles attenuate apoptosis and neuroinflammation after traumatic spinal cord injury by activating autophagy," *Cell Death & Disease*, vol. 10, no. 5, pp. 1–18, 2019.

[106] F. Naaz, M. R. Haider, S. Shafi, and M. S. Yar, "Anti-tubulin agents of natural origin: targeting taxol, vinca, and colchicine binding domains," *European Journal of Medicinal Chemistry*, vol. 171, pp. 310–331, 2019.

[107] D. Cao, Y. Liu, W. Yan et al., "Design, synthesis, and evaluation of in vitro and in vivo anticancer activity of 4-substituted coumarins: a novel class of potent tubulin polymerization inhibitors," *Journal of Medicinal Chemistry*, vol. 59, no. 12, pp. 5721–5739, 2016.

[108] K. H. Altmann, "Microtubule-stabilizing agents: a growing class of important anticancer drugs," *Current Opinion in Chemical Biology*, vol. 5, no. 4, pp. 424–431, 2001.

[109] L. A. Amos, "Microtubule structure and its stabilisation," *Organic & Biomolecular Chemistry*, vol. 2, no. 15, pp. 2153–2160, 2004.

[110] S. Florian and T. J. Mitchison, "Anti-microtubule drugs," *The Mitotic Spindle*, vol. 1413, pp. 403–421, 2016.

[111] J. Bennouna, J. P. Delord, M. Campone, and L. Nguyen, "Vinflunine: a new microtubule inhibitor agent," *Clinical cancer research : an official journal of the American Association for Cancer Research*, vol. 14, no. 6, pp. 1625–1632, 2008.

[112] A. E. Prota, K. Bargsten, D. Zurwerra et al., "Molecular mechanism of action of microtubule-stabilizing anticancer agents," *Science*, vol. 339, no. 6119, pp. 587–590, 2013.

[113] A. Akhmanova and M. O. Steinmetz, "Control of microtubule organization and dynamics: two ends in the limelight," *Nature Reviews. Molecular Cell Biology*, vol. 16, no. 12, pp. 711–726, 2015.

[114] D. Fanale, G. Bronte, F. Passiglia et al., "Stabilizing versus destabilizing the microtubules: a double-edge sword for an effective cancer treatment option?," *Analytical Cellular Pathology*, vol. 2015, Article ID 690916, 19 pages, 2015.

[115] J. J. Field, A. Kanakkanthara, and J. H. Miller, "Microtubule-targeting agents are clinically successful due to both mitotic and interphase impairment of microtubule function," *Bioorganic & Medicinal Chemistry*, vol. 22, no. 18, pp. 5050–5059, 2014.

[116] L. C. Kapitein and C. C. Hoogenraad, "Building the neuronal microtubule cytoskeleton," *Neuron*, vol. 87, no. 3, pp. 492–506, 2015.

[117] A. Sferra, F. Nicita, and E. Bertini, "Microtubule dysfunction: a common feature of neurodegenerative diseases," *International journal of molecular sciences*, vol. 21, no. 19, article 7354, 2020.

[118] R. Altaha, T. Fojo, E. Reed, and J. Abraham, "Epothilones: a novel class of non-taxane microtubule-stabilizing agents," *Current Pharmaceutical Design*, vol. 8, no. 19, pp. 1707–1712, 2002.

[119] F. Hellal, A. Hurtado, J. Ruschel et al., "Microtubule stabilization reduces scarring and causes axon regeneration after spinal cord injury," *Science*, vol. 331, no. 6019, pp. 928–931, 2011.

[120] P. G. Popovich, C. A. Tovar, S. Lemeshow, Q. Yin, and L. B. Jakeman, "Independent evaluation of the anatomical and behavioral effects of Taxol in rat models of spinal cord injury," *Experimental Neurology*, vol. 261, pp. 97–108, 2014.

[121] V. Sengottuvel, M. Leibinger, M. Pfreimer, A. Andreadaki, and D. Fischer, "Taxol facilitates axon regeneration in the mature CNS," *The Journal of neuroscience : the official journal of the Society for Neuroscience*, vol. 31, no. 7, pp. 2688–2699, 2011.

[122] A. R. Duan and H. V. Goodson, "Taxol-stabilized microtubules promote the formation of filaments from unmodified full-length tau in vitro," *Molecular Biology of the Cell*, vol. 23, no. 24, pp. 4796–4806, 2012.

[123] D. Cartelli, F. Casagrande, C. L. Busceti et al., "Microtubule alterations occur early in experimental parkinsonism and the microtubule stabilizer epothilone D is neuroprotective," *Scientific Reports*, vol. 3, article 1837, pp. 1–10, 2013.

[124] B. Zhang, J. Carroll, J. Q. Trojanowski et al., "The microtubule-stabilizing agent, epothilone D, reduces axonal dysfunction, neurotoxicity, cognitive deficits, and Alzheimer-like pathology in an interventional study with aged tau transgenic mice," *The Journal of neuroscience : the official journal of the Society for Neuroscience*, vol. 32, no. 11, pp. 3601–3611, 2012.

[125] P. Mondal, G. Das, J. Khan, K. Pradhan, and S. Ghosh, "Crafting of neuroprotective octapeptide from taxol-binding pocket of β-tubulin," *ACS Chemical Neuroscience*, vol. 9, no. 3, pp. 615–625, 2018.

[126] S. Quraishe, C. M. Cowan, and A. Mudher, "NAP (davunetide) rescues neuronal dysfunction in a Drosophila model of tauopathy," *Molecular Psychiatry*, vol. 18, no. 7, pp. 834–842, 2013.

[127] I. Magen and I. Gozes, "Microtubule-stabilizing peptides and small molecules protecting axonal transport and brain function: focus on davunetide (NAP)," *Neuropeptides*, vol. 47, no. 6, pp. 489–495, 2013.

[128] C. Schinke, V. Fernandez Vallone, A. Ivanov et al., "Modeling chemotherapy induced neurotoxicity with human induced pluripotent stem cell (iPSC) -derived sensory neurons," *Neurobiology of Disease*, vol. 155, article 105391, 2021.

[129] V. Das and J. H. Miller, "Microtubule stabilization by peloruside A and paclitaxel rescues degenerating neurons from okadaic acid-induced tau phosphorylation," *The European Journal of Neuroscience*, vol. 35, no. 11, pp. 1705–1717, 2012.

[130] Y. Zhao, X. Mu, and G. Du, "Microtubule-stabilizing agents: new drug discovery and cancer therapy," *Pharmacology & Therapeutics*, vol. 162, pp. 134–143, 2016.

[131] M. N. Kundranda and J. Niu, "Albumin-bound paclitaxel in solid tumors: clinical development and future directions," *Drug Design, Development and Therapy*, vol. 9, pp. 3767–3777, 2015.

[132] M. Joerger, "Metabolism of the taxanes including nab-paclitaxel," *Expert Opinion on Drug Metabolism & Toxicology*, vol. 11, no. 5, pp. 691–702, 2015.

[133] N. I. Marupudi, J. E. Han, K. W. Li, V. M. Renard, B. M. Tyler, and H. Brem, "Paclitaxel: a review of adverse toxicities and novel delivery strategies," *Expert Opinion on Drug Safety*, vol. 6, no. 5, pp. 609–621, 2007.

[134] L. Zhu and L. Chen, "Progress in research on paclitaxel and tumor immunotherapy," *Cellular & Molecular Biology Letters*, vol. 24, no. 1, pp. 1–11, 2019.

[135] X. Li, C. Fan, Z. Xiao et al., "A collagen microchannel scaffold carrying paclitaxel-liposomes induces neuronal differentiation of neural stem cells through Wnt/β-catenin signaling for spinal cord injury repair," *Biomaterials*, vol. 183, pp. 114–127, 2018.

[136] J. Mulzer and K. Prantz, "Total synthesis of epothilones AF," in *The Epothilones: An Outstanding Family of Anti-Tumor Agents*, pp. 55–133, Springer, Vienna, 2009.

[137] R. Long, W. Yang, and G. Huang, "Preparation and separation of epothilones with anticancer activity," *Chemical Biology & Drug Design*, vol. 96, no. 2, pp. 785–789, 2020.

[138] S. Forli, "Epothilones: from discovery to clinical trials," *Current Topics in Medicinal Chemistry*, vol. 14, no. 20, pp. 2312–2321, 2014.

[139] L. T. Vahdat, "Clinical studies with epothilones for the treatment of metastatic breast cancer," *Seminars in Oncology*, vol. 35, 2 Suppl 2, pp. S22–S30, 2008.

[140] K. R. Brunden, B. Zhang, J. Carroll et al., "Epothilone D improves microtubule density, axonal integrity, and cognition in a transgenic mouse model of tauopathy," *The Journal of neuroscience : the official journal of the Society for Neuroscience*, vol. 30, no. 41, pp. 13861–13866, 2010.

[141] W. Xue, H. Zhang, Y. Fan et al., "Upregulation of Apol8 by epothilone D facilitates the neuronal relay of transplanted NSCs in spinal cord injury," *Stem Cell Research & Therapy*, vol. 12, no. 1, pp. 1–12, 2021.

[142] D. Donovan and L. T. Vahdat, "Epothilones: clinical update and future directions," *Oncology (Williston Park)*, vol. 22, no. 4, pp. 408–416, 2008.

[143] C. Kugler, C. Thielscher, B. A. Tambe et al., "Epothilones improve axonal growth and motor outcomes after stroke in the adult mammalian," *Cell Reports.Medicine*, vol. 1, no. 9, article 100159, 2020.

[144] E. L. Schwartz, "Antivascular actions of microtubule-binding drugs," *Clinical cancer research : an official journal of the American Association for Cancer Research*, vol. 15, no. 8, pp. 2594–2601, 2009.

[145] A. D. Tangutur, D. Kumar, K. V. Krishna, and S. Kantevari, "Microtubule targeting agents as cancer chemotherapeutics: an overview of molecular hybrids as stabilizing and destabilizing agents," *Current Topics in Medicinal Chemistry*, vol. 17, no. 22, pp. 2523–2537, 2017.

[146] M. Moudi, R. Go, C. Y. Yien, and M. Nazre, "Vinca alkaloids," *International Journal of Preventive Medicine*, vol. 4, no. 11, pp. 1231–1235, 2013.

[147] E. Martino, G. Casamassima, S. Castiglione et al., "Vinca alkaloids and analogues as anti-cancer agents: looking back, peering ahead," *Bioorganic & Medicinal Chemistry Letters*, vol. 28, no. 17, pp. 2816–2826, 2018.

[148] R. Rahmani and X. J. Zhou, "Pharmacokinetics and metabolism of vinca alkaloids," *Cancer Surveys*, vol. 17, pp. 269–281, 1993.

[149] X. J. Zhou and R. Rahmani, "Preclinical and clinical pharmacology of vinca alkaloids," *Drugs*, vol. 44, no. 4, pp. 1–16, 1992.

[150] S. Lobert, "Neurotoxicity in cancer chemotherapy: vinca alkaloids," *Critical Care Nurse*, vol. 17, no. 4, pp. 71–79, 1997.

[151] C. Angelidis, Z. Kotsialou, C. Kossyvakis et al., "Colchicine pharmacokinetics and mechanism of action," *Current Pharmaceutical Design*, vol. 24, no. 6, pp. 659–663, 2018.

[152] T. Tateishi, P. Soucek, Y. Caraco, F. P. Guengerich, and A. J. Wood, "Colchicine biotransformation by human liver microsomes: identification of cyp3a4 as the major isoform responsible for colchicine demethylation," *Biochemical Pharmacology*, vol. 53, no. 1, pp. 111–116, 1997.

[153] R. Herran-Monge, A. Muriel-Bombin, M. Garcia-Garcia, A. Duenas-Laita, M. L. Fernandez-Rodriguez, and A. M. Prieto de Lamo, "Accidental fatal colchicine overdose," *Medicina Intensiva*, vol. 37, no. 6, pp. 434–436, 2013.

[154] E. Niel and J. M. Scherrmann, "Colchicine today," *Joint Bone Spine*, vol. 73, no. 6, pp. 672–678, 2006.

[155] Y. Finkelstein, S. E. Aks, J. R. Hutson et al., "Colchicine poisoning: the dark side of an ancient drug," *Clinical Toxicology*, vol. 48, no. 5, pp. 407–414, 2010.

[156] A. Urbaniak, F. Jousheghany, S. Pina-Oviedo et al., "Carbamate derivatives of colchicine show potent activity towards primary acute lymphoblastic leukemia and primary breast cancer cells-in vitro and ex vivo study," *Journal of Biochemical and Molecular Toxicology*, vol. 34, no. 6, article e22487, 2020.

[157] B. A. Winn, L. Devkota, B. Kuch et al., "Bioreductively activatable prodrug conjugates of combretastatin A-1 and combretastatin A-4 as anticancer agents targeted toward tumor-associated hypoxia," *Journal of Natural Products*, vol. 83, no. 4, pp. 937–954, 2020.

[158] L. Huang, J. Huang, H. Nie, Y. Li, L. Song, and F. Wu, "Design, synthesis and biological evaluation of combretastatin A-4 sulfamate derivatives as potential anti-cancer agents," *RSC Medicinal Chemistry*, vol. 12, no. 8, pp. 1374–1380, 2021.

[159] L. K. Folkes, M. Christlieb, E. Madej, M. R. Stratford, and P. Wardman, "Oxidative metabolism of combretastatin A-1 produces quinone intermediates with the potential to bind to nucleophiles and to enhance oxidative stress via free radicals," *Chemical Research in Toxicology*, vol. 20, no. 12, pp. 1885–1894, 2007.

[160] M. Weigel, L. Wang, and M. M. Fu, "Microtubule organization and dynamics in oligodendrocytes, astrocytes, and microglia," *Developmental Neurobiology*, vol. 81, no. 3, pp. 310–320, 2021.

[161] A. Roll-Mecak, "The tubulin code in microtubule dynamics and information encoding," *Developmental Cell*, vol. 54, no. 1, pp. 7–20, 2020.

[162] C. M. Waterman-Storer, A. Desai, J. C. Bulinski, and E. D. Salmon, "Fluorescent speckle microscopy, a method to visualize the dynamics of protein assemblies in living cells," *Current Biology*, vol. 8, no. 22, pp. 1227–1230, 1998.

[163] J. M. Cleary and W. O. Hancock, "Molecular mechanisms underlying microtubule growth dynamics," *Current Biology*, vol. 31, no. 10, pp. R560–R573, 2021.

[164] C. Janke and G. Montagnac, "Causes and consequences of microtubule acetylation," *Current Biology*, vol. 27, no. 23, pp. R1287–R1292, 2017.

[165] H. Li and W. Wu, "Microtubule stabilization promoted axonal regeneration and functional recovery after spinal root avulsion," *European Journal of Neuroscience*, vol. 46, no. 1, pp. 1650–1662, 2017.

[166] J. Logie, A. N. Ganesh, A. M. Aman, R. S. Al-Awar, and M. S. Shoichet, "Preclinical evaluation of taxane-binding peptide-modified polymeric micelles loaded with docetaxel in an orthotopic breast cancer mouse model," *Biomaterials*, vol. 123, pp. 39–47, 2017.

Hindawi
Oxidative Medicine and Cellular Longevity
Volume 2022, Article ID 8010670, 18 pages
https://doi.org/10.1155/2022/8010670

Research Article

Sesamol Attenuates Neuroinflammation by Regulating the AMPK/SIRT1/NF-κB Signaling Pathway after Spinal Cord Injury in Mice

Xiaochu Feng, Xianghang Chen, Muhammad Zaeem, Wanying Zhang, Liwan Song, Lulu Chen, Joana Mubwandarikwa, Xiangxiang Chen, Jian Xiao, Ling Xie, and Keyong Ye

Department of Orthopaedics, Affiliated Pingyang Hospital and School of Pharmaceutical Science, Wenzhou Medical University, Wenzhou, Zhejiang 325000, China

Correspondence should be addressed to Jian Xiao; xfxj2000@126.com, Ling Xie; xieling0612@163.com, and Keyong Ye; yeky12600@126.com

Received 21 August 2021; Accepted 23 November 2021; Published 6 January 2022

Academic Editor: Zonghao Tang

Inflammation is one of the crucial mechanisms mediating spinal cord injury (SCI) progress. Sesamol, a component of sesame oil, has anti-inflammatory activity, but its mechanism in SCI remains unclear. We investigated if the AMPK/SIRT1/NF-κB pathway participated in anti-inflammation of sesamol in SCI. Sesamol could inhibit neuronal apoptosis, reduce neuroinflammation, enhance M2 phenotype microglial polarization, and improved motor function recovery in mice after SCI. Furthermore, sesamol increased SIRT1 protein expression and p-AMPK/AMPK ratio, while it downregulated the p-p65/p65 ratio, indicating that sesamol treatment upregulated the AMPK/SIRT1 pathway and inhibited NF-κB activation. However, these effects were blocked by compound C which is a specific AMPK inhibitor. Together, the study suggests that sesamol is a potential drug for antineuroinflammation and improving locomotor functional recovery through regulation of the AMPK/SIRT1/NF-κB pathway in SCI.

1. Introduction

Spinal cord injury (SCI) is severe central nervous system (CNS) damage, and more than 250000 patients suffer from it every year [1]. However, there are few effective treatments for SCI. As a grievous neurological disease, SCI seriously destroys the function of motor and sensory neurons; paralysis caused by SCI brings huge medical and economic burden to the patients and their families [2, 3].

Traumatic SCI involves primary mechanical insult and the secondary injury [4]. The primary insult makes a direct crash to the spinal cord and damages cells, which also leads to a series of complex secondary injury molecular events, including toxic oxidative stress, excessive microglial activation, continuous inflammation, and rampant apoptosis [2, 5]. Neuroinflammation is one of the dominating mechanisms mediating secondary SCI progress. Microglia, the CNS-resident immune cells, maintain a resting state under control condition and become activated in response to local CNS injury [6]. There are two phenotypes of microglia called M1 and M2 after activation [7, 8]. M1 microglia are detrimental and can generate a lot of proinflammatory cytokines, including TNF-α and IL-6, while the M2 phenotype is protective and upregulates anti-inflammatory cytokines, including IL-10, which contribute to tissue regeneration and wound healing [9]. The resident microglia are activated after SCI, and then, a lot of inflammatory cytokines produced in the early stage of SCI, which will cause neuronal apoptosis, aggravate the injury and make recovery more difficult [10–12]. Therefore, it is especially important to alleviate inflammatory response in the early stage of injury.

Sesamol, a component of sesame oil [13], has been proven to have effects of anti-inflammation and neuroprotection [13–15]. As a member of the sirtuin (SIRTs) family,

SIRT1 has been proven to have positive impacts on antiaging, anti-inflammation, and reducing oxidative stress damage [16–19]. AMP-activated protein kinase (AMPK) is a critical modulator of cellular energy, which coordinates numerous pathways to maintain energy homeostasis [20]. A number of evidences have indicated that AMPK upregulates protein expression of SIRT1 and inhibits inflammation under pathological conditions [16, 21, 22]. SIRT1, as a downstream protein of the AMPK signaling pathway, also plays a part in anti-inflammation via inhibiting NF-κB [23–25]. The previous studies have proven that sesamol plays roles in anti-inflammation by suppressing NF-κB activation and upregulating AMPK signaling [26, 27] and attenuating oxidative stress via activation of SIRT1 [28].

Sesamol has potential therapeutic use in SCI, but the underlying mechanism of sesamol in SCI remains poorly understood. This study confirmed the effect and mechanism of sesamol in anti-inflammation in mice following SCI and provided evidence for the potential clinical use of sesamol in SCI.

2. Materials and Methods

2.1. Animals. Healthy 8~10-week-old male C57BL/6J mice (weighing 20~25 g) were used in this study. All mice lived in standard housing conditions and can drink and eat freely. Animal experimental operations were performed according to protocols authorized by the Laboratory Animal Ethics Committee of Wenzhou Medical University (no. wydw2018-0043).

2.2. SCI and Drug Treatments. The SCI protocol for adult mice under sterile conditions is described previously. Shortly, animals were anesthetized with 1% pentobarbital sodium (50 mg/kg, i.p.) before surgery. Skin and muscles near spinous processes were incised to expose the dorsal cord in mice. After a laminectomy at the T9-T10 level, a 10 g weight from 20 mm height was fallen onto the exposed spinal cord by a modified New York University impactor to induce a moderate SCI [29]. As a control, mice in the sham group did not suffer from SCI after laminectomy and did not receive medication. After SCI surgery, the mouse bladders were manually emptied every morning and evening until bladder function returned to normal.

All mice are randomly assigned, and mice suffering from SCI were randomly arranged to two groups: SCI and SCI+sesamol. Mice in the SCI+sesamol group were administrated daily with sesamol (10 mg/kg, i.p.) dissolved in saline for 28 days, and animals in the SCI group received the same volume of normal saline every day. Mice were sacrificed, and the damaged spinal cord was taken out for analysis at the corresponding time point after SCI. The time points of administration and experimental arrangement for mice are shown in Figure 1(a).

2.3. Cell Culture and Intervention. BV2 cells were cultivated in DMEM supplemented with 10% fetal bovine serum and 1% penicillin and streptomycin mixture in a humidified incubator with 5% CO_2 at 37°C. BV2 cells were arranged to control, lipopolysaccharide (LPS), LPS+sesamol, and compound C (LPS+sesamol+compound C) groups. Cells were incubated with 10 μM sesamol dissolved in PBS for 2 h and then suffered from LPS (1 μg/mL) for 24 h to stimulate inflammation. To explore whether the AMPK pathway participates in anti-inflammation of sesamol, cells were pretreated with compound C (a specific AMPK inhibitor) for 2 h before sesamol treatment.

2.4. Cell Viability Test. BV2 cells were incubated in a 96-well cell culture plate with 10000 cells per well for 24 h and then administrated with LPS combined with different concentrations of sesamol. The cell viability was detected with Cell Counting Kit-8 (CCK-8) according to the instructions. Shortly, after incubation, cells were further cultured for 2 h in 90 μL of fresh DMEM supplemented with 10 μL of CCK-8 solution. At last, optical density (OD) values at 450 nm were measured using a microplate reader. Six replicate wells of cells were arranged in each group.

2.5. Western Blot. After transcardial perfusion of saline, approximately 1 cm length of the spinal cord adjacent to the injury center was collected. Tissues and BV2 cells were lysed with a protein extraction reagent containing protease inhibitors and then centrifuged to get proteins. Whole tissue lysate (60 μg) or cell lysate (20 μg) was separated by 8%~12% SDS-PAGE, and then, proteins were blotted onto the PVDF membrane. Blocked with 5% (w/v) nonfat milk, the membrane was incubated at 4°C overnight using primary antibodies corresponding to these proteins: TNF-α, IL-6, Bax, CD86, CD206, p-AMPK (Thr172), AMPK, Bcl-2, SIRT1, p-p65 (S536), p65, and cleaved caspase-3, and further immersed in the corresponding HRP-conjugated secondary antibody for 1.5 h at room temperature (RT). At last, signal was visualized by using the ChemiDoc™ XRS$^+$ imaging system (Bio-Rad), and the band intensity was analyzed by using Image Lab 5.2 software (Bio-Rad).

2.6. Immunofluorescence. For immunofluorescence, haematoxylin-eosin (HE), and Nissl staining, animals underwent transcardial perfusion with 4% (w/v) paraformaldehyde (PFA), and then, the injured spinal cord tissue was taken out and fixed with 4% PFA overnight. BV2 cell climbing slices were also fixed with 4% PFA for 15 min. The tissues were then dehydrated and immersed in paraffin. Next, tissues were sliced up to 5 μm thickness of sections, and then, the slices were dewaxed using xylene and hydrated with 100, 90, 80, and 70% ethanol. After high-pressure antigen retrieval, tissue slices or BV2 cell climbing slices were blocked with 5% (w/v) BSA for 30 min at 37°C. Next, the slices were treated with primary antibodies at 4°C overnight as follows: NeuN, cleaved caspase-3, Iba1, CD206, SIRT1, and p65. Next, the sections or cell climbing slices were further incubated with a proper fluorescence-conjugated secondary antibody at RT for 1 h. Finally, DAPI was used for cellular nuclear staining. The images were visualized by using a Nikon ECLIPSE80i microscope.

2.7. HE Staining and Nissl Staining. Injured spinal cord sections were successively dewaxed and hydrated according to protocols described above. A part of tissue slices was used for HE staining with an HE kit, and other slices were stained

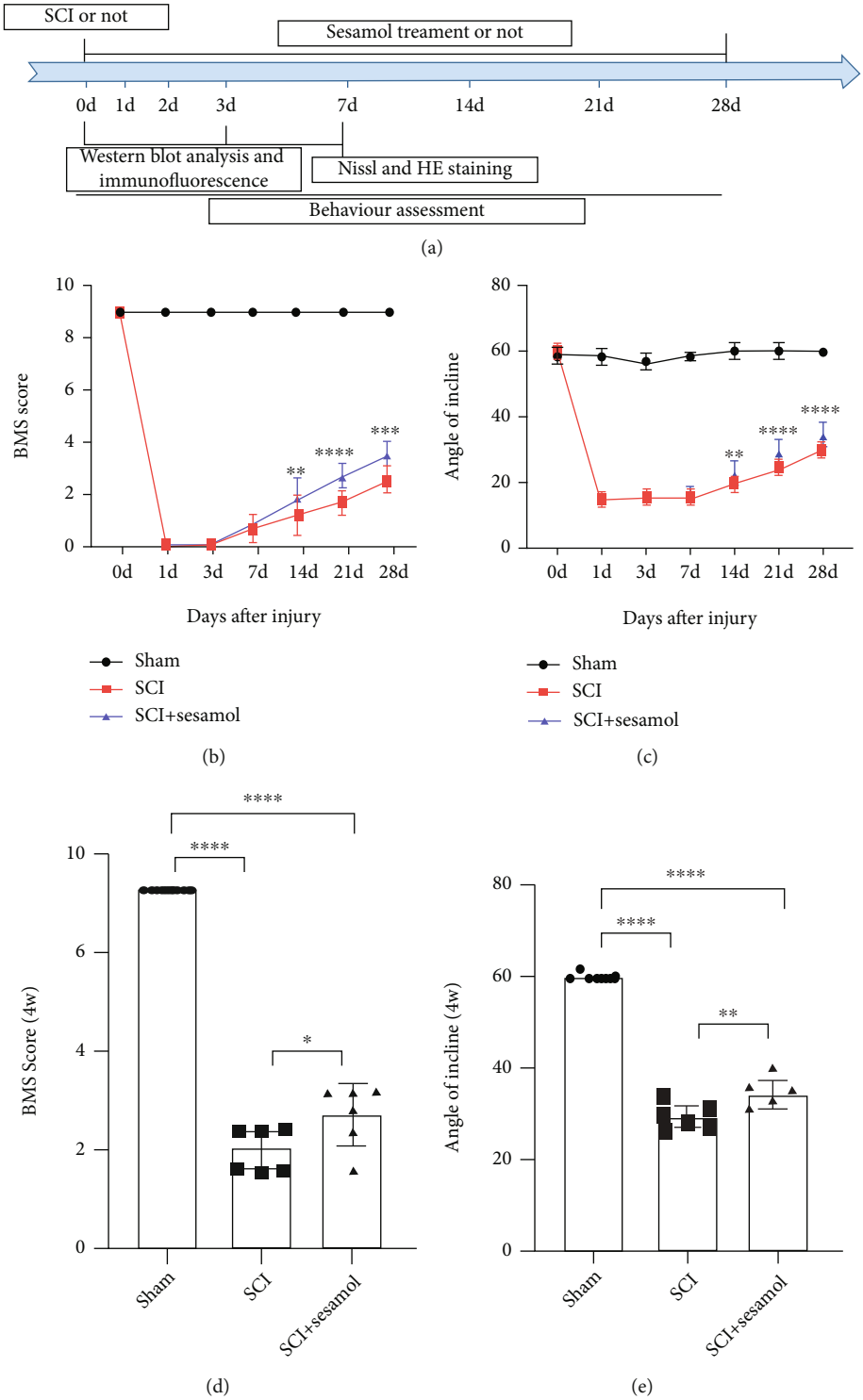

Figure 1: Continued.

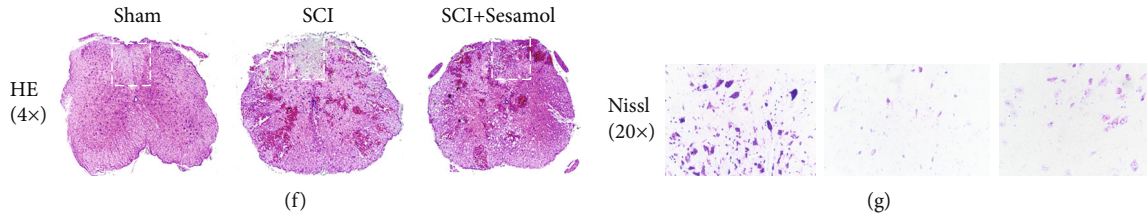

Figure 1: Sesamol evaluates histological outcomes and promotes locomotor functional restoration in mice suffering from SCI. (a) Time schedule of experimental design and analysis in mice. (b) The BMS scores of mice in each group at 0, 1, 3, 7, 14, 21, and 28 dpi. (c) Result of the inclined plane test of mice from different group at 28 dpi. (d, e) Quantitative analysis of the BMS score and incline angle at 28 dpi from (b) and (c), respectively ($n = 6$ per group). (f) H6istological assessment of the injured spinal cord by HE staining at 7 dpi. (g) Nissl staining of the injured spinal cord to evaluate the neuronal survival in each group at 7 dpi. Results are represented as mean ± SEM. $^{\#}P < 0.05$, $^{\#\#}P < 0.01$, $^{\#\#\#}P < 0.001$, and $^{\#\#\#\#}P < 0.0001$.

with cresyl violet acetate for Nissl body staining according to the instructions. After staining, the slices were successively dehydrated and transparentized using 95% alcohol for 2 min and xylene for 5 min, respectively. Finally, the film was sealed with neutral resin. The damage area was photographed by an optical microscope (Olympus, Tokyo, Japan).

2.8. Locomotor Function Recovery Assessment. The hind limb locomotor function of mice was evaluated by the Basso Mouse Scale (BMS) scoring [30] and inclined plane test at 0, 1, 3, 7, 14, 21, and 28 days after injury (dpi). In short, animals were allowed to move freely a period of time in an empty room, and the BMS scores of mice were recorded according to the observation of paw posture, posterior ankle joint mobility, trunk stability, tail posture, and coordination. The BMS score of mice ranges from 0 (completely paralysis) to 9 (normal locomotion). For the inclined plane test, mice were placed on a rubber board, and then, the angles at which the mice could not hold its position for 5 sec were defined as the maximum angles, which could be used to evaluate the hind limb strength of mice [31]. The results of mouse hind limb movements were blindly recorded by two trained investigators.

2.9. ELISA. BV2 cells were coincubated with LPS combined with or without sesamol. IL-6 and TNF-α produced from cells were detected by using a commercial ELISA kit according to the instructions. The OD values at 450 nm and 630 nm were determined by using the SpectraMax microplate reader.

2.10. Statistical Analysis. Results are expressed as the mean ± SEM. The significant difference comparison of two groups was carried out by two-tailed Student's t-test. The statistical significance comparison of multiple groups was conducted by one-way analysis of variance (ANOVA) test with Tukey's multiple comparison test. All statistical analyses were conducted by using GraphPad Prism 8 software. $P < 0.05$ was regarded significant.

3. Results

3.1. Sesamol Improves Locomotor Functional Restoration in Mice after SCI. The BMS score and inclined plane test were applied to assess locomotor functional restoration, and HE staining as well as Nissl staining was carried out to evaluate histological outcomes in mice suffering from SCI. Prospectively, BMS scores of both injury groups were distinctly lower than that of the sham group, while injured mice treated with sesamol exhibited a distinct amelioration of posterior limb motor function with higher BMS scores and better coordinated crawling at 14, 21, and 28 dpi relative to mice suffering from SCI alone (Figures 1(b) and 1(c)). Cavity of necrotic tissue was detected by HE staining, and neuronal survival was measured using Nissl staining at 7 dpi, respectively. Result of HE staining displayed that sesamol treatment decreased SCI-induced cavity of necrotic tissue (Figure 1(f)). Similar to the result, sesamol reduced SCI-induced neuron loss; in other words, dramatically more survival neurons existed in the sesamol-treated group than in mice suffering from SCI alone detected by Nissl staining (Figure 1(g)). Collectively, the above data indicate that sesamol has a neuroprotective role in locomotor function recovery in mice after SCI.

3.2. Sesamol Attenuates Neuronal Apoptosis following SCI. To confirm whether sesamol could reduce apoptosis induced by SCI, the level of apoptosis was measured by western blot and immunofluorescence at 7 dpi. Our results showed that traumatic SCI upregulated cleaved caspase-3 and Bax (markers of proapoptotic proteins) protein expression and weakened the protein level of Bcl-2 (an antiapoptotic protein), which were dramatically reversed by sesamol administration (Figures 2(a)–2(d)). These above data were confirmed by immunofluorescence staining of NeuN (marker for neuron) and cleaved caspase-3. Similarly, SCI increased cleaved caspase-3-positive neurons, but that was decreased by sesamol (Figure 2(e)). These results indicate that sesamol can prevent neuron apoptosis after SCI in vivo.

3.3. Sesamol Reduces Proinflammatory Cytokine Release and Regulates Phenotypic Polarization of Microglia. Accumulating evidences have revealed that inflammatory responses play key roles in secondary SCI. Therefore, levels of IL-6 and TNF-α were determined using western blot in vivo at 3 dpi and by ELISA in LPS-mediated BV2 cells. Compared with uninjured mice, acute SCI induced dramatic increase protein level of IL-6 and TNF-α in the damaged spinal cord, while the level of cytokines was significantly decreased by sesamol (Figures 3(a)–3(c)). Consistent with the result,

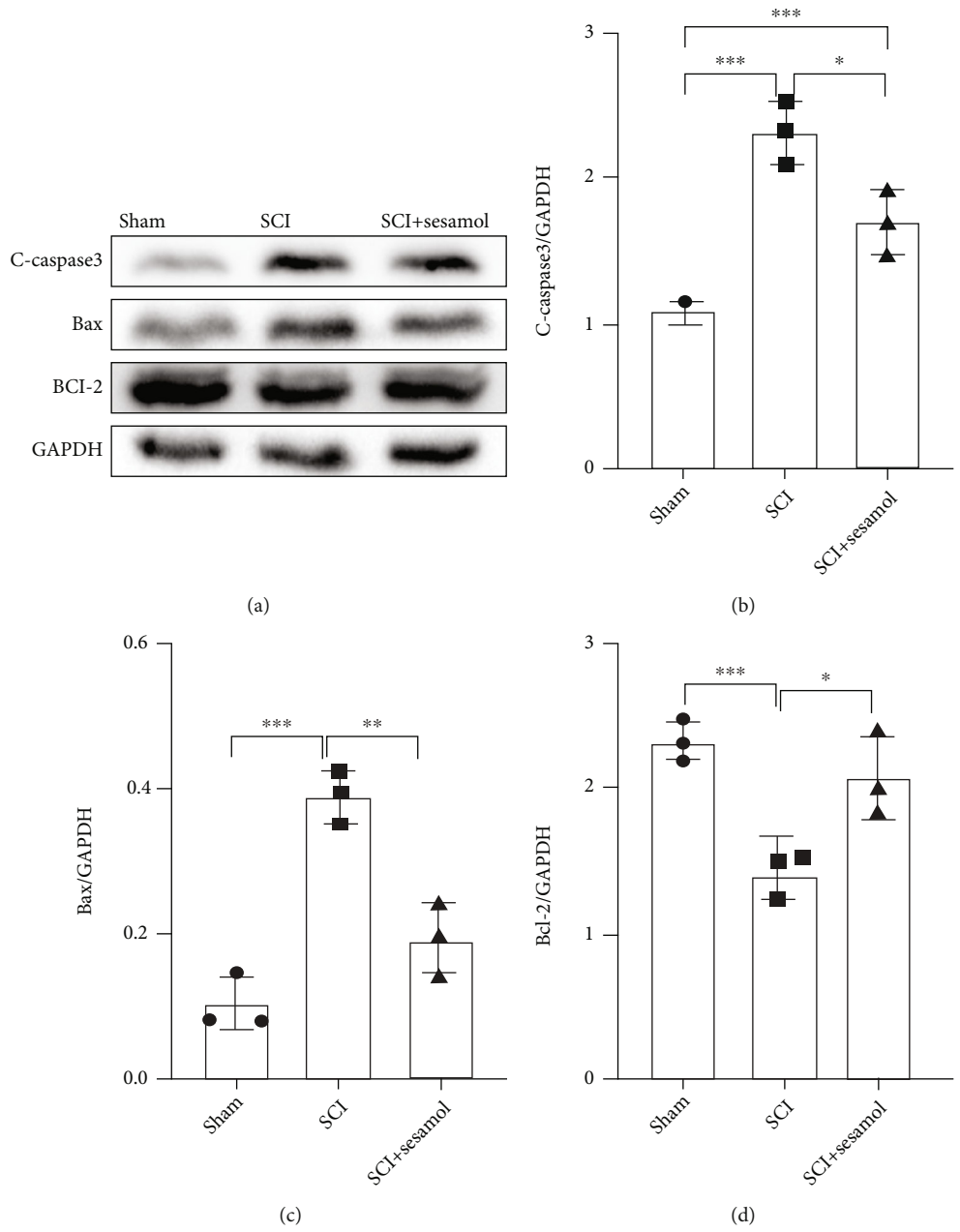

Figure 2: Continued.

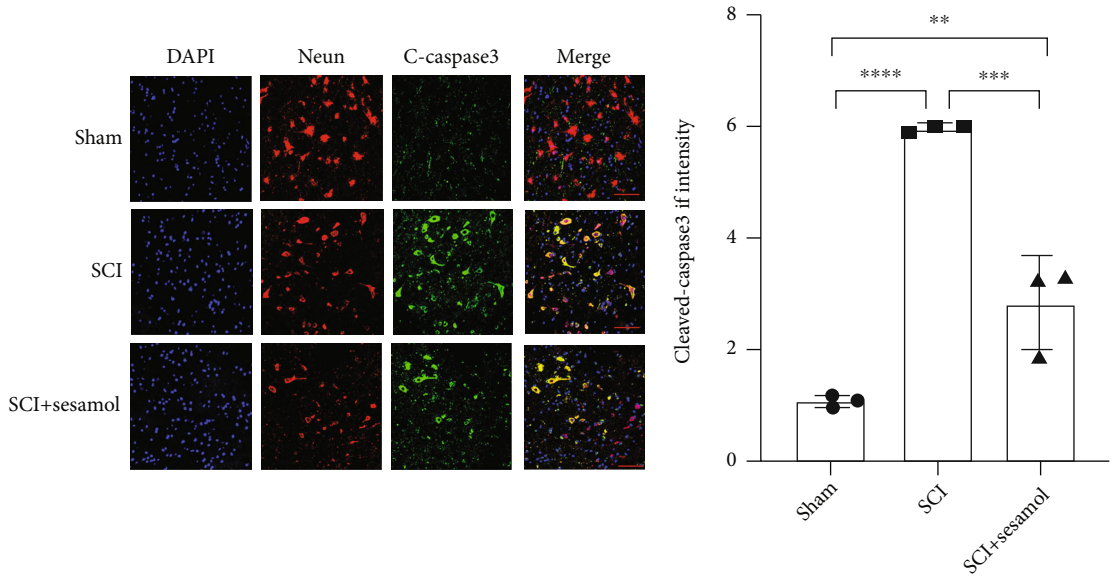

Figure 2: Sesamol protects neurons from apoptosis in mice after SCI. (a) Western blot images exhibiting apoptosis-related protein levels in the injured spinal cord of mice from each group at 7 dpi. (b–d) Quantitative analysis of the expression these proteins from (a) normalized to GAPDH. $n = 3$ per group. (e) Sesamol reduced the fluorescence degree of cleaved caspase-3 (green) in neurons (established by NeuN, red), and DAPI (blue) is for the nuclear staining (scale bar = 50 μm). (f) Quantitative analysis of the fluorescence degree of cleaved caspase-3. Results are expressed as mean ± SEM ($n = 3$ per group). $^{\#\#}P < 0.05$, $^{\#\#\#}P < 0.001$, and $^{\#\#\#\#}P < 0.0001$.

increase in TNF-α and IL-6 was also distinctly overturned by sesamol in LPS-induced BV2 cells (Figures 3(d) and 3(e)).

To further understand the anti-inflammation role of sesamol in mice after SCI, phenotypic polarization of microglia was determined at 3 dpi. The data obtained by western blot analysis showed that sesamol administration prevented M1 microglia-related protein (CD86) expression and increased protein levels of M2 microglial mediators, including CD206 and arginase 1 (Arg1) (Figures 3(a) and 3(f)–3(h)). Consistent with the results, immunofluorescence analysis also verified that sesamol improved the CD206 protein expression in IBA1$^+$ microglia after SCI (Figure 3(i)). These above data indicate that sesamol inhibits production of proinflammatory factors and induces M2 phenotype microglial polarization.

3.4. Effect of Sesamol on AMPK/SIRT1/NF-κB Pathways in SCI. To understand the underlying mechanism of sesamol alleviating inflammation and promoting SCI restoration, effects of sesamol on regulating AMPK/SIRT1/NF-κB pathways at 3 dpi were evaluated. Compared with uninjured mice, SCI resulted in significant decreases in SIRT1 protein expression and the p-AMPK/AMPK ratio, which was reversed by sesamol treatment (Figures 4(a)–4(c)). Activation of NF-κB is connected with proinflammatory factor secretion and phenotypic changes of microglia [32]; thus, protein level of NF-κB p65 and its phosphorylation level (p-p65) were determined by western blot analysis. The result exhibited that the ratio of p-p65/p65 was remarkably increased in mice following SCI relative to uninjured mice, which was dramatically inhibited by sesamol administration (Figures 4(a) and 4(d)). Similar to the result, SIRT1 was upregulated and P65 was downregulated in Iba1$^+$ microglia after SCI with sesamol administration (Figures 4(e) and 4(f)). These above data indicate that sesamol may activate AMPK/SIRT1 and suppress activation of NF-κB pathways in mice after SCI.

3.5. AMPK Participates in Sesamol Alleviating Inflammation in LPS-Stimulated Microglia. To further confirm whether sesamol inhibited inflammation by activating the AMPK pathway following SCI, a specific AMPK inhibitor (compound C) was applied in LPS-induced BV2 cells. Then, protein expression of proinflammatory cytokines was examined by western blot and ELISA. Results in Figures 5(a)–5(e) showed that sesamol (10 μM) significantly reduced the protein expression of IL-6 and TNF-α in LPS-induced BV2 cells, which was reversed by compound C (5 μM). Collectively, these results reveal that AMPK may participate in anti-inflammation of sesamol in microglia stimulated by LPS.

3.6. AMPK Activation Participates in Sesamol-Induced M2 Microglial Polarization. M1 phenotype microglia have been proven to be neurotoxic and induce inflammation response, while M2 microglia perform anti-inflammation. In this study, western blot and immunofluorescence were applied to further determine whether AMPK activation participates in sesamol-induced M2 microglial polarization in vitro. The results showed that both CD86 (a M1 microglia indicator) and CD206 (an established marker for M2 microglia) were significantly increased in LPS-stimulated BV2 cells. However, sesamol administration decreased dramatically

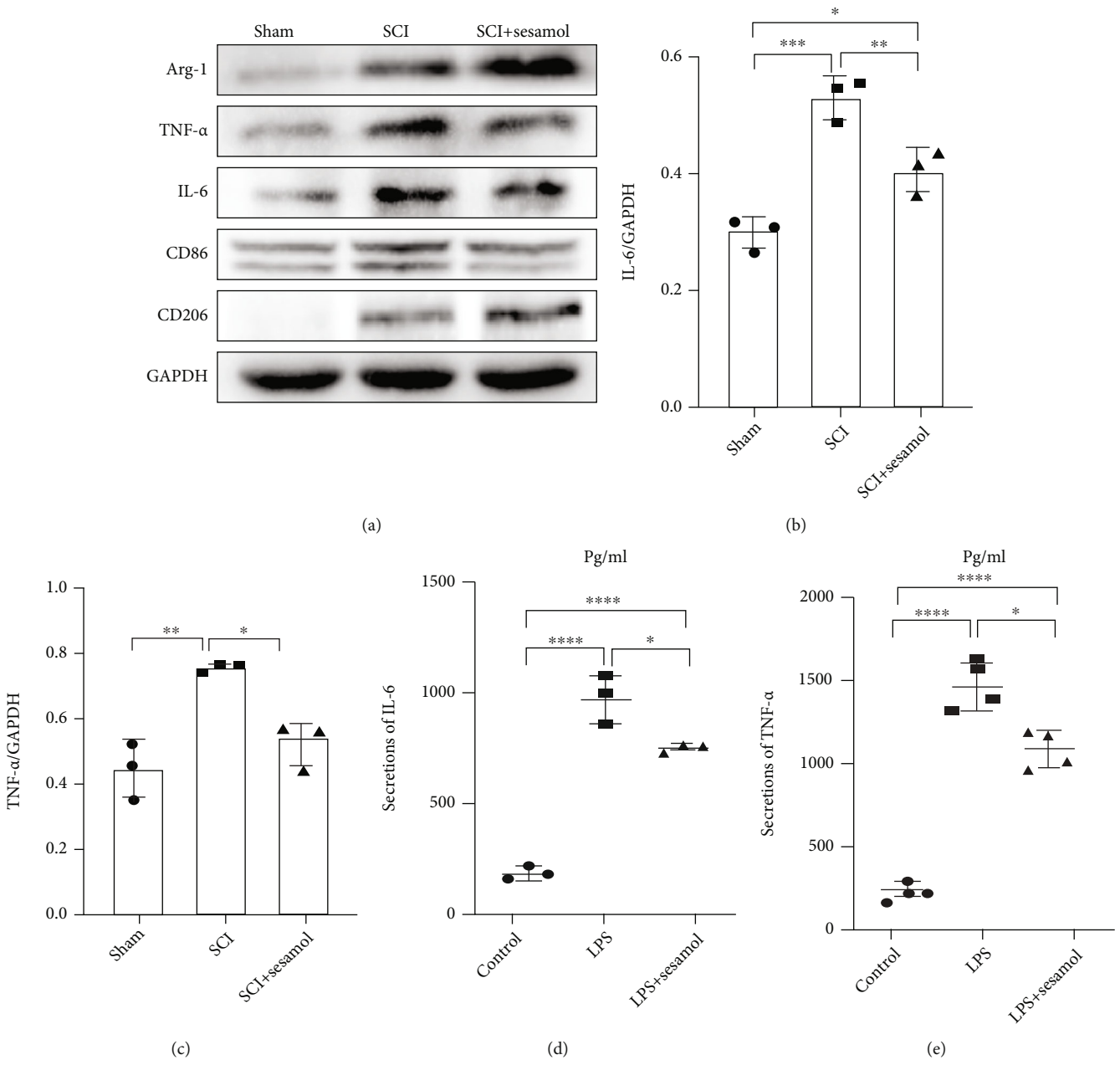

Figure 3: Continued.

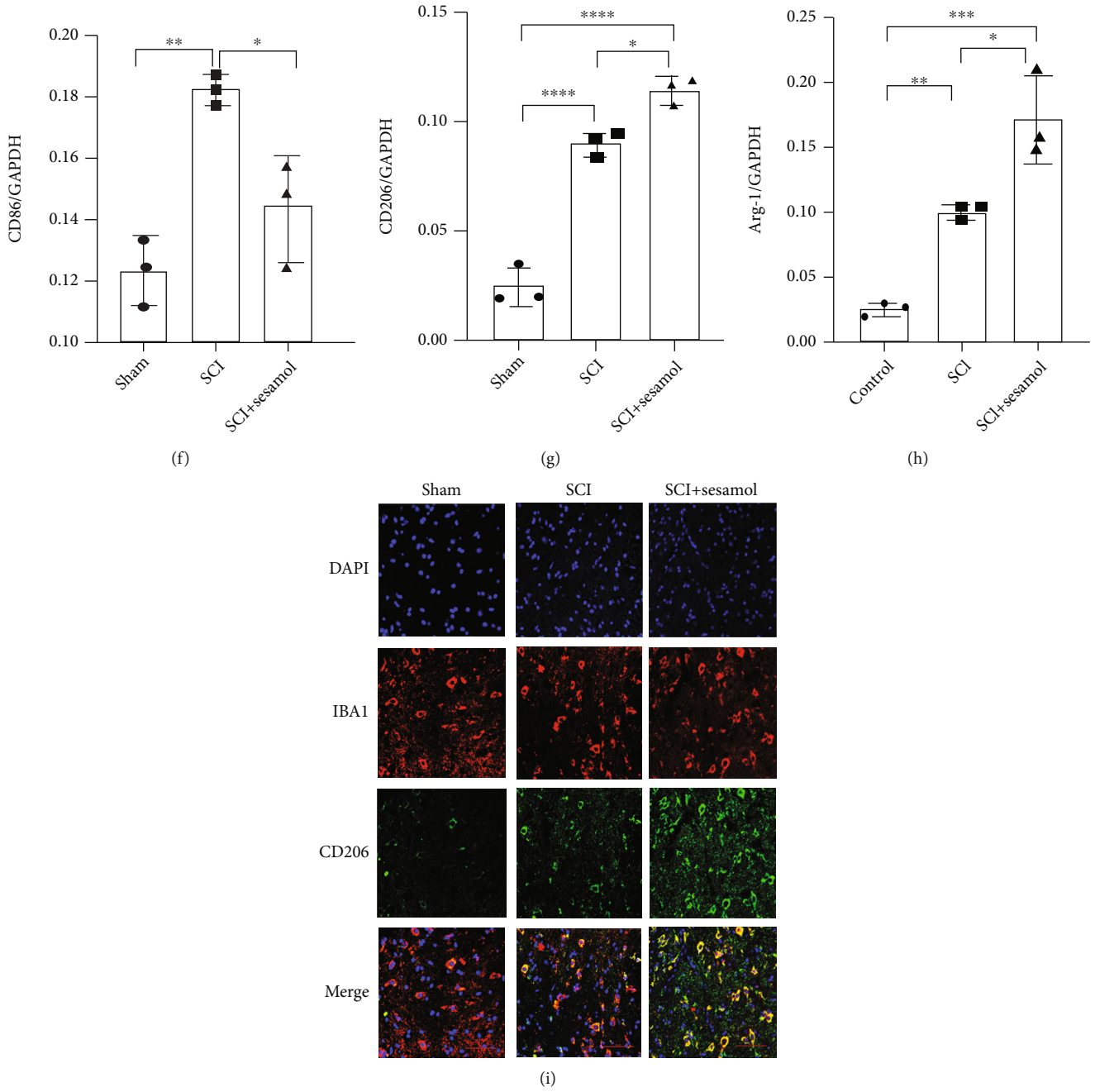

Figure 3: Sesamol attenuates inflammation and induces M2 phenotype microglial polarization in mice suffering from SCI. (a) Western blot images showing protein levels of IL-6, TNF-α, CD86, Arg-1, and CD206 in the injured spinal cord of mice at 3 dpi. (b, c) Quantification of TNF-α and IL-6 from (a), respectively ($n = 3$). (d, e) Statistical analysis of IL-6 and TNF-α concentrations determined by ELISA in BV2 cells suffering from LPS ($n = 4$ per group). (f–h) The quantitative analysis of CD86, CD206, and Arg-1 from (a) ($n = 3$ per group). (i) Sesamol increased the fluorescence degree of CD206 (green) in activated microglia (established by IBA1, red), and DAPI (blue) is for the nuclear staining (scale bar = 50 μm). Values are represented as the mean ± SEM. $^{\#}P < 0.05$, $^{\#\#}P < 0.01$, $^{\#\#\#}P < 0.001$, and $^{\#\#\#\#}P < 0.0001$.

CD86 protein level and further induced CD206 protein expression, which were significantly reversed by the AMPK inhibitor compound C (Figures 6(a)–6(e)). Consistent with the result, fluorescence intensity of CD206 in LPS-mediated BV2 cells was also remarkably increased by sesamol treatment, which was notably reduced by compound C (Figure 6(f)). These results confirm that sesamol promotes M2 polarization in BV2 cells partly regulated by the AMPK pathway.

3.7. Sesamol Alleviating Inflammation Response in Microglia Is Regulated via the AMPK/SIRT1/NF-κB p65 Pathway. Evidences have shown that SIRT1 is a downstream target of the AMPK signaling pathway and participates in anti-inflammation via suppression of NF-κB p65 activation [23–25]. To further verify sesamol playing an anti-inflammatory role in microglia via the AMPK/SIRT1/NF-κB pathway, compound C was applied in BV2 cells, and

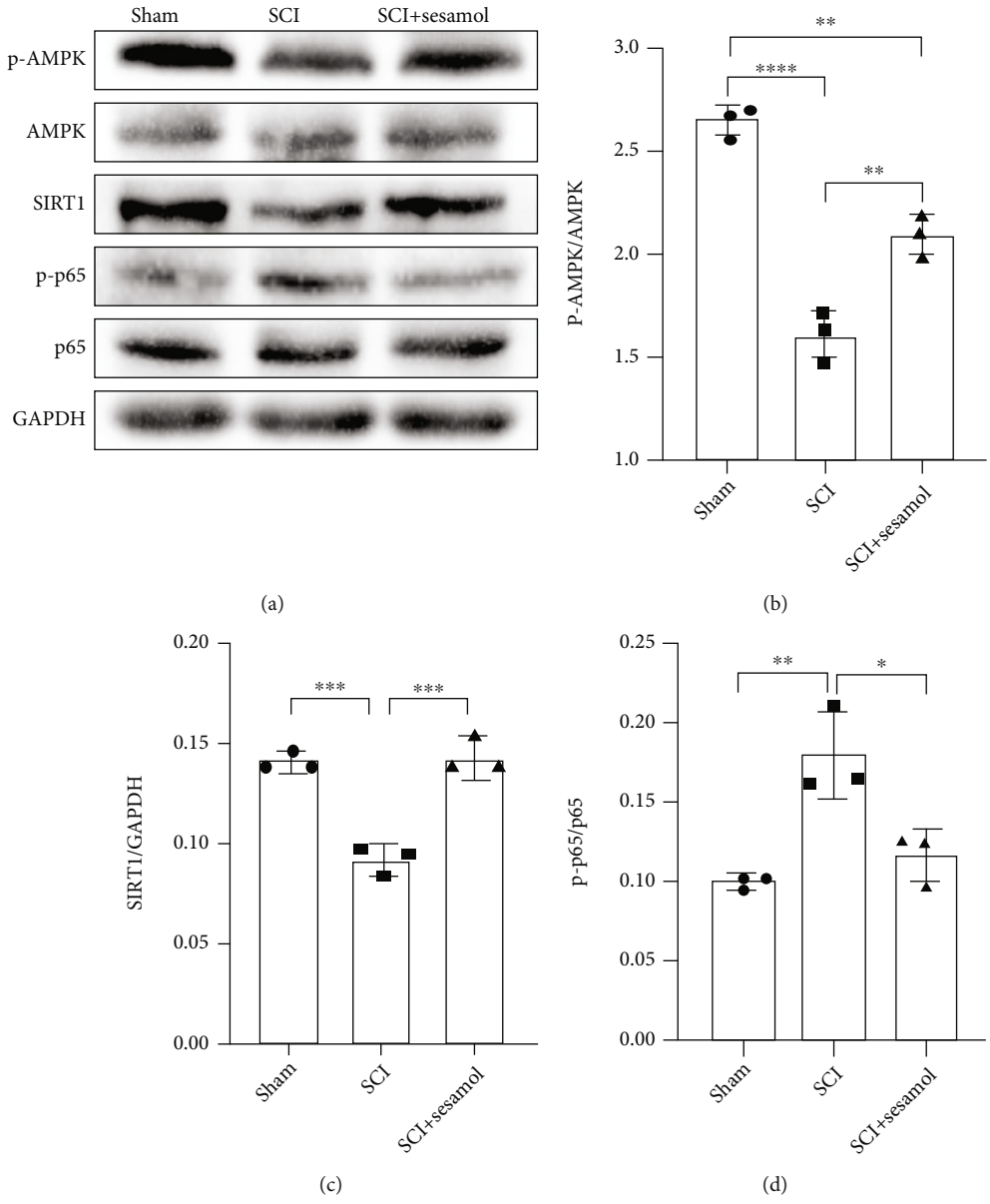

Figure 4: Continued.

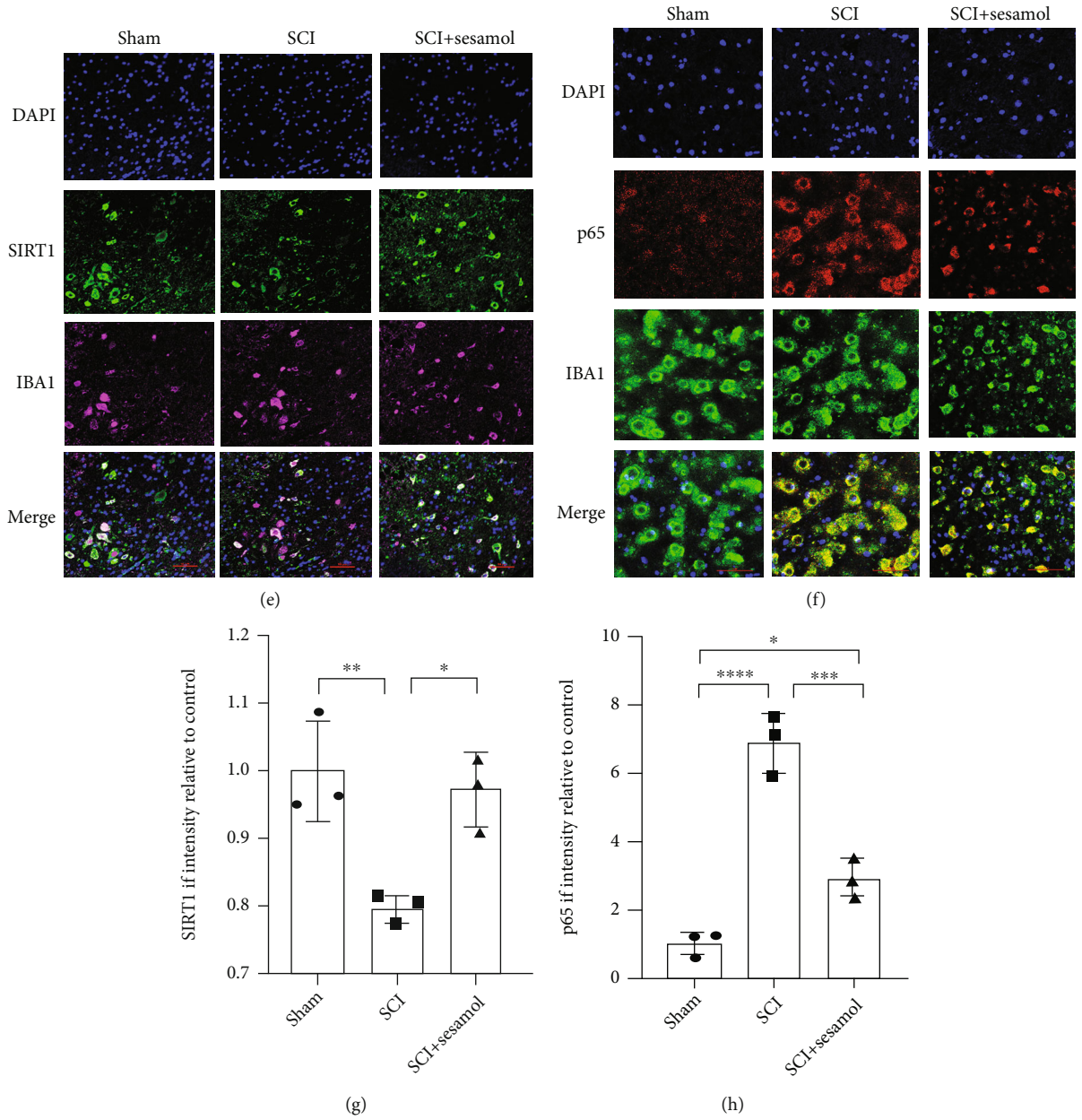

FIGURE 4: Sesamol regulates AMPK/SIRT1/NF-κB pathways in mice following SCI. (a) Western blot images showing protein expressions of p-AMPK, AMPK, SIRT1, p-p65, and p65 in the spinal cord of mice from uninjured, SCI, and sesamol-treated group at 3 dpi. (b–d) Quantitative analysis of western blot results from (a) ($n = 3$ per group). (e) Representative images showing that sesamol increased the fluorescence degree of SIRT1 (green) in activated microglia (established by IBA1, purple), and DAPI (blue) is for the nuclear staining (scale bar = 50 μm). (f) Sesamol reduced the fluorescence degree of p65 (red) in activated microglia (scale bar = 50 μm). (g, h) Quantification of the fluorescence degree of SIRT1 and p65 in activated microglia from (e) and (f), respectively. Data are represented as the mean ± SEM ($n = 3$ per group). $^{\#\#}P < 0.01$, $^{\#\#\#}P < 0.001$, and $^{\#\#\#\#}P < 0.0001$.

then, protein expression of SIRT1, AMPK, and NF-κB was analyzed using western blot. Results from Figures 7(a)–7(d) showed that the SIRT1 protein level and p-AMPK/AMPK ratio increased significantly while the p-p65/p65 ratio reduced remarkably in sesamol-treated BV2 cells compared with cells exposed to LPS only. However, these trends caused by sesamol were apparently overturned by compound C. Moreover, sesamol also resulted in distinct enhancement of fluorescence intensity of SIRT1 and a remarkable reduction of p65 fluorescence intensity, which were reversed by compound C (Figures 7(e) and 7(f)). Combined with data from Figure 5, these data further confirm that sesamol prevents inflammation through regulation of the AMPK/SIRT1/NF-κB pathway.

4. Discussion

Secondary SCI is accompanied by long-term neuroinflammation, oxidative stress, and apoptosis [33]. Sesamol is a kind of excipient used in food and medicine and plays roles

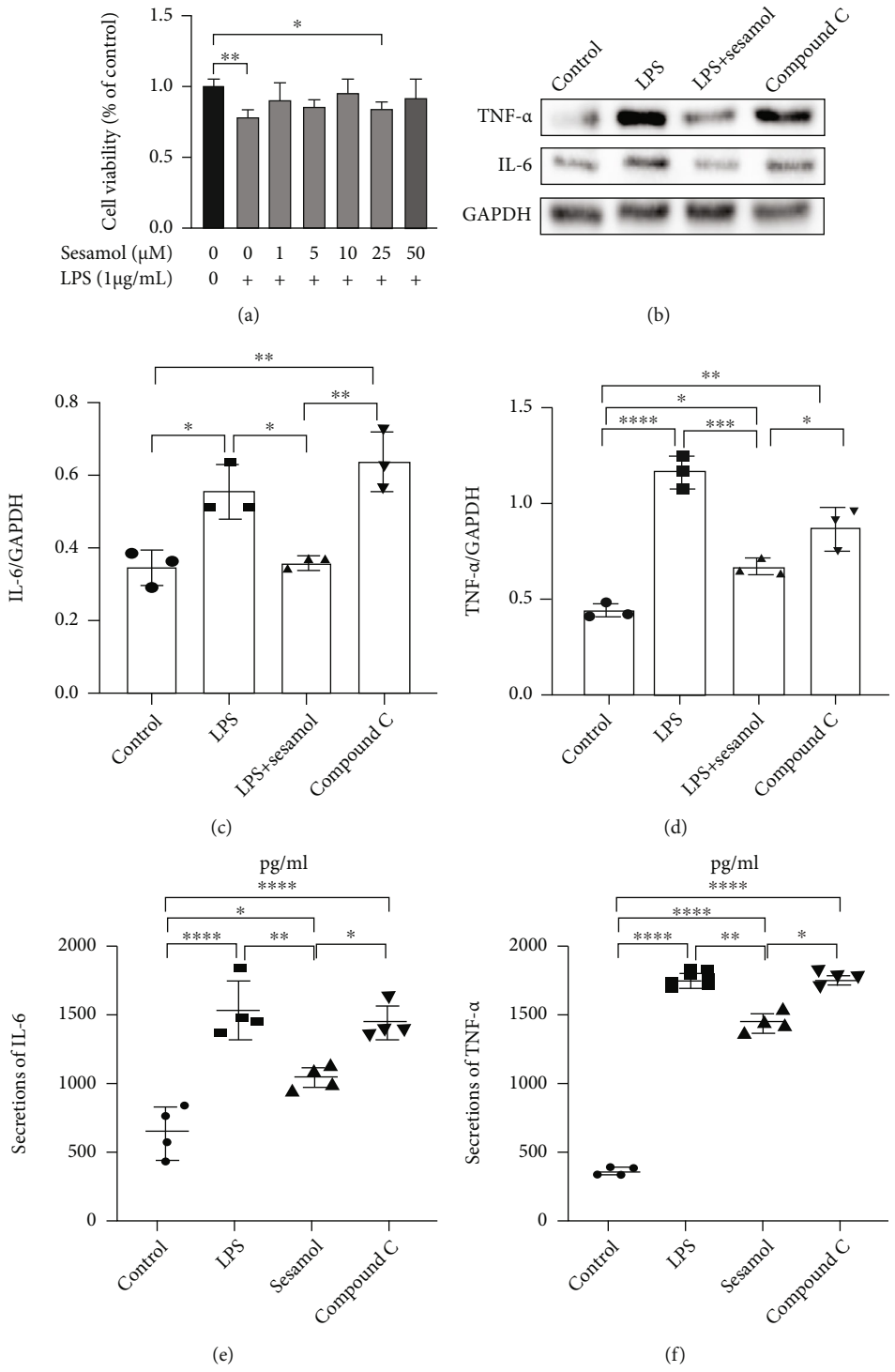

Figure 5: Sesamol-reduced proinflammatory cytokine secretions are reversed by compound C in LPS-mediated BV2 cells. (a) Quantification cell viability of BV2 cells incubated with LPS or (and) sesamol determined by using the CCK-8 kit. (b) Western blot images showing protein expressions of TNF-α and IL-6 in BV2 cells exposed to different conditions. (c, d) Quantitative assessment of TNF-α and IL-6 from (a), respectively ($n = 3$ per group). (e, f) Statistical analysis of IL-6 and TNF-α concentrations determined using ELISA in BV2 cells suffering from different conditions ($n = 4$ per group). Values are expressed as mean ± SEM. $^{\#}P < 0.05$, $^{\#\#}P < 0.01$, $^{\#\#\#}P < 0.001$, and $^{\#\#\#\#}P < 0.0001$.

in antioxidant stress, antiaging, and anti-inflammation [34–36]. Nevertheless, the protective roles and the underlying mechanism of sesamol in SCI repair remain poorly understood. The current study examined the neuroprotective, antineuroinflammatory, and antiapoptotic roles of sesamol in mice following SCI and further explored the underlying mechanisms both in mice and in BV2 cells. Our results indicate that sesamol can ameliorate neuronal

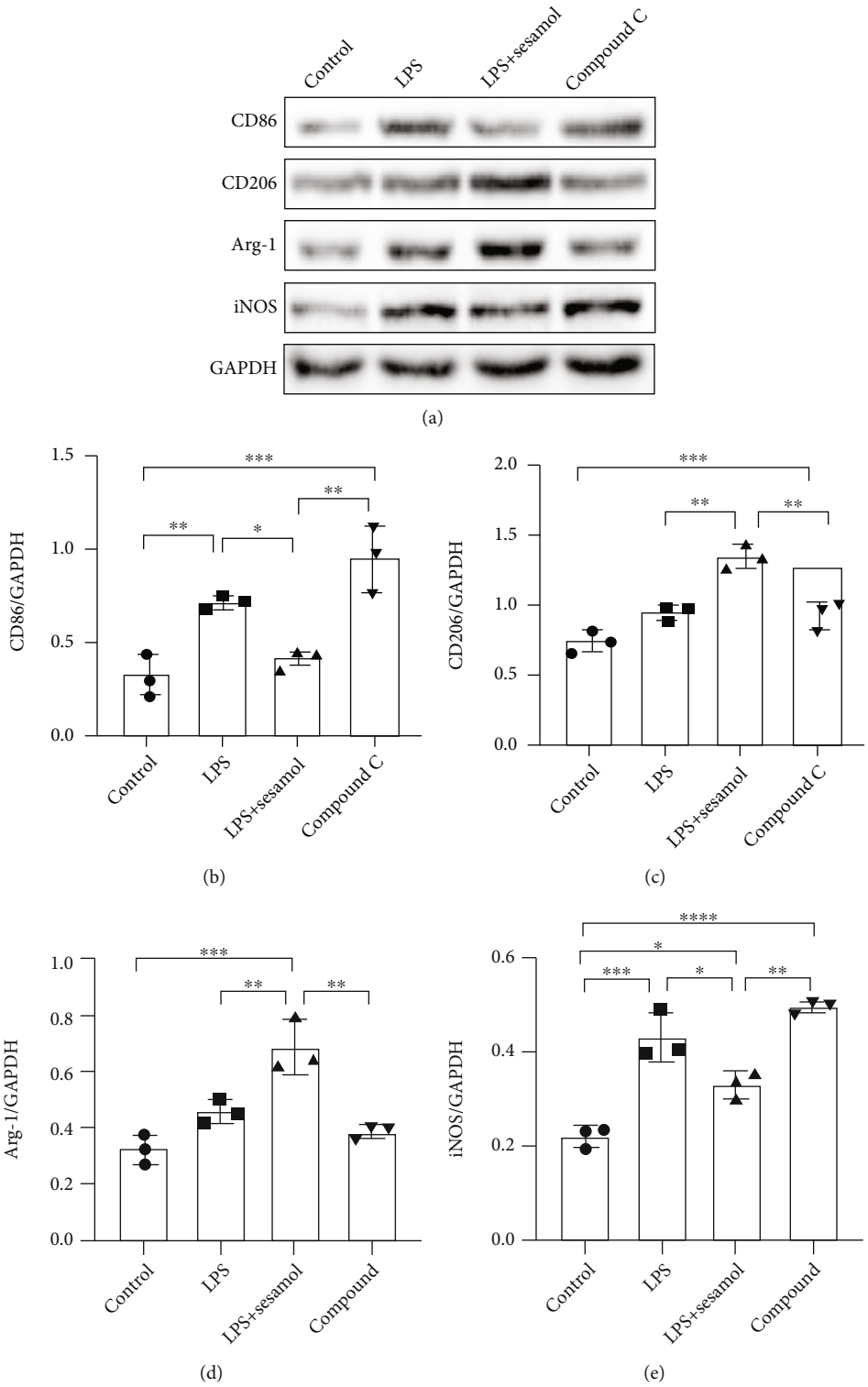

Figure 6: Continued.

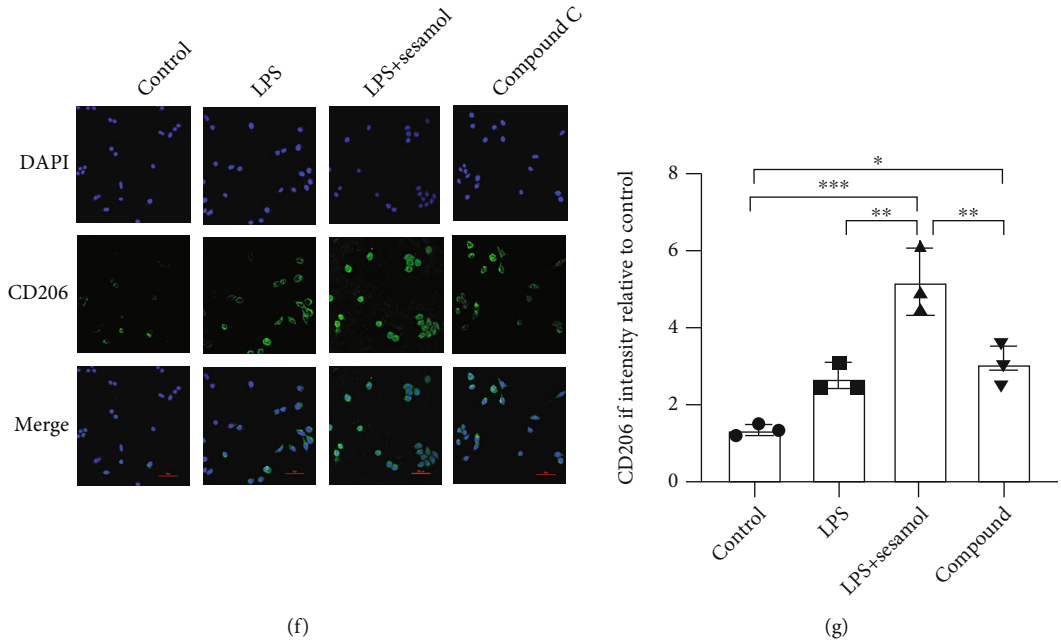

Figure 6: AMPK participates in sesamol-stimulated M2 microglial polarization. (a) Western blot images showing that compound C reversed effects of sesamol on protein levels of CD86, iNOS, Arg-1, and CD206 in BV2 cells. (b–e) Quantitative analysis of CD86, CD206, Arg-1, and iNOS from (a) normalized to GAPDH. (f) Compound C overturned fluorescence intensity of CD206 (green) increased by sesamol in microglia (scale bar = 50 μm). (g) Quantification of the fluorescence degree of CD206 from (f). Results are represented as the mean ± SEM ($n = 3$ per group). $^{\#}P < 0.05$, $^{\#\#}P < 0.01$, $^{\#\#\#}P < 0.001$, and $^{\#\#\#\#}P < 0.0001$.

apoptosis, reduce inflammatory response, promote M2 microglial polarization, and improve neurological function restoration in mice after SCI. Furthermore, our data provide mechanistic evidence for the hypothesis that the AMPK/SIRT1/NF-κB pathway might be important to the antineuroinflammatory ability of sesamol in microglia.

SCI leads to direct or indirect damage to neurons, causing rampant neuronal apoptosis at early stages of injury, which is one of key obstacles to the SCI restoration. Thus, preventing neuron against apoptosis is believed to be an effective approach to promote neural restoration after SCI. In the current study, sesamol could promote locomotor functional recovery and histological outcomes in mice after SCI. Our further results demonstrated that sesamol caused dramatic reduction of cleaved caspase-3 and Bax but a significant upregulation of Bcl-2, particularly within neurons in mice after SCI. Ample evidences indicate that Bax and cleaved caspase-3 participate in proapoptosis, while Bcl-2 has an antiapoptotic role [29, 37]. This work provides novel evidence that sesamol plays an important role of antiapoptosis within neurons in mice suffering from SCI.

Immune response is activated after SCI, and NF-κB (p65) is one of the important regulators participating in infiltration of monocytes, neutrophils, and activated microglia into the damaged site and secretion of a lot of proinflammatory cytokines, including IL-6 and TNF-α [38, 39]. Ample evidences have demonstrated that microglia in CNS contribute to neuroinflammation progress [40, 41]. Our results revealed that sesamol significantly reduced TNF-α and IL-6 protein levels in mice suffering from SCI and in LPS-mediated microglia. This is consistent with the previous study showing that sesamol inhibits dextran sulphate sodium-induced inflammation in colitis mice [35]. After CNS injury, microglia are activated and polarized to the M1 phenotype with proinflammatory function and the M2 phenotype with anti-inflammatory effect [42, 43]. However, whether sesamol alleviates neuroinflammation related to regulating polarization of the microglial phenotype is still unknown. In our study, the protein level of CD86, an indicator of M1 microglia, was significantly increased after SCI and then dramatically reduced after sesamol administration. In contrast, the protein levels of Arg-1 and CD206 specially expressed in M2 microglia were increased at early days after SCI and further increased after sesamol administration. These data indicate that sesamol treatment decreases the proportion of M1 but increases M2 phenotype cells in activated microglia, which may contribute to antineuroinflammation.

Sesamol is extracted from sesame oil and can be used as an antioxidant in foods and medicines [44]. Several studies have revealed that sesamol protects the body from various disease conditions such as obesity, hyperlipidemia, and diabetic foot ulcer mainly through regulating lipid as well as energy metabolism and reducing inflammatory cell infiltration [45–47]. Ample previous studies have also documented that sesamol has anti-inflammatory effects via upregulating AMPK signaling and inhibiting NF-κB activation [26, 27]. Moreover, sesamol can activate SIRT1 signaling to attenuate oxidative stress which will lead to cell apoptosis [28]. It is well known that AMPK is a key energy sensor that mediates cellular energy balance in the body [48]. AMPK also is found to be an important regulator participating in the

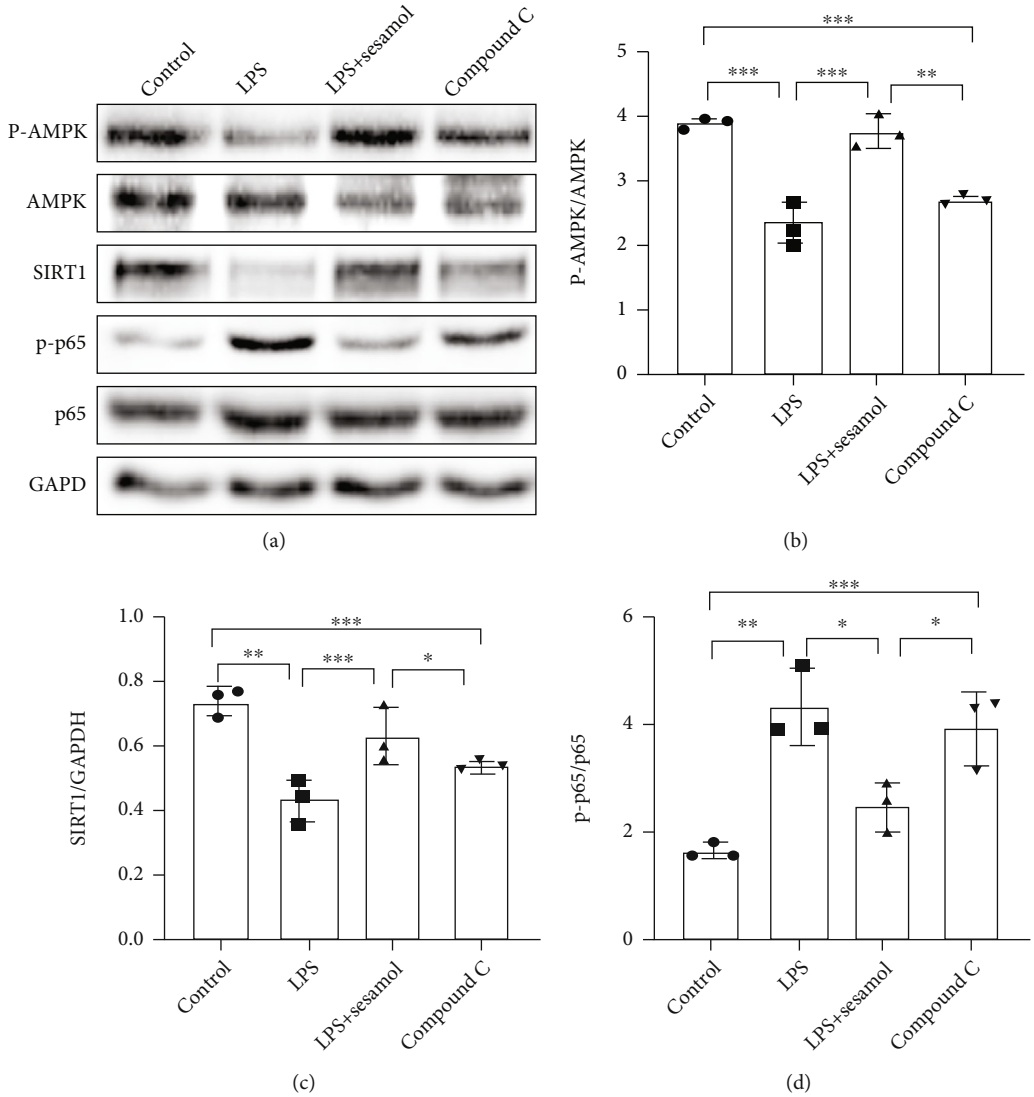

Figure 7: Continued.

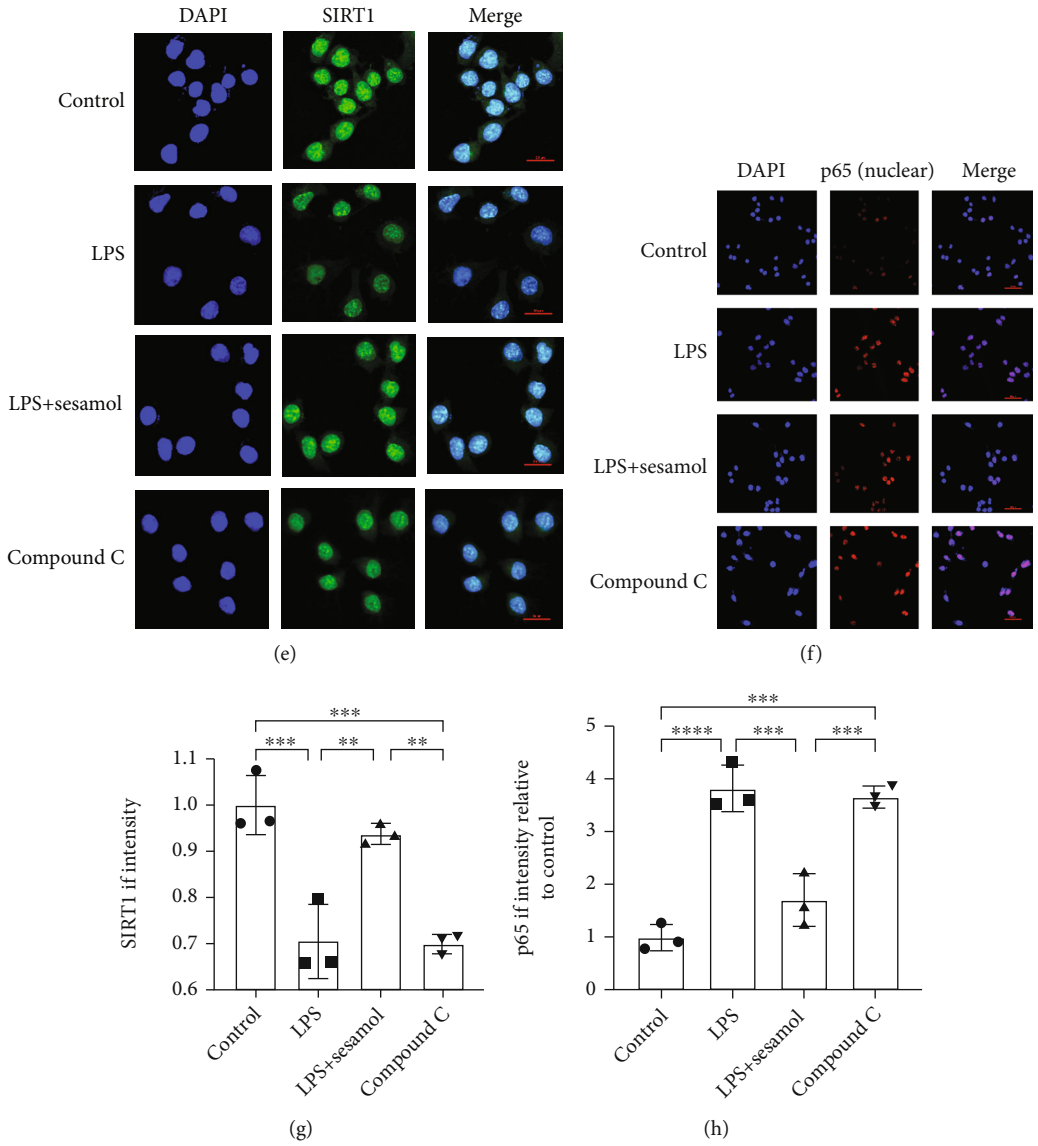

Figure 7: Sesamol regulates the AMPK/SIRT1/NF-κB pathway in BV2 cells suffering from LPS. (a) Western blot images showing that compound C reversed p-AMPK, AMPK, SIRT1, p-p65, and p65 protein expression regulated by sesamol in BV2 cells incubated with LPS. (b–d) Quantification of p-AMPK/AMPK ratio, SIRT1, and p-p65/p65 ratio data from (a) ($n = 3$ per group). (e) Representative images showing that compound C counteracted fluorescence intensity of SIRT1 (green) increased by sesamol (scale bar = 20 μm). (f) Representative images showing that sesamol decreased fluorescence intensity of nuclear p65 (red) while it was reversed by compound C (scale bar = 50 μm). (g, h) Quantification of the fluorescence degree of SIRT1 and p65 in BV2 from (e) and (f), respectively ($n = 3$ per group). Results are represented as the mean ± SEM. $^{\#}P < 0.05$, $^{\#\#}P < 0.01$, $^{\#\#\#}P < 0.001$, and $^{\#\#\#\#}P < 0.0001$.

macrophage phenotype [49]. SIRT1, a member of the SIRT family, has antiaging and anti-inflammatory effects [50]. SIRT1 acts as a downstream target of the AMPK pathway, and it also inhibits the activation of NF-κB [27]. Many evidences verify the inhibitory effect of the AMPK/SIRT1/NF-κB pathway on inflammation [22, 25, 48]. In the present study, compound C, a specific inhibitor of AMPK, was used in BV2 cells suffering from LPS. Our results reveal that AMPK participates in inhibitory effect of sesamol on inflammation. Moreover, our data found that sesamol reduced protein levels of CD86 and iNOS which established M1 microglia, while it increased M2 phenotype microglial protein (CD206 and Arg-1) expressions in BV2 cells exposed to LPS, but these results could be reversed by compound C. Microglia are activated as M1-type microglia after SCI and then secrete proinflammatory factors, which aggravate neuronal apoptosis in an inflammatory environment and make tissue repair difficult [51]. Excitingly, sesamol can promote M2 phenotype polarization and decrease proinflammatory cytokine secretion, sequentially improve the inflammatory environment around the tissue, and consequently inhibit neuronal apoptosis and exert a neuroprotective role in mice following SCI. Finally, this study confirmed that sesamol could activate the AMPK/SIRT1 pathway and inhibit NF-κB activation in vitro (Figure 7). Therefore, this study indicates that sesamol attenuates

neuroinflammation and improves neuron survival partly through regulating the AMPK/SIRT1/NF-κB pathway in mice following SCI.

5. Conclusion

This study suggests that sesamol promotes polarization of M2 phenotype microglia, inhibits neuroinflammation, alleviates neuronal apoptosis, and improves locomotor functional recovery by activating the AMPK/SIRT1 pathway and inhibiting NF-κB activation in mice after SCI. Our results support the antineuroinflammatory effect of sesamol in SCI, and sesamol may be a potential therapeutic agent for the treatment of SCI.

Data Availability

All data supporting the conclusions of this manuscript are provided in the text and figures. Please contact the author for data requests.

Conflicts of Interest

The authors declare that the research was conducted in the absence of any commercial or financial relationships that could be construed as a potential conflict of interest.

Authors' Contributions

Xiaochu Feng, Xianghang Chen, Jian Xiao, and Keyong Ye conceived and designed the research. Xianghang Chen, Muhammad Zaeem, Lulu Chen, and Xiangxiang Chen performed the experiments. Xianghang Chen, Wanying Zhang, Liwan Song, and Ling Xie analyzed the data. Xianghang Chen and Ling Xie wrote the original manuscript. Joana Mubwandarikwa and Jian Xiao revised the manuscript. Xiaochu Feng and Xianghang Chen are the first two authors who contributed equally to this work.

Acknowledgments

This work was partially supported by a research grant from the National Natural Science Foundation of China (81972150, 81801233) and Zhejiang Provincial Natural Science Foundation (LR18H150001, LQ18H090008).

References

[1] C. Tohda and T. Kuboyama, "Current and future therapeutic strategies for functional repair of spinal cord injury," *Pharmacology & Therapeutics*, vol. 132, pp. 57–71, 2011.

[2] K. L. Zhou, Y. F. Zhou, K. Wu et al., "Stimulation of autophagy promotes functional recovery in diabetic rats with spinal cord injury," *Scientific Reports*, vol. 5, no. 1, p. 17130, 2015.

[3] B. Yang, F. Zhang, F. Cheng et al., "Strategies and prospects of effective neural circuits reconstruction after spinal cord injury," *Cell Death & Disease*, vol. 11, no. 6, p. 439, 2020.

[4] J. Dai, G. Y. Yu, H. L. Sun et al., "MicroRNA-210 promotes spinal cord injury recovery by inhibiting inflammation via the JAK-STAT pathway," *European Review for Medical and Pharmacological Sciences*, vol. 22, no. 20, pp. 6609–6615, 2018.

[5] T. Gaojian, Q. Dingfei, L. Linwei et al., "Parthenolide promotes the repair of spinal cord injury by modulating M1/M2 polarization via the NF-kappaB and STAT 1/3 signaling pathway," *Cell death discovery*, vol. 6, p. 97, 2020.

[6] Z. Zheng, Y. Wu, Z. Li et al., "Valproic acid affects neuronal fate and microglial function via enhancing autophagic flux in mice after traumatic brain injury," *Journal of Neurochemistry*, vol. 154, no. 3, pp. 284–300, 2020.

[7] H. Nakajima, K. Honjoh, S. Watanabe, A. Kubota, and A. Matsumine, "Distribution and polarization of microglia and macrophages at injured sites and the lumbar enlargement after spinal cord injury," *Neuroscience Letters*, vol. 737, article 135152, 2020.

[8] D. J. Hellenbrand, K. A. Reichl, B. J. Travis et al., "Sustained interleukin-10 delivery reduces inflammation and improves motor function after spinal cord injury," *Journal of Neuroinflammation*, vol. 16, no. 1, p. 93, 2019.

[9] Y. Ren and W. Young, "Managing inflammation after spinal cord injury through manipulation of macrophage function," *Neural Plasticity*, vol. 2013, Article ID 945034, 2013.

[10] L. Fan, K. Wang, Z. Shi, J. Die, C. Wang, and X. Dang, "Tetramethylpyrazine protects spinal cord and reduces inflammation in a rat model of spinal cord ischemia-reperfusion injury," *Journal of Vascular Surgery*, vol. 54, no. 1, pp. 192–200, 2011.

[11] J. L. Wang, C. H. Ren, J. Feng, C. H. Ou, and L. Liu, "Oleanolic acid inhibits mouse spinal cord injury through suppressing inflammation and apoptosis via the blockage of p38 and JNK MAPKs," *Biomedicine & Pharmacotherapy*, vol. 123, article 109752, 2020.

[12] Y. Y. Wang, D. Shen, L. J. Zhao, N. Zeng, and T. H. Hu, "Sting is a critical regulator of spinal cord injury by regulating microglial inflammation via interacting with TBK1 in mice," *Biochemical and Biophysical Research Communications*, vol. 517, no. 4, pp. 741–748, 2019.

[13] K. Chopra, V. Tiwari, V. Arora, and A. Kuhad, "Sesamol suppresses neuro-inflammatory cascade in experimental model of diabetic neuropathy," *The Journal of Pain*, vol. 11, pp. 950–957, 2010.

[14] B. Ren, T. Yuan, Z. Diao, C. Zhang, Z. Liu, and X. Liu, "Protective effects of sesamol on systemic oxidative stress-induced cognitive impairments via regulation of Nrf2/Keap1 pathway," *Food & Function*, vol. 9, no. 11, pp. 5912–5924, 2018.

[15] A. F. Majdalawieh and Z. R. Mansour, "Sesamol, a major lignan in sesame seeds (Sesamum indicum): anti-cancer properties and mechanisms of action," *European Journal of Pharmacology*, vol. 855, pp. 75–89, 2019.

[16] N. D'Onofrio, L. Servillo, and M. L. Balestrieri, "SIRT1 and SIRT6 signaling pathways in cardiovascular disease protection," *Antioxidants & Redox Signaling*, vol. 28, pp. 711–732, 2018.

[17] P. K. Bagul, N. Deepthi, R. Sultana, and S. K. Banerjee, "Resveratrol ameliorates cardiac oxidative stress in diabetes through deacetylation of NFkB-p65 and histone 3," *The Journal of Nutritional Biochemistry*, vol. 26, pp. 1298–1307, 2015.

[18] G. Hasko and P. Pacher, "Endothelial Nrf2 activation: a new target for resveratrol?," *American Journal of Physiology. Heart and Circulatory Physiology*, vol. 299, pp. H10–H12, 2010.

[19] A. J. Donato, K. A. Magerko, B. R. Lawson, J. R. Durrant, L. A. Lesniewski, and D. R. Seals, "SIRT-1 and vascular endothelial

dysfunction with ageing in mice and humans," *The Journal of Physiology*, vol. 589, no. 18, pp. 4545–4554, 2011.

[20] M. Li, N. Meng, X. Guo et al., "Dl-3-n-butylphthalide promotes remyelination and suppresses inflammation by regulating AMPK/SIRT1 and STAT3/NF-κB signaling in chronic cerebral hypoperfusion," *Frontiers in Aging Neuroscience*, vol. 12, p. 137, 2020.

[21] Z. Liu, M. Zhang, T. Zhou, Q. Shen, and X. Qin, "Exendin-4 promotes the vascular smooth muscle cell re-differentiation through AMPK/SIRT1/FOXO3a signaling pathways," *Atherosclerosis*, vol. 276, pp. 58–66, 2018.

[22] L. Chen and Z. Lan, "Polydatin attenuates potassium oxonate-induced hyperuricemia and kidney inflammation by inhibiting NF-kappaB/NLRP3 inflammasome activation via the AMPK/SIRT1 pathway," *Food & Function*, vol. 8, pp. 1785–1792, 2017.

[23] S. Bansod and C. Godugu, "Nimbolide ameliorates pancreatic inflammation and apoptosis by modulating NF-kappaB/SIRT1 and apoptosis signaling in acute pancreatitis model," *International Immunopharmacology*, vol. 90, article 107246, 2021.

[24] Z. K. Wang, R. R. Chen, J. H. Li et al., "Puerarin protects against myocardial ischemia/reperfusion injury by inhibiting inflammation and the NLRP3 inflammasome: The role of the SIRT1/NF-κB pathway," *International Immunopharmacology*, vol. 89, article 107086, 2020.

[25] C. Wang, Y. Gao, Z. Zhang et al., "Safflower yellow alleviates osteoarthritis and prevents inflammation by inhibiting PGE2 release and regulating NF-κB/SIRT1/AMPK signaling pathways," *Phytomedicine*, vol. 78, article ???, 2020.

[26] Y. C. Lu, T. Jayakumar, Y. F. Duann et al., "Chondroprotective role of sesamol by inhibiting MMPs expression via retaining NF-κB signaling in activated SW1353 cells," *Journal of Agricultural and Food Chemistry*, vol. 59, no. 9, pp. 4969–4978, 2011.

[27] X. L. Wu, C. J. Liou, Z. Y. Li, X. Y. Lai, L. W. Fang, and W. C. Huang, "Sesamol suppresses the inflammatory response by inhibiting NF-κB/MAPK activation and upregulating AMP kinase signaling in RAW 264.7 macrophages," *Inflammation Research*, vol. 64, no. 8, pp. 577–588, 2015.

[28] W. Ruankham, W. Suwanjang, P. Wongchitrat, V. Prachayasittikul, S. Prachayasittikul, and K. Phopin, "Sesamin and sesamol attenuate H2O2-induced oxidative stress on human neuronal cells via the SIRT1-SIRT3-FOXO3a signaling pathway," *Nutritional neuroscience.*, vol. 24, no. 2, pp. 90–101, 2021.

[29] A. Sekiguchi, H. Kanno, H. Ozawa, S. Yamaya, and E. Itoi, "Rapamycin promotes autophagy and reduces neural tissue damage and locomotor impairment after spinal cord injury in mice," *Journal of Neurotrauma*, vol. 29, no. 5, pp. 946–956, 2012.

[30] D. M. Basso, L. C. Fisher, A. J. Anderson, L. B. Jakeman, D. M. Mctigue, and P. G. Popovich, "Basso mouse scale for locomotion detects differences in recovery after spinal cord injury in five common mouse strains," *Journal of Neurotrauma*, vol. 23, no. 5, pp. 635–659, 2006.

[31] Y. Li, J. Xiang, J. Zhang, J. Lin, Y. Wu, and X. Wang, "Inhibition of Brd4 by JQ1 promotes functional recovery from spinal cord injury by activating autophagy," *Frontiers in Cellular Neuroscience*, vol. 14, article 555591, 2020.

[32] T. Taetzsch, S. Levesque, C. McGraw et al., "Redox regulation of NF-κB p50 and M1 polarization in microglia," *Glia*, vol. 63, no. 3, pp. 423–440, 2015.

[33] Y. An, J. Li, Y. Liu, and M. Fan, "Neuroprotective effect of novel celecoxib derivatives against spinal cord injury via attenuation of COX-2, oxidative stress, apoptosis and inflammation," *Bioorganic Chemistry*, vol. 101, article 104044, 2020.

[34] B. Zhao, B. Xia, X. Li et al., "Sesamol supplementation attenuates DSS-induced colitis via mediating gut barrier integrity, inflammatory responses, and reshaping gut microbiome," *Journal of Agricultural and Food Chemistry*, vol. 68, no. 39, pp. 10697–10708, 2020.

[35] B. Ren, T. Yuan, X. Zhang et al., "Protective effects of sesamol on systemic inflammation and cognitive impairment in aging mice," *Journal of Agricultural and Food Chemistry*, vol. 68, no. 10, pp. 3099–3111, 2020.

[36] J. S. Wang, P. H. Tsai, K. F. Tseng, F. Y. Chen, W. C. Yang, and M. Y. Shen, "Sesamol Ameliorates Renal Injury-Mediated Atherosclerosis via Inhibition of Oxidative Stress/IKKα/p53," *Nutritional Neuroscience*, vol. 10, no. 10, p. 1519, 2021.

[37] W. Han, Y. Li, J. Cheng et al., "Sitagliptin improves functional recovery via GLP-1R-induced anti-apoptosis and facilitation of axonal regeneration after spinal cord injury," *Journal of Cellular and Molecular Medicine*, vol. 24, no. 15, pp. 8687–8702, 2020.

[38] M. Srinivasan, B. Bayon, N. Chopra, and D. K. Lahiri, "Novel nuclear factor-kappaB targeting peptide suppresses beta-amyloid induced inflammatory and apoptotic responses in neuronal cells," *PLoS One*, vol. 11, article e0160314, 2016.

[39] K. Karova, J. V. Wainwright, L. Machova-Urdzikova et al., "Transplantation of neural precursors generated from spinal progenitor cells reduces inflammation in spinal cord injury via NF-κB pathway inhibition," *Journal of Neuroinflammation*, vol. 16, no. 1, p. 12, 2019.

[40] D. J. Hines, R. M. Hines, S. J. Mulligan, and B. A. Macvicar, "Microglia processes block the spread of damage in the brain and require functional chloride channels," *Glia*, vol. 57, pp. 1610–1618, 2009.

[41] C. J. Heijnen and A. Kavelaars, "Neuro-immune, behavioral and molecular aspects of brain damage," *Brain, Behavior, and Immunity*, vol. 24, pp. 705–707, 2010.

[42] G. Khayrullina, S. Bermudez, and K. R. Byrnes, "Inhibition of NOX2 reduces locomotor impairment, inflammation, and oxidative stress after spinal cord injury," *Journal of Neuroinflammation*, vol. 12, p. 172, 2015.

[43] S. Xu, W. Zhu, M. Shao et al., "Ecto-5'-nucleotidase (CD73) attenuates inflammation after spinal cord injury by promoting macrophages/microglia M2 polarization in mice," *Journal of Neuroinflammation*, vol. 15, no. 1, p. 155, 2018.

[44] Y. Yang, Y. Qu, X. Lv et al., "Sesamol supplementation alleviates nonalcoholic steatohepatitis and atherosclerosis in high-fat, high carbohydrate and high-cholesterol diet-fed rats," *Food & Function*, vol. 12, no. 19, pp. 9347–9359, 2021.

[45] K. Gourishetti, R. Keni, P. G. Nayak et al., "Sesamol-loaded PLGA nanosuspension for accelerating wound healing in diabetic foot ulcer in rats," *International Journal of Nanomedicine*, vol. 15, pp. 9265–9282, 2020.

[46] D. H. Lee, S. H. Chang, D. K. Yang, N. J. Song, U. J. Yun, and K. W. Park, "Sesamol increases Ucp1 expression in white adipose tissues and stimulates energy expenditure in high-fat diet-fed obese mice," *Nutrients*, vol. 12, no. 5, p. 1459, 2020.

[47] H. Qin, H. Xu, L. Yu, L. Yang, C. Lin, and J. Chen, "Sesamol intervention ameliorates obesity-associated metabolic

disorders by regulating hepatic lipid metabolism in high-fat diet-induced obese mice," *Food Nutrition Research*, vol. 63, 2019.

[48] Y. Wang, Z. Yang, L. Yang et al., "Liuweidihuang pill alleviates inflammation of the testis via AMPK/SIRT1/NF-kappaB pathway in aging rats," *Evidence-based Complementary and Alternative Medicine*, vol. 2020, Article ID 2792738, 2020.

[49] X. Q. Xiong, Z. Geng, B. Zhou et al., "FNDC5 attenuates adipose tissue inflammation and insulin resistance via AMPK-mediated macrophage polarization in obesity," *Metabolism*, vol. 83, pp. 31–41, 2018.

[50] X. Huang, Y. Shi, H. Chen et al., "Isoliquiritigenin prevents hyperglycemia-induced renal injuries by inhibiting inflammation and oxidative stress via SIRT1-dependent mechanism," *Cell Death & Disease*, vol. 11, no. 12, p. 1040, 2020.

[51] X. Lu, F. Lu, J. Yu et al., "Gramine promotes functional recovery after spinal cord injury via ameliorating microglia activation," *Journal of Cellular and Molecular Medicine*, vol. 25, no. 16, pp. 7980–7992, 2021.

Hindawi
Oxidative Medicine and Cellular Longevity
Volume 2022, Article ID 3235524, 15 pages
https://doi.org/10.1155/2022/3235524

Review Article

Role of NETosis in Central Nervous System Injury

Yituo Chen,[1,2,3] Haojie Zhang,[1,2,3] Xinli Hu,[1,2,3] Wanta Cai,[1,2,3] Wenfei Ni,[1,2,3] and Kailiang Zhou[1,2,3]

[1]*Department of Orthopaedics, The Second Affiliated Hospital and Yuying Children's Hospital of Wenzhou Medical University, Wenzhou 325027, China*
[2]*Zhejiang Provincial Key Laboratory of Orthopaedics, Wenzhou 325027, China*
[3]*The Second Clinical Medical College of Wenzhou Medical University, Wenzhou 325027, China*

Correspondence should be addressed to Wenfei Ni; niwenfei@126.com and Kailiang Zhou; zhoukailiang@wmu.edu.cn

Received 22 September 2021; Accepted 18 November 2021; Published 4 January 2022

Academic Editor: Yanqing Wu

Central nervous system (CNS) injury is divided into brain injury and spinal cord injury and remains the most common cause of morbidity and mortality worldwide. Previous reviews have defined numerous inflammatory cells involved in this process. In the human body, neutrophils comprise the largest numbers of myeloid leukocytes. Activated neutrophils release extracellular web-like DNA amended with antimicrobial proteins called neutrophil extracellular traps (NETs). The formation of NETs was demonstrated as a new method of cell death called NETosis. As the first line of defence against injury, neutrophils mediate a variety of adverse reactions in the early stage, and we consider that NETs may be the prominent mediators of CNS injury. Therefore, exploring the specific role of NETs in CNS injury may help us shed some light on early changes in the disease. Simultaneously, we discovered that there is a link between NETosis and other cell death pathways by browsing other research, which is helpful for us to establish crossroads between known cell death pathways. Currently, there is a large amount of research concerning NETosis in various diseases, but the role of NETosis in CNS injury remains unknown. Therefore, this review will introduce the role of NETosis in CNS injury, including traumatic brain injury, cerebral ischaemia, CNS infection, Alzheimer's disease, and spinal cord injury, by describing the mechanism of NETosis, the evidence of NETosis in CNS injury, and the link between NETosis and other cell death pathways. Furthermore, we also discuss some agents that inhibit NETosis as therapies to alleviate the severity of CNS injury. NETosis may be a potential target for the treatment of CNS injury, so exploring NETosis provides a feasible therapeutic option for CNS injury in the future.

1. Introduction

Neutrophils, which originate from hematopoietic stem cells, account for almost 50-70% of all white blood cells. Neutrophils are the primary line of defence of the innate immune system to fight against infection. These inflammatory cells are extensively involved in all kinds of inflammatory reactions. Once the host is infected by microorganisms, neutrophils immediately move from the bloodstream to the target of infection, serving as a "first line" of defence against foreign invaders. This process is called innate immunity. Neutrophils display antimicrobial functions through phagocytosis, degranulation, and NETs (neutrophil extracellular traps). NETs contain modified chromatin with histones and granular proteins, which kill microbes through oxidative or nonoxidative mechanisms and propagate inflammatory and immune responses [1]. The formation of NETs accompanied by cell death is called NETosis, which was first reported by Takei et al. [2]. NETosis is produced by immune complexes, microcrystals, antibodies, chemokines, cytokines, and physiological factors [3]. In recent studies, two different types of NETosis have been discovered: suicidal NETosis and vital NETosis [1]. Suicidal NETosis will cause cell death after the release of NETs, while cells remain alive in vital NETosis. These two different types of NETosis have their own functions and play an important role in immune defensive reactions.

CNS injury is one of the most serious organ injuries and has been very common worldwide in recent years [4]. According to clinical need, CNS injury comprises many

types. CNS injury even causes paralysis in severe cases, seriously influencing individuals' physical and psychological health. Therefore, understanding with the mechanisms of neurotrauma and inventing effective pharmaceutical therapies are vital to improve patients' quality of life. Many cells are involved in the process of CNS injury, including meningeal cells, Schwann cells, endothelial cells, astrocytes, fibroblasts, pericytes, microglia, and other glia cells, which collectively attenuate damage or prompt repair [5]. CNS cells release DAMPs (damage-associated molecular patterns) after injury, which are sensed by macrophages or microglia. Admittedly, injury is a cause of inflammation activation. Damage of the CNS results in inflammatory responses from peripheral immune cells (such as T cells, monocytes, and neutrophils), macrophages, and resident microglia [6]. In addition, the migration of macrophages to injured areas and microglial activation are due to stimulation by chemokines, proinflammatory cytokines, or CNS environmental alterations [7]. Activation of macrophages and microglia has been proven to be related to CNS injury [8]. Neuroinflammation is a sign of spinal cord and brain injury. A large number of endogenous microglia and systemic macrophages migrate to injury sites to assist in clearing cellular debris after stroke, SCI, or TBI. In addition, CNS macrophages have the capability to dichotomously facilitate repairs while concurrently causing injury deterioration [8]. Neutrophils are the earliest inflammatory cells arriving at the injured region, and they possess a variety of toxic compounds. Studies show that CNS infiltration induced by neutrophils under different pathological conditions, such as brain ischaemia, trauma, neurodegeneration, infection, and autoimmunity, is a prominent phenomenon [9]. Previous studies have reported that classic cell death types, including autophagic cell death [10], apoptosis [11], necrosis [12], and pyroptosis [13], are involved in the process of CNS trauma. Macrophages are now widely researched in pyroptosis, while apoptosis occurs in neurons during invasion by viruses or other pathogens. In autophagy and necroptosis, we found neurons, astrocytes, and microglia implicated after CNS trauma [7]. Many cells mediated by various pathways of cell death have been identified in injury diseases, but the role of NETosis by neutrophils in CNS trauma remains unclear. We reasonably assume that NETosis probably regulates the mechanism of injury during inflammation. In this review, we summarize recent studies of NETosis in CNS trauma to provide a feasible future therapeutic method for CNS injury.

2. Mechanism of NETosis

As a specific type of cell death, NETosis is characterized by the release of web-like DNA structures decorated with histones and cytotoxic proteins from activated neutrophils [14]. This substance called NETs is triggered by microcrystals, cholesterol, antibodies, specific cytokines, and pharmacological stimuli containing calcium, potassium ionophores, and PMA [15]. The formation of NETs needs a variety of substances, such as NADPH oxidase, myeloperoxidase (MPO), c-Raf, MEK, ERK, and ROS (reactive oxygen species) [16]. NETosis is divided into suicidal NETosis and vital NETosis. In both, the nuclear membrane dissolves and decondensed chromatin exits the cell mixed with granular antimicrobial factors under the influence of all kinds of enzymes, which collectively form NETs [17]. After that, NETs trap almost all pathogens, even those that cannot be phagocytosed (such as viruses, yeasts, and protozoan parasites), killing them with a cocktail of bactericidal enzymes [3, 18]. Suicidal NETosis extrudes NETs accompanied by cell death; in vital NETosis, the cell is viable and retains its effector functions. Moreover, vital NETosis is induced by bacterial-specific molecular features identified by individual pattern recognition receptors (PRRs), whereas suicidal NETosis is typically attributed to PMA [19]. With regard to this newly described form of NETosis, we lack corresponding studies detailing its exact mechanism.

2.1. Suicidal NETosis. In 1996, Takei et al. found a new method of cell death, differing from necrosis and apoptosis, that is caused by phorbol 12-myristate 13-acetate (PMA) [2]. Subsequently, this method of cell death has been named suicidal NETosis [14]. This form of suicide includes nuclear swelling, chromatin decondensation, membrane perforation, and spilling of the nucleoplasm into the cytoplasm (Figure 1). In vivo, many kinds of pathogens trigger suicidal NETosis. First step is formation of NETs. Recent studies revealed the mechanism of NET formation. Fuchs et al. [20] speculated that ROS (including superoxide anions, dioxygen, and hydrogen peroxide) produced by NADPH oxidase may participate in NET formation and by using detailed cellular experiments in vitro. In his research, inhibition of NADPH oxidase by diphenylene iodonium (DPI) impaired the formation of NETs normally induced by PMA and live bacteria [20]. In addition, hydrogen peroxide was exogenously generated by glucose oxidase (GO) and used to stimulate neutrophils downstream of NADPH oxidase. The results indicated that the stimulation of hydrogen peroxide (membrane permeable) could produce NETs. In addition, studies have demonstrated that the Raf-MEK-ERK pathway activates protein kinase C (PKC), leading to membrane assembly with NADPH oxidase (Figure 1) [21, 22]. Another activation mechanism of NADPH oxidase in neutrophils relates to the ROS-dependent relationship between the p47phox subunit and the disulfide isomerase protein, which results in its migration onto the membrane to induce the release of NADPH oxidase [23]. In addition to ROS induced by NADPH oxidase, researchers also noticed an interesting phenomenon in which chronic granulomatous disease (CGD) patients, who lack NADPH oxidase to produce ROS, still demonstrate NET formation caused by A23187 but not PMA [15]. A23187 is a calcium ionophore that increases the intracellular Ca^{2+} concentration. Further studies indicated that Ca^{2+} overload induced by A23187 leads to increased mitochondrial ROS (mtROS) generation, while mtROS is not only cause NETosis by activating NADPH oxidase but also other pathways that do not involve NADPH oxidase, and mtROS is produced under the influence of the mitochondrial permeability transition pore (mPTP) (Figure 1) [15, 20, 24, 25]. These discoveries explain why CGD patients are able to also demonstrate NETosis.

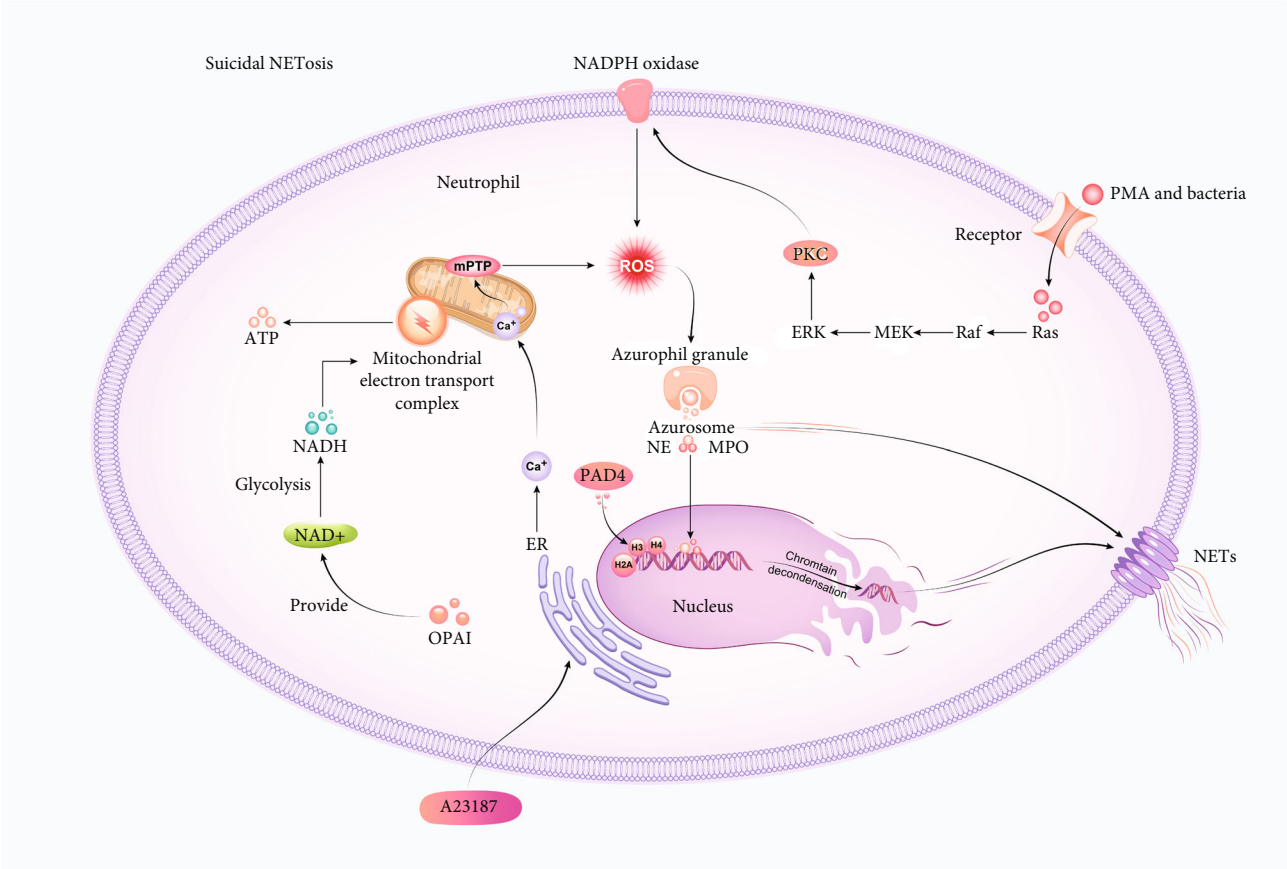

Figure 1: Mechanism of suicidal NETosis and induction of NETosis. PMA or bacteria combine with receptors and activate Ras and then activate PKC through the Raf-MEK-ERK pathway. PKC induces production of ROS by NADPH oxidase. ROS trigger rupture of azurephil granules and release azurosomes, which include NE and MPO. NE and MPO implicated in decondensation of chromatin. Finally, NETs are released through formation of GSDMD. A23187 induces an increase in Ca^{2+} concentration in mitochondria, which activate the opening of mPTP and produce mtROS. PAD4 moves into the nucleus and catalyses citrullination of histones (H3, H2A, and H4), through which it induces chromatin decondensation. OAP1 maintains the supply of NAD+, which later turns into NADH under the influence of glycolysis, and finally, NADH transfers electrons in the mitochondrial electron transport complex, which provides ATP for NET formation.

Generation of ROS leads to tubulin and actin glutathionylation regulated by glutaredoxin 1 (Grx1) [26]. Grx1 is a required enzyme during the process of microtubulin and actin deglutathionylation [26, 27]. Stojkov et al. and Amini et al. [26, 27] thought that an intact cytoskeleton is required for the formation of NETs. Lack of Grx1 leads to impaired cytoskeletal dynamics and causes defective degranulation. Additionally, active cytoskeletal rearrangements and glycolytic ATP production through an entire cytoskeleton are required elements in the formation of NETs. Successful NET formation requires energy from ATP released by glycolysis in the cytoplasm; since OPA1, as an inner mitochondrial membrane protein, maintains the supply of NAD+, NET formation also is indirectly regulated by OPA1 [26, 27]. The shortage of OPA1 leads to a decrease in mitochondrial electron transport complex I activity in neutrophils and consequently reduces ATP generation via glycolysis because of the lack of NAD+ [26, 27]. NET formation and the active assembly of the cytoskeletal network require OPA1-dependent ATP production (Figure 1) [26, 27]. Additionally, ROS participate in the dissociation of azurosomes, which are from Azurophil granules [28]. Azurosomes contain 8 categories of proteins. Three types of the proteins are serine proteases with high homology, namely, cathepsin G and azurocidin, neutrophilic elastase (NE), and myeloperoxidase (MPO) [28]. MPO and NE are associated with NETosis because they are implicated in the decondension of chromatin and the breakdown of cytoskeletal elements [28]. Under the influence of various mechanisms, NE in cytoplasmic granules migrates to the nucleus, incites nuclear envelope damage, and degrades chromatin by histone cleavage (Figure 1). Furthermore, myeloperoxidase (MPO) plays a role in decondensing nuclear DNA, but NET formation is independent of its enzymatic activity at this stage. It has been reported that the decondensation of chromatin is induced by MPO through enhancing the uncoiling of chromatin; however, the molecular mechanism is still unclear [29]. In addition, posttranslational modification may also contribute to the process of chromatin decondensation. Since posttranslational modifications occur in histone proteins (e.g., methylation, acetylation, and phosphorylation), various chromatin functions are altered, such as DNA damage

repair, transcription, and the condensation/decondensation of chromatin [30, 31]. Through an HL-60 cell model, Wang et al. [32] indicated that peptidylarginine deiminase 4 (PAD4) in the cytoplasm migrates into the nucleus and catalyse histone citrullination, causing the decondensation of chromatin. PAD4, which is highly expressed in peripheral blood neutrophils, predominantly moves into the nucleus and is aimed at citrullinate histones H2A, H3, and H4. Inhibition of PAD4 Cl-amidine prevented chromatin from decondensing; neutrophils from PAD4 knockout mice and NETosis induced by Shigella flexneri or Ca^{2+} ionophores in HL-60 cells did not lead to the response of NETosis when induced by PMA [32–35]. It is found that PMA prompts the expression of PAD4 in cells [36]. In addition, transfection with a mimic of miR-155 and an antagomiR-155 increased and decreased PAD4 mRNA expression, respectively, in neutrophils, indicating that miR-155 is a potent regulator of PAD4 in neutrophils [36]. This finding reveals that miR-155 controls PAD4-dependent NET formation [36]. PAD4 also requires a high concentration of calcium for its activation [37]. Finally, nuclear DNA and antimicrobial compounds are released to the extracellular environment, accompanied by cell death via pores formed in the plasma membrane. Gasdermin D protein (GSDMD) contributes to the formation of pores on the plasma membrane (Figure 1). In contrast to pyroptosis in macrophages, typical NETosis hallmarks, involving histone citrullination, nuclear delobulation, DNA extrusion, the destruction of the plasma membrane, granules, and nucleus, which could be triggered after GSDMD activation. Previous studies demonstrated that GSDMD forms pores in the macrophage membrane during pyroptosis by activating caspase-1 and caspase-4/5, while it is activated and cleaved by NE in NETosis [38, 39]. This could also be accompanied by neutrophil lysis. Whether another mechanism causes neutrophil lysis after release of NETs remains unknown.

2.2. Vital NETosis. Suicidal NETosis needs cell death to play a role in antimicrobial function, but is there any other way to kill pathogens while keeping neutrophils alive? Some research groups have discovered a novel mechanism of NETosis without cell death. Pilsczek et al. found that neutrophils could distinctively respond to *Staphylococcus aureus* by a novel process of NET formation, during which neutrophil lysis and plasma membrane breakage were not required [40]. Morphologically, the multilocular neutrophil nucleus rapidly became round and compact. During the process, budding of vesicles and separation of the outer and inner nuclear membranes were observed, and the vesicles and separated membranes were filled with nuclear DNA. In addition to the mechanism whereby NETosis is caused by PMA, suicidal NETosis occurs much slower than vital NETosis, and this indicates that vital NETosis is a rapid mechanism [40]. Some studies have proven that platelet TLR4 recognizes TLR4 ligands in blood and binds to adherent neutrophils, contributing to the formation of NETs and the robustness of neutrophil activation [19, 41]. The NETs retained their integrity under flow conditions and ensnared bacteria within the vasculature. This phenomenon reveals that LPS may be an activator of rapid NETosis [41]. Whether a lack of nuclear DNA induces cell death is an important consideration. IFN-γ- or IL-5-primed eosinophils could rapidly respond to LPS by catapulting their DNA, which did not cause eosinophil apoptosis [42]. The authors explained that this phenomenon was primarily attributed to mitochondrial but not nuclear DNA extruded by eosinophils [42]. Therefore, we assume that neutrophils retain their viability after NETosis in the same manner as eosinophils. Interestingly, a group found that neutrophils treated with GM-CSF could then respond to C5a or LPS by emitting mitochondrial DNA due to oxidant mediation [1]. In this manner, a neutrophil could emit NETs, while its nucleus and other antimicrobial functions were retained. It is paradoxical to the outcome that vital NETosis does not need oxidants, and simultaneous centrifugation of neutrophils forms nuclear cytoplasts, which is cryopreserved and maintain their ability to inactivate phagocytosed bacteria (e.g., *S. aureus*) and exhibit chemotaxis [43, 44]. Considering that erythrocytes live for more than 120 days without nuclei, we believe neutrophils also retain their function even if their nuclei are unavailable. Therefore, relevant studies are needed to describe this mechanism.

2.3. How NETs Play a Role in Immune Defence. NETs comprise numerous antimicrobial compounds, such as MPO and NE, which kill pathogens directly. As the most abundant proteins of NETs, histones possess a strong ability to kill microorganisms [45]. At the same time, as a component of NETs, DNA is also able to inhibit microorganisms. Generally, neutrophils are deemed to possess antimicrobial ability through phagocytosis, but recent studies show that neutrophils whose phagocytosis function was inhibited via treatment with cytochalasin D retained bactericidal activities and failed to function when treated with DNase or antihistone antibodies against H2A [3]. However, the considerable mechanism by which DNA and histones kill microbes is still unclear. Furthermore, physically attaching to pathogen cells and then trapping them are proposed as a mechanism for antimicrobial effects. The initial description of NETs was initially proposed following observations by electron microscopy and immunofluorescence [19]. Extracellular nucleic acids after NETosis stimulation have the ability to bind to exogenous *Salmonella typhimurium*, *S. aureus*, and *Shigella flexneri* [19]. Furthermore, in a model of rabbit shigellosis, bacteria were found to adhere to the NET structure [19]. In total, multiple bacteria have been shown to bind directly to extracellular DNA in vitro, including *Streptococcus pneumoniae*, *S aureus*, and *Escherichia coli* [19]. Therefore, we assume that the primary function of NETs is to trap bacteria, through DNA combinations, but it is not ruled out whether there are other methods to trap bacteria. In addition, components in NETs have also been proven to potentially kill bacteria. For example, histone H2B is able to penetrate through the E. coli membrane, histones H3 and H4 destroy the bacterial cell wall, NET-associated proteases (NE or PR3) inactivate and kill pathogens by cleaving their virulence factors, and LL37, a unique member of human cathelicidin antimicrobial peptides composed of 37 amino acids,

disintegrates pathogen cell membranes, challenging pathogen viability; MPO is an effective antimicrobial material [46, 47]. Pretexts describe TLR4 function in NET formation. The activation of platelet TLR4 leads to a specific platelet response—specifically, attaching to adherent neutrophils in the sinusoids, resulting the formation of NETs, and enhancing the robustness of neutrophil activation [41, 48]. As a haemostatic regulator, platelet functions is only activated by very serious systemic infections that stimulate neutrophils to emit chromatin and proteolytic materials, thereby enhancing the innate immune system's ability to trap and kill microbial cells in circulation [41, 48]. Although LPS causes unconventional platelet activation, and the prevailing view is that during sepsis, the LPS emitted by bacteria activates neutrophils inappropriately and lock them in liver sinusoids and lung capillaries where the proteolysis improperly damages the tissues [41, 48]. It has also been reported that platelets are less sensitive to LPS than neutrophils, and NETs may damage the vascular endothelium [41, 48]. Therefore, NETs are vital to the immune defence response. However, when NETs are out of control, they may cause autoimmune diseases, such as systemic lupus erythematosus (SLE) [49–51]. DNase1 is important for the physiological degradation of NETs [49–51]. The degradation of PMA–NET induced by macrophages occurs in lysosomes [49–51]. If degradation of NETs is incomplete, residual NETs mediate inflammasome and complement activation; for example, lower concentrations of complement factors C3 and C4 were found in SLE patients, indicating consumption of complement and SLE-related NET complement activation, triggering the accumulation of C1q on NETs, which further inhibits DNase1 [52, 53]. Knowing the detailed defence mechanism of NETs in the immune system should be the focus of subsequent studies.

3. Linkage between NETosis and Other Cell Death Pathways

Programmed cell death mainly includes pyroptosis, necroptosis, apoptosis, and NETosis. There are many differences among these cell death pathways. In inflammatory cells, pyroptosis mainly occurs in specialized immune cells (such as macrophages, monocytes, and dendritic cells) and nonimmune cell types (such as intestinal epithelial cells, human trophoblasts, and hepatocyte cells), while NETosis takes place in the PMN [19, 54]. Morphologically, it was found that in NETosis, the cell membrane remains intact until the release of NETs, the cytoplasm remains unchanged or swollen, and the nucleus decondenses and mixes with cytoplasmic contents [55]. In apoptosis, the membrane blebs, but cell integrity is maintained, the cytoplasm becomes shrunk, and the nucleus condenses to form apoptotic bodies [55]. In necroptosis, the membrane loses its integrity, the cytoplasm becomes swollen, and the nucleus remains intact [55]. We explored whether there is a relationship between NETosis and these three cell death pathways. Neutrophils are involved in inflammation, so the formation of NETs is related to inflammatory reactions. Previous study indicated that inflammatory factors are implicated in the process of programmed cell death [56], so we predict that NETosis may trigger other death pathways by releasing NETs. Pyroptosis is an inflammatory form of cell death triggered by certain inflammasomes, leading to the cleavage of gasdermin D (GSDMD) and activation of inactive cytokines such as IL-18 and IL-1β [57]. DAMPs in pathogens are recognized by nucleotide oligomerization domain- (NOD-) like receptors (NLRs), which recruit caspase-1 to cleave pro-IL-18 and prointerleukin-1β (IL-1β) into their mature patterns and rupture GSDMD (encoded by GSDMD) to prompt pyroptosis and pore opening [56]. NE in NETs released during NETosis cleaves and activates GSDMD and induces neutrophil lysis [38, 39]. GSDMD could be a crosslink between pyroptosis and NETosis. The activation of the noncanonical inflammasome occurs during the recognition of LPS by caspase-4, stimulating its activation, caspase-1 activation, and GSDMD pore formation via the NLRP3 inflammasome. Noncanonical inflammasome stimulation through the transportation of LPS to the neutrophil cytoplasm activates caspase-4/-11 and causes the release of NETs in a GSDMD-dependent manner [58]. Related studies showed that NET-primed macrophages improved the IL-1β/Th17 response, causing atherogenesis [59]. IL-1β plays an important role in the canonical pyroptosis pathway, and NETosis may trigger pyroptosis by activating caspase-4 and IL-1β. In addition, a study has documented that apoptotic caspase-8 triggers the formation of GSDMD pores [60]. If NETs are able to activate caspase-8, NETs may trigger apoptosis [56]. In contrast to apoptosis, inhibition of caspase-8 induces necroptosis through recruiting and phosphorylating RIPK3 by RHIM-RHIM under the influence of continued RIPK1 kinase activity [56, 61, 62]. If NETs inhibit caspase-8 activity, NETosis may also cause necroptosis. Overall, GSDMD and caspase-8 may be central points in NETosis, pyroptosis, necroptosis, and apoptosis. Further studies are needed to prove this hypothesis.

4. Evidence of NETosis in CNS Injury

4.1. NETs in Traumatic Brain Injury (TBI). TBI is often attributed to the application of mechanical force to the head. TBI has two stages. One is primary injuries, which occur at the time of impact. Another is secondary injuries developing under the circumstance of supervised medical care [63]. TBI is often considered to be involved in various chronic degenerative processes. After external violence, intracranial haemorrhage will result in increased neurological deterioration, cerebral hypoperfusion, and altered intracranial pressure (ICP) because the volume of the skull is limited. In addition to the influence of external factors and local compression by haematoma, inflammatory cells are also involved in the traumatic process. Therefore, as a diverse group of sterile injuries, TBI is generally induced by primary and secondary mechanisms, and it leads to neurologic dysfunction, inflammation, and cell death in patients of all demographics [64]. Studies have shown that after TBI, the CNS rapidly recruits neutrophils which enter through the choroid plexus and the vessels of meninges [65, 66]. As such, we confirm that neutrophils are implicated in the process of TBI, but whether

NETs are required for the injury process remains to be further researched. Early signs of TBI pathogenesis are tissue destruction, hypoxia, and edema, through which the earliest soluble mediators, ROS, are produced [65]. As described in the pretext, ROS are critical mediators participating in the formation of NETs, so there are enough reasons to assume this hypothesis. Vaibhav et al. [67] discovered NETs in hypoperfused brain tissue through a mouse controlled cortical impact (CCI) model [67]. After that, to further explore the mechanism of NETs in TBI, researchers used C3H/HeJ mice lacking functional TLR4 compared to wild-type C3H/OuJ mice [67]. The results showed that C3H/HeJ mice displayed less NET formation and edema development after TBI. After TBI, the isolated C3H/OuJ neutrophils were transferred to either C3H/HeJ (WT>mutant (MUT)) mice or C3H/OuJ (wild type (WT)>WT) mice, which caused increases in NETs, indicating that TLR4 activation improves the generation of NETs [67]. Additionally, after TBI, TLR4 activation increased histone hypercitrullination and NET formation via a PAD4-dependent mechanism in isolated human neutrophils, and circulating levels of Cit-H3, a product of PAD4 activity, was noted [67]. Administration of Cl-amidine, an inhibiting agent of PAD4, dose-dependently reduced CNS neutrophil infiltration, attenuated NET production after TBI, reduced cerebral edema, improved CSF, and ameliorated neurological deficits after TBI. In addition, paroxysmal sympathetic hyperactivity (PSH) plays an important role in the high morbidity and mortality of TBI [67]. A research group used enzyme-linked immunosorbent assay with a rat diffuse axonal injury (DAI) model to evaluate the concentrations of plasma normetanephrine and metanephrine [68]. These values are indices of sympathetic system variation after TBI [68]. Study shows that after TBI, the levels of normetanephrine and metanephrine initially increased at 9 h and reached their highest values at 72 h [68]. After injury, in the paraventricular nucleus (PVN), a continuous increase in the concentration of NETs was observed at 24 and 72 h [68–71]. A positive connection between blood catecholamine and PVN or NET levels was found [68–71]. The flow cytometry assay of peripheral blood cells demonstrated that compared with the control group, there was a much higher level of NETs in the injury group [68–71]. The immunofluorescence results proved that NETs appeared in the PVN after TBI, the positive immunoprecipitation results indicated that LL37 was correlated with P2 × 7 [68–71]. As a portion of NETs, LL37 is an agonist of the P 2 × 7 receptor, which is a trimer ATP-gated cationic channel and highly expressed on the cell membrane of microglia and monocytes [68–71]. LL37 could enhance IL-1β secretion in monocytes through the P2 × 7 receptor [68–71]. IL-1β, an important inflammatory mediator, takes part in sympathetic excitation by mediating neuronal activity and inhibitory/excitatory neurotransmitter levels [68–71]. The expression levels of IL-1β could be inhibited by PAD4 and Hippo/MST1 pathway inhibitors; furthermore, PAD4 inhibitors could also prevent MST1 expression [68–71]. This evidence reveals that IL-1β secretion is regulated by LL37 in NETs through the Hippo/MST1 pathway, under the influence of PSH, and microglial activation after TBI to eventually cause sympathetic hyperactivity. Moreover, since proteolytic proteins (e.g., metalloproteinases (MMPs) and cathepsin G and NE) are released, intravascular NETs directly lead to toxic effects on the endothelium [9]. MMPs and NE are related to the retraction of endothelial cells and the disruption of junctional complexes [9]. The permeability of endothelial cells was improved by NE itself, while the death of endothelial cells was caused by MPO and histones [9]. In this case, the production of NETs may damage cerebral vascular endothelial cells and brain cells, going a step further to exacerbate the destruction of the brain by hypoxia after TBI.

4.2. NETs in Cerebral Ischaemia. There are many reasons for cerebral ischaemia, including cerebral atherosclerotic plaque formation, cerebral artery thromboembolism, and cerebral artery stenosis. Chronic inflammation induced by neutrophils is considered to be a potential cause of atherosclerosis. A previous perspective is that the underlying pathophysiology termed atherosclerosis is a lipid-driven inflammatory disease of arteries developing at predilection sites with disturbed flow, in which endothelial activation contributes to intimal retention of lipoproteins [72]. Oxidized low-density lipoprotein and modified lipoproteins augment the damage to endothelial cells and cause the recruitment of leukocytes once they fail to pass through cell death, retain inflammation, and eliminate lipoproteins [72]. The growing lesions caused by chronic inflammation will induce vessel occlusion and subsequent arterial or ischaemic thrombosis [72]. Finding the linkage between NETs and atherosclerosis induced by chronic inflammation will further explain the pathophysiological mechanism. In research studies, NETs activated plasmacytoid dendritic cells in the vessel wall, leading to a strong response to type I interferon (IFN I), subsequently causing atherogenesis. After treatment with chloramidine to inhibit PAD4, thrombosis of the carotid artery and the size of atherosclerotic lesions were reduced in an atherosclerotic mouse model [73, 74]. In addition, NETs have a direct effect on inducing endothelial dysfunction (as a starting point of atherosclerosis) via endothelial cell activation and damage [75–77]. Some authors think that NET-mediated priming of macrophages induces PR3-mediated cytokine maturation or a strong IL-1β/Th17 response driving atherogenesis [59, 78]. Regardless, evidence reveals the potential correlation between NETs and cerebral atherosclerosis. Fuchs et al. have proved the relationship between NETs and thrombosis [79]. Extracellular DNA secreted by NETs served as a net for red blood cells and platelets, and high levels of histones and DNA render NETs highly procoagulant by activating and accumulating platelets [79]. Activated platelets adhere to procoagulant molecules, such as fibrinogen, von Willebrand factor (VWF), and fibronectin, which are immobilized on NETs [79]. Meanwhile, components in NETs also trigger procoagulant molecules or block inhibitors of the tissue factor pathway to accelerate the process of coagulation [80]. Moreover, it is well known that extracellular DNA induces coagulation and activates innate immune responses after infection [81]. Therefore, these studies showed that a variety of NET components present in the plasma of stroke patients are possibly required for NET

prothrombotic effects and are assayed to assess disease severity. New studies are needed to further explore the relationship between thrombosis and NETosis in cerebral ischaemia. In addition, experiments by Kim and colleagues suggested that high-mobility group box-1 (HMGB1), a prototypic DAMP, is involved in NET-mediated neuronal damage in the ischaemic brain [82]. HMGB1 is a nonhistone chromosomal protein localized in the nucleus under normal physiological conditions that is considered to activate platelets and induce NETosis [82]. HMGB1 is not only emitted from NETosed neutrophils but also activated platelets [83–85]. The myocardial repair process is interfered with, by activated platelet-derived HMGB1 via decreasing the accumulation of mesenchymal stem cells through downregulating the hepatocyte growth factor receptor MET in a TLR4-dependent process [83–85]. Furthermore, NET formation and autophagy is enhanced by activated platelet-derived HMGB1 in a RAGE-dependent manner [83–85]. Therefore, NETosed neutrophil- or activated platelet-derived extracellular HMGB1 initiates thrombosis and further promotes NETosis, which mediates the aggravation cascade resulting in cerebral ischaemia and various other diseases associated with immunothrombosis [83–85]. In addition, NETosis caused by HMGB1 exacerbates ischaemic brain damage in the MACO model [82]. The results show that HMGB1 induces NETosis via TLR4 and CXCR4, which is consistent with the results described in the pretext that TLR4 is able to trigger the release of NETs [82]. When HMGB1 was emitted from neutrophils and aggregated in culture media and cell lysates, NETosis was triggered by circulating neutrophils treated with NCM, and those blood neutrophils treated with NCM were cocultivated with primary cortical neurons, increasing the levels of PI-positive neurons, suggesting that HMGB1 released from neutrophils after NETosis leads to NETosis-induced neuronal death and the presence of a reciprocal aggravating cycle between NETosis and neuronal cell death [82]. Some researchers also proved that the accumulation of ATP during cerebral ischaemia could lead to NETosis [86]. A prototypic P2X7R agonist (BzATP) or ATP dramatically induced CitH3 and PAD4 in a P2X7R-dependent manner, and NADPH oxidase-dependent ROS production, PKCα activation, and intracellular Ca^{2+} influx are critical in ATP-P2X7R-mediated NETosis [86]. Within the process of NETosis, the most effective component is NETs, so we assume damage in cerebral ischaemia is mainly ascribed to NETs. Many studies have shown an increase in NETs after cerebral ischaemia [87]. Kang et al. [87] through a middle cerebral artery occlusion (MACO) model indicated that stroke resulted in the accumulation of neutrophils in the brain, creating toxic signals (such as NETs), which subsequently improved the production of STING-dependent type I IFN-β activation. Remarkably, they also found that the increased generation and impaired clearance of NETs were detrimental to vascular repair and revascularization after stroke [87]. Additionally, active components in NETs destroy the viability of neurons. In vitro, coculturing transmigrated neutrophils with neurons for 3 h significantly reduced the viability of neurons [88]. However, DNase treatment of conditioned medium from transmigrated granulocytes did not evidently diminish the viability of neurons; therefore, the decrease in the viability of neurons was not ascribed to extracellular DNA [88]. Moreover, inhibiting neutrophil-derived extracellular proteases (such as neutrophilic proteases) related to NETs remarkably reduced neutrophil-mediated neurotoxicity [88]. Interestingly, as shown in experiments, the key neutrophilic proteases, cathepsin-G, NE, proteinase-3, and MMP-9, seem to attack neurons when a mixture of their inhibitors, but not any single specific inhibitor, nearly completely reversed the neutrophil-dependent neurotoxic effect [9, 88]. Altogether, these authors identified a novel neuroinflammatory mechanism: the development of rapid neurotoxicity of neutrophils initiated by IL-1-induced cerebrovascular transmigration [9, 88]. Consistently, Allen et al. [9, 88] proved that rapidly developed (30 min) neutrophil-dependent neurotoxicity is mediated by neutrophil-derived proteases released upon degranulation or associated with NETs. This result indicates that NETs may have toxic effects on neurons, which may be the reason for defects and nerve damage after stroke.

4.3. NETs in CNS Infection. CNS infection is uncommon in the presence of BBB (blood-brain barrier), but individuals may suffer from CNS infection, such as meningitis or encephalitis, under circumstances of low immunity. Local failure of the immune response mechanism leads to these devastating conditions, which consequently result in irreversible brain damage. The critical role of NETs in antimicrobial activity is clear [3], so we assume that NETs may participate in CNS infection. As described previously, NETs mainly kill bacteria through phagocytosis and oxidative stress as bactericidal mechanisms in CNS infection. In the clinic, neutrophils are observed crossing the BBB in bacterial meningitis upon the examination of CSF by lumbar puncture [89]. As described in the pretext, NETs capture both gram-positive and gram-negative microbes, and active components in NETs not only kill bacteria but also inhibit the spread of infection and retain homeostasis at the point of entry, even in unexpected body compartments [19]. By engulfing and immobilizing viruses, NETs also prevent virus entry into cells and spreading [90]. There are many antimicrobial compounds. Mohanty et al. [91] discovered that DNase1 significantly cleared bacteria in affected organs (lungs, brain, and spleen) and decreased bacterial viability in the presence of neutrophils in vitro. The eradication of bacteria from the brains of DNase-treated rats correlated with a decrease in IL-1β levels [91]. These findings indicated that DNA in NETs has antimicrobial activity. The antimicrobial activity effect was also annulled by inhibitors of phagocytosis, NADPH oxidase, and MPO [9, 91]. In addition, much evidence has revealed that NETs occur in CNS infection. From statistical data, increases in NETs were detected in children with enteroviral meningitis (EVM), tick-borne encephalitis (TBE), and Lyme neuroborreliosis (LNB), and the highest median levels of polynuclear cells were present in TBE [92]. Since monocytes play a primary role in viral encephalitis and are also able to release analogues of NETs, the authors determined the proportions of

mononuclear and polynuclear cells in NET-positive samples [92]. The results confirmed that polynuclear cells are specifically related to NET levels rather than pleocytosis. In addition, the activity of NE and the levels of NETs displayed a high degree of correlation [92]. Therefore, they concluded that the NET structures mainly originated from neutrophils [92]. When the researchers tested chemokines and cytokines in CSF sample, the result showed that the levels of CXCL1, CXCL6, CXCL8, CXCL10, MMP-9, IL-6, and TNF were raised in the sample. Therefore, the recruitment of neutrophils into the CNS is a prerequisite in infections resulting from enterovirus and *B. burgdorferi*. The combination of CXC-receptor 2 on neutrophils and chemokines CXCL8, CXCL6, and CXCL1 could result in autoactivation and enable neutrophils to enter the CNS during infections [92]. The highest median levels of NETs/neutrophil-associated cytokines and chemokines were also determined in the CSF samples of children with EVM [92]. However, Mohanty et al. [91] noted that NETs hinder the clearance of bacteria in pneumococcal meningitis, and the application of DNase1 reduces pneumococcal viability in the brain and enhances the clearance of bacteria in a meningitis mouse model. Further data showed that suppression of NADPH, MPO, and phagocytosis caused the death of bacteria due to DNase treatment. Therefore, the authors assume that when encountering neutrophils, bacteria lead to NET generation in the brain; however, not all bacteria are associated with NETs [91]. Therefore, bound/unbound bacteria enhance their viable loading and induce leakage of the BBB. Ultimately, the bacteria go through the defective BBB and spread into other organs. Treatment with DNase degrades DNA in NETs, resulting in the release of bacteria and allows other defence mechanisms of neutrophils to control and promote the process of microbial clearance [91]. Elucidation of the relevant mechanisms still needs further research to provide appropriate future therapeutic targets.

4.4. NETs in Alzheimer's Disease (AD). AD, which tends to occur in the elderly, is a neurodegenerative disorder characterized by the progressive degeneration of cognitive functions. Previous research indicated that the molecular pathogenesis of the disease is mainly ascribed to the loss of synapses and neurons, plaques composed of amyloid beta (Abeta), and tangles composed of hyperphosphorylated tau [93]. Chronic neuroinflammation is a typical feature of AD pathogenesis [94]. Since inflammation occurs in AD, we speculate that leukocytes may be implicated in the pathological process. Compelling evidence indicates that neutrophils are able to pass through the BBB and have been discovered inside the parenchyma and brain vessels of AD subjects. Moreover, recent data from two transgenic animal models of AD indicate that neutrophils bind to blood vessels and intrude into the brain parenchyma, causing neuropathological alterations and cognitive deficits [95]. Further studies have proven the production of NETs in an AD mouse model and in individuals with AD [94, 96]. Aβ is broadly considered a marker of Alzheimer's disease. Aβ promotes the generation of ROS by activating NADPH oxidase in both human and mouse neutrophils in vitro, and several reports have demonstrated that ROS production is a necessary step in the formation of NETs [9]. In addition to Aβ, some studies have demonstrated that NET formation in human neutrophils in vitro is also driven by the fibrillary form of amyloids from other sources, such as α-synuclein, Sup35, and transthyretin [9, 95]. In the same study, the presence of NETs was observed near amyloid deposits in patients with systemic amyloidosis, and NET-associated elastase was able to degrade amyloid fibrils into short toxic oligomeric species, suggesting that amyloid fibrils act as a reservoir of toxic peptides that may promote amyloid disease pathogenesis [95]. Studies have revealed that Aβ1–42 triggers the states of high affinity and intermediate affinity of LFA-1 (lymphocyte function-associated antigen 1) integrin, which modulates intraparenchymal motility and the intravascular adhesion of neutrophils [94, 96]. Then, Aβ improves the interaction between its endothelial ligands and LFA-1 [94, 96]. Although neutrophils were eliminated by injecting an anti-Ly6G antibody (clone 1A8) into the peripheral circulation of 6-month-old 3xTg-AD mice, the authors found that in comparison with the control group, the levels of cognitive function of mice in other groups were improved by treatment with anti-Ly6G [94, 96]. Cognitive deficits and pathology were induced due to inhibition of LFA-1. The results showed the role of neutrophils in Alzheimer's disease-like cognitive decline and pathology through LFA-1 integrin [94, 96]. Although NETs have been discovered in the AD brain, articles have failed to describe the relationship between NETs and AD [94, 96]. Aβ, as a DAMP, has been proven to be recognized by the complement system (CS) [94, 97]. Compliments such as C5a, CR1, and C1q may be related to NETs and AD [98]. Neutrophils may cause extrusion of NETs by recognizing Aβ. With the progression of inflammation and the accumulation of NETs, NETs trigger CS activation, especially C5a, via properdin binding and alternative pathways, eventually resulting in neurodegeneration [99, 100]. A study showed that there is a noticeable decline in the features of neuropathology and inflammation in an AD mouse model lacking C1q. Increases in C1q deposition suppress the activity of DNase, leading to the accumulation of NETs. After inhibition of C1q, the complement cascade reaction stops, and no NETs appear [101, 102]. Furthermore, the constituents of NETs damage neural cells within the brain parenchyma because they proteolytically activate inflammasome pathways and mitochondrial apoptosis and destroy extracellular matrix proteins [9]. The research on NETs is insufficient and needs further experimental elaboration.

4.5. NETs in SCI. SCI has many similarities with TBI. Typically, SCI is induced due to external physical impacts, called the primary injury. Violence causes an increase in interstitial pressure and haemorrhage, which press on the surrounding vessels and subsequently induce local ischaemia [103, 104]. The primary injury induces secondary injury, which further causes mechanical and chemical damage to spinal tissues, resulting in neuronal excitotoxicity due to the increasing level of reactive oxygen and high concentrations of calcium accumulated in cells [104]. Elevated levels of cytosolic Ca^{2+}

Table 1: Potential drugs targeted to NETosis.

Drugs	Target	Model	Potential mechanism	Reference
Apocynin	NOX2	Primary human neutrophils	Decrease production of ROS by inhibiting NOX2	[15]
VAS2870	NOX2	Primary human neutrophils	Decrease production of ROS by inhibiting NOX2	[15]
DNase1	DNA	NZB/W F1 hybrid mice	Endonuclease to digest extracellular DNA and degrade NETs	[114]
Cl-Amidine	Cys645	Mice	Irreversible inhibition of PAD4	[117, 118]
F-Amidine	Cys645	Mice	Irreversible inhibition of PAD4	[117, 118]
GSK484	Low-calcium (2 mM Ca) form of PAD4	Mice	Reversible inhibition of PAD4	[116, 118]
CsA	PPIase	Primary human neutrophils and CGD neutrophils	Inhibit mPTP open by blocking the PPIase activity of mitochondrial cyclophilin CypD	[15]
SfA	PPIase	Primary human neutrophils and CGD neutrophils	Inhibit mPTP open by blocking the PPIase activity of mitochondrial cyclophilin CypD	[15]
MeVal4CsA	PPIase	Primary human neutrophils and CGD neutrophils	Inhibit mPTP open by blocking PPIase activity of mitochondrial cyclophilin CypD	[15]
BKA	ANT	Primary human neutrophils and CGD neutrophils	Inhibit mPTP open by freezing adenine nucleotide ANT in the matrix-oriented conformation	[124]

enhance the activity of complex 1 and increase the production of ATP and ROS [104]. Early signs of TBI pathogenesis are tissue destruction, edema, and hypoxia, through which the earliest soluble mediators, ROS, are produced [67]. ROS are critical mediators in the formation of NETs. Therefore, we assume that SCI and TBI may share the same mechanism to induce NETosis. Apart from that, via the mitochondrial calcium uniporter, Ca^{2+} crossovers into the mitochondria. High levels of cytosolic Ca^{2+} induce increases in mPTPs and enhance membrane permeabilization [105]. Interestingly, mPTP is involved in NET formation and oxidative burst through activation of NADPH oxidase or other nonoxidative pathways [15]. Therefore, we reasonably speculate that NETs occur in the process of SCI. Sterile inflammation caused by spinal cord damage is characterized by infiltration of neutrophils in the spinal cord [106, 107]. As the main component in NETs, MPO is regarded as the primary cause of secondary injury due to its ability to generate HOCl [108, 109]. This cytotoxic substance strengthens apoptosis and necrosis, promotes the inflammatory response, and causes myelin degradation, thereby resulting in increased lesion size and further deteriorating neurological function [108, 109]. MPO exacerbates secondary injury and impairs functional recovery by enhancing neutrophil infiltration after SCI [110]. As an essential component of spinal cord edema, spinal cord astrocyte swelling is related to therapeutic resistance and poor functional recovery after SCI. Sun et al. [111, 112] revealed that an oxygen-glucose deprivation/reoxygenation (OGD/R) model improved the expression of HMGB1 and AQP4 and spinal cord astrocytic swelling, while HMGB1 inhibition by either ethyl pyruvate or HMGB1 shRNA led to a decrease in AQP4 expression and rat spinal cord astrocytic swelling after oxygen-glucose deprivation. HMGB1 upregulates AQP4 expression and promotes cell swelling in cultured spinal cord astrocytes after OGD/R, which is mediated through HMGB1/TLR4/MyD88/NF-κB signalling and in an IL-6-dependent manner [111]. It has been reported that activation impacts are restrained by NF-κB inhibition via the utilization of BAY 11-7082 or TLR4 inhibition via the utilization of C34 or CLI-095 [111, 112]. HMGB1 induces NETosis via TLR4 and exacerbates damage after cerebral ischaemia and cerebral thrombosis [85], and TLR4 is also an important signal for activating NETosis [112]. Therefore, we speculate that NET formation may mediate the process of injury in SCI, although evidence is still insufficient. However, some publications refute the damaging effect of neutrophils in SCI and hold the idea that the inflammatory function of neutrophils could reversely offer valuable outcomes for tissue repair in SCI [113]. There are still many unclear areas about neutrophil function in SCI. Therefore, further information about their cellular and molecular mechanisms of action is required to provide new insights in the field of SCI.

5. Therapy Methods of NETosis

Generally, NETosis has a greater impact on damage to CNS injuries, so preventing the progression of NETosis is vital to cure CNS injuries. Inhibition of NADPH oxidase, DNase, and PAD4 seems feasible to block NET formation, and we have provided details about potential drugs of NETosis in the table (Table 1). Apocynin (a naturally existing methoxy-substituted catechol) and VAS2870 (a triazolopyrimidine), which have been proven to be effective in primary human neutrophils, inhibit NADPH oxidase 2 (NOX2) and prevent the occurrence of NETosis induced by PMA and A23187 [15]. Inhibition of NADPH oxidase is rarely used in the clinic, and ROS produced by NADPH oxidase induces not only NETosis but also other harmful reactions. Therefore, we need to find a more specific medicine for application in the clinic. Recombinant DNase1 has been successfully implemented in pathological mouse models related to NETosis, such as SLE [114]. A formulation of DNase1 (Pulmozyme®) has been approved for

cystic fibrosis treatment in NZB/WF1 hybrid mice [115]. Although the function of extracellular DNA extruded from neutrophils in CNS injury remains unknown, the application of DNase in autoimmune disease and mouse infection models has proven to be effective, yet further studies still need to explore the relationship between DNase and CNS injury. PAD4 prompts decondensation by catalysing citrullination of histones [32], and the binding of calcium and PAD4 enhances the bioactive conformation, causing the activity of PAD4 to be increased by 10,000 times [116]. F-amidine leads to irreversible inhibition of PAD4 by altering the active site of cysteine (Cys645), which is essential for catalysis [117, 118]. Cl-amidine is also a form of irreversible inhibitor that functions in the same manner as F-amidine [117, 119]. Both Cl-amidine and F-amidine have been shown to inhibit NETosis in mice [117, 118]. Moreover, the PAD4 inhibitory potency of Cl-amidine over F-amidine has also been proven in in vitro and in vivo experiments [118]. These compounds are extensively used in experiments to inhibit NET formation and are greatly effective. GSK484, a benzimidazole derivative, also reversibly inhibits PAD4, which tightly and reversibly attaches to the low-calcium (2 mM Ca) form of PAD4 and competes with the substrate. GSK484 is able to diminish histone citrullination and NET formation in mice treated with ionomycin [116, 118]. In addition, mPTP probably participates in NET formation, which is substantially decreased after using MeVal4CsA, bongkrekic acid (BKA), cyclosporine A (CsA), and sanglifehrin A (SfA) [15]. As an immunosuppressant, CsA inhibits mPTP opening by blocking the peptidyl-prolyl cis-trans isomerase (PPIase) activity of mitochondrial cyclophilin CypD, which is a critical regulatory component of the mPTP [15]. However, CsA inactivates the essential Ca^{2+}-dependent protein phosphatase calcineurin, accordingly interrupting various signalling pathways [120–123]. MeVal4CsA and sanglifehrin A (SfA) have the same effect as CsA without the ability to inhibit calcineurin [120–123]. BKA is a form of adenine nucleotide translocase (ANT) inhibitor that inactivates translocase by freezing adenine nucleotide ANT in the matrix-oriented conformation, thereby suppressing the opening of mPTP [124]. All of these drugs have been proven to be effective in inhibiting NET formation in primary human neutrophils and CGD neutrophils [15]. Drugs related to NETosis inhibition are still rarely used in the clinic, so further studies are needed enable their use for the treatment of CNS injury.

6. Conclusion

In summary, NETosis is closely related to inflammatory reactions, and the function of damage outweighs the capability of repair in CNS injuries. The formation of NETs is boosted by diverse physiological stimuli, including lipopolysaccharides, protozoa, viruses, fungi, and bacteria. In addition, NETs are triggered by microcrystals, cholesterol, antibodies, specific cytokines (e.g., TNF-α and IL-8), and pharmacological stimuli containing calcium, potassium ionophores, and PMA. PAD4 is used to citrullinate histones, which will cause chromatin decondensation and NET release. NETs are the main components in the process of NETosis and have a negative effect on the CNS. We found that GSDMD and caspase-8 may be central points in NETosis, pyroptosis, necroptosis, and apoptosis. This will contribute to understanding the reciprocal relationships in all kinds of cell death in various diseases. In addition, we discuss the mechanism and existing evidence of NETosis in TBI, CNS infection, cerebral ischaemia, Alzheimer's disease, and SCI. TLR4, HMGB1, MPO, and NE have critical roles in these diseases. Finally, we expound on probable effective drugs to inhibit NETosis, in order to cure or alleviate CNS injury according to the NETosis mechanism, but most drugs are mainly used in experimental form, and few have progressed to the clinic.

Although NETosis is divided into suicidal NETosis and vital NETosis, the form that occurs in CNS injury remains unknown. DNA is vital to the viability of cells, and those in suicidal NETosis die because of the loss of DNA, while cells in vital NETosis remain alive after the release of NETs. We speculate that DNA in NETs may come from mitochondrial DNA; however, some cells will survive without the presence of nuclear DNA. Therefore, we wanted to know the exact mechanism of vital NETosis and whether the effects and events that occur between vital NETosis and suicidal NETosis are different. Moreover, we always discuss the effect of NETosis based on the function of NETs, but whether NETosis directly activates other cell death pathways or rather produces associate effective proteins or substances that contribute to the damage functions is still unclear. In this review, we discuss the function of NETosis in CNS injury and found much evidence about the occurrence of NETosis in CNS injury. However, what triggers NETosis is still unclear. TLR4 may be a recognized receptor, but whether other receptors recognize injury signals remains unknown. In addition, we focused on the damage of NETs to neurons but did not know whether NETosis influences other CNS cells. For example, if NETs can contribute to recovery of the spinal cord after SCI, did NETs activate Schwann cells or other cells? Or do NETs aggravate damage of other cells? Moreover, even though various biological events triggering the release of NETs have been excessively explored at present, their regulatory mechanisms are still unclear. In addition, related studies in vivo are rare. With regard to drugs, most inhibition of NETosis is mainly applied in experiments but rarely used in the clinic, and exploring the concrete mechanism of NETosis is fundamental on clinical trials. Therefore, further investigations are required to shed sufficient light on the underlying processes. We believe that studies concerning targets of NETosis will contribute to the therapy of a variety of diseases in the future.

Abbreviations

AD: Alzheimer's disease
BBB: Blood-brain barrier
CBF: Cerebral blood flow
CCI: Controlled cortical impact
CGD: Chronic granulomatous disease

CNS: Central nervous system
CS: Complement system
CSF: Cerebrospinal fluid
CXCL: Chemokine (C-X-C motif) ligand
DAI: Diffuse axonal injury
DAMP: Damage-associated molecular pattern
DPI: Diphenylene iodonium
fMLP: N-Formyl-L-methionyl-L-leucyl-L-phenylalanine
GM-CSF: Granulocyte-macrophage colony-stimulating factor
GO: Glucose oxidase
Grx1: Glutaredoxin 1
GSDMD: Gasdermin D protein
HMGB1: High-mobility group box-1
IFN: Interferon
LFA-1: Lymphocyte function-associated antigen 1
MAPK: Mitogen-activated protein kinase
MEK: Mitogen-activated protein kinase
MMP: Metalloproteinase
MPO: Myeloperoxidase
mPTP: Mitochondrial permeability transition pore
NE: Neutrophilic elastase
NETs: Neutrophil extracellular traps
NLRP: NOD-like receptor family pyrin domain containing 3
NOX2: NADPH oxidase 2
OGD/R: Oxygen-glucose deprivation/reoxygenation
PAD4: Peptidylarginine deiminase 4
PAF: Platelet-activating factor
PI3K: Phosphoinositide 3-kinase
PKC: Protein kinase C
PMA: Phorbol 12-myristate 13-acetate
PMN: Polymorphonuclear neutrophil
PRR: Pattern recognition receptors
PSH: Paroxysmal sympathetic hyperactivity
PVN: Paraventricular nucleus
RIPK: Receptor-interacting serine-threonine kinase
ROS: Reactive oxygen species
SCI: Spinal cord injury
SLE: Systemic lupus erythematosus
TBI: Traumatic brain injury
TLR: Toll-like receptors
VWF: von Willebrand factor.

Data Availability

The datasets used and analysed during the current study are available from the corresponding authors on reasonable request.

Conflicts of Interest

The authors have declared that no competing interests exist.

Authors' Contributions

Yituo Chen and Haojie Zhang searched and reviewed the literature and drafted and revised the manuscript. Xinli Hu and Wanta Cai discussed and revised the manuscript. Wenfei Ni and Kailiang Zhou designed and formulated the review theme and revised and finalized the manuscript. Yituo Chen and Haojie Zhang contributed equally to this work.

Acknowledgments

This work was supported by grants from National Natural Science Foundation of China (No. 8207219 to Kailiang Zhou), Public Welfare Technology Research Project of Zhejiang Province (No. LGF20H150003 to Kailiang Zhou), Zhejiang Provincial Natural Science Foundation (Nos. LY17H060009 and Y21H060050 to Wenfei Ni), and Wenzhou Science and Technology Bureau Foundation (No. Y20210438 to Kailiang Zhou).

References

[1] N. V. Vorobjeva and B. V. Chernyak, "NETosis: molecular mechanisms, role in physiology and pathology," *Biochemistry*, vol. 85, no. 10, pp. 1178–1190, 2020.

[2] H. Takei, A. Araki, H. Watanabe, A. Ichinose, and F. Sendo, "Rapid killing of human neutrophils by the potent activator phorbol 12-myristate 13-acetate (PMA) accompanied by changes different from typical apoptosis or necrosis," *Journal of Leukocyte Biology*, vol. 59, no. 2, pp. 229–240, 1996.

[3] V. Brinkmann, U. Reichard, C. Goosmann et al., "Neutrophil extracellular traps kill bacteria," *Science*, vol. 303, no. 5663, pp. 1532–1535, 2004.

[4] X. Hu, H. Chen, H. Xu et al., "Role of pyroptosis in traumatic brain and spinal cord injuries," *International Journal of Biological Sciences*, vol. 16, no. 12, pp. 2042–2050, 2020.

[5] M. B. Orr and J. C. Gensel, "Spinal cord injury scarring and inflammation: therapies targeting glial and inflammatory responses," *Neurotherapeutics*, vol. 15, no. 3, pp. 541–553, 2018.

[6] M. V. Russo and D. B. McGavern, "Inflammatory neuroprotection following traumatic brain injury," *Science*, vol. 353, no. 6301, pp. 783–785, 2016.

[7] J. Wu and M. M. Lipinski, "Autophagy in neurotrauma: good, bad, or dysregulated," *Cell*, vol. 8, no. 7, p. 693, 2019.

[8] N. A. Devanney, A. N. Stewart, and J. C. Gensel, "Microglia and macrophage metabolism in CNS injury and disease: the role of immunometabolism in neurodegeneration and neurotrauma," *Experimental Neurology*, vol. 329, article 113310, 2020.

[9] A. Manda-Handzlik and U. Demkow, "The brain entangled: the contribution of neutrophil extracellular traps to the diseases of the central nervous system," *Cell*, vol. 8, no. 12, p. 1477, 2019.

[10] C. Luo and L. Tao, "The function and mechanisms of autophagy in traumatic brain injury," *Advances in Experimental Medicine and Biology*, vol. 1207, pp. 635–648, 2020.

[11] I. L. McWilliams, J. L. Kielczewski, D. D. C. Ireland et al., "Pseudovirus rVSVΔG-ZEBOV-GP infects neurons in retina and CNS, causing apoptosis and neurodegeneration in neonatal mice," *Cell Reports*, vol. 26, no. 7, pp. 1718–1726.e4, 2019.

[12] S. J. Schimmel, S. Acosta, and D. Lozano, "Neuroinflammation in traumatic brain injury: a chronic response to an acute injury," *Brain Circulation*, vol. 3, no. 3, pp. 135–142, 2017.

[13] A. al Mamun, Y. Wu, I. Monalisa et al., "Role of pyroptosis in spinal cord injury and its therapeutic implications," *Journal of Advanced Research*, vol. 28, pp. 97–109, 2021.

[14] B. E. Steinberg and S. Grinstein, "Unconventional roles of the NADPH oxidase: signaling, ion homeostasis, and cell death," *Science's STKE*, vol. 2007, no. 379, 2007.

[15] N. Vorobjeva, I. Galkin, O. Pletjushkina et al., "Mitochondrial permeability transition pore is involved in oxidative burst and NETosis of human neutrophils," *Biochimica et Biophysica Acta - Molecular Basis of Disease*, vol. 1866, no. 5, article 165664, 2020.

[16] O. Tatsiy and P. P. McDonald, "Physiological stimuli induce PAD4-dependent, ROS-independent NETosis, with early and late events controlled by discrete signaling pathways," *Frontiers in Immunology*, vol. 9, 2018.

[17] V. Brinkmann and A. Zychlinsky, "Neutrophil extracellular traps: is immunity the second function of chromatin?," *The Journal of Cell Biology*, vol. 198, no. 5, pp. 773–783, 2012.

[18] T. Lu, S. D. Kobayashi, M. T. Quinn, and F. R. DeLeo, "A NET outcome," *Frontiers in Immunology*, vol. 3, 2012.

[19] B. G. Yipp and P. Kubes, "NETosis: how vital is it?," *Blood*, vol. 122, no. 16, pp. 2784–2794, 2013.

[20] T. A. Fuchs, U. Abed, C. Goosmann et al., "Novel cell death program leads to neutrophil extracellular traps," *The Journal of Cell Biology*, vol. 176, no. 2, pp. 231–241, 2007.

[21] D. J. Lu, W. Furuya, and S. Grinstein, "Involvement of multiple kinases in neutrophil activation," *Blood Cells*, vol. 19, no. 2, 1993.

[22] A. Hakkim, T. A. Fuchs, N. E. Martinez et al., "Activation of the Raf-MEK-ERK pathway is required for neutrophil extracellular trap formation," *Nature Chemical Biology*, vol. 7, no. 2, pp. 75–77, 2011.

[23] S. C. Trevelin and L. R. Lopes, "Protein disulfide isomerase and Nox: new partners in redox signaling," *Current Pharmaceutical Design*, vol. 21, no. 41, pp. 5951–5963, 2015.

[24] A. E. Dikalova, A. T. Bikineyeva, K. Budzyn et al., "Therapeutic targeting of mitochondrial superoxide in hypertension," *Circulation Research*, vol. 107, no. 1, pp. 106–116, 2010.

[25] N. Vorobjeva, A. Prikhodko, I. Galkin et al., "Mitochondrial reactive oxygen species are involved in chemoattractant-induced oxidative burst and degranulation of human neutrophils in vitro," *European Journal of Cell Biology*, vol. 96, no. 3, pp. 254–265, 2017.

[26] D. Stojkov, P. Amini, K. Oberson et al., "ROS and glutathionylation balance cytoskeletal dynamics in neutrophil extracellular trap formation," *The Journal of Cell Biology*, vol. 216, no. 12, pp. 4073–4090, 2017.

[27] P. Amini, D. Stojkov, A. Felser et al., "Neutrophil extracellular trap formation requires OPA1-dependent glycolytic ATP production," *Nature Communications*, vol. 9, no. 1, p. 2958, 2018.

[28] V. Papayannopoulos, K. D. Metzler, A. Hakkim, and A. Zychlinsky, "Neutrophil elastase and myeloperoxidase regulate the formation of neutrophil extracellular traps," *The Journal of Cell Biology*, vol. 191, no. 3, pp. 677–691, 2010.

[29] K. D. Metzler, C. Goosmann, A. Lubojemska, A. Zychlinsky, and V. Papayannopoulos, "A myeloperoxidase-containing complex regulates neutrophil elastase release and actin dynamics during NETosis," *Cell Reports*, vol. 8, no. 3, pp. 883–896, 2014.

[30] A. Shilatifard, "Chromatin modifications by methylation and ubiquitination: implications in the regulation of gene expression," *Annual Review of Biochemistry*, vol. 75, no. 1, pp. 243–269, 2006.

[31] T. Kouzarides, "Chromatin modifications and their function," *Cell*, vol. 128, no. 4, pp. 693–705, 2007.

[32] Y. Wang, M. Li, S. Stadler et al., "Histone hypercitrullination mediates chromatin decondensation and neutrophil extracellular trap formation," *The Journal of Cell Biology*, vol. 184, no. 2, pp. 205–213, 2009.

[33] K. Nakashima, T. Hagiwara, and M. Yamada, "Nuclear localization of peptidylarginine deiminase V and histone deimination in granulocytes," *The Journal of Biological Chemistry*, vol. 277, no. 51, pp. 49562–49568, 2002.

[34] A. I. Su, T. Wiltshire, S. Batalov et al., "A gene atlas of the mouse and human protein-encoding transcriptomes," *Proceedings of the National Academy of Sciences of the United States of America*, vol. 101, no. 16, pp. 6062–6067, 2004.

[35] P. Li, M. Li, M. R. Lindberg, M. J. Kennett, N. Xiong, and Y. Wang, "PAD4 is essential for antibacterial innate immunity mediated by neutrophil extracellular traps," *The Journal of Experimental Medicine*, vol. 207, no. 9, pp. 1853–1862, 2010.

[36] A. Hawez, A. al-Haidari, R. Madhi, M. Rahman, and H. Thorlacius, "MiR-155 regulates PAD4-dependent formation of neutrophil extracellular traps," *Frontiers in Immunology*, vol. 10, p. 2462, 2019.

[37] P. L. Kearney, M. Bhatia, N. G. Jones et al., "Kinetic characterization of protein arginine deiminase 4: a transcriptional corepressor implicated in the onset and progression of rheumatoid arthritis," *Biochemistry*, vol. 44, no. 31, pp. 10570–10582, 2005.

[38] H. Kambara, F. Liu, X. Zhang et al., "Gasdermin D exerts anti-inflammatory effects by promoting neutrophil death," *Cell Reports*, vol. 22, no. 11, pp. 2924–2936, 2018.

[39] G. Sollberger, A. Choidas, G. L. Burn et al., "Gasdermin D plays a vital role in the generation of neutrophil extracellular traps," *Sci Immunol*, vol. 3, no. 26, 2018.

[40] F. H. Pilsczek, D. Salina, K. K. H. Poon et al., "A novel mechanism of rapid nuclear neutrophil extracellular trap formation in response to Staphylococcus aureus," *Journal of Immunology*, vol. 185, no. 12, pp. 7413–7425, 2010.

[41] S. R. Clark, A. C. Ma, S. A. Tavener et al., "Platelet TLR4 activates neutrophil extracellular traps to ensnare bacteria in septic blood," *Nature Medicine*, vol. 13, no. 4, pp. 463–469, 2007.

[42] S. Yousefi, J. A. Gold, N. Andina et al., "Catapult-like release of mitochondrial DNA by eosinophils contributes to antibacterial defense," *Nature Medicine*, vol. 14, no. 9, pp. 949–953, 2008.

[43] S. E. Malawista, G. Van Blaricom, and M. G. Breitenstein, "Cryopreservable neutrophil surrogates. Stored cytoplasts from human polymorphonuclear leukocytes retain chemotactic, phagocytic, and microbicidal function," *The Journal of Clinical Investigation*, vol. 83, no. 2, pp. 728–732, 1989.

[44] S. E. Malawista, R. R. Montgomery, and G. van Blaricom, "Evidence for reactive nitrogen intermediates in killing of staphylococci by human neutrophil cytoplasts. A new microbicidal pathway for polymorphonuclear leukocytes," *The*

Journal of Clinical Investigation, vol. 90, no. 2, pp. 631–636, 1992.

[45] H. Parker, A. M. Albrett, A. J. Kettle, and C. C. Winterbourn, "Myeloperoxidase associated with neutrophil extracellular traps is active and mediates bacterial killing in the presence of hydrogen peroxide," *Journal of Leukocyte Biology*, vol. 91, no. 3, pp. 369–376, 2012.

[46] Y. Song, U. Kadiyala, P. Weerappuli et al., "Antimicrobial microwebs of DNA-histone inspired from neutrophil extracellular traps," *Advanced Materials*, vol. 31, no. 14, article e1807436, 2019.

[47] M. Zawrotniak and M. Rapala-Kozik, "Neutrophil extracellular traps (NETs) - formation and implications," *Acta Biochimica Polonica*, vol. 60, no. 3, pp. 277–284, 2013.

[48] B. C. Sheridan, R. C. McIntyre, E. E. Moore, D. R. Meldrum, J. Agrafojo, and D. A. Fullerton, "Neutrophils mediate pulmonary vasomotor dysfunction in endotoxin-induced acute lung injury," *The Journal of Trauma*, vol. 42, no. 3, pp. 391–397, 1997.

[49] A. Hakkim, B. G. Furnrohr, K. Amann et al., "Impairment of neutrophil extracellular trap degradation is associated with lupus nephritis," *Proceedings of the National Academy of Sciences of the United States of America*, vol. 107, no. 21, pp. 9813–9818, 2010.

[50] C. Farrera and B. Fadeel, "Macrophage clearance of neutrophil extracellular traps is a silent process," *Journal of Immunology*, vol. 191, no. 5, pp. 2647–2656, 2013.

[51] B. Lazzaretto and B. Fadeel, "Intra- and extracellular degradation of neutrophil extracellular traps by macrophages and dendritic cells," *Journal of Immunology*, vol. 203, no. 8, pp. 2276–2290, 2019.

[52] H. Wang, C. Wang, M. H. Zhao, and M. Chen, "Neutrophil extracellular traps can activate alternative complement pathways," *Clinical and Experimental Immunology*, vol. 181, no. 3, pp. 518–527, 2015.

[53] E. Fousert, R. Toes, and J. Desai, "Neutrophil extracellular traps (NETs) take the central stage in driving autoimmune responses," *Cell*, vol. 9, no. 4, 2020.

[54] Z. Zheng and G. Li, "Mechanisms and therapeutic regulation of pyroptosis in inflammatory diseases and cancer," *International Journal of Molecular Sciences*, vol. 21, no. 4, p. 1456, 2020.

[55] S. Gupta, D. W. Chan, K. J. Zaal, and M. J. Kaplan, "A high-throughput real-time imaging technique to quantify NETosis and distinguish mechanisms of cell death in human neutrophils," *Journal of Immunology*, vol. 200, no. 2, pp. 869–879, 2018.

[56] I. Jorgensen, M. Rayamajhi, and E. A. Miao, "Programmed cell death as a defence against infection," *Nature Reviews. Immunology*, vol. 17, no. 3, pp. 151–164, 2017.

[57] T. Bergsbaken, S. L. Fink, and B. T. Cookson, "Pyroptosis: host cell death and inflammation," *Nature Reviews. Microbiology*, vol. 7, no. 2, pp. 99–109, 2009.

[58] T. Rosazza, J. Warner, and G. Sollberger, "NET formation - mechanisms and how they relate to other cell death pathways," *The FEBS Journal*, vol. 288, no. 11, pp. 3334–3350, 2021.

[59] A. Warnatsch, M. Ioannou, Q. Wang, and V. Papayannopoulos, "Neutrophil extracellular traps license macrophages for cytokine production in atherosclerosis," *Science*, vol. 349, no. 6245, pp. 316–320, 2015.

[60] P. Orning, D. Weng, K. Starheim et al., "Pathogen blockade of TAK1 triggers caspase-8-dependent cleavage of gasdermin D and cell death," *Science*, vol. 362, no. 6418, pp. 1064–1069, 2018.

[61] M. Feoktistova, P. Geserick, B. Kellert et al., "cIAPs block Ripoptosome formation, a RIP1/caspase-8 containing intracellular cell death complex differentially regulated by cFLIP isoforms," *Molecular Cell*, vol. 43, no. 3, pp. 449–463, 2011.

[62] M. Pasparakis and P. Vandenabeele, "Necroptosis and its role in inflammation," *Nature*, vol. 517, no. 7534, pp. 311–320, 2015.

[63] T. Araki, H. Yokota, and A. Morita, "Pediatric traumatic brain injury: characteristic features, diagnosis, and management," *Neurologia Medico-Chirurgica (Tokyo)*, vol. 57, no. 2, pp. 82–93, 2017.

[64] K. N. Corps, T. L. Roth, and D. B. McGavern, "Inflammation and neuroprotection in traumatic brain injury," *JAMA Neurology*, vol. 72, no. 3, pp. 355–362, 2015.

[65] T. M. Carlos, R. S. B. Clark, D. Franicola-Higgins, J. K. Schiding, and P. M. Kochanek, "Expression of endothelial adhesion molecules and recruitment of neutrophils after traumatic brain injury in rats," *Journal of Leukocyte Biology*, vol. 61, no. 3, pp. 279–285, 1997.

[66] J. Szmydynger-Chodobska, N. Strazielle, B. J. Zink, J. F. Ghersi-Egea, and A. Chodobski, "The role of the choroid plexus in neutrophil invasion after traumatic brain injury," *Journal of Cerebral Blood Flow and Metabolism*, vol. 29, no. 9, pp. 1503–1516, 2009.

[67] K. Vaibhav, M. Braun, K. Alverson et al., "Neutrophil extracellular traps exacerbate neurological deficits after traumatic brain injury," *Science Advances*, vol. 6, no. 22, 2020.

[68] Y. Wang, J. Yin, C. Wang et al., "Microglial Mincle receptor in the PVN contributes to sympathetic hyperactivity in acute myocardial infarction rat," *Journal of Cellular and Molecular Medicine*, vol. 23, no. 1, pp. 112–125, 2019.

[69] A. Elssner, M. Duncan, M. Gavrilin, and M. D. Wewers, "A novel P2X7 receptor activator, the human cathelicidin-derived peptide LL37, induces IL-1 beta processing and release," *Journal of Immunology*, vol. 172, no. 8, pp. 4987–4994, 2004.

[70] M. Monif, G. Burnstock, and D. A. Williams, "Microglia: proliferation and activation driven by the P2X7 receptor," *The International Journal of Biochemistry & Cell Biology*, vol. 42, no. 11, pp. 1753–1756, 2010.

[71] K. Zhu, Y. Zhu, X. Hou et al., "NETs Lead to sympathetic hyperactivity after traumatic brain injury through the LL37-hippo/MST1 pathway," *Frontiers in Neuroscience*, vol. 15, article 621477, 2021.

[72] G. Lippi, M. Franchini, and G. Targher, "Arterial thrombus formation in cardiovascular disease," *Nature Reviews. Cardiology*, vol. 8, no. 9, pp. 502–512, 2011.

[73] Y. Döring, H. D. Manthey, M. Drechsler et al., "Auto-antigenic protein-DNA complexes stimulate plasmacytoid dendritic cells to promote atherosclerosis," *Circulation*, vol. 125, no. 13, pp. 1673–1683, 2012.

[74] J. S. Knight, W. Luo, A. A. O'Dell et al., "Peptidylarginine deiminase inhibition reduces vascular damage and modulates innate immune responses in murine models of atherosclerosis," *Circulation Research*, vol. 114, no. 6, pp. 947–956, 2014.

[75] A. K. Gupta, M. B. Joshi, M. Philippova et al., "Activated endothelial cells induce neutrophil extracellular traps and

are susceptible to NETosis-mediated cell death," *FEBS Letters*, vol. 584, no. 14, pp. 3193–3197, 2010.

[76] E. Villanueva, S. Yalavarthi, C. C. Berthier et al., "Netting neutrophils induce endothelial damage, infiltrate tissues, and expose immunostimulatory molecules in systemic lupus erythematosus," *Journal of Immunology*, vol. 187, no. 1, pp. 538–552, 2011.

[77] C. Carmona-Rivera, W. Zhao, S. Yalavarthi, and M. J. Kaplan, "Neutrophil extracellular traps induce endothelial dysfunction in systemic lupus erythematosus through the activation of matrix metalloproteinase-2," *Annals of the Rheumatic Diseases*, vol. 74, no. 7, pp. 1417–1424, 2015.

[78] O. Soehnlein, A. Ortega-Gómez, Y. Döring, and C. Weber, "Neutrophil-macrophage interplay in atherosclerosis: protease-mediated cytokine processing versus NET release," *Thrombosis and Haemostasis*, vol. 114, no. 4, pp. 866-867, 2015.

[79] T. A. Fuchs, A. Brill, D. Duerschmied et al., "Extracellular DNA traps promote thrombosis," *Proceedings of the National Academy of Sciences*, vol. 107, no. 36, pp. 15880–15885, 2010.

[80] M. L. von Brühl, K. Stark, A. Steinhart et al., "Monocytes, neutrophils, and platelets cooperate to initiate and propagate venous thrombosis in mice in vivo," *The Journal of Experimental Medicine*, vol. 209, no. 4, pp. 819–835, 2012.

[81] B. Altincicek, S. Stötzel, M. Wygrecka, K. T. Preissner, and A. Vilcinskas, "Host-derived extracellular nucleic acids enhance innate immune responses, induce coagulation, and prolong survival upon infection in insects," *Journal of Immunology*, vol. 181, no. 4, pp. 2705–2712, 2008.

[82] S. W. Kim, H. Lee, H. K. Lee, I. D. Kim, and J. K. Lee, "Neutrophil extracellular trap induced by HMGB1 exacerbates damages in the ischemic brain," *Acta Neuropathologica Communications*, vol. 7, no. 1, 2019.

[83] S. Vogel, M. Chatterjee, K. Metzger et al., "Activated platelets interfere with recruitment of mesenchymal stem cells to apoptotic cardiac cells via high mobility group box 1/Toll-like receptor 4-mediated down-regulation of hepatocyte growth factor receptor MET," *The Journal of Biological Chemistry*, vol. 289, no. 16, pp. 11068–11082, 2014.

[84] N. Maugeri, L. Campana, M. Gavina et al., "Activated platelets present high mobility group box 1 to neutrophils, inducing autophagy and promoting the extrusion of neutrophil extracellular traps," *Journal of Thrombosis and Haemostasis*, vol. 12, no. 12, pp. 2074–2088, 2014.

[85] S. W. Kim and J. K. Lee, "Role of HMGB1 in the interplay between NETosis and thrombosis in ischemic stroke: A Review," *Cells*, vol. 9, no. 8, p. 1794, 2020.

[86] S. W. Kim, D. Davaanyam, S. I. Seol, H. K. Lee, H. Lee, and J. K. Lee, "Adenosine triphosphate accumulated following cerebral ischemia induces neutrophil extracellular trap formation," *International Journal of Molecular Sciences*, vol. 21, no. 20, p. 7668, 2020.

[87] L. Kang, H. Yu, X. Yang et al., "Neutrophil extracellular traps released by neutrophils impair revascularization and vascular remodeling after stroke," *Nature Communications*, vol. 11, no. 1, p. 2488, 2020.

[88] C. Allen, P. Thornton, A. Denes et al., "Neutrophil cerebrovascular transmigration triggers rapid neurotoxicity through release of proteases associated with decondensed DNA," *Journal of Immunology*, vol. 189, no. 1, pp. 381–392, 2012.

[89] J. M. Conly and A. R. Ronald, "Cerebrospinal fluid as a diagnostic body fluid," *The American Journal of Medicine*, vol. 75, no. 1, pp. 102–108, 1983.

[90] G. Schönrich and M. J. Raftery, "Neutrophil extracellular traps go viral," *Frontiers in Immunology*, vol. 7, 2016.

[91] T. Mohanty, J. Fisher, A. Bakochi et al., "Neutrophil extracellular traps in the central nervous system hinder bacterial clearance during pneumococcal meningitis," *Nature Communications*, vol. 10, no. 1, p. 1667, 2019.

[92] D. Appelgren, H. Enocsson, B. H. Skogman et al., "Neutrophil extracellular traps (NETs) in the cerebrospinal fluid samples from children and adults with central nervous system infections," *Cell*, vol. 9, no. 1, p. 43, 2020.

[93] K. Blennow, M. J. de Leon, and H. Zetterberg, "Alzheimer's disease," *Lancet*, vol. 368, no. 9533, pp. 387–403, 2006.

[94] T. Wyss-Coray and J. Rogers, "Inflammation in Alzheimer disease-a brief review of the basic science and clinical literature," *Cold Spring Harbor Perspectives in Medicine*, vol. 2, no. 1, article a006346, 2012.

[95] E. C. Pietronigro, V. Della Bianca, E. Zenaro, and G. Constantin, "NETosis in Alzheimer's Disease," *Frontiers in Immunology*, vol. 8, 2017.

[96] E. Zenaro, E. Pietronigro, V. D. Bianca et al., "Neutrophils promote Alzheimer's disease-like pathology and cognitive decline via LFA-1 integrin," *Nature Medicine*, vol. 21, no. 8, pp. 880–886, 2015.

[97] P. L. McGeer, H. Akiyama, S. Itagaki, and E. G. McGeer, "Activation of the classical complement pathway in brain tissue of Alzheimer patients," *Neuroscience Letters*, vol. 107, no. 1-3, pp. 341–346, 1989.

[98] Y. Gottlieb, R. Elhasid, S. Berger-Achituv, E. Brazowski, A. Yerushalmy-Feler, and S. Cohen, "Neutrophil extracellular traps in pediatric inflammatory bowel disease," *Pathology International*, vol. 68, no. 9, pp. 517–523, 2018.

[99] C. Lebrero-Fernández, J. H. Bergström, T. Pelaseyed, and A. Bas-Forsberg, "Murine butyrophilin-like 1 and Btnl6 form heteromeric complexes in small intestinal epithelial cells and promote proliferation of local T lymphocytes," *Frontiers in Immunology*, vol. 7, 2016.

[100] C. M. de Bont, W. C. Boelens, and G. J. M. Pruijn, "NETosis, complement, and coagulation: a triangular relationship," *Cellular & Molecular Immunology*, vol. 16, no. 1, pp. 19–27, 2019.

[101] J. Leffler, M. Martin, B. Gullstrand et al., "Neutrophil extracellular traps that are not degraded in systemic lupus erythematosus activate complement exacerbating the disease," *Journal of Immunology*, vol. 188, no. 7, pp. 3522–3531, 2012.

[102] S. Hu, C. Marshall, J. Darby, W. Wei, A. B. Lyons, and H. Körner, "Absence of tumor necrosis factor supports alternative activation of macrophages in the liver after infection with Leishmania major," *Frontiers in Immunology*, vol. 9, 2018.

[103] B. Fan, Z. Wei, X. Yao et al., "Microenvironment imbalance of spinal cord injury," *Cell Transplantation*, vol. 27, no. 6, pp. 853–866, 2018.

[104] A. Anjum, M. D. Yazid, M. Fauzi Daud et al., "Spinal cord injury: pathophysiology, multimolecular interactions, and underlying recovery mechanisms," *International Journal of Molecular Sciences*, vol. 21, no. 20, p. 7533, 2020.

[105] Y. Cao, G. Lv, Y. S. Wang et al., "Mitochondrial fusion and fission after spinal sacord injury in rats," *Brain Research*, vol. 1522, pp. 59–66, 2013.

[106] H. Saiwai, Y. Ohkawa, H. Yamada et al., "The LTB4-BLT1 axis mediates neutrophil infiltration and secondary injury in experimental spinal cord injury," *The American Journal of Pathology*, vol. 176, no. 5, pp. 2352–2366, 2010.

[107] F. Bao, J. C. Fleming, R. Golshani et al., "A selective phosphodiesterase-4 inhibitor reduces leukocyte infiltration, oxidative processes, and tissue damage after spinal cord injury," *Journal of Neurotrauma*, vol. 28, no. 6, pp. 1035–1049, 2011.

[108] Y. W. Yap, M. Whiteman, B. H. Bay et al., "Hypochlorous acid induces apoptosis of cultured cortical neurons through activation of calpains and rupture of lysosomes," *Journal of Neurochemistry*, vol. 98, no. 5, pp. 1597–1609, 2006.

[109] Y. W. Yap, M. Whiteman, and N. S. Cheung, "Chlorinative stress: an under appreciated mediator of neurodegeneration?," *Cellular Signalling*, vol. 19, no. 2, pp. 219–228, 2007.

[110] K. Kubota, H. Saiwai, H. Kumamaru et al., "Myeloperoxidase exacerbates secondary injury by generating highly reactive oxygen species and mediating neutrophil recruitment in experimental spinal cord injury," *Spine*, vol. 37, no. 16, pp. 1363–1369, 2012.

[111] L. Sun, M. Li, X. Ma et al., "Inhibition of HMGB1 reduces rat spinal cord astrocytic swelling and AQP4 expression after oxygen-glucose deprivation and reoxygenation via TLR4 and NF-κB signaling in an IL-6-dependent manner," *Journal of Neuroinflammation*, vol. 14, no. 1, 2017.

[112] T. D. Tsourouktsoglou, A. Warnatsch, M. Ioannou, D. Hoving, Q. Wang, and V. Papayannopoulos, "Histones, DNA, and citrullination promote neutrophil extracellular trap inflammation by regulating the localization and activation of TLR4," *Cell Reports*, vol. 31, no. 5, article 107602, 2020.

[113] V. Neirinckx, C. Coste, R. Franzen, A. Gothot, B. Rogister, and S. Wislet, "Neutrophil contribution to spinal cord injury and repair," *Journal of Neuroinflammation*, vol. 11, no. 1, 2014.

[114] M. Macanovic, D. Sinicropi, S. Shak, S. Baughman, S. Thiru, and P. J. Lachmann, "The treatment of systemic lupus erythematosus (SLE) in NZB/W F1 hybrid mice; studies with recombinant murine DNase and with dexamethasone," *Clinical and Experimental Immunology*, vol. 106, no. 2, pp. 243–252, 1996.

[115] P. J. Mogayzel Jr., E. T. Naureckas, K. A. Robinson et al., "Cystic fibrosis pulmonary guidelines. Chronic medications for maintenance of lung health," *American Journal of Respiratory and Critical Care Medicine*, vol. 187, no. 7, pp. 680–689, 2013.

[116] H. D. Lewis, J. Liddle, J. E. Coote et al., "Inhibition of PAD4 activity is sufficient to disrupt mouse and human NET formation," *Nature Chemical Biology*, vol. 11, no. 3, pp. 189–191, 2015.

[117] Y. Luo, K. Arita, M. Bhatia et al., "Inhibitors and inactivators of protein arginine deiminase 4: functional and structural characterization," *Biochemistry*, vol. 45, no. 39, pp. 11727–11736, 2006.

[118] S. Koushik, N. Joshi, S. Nagaraju et al., "PAD4: pathophysiology, current therapeutics and future perspective in rheumatoid arthritis," *Expert Opinion on Therapeutic Targets*, vol. 21, no. 4, pp. 433–447, 2017.

[119] B. Knuckley, C. P. Causey, J. E. Jones et al., "Substrate specificity and kinetic studies of PADs 1, 3, and 4 identify potent and selective inhibitors of protein arginine deiminase 3," *Biochemistry*, vol. 49, no. 23, pp. 4852–4863, 2010.

[120] A. Nicolli, E. Basso, V. Petronilli, R. M. Wenger, and P. Bernardi, "Interactions of Cyclophilin with the Mitochondrial Inner Membrane and Regulation of the Permeability Transition Pore, a Cyclosporin A-sensitive Channel (*)," *The Journal of Biological Chemistry*, vol. 271, no. 4, pp. 2185–2192, 1996.

[121] J. J. Sanglier, V. Quesniaux, T. FEHR et al., "Sanglifehrins A, B, C and D, novel cyclophilin-binding compounds isolated from Streptomyces sp. A92-308110. I. Taxonomy, fermentation, isolation and biological activity," *Journal of Antibiotics*, vol. 52, no. 5, pp. 466–473, 1999.

[122] G. Zenke, U. Strittmatter, S. Fuchs et al., "Sanglifehrin A, a novel cyclophilin-binding compound showing immunosuppressive activity with a new mechanism of action," *Journal of Immunology*, vol. 166, no. 12, pp. 7165–7171, 2001.

[123] P. Bernardi, A. Rasola, M. Forte, and G. Lippe, "The mitochondrial permeability transition pore: channel formation by F-ATP synthase, integration in signal transduction, and role in pathophysiology," *Physiological Reviews*, vol. 95, no. 4, pp. 1111–1155, 2015.

[124] A. P. Halestrap and A. M. Davidson, "Inhibition of Ca2(+)-induced large-amplitude swelling of liver and heart mitochondria by cyclosporin is probably caused by the inhibitor binding to mitochondrial-matrix peptidyl-prolyl cis-trans isomerase and preventing it interacting with the adenine nucleotide translocase," *The Biochemical Journal*, vol. 268, no. 1, pp. 153–160, 1990.

Hindawi
Oxidative Medicine and Cellular Longevity
Volume 2021, Article ID 4280951, 17 pages
https://doi.org/10.1155/2021/4280951

Research Article

Controlled Decompression Attenuates Compressive Injury following Traumatic Brain Injury via TREK-1-Mediated Inhibition of Necroptosis and Neuroinflammation

Tao Chen, Xiao Qian, Jie Zhu, Li-Kun Yang, and Yu-Hai Wang

Department of Neurosurgery, The 904th Hospital of PLA, Medical School of Anhui Medical University, Wuxi, Jiangsu 214044, China

Correspondence should be addressed to Li-Kun Yang; yanglikun904@163.com and Yu-Hai Wang; prof_wyh101@163.com

Received 12 August 2021; Accepted 24 September 2021; Published 8 November 2021

Academic Editor: Yanqing Wu

Decompressive craniectomy is an effective strategy to reduce intracranial hypertension after traumatic brain injury (TBI), but it is related to many postoperative complications, such as delayed intracranial hematoma and diffuse brain swelling. Our previous studies have demonstrated that controlled decompression (CDC) surgery attenuates brain injury and reduces the rate of complications after TBI. Here, we investigated the potential molecular mechanisms of CDC in experimental models. The in vitro experiments were performed in a traumatic neuronal injury (TNI) model following compression treatment in primary cultured cortical neurons. We found that compression aggravates TNI-induced neuronal injury, which was significantly attenuated by CDC for 2 h or 3 h. The results of immunocytochemistry showed that CDC reduced neuronal necroptosis and activation of RIP3 induced by TNI and compression, with no effect on RIP1 activity. These protective effects were associated with decreased levels of inflammatory cytokines and preserved intracellular Ca^{2+} homeostasis. In addition, the expression of the two-pore domain K^+ channel TREK-1 and its activity was increased by compression and prolonged by CDC. Treatment with the TREK-1 blockers, spadin or SID1900, could partially prevent the effects of CDC on intracellular Ca^{2+} metabolism, necroptosis, and neuronal injury following TNI and compression. Using a traumatic intracranial hypertension model in rats, we found that CDC for 20 min or 30 min was effective in alleviating brain edema and locomotor impairment in vivo. CDC significantly inhibited neuronal necroptosis and neuroinflammation and increased TREK-1 activation, and the CDC-induced protection in vivo was attenuated by spadin and SID1900. In summary, CDC is effective in alleviating compressive neuronal injury both in vitro and in vivo, which is associated with the TREK-1-mediated attenuation of intracellular Ca^{2+} overload, neuronal necroptosis, and neuroinflammation.

1. Introduction

Traumatic brain injury (TBI) has been considered as one of the most complex human diseases because of the complexity of brain damage mechanisms and poor prognosis. For patients with uncontrollable high intracranial pressure, decompressive craniectomy is an effective strategy to reduce traumatic intracranial hypertension and improve prognosis [1]. However, the standard procedure of rapid decompression is associated with many postoperative complications, such as delayed intracranial hematoma and diffuse brain swelling [2, 3]. Our previous studies have demonstrated that the controlled decompression (CDC) surgery attenuates brain injury and reduces the rates of complications after TBI [4–6]. However, the underlying molecular mechanism has not been determined.

In the central nervous system (CNS), a variety of cellular physiological processes, including neurotransmitter release, neuronal excitability, and plasticity, are regulated by ion channels, especially Ca^{2+} and K^+ ions [7]. The tandem of pore domain in weak inwardly rectifying K^+ channel- (TWIK-) related K^+ channels (TREK) belongs to the recently discovered two-pore domain K^+ (K_{2P}) channels, which include 15 members grouped in six subfamilies and are responsible for

maintaining the neuronal resting membrane potential [8]. TREK-1, also known as KCNK2 or $K_{2P}2.1$, is highly expressed in the lung and brain, from the prefrontal cortex, hippocampus, and midbrain to the spinal cord [9]. Since its cloning two decades ago, the physiological importance of TREK-1 is constantly being discovered. TREK-1 is located at both presynaptic and postsynaptic components, which are its key roles in maintaining the resting membrane potential and neurotransmitter release. Its activation is regulated by various physical and chemical stimuli, such as mechanical stretch, Gq-coupled group I mGluRs, and Gs-coupled 5-HR4 receptor serotonin [10]. Increasing evidence has been demonstrated that dysfunction of TREK-1 channels is involved in multiple neurological pathologies, including depression, pain, epilepsy, and ischemia [11]. In TREK-1 gene knockout mice, TREK-1 null was found to increase neuronal excitability and enhance excitatory and inhibitory postsynaptic currents, thereby impairing cognitive function [12]. In addition, TREK-1 was found to be upregulated by ischemia in astrocytes to enhance glutamate clearance and block neuronal death [13]. However, the role of TREK-1 in traumatic intracranial hypertension conditions has not been fully determined.

In the current study, we investigated the effect of CDC on compressive injury following neuronal trauma in an in vitro model using primary cultured cortical neurons and also in an in vivo traumatic intracranial hypertension model in rats. Considering the effect of mechanical force on TREK-1 activation, we assessed the potential role of TREK-1 in CDC-induced protection.

2. Materials and Methods

2.1. Primary Culture of Cortical Neurons. Because neurons in the cerebral cortex are most vulnerable under traumatic intracranial hypertension, primary cultured cortical neurons were obtained from SD rats to establish the experimental models as previously described [14]. All the animal research procedures were approved by the Anhui Medical University Committee of Animal Research.

2.2. In Vitro Model and Treatments. The TNI model was performed according to our previously published method [15]. In brief, traumatic injury was performed on cultured neurons by using a rotating scribe injury device, which consisted of a rotating cylinder with ten holes, steel needles, and a permanent magnet. The cylinder holes are distributed at the same interval from the center, and these holes allowed the ten steel needles to freely cross through. A magnet is placed under the culture dish, which ensured that the steel needles could cling to the cell layer as the cylinder rotated. After one turn of this device, ten concentric circular scratches were produced in the neuronal layer with equal distances (1.5 mm) between the scratches. After TNI, neurons were exposed to continuous high pressure of 0.5 MPa according to our previous published paper [16]. Briefly, a custom-made compression apparatus in vitro was applied to expose neurons to continuous high pressure for 3 h. The TREK-1 blockers, spadin and SID1900, were obtained from the Mycell Biotech Company (Shanghai, China) and diluted in neurobasal medium to achieve the final concentration of 1 μM or 30 μM, respectively.

2.3. Hematoxylin-Eosin (H&E) Staining. At 12 h after TNI and compression treatment, cortical neurons were washed with phosphate buffer saline (PBS) and fixed with 4% paraformaldehyde for 30 min. Neurons were deparaffinized with xylene, stained by H&E, and then assessed by a pathologist for neuronal loss under an Olympus U-DO3 light microscope (Tokyo, Japan).

2.4. LDH Release. The neurotoxicity in cortical neurons was determined by measuring LDH release at 12 h after TNI and compression using a kit according to the manufacturer's protocol (Jiancheng Bioengineering Institute, Nanjing, Jiangsu, China).

2.5. Cell Viability Assay. Cell viability of cortical neurons was determined by calcein AM assay at 12 h after TNI and compression using a kit according to the manufacturer's protocol (Enzo Life Sciences, Farmingdale, NY, USA).

2.6. Immunocytochemistry. For immunocytochemistry, the neurons were cultured in poly-D-lysine-coated coverslips and treated with TNI, compression, or CDC. After being fixed with 4% paraformaldehyde, permeabilized with 0.1% Triton X-100, and washed with PBS for three times, neurons were blocked by 5% bovine serum albumin. Incubation with the RIP1 (1 : 100, #3493, Cell Signaling), RIP3 (1 : 200, ab62344, Abcam), and TREK-1 (1 : 50, sc-398449, Santa Cruz) primary antibodies was performed at 4°C overnight. After being washed by PBS with Tween-20 (PBST) for three times, the samples were incubated with the secondary antibody at 37°C for 1 h. Then, incubation with 4′,6-diamidino-2-phenylindole (DAPI) was performed to stain the nuclei, and the images were obtained using a Leica SP5 II confocal microscope.

2.7. Enzyme-Linked Immunosorbent Assay (ELISA). The levels of inflammatory cytokines, including TNF-α, IL-1β, IL-6, INF-γ, and IL-18, were measured by ELISA kits following the manufacturer's protocols (Anoric-Bio, Tianjin, China).

2.8. Ca^{2+} Imaging. Ca^{2+} imaging was performed using the Ca^{2+} indicator Fura-2 AM to measure the intracellular Ca^{2+} concentrations [17]. The neurons cultured in coverslips were loaded with 5 μM Fura-2 AM in HBSS solution for 30 min and equilibrated lucifugally for 30 min. Cells were excited at 345 and 385 nm using a confocal laser scanning microscope, and the emission fluorescence at 510 nm was recorded. The fluorescence values were then plotted against time and shown as F/F_0.

2.9. Patch Clamp Electrophysiology. The single TREK-1 channel currents were recorded in cortical neurons using the inside-out patch clamp configuration, and the bath solution contained the following: 130 mM KCl, 10x HEPES, 1 mM $MgCl_2$, 5 mM EGTA, and 10 μM Ca^{2+}. The experiments were

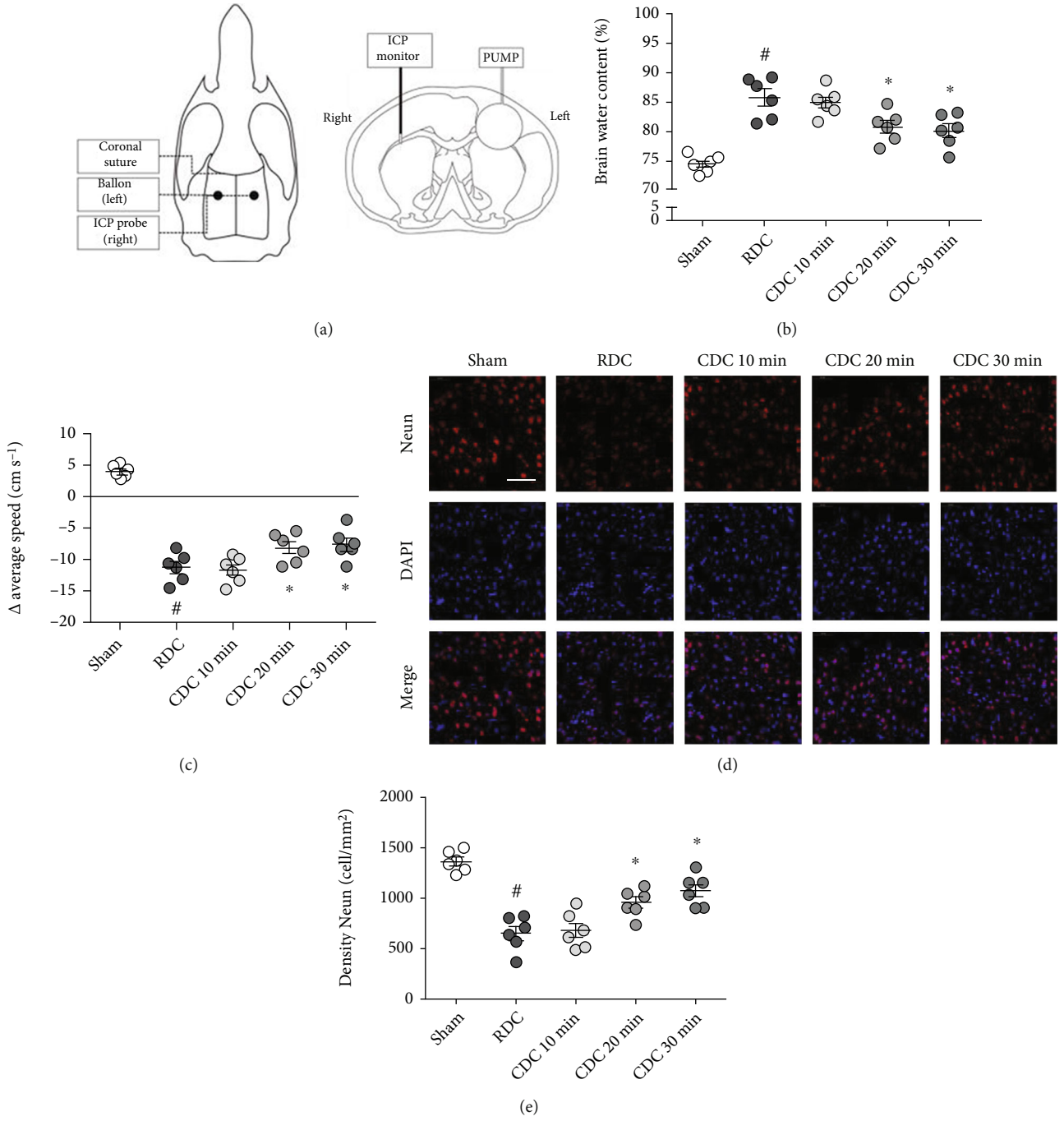

Figure 1: CDC attenuates brain damage after traumatic intracranial hypertension. (a) The horizontal and coronal schematic diagrams of the traumatic intracranial hypertension model. (b) Brain water content assay shows that CDC for 20 min or 30 min reduced brain edema compared to RDC. (c) The neurological assay shows that CDC for 20 min or 30 min attenuates locomotor impairment compared to RDC. (d, e) Typical pictures of NeuN staining (d) and quantification (e) show that CDC for 20 min or 30 min decreases neuronal loss compared to RDC. The data was represented as means ± SEM. $^{\#}p < 0.05$ vs. sham group and $^{*}p < 0.05$ vs. RDC group.

performed at membrane voltages of -40 mV. TREK-1 currents were filtered at 1 kHz and digitized at 5 kHz. Analysis was performed using Clampfit 9.2 (MDS Analytical Technologies).

2.10. Traumatic Intracranial Hypertension Model. Traumatic intracranial hypertension was induced using a balloon compression method in SD rats. Briefly, anesthesia was induced via 5% isoflurane (RWD, Guangdong, China) with a 1 : 1 N_2O/O_2 mixture and was then maintained with a 2.5% isoflurane with 1 : 1 N_2O/O_2 mixture by a face mask. The rats were placed on a fixing frame in the prone position. 2% lidocaine was injected subcutaneously near the midline of the skull to minimize the influence of skin incision on blood pressure. The fur around the midline of the skull was cleared with an electronic clipper and the skin of the rat was disinfected by using 75% alcohol. We incised the scalp along

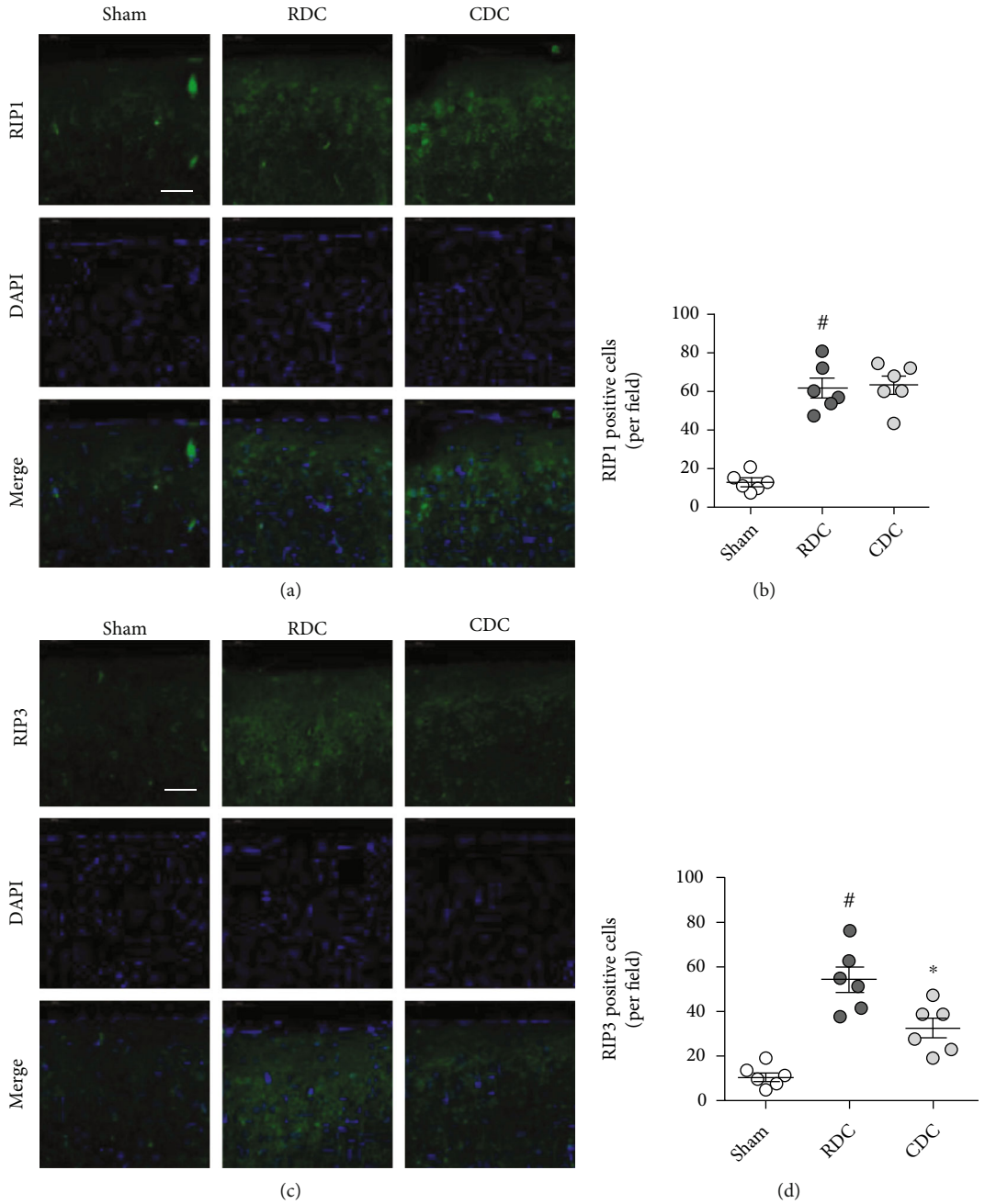

Figure 2: Continued.

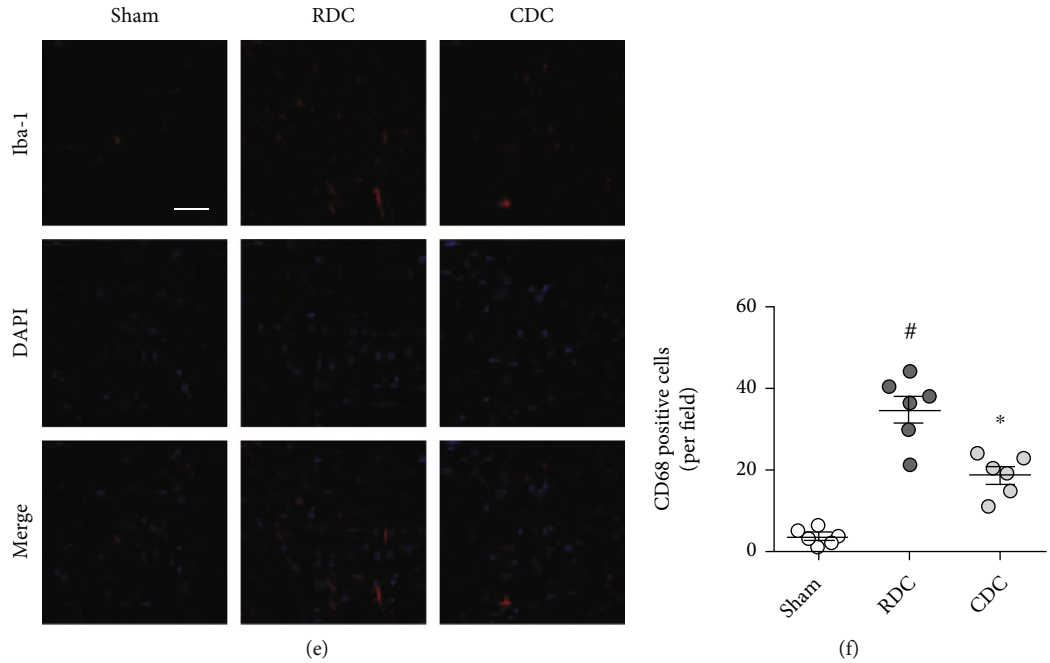

Figure 2: CDC alleviates neuronal necroptosis and neuroinflammation. (a, b) Typical pictures of RIP1 staining (a) and quantification (b) show that CDC had no effect on the RDC-induced increase of RIP1 expression. The scale bar is 50 μm. (c, d) Typical pictures of RIP3 staining (c) and quantification (d) show that CDC attenuates the RIP3 expression compared to RDC. The scale bar is 50 μm. (e, f) Typical pictures of CD68 staining (e) and quantification (f) show that CDC attenuates microglial activation compared to RDC. The scale bar is 50 μm. The data was represented as means ± SEM. $^{\#}p < 0.05$ vs. sham group and $^{*}p < 0.05$ vs. RDC group.

the midline for 2.5 cm, separated the subcutaneous tissue, and striped the periosteum to expose the anterior- and posterior-sagittal suture adequately. We made two holes using a dental drill (JSDA, JD700, China) bilaterally in the position of 0.5 cm by the side of the midline and 0.6 cm behind the anterior-sagittal suture and carefully removed the skull fragment to expose the cerebral dura mater without inflicting additional damage. The balloon system is composed of an embolization balloon (Balt 2, Montmorency, France) mounted on an intervention catheter (MAGIC, Montmorency, France). The balloon was inserted into the left hole carefully towards the frontotemporal side, and the dura mater was kept intact during the insertion so that the balloon would only lead to epidural compression. The catheter was connected to a pressure pump (Merit Basix Touch Inflation Device, IN4130, USA) to control the amount of injection fluid accurately. The ICP transducer was inserted into the brain at the depth of around 0.5 cm and was connected to an ICP monitoring device (Codman, Johnson and Johnson Medical, 82-6635, USA). After the insertions of the ICP probe and balloon, the bone holes were sealed using dental cement (Dentsply, Jeltrate Alginate Impression Material, USA) (Figure 1(a)). When the balloon was inflated by the pressure pump gradually, the variation trend of ICP and CPP was recorded.

2.11. In Vivo Experimental Design. Experiment 1 (Figure 1): the animals were randomly assigned into five groups: the sham group, rapid decompression group (RDC), controlled decompression for 10 min group (CDC 10 min), controlled decompression for 20 min group (CDC 20 min), and controlled decompression for 30 min group (CDC 30 min). The surgery of the sham group merely included skin incision, skull exposure, bone hole drilling, and the insertion of the ICP probe and balloon for 30 min without inflation. For the other four groups, we inflated the balloon with a pump until the value of ICP reached to the level of 30 mmHg which was maintained for 30 min. As for the RDC group, normal saline (NS) was pumped out rapidly within 3 seconds to reduce ICP suddenly after 30 min balloon-inflation. On the contrary, the ICP was lowered gradually in the CDC group, and the whole process lasted for 10 min, 20 min, or 30 min.

Experiment 2 (Figures 2 and 3(a) and 3(b)): the animals were randomly assigned into three groups: Sham group, RDC group and CDC group. The rats in Sham and RDC group were treated as mentioned in experiment 1. The animals in CDC group were treated with CDC procedure for 30 min as mentioned in experiment 1.

Experiment 3 (Figures 3(c) and 3(d)): the animals were randomly assigned into five groups: the sham group, RDC group, CDC group, CDC and spadin group (CDC+spadin), and CDC and SID1900 group (CDC+SID1900). The rats in the first three groups were treated as experiment 2. For the other two groups, rats were pretreated with spadin or SID1900 via the left cerebral ventricle (coordinates relative to bregma: 0.1 mm posterior, 1 mm lateral, and 2 mm deep) before the surgery.

2.12. Measurement of Brain Edema. Brian edema was determined by measuring brain water content using the standard wet and dry method [18].

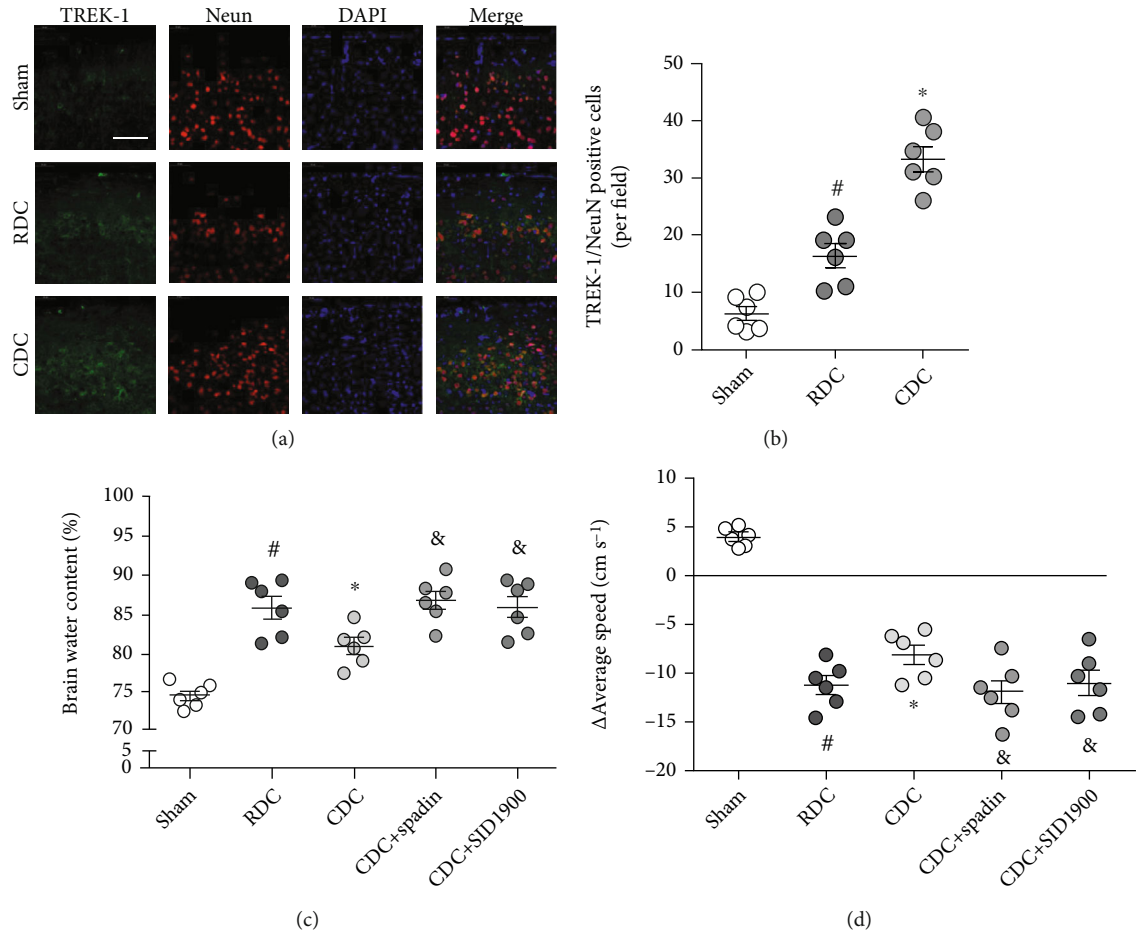

Figure 3: CDC exerts neuroprotective effects via activating TREK-1 in vivo. (a, b) Typical pictures of TREK-1 staining (a) and quantification (b) show that CDC further increased the expression of TREK-1 in cortical neurons compared to RDC. The scale bar is 50 μm. (c) Brain water content assay shows that the CDC-induced inhibition of brain edema was prevented by spadin and SID1900. (d) The neurological assay shows that the CDC-induced preservation of locomotor function was reversed by spadin and SID1900. The data was represented as means ± SEM. $^{\#}p < 0.05$ vs. sham group, $^{*}p < 0.05$ vs. RDC group, and $^{\&}p < 0.05$ vs. CDC group.

2.13. Neurological Function Assay. The CatWalk XT automated gait analysis system (Noldus Information Technology, Wageningen, the Netherlands) was used to measure the locomotor function as previously described [19].

2.14. Immunostaining in Brain Sections. The sections were washed three times with PBST for 5 min and were blocked by 10% normal bovine serum (Gibco, United States) in PBST for 1 h at room temperature. After that, the sections were incubated at 4°C overnight in 5% normal goat serum (NGS) in PBST with the following primary antibodies: NeuN (1 : 200, #24307, Cell Signaling), RIP1 (1 : 100, #3493, Cell Signaling), RIP3 (1 : 200, ab62344, Abcam), CD68 (1 : 200, ab125212, Abcam), and TREK-1 (1 : 50, sc-398449, Santa Cruz). After being washed for three times by PBST, the sections were incubated with secondary antibodies conjugated to Alexa Fluor (1 : 800, Invitrogen, United States) for 1 h at 37°C. DAPI was administrated to counterstain the nuclei, and the images were obtained using a Leica SP5 II confocal microscope.

2.15. Statistical Analysis. Data represent the mean and standard error of the mean (SEM). Student's *t* test and repeated measure analysis of variance with Student-Newman-Keuls post hoc test were performed for all statistical significance analyses using GraphPad Prism 6.0 software. All experiments were repeated at least for three times.

3. Results

3.1. Compression Aggravates Neuronal Injury after TNI in Cortical Neurons. To mimic intracranial hypertension after TBI in vitro, primary cultured cortical neurons were treated with traumatic injury and compression of 0.5 MPa pressure for 3 h. The results of H&E staining showed that the neuronal loss induced by TNI was significantly increased by compression (Figure 4(a)). LDH release was measured to determine cytotoxicity, and the TNI-induced increase in LDH release in cortical neurons was enhanced by compression (Figure 4(b)). In addition, the neuronal viability was assayed by measuring the calcein AM signaling (Figure 4(c)).

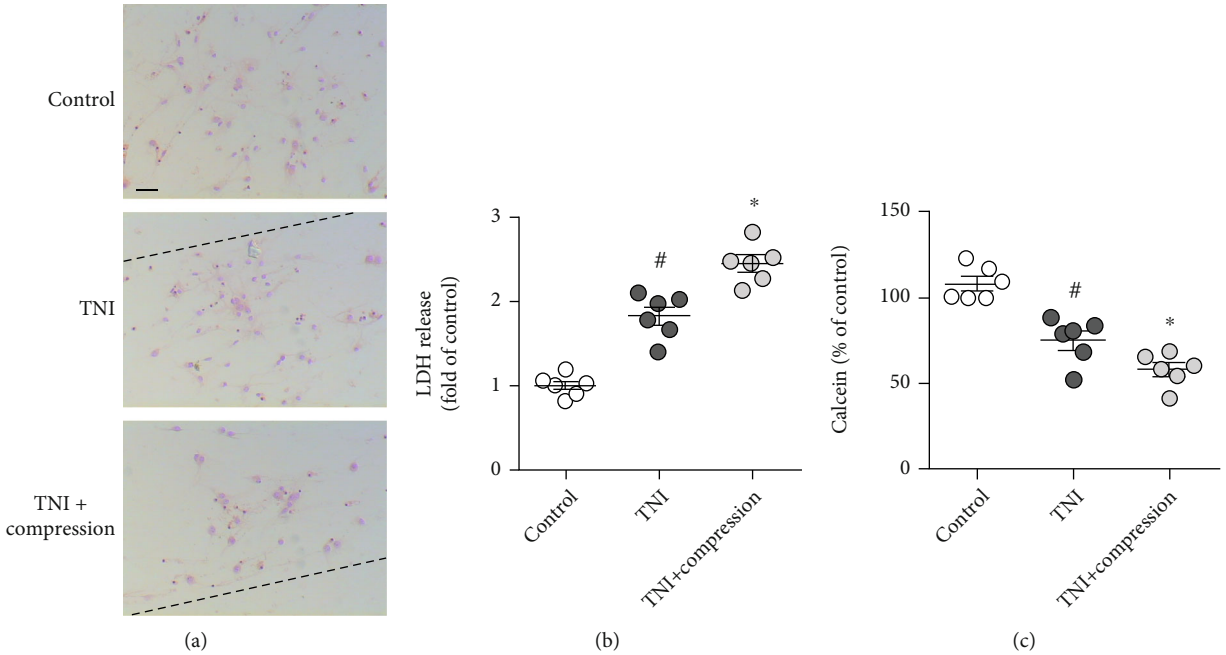

Figure 4: Compression aggravates neuronal injury after TNI in cortical neurons. (a) Typical pictures of H&E staining show that compression aggravates neuronal loss after TNI. The dotted line indicates the edge of the scratch injury. The scale bar is 50 μm. (b) Compression increases LDH release after TNI. (c) Compression decreases calcein signal after TNI. The data was represented as means ± SEM. $^{\#}p < 0.05$ vs. control group and $^{*}p < 0.05$ vs. TNI group.

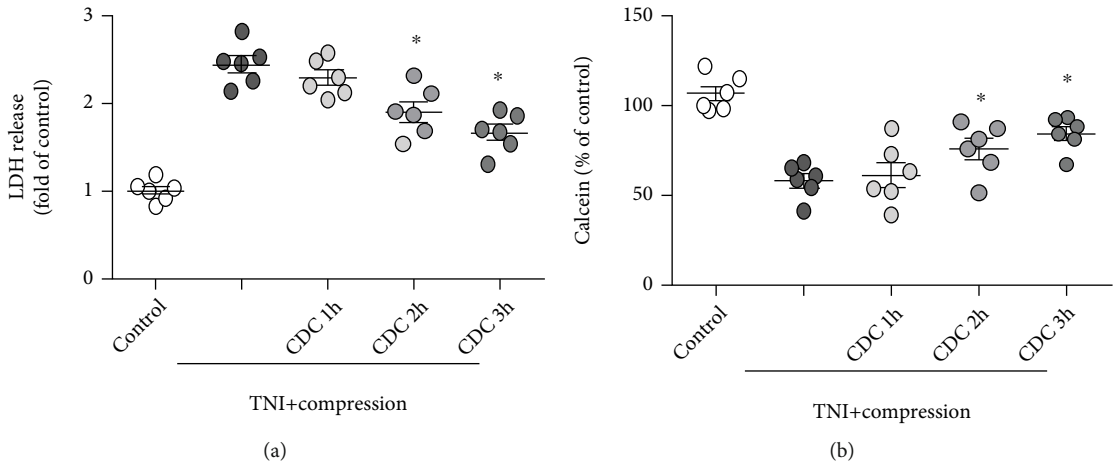

Figure 5: CDC attenuates compressive injury following TNI. (a) CDC for 2 h or 3 h, but not 1 h, attenuates compression-induced increase in LDH release following TNI. (b) CDC for 2 h or 3 h, but not 1 h, attenuates compression-induced decrease in calcein signal following TNI. The data was represented as means ± SEM. $^{*}p < 0.05$ vs. TNI+compression group.

The results showed that TNI markedly decreased the calcein signal in cortical neurons, which was further aggravated by compression.

3.2. CDC Attenuates Compressive Injury following TNI. To mimic controlled decompression in vitro, the 0.5 MPa pressure was gradually released within 1 h (CDC 1 h group), 2 h (CDC 2 h group), or 3 h (CDC 3 h group), while the pressure was completely released at once as control. The results showed that CDC 2 h and CDC 3 h significantly decreased the LDH release induced by TNI and compression, whereas CDC 1 h had no effect (Figure 5(a)). In congruent, CDC 2 h and CDC 3 h, but not CDC 1 h, obviously increased the calcein signal after TNI and compression (Figure 5(b)). CDC 2 h was used in following experiments (represented as CDC).

3.3. CDC Alleviates Neuronal Necroptosis. Double staining with PI and DAPI was performed to detect necrotic cell death in cortical neurons (Figure 6(a)), and the results showed that the number of PI-positive cells was increased by TNI and compression but significantly decreased by CDC (Figure 6(b)). To investigate the role of necroptosis

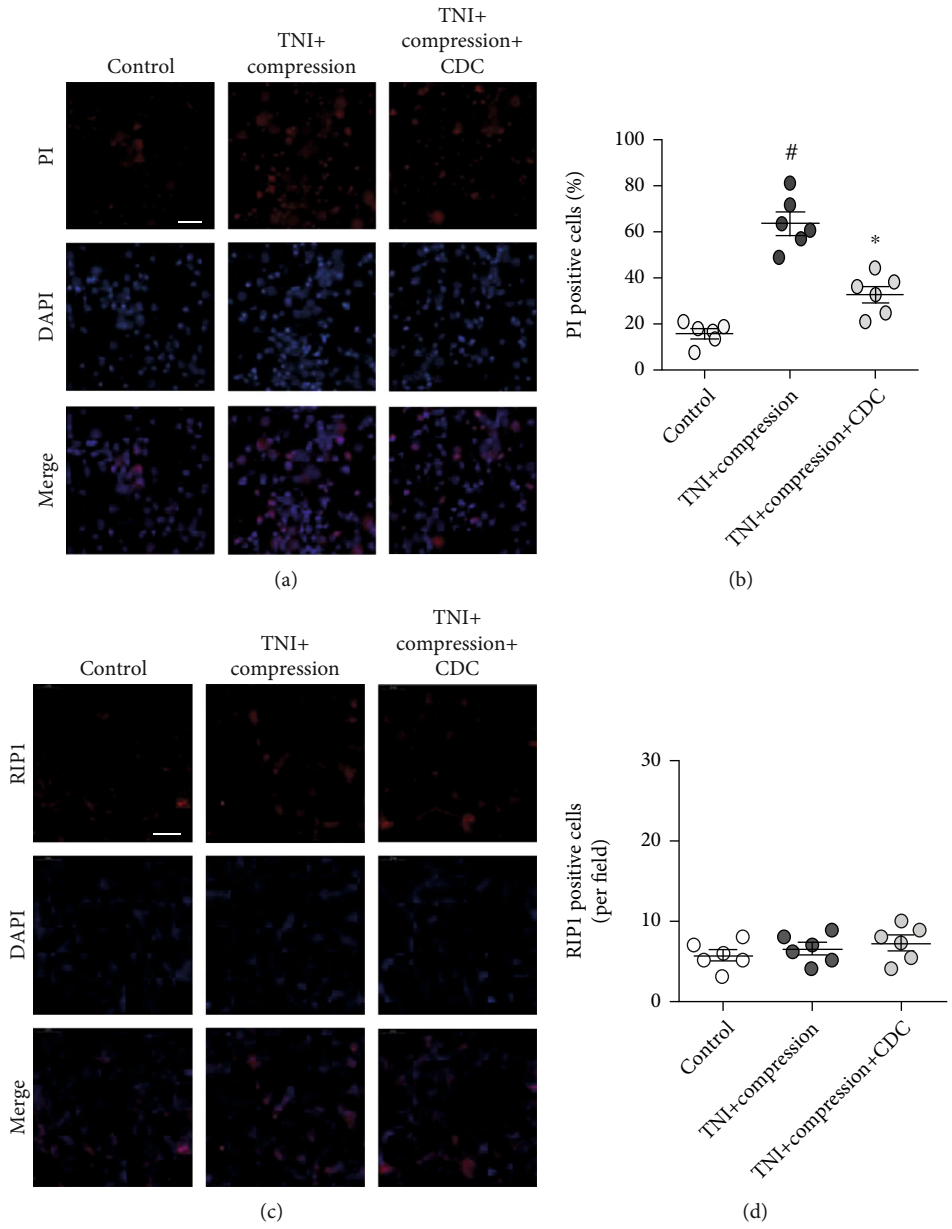

Figure 6: Continued.

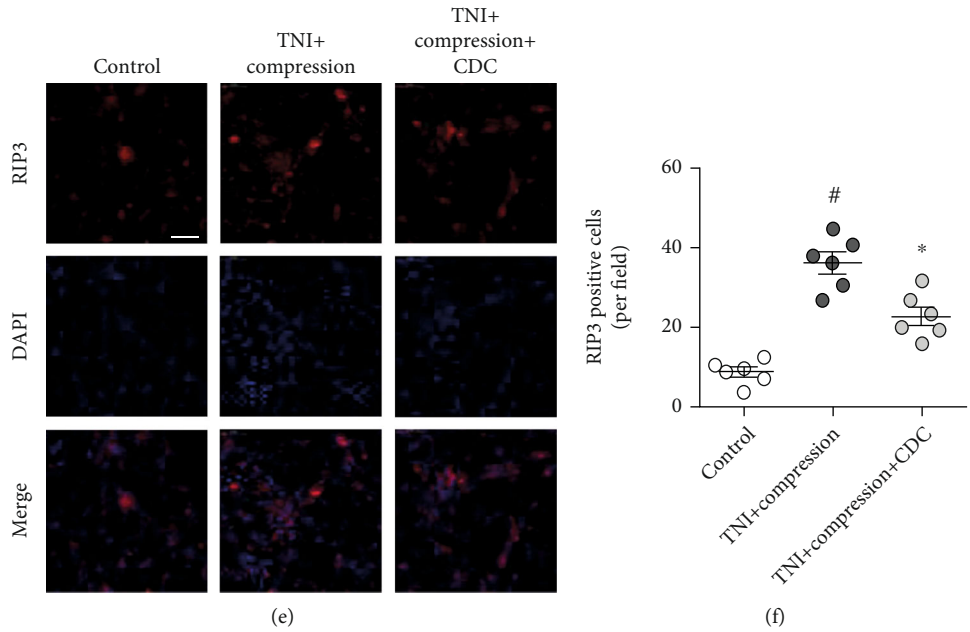

Figure 6: CDC alleviates neuronal necroptosis. (a, b) Typical pictures of PI staining (a) and quantification (b) show that CDC inhibits neuronal necrosis following TNI and compression. The scale bar is 50 μm. (c, d) Typical pictures of RIP1 staining (c) and quantification (d) show that CDC or compressive injury after TNI has no effect on RIP1 expression. The scale bar is 50 μm. (e, f) Typical pictures of RIP3 staining (e) and quantification (f) show that CDC attenuates RIP3 activation after TNI and compression. The scale bar is 50 μm. The data was represented as means ± SEM. $^{\#}p < 0.05$ vs. control group and $^{*}p < 0.05$ vs. TNI+compression group.

in our in vitro experiments, we detected the expression of RIP1 (Figure 6(c)) and RIP3 (Figure 6(e)) using immunostaining. The results showed that neither TNI+compression nor CDC had effects on the number of RIP1-positive cells (Figure 6(d)). However, the increased number of RIP3-positive cells was reduced by CDC (Figure 6(f)).

3.4. CDC Decreases the Levels of Inflammatory Cytokines. Necroptotic cell death was associated with inflammatory responses. Thus, we measured the levels of inflammatory cytokines in cortical neurons treated with TNI, compression, and/or CDC. The results showed that TNI increased the levels of TNF-α (Figure 7(a)) and IL-1β (Figure 7(b)), which were further increased by compression. However, these increases were significantly attenuated by CDC. The level of IL-6 was increased by TNI and compression, which was decreased by CDC (Figure 7(c)). In contrast, the increased level of INF-γ induced by TNI and compression was not altered by CDC (Figure 7(d)). As shown in Figure 7(e), the increased level of IL-18 after TNI and compression was markedly attenuated by CDC.

3.5. CDC Preserves Intracellular Ca^{2+} Homeostasis. Next, we performed Ca^{2+} imaging to examine the effect of TNI, compression, and CDC on calcium homeostasis (Figure 8(a)). The representative pictures of Ca^{2+} imaging are shown in Figure 8(b). The results showed that TNI and compression-induced Ca^{2+} overload were reduced by CDC (Figure 8(c)). The time of Ca^{2+} signaling to baseline in the CDC group was shorter than that in the TNI and compression group (Figure 8(d)).

3.6. CDC Activates TREK-1 Channels. To detect the potential involvement of TREK-1 in our findings, we performed immunostaining using the TREK-1 antibody (Figure 9(a)). The results showed that TNI did not change the fluorescence intensity of TREK-1 in cortical neurons, whereas compression significantly increased the TREK-1 signal after TNI (Figure 9(b)). The compression-induced increase in TREK-1 fluorescence intensity after TNI was further enhanced by CDC. In addition, we investigated whether TNI or compression has effects on TREK-1 channel activity, which was detected by inside-out membrane patches at a physiological steady membrane voltage of -40 mV (Figure 9(c)). The results showed that the TREK-1 channel activation was markedly increased by compression, but not by TNI (Figure 9(d)).

3.7. CDC Inhibits Ca^{2+} Responses via TREK-1 in Cortical Neurons. To investigate the role of the TREK-1 channel in CDC-induced regulation of intracellular Ca^{2+} homeostasis after TNI, we repeated the Ca^{2+} imaging experiments using the TREK-1 blockers, spadin and SID1900. The results showed that the decreased intracellular Ca^{2+} concentration induced by compression after TNI was significantly preserved by both spadin (1 μM, Figure 10(a)) and SID1900 (30 μM, Figure 10(b)).

3.8. Involvement of TREK-1 in CDC-Induced Protection In Vitro. Treatment with spadin and SID1900 (at the beginning of CDC) was used to investigate the involvement of TREK-1 in CDC-induced protection and related mechanisms. The results showed that the CDC-induced decrease in cytotoxicity, as evidenced by decreased LDH release, was prevented

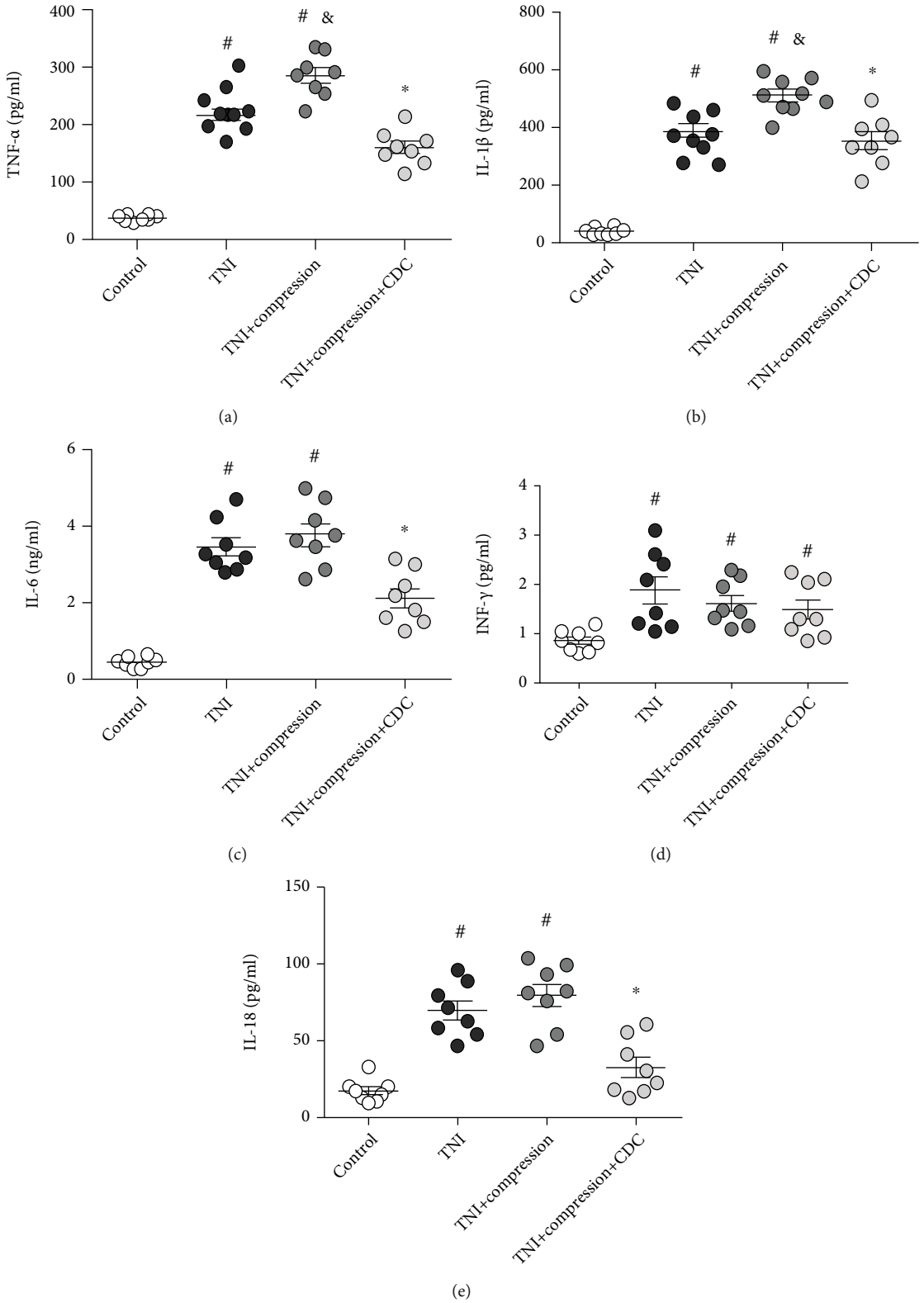

Figure 7: CDC decreases the levels of inflammatory cytokines. (a–c) ELISA assay shows that CDC decreases the levels of TNF-α (a), IL-1β (b), and IL-6 (c) after TNI and compression. (d) CDC has no effect on INF-γ level in cortical neurons after TNI and compression treatment. (e) The TNI and compression-induced increase in IL-18 levels is attenuated by CDC. The data was represented as means ± SEM. $^{\#}p < 0.05$ vs. control group, $^{\&}p < 0.05$ vs. TNI group, and $^{*}p < 0.05$ vs. TNI+compression group.

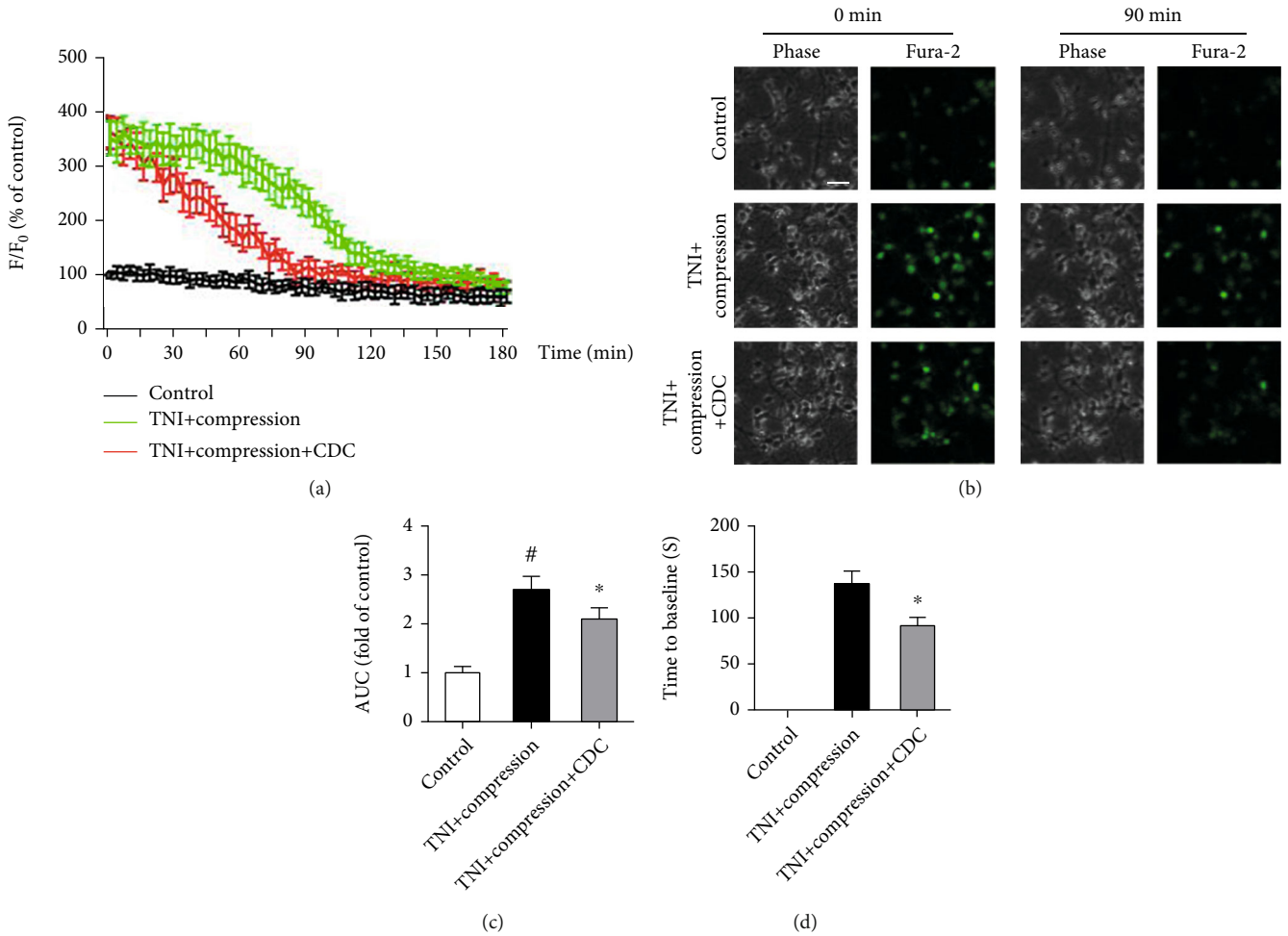

Figure 8: CDC preserves intracellular Ca^{2+} homeostasis. (a) Ca^{2+} imaging shows the intracellular Ca^{2+} levels up to 180 min after TNI and compression. (b) Typical pictures of Ca^{2+} imaging at 0 and 90 min following TNI and compression. The scale bar is 20 μm. (c) CDC attenuates intracellular Ca^{2+} overload up to 180 min following TNI and compression. (d) CDC reduces the time of Ca^{2+} levels to the baseline. The data was represented as means ± SEM. $^{\#}p < 0.05$ vs. control group and $^{*}p < 0.05$ vs. TNI+compression group.

by spadin and SID1900 (Figure 11(a)). Congruently, the CDC-induced increase in calcein signal (Figure 11(b)), as well as the CDC-induced decrease in the number of PI-positive cells (Figure 11(c)), was apparently reversed by spadin and SID1900. In addition, the CDC-induced inhibition of RIP3 expression was markedly attenuated by spadin, but not by SID1900 (Figure 11(d)).

3.9. CDC Attenuates Brain Damage after Traumatic Intracranial Hypertension. To confirm the above findings in in vivo conditions, we established a traumatic intracranial hypertension model in rats, and the horizontal and coronal schematic diagrams are shown in Figure 1(a). The results of the brain water content assay showed that CDC for 20 min or 30 min, but not CDC for 10 min, significantly reduced brain edema compared to the RDC group (Figure 1(b)). The neurological assay showed that CDC for 20 min or 30 min, but not CDC for 10 min, preserved locomotor function compared to RDC (Figure 1(c)). Next, we performed immunostaining using the NeuN antibody to detect the neuronal loss following traumatic intracranial hypertension (Figure 1(d)), and the results showed that CDC for 20 min or 30 min, but not CDC for 10 min, inhibited neuronal loss compared to RDC (Figure 1(e)). The CDC for 30 min was used in the following experiments.

3.10. CDC Alleviates Neuronal Necroptosis and Neuroinflammation In Vivo. To investigate the effects of CDC on neuronal necroptosis following traumatic intracranial hypertension, the expression of RIP1 (Figure 2(a)) and RIP3 (Figure 2(c)) on brain sections was detected by immunostaining using corresponding antibodies. The results showed that RDC and CDC both increased the expression of RIP1 compared to the sham group, but there is no difference between these two groups (Figure 2(b)). However, CDC markedly decreased the expression of RIP3 compared to RDC (Figure 2(d)). The activation of microglia was determined by immunostaining using the CD68 antibody (Figure 2(e)), and the results showed that microglial activation in the CDC group was lower than that in the RDC group (Figure 2(f)).

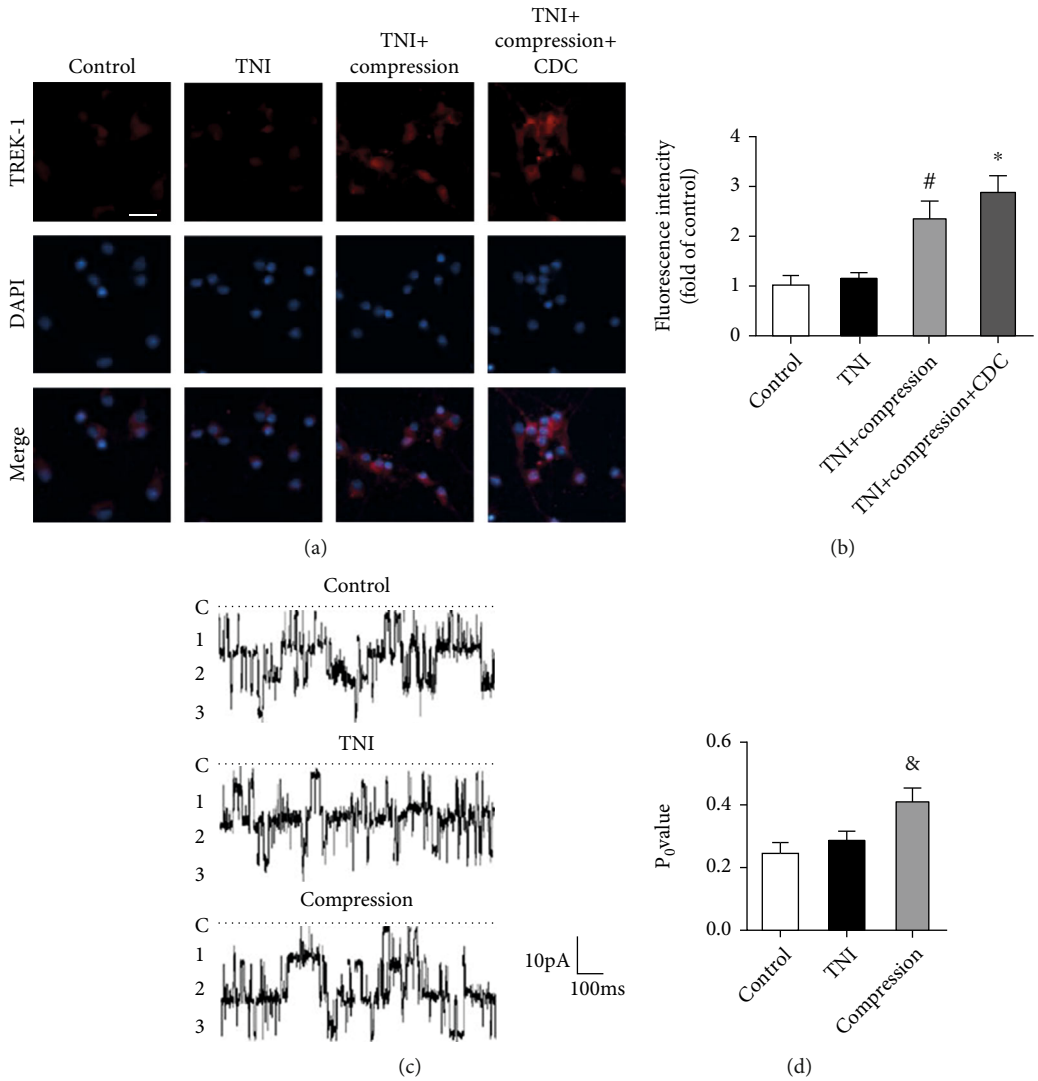

Figure 9: CDC activates TREK-1 channels. (a, b) Typical pictures of TREK-1 staining (a) and quantification (b) show that CDC further enhances the activation of TREK-1 channels following TNI and compression. The scale bar is 20 μm. (c, d) Typical recordings from the inside-out patch illustrating TREK-1 channel activation (c) and quantification (d) show that compression, but not TNI, activates TREK-1 channels in cortical neurons. The data was represented as means ± SEM. $^{\#}p < 0.05$ vs. TNI group, $^{*}p < 0.05$ vs. TNI+compression group, and $^{\&}p < 0.05$ vs. control group.

3.11. CDC Exerts Neuroprotective Effects via Activating TREK-1 In Vivo. We also performed immunostaining using the TREK-1 antibody in brain sections after traumatic intracranial hypertension (Figure 3(a)), and the results showed that RDC and CDC both increased the expression of TREK-1 with the higher levels of TREK-1 in the CDC group (Figure 4(b)). It was shown that the increased expression of TREK-1 was mainly in neurons, as evidenced by colocalization with NeuN staining (Figure 3(a)). To further confirm the involvement of TREK-1 in vivo, we repeated the brain water content assay (Figure 3(c)) and neurological function assay (Figure 3(d)) using spadin and SID9100. The result showed that the effects of CDC on brain edema and locomotor impairment were weakened by spadin and SID9100.

4. Discussion

Uncontrollable intracranial hypertension is one of the most important causes of death in TBI patients, but rapid decompression during the standard decompressive craniectomy surgery has been reported to be associated with many postoperative complications [20, 21]. In this study, we demonstrated that compression aggravates neuronal injury after TNI in cortical neurons and identified CDC as an effective strategy to prevent this kind of neuronal injury. We found that (a) CDC (2 h and 3 h) effectively reduces compressive neuronal damage following TNI, (b) CDC significantly inhibits neuronal necrosis and RIP3 activation;,(c) CDC markedly decreases the levels of inflammatory cytokines, (d) compression-induced intracellular Ca^{2+} overload is

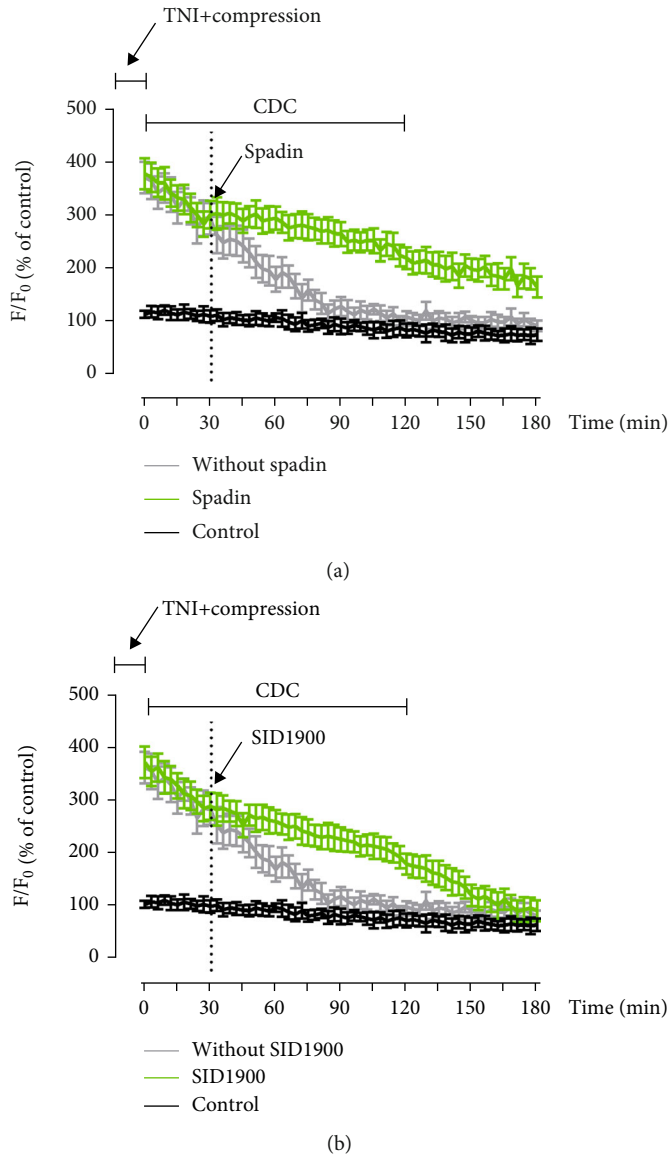

Figure 10: CDC inhibits Ca^{2+} responses via TREK-1. (a) Ca^{2+} imaging shows that CDC-induced attenuation of intracellular Ca^{2+} overload was ablated by the TREK-1 blocker spadin. (b) Ca^{2+} imaging shows that CDC-induced attenuation of intracellular Ca^{2+} overload was ablated by the TREK-1 blocker SID1900. The data was represented as means ± SEM.

attenuated by CDC in vitro, (e) CDC enhances the expression and activity of TREK-1 channel induced by compression, (f) the CDC-induced effects on Ca^{2+} metabolism and neuronal injury following TNI and compression are decreased by TREK-1 blockers, (g) CDC (20 min and 30 min) is effective in alleviating brain edema and locomotor impairment in vivo, (h) CDC inhibits neuronal necroptosis and microglial activation and increases TREK-1 expression, and (i) the CDC-induced protection in vivo is reversed by TREK-1 blockers.

At the beginning of the 19th century, decompressive craniectomy was firstly described by Kocher T and Harvey Cushing to treat patients with low Glasgow coma scale (GCS) score and dilated pupils following TBI. However, the standard procedure of rapid decompression was found to be associated with many intraoperative and postoperative complications, including delayed intracranial hematoma and diffuse brain swelling. In the past few decades, neurosurgeons have made a lot of improvements to the surgical procedures. Alves et al. used "Basal durotomy", a novel design of dural opening with a "reversed U-shaped" durotomy incision, to minimize the risk of massive intraoperative swelling [22]. In 2013, decompressive craniectomy with multi-dural stabs (also called SKIMS technique) was introduced to be effective in increasing survival of low GCS score and severe TBI patients with acute subdural hematoma [23]. Our previous studies showed that decompressive craniectomy using the CDC strategy, a method to gradually reduce the intracranial pressure (ICP) with the ventricular or brain tissue ICP detector, significantly improved outcomes and reduced complications in severe TBI patients [5]. Here, we used the in vitro model to confirmed the effectiveness of CDC in

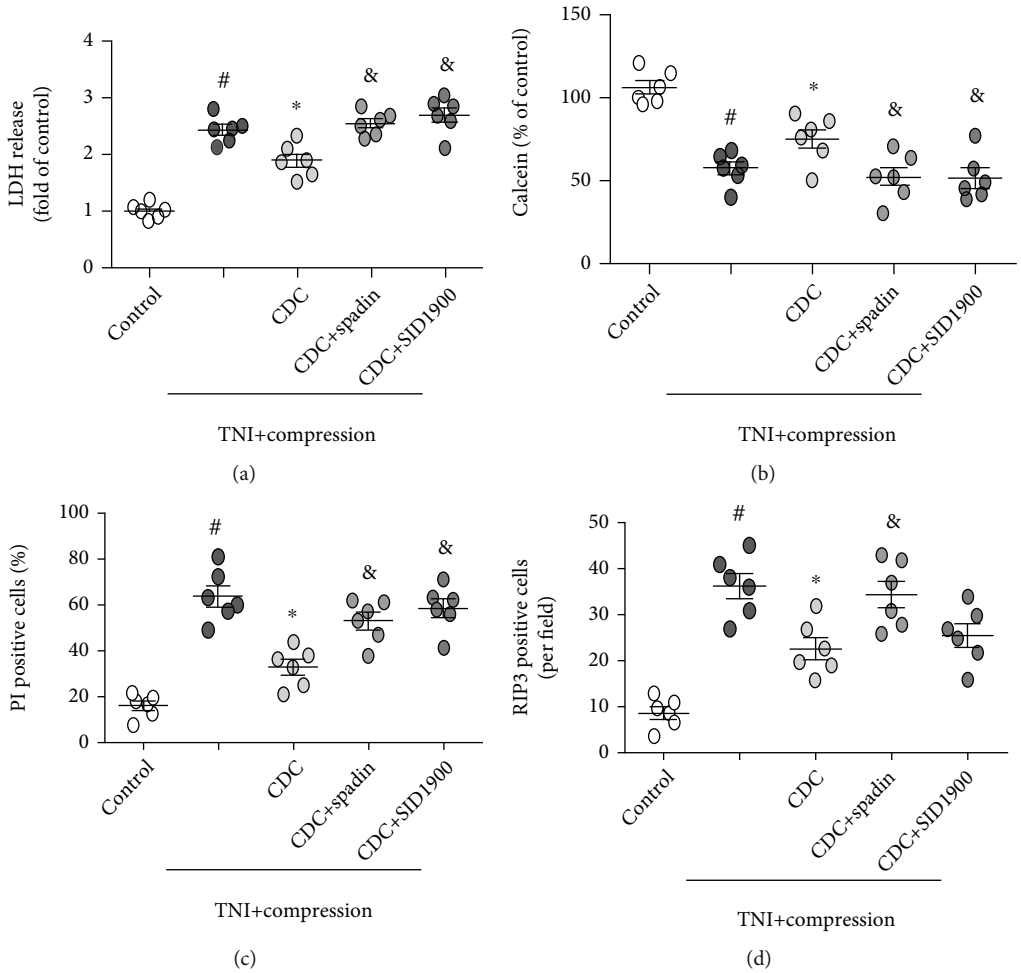

Figure 11: Involvement of TREK-1 in CDC-induced protection. (a) The CDC-induced decrease in LDH release was prevented by spadin and SID1900. (b) The CDC-induced increase in calcein signal was prevented by spadin and SID1900. (c) The CDC-induced inhibition of RIP3 activation was prevented by spadin and SID1900. (d) The CDC-induced inhibition of neuronal necrosis was prevented by spadin, but not by SID1900. The data was represented as means ± SEM. $^{\#}p < 0.05$ vs. control group, $^{*}p < 0.05$ vs. TNI+compression group, and $^{\&}p < 0.05$ vs. CDC+TNI+compression group.

TNI- and compression-treated cortical neurons. Our results showed that CDC for 2 and 3 h markedly reduced LDH release and increased calcein signal, which were accompanied by inhibited neuronal death. In addition, these protective effects were also confirmed in an in vivo traumatic intracranial hypertension model in rats with the CDC procedure for 20 min or 30 min. Thus, CDC could be an effective strategy for the treatment of compressive neuronal injury following TBI both in vitro and in vivo.

Regulated neuronal death is thought to be an ideal therapeutic target for neurological disorders. However, the primary brain damage following TBI is mainly due to neuronal necrosis, an uncontrollable cell death characterized by ATP depletion, intracellular organelle swelling, and loss of membrane integrity [24–26]. Necroptosis is the first form of programmed necrosis with an important role in both physiological and pathological conditions [27]. More recently, the necroptosis inhibitor necrostatin-1 was predicted to have the potential to protect against the complications of coronavirus disease 2019 (COVID-19) [28]. In addition, necroptosis has been demonstrated to contribute to the delayed neuronal death in multiple neurological disorders, ranging from chronic neurodegenerative disorders such as Alzheimer's disease (AD) and Parkinson's disease (PD) to acute insults, including stroke and TBI [29, 30]. The necroptosis inhibitors were found to exert neuroprotective effects against TBI [31], and blocking necroptotic neuronal death was shown to mediate the therapeutic potential of many treatments for TBI, such as hypothermia [32]. In this study, increased number of PI-positive cells was found in TNI- and compression-treated neurons, confirming the involvement of necroptosis in our in vitro traumatic intracranial hypertension conditions. The necroptotic pathway depends on the assembly of the apical protein kinases, receptor-interacting protein kinase 1 (RIP1) and RIP3, to form the high molecular weight complex necrosome, which in turn governs the oligomerization and translocation of the cell death executor mixed lineage kinase domain-like (MLKL) [33]. Intriguingly, our results showed that TNI and compression increased RIP3 (but not RIP1) activation,

which was partially prevented by CDC. In addition, increased expression of RIP1 and RIP3 was found after traumatic intracranial hypertension in vivo, while CDC only decreased RIP3 expression. These data indicated that CDC-induced inhibition of neuronal necroptosis might be mediated by a RIP1-independent mechanism, which was also previously reported [34, 35].

As the stretch-dependent K^+ channels (with TREK-2 and TRAAK), TREK-1 was originally described in rat cardiac ventricular muscle, where mechanical stretch could increase its expression in mechanoelectrical coupling [36]. Following researches demonstrated that the mechanogating activity of TREK-1 channels was also important for the sensation of pain in sensory neurons [37]. Thus, to determine the potential involvement of TREK-1, we detected the expression and activity of TREK-1. We found that TNI had no effect on the expression and activity of TREK-1, but compression significantly potentiated TREK-1 activation, which was prolonged by CDC strategy. Immunostaining results in brain sections also showed that CDC markedly increased the expression of TREK-1 in neurons. The TREK-1-induced K^+ efflux could counter-balance the detrimental arrhythmogenic cation influx through nonselective cation channels, such as Na^+ channels [38]. In addition, TREK-1 was demonstrated to mediate the fast glutamate release in astrocytes via the activation of G-protein-coupled receptors (GPCRs) [39]. These data suggest that TREK-1 might be involved in glutamate-associated neurotoxicity. To confirm this hypothesis, we used two TREK-1 specific inhibitors, spadin and SID1900. Spadin is a synthetic peptide derived from sortilin which was shown to inhibit TREK-1 with high affinity [11]. The small molecule SID1900 was found to inhibit TREK-1 with an IC_{50} of 29.72 μM, comparing that of spadin is 40 nM [40]. The results showed that CDC-induced effects on Ca^{2+} regulation, neuronal injury, as well as the in vivo protective effects, were all partially reversed by spadin and SID1900, confirming the role of TREK-1 in CDC-induced neuroprotection. Intriguingly, a previous study has reported the negative results of TBI-related brain damage in mice lacking TREK-1 [41]. However, deficiency of TREK-1 was shown to exacerbate BBB injury and neuroinflammation in intracranial hemorrhage [42]. The role of TREK-1 in neuronal injury seems to be controversial in different experimental models, where mechanical force could be an important factor.

As the most abundant divalent cation in mammalian cells, Ca^{2+} serves as the key intracellular signaling molecule with a striking 10000-fold concentration gradient larger than other ions, including Na^+ and K^+ [43]. The physiological function of Ca^{2+} in the central nervous system depends on where, when, and how it enters and exits the neurons and glial cells. Increasing evidence indicate that dysfunction of intracellular Ca^{2+} homeostasis is involved in TBI-induced brain damage, and many Ca^{2+} channel blockers are thought to exert neuroprotective potential [44]. Our previous study showed that compression resulted in intracellular Ca^{2+} overload via promoting intracellular Ca^{2+} release in primary cultured cortical neurons [16]. Here, we detected the changes in intracellular Ca^{2+} concentrations using Ca^{2+} imaging, and the results showed that compressive injury following TNI caused an increase in the F/F_0 signal, which was attenuated by CDC. A previous study showed that TREK-1 gene knockout impairs neuronal excitability, synaptic plasticity, and cognitive function [12]. The activity of TREK-1 channels can be regulated by various chemical stimuli, including Gq-coupled group I mGluRs, mGluR1, and mGluR5, which enhance the release of Ca^{2+} from the intracellular calcium stores by stimulating 1,4,5-trisphosphate receptors (IP_3R) on the endoplasmic reticulum (ER) membrane [45]. Thus, we repeated the Ca^{2+} imaging experiments using TREK-1 inhibitors, and the intracellular Ca^{2+} overload was found to be prolonged after blocking TREK-1 activation. Congruently, TREK-1 was shown to regulate pressure sensitivity and Ca^{2+} signaling in trabecular meshwork cells [46], and the TREK-1-specific blocker spadin was found to potentiate Ca^{2+} influx and insulin secretion in pancreatic beta cells [47]. These data strongly suggest that the TREK-1-mediated neuroprotective mechanism was associated with the preservation of intracellular Ca^{2+} homeostasis, possibly via regulating Ca^{2+} release form intracellular Ca^{2+} stores, which needs to be further determined.

5. Conclusions

In summary, our present data indicate that CDC for 2 h or 3 h in vitro and CDC for 20 min or 30 min in vivo exert neuroprotective effects. The potential underlying mechanisms involve in TREK-1 mediated regulation of intracellular Ca^{2+} homeostasis and inhibition of neuronal necroptosis.

Data Availability

The research data used to support the findings of this study are included within the article.

Ethical Approval

All experimental procedures used in this study were approved by the Ethics Review Committee of Anhui Medical University (Hefei, China).

Conflicts of Interest

The authors declare that they have no conflict of interest.

Authors' Contributions

YHW and LKY conceived and designed the study. TC, XQ, and JZ performed the experiments. JZ analyzed the data. TC wrote the manuscript. YHW and LKY reviewed and revised the manuscript and supervised the study. All authors read and approved the manuscript. Tao Chen and Xiao Qian contributed equally to this work.

Acknowledgments

This work was supported by the National Natural Science Foundation of China (No. 81701932, No. 81871589, and No. 82072168), the Natural Science Foundation of Jiangsu

Province (No. MS2022200), the Major Scientific Research Project of the Wuxi Health Commission (No. Z202001), the Top Talent Support Program for Young and Middle-Aged People of the Wuxi Health Committee (BJ2020118), the Translational Medicine Research Major Project of the Wuxi Health Commission (No. ZH201901), the China Postdoctoral Science Foundation Funded Project (No. 2019M651803), the Key Scientific Research Project of the Jiangsu Health Commission (No. K2019018), the Research Project of the Wuxi Health Commission (No. MS201910), and the Logistics Scientific Research Project of the PLA (No. CLB20J027).

References

[1] Z. Rossini, F. Nicolosi, A. G. Kolias, P. J. Hutchinson, P. de Sanctis, and F. Servadei, "The history of decompressive craniectomy in traumatic brain injury," *Frontiers in Neurology*, vol. 10, p. 458, 2019.

[2] N. Fatima, G. al Rumaihi, A. Shuaib, and M. Saqqur, "The role of decompressive craniectomy in traumatic brain injury: a systematic review and meta-analysis," *Asian J Neurosurg*, vol. 14, no. 2, pp. 371–381, 2019.

[3] A. G. Kolias, H. Adams, I. Timofeev et al., "Decompressive craniectomy following traumatic brain injury: developing the evidence base," *British Journal of Neurosurgery*, vol. 30, no. 2, pp. 246–250, 2016.

[4] H. Guan, C. Zhang, T. Chen et al., "Controlled decompression attenuates brain injury in a novel rabbit model of acute intracranial hypertension," *Medical Science Monitor*, vol. 25, pp. 9776–9785, 2019.

[5] J. Chen, M. Li, L. Chen et al., "The effect of controlled decompression for severe traumatic brain injury: a randomized controlled trial," *Frontiers in Neurology*, vol. 11, p. 107, 2020.

[6] Y. Wang, W. Chunli, Y. Likun et al., "Controlled decompression for the treatment of severe head injury: a preliminary study," *Turkish Neurosurgery*, vol. 24, no. 2, pp. 214–220, 2014.

[7] R. Santos, O. Ursu, A. Gaulton et al., "A comprehensive map of molecular drug targets," *Nature Reviews Drug Discovery*, vol. 16, no. 1, pp. 19–34, 2017.

[8] C. Heurteaux, N. Guy, C. Laigle et al., "TREK-1, a K+ channel involved in neuroprotection and general anesthesia," *The EMBO Journal*, vol. 23, no. 13, pp. 2684–2695, 2004.

[9] M. Fink, F. Duprat, F. Lesage et al., "Cloning, functional expression and brain localization of a novel unconventional outward rectifier K+ channel," *The EMBO Journal*, vol. 15, no. 24, pp. 6854–6862, 1996.

[10] E. Honore, "The neuronal background K_{2P} channels: focus on TREK1," *Nature Reviews Neuroscience*, vol. 8, no. 4, pp. 251–261, 2007.

[11] A. Djillani, J. Mazella, C. Heurteaux, and M. Borsotto, "Role of TREK-1 in Health and Disease focus on the central nervous system," *Frontiers in Pharmacology*, vol. 10, p. 379, 2019.

[12] W. Wang, C. M. Kiyoshi, Y. du et al., "TREK-1 null impairs neuronal excitability, synaptic plasticity, and cognitive function," *Molecular Neurobiology*, vol. 57, no. 3, pp. 1332–1346, 2020.

[13] X. Wu, Y. Liu, X. Chen et al., "Involvement of TREK-1 activity in astrocyte function and neuroprotection under simulated ischemia conditions," *Journal of Molecular Neuroscience*, vol. 49, no. 3, pp. 499–506, 2013.

[14] T. Chen, F. Fei, X. F. Jiang et al., "Down-regulation of Homer1b/c attenuates glutamate-mediated excitotoxicity through endoplasmic reticulum and mitochondria pathways in rat cortical neurons," *Free Radical Biology and Medicine*, vol. 52, no. 1, pp. 208–217, 2012.

[15] W. Rao, L. Zhang, C. Peng et al., "Downregulation of STIM2 improves neuronal survival after traumatic brain injury by alleviating calcium overload and mitochondrial dysfunction," *Biochimica et Biophysica Acta (BBA) - Molecular Basis of Disease*, vol. 1852, no. 11, pp. 2402–2413, 2015.

[16] T. Chen, J. Zhu, Y. H. Wang, and C. H. Hang, "ROS-mediated mitochondrial dysfunction and ER stress contribute to compression-induced neuronal injury," *Neuroscience*, vol. 416, pp. 268–280, 2019.

[17] T. Chen, J. Zhu, Y. H. Wang, and C. H. Hang, "Arc silence aggravates traumatic neuronal injury via mGluR1-mediated ER stress and necroptosis," *Cell Death & Disease*, vol. 11, no. 1, p. 4, 2020.

[18] T. Chen, W. B. Liu, X. D. Chao et al., "Salvianolic acid B attenuates brain damage and inflammation after traumatic brain injury in mice," *Brain Research Bulletin*, vol. 84, no. 2, pp. 163–168, 2011.

[19] R. Campos-Pires, H. Onggradito, E. Ujvari et al., "Xenon treatment after severe traumatic brain injury improves locomotor outcome, reduces acute neuronal loss and enhances early beneficial neuroinflammation: a randomized, blinded, controlled animal study," *Critical Care*, vol. 24, no. 1, p. 667, 2020.

[20] A. F. de Andrade, R. L. Amorim, D. J. F. Solla et al., "New technique for surgical decompression in traumatic brain injury: merging two concepts to prevent early and late complications of unilateral decompressive craniectomy with dural expansion," *International Journal of Burns and Trauma*, vol. 10, no. 3, pp. 76–80, 2020.

[21] P. Grille and N. Tommasino, "Decompressive craniectomy in severe traumatic brain injury: prognostic factors and complications," *Revista Brasileira de Terapia Intensiva*, vol. 27, no. 2, pp. 113–118, 2015.

[22] O. L. Alves and R. Bullock, ""Basal durotomy" to prevent massive intra-operative traumatic brain swelling," *Acta Neurochirurgica*, vol. 145, no. 7, pp. 583–586, 2003.

[23] A. R. Bhat, A. R. Kirmani, and M. A. Wani, "Decompressive craniectomy with multi-dural stabs - a combined (SKIMS) technique to evacuate acute subdural hematoma with underlying severe traumatic brain edema," *Asian Journal of Neurosurgery*, vol. 8, no. 1, pp. 15–20, 2013.

[24] M. Desai and A. Jain, "Neuroprotection in traumatic brain injury," *J Neurosurg Sci*, vol. 62, no. 5, pp. 563–573, 2018.

[25] D. J. Loane, B. A. Stoica, and A. I. Faden, "Neuroprotection for traumatic brain injury," *Handbook of Clinical Neurology*, vol. 127, pp. 343–366, 2015.

[26] R. Watzlawick, D. W. Howells, and J. M. Schwab, "Neuroprotection after traumatic brain injury," *JAMA Neurology*, vol. 73, no. 2, pp. 149-150, 2016.

[27] L. Della Torre, A. Nebbioso, H. G. Stunnenberg, J. H. A. Martens, V. Carafa, and L. Altucci, "The role of necroptosis: biological relevance and its involvement in cancer," *Cancers (Basel)*, vol. 13, no. 4, p. 684, 2021.

[28] L. Cao and W. Mu, "Necrostatin-1 and necroptosis inhibition: pathophysiology and therapeutic implications," *Pharmacological Research*, vol. 163, p. 105297, 2021.

[29] Z. Bao, L. Fan, L. Zhao et al., "Silencing of A20 aggravates neuronal death and inflammation after traumatic brain injury: a potential trigger of necroptosis," *Frontiers in Molecular Neuroscience*, vol. 12, p. 222, 2019.

[30] H. Ni, Q. Rui, X. Lin, D. Li, H. Liu, and G. Chen, "2-BFI provides neuroprotection against inflammation and necroptosis in a rat model of traumatic brain injury," *Frontiers in Neuroscience*, vol. 13, p. 674, 2019.

[31] Y. Q. Wang, L. Wang, M. Y. Zhang et al., "Necrostatin-1 suppresses autophagy and apoptosis in mice traumatic brain injury model," *Neurochemical Research*, vol. 37, no. 9, pp. 1849–1858, 2012.

[32] T. Liu, D. X. Zhao, H. Cui et al., "Therapeutic hypothermia attenuates tissue damage and cytokine expression after traumatic brain injury by inhibiting necroptosis in the rat," *Scientific Reports*, vol. 6, no. 1, 2016.

[33] Y. Meng, J. J. Sandow, P. E. Czabotar, and J. M. Murphy, "The regulation of necroptosis by post-translational modifications," *Cell Death & Differentiation*, vol. 28, no. 3, pp. 861–883, 2021.

[34] J. P. Ingram, R. J. Thapa, A. Fisher et al., "ZBP1/DAI drives RIPK3-mediated cell death induced by IFNs in the absence of RIPK1," *The Journal of Immunology*, vol. 203, no. 5, pp. 1348–1355, 2019.

[35] D. M. Moujalled, W. D. Cook, T. Okamoto et al., "TNF can activate RIPK3 and cause programmed necrosis in the absence of RIPK1," *Cell Death & Disease*, vol. 4, no. 1, article e465, 2013.

[36] F. Zhao, L. Dong, L. Cheng, Q. Zeng, and F. Su, "Effects of acute mechanical stretch on the expression of mechanosensitive potassium channel TREK-1 in rat left ventricle," *Journal of Huazhong University of Science and Technology*, vol. 27, no. 4, pp. 385–387, 2007.

[37] A. Mathie and E. L. Veale, "Two-pore domain potassium channels: potential therapeutic targets for the treatment of pain," *Pflügers Archiv-European Journal of Physiology*, vol. 467, no. 5, pp. 931–943, 2015.

[38] K. Monaghan, S. A. Baker, L. Dwyer et al., "The stretch-dependent potassium channel TREK-1 and its function in murine myometrium," *The Journal of physiology*, vol. 589, no. 5, pp. 1221–1233, 2011.

[39] D. H. Woo, K. S. Han, J. W. Shim et al., "TREK-1 and Best1 channels mediate fast and slow glutamate release in astrocytes upon GPCR activation," *Cell*, vol. 151, no. 1, pp. 25–40, 2012.

[40] A. Djillani, M. Pietri, J. Mazella, C. Heurteaux, and M. Borsotto, "Fighting against depression with TREK-1 blockers: past and future. A focus on spadin," *Pharmacology & Therapeutics*, vol. 194, pp. 185–198, 2019.

[41] K. Namiranian, C. D. Brink, J. C. Goodman, C. S. Robertson, and R. M. Bryan Jr., "Traumatic brain injury in mice lacking the K channel, TREK-1," *Journal of Cerebral Blood Flow & Metabolism*, vol. 31, no. 3, pp. e1–e6, 2011.

[42] Y. Fang, Y. Tian, Q. Huang et al., "Deficiency of TREK-1 potassium channel exacerbates blood-brain barrier damage and neuroinflammation after intracerebral hemorrhage in mice," *Journal of Neuroinflammation*, vol. 16, no. 1, p. 96, 2019.

[43] A. De Loof, "The essence of female-male physiological dimorphism: differential Ca^{2+}-homeostasis enabled by the interplay between farnesol-like endogenous sesquiterpenoids and sex-steroids? The Calcigender paradigm," *General And Comparative Endocrinology*, vol. 211, pp. 131–146, 2015.

[44] S. L. Zup and A. M. Madden, "Gonadal hormone modulation of intracellular calcium as a mechanism of neuroprotection," *Frontiers in Neuroendocrinology*, vol. 42, pp. 40–52, 2016.

[45] V. Bruno, G. Battaglia, A. Copani et al., "Metabotropic glutamate receptor subtypes as targets for neuroprotective drugs," *Journal of Cerebral Blood Flow & Metabolism*, vol. 21, no. 9, pp. 1013–1033, 2001.

[46] O. Yarishkin, T. T. T. Phuong, C. A. Bretz et al., "TREK-1 channels regulate pressure sensitivity and calcium signaling in trabecular meshwork cells," *Journal of General Physiology*, vol. 150, no. 12, pp. 1660–1675, 2018.

[47] C. Hivelin, S. Béraud-Dufour, C. Devader et al., "Potentiation of calcium influx and insulin secretion in pancreatic beta cell by the specific TREK-1 blocker spadin," *Journal of Diabetes Research*, vol. 2016, Article ID 3142175, 9 pages, 2016.

Hindawi
Oxidative Medicine and Cellular Longevity
Volume 2021, Article ID 8186877, 31 pages
https://doi.org/10.1155/2021/8186877

Research Article

GDF-11 Protects the Traumatically Injured Spinal Cord by Suppressing Pyroptosis and Necroptosis via TFE3-Mediated Autophagy Augmentation

Yu Xu,[1,2,3] Xinli Hu,[1,2,3] Feida Li,[1,2,3] Haojie Zhang,[1,2,3] Junsheng Lou,[1,2,3] Xingyu Wang,[1,2,3] Hui Wang,[1,2,3] Lingyan Yin,[3] Wenfei Ni,[1,2,3] Jianzhong Kong,[1,2,3] Xiangyang Wang,[1,2,3] Yao Li,[1,2,3] Kailiang Zhou,[1,2,3] and Hui Xu[1,2,3]

[1]*Department of Orthopaedics, The Second Affiliated Hospital and Yuying Children's Hospital of Wenzhou Medical University, Wenzhou 325027, China*
[2]*Zhejiang Provincial Key Laboratory of Orthopaedics, Wenzhou 325027, China*
[3]*The Second Clinical Medical College of Wenzhou Medical University, Wenzhou 325027, China*

Correspondence should be addressed to Yao Li; yaoli@wmu.edu.cn, Kailiang Zhou; zhoukailiang@wmu.edu.cn, and Hui Xu; 13968800082@163.com

Yu Xu and Xinli Hu contributed equally to this work.

Received 11 June 2021; Accepted 27 August 2021; Published 19 October 2021

Academic Editor: Xu Ke

Spinal cord injury (SCI) refers to a major worldwide cause of accidental death and disability. However, the complexity of the pathophysiological mechanism can result in less-effective clinical treatment. Growth differentiation factor 11 (GDF-11), an antiageing factor, was reported to affect the development of neurogenesis and exert a neuroprotective effect after cerebral ischaemic injury. The present work is aimed at investigating the influence of GDF-11 on functional recovery following SCI, in addition to the potential mechanisms involved. We employed a mouse model of spinal cord contusion injury and assessed functional outcomes via the Basso Mouse Scale and footprint analysis following SCI. Using western blot assays and immunofluorescence, we analysed the levels of pyroptosis, autophagy, necroptosis, and molecules related to the AMPK-TRPML1-calcineurin signalling pathway. The results showed that GDF-11 noticeably optimized function-related recovery, increased autophagy, inhibited pyroptosis, and alleviated necroptosis following SCI. Furthermore, the conducive influences exerted by GDF-11 were reversed with the application of 3-methyladenine (3MA), an autophagy suppressor, indicating that autophagy critically impacted the therapeutically related benefits of GDF-11 on recovery after SCI. In the mechanistic study described herein, GDF-11 stimulated autophagy improvement and subsequently inhibited pyroptosis and necroptosis, which were suggested to be mediated by TFE3; this effect resulted from the activity of TFE3 through the AMPK-TRPML1-calcineurin signalling cascade. Together, GDF-11 protects the injured spinal cord by suppressing pyroptosis and necroptosis via TFE3-mediated autophagy augmentation and is a potential agent for SCI therapy.

1. Introduction

Spinal cord injury (SCI) refers to a destructive disease that causes serious neurological and motor dysfunctions when the structure is injured [1]. Clinically, a few SCI therapies, including surgeries, increased blood pressure, and methylprednisolone administration, are able to decompress and stabilize injuries, preventing secondary complications and managing symptoms [2–4]. The SCI pathology is complicated and operationally falls into two states: primary injury triggered by mechanical damage, which includes demyelination and necrosis of axons and neurons, and secondary injury initiated by a variety of pathophysiologies, including autophagy, apoptosis, oxidative stress, inflammation, and other factors, which primarily aggravate neurological dysfunction and could be reversible and regulated [5–7]. Thus,

secondary injury prevention and intervention are considered promising treatments for SCI [8]. Among the mentioned pathophysiologic events in secondary injury, cell death and inflammation are considered to be two critical targets for SCI treatment [9, 10].

Pyroptosis, a proinflammation-related programmed cell death pathway, markedly impacts neuroinflammation, a critical element that drives secondary injury post-SCI and is induced through inflammasome activation [11, 12]. The inflammasome refers to a complex of multimeric proteins that include a cytosolic sensor (e.g., NLRP1, NLRP2, NLRP3, etc.), an adaptor protein (ASC), and an effector caspase (caspase-1) [13, 14]. By stimulating the cytoplasmic inflammasome complex, caspase-1/4/5/11 are activated and the gasdermin- (GSDMD-) *N* domain is translocated to the cell membrane, thereby inducing pore formation and causing pyroptosis [15–17]. Necroptosis, another type of proinflammation-related programmed cell death, is activated by the binding of tumour necrosis factor-α (TNF-α) to tumour necrosis factor receptor 1 (TNFR1) and is involved in the intracellular signalling cascade involving receptor-interacting protein kinase 1/3 (RIPK1/3) and mixed lineage kinase domain-like (MLKL) protein [18]. Moreover, it was demonstrated that caspase-8 suppresses the occurrence of necroptosis [19]. An increasing number of studies have shown that necroptosis and pyroptosis cause numerous neurological diseases, including neurodegenerative disorders, ischaemic brain injury, and psychiatric diseases [20, 21]. Additionally, necroptosis and pyroptosis aggravate neuronal and glial cell death after SCI [22, 23]. Therefore, targeting necroptosis and pyroptosis is promising as a potential therapy for SCI.

Macroautophagy (hereafter named autophagy) is a dynamic regulatory mechanism that maintains the stability of intracellular environments and degrades long-lived proteins and damaged organelles in a selective manner [24, 25]. According to accumulating evidence, autophagy has a critical effect after neurological diseases by regulating neural cell death [26, 27]. According to SCI pathogenesis, lysosomal injury and dysfunction can trigger defects within autophagy fluxes and messy environments, triggering an inflammatory response [28]. Subsequently, the activation of NLRP3 inflammasomes facilitates the cleavage of pro-IL-1β/18 and cleaves GSDMD into 2 parts, ultimately initiating pyroptosis [29–32]. Moreover, it has been found that lysosomal damage decreases autophagy flux, leading to rapid increases in the necroptosis activators RIPK1, RIPK3, and MLKL in neurons [33]. Moreover, recent studies have also demonstrated that autophagy can suppress pyroptosis and necroptosis by degrading key activators [34–36]. Thus, we hypothesized that autophagy may modulate the death of neural cells for neuroprotection by suppressing pyroptosis and necroptosis and it may improve functional recovery after SCI. Accordingly, active drugs capable of inhibiting pyroptosis and necroptosis through the activation of autophagy should be identified.

Growth differentiation factor 11 (GDF-11) pertains to the transforming growth factor β (TGF-β) superfamily, members of which impact numerous processes, such as histogenesis, embryonic development, cancer, and metabolic disorders [37, 38]. A recent study has indicated that GDF-11 exerts its neuroprotective effect in cerebral ischaemic injury to reduce neuronal apoptosis [39]. GDF-11 treatment also improves functional outcomes and stimulates neurogenesis and angiogenesis in mice by activating autophagy in ischaemic stroke [40]. However, the effects exerted by GDF-11 in the treatment of SCI have never been investigated. Furthermore, whether GDF-11 inhibits pyroptosis and necroptosis by activating autophagy remains unknown. Therefore, we assessed the effect of GDF-11 on autophagy, pyroptosis, and necroptosis and assessed its effects on the functional recovery following SCI using a mouse model of SCI injected with GDF-11.

2. Material and Method

2.1. Animals and Ethics Statement. Healthy adult C57BL/6 mice (female, average weight 20–30 g) originated from Wenzhou Medical University's Experimental Animal Center (license no. SCXK [ZJ] 2015-0001), Zhejiang province, China. All animals were housed under standard conditions (temperature: 21–25°C, 12 h light/dark cycle, humidity: 50–60%) with free access to water and food. The experimental procedure related to animals followed the Guide for the Care and Use of Laboratory Animals of the China National Institutes of Health, as accepted by the Animal Care and Use Committee of Wenzhou Medical University (wydw 2017-0022).

2.2. Antibodies and Reagents. The chemicals listed below were used herein: GDF-11 was acquired from PeproTech (Rocky Hill, the United States of America; Cat# 120-11). Solarbio Science & Technology (Beijing, China) provided the pentobarbital sodium, diaminobenzidine (DAB) developer, Masson staining tool, and haematoxylin and eosin (HE) staining tools. Sigma-Aldrich (St. Louis, MO, the United States of America; Cat# M9281) supplied the 3-methyladenine (3MA). MedChemExpress (Monmouth Junction, NJ, the United States of America; Cat# HY-13418A) provided the dorsomorphin (Compound C, C24H25N5O; purity ≥98.14%). Shanghai Genechem Co. Ltd. (Shanghai, China) developed the adeno-associated virus transcription factor E3 (AAV-TFE3) shRNA (serotype 9, with no fluorescent reporter gene). Thermo Fisher Scientific (Rockford, IL, United States of America) provided the Cytoplasmic Extraction Reagent and NE-PER™ Nuclear and BCA tools. Cell Signaling Technology (Beverly, MA, United States of America; Cat# 3738, Cat# 15101, Cat# 5832, Cat# 2535, Cat# 2983, and Cat# 5536) supplied the primary antibodies against Beclin1, NLRP3, AMPK, p-AMPK, p-mTOR, and mTOR. Proteintech Cohort (Chicago, IL, United States of America; Cat# 12452-1, Cat# 21327-1, Cat# 22915-1, Cat# 17168-1, and Cat# 10494-1) provided the VPS34, CTSD, CASP1, histone H3, and GAPDH antibodies. Abcam (Cambridge, UK; Cat# ab106393, Cat# ab62344, Cat# ab180799, Cat# ab207323, Cat# ab52761, Cat# ab52636, Cat# ab183830, Cat# ab104224, Cat# ab272608, Cat# ab56416, Cat# ab150077, and Cat# ab150115) provided the goat anti-mouse IgG H&L (Alexa Fluor® 647), RIPK1, RIPK3, ASC, IL-18, calcineurin, synaptophysin (SYN), microtubule-associated protein-2 (MAP2), NeuN, TRPML1/MG-2, p62/SQSTM1, and goat anti-rabbit IgG H&L (Alexa Fluor® 488) antibodies.

The primary antibody against TFE3 was purchased from Sigma-Aldrich Chemical Company (Milwaukee, WI, United States of America; Cat# HPA023881). LC3B was purchased from Novus Biologicals (Littleton, CO, United States of America; Cat# NB600-1384). IL-1β was purchased from ABclonal Technology (Cambridge, MA, United States of America; Cat# A1112). MLKL, GSDMD, and NLRP1 were from Affinity Biosciences (OH, United States of America; Cat# DF7412, Cat# AF4013, and Cat#DF13187). Santa Cruz Biotechnology (Dallas, TX, the United States of America) provided the horseradish peroxidase- (HRP-) conjugated IgG secondary antibody. Boyun Biotechnology (Nanjing, the People's Republic of China) provided the fluorescein isothiocyanate- (FITC-) conjugated IgG secondary antibody. Furthermore, Beyotime Biotechnology (Jiangsu, the People's Republic of China) supplied the 4′,6-diamidino-2-phenylindole (DAPI) solution.

2.3. Animal Model of SCI. In advance of the procedures, anaesthesia was administered to animals by intraperitoneal injection with 1% (*w*/*v*) pentobarbital sodium (50 mg/kg). Next, a standard laminectomy was performed in the T9-T10 vertebra to expose a dura circle. Subsequently, a weight drop injury model was adopted to trigger spinal cord contusion injury following a previous description [41]. Briefly, we dropped a bar (10 g in weight and 1.2 mm in diameter) from 15 mm onto the exposed spinal cord to induce moderate SCI contusion while keeping the dura intact. After the injury, the layers of the skin, fascia, and muscle were closed with 4–0 nonabsorbable silk sutures. Mice in the sham group underwent the same operation as mentioned above, with no injury caused by a weight drop. Following the procedure, the mice were artificially urinated three times per day.

2.4. Adeno-Associated Virus (AAV) Vector Packaging. The Shanghai Genechem Company developed the AAV-TFE3-shRNA. The shRNA sequence of TFE3-stimulated protein kinase was constructed, cloned, and then processed into the pAV-U6-shRNA-CMV-EGFP plasmid, and pAV-U6-shRNA(TFE3)-CMV-EGFP was obtained. AAV-293 cells were transfected to produce AAV9-U6-shRNA(TFE3)-CMVEGFP based on the AAV Rep/Cap expression plasmid, adenovirus helper plasmid (Ad helper), and pAV-U6-shRNA(TFE3)-CMV-EGFP. Likewise, AAV9-U6-shRNA(scramble)-CMV-EGFP was used as a scramble control. Viral particles were purified using the iodixanol gradient approach. Using quantitative PCR, we detected the titres of AAV9-U6-shRNA(TFE3)-CMV-EGFP and AAV9-U6-shRNA(scramble)-CMV-EGFP, i.e., 4.82×10^{12} and 6.56×10^{12} genomic copies per ml, respectively.

2.5. Drug and AAV Vector Administration. We separated 114 mice in a random manner into seven groups: sham ($n = 18$), SCI ($n = 18$), GDF-11 ($n = 18$), GDF − 11 + 3MA ($n = 18$), GDF − 11 + scrambled shRNA control ($n = 18$), GDF − 11 + TFE3 shRNA ($n = 18$), and GDF − 11 + CC ($n = 6$). The GDF-11 group was treated with GDF-11 (100 ng/kg/day) via daily intraperitoneal injection for 3 days after SCI [42]. An equal volume of saline was given to the sham and SCI groups. Daily intraperitoneal injection of 3-methyladenine (3MA, 15 mg/kg) and dorsomorphin (compound C, 1.5 mg/kg) was performed 30 min prior to GDF-11 administration for 3 days. The GDF − 11 + scrambled shRNA control and GDF − 11 + TFE3 shRNA groups received a 100 μl intravenous injection of the viral vectors in PBS with 1×10^{10} packaged genomic particles 14 days before SCI. After 14 days, the GDF − 11 + scrambled shRNA control and GDF − 11 + TFE3 shRNA groups received the same treatment as the GDF-11 group. The animals were killed by overdosing them with pentobarbital sodium, and histological samples were acquired for corresponding experiments on days 3 and 28.

2.6. Functional Behavioural Assessment. We administered the Basso Mouse Scale (BMS) to measure locomotion on days 0, 1, 3, 7, 14, 21, and 28 following SCI to evaluate functional recovery [43]. BMS scores ranged from 0 to 9, with 0 indicating normal motor function and 9 indicating overall paralysis. We carried out a footprint investigation at 28 days after surgery. Hind limbs (red) and mouse forelimbs (blue) were stained using dyes of various colours [44]. Two independent testers without any knowledge of the experimental conditions measured the results.

2.7. Tissue Slide Preparation for HE and Masson Staining. On day 28 after surgery, the mice underwent reanaesthetization using 2% (*w*/*v*) pentobarbital sodium, perfusion using normal saline, and introduction of 4% (*w*/*v*) paraformaldehyde in phosphate-buffered saline. Next, we split the overall parts (10 mm long, epicentre in the centre) and fixed the mentioned parts in 4% (*w*/*v*) paraformaldehyde over a period of 24 h. Next, we developed the respective longitudinal paraffin sections after embedding the samples in paraffin. Using a microtome, 4 μm sections were cut and mounted onto slides coated with poly-L-lysine to carry out HE staining-based histopathological tests following reported descriptions [45, 46]. For Masson staining, we employed 10% trichloroacetic acid and 10% potassium dichromate for mordant longitudinal sections. Haematoxylin was used to stain nuclei. Next, using ethanol and hydrochloric acid, the slides were differentiated, returned to blue with reduced ammonia, and stained with Masson solution. Staining was performed as described previously [47]. Finally, a light microscope (Olympus, Tokyo, Japan) was used to acquire images.

2.8. Western Blot (WB)Analysis. Mice were euthanized on day 3 under SCI, and the spinal cord parts from mice (1.5 cm; covering the injury epicentre) were dissected and stored at −80°C prior to WB. Partial samples were processed by extracting proteins with lysis buffer. Other samples were processed for extraction of cytoplasmic and nuclear proteins with Cytoplasmic Extraction Reagent and NE-PER™ Nuclear. We employed the protein extraction reagents to purify overall proteins from the spinal cord specimens. BCA assays were used for protein quantification. We performed 12% (*w*/*v*) gel electrophoresis to separate equal amounts of protein (60 μg); the samples were then transferred to polyvinylidene fluoride membranes (Roche Applied

Science, Indianapolis, IN, the United States of America), which were blocked in 5% (*w*/*v*) skimmed milk and probed with the following antibodies overnight at 4°C: ASC (1 : 1000), NLRP1 (1 : 1000), NLRP3 (1 : 1000), IL-18 (1 : 1000), IL-1β (1 : 1000), GSDMD (1 : 1000), CASP1 (1 : 1000), Beclin1 (1 : 1000), SQSTM1/p62 (1 : 1000) LC3B (1 : 1000), VPS34 (1 : 1000), CTSD (1 : 1000), RIPK1 (1 : 1000), RIPK3 (1 : 1000), MLKL (1 : 1000), CASP8 (1 : 1000), p-mTOR (1 : 1000), mTOR (1 : 1000), p-AMPK (1 : 1000), AMPK (1 : 1000), GAPDH (1 : 1000), CaPML1 (1 : 1000), histone (1 : 1000), p-AMPK (1 : 1000), and AMPK (1 : 1 : 1000). The membranes were subsequently incubated with HRP-conjugated IgG secondary antibodies at an ambient temperature for 2 h. Using a Chemi-Doc™ XRS+ Imaging System (Bio-Rad) based on an ECL immune-detection tool, band signals were visualized and investigated.

2.9. Immunofluorescence (IF) Staining. On day 3 after SCI, spinal cord specimens from mice were dissected and collected for IF staining. We performed IF staining on the tissue side according to the rostral spinal cord (1 mm long, 4 mm from the epicentre) following a previous description [48]. We deparaffinized, rehydrated, washed, and then treated the sections with 10.2 mM sodium citrate buffer for 20 min at 95°C. Subsequently, we permeabilized the sections with 0.1% (*v*/*v*) PBS-Triton X-100 (10 min). Next, we blocked the sections with 10% (*v*/*v*) bovine serum albumin in PBS (1 h). The slides were then incubated overnight at 4°C with antibodies against Caspase-1 (1 : 200)/NeuN (1 : 400), GSDMD (1 : 150)/NeuN (1 : 400), LC3 (1 : 200)/NeuN (1 : 400), p62 (1 : 200)/NeuN (1 : 400), RIPK1 (1 : 200)/NeuN (1 : 400), RIPK3 (1 : 200)/NeuN (1 : 400), SYN (1 : 200)/NeuN (1 : 400), and MAP2 (1 : 200). Next, we washed the sections for 10 min at an ambient temperature 3 times and incubated them at an ambient temperature for 1 h with FITC-conjugated secondary antibody. Finally, we captured and evaluated images with a fluorescence microscope (Olympus, Tokyo, Japan) within six fields taken in a random manner in three random sections pertaining to the respective sample.

2.10. Statistical Analysis. We completed all statistical investigations using SPSS ver. 19 software (SPSS, Chicago, IL) and adopted a double-blind approach during the analysis process. Values are expressed as the mean ± standard error of the mean (SEM). To control for unwanted sources of variation, data normalization was performed in this study. Analysis of variance (ANOVA) based on the least significance difference (LSD) (equal variances assumed) post hoc investigation or Dunnett's T3 (equal variances without any assumption) approach was conducted to assess notable distinctions of two groups among three or four groups. We employed an independent sample *t*-test to compare two independent groups. The p values less than 0.05 indicated statistical significance.

3. Results

3.1. GDF-11 Facilitates Functional Recovery after SCI. HE and Masson staining, IF staining, footprint analysis, and BMS scores were used to evaluate motor function following SCI. The lesion area in the injured spinal cord was assessed by HE and Masson staining, which showed a glial scar area with marked expansion ($p < 0.01$) in the SCI group compared with the sham group. Additionally, IF staining revealed reduced MAP2 expression ($p < 0.01$) and a smaller number of SYN-positive synapses on neurons ($p < 0.01$) in the SCI group than in the sham group. With GDF-11 treatment, the animals had fewer glial scars, greater neuronal MAP2 expression levels, and a greater number of SYN-positive synapses on neurons than the SCI group without any treatment ($p < 0.01$ for all; Figures 1(a)–1(f)). Next, in the footprint investigation, the GDF-11 group outperformed the SCI group in terms of functional recovery on day 28 after injury (Figure 1(g)). In the sham group, the BMS score markedly exceeded that in the SCI group on days 1, 3, 7, 14, 21, and 28 following the procedure ($p < 0.01$ for all). An insignificant difference was reported for the BMS score between the SCI and GDF-11 groups on days 1 and 3. Likewise, the GDF-11 group achieved greater BMS scores on days 7, 14, 21, and 28 following the procedure compared with the SCI group ($p = 0.02$, <0.01, <0.01, and <0.01, respectively; Figure 1(h)). Overall, the mentioned outcomes confirmed that GDF-11 facilitated functional recovery following SCI.

3.2. GDF-11 Attenuates Pyroptosis after SCI. IL-18, IL-1β, NLRP1, NLRP3, Caspase-1, GSDMD, and ASC were assessed within the spinal cord following SCI to evaluate the pyroptotic activity in the GDF-11, SCI, and sham groups. As revealed by IF staining, compared with that in the sham group, GSDMD and Caspase-1 achieved marked increases in density in neurons within spinal cord lesions in the SCI group ($p < 0.01$ for both), whereas GDF-11 showed a downregulation of GSDMD and Caspase-1 density in comparison to that in the SCI group ($p < 0.01$ for both), as shown in Figures 2(a)–2(d). WB analysis of IL-18-, IL-1β-, NLRP1-, NLRP3-, Caspase-1-, GSDMD-, and ASC-expressing states was performed (Figure 2(e)). As revealed by the results, in contrast to the sham group, the SCI group achieved higher optical density (OD) values in terms of IL-18, IL-1β, GSDMD, Caspase-1, ASC, NLRP3, and NLRP1 ($p < 0.01$ for all) and GDF-11 showed decreased OD values for the mentioned markers compared with the SCI group ($p = 0.02$, =0.02, <0.01, <0.01, =0.04, <0.01, and <0.01, separately; Figure 2(f)). These results indicated that GDF-11 could reduce pyroptosis-associated markers, demonstrating suppression of pyroptosis after SCI.

3.3. GDF-11 Inhibits Necroptosis after SCI. We examined the states of necroptosis through WB and IF. As revealed by IF staining, relative to that in the sham group, the RIPK3 and RIPK1 density in neurons increased markedly within the spinal cord lesions in the SCI group ($p < 0.01$ for both), whereas GDF-11 showed a decreased density of RIPK3- and RIPK1-positive neurons in comparison to that in the SCI group ($p < 0.01$ for both), as shown in Figures 3(a)–3(d). Moreover, the expression levels of Caspase-8, MLKL, RIPK3, and RIPK1 were analysed by WB (Figure 3(e)). In

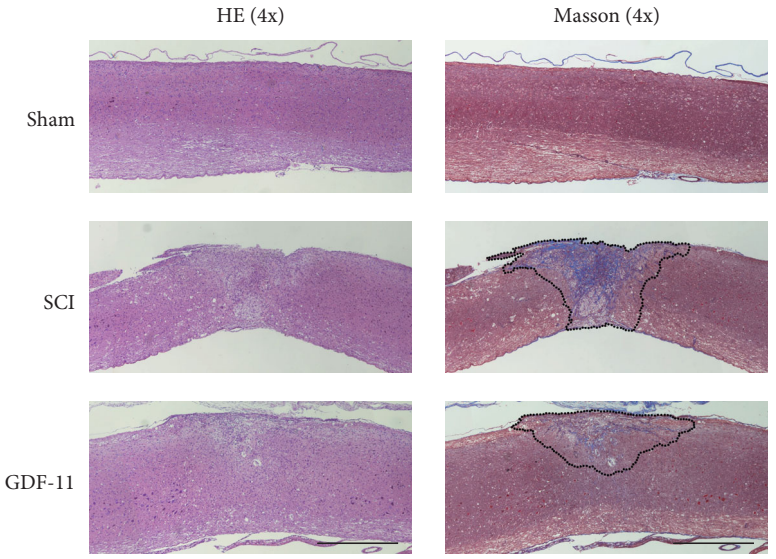

(a)

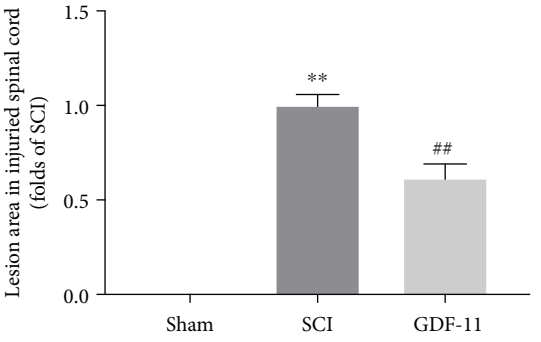

(b)

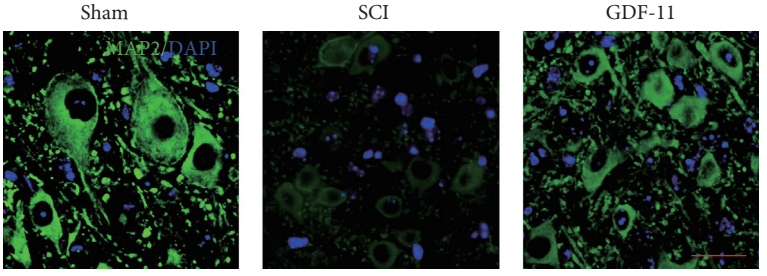

(c)

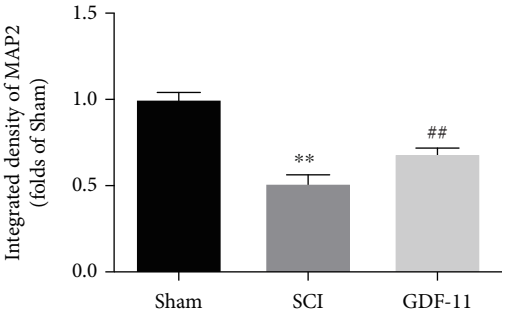

(d)

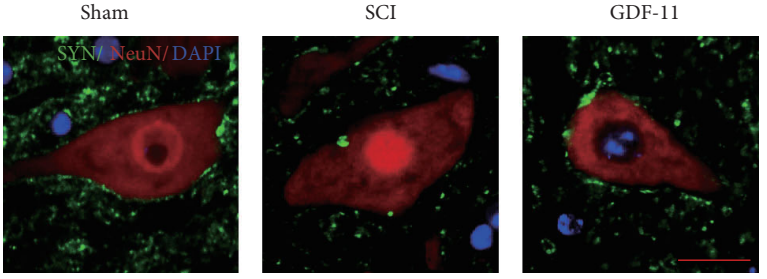

(e)

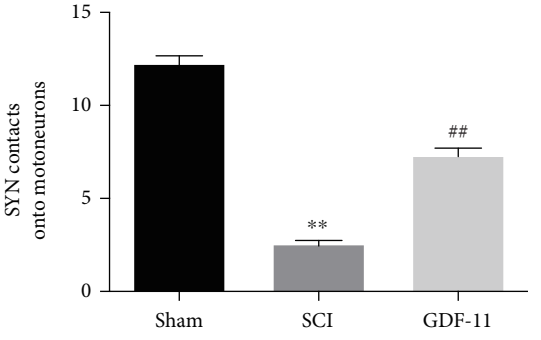

(f)

Figure 1: Continued.

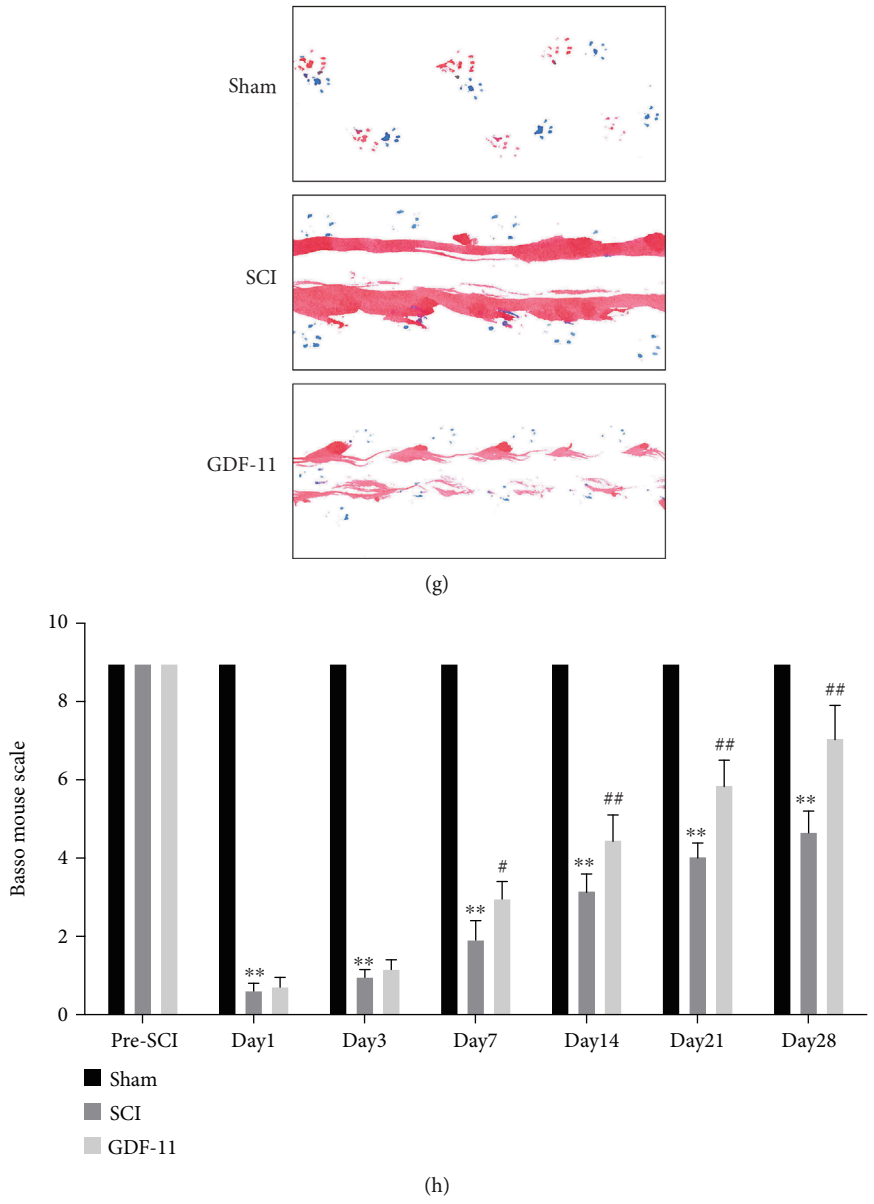

Figure 1: GDF-11 facilitates functional recovery following spinal cord injury. (a) Longitudinal spinal cord sections in the indicated groups on day 28 following SCI were analysed on the basis of Masson staining and HE staining (scale bar = 1000 μm). (b) Quantitative investigations of Masson-positive lesions within the spinal cord of the respective groups. (c) Photographs (×30) of spinal cord sections in the respective groups stained with an antibody against MAP2 (scale bar = 25 μm). (d) MAP2 optical density within a spinal cord subjected to injury on day 28. (e) Photographs (×150) of spinal cord sections subjected to injury (T11-T12) and stained on day 28 with an antibody against SYN/NeuN (scale bar = 5 μm). (f) Relevant quantitative results for neuron-contacting synapse amounts. (g) Photographs of mouse footprints on day 28 following spinal cord injury. (h) Basso mouse scale (BMS) scores in the indicated groups and time points. Data are expressed as the mean ± SEM, $n = 6$ per group. $^{**}p < 0.01$ vs. the sham group. $^{\#}p < 0.05$ and $^{\#\#}p < 0.01$ vs. the SCI group.

comparison to those within the sham group, RIPK1, RIPK3, and MLKL showed greater OD values within the SCI group, while those for Caspase-8 were lower ($p < 0.01$ for all). In comparison to those in the SCI group, the expression levels of MLKL, RIPK3, and RIPK1 were markedly reduced in the GDF-11 group, while the expression of Caspase-8 was increased ($p = 0.04$, <0.01, <0.01, and =0.02; Figure 2(f)). Overall, these results indicated that the restorative effect of GDF-11 after SCI was partly due to the suppression of necroptosis.

3.4. GDF-11 Enhances Autophagy after SCI. For the evaluation of autophagic activity within spinal cord lesions following SCI, we determined the expression profiles of the autophagic substrate protein (p62), an autolysosome-related marker (CTSD), and autophagosomal markers (Vps34,

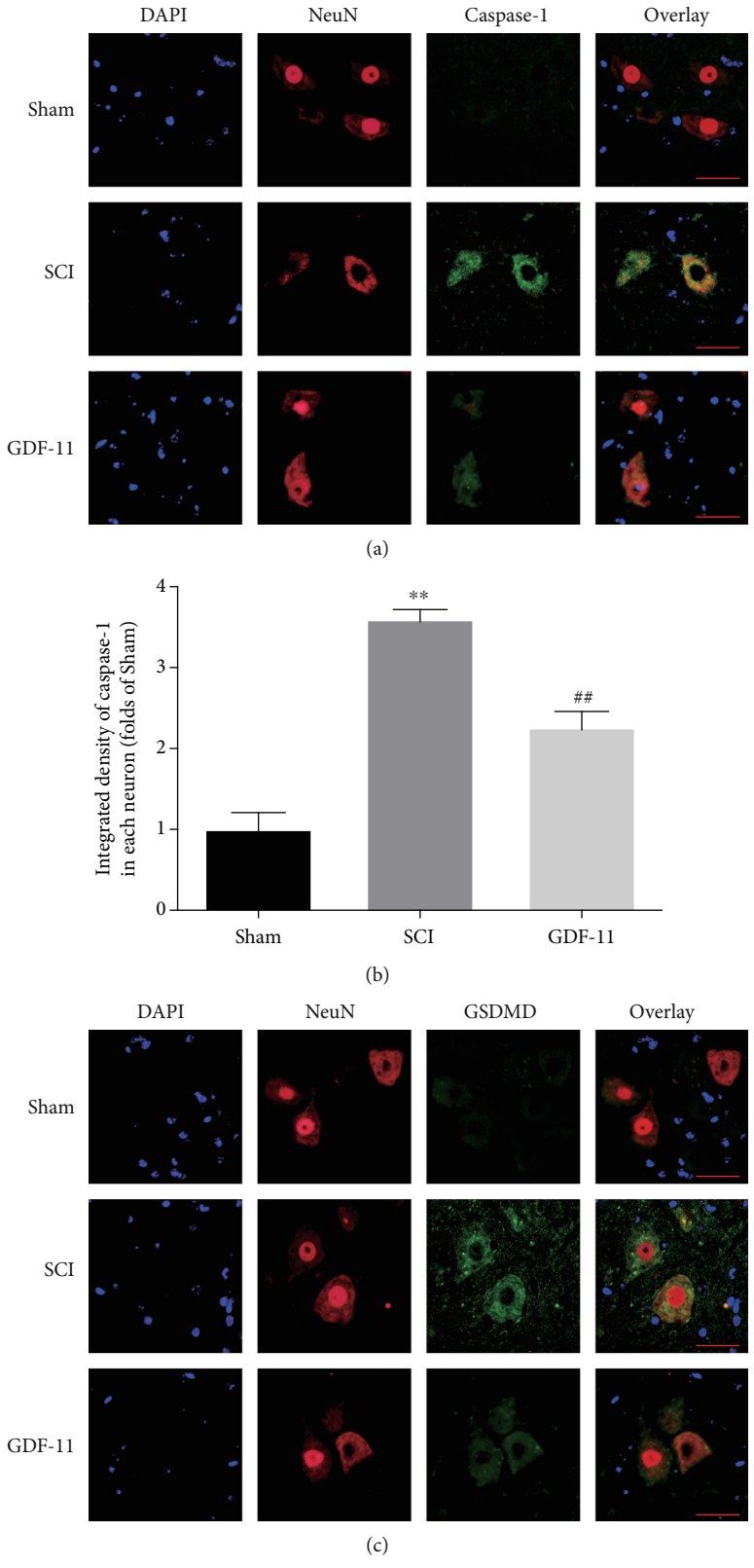

Figure 2: Continued.

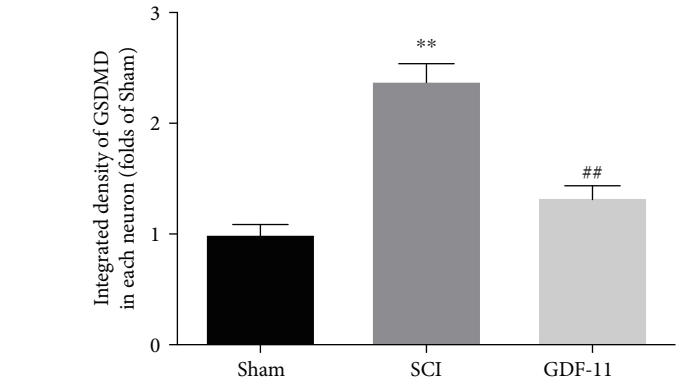

(d)

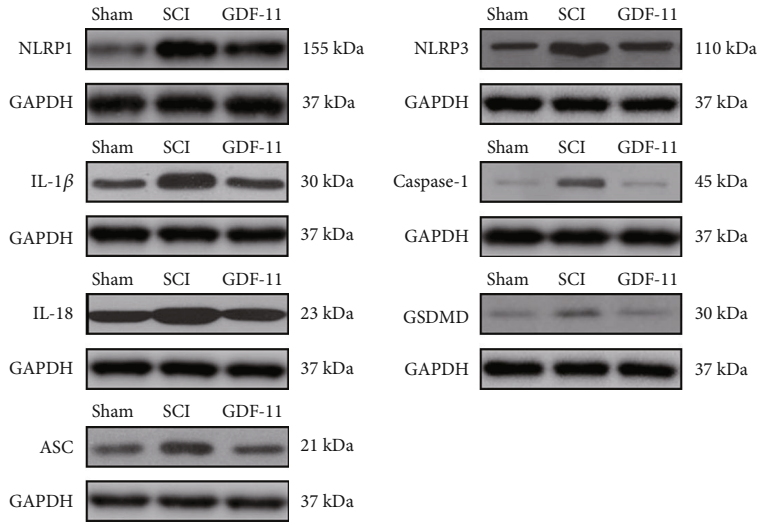

(e)

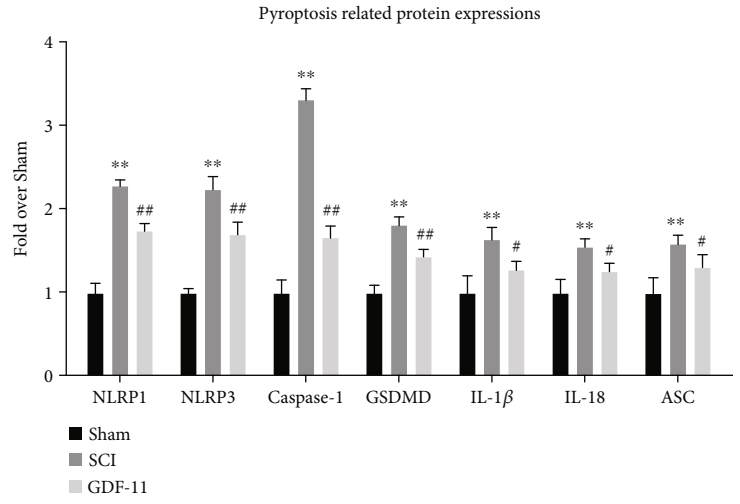

(f)

Figure 2: GDF-11 attenuates pyroptosis following spinal cord injury. (a) Immunofluorescence staining for Caspase-1 and NeuN colocalization in the spinal cords of the GDF-11, SCI, and sham groups (scale bar = 25 μm). (b) The quantitative mean optical density of Caspase-1 in neurons of spinal cord lesions. (c) Immunofluorescence staining for GSDMD and NeuN colocalization in the spinal cords of the GDF-11, SCI, and sham groups (scale bar = 25 μm). (d) The quantitative average optical density of GSDMD within neurons of spinal cord lesions. (e) Western blot assay for IL-18, IL-1β, GSDMD, Caspase-1, ASC, NLRP3, and NLRP1 expression levels in the three groups. Gels were subjected to identical experimental conditions, with cropped blots presented. (f) Optical densities of the IL-18, IL-1β, GSDMD, Caspase-1, ASC, NLRP3, and NLRP1 expression levels were quantified and investigated in the respective groups. Data are expressed as the mean ± SEM, $n = 6$ per group. $^{**}p < 0.01$ vs. the sham group. $^{\#}p < 0.05$ and $^{\#\#}p < 0.01$ vs. the SCI group.

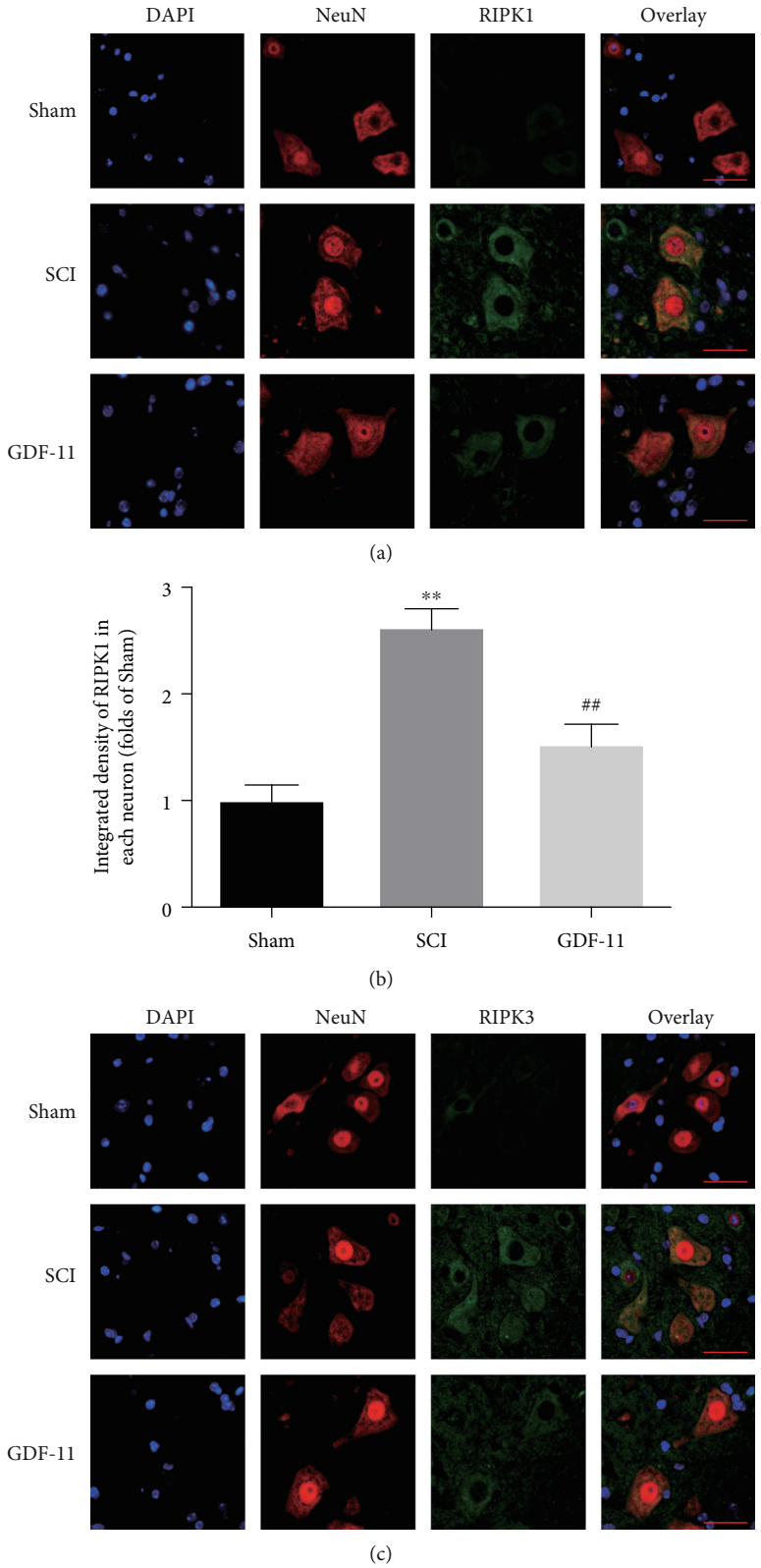

Figure 3: Continued.

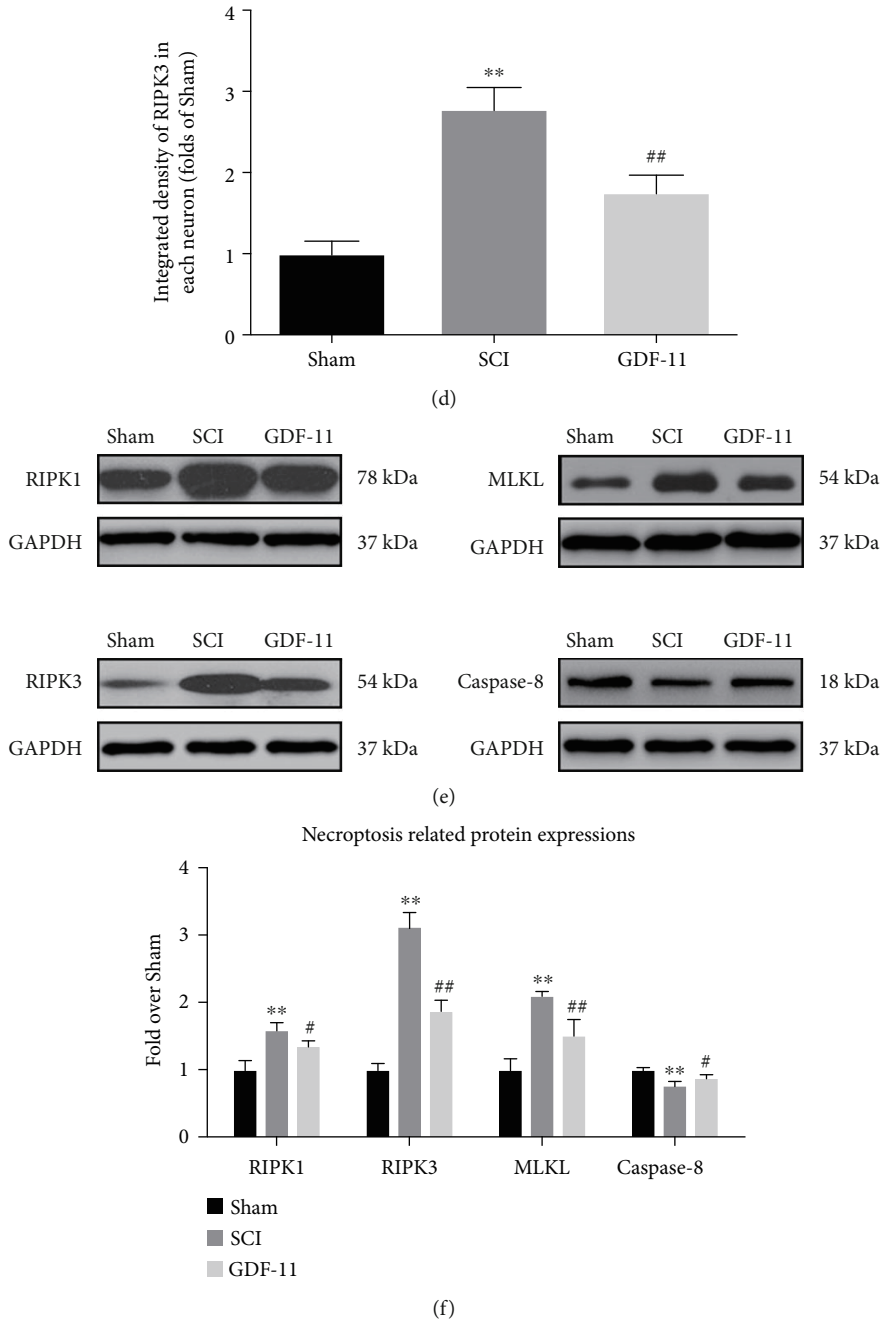

Figure 3: GDF-11 inhibits necroptosis following spinal cord injury. (a) Immunofluorescence staining for RIPK1 and NeuN colocalization in the spinal cords of the GDF-11, SCI, and sham groups (scale bar = 25 μm). (b) Quantification of the optical density of RIPK1 in neurons of spinal cord lesions. (c) Immunofluorescence staining for RIPK3 and NeuN colocalization in spinal cords belonging to the GDF-11, SCI, and sham groups (scale bar = 25 μm). (d) Quantification of the optical density of RIPK3 in neurons of spinal cord lesions. (e) Western blot assay for Caspase-8, MLKL, RIPK3, and RIPK1 expression levels in the GDF-11, SCI, and sham groups. Gels were subjected to identical experimental conditions, with cropped blots presented. (f) Optical densities of Caspase-8, MLKL, RIPK3, and RIPK1 expression levels were quantified and investigated in the respective groups. Data are expressed as the mean ± SEM, $n = 6$ per group. $^{**}p < 0.01$ vs. the sham group. $^{\#}p < 0.05$ and $^{\#\#}p < 0.01$ vs. the SCI group.

Beclin1, and LC3II). As shown in Figure 4(a), IF staining revealed that p62 was expressed within neurons in the lesions. According to the quantitative investigation, following SCI, the p62 density in neurons increased markedly ($p < 0.01$); however, the GDF-11 group achieved a relatively low p62 density in neurons in contrast to the SCI group ($p < 0.01$; Figure 4(b)). As shown in Figure 4(c), the spinal cord showed a greater percentage of LC3II-positive neurons in the SCI group than in the sham group ($p < 0.01$); compared with that of the SCI group, GDF-11 treatment upregulated LC3II-positive neurons ($p < 0.01$; Figure 3(d)). WB was performed to ascertain the amounts of CTSD, VPS34,

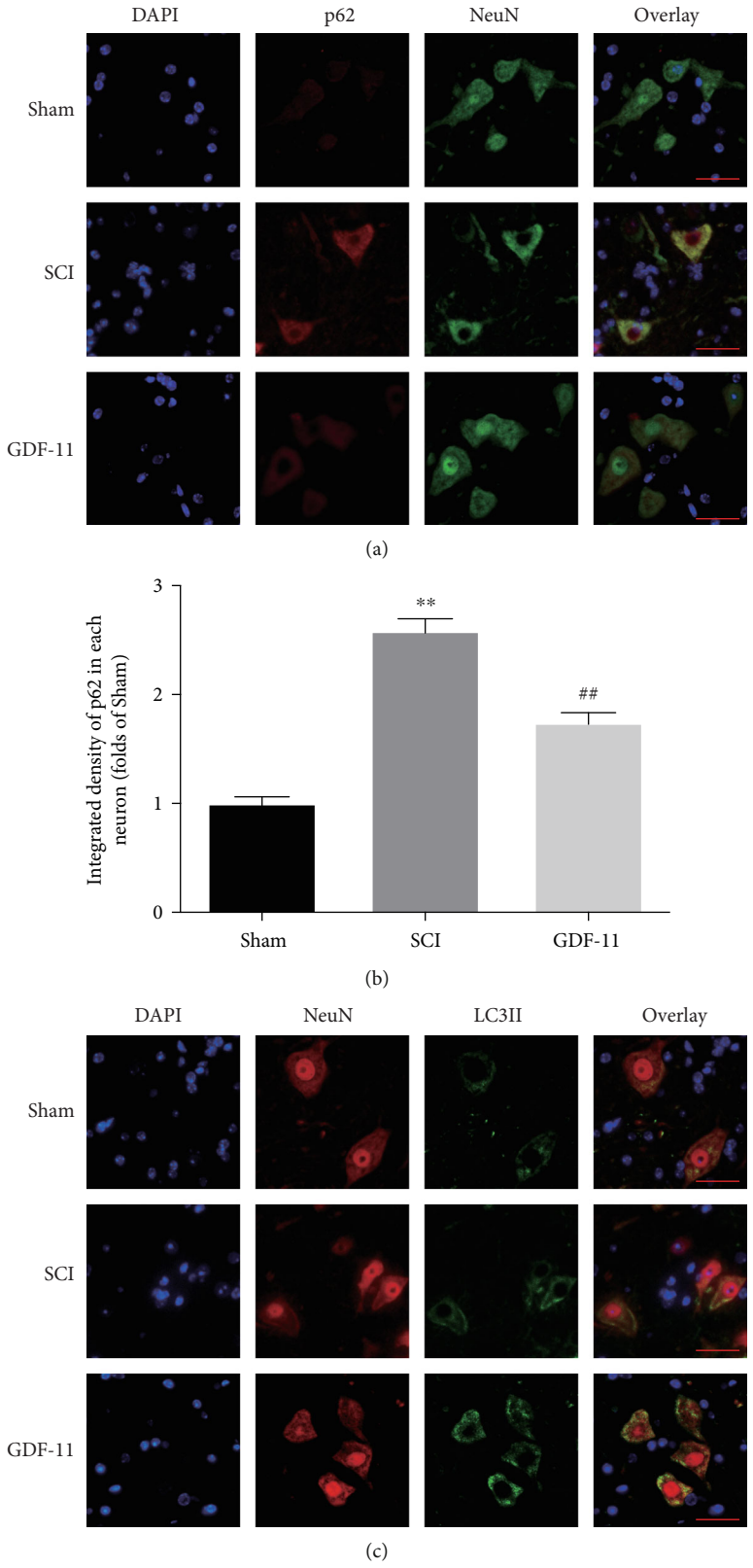

Figure 4: Continued.

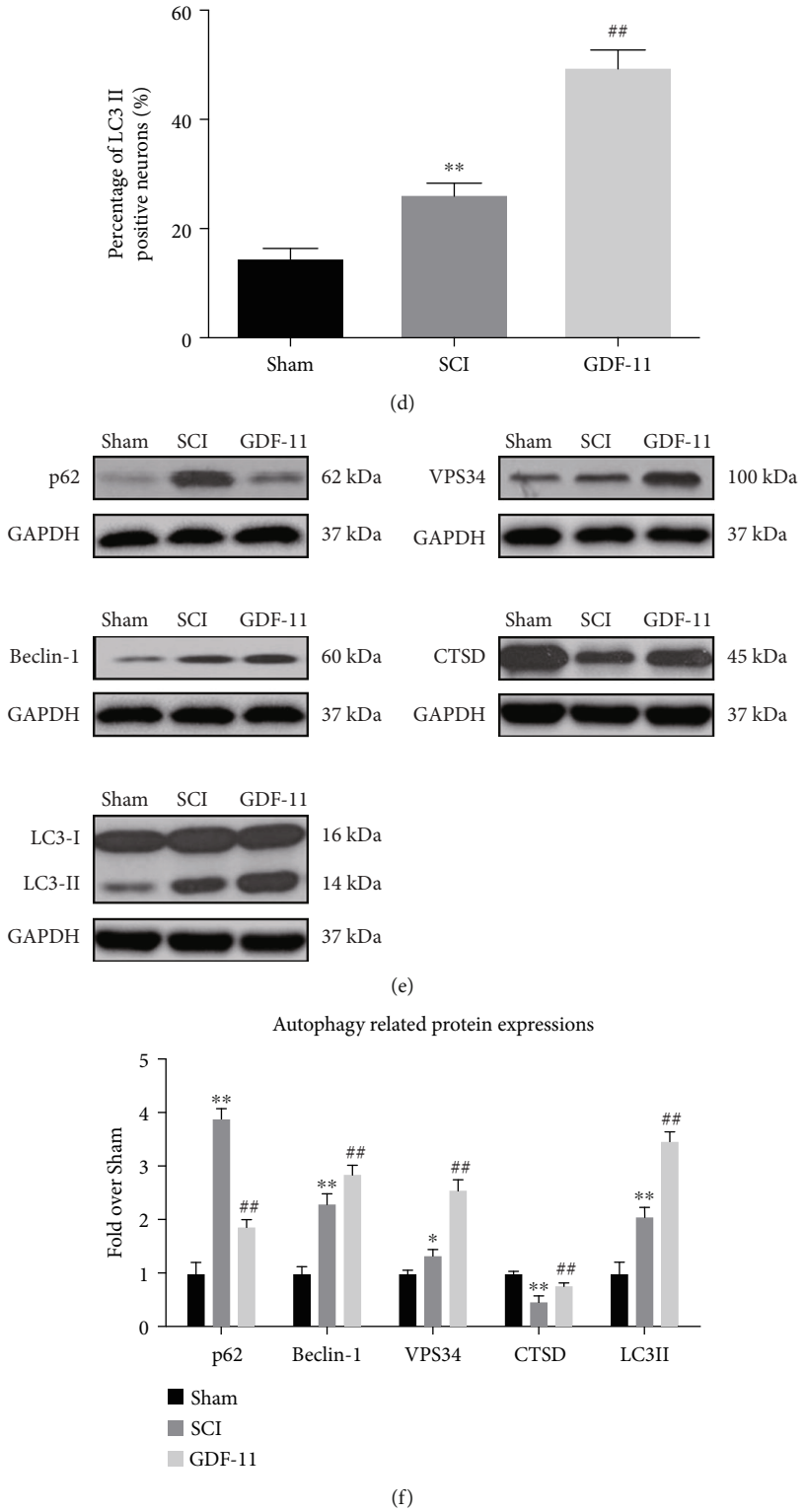

Figure 4: GDF-11 enhances autophagy following spinal cord injury. (a) Immunofluorescence staining for p62 and NeuN colocalization at the spinal cord lesion following spinal cord injury (scale bar = 25 μm). (b) The quantitative mean optical density of p62 in neurons of spinal cord lesions in the respective groups. (c) Staining based on immunofluorescence in terms of the colocalization of NeuN and LC3II within spinal cord lesions following spinal cord injury (scale bar = 25 μm). (d) The percentage of LC3II-positive neurons in neurons of spinal cord lesions in the respective groups. (e) Western blot assay for CTSD, VPS34, Beclin1, LC3II, and p62 expression levels in the sham, SCI, and GDF-11 groups. Gels were subjected to identical experimental conditions, with cropped blots presented. (f) Optical densities of CTSD, VPS34, Beclin1, LC3II, and p62 expression levels were quantified and investigated in the respective groups. Data are expressed as the mean ± SEM, $n = 6$ per group. $^{*}p < 0.05$ and $^{**}p < 0.01$ vs. the sham group. $^{\#\#}p < 0.01$ vs. the SCI group.

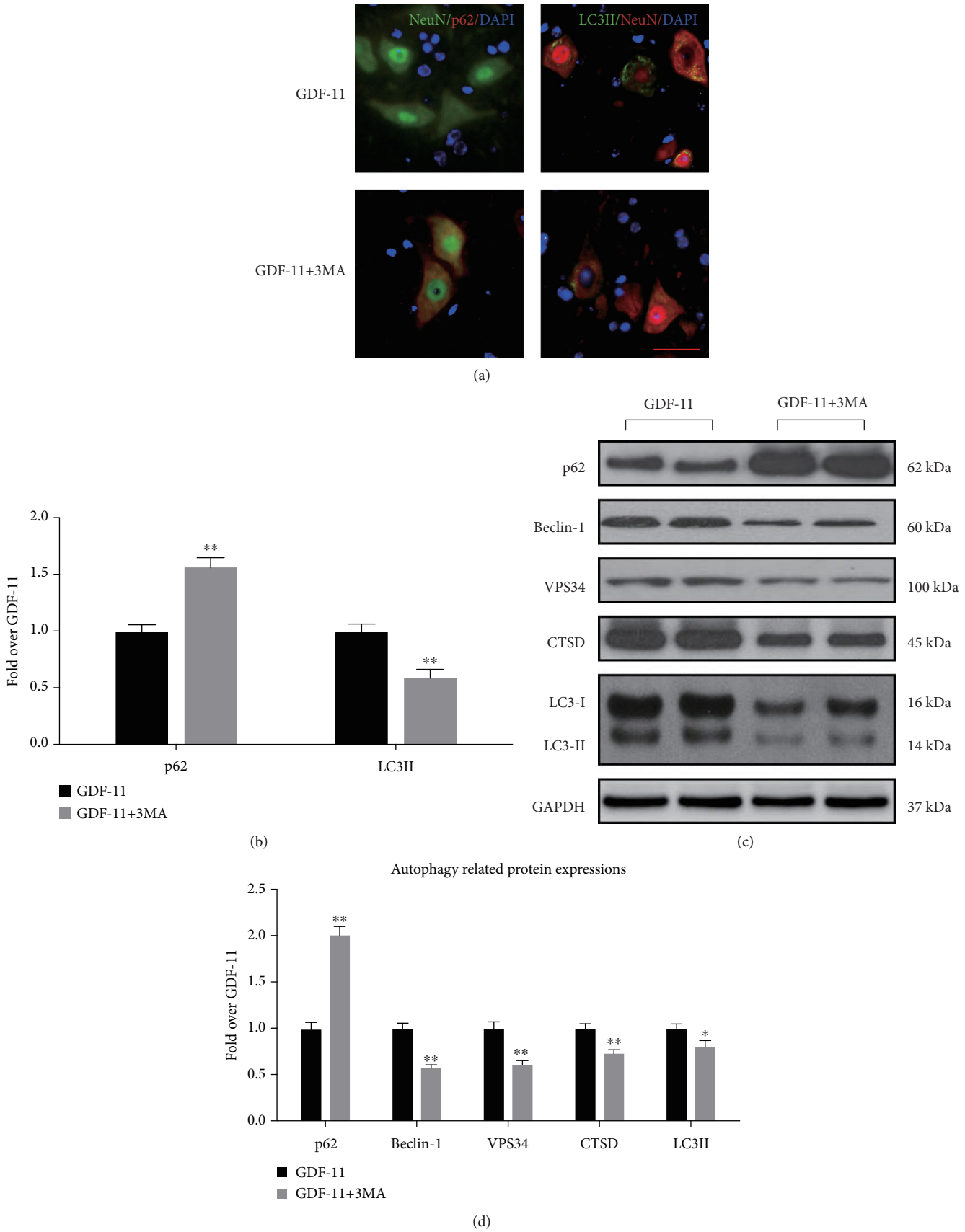

Figure 5: Continued.

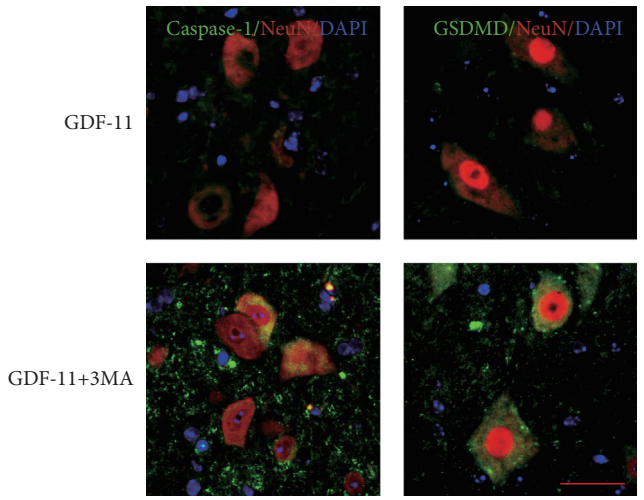

(e)

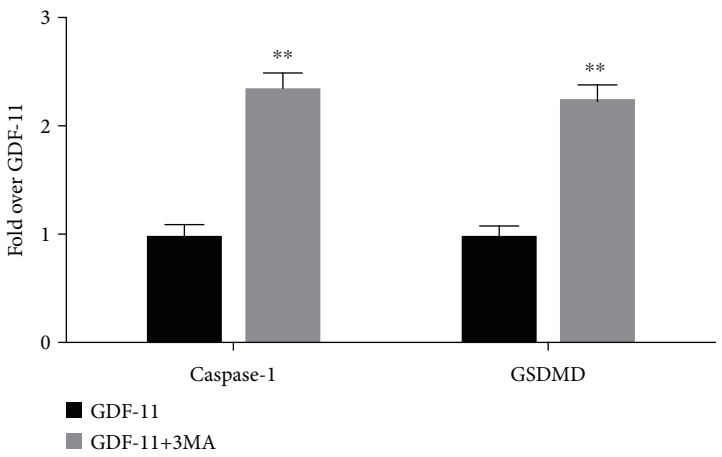

(f)

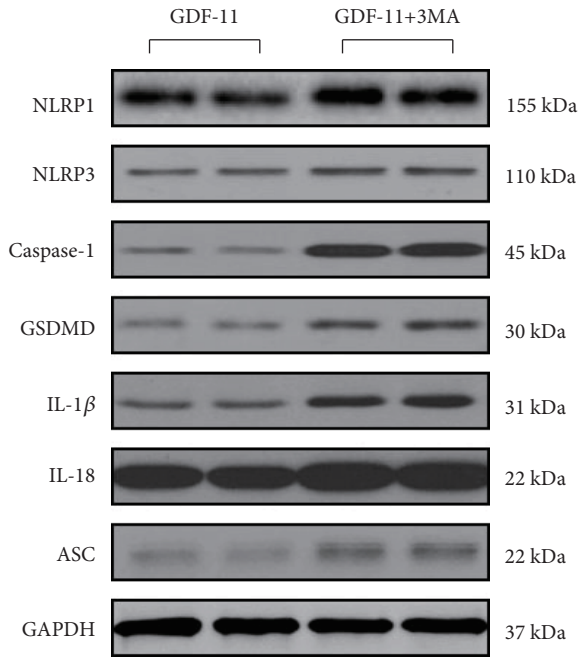

(g)

Figure 5: Continued.

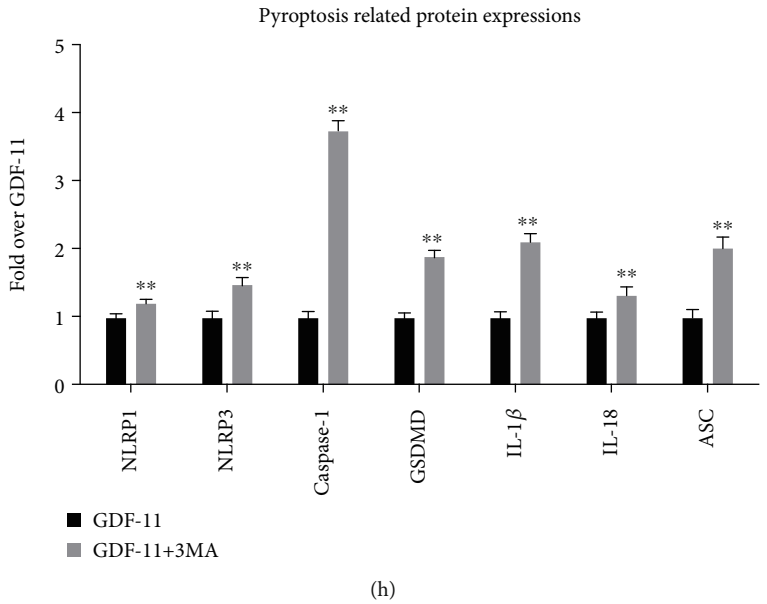

(h)

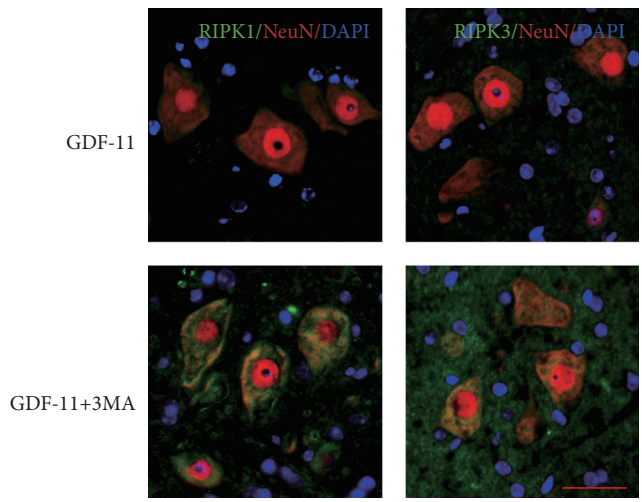

(i)

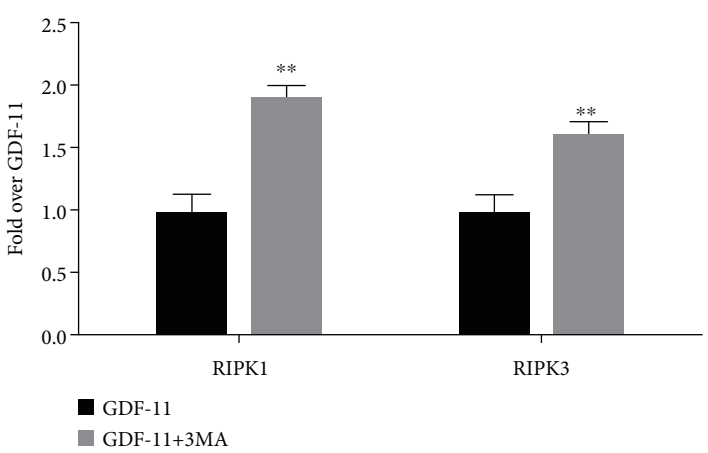

(j)

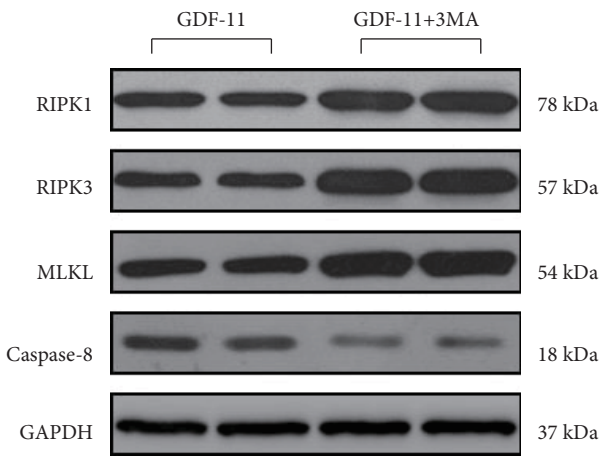

(k)

Figure 5: Continued.

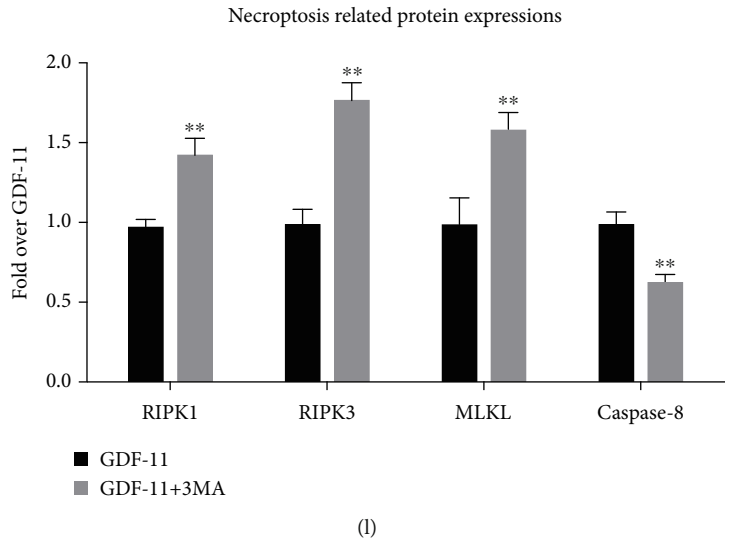

(l)

Figure 5: Suppression of autophagy reverses the influence exerted by GDF-11 on pyroptosis and necroptosis following spinal cord injury. (a) Neuron colocalization and immunofluorescence staining for p62 and LC3II at the spinal cord lesion following spinal cord injury (scale bar = 25 μm). (b) The quantitative mean optical density of p62 and the number of LC3II-positive neurons in neurons of spinal cord lesions in the respective groups. (c) Western blot assay for CTSD, VPS34, Beclin1, LC3II, and p62 expression levels in the respective groups. (d) Optical densities of CTSD, VPS34, Beclin1, LC3II, and p62 expression levels were quantified and investigated in the respective groups. (e) Neuron colocalization and immunofluorescence staining for Caspase-1 and GSDMD in the spinal cords of each group (scale bar = 25 μm). (f) The quantitative mean optical density of Caspase-1 and GSDMD in neurons of spinal cord lesions. (g) Western blot assay for IL-18, IL-1β, GSDMD, Caspase-1, ASC, NLRP3, and NLRP1 expression levels in the respective groups. (h) Optical densities of IL-18, IL-1β, GSDMD, Caspase-1, ASC, NLRP3, and NLRP1 expression levels were quantified and investigated in the respective groups. (i) Neuron colocalization and immunofluorescence staining for RIPK1 and RIPK3 in the spinal cords of each group (scale bar = 25 μm). (j) Quantification of the optical density of RIPK1 and RIPK3 in neurons of spinal cord lesions. (k) Western blot assay for Caspase-8, MLKL, RIPK3, and RIPK1 expression levels in the respective groups. (l) Optical densities of Caspase-8, MLKL, RIPK3, and RIPK1 expression levels were quantified and investigated in the respective groups. Data are expressed as the mean ± SEM, $n = 6$ per group. $^{*}p < 0.05$ and $^{**}p < 0.01$ vs. the GDF-11 group.

Beclin1, LC3II, and p62 (Figure 3(e)). As revealed by the results, compared with that within the sham group, VPS34, Beclin1, LC3II, and p62 had a higher OD within the SCI group ($p = 0.02$, <0.01, <0.01, and <0.01, respectively), with smaller OD values for CTSD within the SCI group ($p < 0.01$). Compared with the SCI group, the GDF-11 group showed increases in CTSD, VPS34, Beclin1, and LC3II levels but decreases in p62 levels ($p < 0.01$ for all; Figure 3(f)). These results summarize the phenomenon of autophagy substrate accumulation that occurs following SCI, despite the upregulation of autophagosome- and autophagolysosomal-related markers. In addition, as revealed by the abovementioned results, GDF-11 could upregulate autolysosome- and autophagosome-associated markers and alleviate autophagy substrate pressure, which is likely to result from a complete improvement in autophagic flux following SCI.

3.5. Suppression of Autophagy Reverses the Influence Exerted by GDF-11 on Pyroptosis and Necroptosis after SCI. The 3MA, an autophagy suppressor, was coadministered with GDF-11 to assess whether GDF-11 had a conducive influence on the results after SCI resulting from the activation of autophagy. Neuron colocalization analysis and IF revealed an upregulation of the p62 density and downregulation of the percentage of neurons positive for LC3II in the GDF − 11 + 3MA group compared with the GDF-11 group ($p < 0.01$ for both; Figures 5(a) and 5(b)). WB was employed to detect the expression levels of CTSD, VPS34, Beclin1, LC3II, and p62 (Figure 5(c)). Compared with the GDF-11 group, the CTSD, VPS34, Beclin1, and LC3II groups had lower OD values within the GDF − 11 + 3MA group ($p < 0.01$, ≤0.01, <0.01, and =0.01, respectively), with larger OD values for p62 within the GDF − 11 + 3MA group ($p < 0.01$; Figure 5(d)). Thus, 3MA significantly suppressed autophagy during coadministration with GDF-11.

For an in-depth verification of autophagy as the main factor allowing GDF-11 to facilitate neuronal function recovery following SCI, we delved into the influences exerted by 3MA on necroptosis and pyroptosis. As shown in the IF analysis, compared with those within the GDF-11 group, the densities of GSDMD and Caspase-1 within neurons exceeded those within the GDF − 11 + 3MA group ($p < 0.01$ for both; Figures 5(e) and 5(f)). The expression levels of pyroptosis-related proteins (IL-18, IL-1β, GSDMD, Caspase-1, ASC, NLRP3, and NLRP1) were higher in the GDF − 11 + 3MA group than in the GDF-11 group ($p < 0.01$ for all; Figures 5(g) and 5(h)). IF also showed that the RIPK1 and RIPK3 densities in neurons were markedly increased in the GDF − 11 + 3MA group compared with the GDF-11 group ($p < 0.01$ for both; Figures 5(i) and 5(j)). The OD values for necroptosis-related proteins (MLKL, RIPK3, and RIPK1) were higher in the GDF − 11 + 3MA group than in the

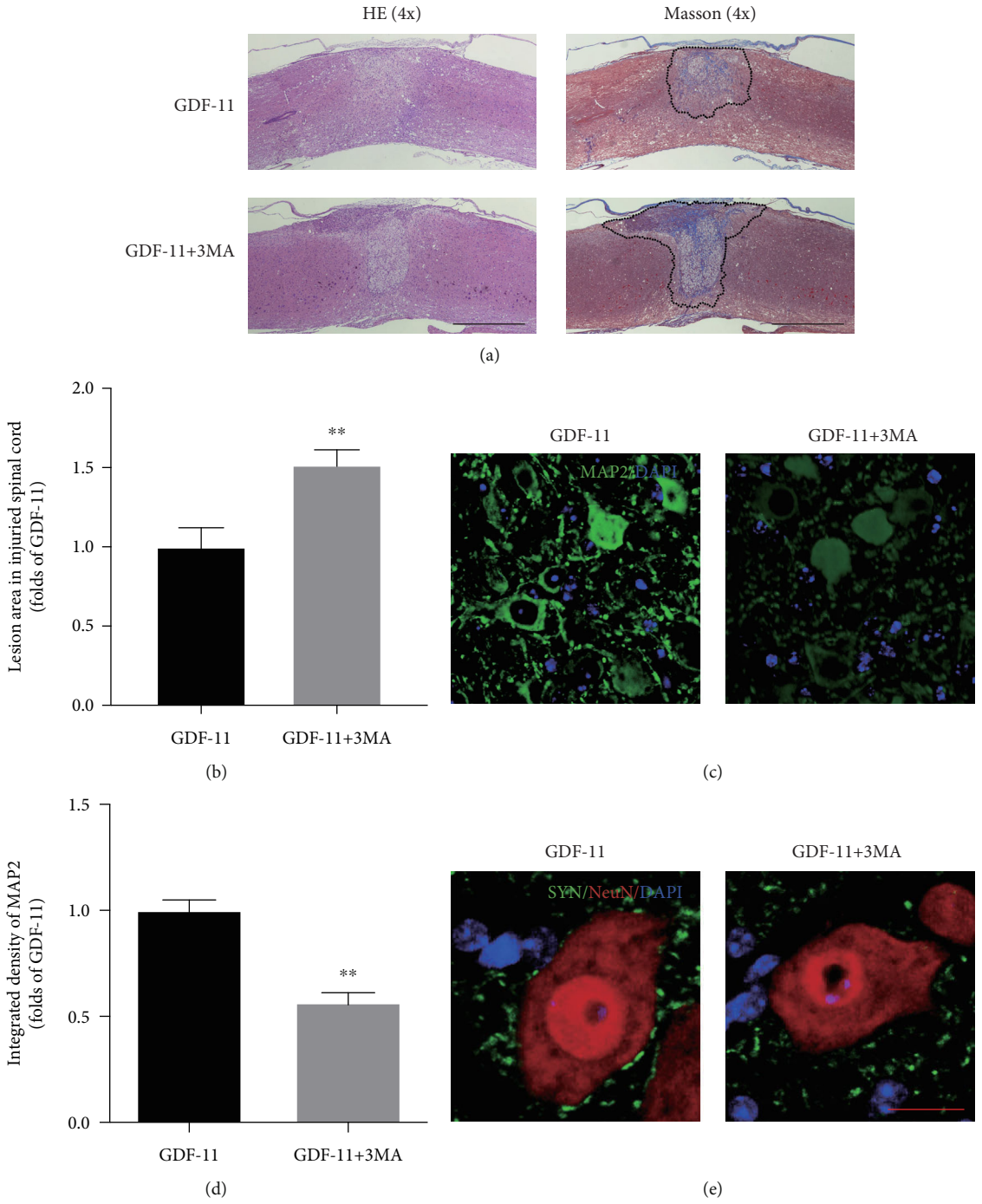

Figure 6: Continued.

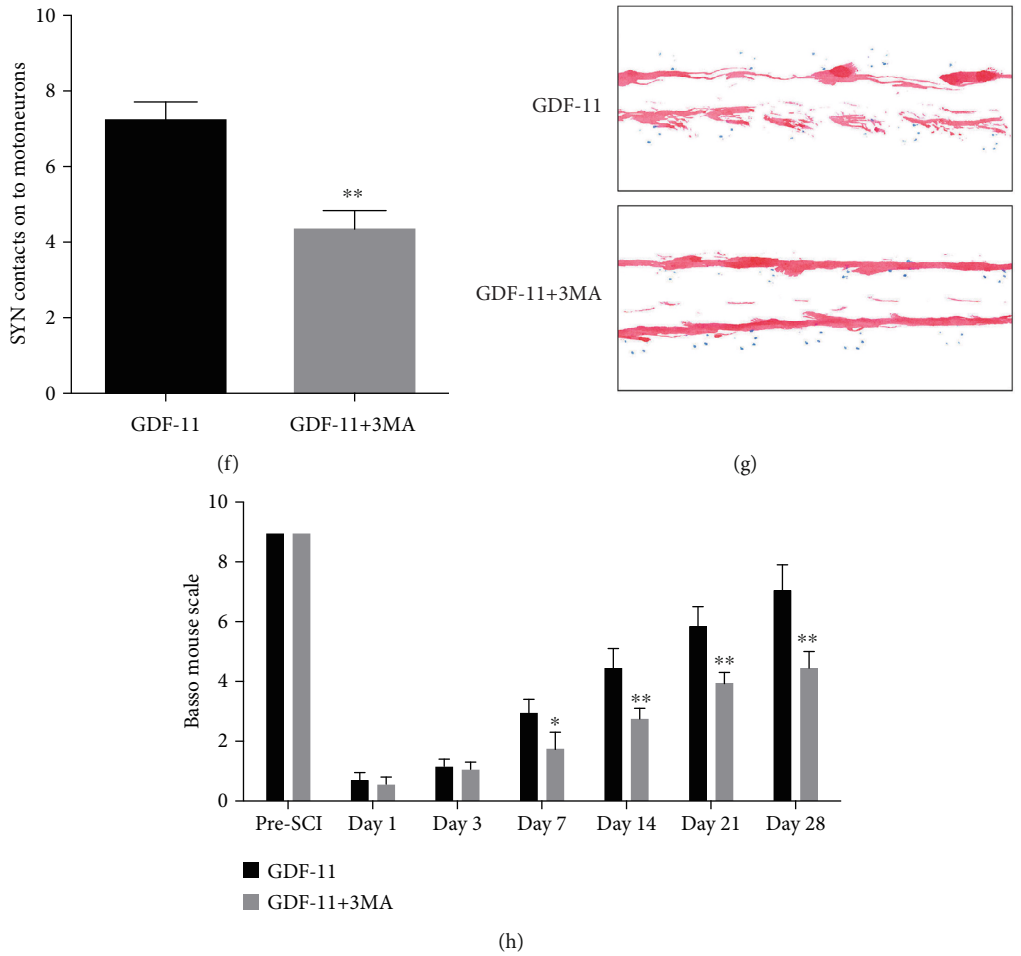

Figure 6: Suppression of autophagy reverses the influence exerted by GDF-11 on functional recovery following spinal cord injury. (a) Longitudinal spinal cord sections in the indicated groups on day 28 were analysed on the basis of Masson staining and HE staining (scale bar = 1000 μm). (b) Quantitative investigation of Masson-positive lesions within the spinal cords of the respective groups. (c) Photographs (×30) of spinal cord sections in the respective groups stained with an antibody against MAP2 (scale bar = 25 μm). (d) MAP2 optical density within spinal cords subjected to injury on day 28. (e) Photographs (×150) of spinal cord sections following injury (T11-T12) and stained on day 28 with an antibody against SYN/NeuN (scale bar = 5 μm). (f) Relevant quantitative results for numbers of neuron-contacting synapses. (g) Photographs of mouse footprints on day 28 following spinal cord injury. (h) Basso mouse scale (BMS) scores for the indicated groups and time points. Data are expressed as the mean ± SEM, $n = 6$ per group. $^{*}p < 0.05$ and $^{**}p < 0.01$ vs. the GDF-11 group.

GDF-11 group ($p < 0.01$ for all), with a lower OD value for Caspase-8 in the GDF − 11 + 3MA group ($p < 0.01$; Figures 5(k) and 5(l)). These results indicated that coadministration of 3MA with GDF-11 led to a weakening of the reducing effect of GDF-11 on pyroptosis and necroptosis, thereby demonstrating the underlying autophagy-enhancing effects of GDF-11 in the mechanism by which it inhibited pyroptosis and necroptosis.

3.6. Autophagy Inhibition Reverses the Neuroprotective Effects of GDF-11 on SCI. The lesion area in the injured spinal cord was assessed by HE and Masson staining, which revealed a broadened area of glial scars ($p < 0.01$, Figures 6(a) and 6(b)) in the GDF − 11 + 3MA group compared with the GDF-11 group. Additionally, IF staining revealed decreased MAP2 states ($p < 0.01$, Figures 6(c) and 6(d)) and a smaller number of SYN-positive synapses on neurons ($p < 0.01$, Figures 6(e) and 6(f)) in the GDF − 11 + 3MA group than in the GDF-11 group. On day 28 following injury, the GDF-11 group displayed a marked restoration of hind leg action, with coordinated crawling, while the GDF − 11 + 3MA group continued to drag their hind legs (Figure 6(g)). An insignificant difference was reported for the BMS score between the GDF-11 and GDF − 11 + 3MA groups on days 1 and 3. In the GDF − 11 + 3MA group, the BMS scores were markedly lower than those in the GDF-11 group after SCI on days 7, 14, 21, and 28 ($p = 0.04$, <0.01, <0.01, and <0.01, respectively; Figure 6(h)). Therefore, the autophagy-improving influence of GDF-11 likely accounted for the optimized results with GDF-11 treatment following SCI.

3.7. GDF-11 Facilitates Autophagy by Upregulating TFE3 Activity and Subsequently Depresses Pyroptosis and Necroptosis following SCI. We then explored TFE3

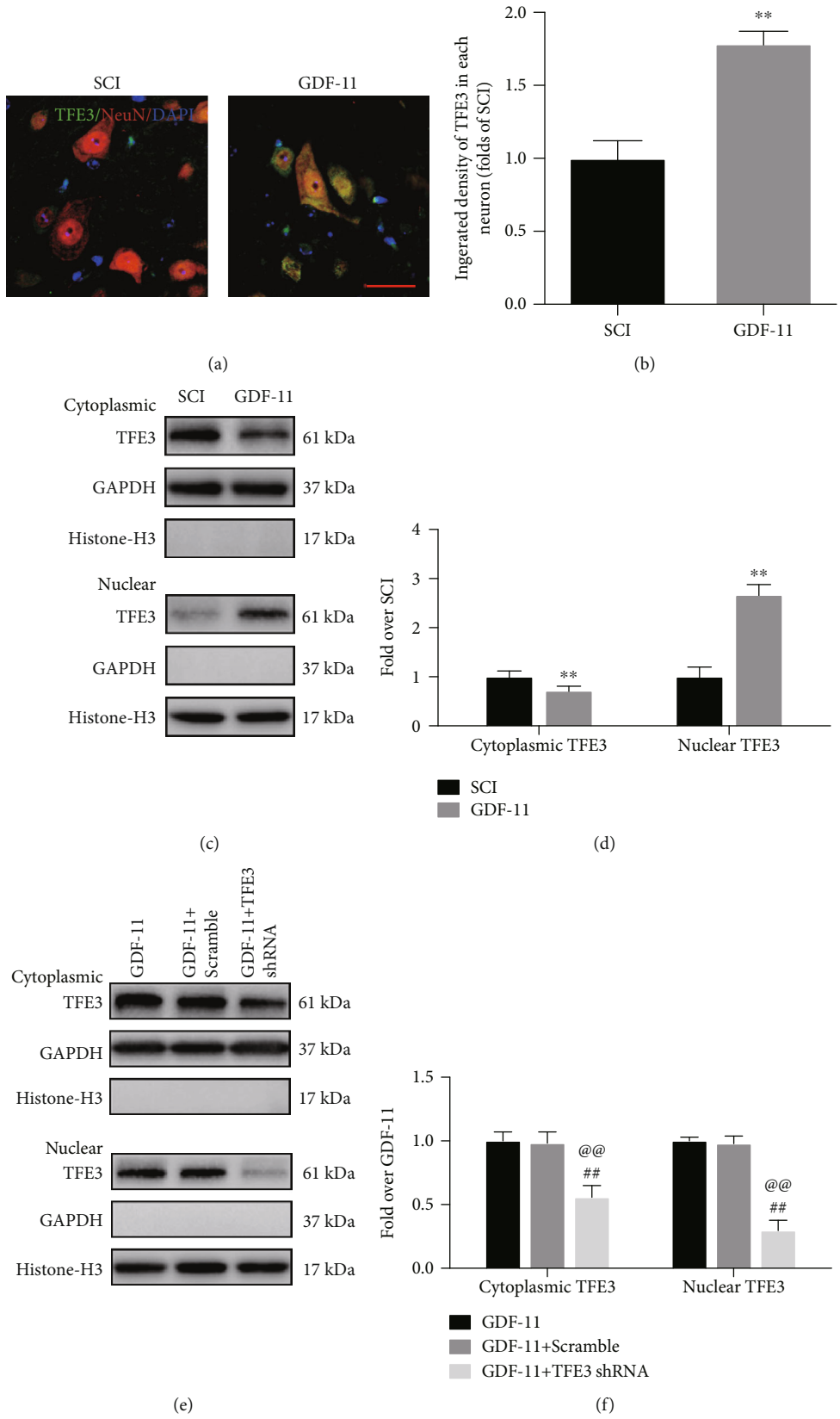

Figure 7: Continued.

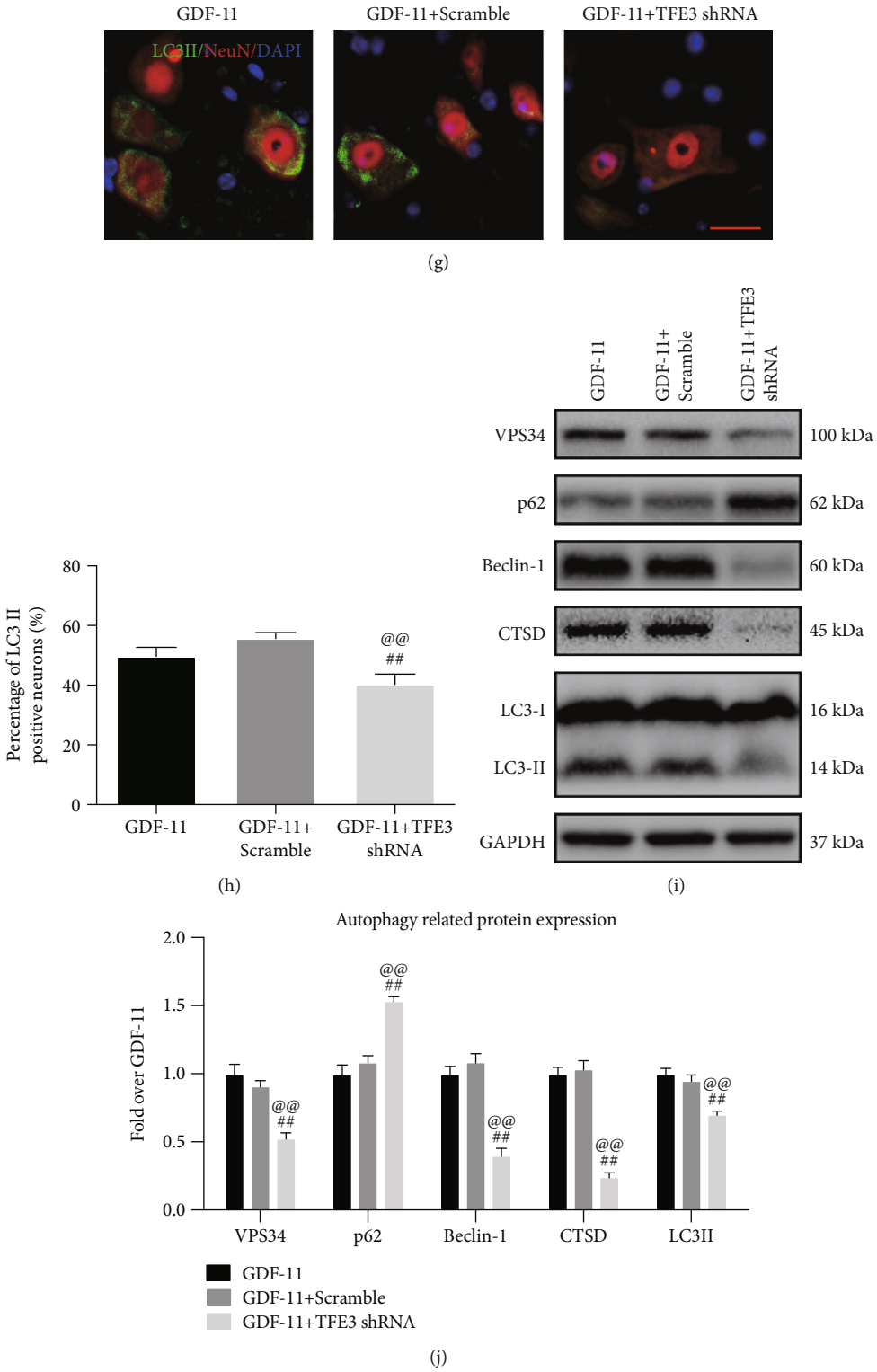

Figure 7: Continued.

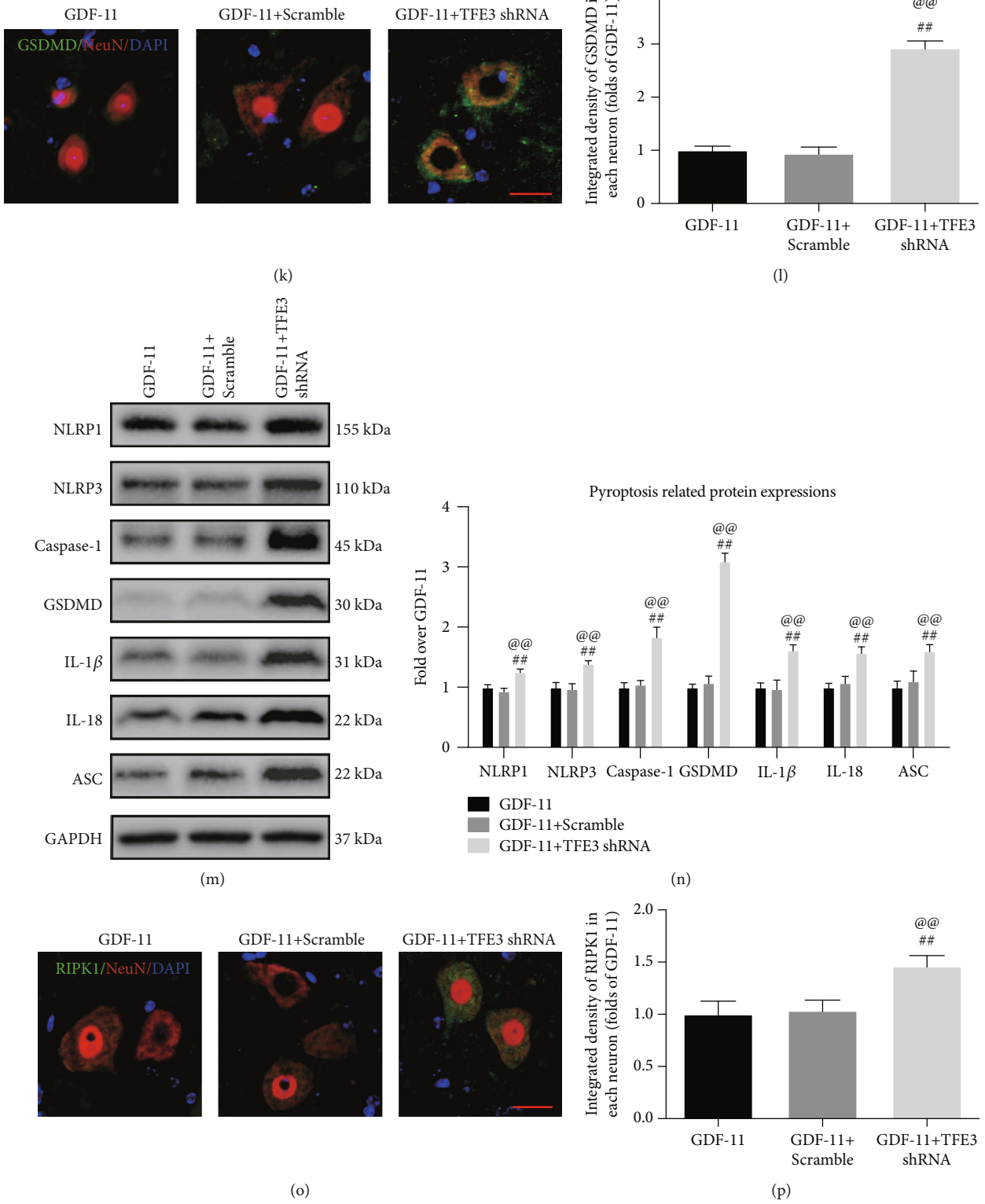

Figure 7: Continued.

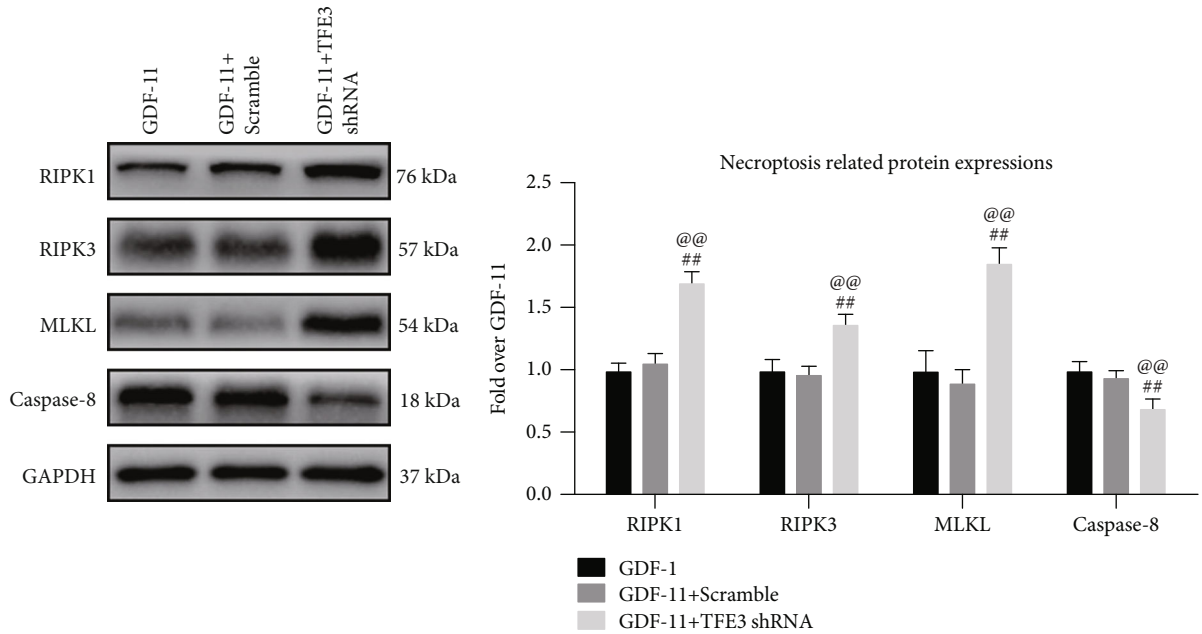

(q) (r)

Figure 7: GDF-11 enhances autophagy by upregulating TFE3 activity and inhibiting pyroptosis and necroptosis. (a) Immunofluorescence to detect TFE3 within spinal cord lesions (scale bar = 25 μm). (b) Quantification of the optical density of TFE3 expression in neurons. (c) Western blot assay of nuclear TFE3 and cytoplasmic TFE3 expression. (d) Quantification results for optical densities pertaining to nuclear TFE3 and cytoplasmic TFE3. (e) Western blot assay reporting nuclear TFE3 and cytoplasmic TFE3 expression levels in the GDF-11, GDF − 11 + scramble and GDF − 11 + TFE3 shRNA groups. (f) Quantification results for optical densities pertaining to nuclear TFE3 and cytoplasmic TFE3. (g) Staining based on immunofluorescence in terms of the colocalization of NeuN and LC3II within spinal cord lesions (scale bar = 25 μm). (h) Percentage of LC3II-positive neurons in spinal cord lesions in the respective groups. (i) Western blot assay for CTSD, VPS34, Beclin1, LC3II, and p62 expression levels in the GDF-11, GDF − 11 + scramble, and GDF − 11 + TFE3 shRNA groups. (j) Optical densities of CTSD, VPS34, Beclin1, LC3II, and p62 expression levels were quantified and investigated in the respective groups. (k) Immunofluorescence staining for GSDMD and NeuN colocalization in spinal cord lesions (scale bar = 25 μm). (l) Quantitative average optical density of GSDMD within neurons of spinal cord lesions. (m) Western blot assay for IL-18, IL-1β, GSDMD, Caspase-1, ASC, NLRP3, and NLRP1 expression levels in each group. (n) Optical densities of IL-18, IL-1β, GSDMD, Caspase-1, ASC, NLRP3, and NLRP1 expression levels were quantified and investigated in the respective groups. (o) Immunofluorescence staining for RIPK1 and NeuN colocalization in spinal cord lesions (scale bar = 25 μm). (p) Quantification of the optical density of RIPK1 in neurons of spinal cord lesions. (q) Western blot assay for Caspase-8, MLKL, RIPK3, and RIPK1 expression levels in the three groups. (r) Optical densities of Caspase-8, MLKL, RIPK3, and RIPK1 expression levels were quantified and investigated in the respective groups. Data are expressed as the mean ± SEM, $n = 6$ per group. $^{*}p < 0.05$ and $^{**}p < 0.01$ vs. the SCI group. $^{\#}p < 0.05$ and $^{\#\#}p < 0.01$ vs. the GDF-11 group. $^{@}p < 0.05$ and $^{@@}p < 0.01$ vs. the GDF − 11 + scramble group.

expression in the cytoplasm and nucleus to determine whether GDF-11 had a regulatory effect on TFE3. As shown in Figures 7(a) and 7(b), after GDF-11 treatment, TFE3 expression in neurons was markedly increased ($p < 0.01$). Next, according to the WB results, intranuclear TFE3 expression rose markedly in the GDF-11 group, while TFE3 expression in the cytoplasm was decreased ($p < 0.01$ for both; Figures 7(c) and 7(d)). For an in-depth confirmation of the effect of TFE3 activation in promoting autophagy and inhibiting pyroptosis and necroptosis through GDF-11, we silenced the TFE3 activity using TFE3 shRNA and designed a trial to compare the following three groups: GDF-11 only, GDF − 11 + scrambled shRNA, and GDF − 11 + TFE3 shRNA. The results showed that both cytoplasmic TFE3 expression and nuclear TFE3 expression in the TFE3 shRNA group were markedly lower than those in the scramble group, whereas an insignificant difference was reported for the nuclear TFE3 expression status between the GDF-11 and GDF − 11 + scramble groups ($p < 0.01$ for all; Figures 7(e) and 7(f)). These results indicated that TFE3 shRNA transfection suppressed TFE3 expression and nuclear translocation.

Subsequently, we conducted studies to determine whether TFE3 nuclear translocation induced by GDF-11 was responsible for the regulation of autophagy, pyroptosis, and necroptosis. IF revealed an insignificant distinction in the percentage of neurons positive for LC3II between the GDF-11 and GDF − 11 + scramble groups, while the proportion in the GDF − 11 + TFE3 shRNA group was markedly reduced ($p < 0.01$ for both; Figures 7(g) and 7(h)). Likewise, according to the WB results, the expression levels of p62, LC3II, CTSD, VPS34, and Beclin1 were not markedly different between the GDF-11 and GDF − 11 + scramble groups and the expression levels of VPS34, Beclin1, CTSD, and LC3II were markedly lower in the GDF − 11 + TFE3 shRNA group than in the GDF − 11 + scramble group, while

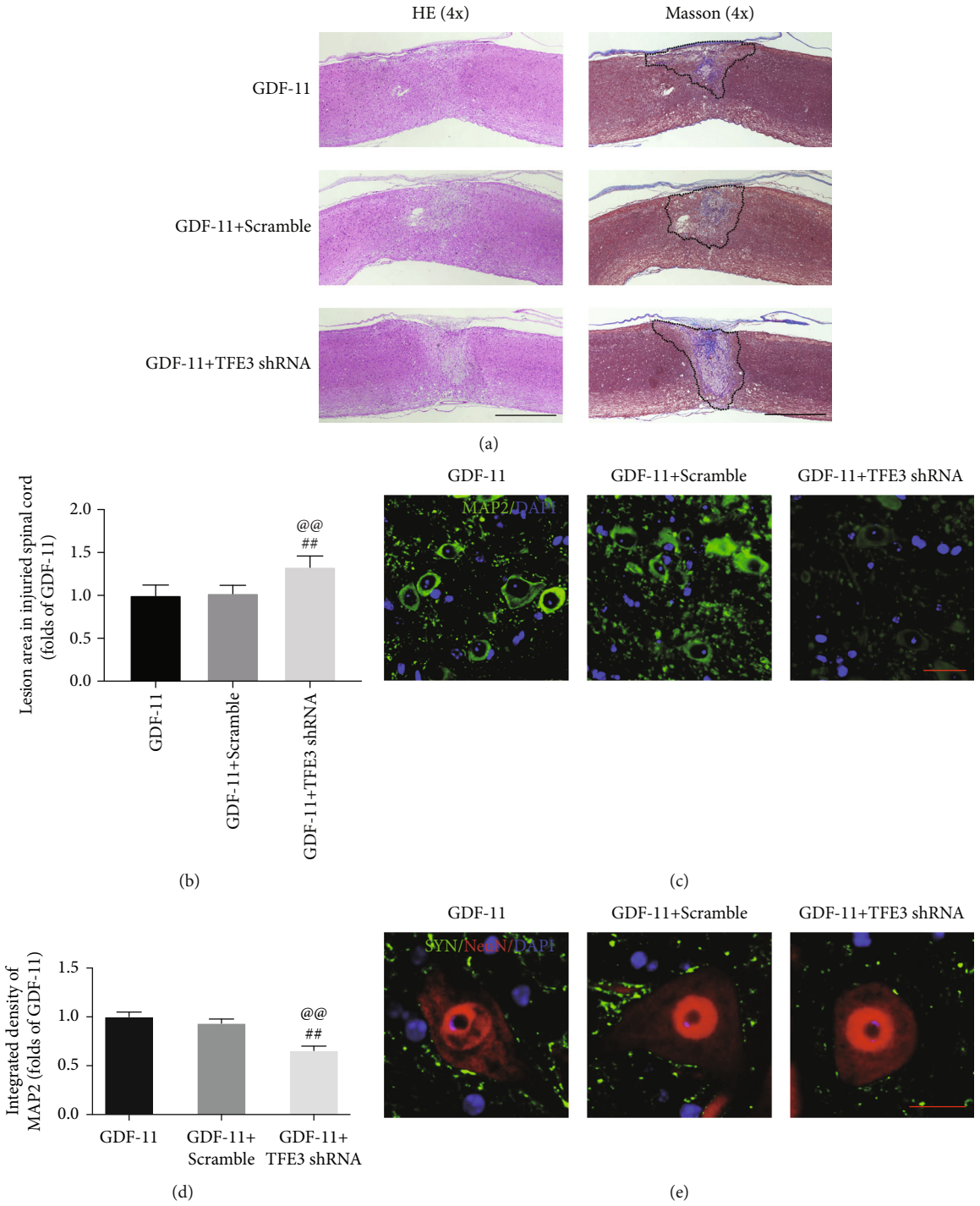

Figure 8: Continued.

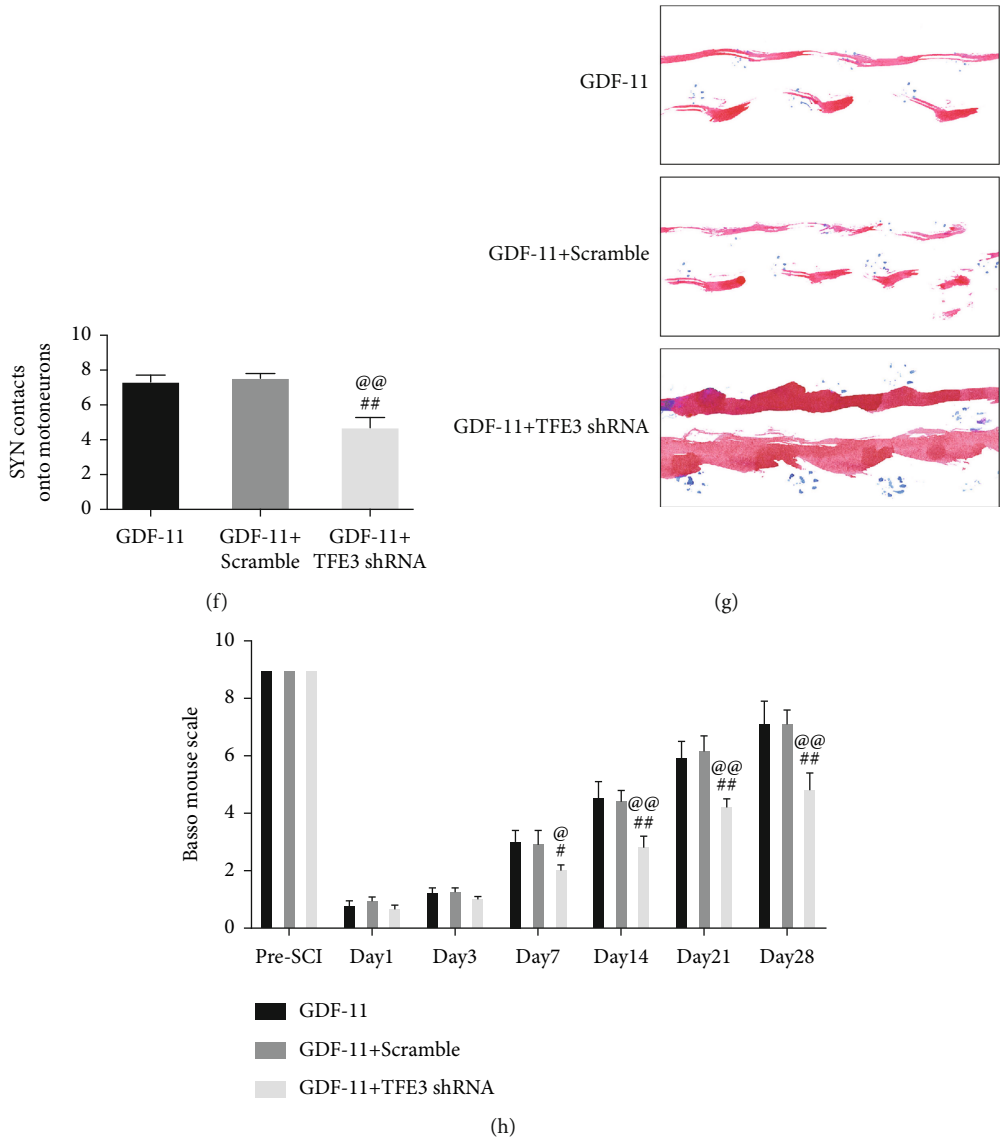

Figure 8: Autophagy inhibition reverses the neuroprotective effects of GDF-11 on SCI. (a) Longitudinal spinal cord sections in the indicated groups on day 28 were analysed on the basis of Masson staining and HE staining (scale bar = 1000 μm). (b) Quantitative investigation of Masson-positive lesions within the spinal cords of the respective groups. (c) Photographs (×30) of spinal cord sections in the respective groups stained using an antibody against MAP2 (scale bar = 25 μm). (d) MAP2 optical density within spinal cords subjected to injury on day 28. (e) Photographs (×150) of spinal cord sections following injury (T11-T12) and stained on day 28 with an antibody against SYN/NeuN (scale bar = 5 μm). (f) Relevant quantification results for numbers of neuron-contacting synapses. (g) Photographs of mouse footprints on day 28 following spinal cord injury. (h) Basso mouse scale (BMS) scores in terms of the indicated groups and time points. Data are expressed as the mean ± SEM, $n = 6$ per group. $^{\#}p < 0.05$ and $^{\#\#}p < 0.01$ vs. the GDF-11 group. $^{@}P < 0.05$ and $^{@@}P < 0.01$ vs. the GDF − 11 + scramble group.

opposite results were obtained for p62 ($p < 0.01$ for all; Figures 7(i) and 7(j)). TFE3 shRNA treatment increased the expression levels of pyroptosis-associated markers (ASC, IL-18, IL-1β, GSDMD, Caspase-1, NLRP3, and NLRP1) and necroptosis-related markers (RIPK1, RIPK3, MLKL, and opposite Caspase-8), as shown in Figures 7(k)–7(r) ($p < 0.01$ for all). The GDF − 11 + TFE3 shRNA group showed a broadened area of glial scarring ($p = 0.01$, Figures 8(a) and 8(b)), decreased MAP2 expression ($p < 0.01$, Figures 8(c) and 8(d)), and fewer SYN-positive synapses ($p < 0.01$, Figures 8(e) and 8(f)) on neurons compared with the GDF-11 group following SCI. On day 28 following injury, the GDF − 11 + TFE3 shRNA group was still dragging their hind legs (Figure 8(g)). An insignificant difference was reported for the BMS score among the GDF-11, the GDF − 11 + scramble, and GDF − 11 + TFE3 shRNA groups on days 1 and 3. In the GDF − 11 + TFE3 shRNA group, the BMS scores were markedly lower than those in the GDF-11 and GDF − 11 + scramble groups on days 7, 14, 21, and 28 after SCI ($p = 0.03$, <0.01, <0.01, and <0.01; Figure 8(h)). Together, these results suggested that TFE3 activation and nuclear translocation were the major mechanisms by which

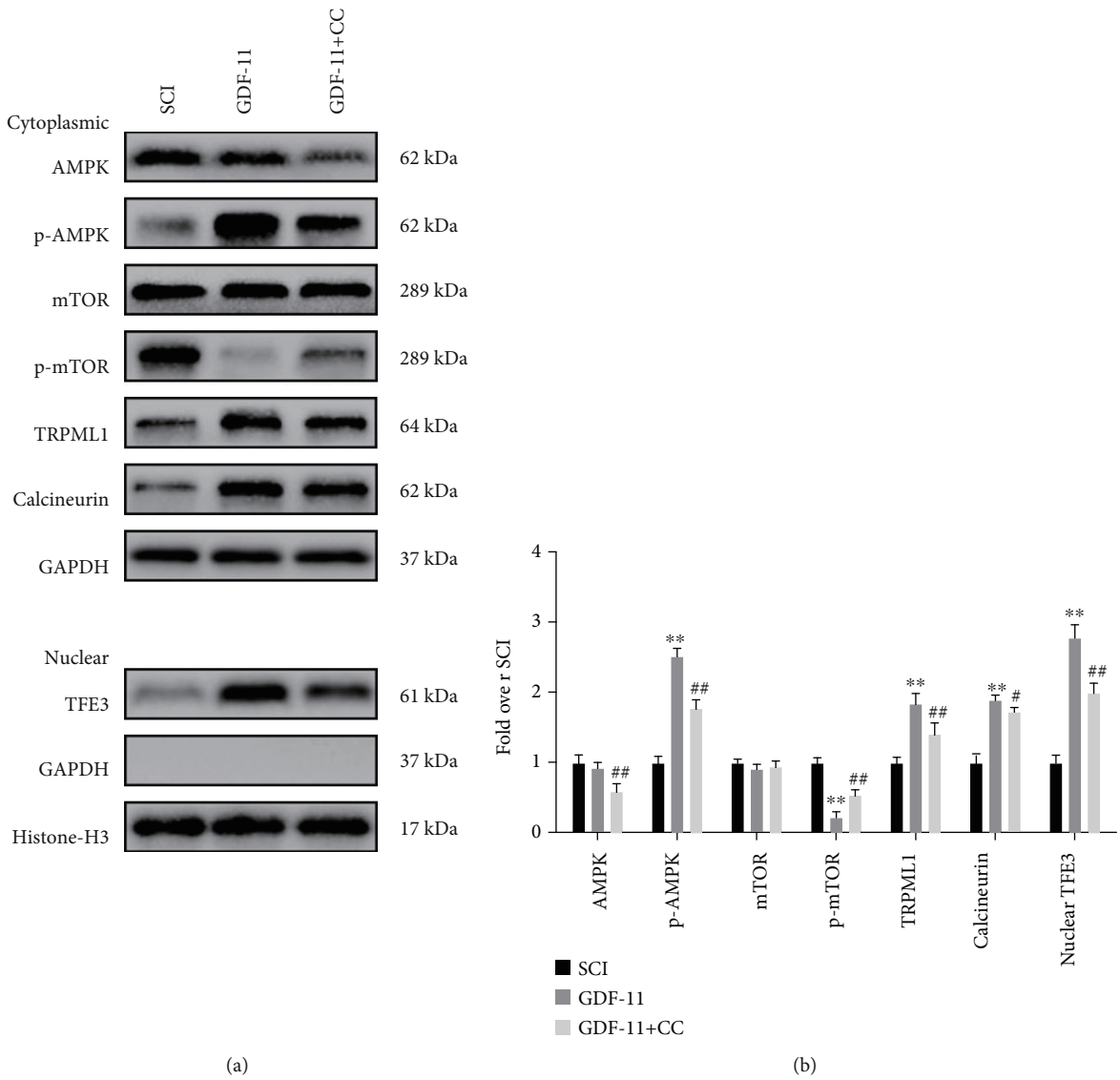

Figure 9: Continued.

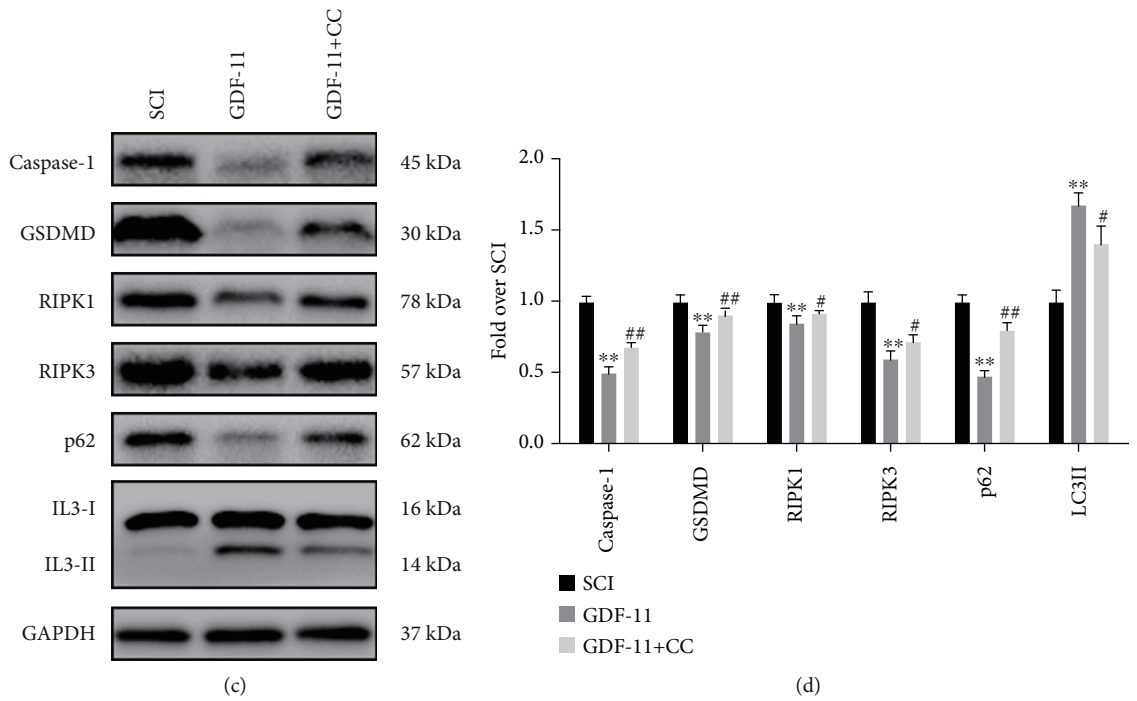

Figure 9: GDF-11 activates TFE3 through the AMPK-TRPML1-calcineurin signalling pathway. (a) Western blot assay showing the cytoplasmic expression levels of p-mTOR, mTOR, p-AMPK, AMPK, TRPML1, and calcineurin, normalized to GAPDH as an internal control; nuclear expression of TFE3, normalized to histone H3 as an internal control. (b) Optical densities of TRPML1, p-mTOR, mTOR, p-AMPK, AMPK, calcineurin, and nuclear TFE3. (c) Western blot assay showing the expression levels of Caspase-1, GSDMD, RIPK1, RIPK3, p62, and LC3II normalized to GAPDH as an internal control. (d) Optical densities of Caspase-1, GSDMD, RIPK1, RIPK3, p62, and LC3II. Data are expressed as the mean ± SEM, $n = 6$ per group. $^{*}p < 0.05$ and $^{**}p < 0.01$ vs. the SCI group. $^{\#}p < 0.05$ and $^{\#\#}p < 0.01$ vs. the GDF-11 group.

GDF-11 increased autophagy and inhibited pyroptosis and necroptosis.

3.8. GDF-11 Activates TFE3 through the AMPK-TRPML1-Calcineurin Signalling Pathway after SCI. According to published reports, there is an important calcium signalling pathway that modulates TFE3: the AMPK-TRPML1-calcineurin signalling cascade. Our results showed that GDF-11 increased p-AMPK expression and TFE3 nuclear translocation, while p-mTOR was inhibited ($p < 0.01$ for all, Figures 9(a) and 9(b)). As downstream signalling molecules, Western blot analysis revealed that the expression states of TRPML1 and calcineurin were markedly increased ($p < 0.01$ for both, Figures 9(a) and 9(b)). To further investigate whether TFE3 activation after GDF-11 treatment was modulated by the AMPK-TRPML1-calcineurin signalling pathway, we explored the effects of compound C (CC), an AMPK blocker, on the GDF-11 group. Here, p-AMPK expression and TFE3 nuclear translocation states were lower in the GDF − 11 + CC group than in the GDF-11 group ($p < 0.01$ for both), while p-mTOR expression was higher in the GDF − 11 + CC group ($p < 0.01$, Figures 9(a) and 9(b)). Likewise, the expression levels of TRPML1 and calcineurin were markedly decreased ($p < 0.01$ and $p = 0.04$, respectively, Figures 9(a) and 9(b)). We further evaluated whether the AMPK-TRPML1-calcineurin axis was also involved in the mechanism by which GDF-11 modulated pyroptosis-, necroptosis-, and autophagy-related proteins. The WB results showed that the expression levels of Caspase-1, GSDMD, RIPK1, RIPK3, and p62 were markedly higher in the GDF − 11 + CC group than in the GDF-11 group, while LC3II expression levels showed the opposite pattern ($p < 0.01$, <0.01, =0.04, =0.03, <0.01, and =0.01, Figures 9(c) and 9(d)). Together, our results confirmed that GDF-11 activated TFE3 through the AMPK-TRPML1-calcineurin signalling cascade.

4. Discussion

Significant damage to the spinal cord is capable of causing sensorimotor disorder or permanent paralysis [49]. A decreased regenerative capacity (neuronal death) after SCI is capable of disrupting the continuing signal transmission property within the limbs and brain, as well as hindering functional recovery [50, 51]. Thus, it is essential to inhibit neuronal death and facilitate neuronal regeneration, which is capable of forming novel relay circuits to replace ruptured circuits. GDF-11 is an important regulator of central nervous system formation and fate throughout life [52]. In previous studies, GDF-11 exerted neuroprotective and neurorestorative effects on cerebral ischaemic injury [39, 53]. Programmed cell death, including the pyroptosis, necroptosis, and autophagy, is found to facilitate neurological deficits [54–57]. Thus, we hypothesized that GDF-11 regulates pyroptosis, necroptosis, and autophagy following SCI. In this study, our results showed that the therapeutic effect of

GDF-11 was due to the activity of TFE3 through the AMPK-TRPML1-calcineurin signalling pathway, which subsequently enhanced autophagy and further attenuated pyroptosis and inhibited necroptosis.

Pyroptosis refers to one proinflammatory form of programmed cell death that is regulated during the process of activating caspase-1-, caspase-4/5/11-, and GSDMD-regulated signalling pathways and the release of several inflammatory mediators, such as IL-1β and IL-18 [58–61]. By assembling inflammasome-related sensor proteins (NLRP1, NLRP3, AIM2, and pyrin), the scaffolding protein apoptosis-related speck-like protein covering CARD (ASC), and proinflammatory caspase (caspase-1 and -4/5 in humans) into inflammasomes, the autoactivating process for caspase and subsequent proteolytic gasdermin D (GSDMD) cleavage can be promoted, thereby triggering cell pyroptosis [12]. To evaluate GDF-11 activity in pyroptosis, we performed IF staining to assess the Caspase-1 and GSDMD density in neurons and found diminished GDF-11 densities in spinal cord lesions. According to the WB results, following GDF-11 treatment, IL-1B, IL-1β, Caspase-1, GSDMD, NLRP1, NLRP3, and ASC expression levels were all decreased, thereby demonstrating that GDF-11 was an effective suppressor of pyroptosis in the mouse SCI model.

Necroptosis is regulated by classical necrosomes that comprise mixed-lineage kinase domain-like protein (MLKL) and receptor-interacting protein kinase 1/3 (RIPK1/3) via TNF/TNFR1 signalling or other stimuli [18]. RIPK1, an upstream mediator of necrosis, is a key regulator of innate immune responses involved in inflammation and cell death [33]. RIPK3 plays a pivotal role in the recruitment and phosphorylation of MLKL, which is the executor of necroptosis to recruit Ca^{2+} and Na^{+} ion pathways and form pores at the plasma membrane, leading to cell rupture [62]. Therefore, they may be ideal targets for reducing cell death and inflammation in the central nervous system [63]. Thus, we hypothesized that GDF-11 might inhibit necroptosis following SCI. In this study, we showed via both IF and WB that GDF-11 decreased expression levels of MLKL, RIPK3, and RIPK1, while Caspase-8 expression was increased. Therefore, our results demonstrated that GDF-11 could inhibit necroptosis in SCI.

Autophagy, a major process of degrading intracellular waste, has an important role in maintaining cellular homeostasis [64]. After SCI, lysosomal damage and dysfunction can occur within affected cells, leading to autophagy flux defects, an accumulation of autophagosomes, and active cell death, which is not conducive to the survival of neurons [65]. A previous study has demonstrated that autophagy is suppressed by knocking out the ATG5 gene, further demonstrating that functional recovery can be limited by blocking autophagy after SCI [66]. Here, from the results of increased expressions of Beclin1, VPS34, CTSD, LC3II, and decreased p62 expression via both IF and WB, we revealed that GDF-11 functioned as an effective activator of autophagy by improving the states of autophagy flux.

Neuronal death via pyroptosis or necroptosis is regulated through the activities of host proteins that induce different biological outcomes [67]. Autophagy, a prosurvival mechanism, has been found to suppress pyroptosis and necroptosis by degradation of various proteins (e.g., NLRP3, ASC, and RIPK1) [35, 36, 68]. Previous studies of SCI have confirmed that the induction of autophagy plays a neuroprotective role by suppressing apoptosis [69]. However, few studies investigated the effect of autophagy on cosuppression of pyroptosis and necroptosis following SCI. In the current study, we used 3MA to inhibit autophagy in SCI with GDF-11 treatment to demonstrate that GDF-11 inhibited pyroptosis and necroptosis via autophagy enhancement. After autophagy was suppressed, pyroptosis-associated and necroptosis-associated markers were partially adjusted and functional recovery was inhibited in SCI with GDF-11 treatment. However, the specific connection and biochemical mechanism need to be further studied. Altogether, these results suggest that GDF-11 suppresses pyroptosis and necroptosis by activating autophagy, which plays a critical role in the therapeutic effect of GDF-11 after SCI.

To elucidate the GDF-11 action system and how it facilitates autophagy in SCI, we also explored upstream mechanisms of autophagy activity. Previous reports have shown that autophagy is regulated by TFE3, which is a member of the MiT/TFE subfamily of the bHLH-LZ transcription factor family [70, 71]. Therefore, in this study, we investigated the relationship between tissue TFE3 and autophagy activity. From a mechanistic perspective, within a normal physiological environment, phosphorylated TFE3 interacts with 14–3–3 cytosolic chaperones to form the TFE3-14-3-3 complex; if cells receive stimulation from environmental signals (starvation, hypoxia, or toxins), TFE3 dephosphorylation inhibits the activity of mTOR and causes it to separate from the TFE3-14-3-3 complex [72]. In our study, we showed that GDF-11 increased TFE3 expression. Simultaneously, activated TFE3 markedly enhanced autophagy, attenuated pyroptosis, inhibited necroptosis, and promoted functional recovery in the SCI group. Taken together, these results demonstrated that the therapeutic effect of GDF-11 was regulated by promoting the nuclear translocation of TFE3.

Next, we also investigated how GDF-11 regulated TFE3 states. AMPK, which is capable of responding to a low-energy state and starvation, can be activated by the ratio of AMP/ATP, Ca^{2+}-activated Ca^{2+}/calmodulin-dependent kinase (CaMKII), and converting growth factor-β-activated kinase 1 (TAK1) [73]. Activation of the AMPK-mTOR pathway also facilitates the release of Ca^{2+} via the TRPML1 pathway, thereby activating calcineurin [74, 75]. In the past few years, it has been reported that the PPP3/calcineurin-activating process and increased intracellular Ca^{2+} states may stimulate TFE3 dephosphorylation and the translocation of TFE3 to the nucleus following SCI [76, 77]. Here, our results suggested that the AMPK-TRPML1-calcineurin signalling pathway was activated after GDF-11 treatment in SCI. With the use of CC, suppressing the AMPK-TRPML1-calcineurin signalling pathway could reduce the influence exerted by GDF-11 on autophagy, pyroptosis, and necroptosis.

This work has several limitations that will require in-depth analyses. Specifically, in a previous study, TFE3 activation during SCI was found to be partially regulated by AMPK-SKP2-CARM1 and AMPK-mTOR signalling

pathways [2, 68]. In-depth investigations can delve into whether GDF-11 also acts through AMPK-SKP2-CARM1 and AMPK-mTOR signalling pathways and the differences among them in SCI. The expression of GDF-11 decreases gradually with age, and more work should be performed to investigate whether the recovery of patients of different ages depends on the expression of GDF-11. The optimal dose and regimen of GDF-11 will require in-depth assessments to improve its therapeutic value.

We also have several prospects for further research on GDF-11. A previous study has demonstrated that TFE3 and TFEB share partial common mechanisms [70]. Therefore, we speculate that GDF-11 is also likely to activate autophagy through TFEB enhancement after SCI but the details require further study. It was found that the treatment of GDF-11 for central nervous system injury is promising [53, 78]. However, there is a lack of clinical experimental reports related to GDF-11 in CNS injury. Therefore, the possibility of clinical transformation of GDF-11 for SCI requires further research. Many other mechanisms may also cause neuronal death following SCI, such as parthanatos. Parthanatos have a close relationship with nervous system diseases and neurologic disorders and have been described in nervous system neoplasms [79]. The effect of GDF-11 on parthanatos after SCI is an issue worthy of further discussion.

In conclusion, our study demonstrated that GDF-11 facilitated the nuclear translocation of TFE3 by activating the AMPK-TRPML1-calcineurin signalling pathway, which enhanced autophagy. Subsequently, increased autophagy attenuated pyroptosis and inhibited necroptosis. Ultimately, the effects of GDF-11 that were evaluated facilitate functional recovery following SCI. In conclusion, we not only focused on the effect of GDF-11 on autophagy, pyroptosis, and necroptosis but also demonstrated the connection among them. The results of our studies show that replenishment with GDF-11 may be a novel therapeutic approach with broad clinical potential for the treatment of SCI patients.

Data Availability

The datasets used and analysed during the current study are available from the corresponding authors upon reasonable request.

Conflicts of Interest

The authors have declared that no competing interests exist.

Authors' Contributions

Yu Xu and Xinli Hu wrote the manuscript text. Yu Xu, Feida Li, Haojie Zhang, Junsheng Lou, Xingyu Wang, and Hui Wang prepared the figures and collected the samples. Wenfei Ni, Jianzhong Kong, and Xiangyang Wang analysed the data. Yao Li, Kailiang Zhou, and Hui Xu designed the experiment. Kailiang Zhou and Hui Xu revised the manuscript. All authors reviewed and approved the final manuscript. Yu Xu and Xinli Hu contributed equally to this work.

Acknowledgments

This study was supported by grants from the Zhejiang Provincial Science and Technology Project of Traditional Chinese Medicine (Grant no. 2021ZB183 to Hui Xu), the Natural Science Foundation of China (Grant no. 82072192 to Kailiang Zhou and Grant no. 82102674 to Yao Li), Zhejiang Provincial Public Welfare Technology Application Research Project (Grant no. LGF20H150003 to Kailiang Zhou), and Wenzhou Science and Technology Bureau Foundation (no. Y20210438 to Kailiang Zhou).

References

[1] M. Tariq, C. Morais, P. N. Kishore, N. Biary, S. A. Deeb, and K. A. Moutaery, "Neurological recovery in diabetic rats following spinal cord injury," *Journal of Neurotrauma*, vol. 15, no. 4, pp. 239–251, 1998.

[2] L. Bai, X. Mei, Y. Wang et al., "The role of netrin-1 in improving functional recovery through autophagy stimulation following spinal cord injury in rats," *Frontiers in Cellular Neuroscience*, vol. 11, p. 350, 2017.

[3] Y. Zhou, Z. Wang, J. Li, X. Li, and J. Xiao, "Fibroblast growth factors in the management of spinal cord injury," *Journal of Cellular and Molecular Medicine*, vol. 22, no. 1, pp. 25–37, 2018.

[4] V. Tardivo, E. Crobeddu, G. Pilloni et al., "Say "no" to spinal cord injury: is nitric oxide an option for therapeutic strategies?," *The International Journal of Neuroscience*, vol. 125, no. 2, pp. 81–90, 2015.

[5] H. Kim, H. Kumar, M. J. Jo et al., "Therapeutic efficacy-potentiated and diseased organ-targeting nanovesicles derived from mesenchymal stem cells for spinal cord injury treatment," *Nano Letters*, vol. 18, no. 8, pp. 4965–4975, 2018.

[6] S. Ko, E. C. Apple, Z. Liu, and L. Chen, "Age-dependent autophagy induction after injury promotes axon regeneration by limiting NOTCH," *Autophagy*, vol. 16, no. 11, pp. 2052–2068, 2020.

[7] I. Vismara, S. Papa, V. Veneruso et al., "Selective modulation of A1 astrocytes by drug-loaded nano-structured gel in spinal cord injury," *ACS Nano*, vol. 14, no. 1, pp. 360–371, 2020.

[8] P. Boulenguez and L. Vinay, "Strategies to restore motor functions after spinal cord injury," *Current Opinion in Neurobiology*, vol. 19, no. 6, pp. 587–600, 2009.

[9] J. Wu, Z. Zhao, B. Sabirzhanov et al., "Spinal cord injury causes brain inflammation associated with cognitive and affective changes: role of cell cycle pathways," *The Journal of Neuroscience : The Official Journal of the Society for Neuroscience*, vol. 34, no. 33, pp. 10989–11006, 2014.

[10] S. Xu, J. Wang, J. Zhong et al., "CD73 alleviates GSDMD-mediated microglia pyroptosis in spinal cord injury through PI3K/AKT/Foxo1 signaling," *Clinical and Translational Medicine*, vol. 11, no. 1, article e269, 2021.

[11] J. Shi, W. Gao, and F. Shao, "Pyroptosis: gasdermin-mediated programmed necrotic cell death," *Trends in Biochemical Sciences*, vol. 42, no. 4, pp. 245–254, 2017.

[12] L. Vande Walle and M. Lamkanfi, "Pyroptosis," *Current Biology : CB*, vol. 26, no. 13, pp. R568–R572, 2016.

[13] M. Fleshner, M. Frank, and S. Maier, "Danger signals and Inflammasomes: stress-evoked sterile inflammation in mood disorders," *Neuropsychopharmacology : Official Publication of*

the American College of Neuropsychopharmacology, vol. 42, no. 1, pp. 36–45, 2017.

[14] A. Zendedel, S. Johann, S. Mehrabi et al., "Activation and regulation of NLRP3 inflammasome by intrathecal application of SDF-1a in a spinal cord injury model," *Molecular Neurobiology*, vol. 53, no. 5, pp. 3063–3075, 2016.

[15] Q. Fu, J. Wu, X. Y. Zhou et al., "NLRP3/Caspase-1 pathway-induced pyroptosis mediated cognitive deficits in a mouse model of Sepsis-associated encephalopathy," *Inflammation*, vol. 42, no. 1, pp. 306–318, 2019.

[16] F. Marín-Aguilar, J. Ruiz-Cabello, and M. Cordero, "Aging and the Inflammasomes," in *Experientia supplementum*, pp. 303–320, Springer, Cham, 2012.

[17] W. Lin, G. P. Xiong, Q. Lin et al., "Heme oxygenase-1 promotes neuron survival through down-regulation of neuronal NLRP1 expression after spinal cord injury," *Journal of Neuroinflammation*, vol. 13, no. 1, p. 52, 2016.

[18] L. Andera, "Signaling activated by the death receptors of the TNFR family," *Biomedical Papers of the Medical Faculty of the University Palacky, Olomouc, Czechoslovakia*, vol. 153, no. 3, pp. 173–180, 2009.

[19] M. Fritsch, S. D. Günther, R. Schwarzer et al., "Caspase-8 is the molecular switch for apoptosis, necroptosis and pyroptosis," *Nature*, vol. 575, no. 7784, pp. 683–687, 2019.

[20] A. Degterev, D. Ofengeim, and J. Yuan, "Targeting RIPK1 for the treatment of human diseases," *Proceedings of the National Academy of Sciences of the United States of America*, vol. 116, no. 20, pp. 9714–9722, 2019.

[21] B. McKenzie, V. Dixit, and C. Power, "Fiery cell death: pyroptosis in the central nervous system," *Trends in Neurosciences*, vol. 43, no. 1, pp. 55–73, 2020.

[22] J. Kjell and L. Olson, "Rat models of spinal cord injury: from pathology to potential therapies," *Disease Models & Mechanisms*, vol. 9, no. 10, pp. 1125–1137, 2016.

[23] S. Liu, B. Sandner, T. Schackel et al., "Regulated viral BDNF delivery in combination with Schwann cells promotes axonal regeneration through capillary alginate hydrogels after spinal cord injury," *Acta Biomaterialia*, vol. 60, pp. 167–180, 2017.

[24] L. Yu, Y. Chen, and S. Tooze, "Autophagy pathway: cellular and molecular mechanisms," *Autophagy*, vol. 14, no. 2, pp. 207–215, 2018.

[25] C. Behrends, M. E. Sowa, S. P. Gygi, and J. W. Harper, "Network organization of the human autophagy system," *Nature*, vol. 466, no. 7302, pp. 68–76, 2010.

[26] H. Zhang, Z. G. Wang, F. Z. Wu et al., "Regulation of autophagy and ubiquitinated protein accumulation by bFGF promotes functional recovery and neural protection in a rat model of spinal cord injury," *Molecular Neurobiology*, vol. 48, no. 3, pp. 452–464, 2013.

[27] X. Lu, Q. Fan, L. Xu et al., "Ursolic acid attenuates diabetic mesangial cell injury through the up-regulation of autophagy via miRNA-21/PTEN/Akt/mTOR suppression," *PLoS One*, vol. 10, no. 2, article e0117400, 2015.

[28] Y. Rong, W. Liu, J. Wang et al., "Neural stem cell-derived small extracellular vesicles attenuate apoptosis and neuroinflammation after traumatic spinal cord injury by activating autophagy," *Cell Death & Disease*, vol. 10, no. 5, p. 340, 2019.

[29] S. Bedoui, M. Herold, and A. Strasser, "Emerging connectivity of programmed cell death pathways and its physiological implications. Nature reviews," *Molecular cell biology*, vol. 21, no. 11, pp. 678–695, 2020.

[30] K. Tsuchiya, "Inflammasome-associated cell death: pyroptosis, apoptosis, and physiological implications," *Microbiology and Immunology*, vol. 64, no. 4, pp. 252–269, 2020.

[31] N. Kayagaki, S. Warming, M. Lamkanfi et al., "Non-canonical inflammasome activation targets caspase-11," *Nature*, vol. 479, no. 7371, pp. 117–121, 2011.

[32] S. Man, R. Karki, and T. Kanneganti, "Molecular mechanisms and functions of pyroptosis, inflammatory caspases and inflammasomes in infectious diseases," *Immunological Reviews*, vol. 277, no. 1, pp. 61–75, 2017.

[33] S. Liu, Y. Li, H. M. C. Choi et al., "Lysosomal damage after spinal cord injury causes accumulation of RIPK1 and RIPK3 proteins and potentiation of necroptosis," *Cell Death & Disease*, vol. 9, no. 5, p. 476, 2018.

[34] M. Li, X. L. Zhu, B. X. Zhao et al., "Adrenomedullin alleviates the pyroptosis of Leydig cells by promoting autophagy via the ROS-AMPK-mTOR axis," *Cell Death & Disease*, vol. 10, no. 7, p. 489, 2019.

[35] Y. Hongna, T. Hongzhao, L. Quan et al., "Jia-Ji electroacupuncture improves locomotor function with spinal cord injury by regulation of autophagy flux and inhibition of necroptosis," *Frontiers in Neuroscience*, vol. 14, p. 616864, 2021.

[36] C. Shi, K. Shenderov, N. N. Huang et al., "Activation of autophagy by inflammatory signals limits IL-1β production by targeting ubiquitinated inflammasomes for destruction," *Nature Immunology*, vol. 13, no. 3, pp. 255–263, 2012.

[37] J. Liu, "The function of growth/differentiation factor 11 (Gdf11) in rostrocaudal patterning of the developing spinal cord," *Development*, vol. 133, no. 15, pp. 2865–2874, 2006.

[38] A. McPherron, A. Lawler, and S. Lee, "Regulation of anterior/-posterior patterning of the axial skeleton by growth/differentiation factor 11," *Nature Genetics*, vol. 22, no. 3, pp. 260–264, 1999.

[39] Y. Zhao, L. H. Wang, A. Peng et al., "The neuroprotective and neurorestorative effects of growth differentiation factor 11 in cerebral ischemic injury," *Brain Research*, vol. 1737, p. 146802, 2020.

[40] J. Hudobenko, B. P. Ganesh, J. Jiang et al., "Growth differentiation factor-11 supplementation improves survival and promotes recovery after ischemic stroke in aged mice," *Aging*, vol. 12, no. 9, pp. 8049–8066, 2020.

[41] K. Byrnes, B. A. Stoica, S. Fricke, S. di Giovanni, and A. I. Faden, "Cell cycle activation contributes to post-mitotic cell death and secondary damage after spinal cord injury," *Brain : A Journal of Neurology*, vol. 130, no. 11, pp. 2977–2992, 2007.

[42] R. Zheng, L. Xie, W. Liu et al., "Recombinant growth differentiation factor 11 impairs fracture healing through inhibiting chondrocyte differentiation," *Annals of the New York Academy of Sciences*, vol. 1440, no. 1, pp. 54–66, 2019.

[43] Z. He, S. Zou, J. Yin et al., "Inhibition of Endoplasmic Reticulum Stress Preserves the Integrity of Blood- Spinal Cord Barrier in Diabetic Rats Subjected to Spinal Cord Injury," *Scientific Reports*, vol. 7, no. 1, p. 7661, 2017.

[44] D. Jiang, F. Gong, X. Ge et al., "Neuron-derived exosomes-transmitted miR-124-3p protect traumatically injured spinal cord by suppressing the activation of neurotoxic microglia and astrocytes," *Journal of Nanobiotechnology*, vol. 18, no. 1, p. 105, 2020.

[45] K. Zhou, Y. F. Zhou, K. Wu et al., "Stimulation of autophagy promotes functional recovery in diabetic rats with spinal cord injury," *Scientific Reports*, vol. 5, no. 1, 2015.

[46] K. Wu, K. Zhou, Y. Wang et al., "Stabilization of HIF-1α by FG-4592 promotes functional recovery and neural protection in experimental spinal cord injury," *Brain Research*, vol. 1632, pp. 19–26, 2016.

[47] H. Li, C. Wang, T. He et al., "Mitochondrial transfer from bone marrow mesenchymal stem cells to motor neurons in spinal cord injury rats via gap junction," *Theranostics*, vol. 9, no. 7, pp. 2017–2035, 2019.

[48] J. Li, Q. Wang, H. Cai et al., "FGF1 improves functional recovery through inducing PRDX1 to regulate autophagy and anti-ROS after spinal cord injury," *Journal of Cellular and Molecular Medicine*, vol. 22, no. 5, pp. 2727–2738, 2018.

[49] A. Singh, L. Tetreault, S. Kalsi-Ryan, A. Nouri, and M. G. Fehlings, "Global prevalence and incidence of traumatic spinal cord injury," *Clinical Epidemiology*, vol. 6, pp. 309–331, 2014.

[50] D. Seo, J. H. Kim, J. Min et al., "Enhanced axonal regeneration by transplanted Wnt3a-secreting human mesenchymal stem cells in a rat model of spinal cord injury," *Acta Neurochirurgica*, vol. 159, no. 5, pp. 947–957, 2017.

[51] H. Yin, L. Shen, C. Xu, and J. Liu, "Lentivirus-mediated overexpression of miR-29a promotes axonal regeneration and functional recovery in experimental spinal cord injury via PI3K/Akt/mTOR pathway," *Neurochemical Research*, vol. 43, no. 11, pp. 2038–2046, 2018.

[52] K. Chang, C. Sun, E. G. Cameron et al., "Opposing Effects of Growth and Differentiation Factors in Cell-Fate Specification," *Current Biology : CB*, vol. 29, no. 12, pp. 1963–1975.e5, 2019.

[53] W. Chen, H. Wang, J. Feng, and L. Chen, "Overexpression of circRNA circUCK2 attenuates cell apoptosis in cerebral ischemia-reperfusion injury via miR-125b-5p/GDF11 signaling," *Molecular Therapy. Nucleic Acids*, vol. 22, pp. 673–683, 2020.

[54] L. Cabon, A. Martinez-Torres, and S. Susin, "Programmed cell death comes in many flavors," *Medecine Sciences : M/S*, vol. 29, no. 12, pp. 1117–1124, 2013.

[55] M. Föller, S. Huber, and F. Lang, "Erythrocyte programmed cell death," *IUBMB Life*, vol. 60, no. 10, pp. 661–668, 2008.

[56] I. Lekli, D. D. Haines, G. Balla, and A. Tosaki, "Autophagy: an adaptive physiological countermeasure to cellular senescence and ischaemia/reperfusion-associated cardiac arrhythmias," *Journal of Cellular and Molecular Medicine*, vol. 21, no. 6, pp. 1058–1072, 2017.

[57] C. Song, J. F. Guo, Y. Liu, and B. S. Tang, "Autophagy and its comprehensive impact on ALS," *The International Journal of Neuroscience*, vol. 122, no. 12, pp. 695–703, 2012.

[58] V. Ringel-Scaia, D. McDaniel, and I. Allen, "The goldilocks conundrum: NLR Inflammasome modulation of gastrointestinal inflammation during inflammatory bowel disease," *Critical Reviews in Immunology*, vol. 36, no. 4, pp. 283–314, 2016.

[59] W. He, H. Wan, L. Hu et al., "Gasdermin D is an executor of pyroptosis and required for interleukin-1β secretion," *Cell Research*, vol. 25, no. 12, pp. 1285–1298, 2015.

[60] I. Jorgensen and E. Miao, "Pyroptotic cell death defends against intracellular pathogens," *Immunological Reviews*, vol. 265, no. 1, pp. 130–142, 2015.

[61] J. Ruan, "Structural insight of gasdermin family driving pyroptotic cell death," *Advances in Experimental Medicine and Biology*, vol. 1172, pp. 189–205, 2019.

[62] X. Qiu, Y. Zhang, and J. Han, "RIP3 is an upregulator of aerobic metabolism and the enhanced respiration by necrosomal RIP3 feeds back on necrosome to promote necroptosis," *Cell Death and Differentiation*, vol. 25, no. 5, pp. 821–824, 2018.

[63] J. Yuan, P. Amin, and D. Ofengeim, "Necroptosis and RIPK1-mediated neuroinflammation in CNS diseases," *Nature Reviews. Neuroscience*, vol. 20, no. 1, pp. 19–33, 2019.

[64] B. Levine and G. Kroemer, "Biological functions of autophagy genes: a disease perspective," *Cell*, vol. 176, no. 1-2, pp. 11–42, 2019.

[65] S. Liu, C. Sarkar, M. Dinizo et al., "Disrupted autophagy after spinal cord injury is associated with ER stress and neuronal cell death," *Cell Death & Disease*, vol. 6, no. 1, 2015.

[66] S. Saraswat Ohri, A. N. Bankston, S. A. Mullins et al., "Blocking autophagy in oligodendrocytes limits functional recovery after spinal cord injury," *The Journal of Neuroscience : The Official Journal of the Society for Neuroscience*, vol. 38, no. 26, pp. 5900–5912, 2018.

[67] Z. Shi, S. Yuan, L. Shi et al., "Programmed cell death in spinal cord injury pathogenesis and therapy," *Cell Proliferation*, vol. 54, no. 3, article e12992, 2021.

[68] C. Wu, H. Chen, R. Zhuang et al., "Betulinic acid inhibits pyroptosis in spinal cord injury by augmenting autophagy via the AMPK-mTOR-TFEB signaling pathway," *International Journal of Biological Sciences*, vol. 17, no. 4, pp. 1138–1152, 2021.

[69] R. Liu, Z. Peng, Y. Zhang, R. Li, and Y. Wang, "Upregulation of miR-128 inhibits neuronal cell apoptosis following spinal cord injury via FasL downregulation by repressing ULK1," *Molecular Medicine Reports*, vol. 24, no. 3, 2021.

[70] K. Zhou, Z. Zheng, Y. Li et al., "TFE3, a potential therapeutic target for spinal cord injury via augmenting autophagy flux and alleviating ER stress," *Theranostics*, vol. 10, no. 20, pp. 9280–9302, 2020.

[71] J. Martina, H. I. Diab, L. Lishu et al., "The nutrient-responsive transcription factor TFE3 promotes autophagy, lysosomal biogenesis, and clearance of cellular debris," *Science Signaling*, vol. 7, no. 309, p. ra9, 2014.

[72] N. Raben and R. Puertollano, "TFEB and TFE3: linking lysosomes to cellular adaptation to stress," *Annual Review of Cell and Developmental Biology*, vol. 32, pp. 255–278, 2016.

[73] Y. Kim and K. Guan, "mTOR: a pharmacologic target for autophagy regulation," *The Journal of Clinical Investigation*, vol. 125, no. 1, pp. 25–32, 2015.

[74] H. Pi, M. Li, L. Zou et al., "AKT inhibition-mediated dephosphorylation of TFE3 promotes overactive autophagy independent of MTORC1 in cadmium-exposed bone mesenchymal stem cells," *Autophagy*, vol. 15, no. 4, pp. 565–582, 2019.

[75] H. Kim, G. H. Lee, K. R. Bhattarai et al., "TMBIM6 (transmembrane BAX inhibitor motif containing 6) enhances autophagy through regulation of lysosomal calcium," *Autophagy*, vol. 17, no. 3, pp. 761–778, 2021.

[76] C. Yang, Z. Zhu, B. C. K. Tong et al., "A stress response p38 MAP kinase inhibitor SB202190 promoted TFEB/TFE3-dependent autophagy and lysosomal biogenesis independent of p38," *Redox Biology*, vol. 32, p. 101445, 2020.

[77] J. Martina, H. I. Diab, O. A. Brady, and R. Puertollano, "TFEB and TFE3 are novel components of the integrated stress response," *The EMBO Journal*, vol. 35, no. 5, pp. 479–495, 2016.

[78] L. Katsimpardi, N. K. Litterman, P. A. Schein et al., "Vascular and neurogenic rejuvenation of the aging mouse brain by young systemic factors," *Science*, vol. 344, no. 6184, pp. 630–634, 2014.

[79] X. Wang and P. Ge, "Parthanatos in the pathogenesis of nervous system diseases," *Neuroscience*, vol. 449, pp. 241–250, 2020.

Hindawi
Oxidative Medicine and Cellular Longevity
Volume 2021, Article ID 6114132, 8 pages
https://doi.org/10.1155/2021/6114132

Review Article

Contribution of Oxidative Stress to HIF-1-Mediated Profibrotic Changes during the Kidney Damage

Hong Zhang, Renfeng Xu, and Zhengchao Wang

Provincial Key Laboratory for Developmental Biology and Neurosciences, Key Laboratory of Optoelectronic Science and Technology for Medicine of Ministry of Education, College of Life Sciences, Fujian Normal University, Fuzhou 350007, China

Correspondence should be addressed to Zhengchao Wang; zcwang@fjnu.edu.cn

Received 25 August 2021; Accepted 9 October 2021; Published 19 October 2021

Academic Editor: Xu Ke

Hypoxia and oxidative stress are the common causes of various types of kidney injury. During recent years, the studies on hypoxia inducible factor- (HIF-) 1 attract more and more attention, which can not only mediate hypoxia adaptation but also contribute to profibrotic changes. Through analyzing related literatures, we found that oxidative stress can regulate the expression and activity of HIF-1α through some signaling molecules, such as prolyl hydroxylase domain-containing protein (PHD), PI-3K, and microRNA. And oxidative stress can take part in inflammation, epithelial-mesenchymal transition, and extracellular matrix deposition mediated by HIF-1 via interacting with classical NF-κB and TGF-β signaling pathways. Therefore, based on previous literatures, this review summarizes the contribution of oxidative stress to HIF-1-mediated profibrotic changes during the kidney damage, in order to further understand the role of oxidative stress in renal fibrosis.

1. Introduction

The balance of oxygen consumption and supply is essential for all mammalian organs, providing fuel for various physiological metabolic processes and maintaining homeostasis [1]. Kidney, an active metabolic organ, is a great need for oxygen. Thus, there is no doubt that the kidney is also susceptible to hypoxic damage.

There are increasing evidences shown that a variety of pathological factors such as hyperglycemia, hypersaline, hypertension, and infection can induce renal hypoxia and aggravate oxidative stress [2]. Meanwhile, it is demonstrated that acute kidney injury (AKI) and various chronic renal diseases (CKD) are associated with hypoxia and oxidative stress, which are more likely to develop into renal fibrosis eventually [3, 4]. Therefore, we have reasons to believe that hypoxia and oxidative stress may play an important role in the destruction of renal tissue, irreversible loss of kidney function, and the progression of renal fibrosis [5, 6].

Hypoxia inducible factors (HIFs), critical nuclear transcription factors, involved in maintaining O_2 homeostasis were firstly discovered by Semenza in 1992, which have received extensive attention due to their significant role in cellular adaptation to hypoxia in recent years [7, 8]. Based on the difference of α-subunits, HIFs are divided into three subtypes, HIF-1, HIF-2, and HIF-3. The function of HIF-1 and HIF-2 is currently being intensively investigated. An increasing evidence finds that HIF-1 during kidney damage not only mediates hypoxia adaptation but also is associated with inflammation, epithelial-mesenchymal transition (EMT), and extracellular matrix (ECM) deposition, participating in the profibrotic changes [9–12]. And oxidative stress has been also reported to play an important role in this process [2]. HIF-2α plays a dominant role in erythropoietin production [13–15]. Schietke et al. also found that constitutional transgenic overexpression of HIF-2α in distal tubular cells in mice resulted in renal fibrosis [16]. Besides, a recent study has shown that SIRT1 can attenuate renal fibrosis by repressing HIF-2α. The effects of HIFs may be cell type and context dependent. HIF-2α may also be a candidate for studying renal fibrosis [17, 18]. However, HIF-3 is less well known. Other studies have shown that HIF-3α can act as a

target gene of HIF-1 and negatively regulate the activity of HIF-1 and HIF-2 [19].

The present review is aimed at summarizing the profibrotic role and molecular regulation of HIF-1α on kidney damage, illustrating the interaction between HIF-1α and oxidative stress, and providing new insights for renal injury and aberrant tissue repair.

2. The Progression of Renal Fibrosis

Renal fibrosis is the final outcome of various kidney injuries and diseases. Although the reasons for fibrogenesis are diverse in different kidney diseases, the pathological process is similar. Usually, renal fibrosis can be artificially divided into four overlapping stages named as priming, activation, execution, and progression, respectively, according to different characteristics. Priming, the earliest stage of fibrogenesis, inflammatory cells can infiltrate into the kidney and be activated to secrete a variety of factors, such as chemokines, cytokines, and reactive oxygen species because of tissue damage. And then, secreted cytokines stimulate cells to undergo transformation and transdifferentiation to a myofibroblast phenotype, which expresses α-smooth muscle actin and produces a large amount of ECM proteins during the activation phase. In the stage of execution, ECM are accumulated in the interstitials and modified to resist proteolytic enzyme. The last stage of fibrosis is progression, which involves several types of kidney injuries, such as renal tubular atrophy and capillary rarefaction [20–22]. It is worth noting that the pathological process is irreversible once fibrosis emerges. Thus, it is crucial to understand the mechanism of renal fibrosis clearly and prevent fibrogenesis timely at the early stage of renal disease.

3. Oxidative Stress

Under normal physiological conditions, the body can produce a small amount of reactive oxygen species (ROS) [23]. And free radical scavenging enzymes and antioxidants maintain the balance of oxygen metabolism through activating transcription factors, regulating physiological active substances and inflammatory immunity, and promoting cell proliferation and differentiation, which has extensive physiological significance. However, once the levels between ROS and reactive nitrogen species (RNS) and antioxidant defense system cannot keep balance, oxidative stress appears [24, 25].

ROS is the main member inducing oxidative stress *in vivo*, mainly including superoxide anion and hydrogen peroxide. In cells, a large number of ROS are generated by the mitochondrial electron transport chain and cytochrome P450 family, and xanthine oxidoreductase, reduced nicotinamide adenine dinucleotide phosphate oxidase (NOX), nitric oxide synthase, and other catalytic enzymes greatly affect the generation of ROS [26]. RNS is a class of nitric oxide- (NO-) centered derivatives produced by the reaction of NO with ROS, including NO, nitrogen oxygen anion, nitrosothiols, and peroxynitrite. Excessive ROS and RNS can react with intracellular lipids, nucleic acids, and proteins, leading to lipid peroxidation, DNA oxidative damage, and intracellular protein denaturation, causing damage to cellular structure and function [27]. And oxidants can also act as signaling molecules to change intracellular signaling pathways and even gene expression [28]. In addition, oxidative modification can promote abnormal cell growth, inflammation, and other physiological processes [29, 30].

4. Hypoxia Inducible Factor-1

HIF-1 is a basic heterodimeric helix-loop-helix transcription factor and consists of an adjustable oxygen-sensitive α-subunit, HIF-α, and a constitutively expressed β-subunit, HIF-β. Hypoxia is the main regulation factor of physiologic HIF-1 expression. Besides, it is important to notice that HIF-1α overactivation can also be stimulated by some other mechanisms [31, 32].

4.1. Regulation of HIF-1 Hydrolysis. Oxygen-induced hydroxylation is one of the most important regulated pathways for HIF-α. Under normoxia, oxygen-dependent proline degradation domains on HIF-α can be hydroxylated by PHD [33]. Hydroxylated HIF-α can combinate with ubiquitin and be degraded by proteasome following the activation of von Hippel-Lindau tumor suppressor protein (pVHL), with the latter acting as a ubiquitin ligase to promote proteolysis of HIF-α. Factor inhibiting HIF (FIH) can also inhibit the transcriptional activity of HIF-α by hydroxylating asparaginic acid, while, under hypoxic conditions, the activity of PHD and FIH is suppressed, which further inhibits the hydroxylation and hydrolysis of HIF-α. Subsequently, the stabilized HIF-α dimerizes with HIF-β and translocates into the nucleus, activating a targeting gene [34].

4.2. HIF-1 Mediated Profibrotic Change. As a transcription factor, HIF-1 activation can regulate the expression of erythropoietin, vascular endothelial growth factor, endothelin-1, glucose transporters, and some other target genes, affecting erythropoiesis, angiogenesis, and energy metabolism, during which it governs the initial adaptation process to hypoxia, improves tissue oxygenation and cell survival, and to some extent offsets some harmful effects [9–11]. Although HIF-1 can reduce hypoxic-related damage under short-term hypoxia, increasing findings have suggested that HIF-1 can also play a significant role in the initiation and progression of kidney disease [12, 35–37]. Wang et al. demonstrated that chronic ischemia-induced overactivation of HIF-1α in the kidney mediates chronic renal damage [32]. Kimura et al. performed 5/6 nephrectomy on normal and VHL-knockout mice, finding that HIF-1 expression was stable and interstitial fibrosis was significantly severe in tubular epithelial cells of VHL-deleted mice [38]. And Baumann et al. found that knockout of the podocyte HIF-1α gene can prevent glomerular type I collagen accumulation and glomerulosclerosis [35]. Thus, HIF seems to promote the formation and development of fibrosis during kidney damage. Generally, renal fibrosis is characterized by inflammation, myofibroblast transformation, and extracellular matrix deposition [20, 21, 22]. Many researches have also demonstrated that HIF-1 may promote extracellular matrix remodeling to mediate renal fibrosis by

inducing inflammation, EMT, collagen deposition, and ECM stiffening [39–41].

5. Contribution of Oxidative Stress to HIF-1-Mediated Profibrotic Changes

It has been described that during hypoxia, mitochondria increased the production of ROS, leading to inhibition of PHD activity and subsequent stabilization of HIF-1α protein [41]. Wang et al. have also demonstrated that ANG II stimulated H_2O_2 production, which inhibited PHD activity and thereby upregulated HIF-1α levels and consequently activated the tissue inhibitor of metalloproteinase, resulting in collagen I/III accumulation in cultured renal medullary interstitial cells [31]. PHD2 is the main subtype of renal PHD, mainly expressed in renal medulla. High salt intake initially increased renal tubular activity and decreased renal medullary oxygen level, thereby inhibiting PHD2 activity and activating HIF-1α-mediated adaptive genes. Proteins encoded by these genes produced medullary protective factors including NO, which in turn inhibited PHD2 [42]. Additional studies have suggested the involvement of PI-3K and ERK in NO-mediated HIF-1α accumulation [43, 44]. Others have also reported an increase in transcription of HIF-1α under hypoxia by ROS through induction of PI-3K/AKT and ERK phosphorylation [45, 46]. Oxidative factors can regulate the expression and activity of HIF-1 via PHD, ERK, and PI-3K/AKT.

While there is impaired PHD2 response to high salt in Dahl rats, increased oxidant stress might be one of the mechanisms. It is possible that high salt-induced oxidative stress induces PHD2 and thereby reduces HIF-1α levels in the renal medulla in Dahl S rats. Because of superoxide anion, it has been demonstrated to stimulate PHDs and thereby inhibit HIF-1α [47, 48]. Therefore, details of oxidative stress and PHD activity need to be clarified in future investigations. The relationship of oxidative stress and HIF-1 might be complex than our imagination. For example, it may be different in diverse animal models or distinct periods of diseases.

5.1. OS/NF-κB/HIF-1 Signaling. Normally, inflammatory response is a process that the body resists to pathogen infection, which is controllable. However, if inflammatory response lasts a long time, it will cause damage and diseases to the body [49]. It is accepted that hypoxia is a common feature and an important cause of most inflammation. Studies have found that most kidney damage started with inflammation [50]. The nuclear factor-kappa B (NF-κB) pathway is necessary for the expression of various proinflammatory factors under hypoxia, including TNF-α, IL-8, and IL-1β [51].

The study conducted by Jin and his colleagues has demonstrated that the oxidative stress/NF-κB signal pathway contributed to the formation of unilateral ureteral obstruction renal interstitial fibrosis [52]. Under hypoxic environment, excessive ROS can activate the NF/κB signaling pathway and then promote the expression of HIF-1α [53]. HIF-1α and NF-κB signaling is highly dependent. Hypoxia and/or inflammation lead to increased NF-κB and CCAAT/enhancer-binding protein delta (CEBPD) activity. CEBPD subsequently binds to the HIF-1α promoter and regulates HIF-1α signaling, thereby promoting inflammatory cell infiltration and inflammatory cytokine secretion in the renal tubulointerstitial region [54]. Zhao et al. showed that HIF-1α was upregulated in the kidneys of wild-type aristolochic acid nephropathy mice, accompanied by proximal tubular cell G2/M arrest and renal fibrosis [36]. Greijer and van der Wall have suggested that HIF-1 may inhibit the expression of cyclin-dependent kinase 1 and cyclins B1 and D1, leading to cell cycle G2/M arrest and promoting apoptosis in renal tubules [55]. Apoptosis induced by HIF-1 can release inflammatory mediators such as IL-1β and TNF-α, altering local renal microenvironment to trigger inflammation and fibrosis [56–58]. What is more, it has been shown that inflammatory cytokines can upregulate HIF-1α by MAPKp38 and via PI-3K/AKT phosphorylation [59].

Nevertheless, HIF can also inhibit renal inflammation by regulating Bcl-2 family genes, interacting with p53 or targeting mitochondrial enzymes to reduce tubular cell death [60, 61]. It can be seen that due to the complexity of the occurrence and development of inflammation, HIF-1α may play different roles in different stages of its development, which needs further study.

5.2. OS/HIF-1α /TGF-β Signaling. The activation of the NF/kB signaling pathway also plays an important role in the process of EMT and renal interstitial fibrosis in renal tubules [62]. EMT and ECM deposition are the key during renal aberrant trauma repair, which leads to fibrosis [63, 64]. During the process of EMT, proteins, such as e-cadherin, normally expressed by epithelial cells are lost and cell transdifferentiation markers, such as α-smooth muscle actin and fibroblast-specific protein 1, are obtained. An interesting finding shows that HIF-1α inhibited by short hairpin RNA can block the increasing expression of α-smooth muscle actin (SMA) in rats with a clipped kidney [32]. Higgins et al. found that activation of HIF-1 signaling in renal epithelial cells was associated with the development of chronic renal disease [64]. Experimental studies have shown that HIF-1 can activate various transcriptional regulators to promote mesenchymal transition by upregulating lysyl oxidase-like 2, B lymphoma Mo-MLV insertion region homolog1 (Bmi1), and Twist [12, 65, 66]. It has been demonstrated that HIF-1α stimulated collagen accumulation by activation of fibrogenic factors, such as connective tissue growth factor, plasminogen activator inhibitor, tissue inhibitor of metalloproteinase, and collagen proline and lysine hydroxylase [35, 67–69].

Transforming growth factor- (TGF-) β is considered to be the prototypical cytokine in renal fibrosis, which not only regulates the transformation of epithelial-mesenchymal cells to form myofibroblasts but also regulates the production and degradation of ECM [70, 71]. Zhou et al. indicate that ROS and HIF participate in hypoxia-induced TGF-β production [72]. HIF-1 accumulation can significantly enhance TGF-β expression [73–75]. TGF-β can upregulate gene expression of Nox4 NADPH oxidase or directly activate NADPH oxidase to generate ROS, which was reported to stabilize HIF-1α by decreasing PHD2 to reduce HIF-1α prolyl

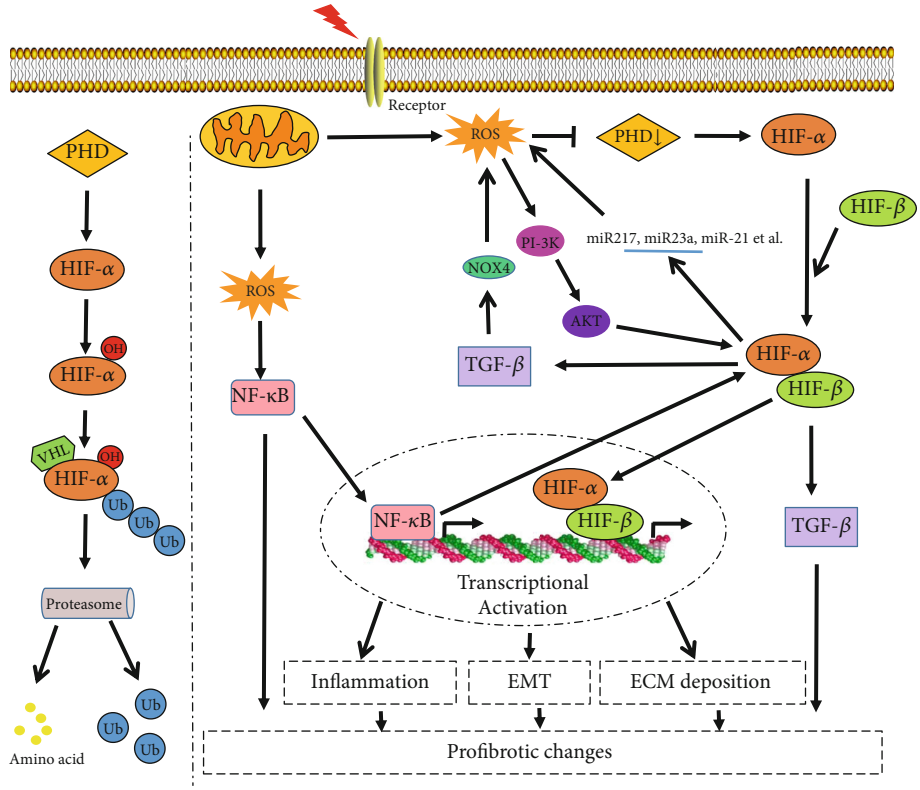

Figure 1: Contribution of oxidative stress to HIF-1-mediated profibrotic changes during the kidney damage. (1) Under normoxia, HIF-α can be hydroxylated by PHD. Hydroxylated HIF-α can combinate with ubiquitin and be degraded following the activation of VHL, (2) while, under stress conditions such as hypoxia or inflammation, the increased ROS can suppress the activity of PHD, which further inhibits the hydroxylation and hydrolysis of HIF-α. (3) Meanwhile, excessive ROS can activate NF/κB signaling and then promote the expression of HIF-α. (4) Stabilized HIF-α dimerizes with HIF-β and translocates into the nucleus, activating a targeting gene. HIF-1 can promote apoptosis and lead to the release of inflammatory mediators such as IL-1β and TNF-α, triggering inflammation, while inflammation can aggravate hypoxia and oxidative stress further. Besides, HIF-1 may promote EMT and ECM deposition to mediate profibrotic changes by activating various transcriptional regulators and fibrogenic factors. (5) HIF-1 accumulation can also significantly enhance TGF-β expression. TGF-β can upregulate gene expression of Nox4 NADPH oxidase or directly activate NADPH oxidase to generate ROS, which may form a vicious cycle to lead to renal fibrosis. (6) In addition, HIF-1 can also regulate the expression of various microRNAs such as miR217, miR23a, and miR-21, then affecting the generation of ROS and promoting the development of fibrosis via activating PI-3K signaling.

hydroxylation [76]. Das et al. found that the expression of NOX4 caused by TGF-β activation can be reduced by blocking Smad2 or Smad3, which suggested that TGF-β/Smad2/3 upregulated NOX4 and induced ROS generation, such as H_2O_2, which played an important role in the progression of renal fibrosis [76–78]. In TGF-β-treated renal tubular epithelial and mesangial cells, mammalian target of rapamycin complex-1 and Smad3 can also interact to increase the expression of HIF-1 and collagen [79]. Thus, TGF-β and ROS/HIF may form a feedback loop to maintain a prolonged signaling cascade initiated by either ROS/HIF or TGF-β.

5.3. miRNA/OS/HIF Signaling. The researches focused on the role of microRNA and HIF-1 during renal disease have also become more and more popular in recent years. MicroRNAs (miRNAs), small noncoding RNA molecules, can combine with 3′ untranslated regions of their target messenger RNA to inhibit their translation and thus regulate gene expression. A large number of studies show that miRNAs, such as miR217, miR23a, and miR-155, are closely related to the occurrence and development of renal fibrosis [80–84]. Recent studies have found that microRNA can regulate the expression or activity of HIF-1 by interfering with ROS production.

Increased miR-217 promotes inflammation and fibrosis in rats' glomerular mesangial cells cultured with high glucose through upregulating ROS, activating HIF-1 signaling pathway, and mediating cell apoptosis [80, 81]. miR-23a regulates cardiomyocyte apoptosis by suppressing the expression of MnSOD [82]. Li et al. also suggested that HIF-1 can induce exosome miR-23a expression, mediating the interaction between tubule epithelial cells and macrophages in tubule interstitial inflammation [83]. Xie et al. demonstrated that HIF-1α can increase the level of miR-155, thus promoting ETM and fibrosis both *in vivo* and *in vitro* [84], while miR-155-5p inhibitor treatment significantly decreased ROS generation and H_2O_2 concentration in HK-2 cells incubated with oxalate [85]. Therefore, we speculate that miR-155-5p mediated EMT by upregulating ROS, thereby activating HIF-1 signaling, which may form a vicious cycle.

In addition, miR-21 in extracellular vesicles may induce EMT through enhancing HIF-1α expression, and caloric restriction alleviates aging-related fibrosis of the kidney through downregulation of miR-21 [86]. It has also been shown that miR-21 is induced by H_2O_2 in vascular smooth muscles [87]. miR-21 silencing enhanced mitochondrial function, which reduced mitochondrial ROS production and thus preserved tubular functions. It is possible that the interplay between miR-21 and ROS may lead to the activation of AKT and ERK pathways and contribute to miR-21 regulation of HIF-1α [88].

6. Conclusion

With the aging of the social population, more and more patients now suffer from diabetes, hypertension, chronic kidney disease, and fibrosis, especially in developed countries [89–91]. Hypoxia and oxidative stress play an indispensable role in the occurrence and development of renal damage induced by these factors [92]. ROS accumulation during hypoxia promotes inflammation through activating NF-κB and mediating crosstalk with HIF-1 signaling. Besides, ROS can stabilize HIF, inducing TGF-β gene expression. Elevated TGF-β levels sustain the ROS production, maintaining prolonged ROS/HIF/TGF-β signaling. The possible interaction between microRNA and HIF-1 may provide a sight for revealing the profibrotic changes of HIF-1. The crosstalk of HIF-1 with other classical intracellular fibrogenic signaling pathways may be necessary to amplify fibrotic pathological response (Figure 1).

However, the results on studying the role of HIF-1 in renal fibrosis seem to be much more complex. Kapitsinou et al. found that the stable expression of HIF can inhibit cell apoptosis and inflammatory response and significantly reduce AKI-related renal fibrosis [93]. In addition, HIF-1 has been found to contribute to the activation of forkhead box O3, leading to increased autophagy and reduced oxidative damage, thus playing a role in renal protection [94]. Inconsistent results may be caused due to diverse experimental conditions, nature and duration of animal models, and methods of manipulating HIF activity. It is worth noting that these harmful or protective mediators are not always easily distinguished. The overall effect depends on the intensity and duration of their expression.

Data Availability

The original contributions presented in the study are included in the article. Further inquiries can be directed to the corresponding author.

Conflicts of Interest

The authors declare that they have no competing interests.

Authors' Contributions

The work was conceived by HZ, RX, and ZW, the draft was written by HZ and RX, and the manuscript was revised by ZW. All authors reviewed and approved the final version of the manuscript for publication.

Acknowledgments

This work was supported by the Key Projects of Scientific and Technological Innovation in Fujian Province (2021G02021 and 2021G02023), Special Funds of the Central Government Guiding Local Science and Technology Development (2020L3008), and Fujian Provincial Natural Science Foundation (2020J01176 and 2021J02028).

References

[1] N. R. Prabhakar and G. L. Semenza, "Oxygen sensing and homeostasis," *Physiology (Bethesda)*, vol. 30, no. 5, pp. 340–348, 2015.

[2] T. Honda, Y. Hirakawa, and M. Nangaku, "The role of oxidative stress and hypoxia in renal disease," *Kidney Research and Clinical Practice*, vol. 38, no. 4, pp. 414–426, 2019.

[3] W. M. Bernhardt, V. Câmpean, S. Kany et al., "Preconditional activation of hypoxia-inducible factors ameliorates ischemic acute renal failure," *Journal of the American Society of Nephrology*, vol. 17, no. 7, pp. 1970–1978, 2006.

[4] Z. L. Li and B. C. Liu, "Hypoxia and renal tubulointerstitial fibrosis," *Advances in Experimental Medicine and Biology*, vol. 1165, pp. 467–485, 2019.

[5] K. Richter and T. Kietzmann, "Reactive oxygen species and fibrosis: further evidence of a significant liaison," *Cell and Tissue Research*, vol. 365, no. 3, pp. 591–605, 2016.

[6] I. A. Darby and T. D. Hewitson, "Hypoxia in tissue repair and fibrosis," *Cell and Tissue Research*, vol. 365, no. 3, pp. 553–562, 2016.

[7] G. L. Semenza, "Hydroxylation of HIF-1: oxygen sensing at the molecular level,," *Physiology (Bethesda)*, vol. 19, pp. 176–182, 2004.

[8] H. Choudhry and A. L. Harris, "Advances in hypoxia-inducible factor biology," *Cell Metabolism*, vol. 27, no. 2, pp. 281–298, 2018.

[9] E. Moore and R. Bellomo, "Erythropoietin (EPO) in acute kidney injury," *Annals of Intensive Care*, vol. 1, no. 1, p. 3, 2011.

[10] A. Agarwal and H. S. Nick, "Renal response to tissue Injury," *Journal of the American Society of Nephrology*, vol. 11, no. 5, pp. 965–973, 2000.

[11] C. Warnecke, Z. Zaborowska, J. Kurreck et al., "Differentiating the functional role of hypoxia-inducible factor (HIF)-1alpha and HIF-2alpha (EPAS-1) by the use of RNA interference: erythropoietin is a HIF-2alpha target gene in Hep3B and Kelly cells," *FASEB Journal*, vol. 18, no. 12, pp. 1462–1464, 2004.

[12] R. Schietke, C. Warnecke, I. Wacker et al., "The Lysyl Oxidases LOX and LOXL2 Are Necessary and Sufficient to Repress E-cadherin in Hypoxia:," *Journal of Biological Chemistry*, vol. 285, no. 9, pp. 6658–6669, 2010.

[13] R. Hafizi, F. Imeri, R. H. Wenger, and A. Huwiler, "S1P stimulates erythropoietin production in mouse renal interstitial fibroblasts by S1P1 and S1P3 receptor activation and HIF-2alpha stabilization," *International Journal of Molecular Sciences*, vol. 22, no. 17, p. 9467, 2021.

[14] S. Zhu, L. Wu, J. Zhang et al., "Collagen hydrolysate corrects anemia in chronic kidney disease via anti-inflammatory renoprotection and HIF-2α-Dependent erythropoietin and

hepcidin regulation," *Journal of Agricultural and Food Chemistry*, vol. 68, no. 42, pp. 11726–11734, 2020.

[15] D. F. Higgins, K. Kimura, M. Iwano, and V. H. Haase, "Hypoxia-inducible factor signaling in the development of tissue fibrosis," *Cell Cycle*, vol. 7, no. 9, pp. 1128–1132, 2008.

[16] R. E. Schietke, T. Hackenbeck, M. Tran et al., "Renal tubular HIF-2α expression requires VHL inactivation and causes fibrosis and cysts," *PLoS One*, vol. 7, no. 1, p. e31034, 2012.

[17] P. Li, Y. Liu, X. Qin et al., "SIRT1 attenuates renal fibrosis by repressing HIF-2α," *Cell Death Discovery*, vol. 7, no. 1, p. 59, 2021.

[18] S. Y. Pan, P. Z. Tsai, Y. H. Chou et al., "Kidney pericyte hypoxia-inducible factor regulates erythropoiesis but not kidney fibrosis," *Kidney International*, vol. 99, no. 6, pp. 1354–1368, 2021.

[19] T. Tanaka, M. Wiesener, W. Bernhardt, K. U. Eckardt, and C. Warnecke, "The human HIF (hypoxia-inducible factor)-3α gene is a HIF-1 target gene and may modulate hypoxic gene induction," *Biochemical Journal*, vol. 424, no. 1, pp. 143–151, 2009.

[20] J. P. Thiery, H. Acloque, R. Y. Huang, and M. A. Nieto, "Epithelial-mesenchymal transitions in development and disease," *Cell*, vol. 139, no. 5, pp. 871–890, 2009.

[21] Y. Liu, "Cellular and molecular mechanisms of renal fibrosis," *Nature Reviews Nephrology*, vol. 7, no. 12, pp. 684–696, 2011.

[22] S. G. Mansour, J. Puthumana, S. G. Coca, M. Gentry, and C. R. Parikh, "Biomarkers for the detection of renal fibrosis and prediction of renal outcomes: a systematic review," *BMC Nephrology*, vol. 18, no. 1, p. 72, 2017.

[23] J. Pi, Q. Zhang, J. Fu et al., "ROS signaling, oxidative stress and Nrf2 in pancreatic beta-cell function," *Toxicology and Applied Pharmacology*, vol. 244, no. 1, pp. 77–83, 2010.

[24] N. S. Chandel, D. S. McClintock, C. E. Feliciano et al., "Reactive Oxygen Species Generated at Mitochondrial Complex III Stabilize Hypoxia-inducible Factor-1α during Hypoxia:," *Journal of Biological Chemistry*, vol. 275, no. 33, pp. 25130–25138, 2000.

[25] H. Zhang, H. M. Zhang, L. P. Wu et al., "Impaired mitochondrial complex III and melatonin responsive reactive oxygen species generation in kidney mitochondria of db/db mice," *Journal of Pineal Research*, vol. 51, no. 3, pp. 338–344, 2011.

[26] M. Sedeek, R. Nasrallah, R. M. Touyz, and R. L. Hebert, "NADPH oxidases, reactive oxygen species, and the kidney: friend and foe," *Journal of the American Society of Nephrology*, vol. 24, no. 10, pp. 1512–1518, 2013.

[27] J. Martinez-Useros, W. Li, M. Cabeza-Morales, and J. Garcia-Foncillas, "Oxidative stress: a new target for pancreatic cancer prognosis and treatment," *Journal of Clinical Medicine*, vol. 6, no. 3, p. 29, 2017.

[28] H. Ha, M. R. Yu, Y. J. Choi, M. Kitamura, and H. B. Lee, "Role of high glucose-induced nuclear factor-kappaB activation in monocyte chemoattractant protein-1 expression by mesangial cells," *Journal of the American Society of Nephrology*, vol. 13, no. 4, pp. 894–902, 2002.

[29] P. D. Ray, B. W. Huang, and Y. Tsuji, "Reactive oxygen species (ROS) homeostasis and redox regulation in cellular signaling," *Cellular Signalling*, vol. 24, no. 5, pp. 981–990, 2012.

[30] J. L. Barnes and Y. Gorin, "Myofibroblast differentiation during fibrosis: role of NAD(P)H oxidases," *Kidney International*, vol. 79, no. 9, pp. 944–956, 2011.

[31] Z. Wang, L. Tang, Q. Zhu et al., "Hypoxia-inducible factor-1α contributes to the profibrotic action of angiotensin II in renal medullary interstitial cells," *Kidney International*, vol. 79, no. 3, pp. 300–310, 2011.

[32] Z. Wang, Q. Zhu, P. Li et al., "Silencing of hypoxia-inducible factor-1α gene attenuates chronic ischemic renal injury in two-kidney, one-clip rats," *American Journal of Physiology - Renal Physiology*, vol. 306, no. 10, pp. F1236–F1242, 2014.

[33] G. H. Fong and K. Takeda, "Role and regulation of prolyl hydroxylase domain proteins," *Cell Death and Differentiation*, vol. 15, no. 4, pp. 635–641, 2008.

[34] A. J. Majmundar, W. J. Wong, and M. C. Simon, "Hypoxia-inducible factors and the response to hypoxic stress," *Molecular Cell*, vol. 40, no. 2, pp. 294–309, 2010.

[35] B. Baumann, T. Hayashida, X. Liang, and H. W. Schnaper, "Hypoxia-inducible factor-1α promotes glomerulosclerosis and regulates _COL1A2_ expression through interactions with Smad3," *Kidney International*, vol. 90, no. 4, pp. 797–808, 2016.

[36] H. Zhao, N. Jiang, Y. Han et al., "Aristolochic acid induces renal fibrosis by arresting proximal tubular cells in G2/M phase mediated by HIF-1α," *FASEB Journal*, vol. 34, no. 9, pp. 12599–12614, 2020.

[37] M. Nangaku, C. Rosenberger, S. N. Heyman, and K. U. Eckardt, "Regulation of hypoxia-inducible factor in kidney disease," *Clinical and Experimental Pharmacology and Physiology*, vol. 40, no. 2, pp. 148–157, 2013.

[38] K. Kimura, M. Iwano, D. F. Higgins et al., "Stable expression of HIF-1alpha in tubular epithelial cells promotes interstitial fibrosis," *American Journal of Physiology - Renal Physiology*, vol. 295, no. 4, pp. F1023–F1029, 2008.

[39] S. Shu, Y. Wang, M. Zheng et al., "Hypoxia and hypoxia-inducible factors in kidney injury and repair," *Cell*, vol. 8, no. 3, p. 207, 2019.

[40] M. Liu, X. Ning, R. Li et al., "Signalling pathways involved in hypoxia-induced renal fibrosis," *Journal of Cellular and Molecular Medicine*, vol. 21, no. 7, pp. 1248–1259, 2017.

[41] K. Louis and A. Hertig, "How tubular epithelial cells dictate the rate of renal fibrogenesis?," *World Journal of Nephrology*, vol. 4, no. 3, pp. 367–373, 2015.

[42] Z. Wang, Q. Zhu, M. Xia, P. L. Li, S. J. Hinton, and N. Li, "Hypoxia-inducible factor prolyl-hydroxylase 2 senses high-salt intake to increase hypoxia inducible factor 1alpha levels in the renal medulla," *Hypertension*, vol. 55, no. 5, pp. 1129–1136, 2010.

[43] K. B. Sandau, H. G. Faus, and B. Brüne, "Induction of hypoxia-inducible-factor 1 by nitric oxide is mediated via the PI 3K pathway," *Biochemical and Biophysical Research Communications*, vol. 278, no. 1, pp. 263–267, 2000.

[44] K. Kasuno, S. Takabuchi, K. Fukuda et al., "Nitric Oxide Induces Hypoxia-inducible Factor 1 Activation That Is Dependent on MAPK and Phosphatidylinositol 3-Kinase Signaling," *Journal of Biological Chemistry*, vol. 279, no. 4, pp. 2550–2558, 2004.

[45] N. Koshikawa, J. Hayashi, A. Nakagawara, and K. Takenaga, "Reactive Oxygen Species-generating Mitochondrial DNA Mutation Up-regulates Hypoxia-inducible Factor-1α Gene Transcription via Phosphatidylinositol 3-Kinase-Akt/Protein Kinase C/Histone Deacetylase Pathway," *Journal of Biological Chemistry*, vol. 284, no. 48, pp. 33185–33194, 2009.

[46] J. du, R. Xu, Z. Hu et al., "PI3K and ERK-induced Rac1 activation mediates hypoxia-induced HIF-1α expression in MCF-7 breast cancer cells," *PLoS One*, vol. 6, no. 9, p. e25213, 2011.

[47] M. Callapina, J. Zhou, T. Schmid, R. Kohl, and B. Brune, "NO restores HIF-1α hydroxylation during hypoxia: Role of reactive oxygen species," *Free Radical Biology and Medicine*, vol. 39, no. 7, pp. 925–936, 2005.

[48] Y. EMORI, T. MIZUSHIMA, N. MATSUMURA et al., "Camostat, an oral trypsin inhibitor, reduces pancreatic fibrosis induced by repeated administration of a superoxide dismutase inhibitor in rats," *Journal of Gastroenterology and Hepatology*, vol. 20, no. 6, pp. 895–899, 2005.

[49] X. M. Meng, G. L. Ren, L. Gao et al., "NADPH oxidase 4 promotes cisplatin-induced acute kidney injury via ROS- mediated programmed cell death and inflammation," *Laboratory Investigation*, vol. 98, no. 1, pp. 63–78, 2018.

[50] O. M. Akchurin and F. Kaskel, "Update on inflammation in chronic kidney disease," *Blood Purification*, vol. 39, no. 1-3, pp. 84–92, 2015.

[51] X. Chen, X. Li, W. Zhang et al., "Activation of AMPK inhibits inflammatory response during hypoxia and reoxygenation through modulating JNK-mediated NF-κB pathway," *Metabolism - Clinical and Experimental*, vol. 83, pp. 256–270, 2018.

[52] H. Jin, Y. Wang, D. Wang, and L. Zhang, "Effects of Qingshen granules on the oxidative stress-NF/kB signal pathway in unilateral ureteral obstruction rats," *Evidence-based Complementary and Alternative Medicine*, vol. 2018, 2018.

[53] A. Quercioli, G. Luciano Viviani, F. Dallegri, F. Mach, and F. Montecucco, "Receptor activator of nuclear factor kappa B ligand/osteoprotegerin pathway is a promising target to reduce atherosclerotic plaque calcification," *Critical Pathways in Cardiology*, vol. 9, no. 4, pp. 227–230, 2010.

[54] J. Yamaguchi, T. Tanaka, N. Eto, and M. Nangaku, "Inflammation and hypoxia linked to renal injury by CCAAT/enhancer-binding protein δ," *Kidney International*, vol. 88, no. 2, pp. 262–275, 2015.

[55] A. E. Greijer and E. van der Wall, "The role of hypoxia inducible factor 1 (HIF-1) in hypoxia induced apoptosis," *Journal of Clinical Pathology*, vol. 57, no. 10, pp. 1009–1014, 2004.

[56] C. C. Scholz, M. A. S. Cavadas, M. M. Tambuwala et al., "Regulation of IL-1 -induced NF- B by hydroxylases links key hypoxic and inflammatory signaling pathways," *Proceedings of the National Academy of Sciences of the United States of America*, vol. 110, no. 46, pp. 18490–18495, 2013.

[57] L. Liu, P. Zhang, M. Bai et al., "p53 upregulated by HIF-1α promotes hypoxia-induced G2/M arrest and renal fibrosis in vitro and in vivo," *Journal of Molecular Cell Biology*, vol. 11, no. 5, pp. 371–382, 2019.

[58] A. Sendoel and M. O. Hengartner, "Apoptotic cell death under hypoxia," *Physiology (Bethesda)*, vol. 29, no. 3, pp. 168–176, 2014.

[59] J. WESTRA, E. BROUWER, R. BOS et al., "Regulation of cytokine-induced HIF-1 Expression in rheumatoid synovial fibroblasts," *Annals of the New York Academy of Sciences*, vol. 1108, no. 1, pp. 340–348, 2007.

[60] R. Provenzano, A. Besarab, C. H. Sun et al., "Oral hypoxia-inducible factor prolyl hydroxylase inhibitor roxadustat (FG-4592) for the treatment of anemia in patients with CKD," *Clinical Journal of the American Society of Nephrology*, vol. 11, no. 6, pp. 982–991, 2016.

[61] B. De Vries, R. A. Matthijsen, T. G. Wolfs, A. A. Van Bijnen, P. Heeringa, and W. A. Buurman, "Inhibition of complement factor C5 protects against renal ischemia-reperfusion injury: inhibition of late apoptosis and inflammation," *Transplantation*, vol. 75, no. 3, pp. 375–382, 2003.

[62] Z. Wang, Z. Chen, B. Li et al., "Curcumin attenuates renal interstitial fibrosis of obstructive nephropathy by suppressing epithelial-mesenchymal transition through inhibition of the TLR4/NF-κB and PI3K/AKT signalling pathways," *Pharmaceutical Biology*, vol. 58, no. 1, pp. 828–837, 2020.

[63] M. Mack and M. Yanagita, "Origin of myofibroblasts and cellular events triggering fibrosis," *Kidney International*, vol. 87, no. 2, pp. 297–307, 2015.

[64] D. F. Higgins, K. Kimura, W. M. Bernhardt et al., "Hypoxia promotes fibrogenesis in vivo via HIF-1 stimulation of epithelial-to-mesenchymal transition," *Journal of Clinical InvestigationJournal of Clinical Investigation*, vol. 117, no. 12, pp. 3810–3820, 2007.

[65] M. H. Yang and K. J. Wu, "TWIST activation by hypoxia inducible factor-1 (HIF-1): implications in metastasis and development," *Cell Cycle*, vol. 7, no. 14, pp. 2090–2096, 2008.

[66] S. Sun, X. Ning, Y. Zhang et al., "Hypoxia-inducible factor-1α induces Twist expression in tubular epithelial cells subjected to hypoxia, leading to epithelial-to-mesenchymal transition," *Kidney International*, vol. 75, no. 12, pp. 1278–1287, 2009.

[67] X. Li, H. Kimura, K. Hirota et al., "Synergistic effect of hypoxia and TNF-α on production of PAI-1 in human proximal renal tubular cells," *Kidney International*, vol. 68, no. 2, pp. 569–583, 2005.

[68] T. Tanaka, "Expanding roles of the hypoxia-response network in chronic kidney disease," *Clinical and Experimental Nephrology*, vol. 20, no. 6, pp. 835–844, 2016.

[69] J. T. Norman, I. M. Clark, and P. L. Garcia, "Hypoxia promotes fibrogenesis in human renal fibroblasts," *Kidney International*, vol. 58, no. 6, pp. 2351–2366, 2000.

[70] S. W. Chea and K. B. Lee, "TGF-beta mediated epithelial-mesenchymal transition in autosomal dominant polycystic kidney disease," *Yonsei Medical Journal*, vol. 50, no. 1, pp. 105–111, 2009.

[71] C. L. Belmiro, R. G. Gonçalves, E. O. Kozlowski et al., "Dermatan sulfate reduces monocyte chemoattractant protein 1 and TGF-β production, as well as macrophage recruitment and myofibroblast accumulation in mice with unilateral ureteral obstruction," *Brazilian Journal of Medical and Biological Research*, vol. 44, no. 7, pp. 624–633, 2011.

[72] G. Zhou, L. A. Dada, M. Wu et al., "Hypoxia-induced alveolar epithelial-mesenchymal transition requires mitochondrial ROS and hypoxia-inducible factor 1," *American Journal of Physiology - Lung Cellular and Molecular Physiology*, vol. 297, no. 6, pp. L1120–L1130, 2009.

[73] R. Kalluri and E. G. Neilson, "Epithelial-mesenchymal transition and its implications for fibrosis," *Journal of Clinical Investigation*, vol. 112, no. 12, pp. 1776–1784, 2003.

[74] C. Sahlgren, M. V. Gustafsson, S. Jin, L. Poellinger, and U. Lendahl, "Notch signaling mediates hypoxia-induced tumor cell migration and invasion," *Proceedings of the National Academy of Sciences of the United States of America*, vol. 105, no. 17, pp. 6392–6397, 2008.

[75] N. Kushida, S. Nomura, I. Mimura et al., "Hypoxia-inducible Factor-1α activates the transforming growth Factor-β/SMAD3 pathway in kidney tubular epithelial cells," *American Journal of Nephrology*, vol. 44, no. 4, pp. 276–285, 2016.

[76] R. Das, S. Xu, X. Quan et al., "Upregulation of mitochondrial Nox4 mediates TGF-β-induced apoptosis in cultured mouse podocytes," *American Journal of Physiology - Renal Physiology*, vol. 306, no. 2, pp. F155–F167, 2014.

[77] R. Das, S. Xu, T. T. Nguyen et al., "ERK1/2-mTORC1-Nox4 Axis in TGF-β1-induced Podocyte Apoptosis," *Journal of Biological Chemistry*, vol. 290, no. 52, pp. 30830–30842, 2015.

[78] H. E. Boudreau, B. W. Casterline, B. Rada, A. Korzeniowska, and T. L. Leto, "Nox4 involvement in TGF-beta and SMAD3-driven induction of the epithelial-to- mesenchymal transition and migration of breast epithelial cells," *Free Radical Biology and Medicine*, vol. 53, no. 7, pp. 1489–1499, 2012.

[79] B. Rozen-Zvi, T. Hayashida, S. C. Hubchak, C. Hanna, L. C. Platanias, and H. W. Schnaper, "TGF-β/Smad3 activates mammalian target of rapamycin complex-1 to promote collagen production by increasing HIF-1α expression," *American Journal of Physiology - Renal Physiology*, vol. 305, no. 4, pp. F485–F494, 2013.

[80] Y. Shao, C. Lv, C. Wu, Y. Zhou, and Q. Wang, "Mir-217 promotes inflammation and fibrosis in high glucose cultured rat glomerular mesangial cells via Sirt1/HIF-1α signaling pathway," *Diabetes/Metabolism Research and Reviews*, vol. 32, no. 6, pp. 534–543, 2016.

[81] J. Sun, Z. P. Li, R. Q. Zhang, and H. M. Zhang, "Repression of miR-217 protects against high glucose-induced podocyte injury and insulin resistance by restoring PTEN-mediated autophagy pathway," *Biochemical and Biophysical Research Communications*, vol. 483, no. 1, pp. 318–324, 2017.

[82] B. Long, T. Y. Gan, R. C. Zhang, and Y. H. Zhang, "miR-23a regulates cardiomyocyte apoptosis by targeting manganese superoxide dismutase," *Molecules and Cells*, vol. 40, no. 8, pp. 542–549, 2017.

[83] Z. L. Li, L. L. Lv, T. T. Tang et al., "HIF-1α inducing exosomal microRNA-23a expression mediates the cross-talk between tubular epithelial cells and macrophages in tubulointerstitial inflammation," *Kidney International*, vol. 95, no. 2, pp. 388–404, 2019.

[84] S. Xie, H. Chen, F. Li, S. Wang, and J. Guo, "Hypoxia-induced microRNA-155 promotes fibrosis in proximal tubule cells," *Molecular Medicine Reports*, vol. 11, no. 6, pp. 4555–4560, 2015.

[85] K. Jiang, J. Hu, G. Luo et al., "miR-155-5p promotes oxalate- and calcium-induced kidney oxidative stress injury by suppressing MGP expression," *Oxidative Medicine and Cellular Longevity*, vol. 2020, 2020.

[86] J. R. Liu, G. Y. Cai, Y. C. Ning et al., "Caloric restriction alleviates aging-related fibrosis of kidney through downregulation of miR-21 in extracellular vesicles," *Aging (Albany NY)*, vol. 12, no. 18, pp. 18052–18072, 2020.

[87] Y. Lin, X. Liu, Y. Cheng, J. Yang, Y. Huo, and C. Zhang, "Involvement of MicroRNAs in Hydrogen Peroxide-mediated Gene Regulation and Cellular Injury Response in Vascular Smooth Muscle Cells," *Journal of Biological Chemistry*, vol. 284, no. 12, pp. 7903–7913, 2009.

[88] I. G. Gomez, D. A. MacKenna, B. G. Johnson et al., "Anti-microRNA-21 oligonucleotides prevent Alport nephropathy progression by stimulating metabolic pathways," *Journal of Clinical Investigation*, vol. 125, no. 1, pp. 141–156, 2015.

[89] L. Zhang, F. Wang, L. Wang et al., "Prevalence of chronic kidney disease in China: a cross-sectional survey," *Lancet*, vol. 379, no. 9818, pp. 815–822, 2012.

[90] P. Romagnani, G. Remuzzi, R. Glassock et al., "Chronic kidney disease," *Nature Reviews. Disease Primers*, vol. 3, no. 1, p. 17088, 2017.

[91] S. G. Coca, S. Singanamala, and C. R. Parikh, "Chronic kidney disease after acute kidney injury: a systematic review and meta-analysis," *Kidney International*, vol. 81, no. 5, pp. 442–448, 2012.

[92] K. Shoji, T. Tanaka, and M. Nangaku, "Role of hypoxia in progressive chronic kidney disease and implications for therapy," *Current Opinion in Nephrology and Hypertension*, vol. 23, no. 2, pp. 161–168, 2014.

[93] P. P. Kapitsinou, J. Jaffe, M. Michael et al., "Preischemic targeting of HIF prolyl hydroxylation inhibits fibrosis associated with acute kidney injury," *American Journal of Physiology - Renal Physiology*, vol. 302, pp. F1172–F1179, 2012.

[94] L. Li, H. Kang, Q. Zhang, V. D. D'Agati, Q. Al-Awqati, and F. Lin, "FoxO3 activation in hypoxic tubules prevents chronic kidney disease," *Journal of Clinical Investigation*, vol. 129, no. 6, pp. 2374–2389, 2019.

Hindawi
Oxidative Medicine and Cellular Longevity
Volume 2021, Article ID 3846122, 5 pages
https://doi.org/10.1155/2021/3846122

Review Article

Effects of Exercise-Induced ROS on the Pathophysiological Functions of Skeletal Muscle

Fan Wang, Xin Wang, Yiping Liu, and Zhenghong Zhang

Provincial University Key Laboratory of Sport and Health Science, Provincial Key Laboratory for Developmental Biology and Neurosciences, Key Laboratory of Optoelectronic Science and Technology for Medicine of Ministry of Education, School of Physical Education and Sport Sciences, Fujian Normal University, Fuzhou 350007, China

Correspondence should be addressed to Yiping Liu; ypliu1966@fjnu.edu.cn and Zhenghong Zhang; zhangzh@fjnu.edu.cn

Received 16 August 2021; Accepted 18 September 2021; Published 1 October 2021

Academic Editor: Yanqing Wu

Oxidative stress is the imbalance of the redox system in the body, which produces excessive reactive oxygen species, leads to multiple cellular damages, and closely relates to some pathological conditions, such as insulin resistance and inflammation. Meanwhile, exercise as an external stimulus of oxidative stress causes the changes of pathophysiological functions in the tissues and organs, including skeletal muscle. Exercise-induced oxidative stress is considered to have different effects on the structure and function of skeletal muscle. Long-term regular or moderate exercise-induced oxidative stress is closely related to the formation of muscle adaptation, while excessive free radicals produced by strenuous or acute exercise can cause muscle oxidative stress fatigue and damage, which impacts exercise capacity and damages the body's health. The present review systematically summarizes the relationship between exercise-induced oxidative stress and the adaptions, damage, and fatigue in skeletal muscle, in order to clarify the effects of exercise-induced oxidative stress on the pathophysiological functions of skeletal muscle.

1. Introduction

Exercise as a common stressor leads to oxygen supply that cannot meet a rapid increase in oxygen demand of the body; then, many tissues and organs produce some highly active molecules, such as reactive nitrogen species (RNS) and reactive oxygen species (ROS). ROS plays a pivotal role in the stress process, including superoxide anion ($O_2^{\cdot-}$), hydroxyl radical ($OH^{\cdot}$), and hydrogen peroxide (H_2O_2) (Figure 1) [1]. The production of ROS exceeds its scavenging capacity, which is the reaction of oxidative stress. Under normal physiological conditions, ROS participates in a number of cell activities, including cell energy metabolism, signal transduction, and gene expression regulation, but high levels of ROS can also damage biomacromolecules in cells, such as lipids, proteins, and nucleic acids, leading to cell senescence even death [2]. A large number of studies have shown that regular or suitable exercise produces low-level ROS, while excessive production of endogenous free radicals during exercise can damage the physiological functions of the entire tissue [1–3], such as skeletal muscle [3]. Skeletal muscle is the dynamic part of the exercise system, and the physiological level ROS is an essential substance for maintaining its function, which is involved in the production of muscle force, the maintenance of muscle content, intracellular signal transduction, gene expression, and other related activities, while excessive ROS causes the dysfunction of contraction and muscle weakness [4]. As is well known, ROS induced by skeletal muscle contraction during exercise can increase the level of oxidative stress and enhance the antioxidant defense system. Although exercise-induced reactive oxygen species are required for normal force production in skeletal muscle, the high levels of ROS can contribute to contractile dysfunction [5]. The sarcoplasmic reticulum Ca^{2+} release channel is highly sensitive to ROS, which will reduce the sensitivity of myofibrils to Ca^{2+} and then affect muscle contraction [5, 6]. In addition, the accumulation of ROS in the body depends on exercise mode, exercise intensity, and duration.

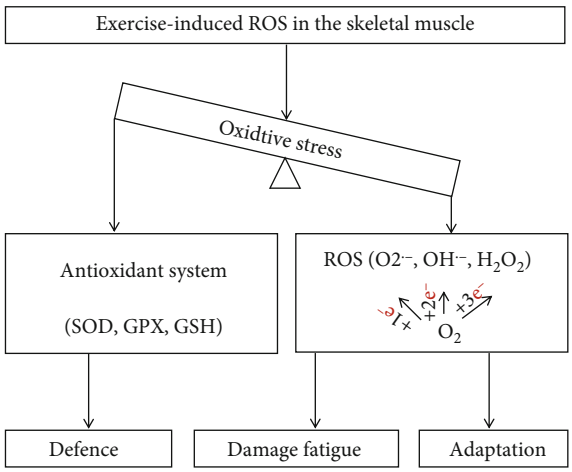

Figure 1: Effects of exercise-induced ROS on the balance of oxidative stress in the skeletal muscle. Exercise-induced oxidative stress occurs as the production of ROS generated in the body, which is excessive to the defense ability of antioxidant system during physical exercise. ROS includes O_2^-, OH^-, and H_2O_2, which affect the adaption, damage, and fatigue in the skeletal muscle.

Therefore, exercise-induced oxidative stress may play an important role in the pathophysiological functions of skeletal muscle.

2. Exercise-Induced Oxidative Stress

In 1978, exercise-induced oxidative stress was firstly proposed, which refers to oxidative stress caused by exercise; that is, the rate of free radicals generated in the body is much greater than its scavenging rate during physical exercise, which will damage tissue, resulting in the decline of the body's working ability [7]. The mitochondrial respiratory chain is the main source of endogenous ROS during exercise, and its excessive production can cause oxidative damage to lipids, proteins, nucleic acids, and other substances [8]. The accumulation of ROS in the body depends on the exercise mode, intensity, and duration. Studies have indicated that a small amount of ROS produced by moderate-intensity exercise can act as a second messenger in cells to mediate growth factor signal transmission [9–11]. Acute exercise can promote the excessive production of ROS, which causes an imbalance in the oxidation-antioxidant homeostasis in cells, because rapidly increasing oxygen consumption inevitably produces more free radicals during strenuous exercise [12]. A large amount of oxygen is consumed to produce a large amount of singlet oxygen ($O_2^{\cdot\cdot}$), which stimulates a series of radical chain reactions [13]. On the other hand, the hypoxia of local tissue and the accumulation of metabolites affect the mitochondrial energy supply. Meanwhile, high-intensity exhaustive exercise can cause a significant increase in the content of malondialdehyde (MDA) and further increase with the extension exercise [14]. MDA can objectively reflect the level of free radicals in the body.

3. ROS in Skeletal Muscle

Skeletal muscle is an important exercise organ in the body; its normal physiological function is the basic prerequisite and important guarantee for health.

3.1. ROS in Different Skeletal Muscle Fibers. Skeletal muscle is composed of three types of muscle fibers: I, IIa, and IIb. The abilities of these different types of muscle fibers to generate ROS and resist oxidative stress are also different [15]. The leakage level of mitochondrial ROS in type IIb muscle fiber is 2-3 times that of type IIa muscle fiber, due to mitochondria in type IIb muscle fiber playing an important role in the production and release of superoxide [4]. High-intensity exercise leads to the excessive production of ROS, which can cause changes in the normal physiological environment of skeletal muscle fibers and vascular endothelial dysfunction. The levels of antioxidant enzymes of type I and IIa muscle fibers enhance the scavenging ability of free radicals and promote the recovery of skeletal muscle motor functions, while there is no significant change in type IIb muscle fibers. In addition, type I muscle fibers are rich in myoglobin with the strongest abilities of aerobic metabolism and antifatigue [16]. These findings indicate that different types of muscle fibers have different effects on antifatigue and ROS production, but they are all related to their antioxidant capacity.

3.2. Sites for ROS in Skeletal Muscle Cells. In the past, mitochondria are the main site of intracellular ROS in contracting skeletal muscle [14]. In mitochondria, 2–5% of the total oxygen consumed may undergo one electron reduction with the generation of superoxide [17]. Mitochondrial complex I in the electron transport chain releases superoxide to the mitochondrial matrix, while complex III to both sides of the inner membrane [18]. Recently, some scholars have discovered that the main source of ROS may not be limited to mitochondria during exercise [14]. The upper limit of the total utilization of oxygen consumed by mitochondria in different tissues to produce ROS is about 0.15% [19]. Simultaneously, a large number of studies have shown that many intracellular enzymes are involved in the production of ROS, such as NADPH oxidases (NOXs), xanthine oxidase (XO), and phospholipase A2 (PLA2) [18]. Regardless of whether muscle is in a resting or contracting state, NOX family proteins can produce more superoxide anions than that of mitochondria in single muscle fibers [20]. Moreover, the NOX2 loss-of-function model indicated that NOX2 may be the main source of cytosolic ROS in skeletal muscle during moderate-intensity exercise [21]. Another study found that there was a correlation between XO content and lactic acid level during anaerobic exercise, producing a large amount of ROS, thereby aggravating skeletal muscle oxidative damage [22]. In addition, muscle damage caused by exercise can also stimulate various cytokines to activate macrophages and neutrophils, leading to the overproduction of ROS [23].

4. Skeletal Muscle Adaptation

Skeletal muscle is a highly plastic tissue. Moderate or regular exercise training can regulate the signaling pathways by

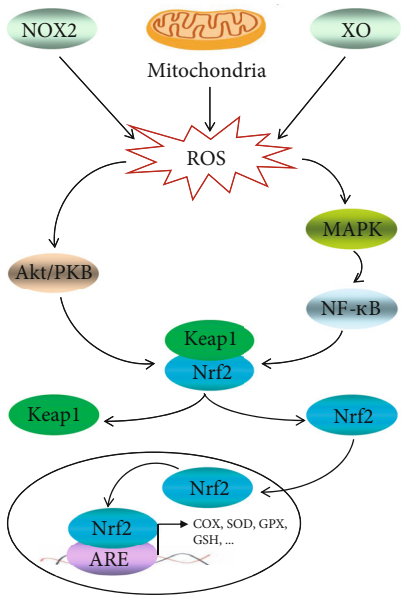

Figure 2: Effects of exercise-induced ROS on the signaling pathway in the skeletal muscle. Exercise-induced ROS can activate MAPK and Akt signaling pathways. Nrf2 dissociates from its cytoplasmic inhibitor Keap1 then translocates to the nucleus and combines with ARE to contribute to some downstream antioxidant gene transactivation, such as the oxidases, COX, SOD, GPX, and GSH.

oxidative stress and ROS to resist oxidative damage and further come true structure-function adaptations in skeletal muscle [19, 24, 25]. ROS can not only activate NF-κB by activating mitogen-activated protein kinase (MAPK) but also stimulate Akt phosphorylation, thereby activating their common downstream molecule nuclear factor erythroid-derived 2-related factor 2 (Nrf2) [25]. Nrf2 as a redox-sensing transcription factor dissociates from its cytoplasmic inhibitor Keap1, then translocates to the nucleus and combines with antioxidant response element (ARE) to contribute to transactivation of some downstream antioxidant genes, especially defense-related enzymes and exercise-adapting-related enzymes, such as oxidase cytochrome oxidase (COX), superoxide dismutase (SOD), glutathione peroxidase (GPX) activities, and glutathione (GSH), thereby upregulating their expressions and activities, alleviating the oxidative damage, and promoting exercise-induced adaptations (Figure 2) [19, 24, 25]. Acute exercise or long-term exercise training may increase the expression of Nrf2 and/or Nrf2-ARE binding activity. After 6 weeks of treadmill training, the transcription activity of Nrf2 in skeletal muscle is increased, and the activity of COX is also increased by 20% [26].

Moreover, exercise-activated Nrf2 may regulate skeletal muscle mitochondria by promoting mitochondrial biogenesis, improving mitochondrial respiratory function, and regulating mitochondrial autophagy. In addition, peroxisome proliferator-activated receptor-γ coactivator-1α (PGC-1α) plays an important role in glucose uptake, mitochondriogenesis, and hypertrophy in skeletal muscle responses to physical exercise [24]. Exercise-induced ROS can couple with lactate metabolism to stimulate PGC-1α production, especially endurance exercise [24]. PGC-1α coactivates nuclear respiratory factor- (NRF-) 1 and NRF-2 to increase their DNA binding in skeletal muscle after acute exercise [24], then activates the genes encoding COX and mitochondrial transcription factor A (TFAM), which activate mitochondrial DNA transcription, thereby increasing mitochondrial synthesis [24]. In addition, exercise-induced ROS are able to stimulate the skeletal muscle to secrete myokines, which also play important roles in the regulation of cell signaling and muscle metabolic adaptation [27, 28], such as interleukin-15 (IL-15). IL-15 is a regulator to control intracellular ROS production and attenuate oxidative stress in skeletal muscle cells [29].

5. Skeletal Muscle Cell Damage

Exhaustive exercise can increase the peroxidation and weaken the antioxidant capacity in skeletal muscles, which can cause the damage of skeletal muscle cells through modification of lipid, protein, and DNA.

Firstly, for lipid damage, biomembrane is the main component of cells. Lipid peroxidation caused by excessive endogenous ROS during exercise can change the liquidity, fluidity, and permeability of the biomembrane, which in turn leads to membrane dysfunction [30]. The lipid bilayer contains a large amount of polyunsaturated fatty acid (PUFA). ROS can deprive the hydrogen at the diallyl position in PUFA to form unsaturated fatty acid free radicals, then combine with oxygen molecules to generate lipid peroxyl radicals $LOO^{\cdot}$ [31]. $LOO^{\cdot}$ can deprive the allyl groups of unsaturated fatty acid hydrogen which forms a new unsaturated fatty acid free radical and lipid peroxide (LOOH), causing oxidative damage to the biomembranes of skeletal muscle cells [31].

Secondly, for protein damage, ROS plays a very important role in the process of protein metabolism, which can promote protein turnover and renewal under physiological conditions. But excessive ROS induced by exercise will cause damage to proteins and induce the inactivation of enzymes, the loss of receptors, and the decline of immune function [31]. The damage of proteins by ROS is mainly to change their activities. $OH^{\cdot}$ can change the primary structure of the protein and contribute to the secondary and tertiary structure modification, so that the polypeptide chain unfolds to form a random structure [32]. These modifications expose the originally shielded peptide bonds to proteolytic enzymes. In addition, a protein is combined with $OH^{\cdot}$ which will increase the production of double tyrosine, further induce the breakage, which is manifested by the effect of extracting hydrogen on the a-carbon atom of the amino acid, and then react with $O_2^{\cdot-}$ to generate LOO^{-}, ultimately forming peroxides [32].

The last is DNA damage. 8-Hydroxydeoxyguanosine (8-OHdG) is an important marker for the detection of oxidative DNA damage. The C-8 position of the base guanine in the DNA chain is susceptible to the attack of $OH^{\cdot}$ and $O_2^{\cdot-}$ and undergoes hydroxylation to form the adduct 8-OHdG [33]. OH^{-} combines with the deoxyguanine nucleotide residues at the C-4, C-5, or C-8 positions of DNA bases to form

8-hydroxy-7,8-dihydroxyguanine nucleotides, which in turn further oxidizes to generate 8-hydroxydeoxyguanine nucleotides. Simultaneously, during the replication process, 8-OHdG on the DNA chain can pair with other bases than C to form point mutations, such as GC→TA [32].

6. Skeletal Muscle Fatigue

The process of sports fatigue is a complex physiological phenomenon; it actually occurs with the consumption of physical energy or the accumulation of metabolites, including skeletal muscle fatigue, visceral fatigue, and nerve fatigue. Skeletal muscle fatigue is the main peripheral manifestation of sports fatigue. The production of skeletal muscle strength depends on its contraction mechanisms, while any disorder of the nerves, ions, blood vessels, and energy systems upstream of the cross bridge will lead to their loss and cause muscle fatigue, especially the energy metabolism factors during the process of muscle contraction, such as H^+, lactic acid, Pi, reactive ROS, heat shock protein (HSP), α-acid glycoprotein (ORM) which also affect muscle fatigue.

Excessive ROS produced by strenuous exercise may cause exercise fatigue by reducing the release of skeletal muscle sarcoplasmic reticulum Ca^{2+} and/or the sensitivity of myofibrils Ca^{2+} [34]. However, under mild oxidative stress induced by physical exercise, the S-glutathionization of troponin can improve contractile apparatus Ca^{2+} sensitivity in fast-twitch fibers, thereby delaying the occurrence of fatigue [35]. However, antioxidants restored Ca^{2+} to release in the sarcoplasmic reticulum, but the decrease in muscle strength during fatigue cannot be eliminated [36], indicating that oxidative stress caused by exercise is closely related to muscle fatigue. Endogenous and exogenous ROS not only may hinder muscle fiber contraction by affecting the release and uptake of Ca^{2+} in the sarcoplasmic reticulum and reducing the activity of troponin but also can promote the occurrence of exercise fatigue by destroying mitochondrial functions and inhibiting aerobic metabolism [6]. In addition, during exercise, the increased energy metabolism rate leads to excessive mitochondrial ROS production in fatigued skeletal muscle cells, which further leads to the occurrence of the oxidative modification of lipids, proteins, and DNA.

7. Conclusion

Together, exercise-induced oxidative stress has dual effects on skeletal muscle tissue. Proper exercise can promote generation of the physiological levels of ROS, maintain the normal skeletal muscle function, and facilitate exercise adaptation, while exhaustive exercise can cause the body to produce too much ROS, which causes excessive oxidative stress, leading to fatigue and cell damage of skeletal muscle. Therefore, further understanding the effect of exercise-induced oxidative stress on the pathophysiological functions of skeletal muscle is very important for guiding exercise to promote health and provides a direction to explore the molecular mechanism of exercise to improve the development of pathophysiological processes in oxidative stress-related diseases.

Data Availability

The original contributions presented in the study are included in the article. Further inquiries can be directed to the corresponding authors.

Conflicts of Interest

The authors declare that they have no competing interests.

Authors' Contributions

The work was conceived by FW, XW, YL, and ZZ; draft writing was performed by FW and XW; and the manuscript was revised by YL and ZZ. All authors reviewed and approved the final version of the manuscript for publication.

Acknowledgments

This work was supported by the Key Projects of Scientific and Technological Innovation in Fujian Province (2021G02021 and 2021G02023), Special Funds of the Central Government Guilding Local Science and Technology Development (2020L3008), Fujian Provincial Natural Science Foundation (2019R1011-3 and 2020J01176), and Scientific Research Talent Project of Fujian Provincial Health Commission (2018-ZQN-20).

References

[1] S. K. Powers, R. Deminice, M. Ozdemir, T. Yoshihara, M. P. Bomkamp, and H. Hyatt, "Exercise-induced oxidative stress: friend or foe?," *Journal of Sport and Health Science*, vol. 9, no. 5, pp. 415–425, 2020.

[2] Z. He, Q. Xu, B. Newland et al., "Reactive oxygen species (ROS): utilizing injectable antioxidative hydrogels and ROS-producing therapies to manage the double-edged sword," *Journal of Materials Chemistry B*, vol. 9, no. 32, pp. 6326–6346, 2021.

[3] S. K. Powers, W. B. Nelson, and M. B. Hudson, "Exercise-induced oxidative stress in humans: cause and consequences," *Free Radical Biology & Medicine*, vol. 51, no. 5, pp. 942–950, 2011.

[4] A. Thirupathi, R. A. Pinho, and Y.-Z. Chang, "Physical exercise: an inducer of positive oxidative stress in skeletal muscle aging," *Life Sciences*, vol. 252, 2020.

[5] F. Magherini, T. Fiaschi, R. Marzocchini et al., "Oxidative stress in exercise training: the involvement of inflammation and peripheral signals," *Free Radical Research*, vol. 53, no. 11-12, pp. 1155–1165, 2019.

[6] A. Cheng, T. Yamada, D. E. Rassier, D. C. Andersson, H. Westerblad, and J. T. Lanner, "Reactive oxygen/nitrogen species and contractile function in skeletal muscle during fatigue and recovery," *The Journal of Physiology*, vol. 594, no. 18, pp. 5149–5160, 2016.

[7] M. C. Fogarty, C. M. Hughes, G. Burke et al., "Exercise-induced lipid peroxidation: implications for deoxyribonucleic acid damage and systemic free radical generation," *Environmental and Molecular Mutagenesis*, vol. 52, no. 1, pp. 35–42, 2011.

[8] A. Sarniak, J. Lipińska, K. Tytman, and S. Lipińska, "Endogenous mechanisms of reactive oxygen species (ROS) generation," *Postępy Higieny I Medycyny Doświadczalnej*, vol. 70, pp. 1150–1165, 2016.

[9] C. R. Reczek and N. S. Chandel, "ROS-dependent signal transduction," *Current Opinion in Cell Biology*, vol. 33, pp. 8–13, 2015.

[10] M. C. Gomez-Cabrera, J. Viña, and L. L. Ji, "Role of redox signaling and inflammation in skeletal muscle adaptations to training," *Antioxidants*, vol. 5, no. 4, p. 48, 2016.

[11] M.-C. Gomez-Cabrera, C. Borrás, F. V. Pallardó, J. Sastre, L. L. Ji, and J. Viña, "Decreasing xanthine oxidase-mediated oxidative stress prevents useful cellular adaptations to exercise in rats," *The Journal of Physiology*, vol. 567, no. 1, pp. 113–120, 2005.

[12] G. Schippinger, W. Wonisch, P. M. Abuja, F. Fankhauser, B. Winklhofer-Roob, and G. Halwachs, "Lipid peroxidation and antioxidant status in professional American football players during competition," *European Journal of Clinical Investigation*, vol. 32, no. 9, pp. 686–692, 2002.

[13] S. G. Sokolovski, E. U. Rafailov, A. Y. Abramov, and P. R. Angelova, "Singlet oxygen stimulates mitochondrial bioenergetics in brain cells," *Free Radical Biology and Medicine*, vol. 163, pp. 306–313, 2021.

[14] S. Joanisse, J. McKendry, C. Lim et al., "Understanding the effects of nutrition and post-exercise nutrition on skeletal muscle protein turnover: insights from stable isotope studies," *Clinical Nutrition Open Science*, vol. 36, pp. 56–77, 2021.

[15] S. K. Powers, Z. Radak, and L. L. Ji, "Exercise-induced oxidative stress: past, present and future," *Journal of Physiology*, vol. 594, no. 18, pp. 5081–5092, 2016.

[16] L. Zhang, Y. Zhou, W. Wu et al., "Skeletal muscle-specific overexpression of PGC-1α induces fiber-type conversion through enhanced mitochondrial respiration and fatty acid oxidation in mice and pigs," *International Journal of Biological Sciences*, vol. 13, no. 9, pp. 1152–1162, 2017.

[17] S. K. Powers and M. J. Jackson, "Exercise-induced oxidative stress: cellular mechanisms and impact on muscle force production," *Physiological Reviews*, vol. 88, no. 4, pp. 1243–1276, 2008.

[18] E. L. Robb, A. R. Hall, T. A. Prime et al., "Complex I reverse electron transport," *Journal of Biological Chemistry*, vol. 293, no. 25, pp. 9869–9879, 2018.

[19] P. Steinbacher and P. Eckl, "Impact of oxidative stress on exercising skeletal muscle," *Biomolecules*, vol. 5, no. 2, pp. 356–377, 2015.

[20] G. K. Sakellariou, A. Vasilaki, J. Palomero et al., "Studies of mitochondrial and nonmitochondrial sources implicate nicotinamide adenine dinucleotide phosphate oxidase(s) in the increased skeletal muscle superoxide generation that occurs during contractile activity," *Antioxidants & Redox Signaling*, vol. 18, no. 6, pp. 603–621, 2013.

[21] C. Henríquez-Olguin, J. R. Knudsen, S. H. Raun et al., "Cytosolic ROS production by NADPH oxidase 2 regulates muscle glucose uptake during exercise," *Nature Communications*, vol. 10, no. 1, p. 4623, 2019.

[22] M.-C. Gomez-Cabrera, E. Domenech, and J. Viña, "Moderate exercise is an antioxidant: upregulation of antioxidant genes by training," *Free Radical Biology & Medicine*, vol. 44, no. 2, pp. 126–131, 2008.

[23] P. Baumert, E. C. Hall, and R. M. Erskine, "The genetic association with exercise-induced muscle damage and muscle injury risk," in *Sports, Exercise, and Nutritional Genomics*, pp. 375–407, Elsevier, 2019.

[24] J. Bouviere, R. S. Fortunato, C. Dupuy, J. P. Werneck-de-Castro, D. P. Carvalho, and R. A. Louzada, "Exercise-stimulated ROS sensitive signaling pathways in skeletal muscle," *Antioxidants*, vol. 10, no. 4, p. 537, 2021.

[25] P. M. Abruzzo, F. Esposito, C. Marchionni et al., "Moderate exercise training induces ROS-related adaptations to skeletal muscles," *International Journal of Sports Medicine*, vol. 34, no. 8, pp. 676–687, 2013.

[26] M. J. Crilly, L. D. Tryon, A. T. Erlich, and D. A. Hood, "The role of Nrf2 in skeletal muscle contractile and mitochondrial function," *Journal of Applied Physiology*, vol. 121, no. 3, pp. 730–740, 2016.

[27] C. Scheele, S. Nielsen, and B. K. Pedersen, "ROS and myokines promote muscle adaptation to exercise," *Trends in Endocrinology and Metabolism*, vol. 20, no. 3, pp. 95–99, 2009.

[28] J. Starnes, T. Parry, S. O'Neal et al., "Exercise-induced alterations in skeletal muscle, heart, liver, and serum metabolome identified by non-targeted metabolomics analysis," *Metabolites*, vol. 7, no. 3, pp. 40–54, 2017.

[29] F. Li, Y. Li, Y. Tang et al., "Protective effect of myokine IL-15 against H_2O_2-mediated oxidative stress in skeletal muscle cells," *Molecular Biology Reports*, vol. 41, no. 11, pp. 7715–7722, 2014.

[30] F. Ito, Y. Sono, and T. Ito, "Measurement and clinical significance of lipid peroxidation as a biomarker of oxidative stress: oxidative stress in diabetes, atherosclerosis, and chronic inflammation," *Antioxidants*, vol. 8, no. 3, pp. 72–100, 2019.

[31] U. N. Das, "Exercise is beneficial: but how and why?," *Circulation Journal*, vol. 75, no. 4, pp. 1010-1011, 2011.

[32] A. Vasilaki, A. Richardson, H. Van Remmen et al., "Role of nerve-muscle interactions and reactive oxygen species in regulation of muscle proteostasis with ageing," *The Journal of Physiology*, vol. 595, no. 20, pp. 6409–6415, 2017.

[33] H. Kasai, N. Iwamoto-Tanaka, T. Miyamoto et al., "Life style and urinary 8-hydroxydeoxyguanosine, a marker of oxidative DNA damage: effects of exercise, working conditions, meat intake, body mass index, and smoking," *Japanese Journal of Cancer Research*, vol. 92, no. 1, pp. 9–15, 2001.

[34] J. Ying, X. Cen, and Y. Peimin, "Effects of eccentric exercise on skeletal muscle injury: from an ultrastructure aspect: a review," *Physical Activity and Health*, vol. 5, no. 1, pp. 15–20, 2021.

[35] J. Osório Alves, L. Matta Pereira, I. Cabral Coutinho do Rêgo Monteiro et al., "Strenuous acute exercise induces slow and fast twitch-dependent NADPH oxidase expression in rat skeletal muscle," *Antioxidants*, vol. 9, no. 1, p. 57, 2020.

[36] L. Delgado-Roche, N. Lagumersindez, and G. Martínez-Sánchez, "Biochemical changes in mitochondria and its role in cell death during myocardial ischemia-reperfusion injury," *Pharmacologyonline*, vol. 2, 2009.

Hindawi
Oxidative Medicine and Cellular Longevity
Volume 2021, Article ID 1764929, 11 pages
https://doi.org/10.1155/2021/1764929

Research Article

HIF-1α Activation Promotes Luteolysis by Enhancing ROS Levels in the Corpus Luteum of Pseudopregnant Rats

Zonghao Tang,[1,2] **Jiajie Chen**,[1] **Zhenghong Zhang**,[1] **Jingjing Bi**,[2] **Renfeng Xu**,[1] **Qingqiang Lin**,[1] **and Zhengchao Wang**[1]

[1]*Provincial Key Laboratory for Developmental Biology and Neurosciences, Provincial University Key Laboratory of Sport and Health Science, Key Laboratory of Optoelectronic Science and Technology for Medicine of Ministry of Education, College of Life Sciences, Fujian Normal University, Fuzhou 350007, China*
[2]*Key Laboratory of Medical Electrophysiology, Ministry of Education, Medical Electrophysiological Key Laboratory of Sichuan Province, Southwest Medical University, Luzhou 646000, China*

Correspondence should be addressed to Zhengchao Wang; zcwang@fjnu.edu.cn

Received 23 June 2021; Accepted 12 August 2021; Published 2 September 2021

Academic Editor: Alin Ciobica

The increase of oxidative stress is one of the important characteristics of mammalian luteal regression. Previous investigations have revealed the essential role of reactive oxygen species (ROS) in luteal cell death during luteolysis, while it is unknown how ROS is regulated in this process. Considering the decrease of blood flow and increase of $PGF_{2\alpha}$ during luteolysis, we hypothesized that the HIF-1α pathway may be involved in the regulation of ROS in the luteal cell of the late corpus luteum (CL). Here, by using a pseudopregnant rat model, we showed that the level of both HIF-1α and its downstream BNIP3 was increased during luteal regression. Consistently, we observed the increase of autophagy level during luteolysis, which is regulated in a Beclin1-independent manner. Comparing with early (Day 7 of pseudopregnancy) and middle CL (Day 14), the level of ROS was significantly increased in late CL, indicating the contribution of oxidative stress in luteolysis. Inhibition of HIF-1α by echinomycin (Ech), a potent HIF-1α inhibitor, ameliorated the upregulation of BNIP3 and NIX, as well as the induction of autophagy and the accumulation of ROS in luteal cells on Day 21 of pseudopregnancy. Morphologically, Ech treatment delayed the atrophy of the luteal structure at the late-luteal stage. An in vitro study indicated that inhibition of HIF-1α can also attenuate $PGF_{2\alpha}$-induced ROS and luteal cell apoptosis. Furthermore, the decrease of cell apoptosis can also be observed by ROS inhibition under $PGF_{2\alpha}$ treatment. Taken together, our results indicated that HIF-1α signaling is involved in the regression of CL by modulating ROS production via orchestrating autophagy. Inhibition of HIF-1α could obviously hamper the apoptosis of luteal cells and the process of luteal regression.

1. Introduction

The corpus luteum (CL) is an ephemeral gland in mammalian ovaries evolved from the remains of ovulated follicles, which is responsible for the maintenance of hormonal homeostasis during the menstrual cycle and pregnancy [1]. Normally, the lifespan of CL is mostly dependent on the presence of pregnancy; this period is termed as the luteal phase. The absence of pregnancy is an essential indicator for the initiation of luteal regression and eventually the removal of CL from the ovarian structure at the end of pregnancy whereupon permitting the initiation of the next menstrual cycle [2]. The regression of CL implicates the degradation of the extracellular matrix, loss of blood vessel, and luteal cell death. The attenuation of CL regression disrupts the ovarian cycle and may create a disordered context impairing thereafter follicular development.

Previous investigations have indicated that the increase of ROS is an essential precursor of rat luteal regression [1]. Furthermore, an in vitro study showed that the level of ROS can also be induced by $PGF_{2\alpha}$, a luteolytic agent [3, 4]. In humans, H_2O_2 treatment is able to generate a luteolytic effect on granulosa-luteal cells [5]. These findings highlighted the important role of ROS in luteal regression.

However, the question in terms of how ROS is generated still remains poorly understood. Physiologically, the degeneration of the vascular network is initiated before the comparable change of the CL structure during luteolysis [6]. Furthermore, precedent evidences also indicate $PGF_{2\alpha}$ as a HIF-1α activator in adipocytes [7], and this effect was also observed in luteal cells [8]. Therefore, it is rational to hypothesize that HIF-1α might be an essential causative factor of ROS generation. Indeed, the prodeath role of HIF-1α on luteal cells has been evaluated in an in vitro model [9]. The level of HIF-1α downstream protein BNIP3, an important factor involved in autophagy regulation in mammalian cells, is also obviously increased under hypoxic conditions in luteal cells [9]. These findings suggest that the dysregulation of autophagy may be involved in ROS production in luteal cells. Consistently, plenty of evidences revealed the involvement of autophagy in luteal regression in diverse species, including rats [10] and humans [11], although the detail of autophagic regulation still remains elusive.

Autophagy is an evolutionarily conserved catabolic mechanism in eukaryotic cells, by which cells can elegantly control the homeostasis of metabolism under stresses so as to inhibit the occurrence of cell dysfunctions. However, autophagy could also promote the apoptosis of cells by excess self-digestions, removal of essential organelles, and autophagosome accumulation [12]. The abnormal induction of autophagy is highly involved in diverse cell diseases, including cancer [13], diabetes [14], and neurodegeneration [15]. In the mammalian ovary, autophagy plays crucial roles in the formation of the primordial pool [16], the transition of oocyte-to-embryo, the development of follicles [17], and the regression of the corpus luteum [10]. However, the evidence is still marginal about how autophagy is involved in luteal regression.

In the present study, we evaluated the expression changes of HIF-1α signaling and its effect on oxidative stress during luteal regression by using a pseudopregnant rat model. We treated rats with echinomycin, a potent HIF-1α inhibitor, and studied the progress of luteal regression by observing luteal morphologies and expressions of apoptotic proteins during luteal regression, aiming to elucidate the role of HIF-1α signaling in autophagy and apoptosis during the luteal regression of pseudopregnant rats.

2. Materials and Methods

2.1. Animals. Female Sprague-Dawley rats (about 21~23 days) were purchased from Wushi Experimental Animal Supply Co. Ltd. (Fuzhou, China). The animals were maintained under a 14 h : 10 h light-dark schedule with a continuous supply of chow and water. These rats were superovulated by i.p. 30 IU pregnant mare serum gonadotrophin (PMSG; Ningbo Second Hormone Factory, Jiangsu). After 48 h, these rats were then treated with human chorionic gonadotrophin (hCG; i.p. 30 IU, Ningbo Second Hormone Factory, Jiangsu) to induce pseudopregnancy. The rats were executed, and the ovaries were excised for further analysis on Days 7, 14, and 21 after hCG treatment. The experimental protocol was approved by the Institutional Animal Care and Use Committee and the Ethics Committee on Animal Experimentation, Fujian Normal University. All efforts were made to minimize animal discomfort and to reduce the number of animals used.

2.2. Immunohistochemistry. The ovaries were fixed in 4% paraformaldehyde. After fixation, the ovaries were embedded in paraffin, and 5 μm sections were cut and mounted on slides. After drying, the sections were dewaxed and rehydrated before antigen retrieval. The sections were then processed for immunohistochemical analysis with anti-LC-3 antibody (1 : 500 dilution, ab48394, Abcam), anti-Beclin1 antibody (1 : 200 dilution, 11306-1-AP, Proteintech), and anti-p62 antibody (1 : 200 dilution, 18420-1-AP). The negative control used serum (Boster Biological Technology, Wuhan) instead of primary antibody. The sections were incubated at 4°C overnight with a primary antibody. The immunoreactivity of the specific protein was visualized by the Elite ABC kit (BioGenex, San Ramon, CA, USA). Then, the sections were counterstained with hematoxylin and mounted with cover slips.

2.3. Western Blotting Analysis. The CLs were separated from ovaries under a dissecting microscope with great care. After that, CLs were homogenized by using ice-cold RIPA buffer with supplemented protease inhibitors (protease inhibitor cocktail, Beyotime Institute of Biotechnology, Haimen, China) for protein extraction. Protein concentrations were determined by a Bio-Rad protein assay (Bio-Rad, Hercules, CA, USA) with bovine serum albumin standards. 20 μg protein samples were subjected to SDS-PAGE gel electrophoresis. The nonspecific binding was blocked by 5% skimmed milk, and the membranes were thereafter incubated overnight in the presence of primary antibodies (Supplemental Table 1). After incubation, the membranes were washed with TBST and then incubated in horseradish peroxidase-conjugated goat anti-rabbit or mouse IgG (1 : 1000 dilution, Beyotime Institute of Biotechnology, Haimen, China) for 1 h at room temperature. Eventually, the bands were visualized by using enhanced chemiluminescence star (ECL, Beyotime Institute of Biotechnology, Haimen, China). The bands were quantified using ImageJ 1.49 software (National Institutes of Health, Bethesda, MD, USA).

2.4. Quantitative RT-PCR (qRT-PCR). Total RNA of luteal samples was extracted with TRIzol (Invitrogen, Carlsbad, CA, USA) and then reverse-transcribed into cDNA using a commercial kit (Bio-Rad, Hercules, CA, USA). Real-time PCR was performed with SYBR Super Mix (Bio-Rad, Hercules, CA, USA) in a reaction volume of 20 μl, and the reaction was processed in the ABI StepOne system (Applied Biosystems, Foster City, CA, USA). Primer sequences include BNIP3 (F: 5′-CTC TGC TGA GTG AAG TTC TAC G-3′, R: 5′-AAC ACA AGT GCT GGA TAC TGA TT-3′), NIX (F: 5′-GCA GTG CCA TTG AAC TGT GG-3′, R: 5′-GGA ACC GCA AAT CGA CAT CG-3′), and GAPDH (F: 5′-CGA CCC CTT CAT TGA CCT CAA C-3′, R: 5′-AAG ACG CCA GTA GAC

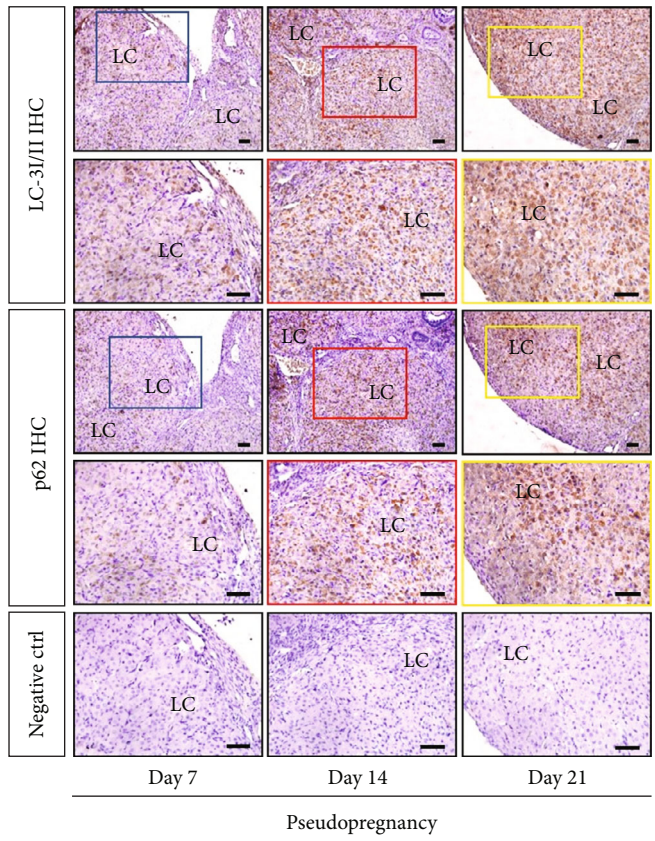

Figure 1: Immunohistochemistry (IHC) of LC-3I/II and p62 on the adjacent section of corpus luteum (CL) from pseudopregnant rats on Days 7, 14, and 21. Negative control (Ctrl) used serum instead of primary antibody. Bar = 100 μm.

TCC ACG AC-3′) primers. Expression data were normalized to the expression level of GAPDH.

2.5. Cell Treatment. To test the effect of HIF-1α on ROS biogenesis, we isolated luteal cells from CL on Day 7 of pseudopregnancy according to the methods provided before [18]. To mimic luteal regression, luteal cells were incubated in OptiMEM (Gibco) medium with the presence of $PGF_{2\alpha}$ (100 μM, Sigma) or $PGF_{2\alpha}$ and 3-MA (2 mM, Sigma) for 24 h.

2.6. ROS Detection. For tissular detection, the equal volume of CLs was dissected from the ovaries and was homogenized in lysis buffer (250 mM sucrose, 20 mM HEPES-NaOH, pH 7.5, 10 mM KCl, 1.5 mM $MgCl_2$, 1 mM EDTA, 1 mM EGTA, and protease cocktail inhibitor) [19] to collect the supernatant at 10000g, 4°C for 5 min. The mixes of DCFH-DA and supernatant were prepared according to the method provided by the manufacturer (Jiancheng Biotech Institute, Nanjing, China). After that, mixes were incubated in the dark at 37°C for 30 min. The DCF fluorescence was determined by a microplate reader at an excitation wavelength of 488 nm and an emission wavelength of 535 nm.

The level of intracellular ROS was measured by using a commercial kit (Beyotime, Institute of Biotechnology, Haimen, China). Briefly, cells were washed with cold PBS. After that, incubate the cells with DCFH-DA at 37°C for 20 min. Cells were washed with PBS before measurement; the DCF fluorescence of 20000 cells was determined by a microplate reader at an excitation wavelength of 488 nm and an emission wavelength of 535 nm (BioTek Synergy HT).

2.7. Statistical Analysis. All data were presented as the mean ± SE. The significant differences within or between groups were evaluated by one-way analysis of variance, followed by Tukey's multiple range test. Statistical analysis was conducted using SPSS version 20 software, and $P < 0.05$ was recognized as a statistically significant difference.

3. Results

3.1. Autophagy Was Induced in Luteal Cells during Luteolysis in a Beclin1-Independent Manner. In order to clarify the induction of autophagy during luteal regression, we detected the expression changes of autophagy-related proteins, including the marker protein (LC-3II, Figure 1) of autophagic induction, the marker protein (p62, Figure 1) of autophagosome degradation, and a scaffold protein (Beclin1, Figure 2(a)) involved in autophagic regulation by immunohistochemical staining analysis. These results demonstrated that LC-3II and p62 were expressed in luteal cells and were concomitantly increased during luteal regression (Figure 1), whereas Beclin1 was decreased on Days 14 and 21 of pseudopregnancy (Figure 2(a)). The results of western

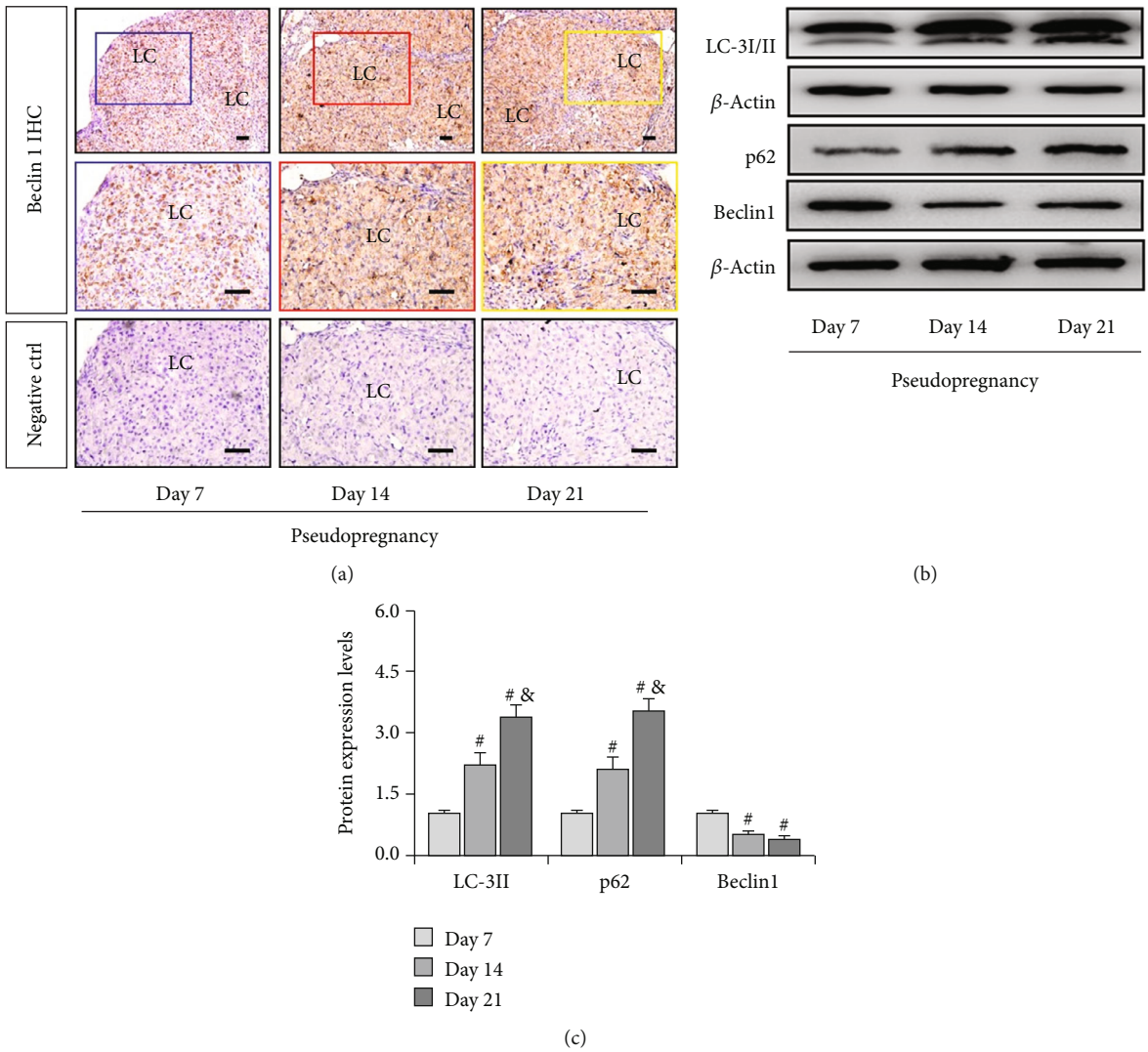

Figure 2: Expressions of LC-3I/II, p62, and Beclin1 in the corpus luteum (CL) from pseudopregnant rats on Days 7, 14, and 21. (a) Immunohistochemistry (IHC) of Beclin1 on the adjacent section of corpus luteum (CL) from pseudopregnant rats on Days 7, 14, and 21. (b) Representative immunoblotting of LC-3I/II, p62, and Beclin1. (c) Densitometric qualification of LC-3I/II, p62, and Beclin1. $P < 0.05$ was considered to indicate a statistically significant difference. $^{\#}P < 0.05$, vs. Day 7. $^{\&}P < 0.05$, vs. Day 14.

blotting also verified the increase of LC-3II and p62 (Figure 2(b)) and the decrease of Beclin1 on Days 14 and 21 of pseudopregnancy (Figure 2(b)). These results indicated the decrease of autophagy flux in luteal cells during CL regression, and autophagy is regulated in a Beclin1-independent manner.

3.2. The Increase of Cell Apoptosis Is Associated with Oxidative Stress and Skewed Mitochondrial Homeostasis. As we have known that apoptosis was induced in luteal cells during regression, the present study thus examined the expressions of apoptosis-related proteins and found a significant increase of cleaved caspase-3 and Bax on Day 21 (Figures 3(a) and 3(b)) and an obvious decrease of Bcl-2 on Day 21 of pseudopregnancy (Figures 3(a) and 3(b)). Furthermore, we also detected a significant increase in the ROS level in CLs, indicating the occurrence of oxidative stress (Figure 3(c)).

The elevation of ROS content implicates the disruption of mitochondrial homeostasis. Under stressful conditions, mitophagy is mobilized to degrade mitochondria so as to maintain its homeostasis [20]. We therefore detected the expressions of PINK1 (Figures 4(a) and 4(b)), a regulator of mitophagy induction, and VDAC1 (Figures 4(a) and 4(b)), a mitochondria marker protein. The results demonstrated that both PINK1 and VDAC1 were obviously decreased on Days 14 and 21 of pseudopregnancy (Figures 4(a) and 4(b)), indicating the curtailment of mitochondrial number, and this effect is dominated in a PINK1-independent manner during luteolysis.

3.3. HIF-1α/BNIP3 Pathway Was Activated during Luteolysis. Previous studies have revealed that hypoxia is involved in the apoptosis of luteal cells *in vitro* [9], implying that HIF-1α may participate in apoptosis during luteal regression *in vivo*. Thus, we detected the expression changes

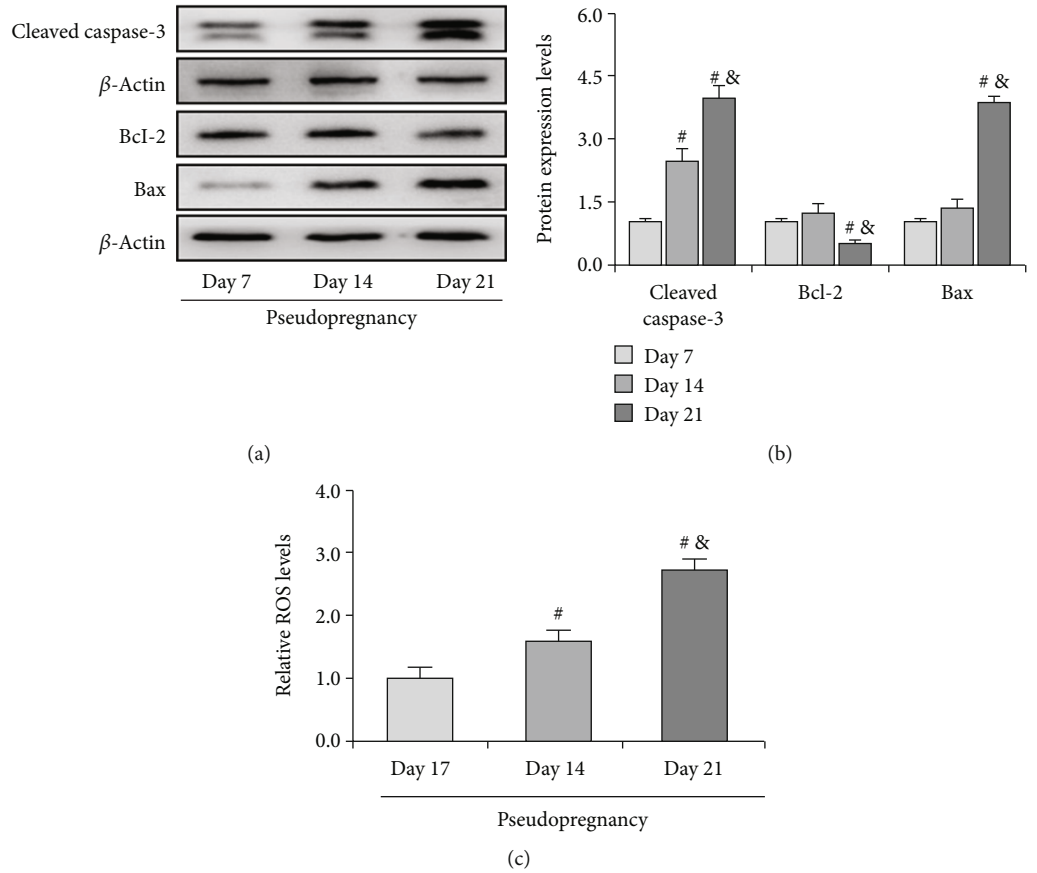

Figure 3: Expressions of cleaved caspase-3, Bcl-2, and Bax in the corpus luteum (CL) from pseudopregnant rats on Days 7, 14, and 21. (a) Representative immunoblotting of cleaved caspase-3, Bcl-2, and Bax. (b) Densitometric qualification of cleaved caspase-3, Bcl-2, and Bax. (c) Relative ROS level in CLs of pseudopregnant rats. $P < 0.05$ was considered to indicate a statistically significant difference. $^{\#}P < 0.05$, vs. Day 7. $^{\&}P < 0.05$, vs. Day 14.

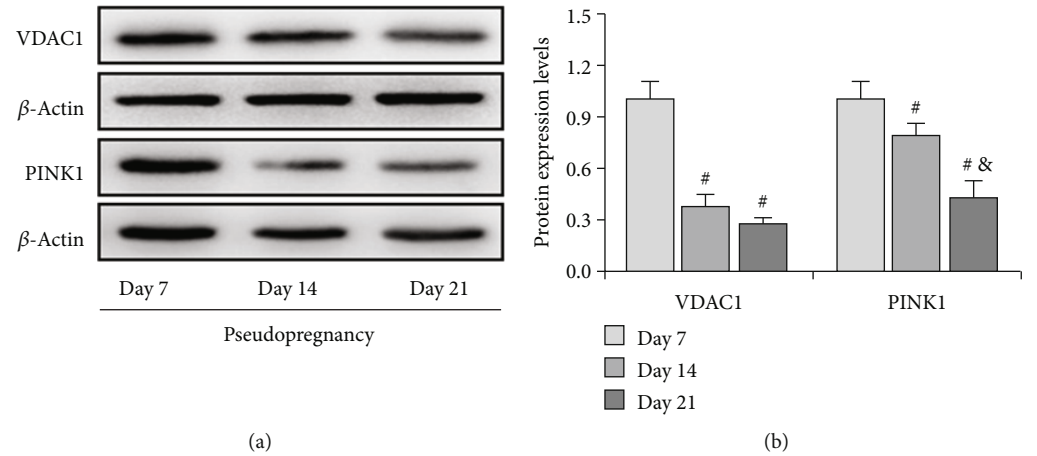

Figure 4: Expressions of VDAC1 and PINK1 in the corpus luteum (CL) from pseudopregnant rats on Days 7, 14, and 21. (a) Representative immunoblotting of VDAC1 and PINK1. (b) Densitometric qualification of VDAC1 and PINK1. Data are presented as the mean ± SE. The significant differences within or between groups were evaluated by one-way analysis of variance, followed by Tukey's multiple range test. $P < 0.05$ was considered to indicate a statistically significant difference. $^{\#}P < 0.05$, vs. Day 7. $^{\&}P < 0.05$, vs. Day 14.

of HIF-1α signaling and then found an obvious increase of HIF-1α on Day 21 of pseudopregnancy (Figures 5(a) and 5(b)), indicating that HIF-1α signaling was activated during luteolysis. Furthermore, we examined the expressions of BNIP3 and NIX, two main downstream factors of HIF-1α that are involved in autophagy induction [21], during luteal

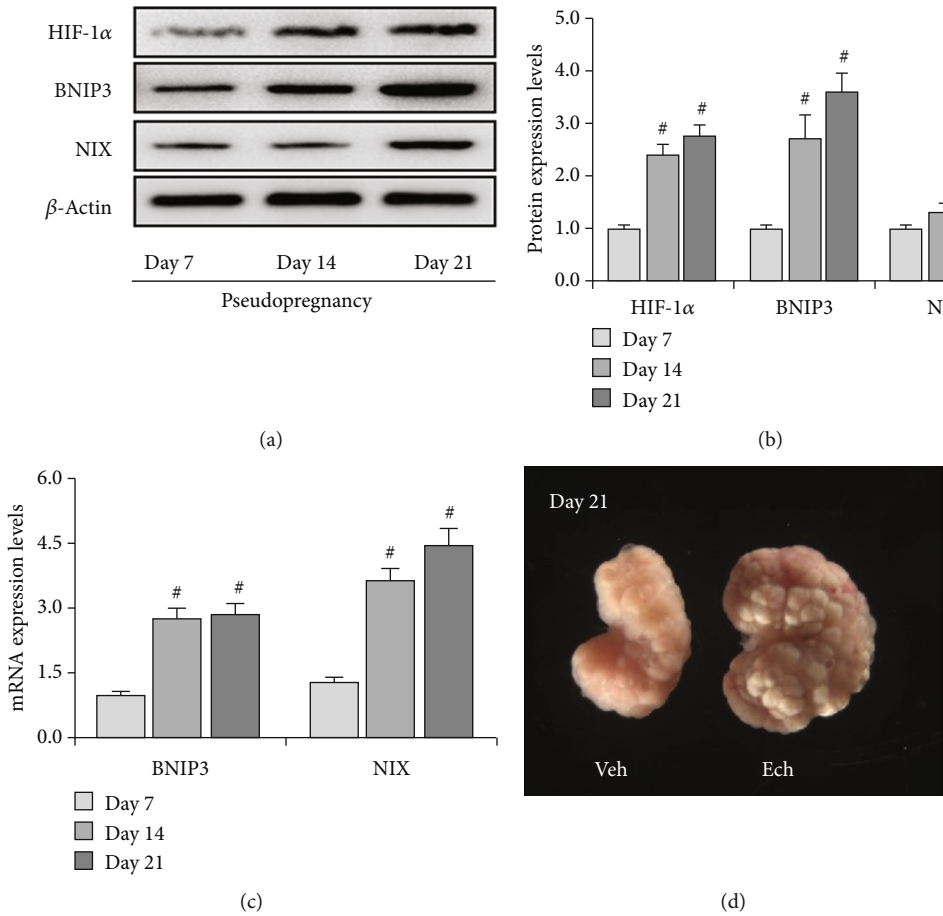

Figure 5: Expressions of HIF-1α, BNIP3, and NIX in the corpus luteum (CL) from pseudopregnant rats on Days 7, 14, and 21. (a) Representative immunoblotting of HIF-1α, BNIP3, and NIX. (b) Densitometric qualification of HIF-1α, BNIP3, and NIX. (c) BNIP3 and NIX mRNA expressions in the corpus luteum (CL) from pseudopregnant rats on Days 7, 14, and 21. (d) Morphology of the ovary on Day 21 from pseudopregnant rats treated with vehicle (Veh) or echinomycin (Ech). $P < 0.05$ was considered to indicate a statistically significant difference. $^{\#}P < 0.05$, vs. Day 7. $^{\&}P < 0.05$, vs. Day 14.

regression. The results showed that the expression of BNIP3 and NIX (Figures 5(a) and 5(b)) is increased in both mRNA and protein levels (Figure 5(c)) on Day 21 of pseudopregnancy, which was consistent with HIF-1α expression changes. Interestingly, treatment with HIF-1α inhibitor echinomycin (Ech) significantly delayed luteal atrophy during luteolysis (Figure 5(d)), further indicating that HIF-1α signaling may play an important role during luteal regression.

3.4. Inhibition of HIF-1α Signaling Alleviated ROS Production and Cell Apoptosis during Luteolysis. Given the fact that Ech retards luteal regression, we thereafter detected the expression of apoptosis-related proteins (Figures 6(a) and 6(b)) and found that Ech treatment obviously inhibited the upregulation of Bax (Figures 6(a) and 6(b)), the decrease of Bcl-2 (Figures 6(a) and 6(b)), and the activation of caspase-3 (Figures 6(a) and 6(b)) on Day 21 of pseudopregnancy. In addition, we also observed a decrease of ROS levels in Ech-treated rats, indicating a positive role of HIF-1α on ROS production (Figure 6(c)). The results demonstrated that inhibition of HIF-1α signaling could obviously diminish the production of ROS and the activation of caspase-3.

3.5. Inhibition of HIF-1α Signaling Ameliorated Autophagosome Accumulation. To verify the involvement of HIF-1α signaling in autophagy induction, we inhibited HIF-1α signaling by Ech and then examined the expressions of autophagy-related proteins (Figures 7 and 8) and HIF-1α downstream proteins (Figure 7). The results demonstrated that inhibition of HIF-1α activity obviously compromised the expressions of BNIP3 and NIX (Figures 7(a) and 7(b)) and also curtailed the levels of LC-3II (Figures 7(a) and 7(b)), which further consolidate that HIF-1α signaling participates in autophagy induction during luteolysis. Besides, we also observed the curb of p62 accumulation and the decrease of mitochondrial aggregation in CLs after Ech treatment (Figures 8(a) and 8(b)). Taken together, these findings indicated that HIF-1α signaling was involved in the degradation of mitochondria by mediating the upregulation of BNIP3 and NIX during the luteal regression.

3.6. Autophagy Is Involved in $PGF_{2\alpha}$-Induced ROS Production and Luteal Cell Death. To test whether dysregulation of autophagy is the causative factor for ROS production, we treated cells with $PGF_{2\alpha}$ to mimic luteal

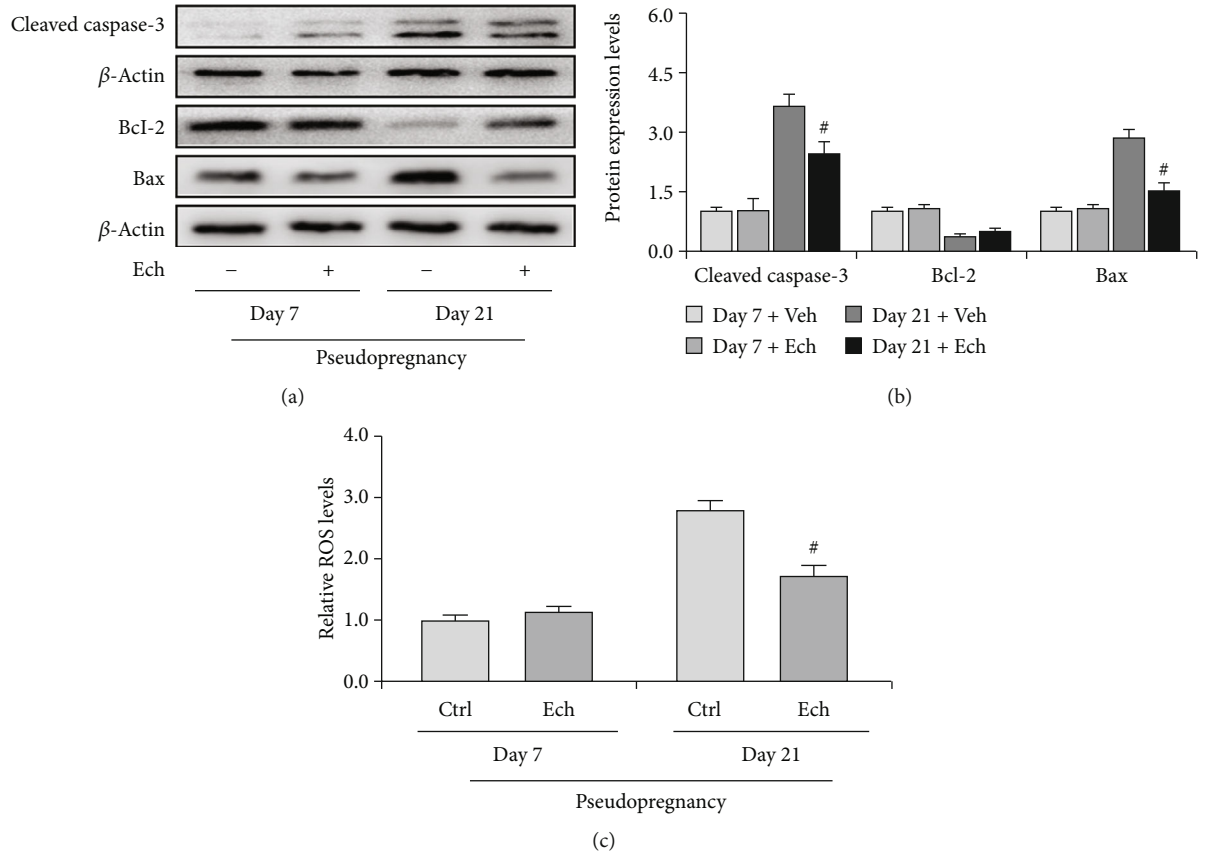

Figure 6: Expressions of cleaved caspase-3, Bcl-2, and Bax in the corpus luteum (CL) on Days 7 and 21 from pseudopregnant rats treated with vehicle (Veh) or echinomycin (Ech). (a) Representative immunoblotting of cleaved caspase-3, Bcl-2, and Bax. (b) Densitometric qualification of cleaved caspase-3, Bcl-2, and Bax. (c) Relative ROS level of CLs with or without Ech treatment on Days 7 and 21 of pseudopregnancy. $P < 0.05$ was considered to indicate a statistically significant difference. $^{\#}P < 0.05$, vs. Day 21 without Ech.

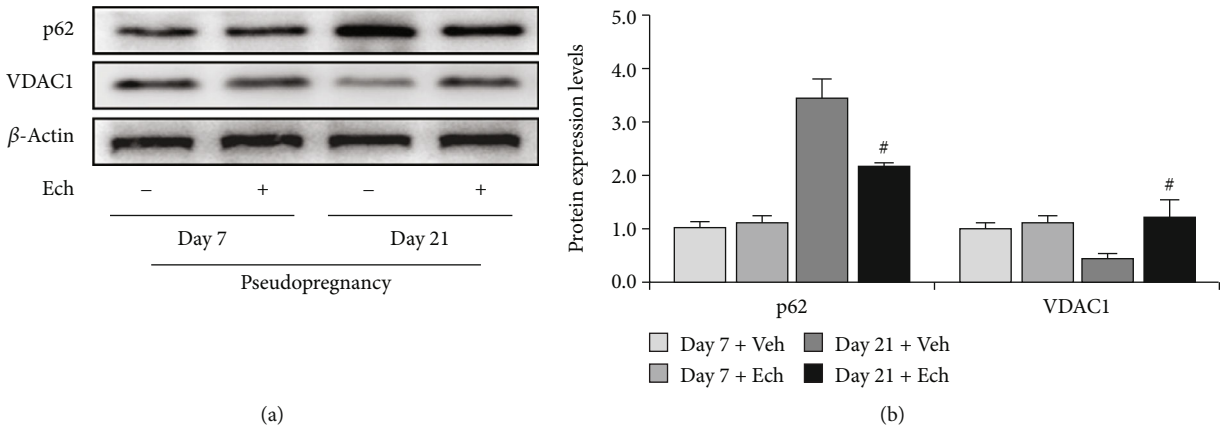

Figure 7: Expressions of LC-3I/II, BNIP3, and NIX in the corpus luteum (CL) on Days 7 and 21 from pseudopregnant rats treated with vehicle (Veh) or echinomycin (Ech). (a) Representative immunoblotting of LC-3I/II, BNIP3, and NIX. (b) Densitometric qualification of LC-3I/II, BNIP3, and NIX. $P < 0.05$ was considered to indicate a statistically significant difference. $^{\#}P < 0.05$, vs. Day 21 without Ech.

regression. Expectedly, we observed the increase of ROS under $PGF_{2\alpha}$ treatment. However, inhibition of autophagy by 3-MA obviously abrogated the increase of ROS (Figure 9(a)). This result indicated that increase of autophagy is, at least in part, the upstream of ROS generation during luteal regression. In addition, we also tested the effect of autophagy inhibition on cell apoptosis by detecting the expression of cleaved caspase-3. The results showed that caspase-3 activation is diminished after 3-MA treatment (Figure 9(b)), which is consistent with the trend of ROS

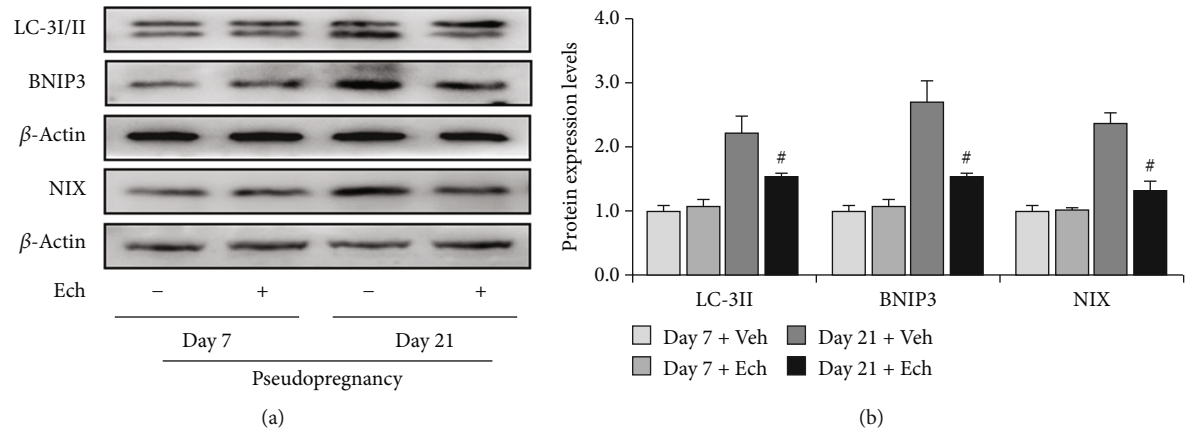

Figure 8: Expressions of p62 and VDAC1 in the corpus luteum (CL) on Days 7 and 21 from pseudopregnant rats treated with vehicle (Veh) or echinomycin (Ech). (a) Representative immunoblotting of p62 and VDAC1. (b) Densitometric qualification of p62 and VDAC1. $P < 0.05$ was considered to indicate a statistically significant difference. $^{\#}P < 0.05$, vs. Day 21 without Ech.

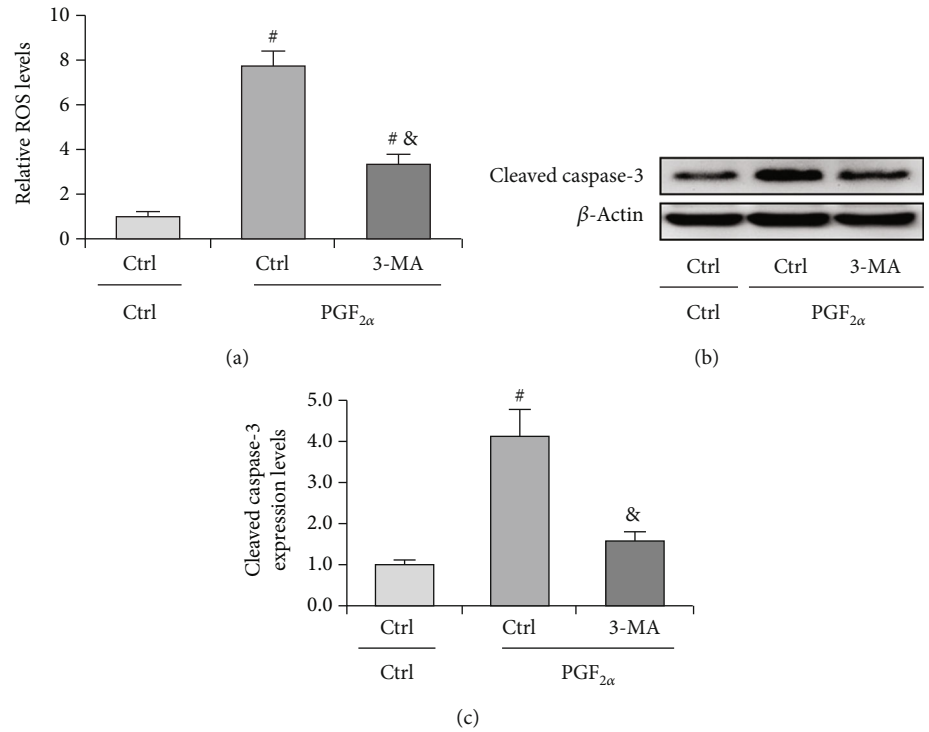

Figure 9: Inhibition of autophagy attenuates $PGF_{2\alpha}$-induced ROS production and cell apoptosis. (a) Inhibition of autophagy attenuates ROS production in luteal cells. Cells were treated with $PGF_{2\alpha}$ for 24 h with or without 3-MA. (b) Representative immunoblotting and (c) densitometric qualification for the effect of autophagy inhibition on caspase-3 activation. Cells were treated with $PGF_{2\alpha}$ for 24 h with or without 3-MA. $^{\#}P < 0.05$, vs. $PGF_{2\alpha}$.

generation. These findings suggested that autophagy can promote luteal cell apoptosis partially in an ROS-dependent manner.

4. Discussion

The corpus luteum is an important temporary gland in the mammalian ovary, the primary function of which is responsible for the production of progesterone and the maintenance of hormonal homeostasis during the menstrual period and pregnancy [1]. At the end of the menstrual period or the absence of pregnancy, CLs cease to produce progesterone and thereafter begin to regress so as to ultimately eliminate luteal structure from the ovary. Several lines of evidence have established that oxidative stress is engaged in luteal regression in rat [4] and human [5]. Furthermore, these findings demonstrated $PGF_{2\alpha}$, a luteal regression inducer, as a critical promoter of ROS production in luteal cells [1]. Particularly, $PGF_{2\alpha}$ can also promote luteal cell death by increasing autophagy [10]. The concomitant increase of autophagy level and ROS

production rise the possibility that the dysregulation of autophagy is an essential contributor to ROS production and luteal regression. In the present study, we showed that HIF-1α enables the upregulation of autophagy levels in luteal cells, which promotes luteal cell death and CL regression by inducing mitochondrial dysregulation and ROS production.

The regression of CL is a multistep biological progress, including functional regression and structural regression [10]. Previously, a wide spectrum of evidence has indicated that apoptosis is the main mechanism that contributes to the atrophy of CLs [11, 22]. Recent investigations also revealed that autophagy is widely involved in the regulation of luteal cell death during luteal regression in cattle [23], human [11], and rat [10]. In mammalian cells, the induction of autophagy plays dual roles in cell survival. The tolerable level of autophagy is required for the resistance of cell death whereas excessive autophagy is deleterious for cell survival. The accumulation of autophagosomes is one of the negative factors induced by autophagy that may disrupt the normal physiology of cells. We here detected the expression of p62, a marker protein indicating autophagosome degradation, Beclin1, an important scaffold protein in the initiation of autophagosomes [24], and LC-3II, a marker protein of autophagy induction. The results revealed that the level of p62 was concomitantly increased with the upregulation of LC-3II, indicating the accumulation of autophagosomes in luteal cells at the late stage of luteal regression. However, we did not observe the upregulation of Beclin1 on Day 14 or 21 of pseudopregnancy, indicating a noncanonical regulation of autophagy in rat CL. Similarly, Gaytan et al. also revealed the curtailment of the Beclin1 level at the late luteal phase of human CL [25], which is consistent with our present finding. Indeed, the induction of Beclin1-independent autophagy was also observed in some cancer cell lines [26–28]. The majority of this noncanonical autophagy regulation was demonstrated to play negative roles in cell survival.

In mammals, the regression of CLs is characterized by the degradation of the capillary network, which induces a hypoxic niche in CLs [1]. Under stressful conditions, cells could mobilize autophagic mechanisms to degrade redundant mitochondria so as to maintain the homeostasis of cellular oxygen consumption under hypoxia [29]. Mechanically, PINK1, BNIP3, and its homologous NIX are recognized as primary mediators involved in the induction of mitophagy in mammalian cells. Among which, BNIP3 mainly undertakes regulatory roles under a hypoxic environment [30–32]. In luteal cells, the expression of BNIP3 is significantly upregulated accompanied by enhanced cell apoptosis under hypoxia, suggesting a positive role in luteal apoptosis [9]. Thus, we examined the change of mitochondrial number during luteal regression and found that the number of mitochondria was decreased on Day 14 and especially Day 21 of pseudopregnancy accompanied by the increase of HIF-1α, BNIP3, and NIX. However, we observed a decrease of PINK1 during regression. These findings suggest that HIF-1α is involved in mitochondrial loss in late CLs by inducing BNIP3.

The dysregulation of mitochondrial homeostasis is a potential contributor to cell apoptosis, especially by initiating oxidative stress [33]. The atrophy and elimination of CLs implicate massive apoptosis of luteal cells during luteal regression [1], while its underlying mechanism still remains largely unknown. We here revealed that the expressions of apoptosis-related proteins, cleaved caspase-3, and Bax were significantly upregulated during luteolysis, which is consistent with previous reports [34]. Also, we verified the role of HIF-1α *in vivo* by treating pseudopregnant rats with Ech. Expectedly, Ech treatment obviously delayed mitochondrial loss, BNIP3 expression, caspase-3 activation, and the pace of luteal regression when compared with the control. These findings indicated that HIF-1α signaling plays a positive role in the apoptosis of luteal cells and the atrophy of CLs during luteolysis. It is noteworthy that autophagy can be regulated by different mechanisms during luteal regression and may also exist divergences between species [23].

Previously, *in vitro* studies have suggested that $PGF_{2\alpha}$, an important trigger of mammalian luteal functional regression, is a crucial inducer of oxidative stress and apoptosis in rat luteal cells [1]. Of note, it also exhibits a positive effect on autophagy regulation [10]. In the present study, we demonstrated that autophagy-induced luteal cell apoptosis is partially dependent on oxidative stress, and inhibition of autophagy can ameliorate ROS production and cell apoptosis.

Taken together, in the present study, we found that the HIF-1α/BNIP3 signaling pathway is involved in the apoptosis of luteal cells and the regression of CL by inducing oxidative stress.

Data Availability

The original contributions presented in the study are included in the article/Supplementary Materials; further inquiries can be directed to the corresponding author.

Conflicts of Interest

The authors declare that they have no competing interests.

Authors' Contributions

The work was conceived by ZT, JC, ZZ, and ZW; the experiment was performed by ZT, JC, ZZ, JB, RX, and QL; the data was analyzed by ZT, JC, ZZ, JB, RX, QL, and ZW; the reagents/materials/analysis tools were contributed by ZT, JC, ZZ, JB, RX, QL, and ZW. Manuscript writing was performed by ZT, JC, ZZ, and ZW. All authors reviewed and approved the final version of the manuscript for publication. Zonghao Tang, Jiajie Chen, and Zhenghong Zhang contributed equally to this work.

Acknowledgments

This work was supported by the Special Funds of the Central Government Guiding Local Science and Technology Development (2020L3008), Open foundation of Medical Electrophysiological Key Laboratory of Sichuan Province and Ministry of Education (Key-ME-2020-006), and Fujian

Provincial Natural Science Foundation of China (2020J01176 and 2021I01010045).

Supplementary Materials

Supplemental Table 1: antibody information for western blotting. *(Supplementary Materials)*

References

[1] H. R. Behrman, T. Endo, R. F. Aten, and B. Musicki, "Corpus luteum function and regression," *Reproductive Medicine Review*, vol. 2, no. 3, pp. 153–180, 1993.

[2] G. D. Niswender, J. L. Juengel, P. J. Silva, M. K. Rollyson, and E. McIntush, "Mechanisms controlling the function and life span of the corpus luteum," *Physiological Reviews*, vol. 80, no. 1, pp. 1–29, 2000.

[3] H. R. Behrman and S. L. Preston, "Luteolytic actions of peroxide in rat ovarian cells," *Endocrinology*, vol. 124, no. 6, pp. 2895–2900, 1989.

[4] J. C. M. Riley and H. R. Behrman, "In vivo generation of hydrogen peroxide in the rat corpus luteum during luteolysis," *Endocrinology*, vol. 128, no. 4, pp. 1749–1753, 1991.

[5] T. Endo, R. F. Aten, L. Leykin, and H. R. Behrman, "Hydrogen peroxide evokes antisteroidogenic and antigonadotropic actions in human granulosa luteal cells," *The Journal of Clinical Endocrinology & Metabolism*, vol. 76, no. 2, pp. 337–342, 1993.

[6] R. Nishimura and K. Okuda, "Multiple roles of hypoxia in ovarian function: roles of hypoxia-inducible factor-related and -unrelated signals during the luteal phase," *Reproduction Fertility & Development*, vol. 28, no. 10, p. 1479, 2015.

[7] L. Liu and N. A. Clipstone, "Prostaglandin F2α induces the normoxic activation of the hypoxia-inducible factor-1 transcription factor in differentiating 3T3-L1 preadipocytes: potential role in the regulation of adipogenesis," *Journal of Cellular Biochemistry*, vol. 105, no. 1, pp. 89–98, 2008.

[8] E. Walewska, K. Wołodko, D. Skarzynski, G. Ferreira-Dias, and A. Galvão, "The interaction between nodal, hypoxia-inducible factor 1 alpha, and thrombospondin 1 promotes luteolysis in equine corpus luteum," *Frontiers in endocrinology*, vol. 10, p. 667, 2019.

[9] R. Nishimura, J. Komiyama, Y. Tasaki, T. J. Acosta, and K. Okuda, "Hypoxia promotes luteal cell death in bovine corpus luteum," *Biology of Reproduction*, vol. 78, no. 3, pp. 529–536, 2008.

[10] J. Choi, M. Jo, E. Lee, and D. Choi, "The role of autophagy in corpus luteum regression in the rat," *Biology of reproduction*, vol. 85, no. 3, pp. 465–472, 2011.

[11] T. Shikone, M. Yamoto, K. Kokawa, K. Yamashita, K. Nishimori, and R. Nakano, "Apoptosis of human corpora lutea during cyclic luteal regression and early pregnancy," *The Journal of clinical endocrinology and metabolism*, vol. 81, no. 6, pp. 2376–2380, 1996.

[12] L. A. Booth, S. Tavallai, H. A. Hamed, N. Cruickshanks, and P. Dent, "The role of cell signalling in the crosstalk between autophagy and apoptosis," *Cellular signalling*, vol. 26, no. 3, pp. 549–555, 2014.

[13] N. Chen and V. Karantza-Wadsworth, "Role and regulation of autophagy in cancer," *Biochimica et Biophysica Acta (BBA)-Molecular Cell Research*, vol. 1793, no. 9, pp. 1516–1523, 2009.

[14] W. M. Kuwabara, R. Curi, and T. C. Alba-Loureiro, "Autophagy is impaired in neutrophils from streptozotocin-induced diabetic rats," *Frontiers in Immunology*, vol. 8, p. 24, 2017.

[15] N. Mizushima and M. Komatsu, "Autophagy: renovation of cells and tissues," *Cell*, vol. 147, no. 4, pp. 728–741, 2011.

[16] T. R. Gawriluk, A. N. Hale, J. A. Flaws, C. P. Dillon, D. R. Green, and E. B. Rucker 3rd., "Autophagy is a cell survival program for female germ cells in the murine ovary," *Reproduction*, vol. 141, no. 6, pp. 759–765, 2011.

[17] J. Zhou, W. Yao, C. Li, W. Wu, Q. Li, and H. Liu, "Administration of follicle-stimulating hormone induces autophagy via upregulation of HIF-1 _α_ in mouse granulosa cells," *Cell death & disease*, vol. 8, no. 8, p. e3001, 2017.

[18] Z. Tang, Z. Zhang, H. Zhang et al., "Autophagy attenuation hampers progesterone synthesis during the development of pregnant corpus luteum," *Cell*, vol. 9, no. 1, p. 71, 2020.

[19] J. Kim, C.-H. Chen, J. Yang, and D. Mochly-Rosen, "Aldehyde dehydrogenase 2 $*$ 2 knock-in mice show increased reactive oxygen species production in response to cisplatin treatment," *Journal of Biomedical Science*, vol. 24, no. 1, pp. 33–38, 2017.

[20] M. Band, A. Joel, A. Hernandez, and A. Avivi, "Hypoxia-induced *BNIP3* expression and mitophagy: *in vivo* comparison of the rat and the hypoxia-tolerant mole rat," *The FASEB Journal*, vol. 23, no. 7, pp. 2327–2335, 2009.

[21] H. R. Mellor and A. L. Harris, "The role of the hypoxia-inducible BH3-only proteins BNIP3 and BNIP3L in cancer," *Cancer and Metastasis Reviews*, vol. 26, no. 3-4, pp. 553–566, 2007.

[22] J. L. Juengel, H. A. Garverick, A. L. Johnson, R. S. Youngquist, and M. F. Smith, "Apoptosis during luteal regression in cattle," *Endocrinology*, vol. 132, no. 1, pp. 249–254, 1993.

[23] M. Aboelenain, M. Kawahara, A. Z. Balboula et al., "Status of autophagy, lysosome activity and apoptosis during corpus luteum regression in cattle," *Journal of Reproduction and Development*, vol. 61, no. 3, pp. 229–236, 2015.

[24] D. J. Klionsky, F. C. Abdalla, H. Abeliovich et al., "Guidelines for the use and interpretation of assays for monitoring autophagy," *Autophagy*, vol. 8, no. 4, pp. 445–544, 2012.

[25] M. Gaytan, C. Morales, J. E. Sanchez-Criado, and F. Gaytan, "Immunolocalization of beclin 1, a bcl-2-binding, autophagy-related protein, in the human ovary: possible relation to life span of corpus luteum," *Cell and tissue research*, vol. 331, no. 2, pp. 509–517, 2008.

[26] Y. Grishchuk, V. Ginet, A. C. Truttmann, P. G. H. Clarke, and J. Puyal, "Beclin 1-independent autophagy contributes to apoptosis in cortical neurons," *Autophagy*, vol. 7, no. 10, pp. 1115–1131, 2011.

[27] L. Sun, N. Liu, S. S. Liu et al., "Beclin-1-independent autophagy mediates programmed cancer cell death through interplays with endoplasmic reticulum and/or mitochondria in colbat chloride-induced hypoxia," *American journal of cancer research*, vol. 5, no. 9, pp. 2626–2642, 2015.

[28] S. Tian, J. Lin, J. Zhou et al., "Beclin 1-independent autophagy induced by a Bcl-XL/Bcl-2 targeting compound, Z18," *Autophagy*, vol. 6, no. 8, pp. 1032–1041, 2010.

[29] L. Liu, D. Feng, G. Chen et al., "Mitochondrial outer-membrane protein FUNDC1 mediates hypoxia-induced mitophagy in mammalian cells," *Nature cell biology*, vol. 14, no. 2, pp. 177–185, 2012.

[30] G. Chen, W. Zhang, Y. P. Li et al., "Hypoxia-induced autophagy in endothelial cells: a double-edged sword in the

progression of infantile haemangioma?," *Cardiovascular research*, vol. 98, no. 3, pp. 437–448, 2013.

[31] S. P. Elmore, T. Qian, S. F. Grissom, and J. J. Lemasters, "The mitochondrial permeability transition initiates autophagy in rat hepatocytes," *Faseb Journal Official Publication of the Federation of American Societies for Experimental Biology*, vol. 15, no. 12, article 2286, pp. 1–17, 2001.

[32] R. Y. Shi, S. H. Zhu, V. Li, S. B. Gibson, X. S. Xu, and J. M. Kong, "BNIP3 interacting with LC3 triggers excessive mitophagy in delayed neuronal death in stroke," *CNS neuroscience & therapeutics*, vol. 20, no. 12, pp. 1045–1055, 2014.

[33] C. García-Ruiz and J. C. Fernández-Checa, "Mitochondrial oxidative stress and antioxidants balance in fatty liver disease," *Hepatology communications*, vol. 2, no. 12, pp. 1425–1439, 2018.

[34] C. Stocco, C. Telleria, and G. Gibori, "The molecular control of corpus luteum formation, function, and regression," *Endocrine reviews*, vol. 28, no. 1, pp. 117–149, 2007.

Hindawi
Oxidative Medicine and Cellular Longevity
Volume 2021, Article ID 5481228, 15 pages
https://doi.org/10.1155/2021/5481228

Research Article

Fibroblast Growth Factor 13 Facilitates Peripheral Nerve Regeneration through Maintaining Microtubule Stability

Rui Li,[1,2] **Xuetao Tao**,[3] **Minghong Huang**,[1] **Yan Peng**,[4] **Jiahong Liang**,[5] **Yanqing Wu**,[6] **and Yongsheng Jiang**[1]

[1]*The Affiliated Xiangshan Hospital of Wenzhou Medial University, No. 291 Donggu Road, Xiangshan County, Zhejiang 315000, China*
[2]*PCFM Lab, GD HPPC Lab, School of Chemistry, Sun Yat-sen University, Guangzhou 510275, China*
[3]*The Second Affiliated Hospital, Zhejiang University School of Medicine, Hangzhou, Zhejiang 310009, China*
[4]*Hangzhou Institute for Food and Drug Control, Hangzhou, Zhejiang 310014, China*
[5]*Betta Pharmaceuticals Co., Ltd, Hangzhou, Zhejiang 310000, China*
[6]*The Institute of Life Sciences, Engineering Laboratory of Zhejiang Province for Pharmaceutical Development of Growth Factors, Biomedical Collaborative Innovation Center of Wenzhou, Wenzhou University, Wenzhou, Zhejiang 325035, China*

Correspondence should be addressed to Rui Li; xiaoerrui1989@163.com, Yanqing Wu; yqwu220946@yeah.net, and Yongsheng Jiang; shenren34127@163.com

Received 18 May 2021; Accepted 2 August 2021; Published 20 August 2021

Academic Editor: Ji Bihl

Peripheral nerve injury (PNI), resulting in the impairment of myelin sheaths and axons, seriously affects the transmission of sensory or motor nerves. Growth factors (GFs) provide a biological microenvironment for supporting nerve regrowth and have become a promising alternative for repairing PNI. As one number of intracellular growth factor family, fibroblast growth factor 13 (FGF13) was regard as a microtubule-stabilizing protein for regulating cytoskeletal plasticity and neuronal polarization. However, the therapeutic efficiency and underlying mechanism of FGF13 for treating PNI remained unknown. Here, the application of lentivirus that overexpressed FGF13 was delivered directly to the lesion site of transverse sciatic nerve for promoting peripheral nerve regeneration. Through behavioral analysis and histological and ultrastructure examinations, we found that FGF13 not only facilitated motor and sense functional recovery but also enhanced axon elongation and remyelination. Furthermore, pretreatment with FGF13 also promoted Schwann cell (SC) viability and upregulated the expression cellular microtubule-associated proteins *in vitro* PNI model. These data indicated FGF13 therapeutic effect was closely related to maintain cellular microtubule stability. Thus, this work provides the evident that FGF13-medicated microtubule stability is necessary for promoting peripheral nerve repair following PNI, highlighting the potential therapeutic value of FGF13 on ameliorating injured nerve recovery.

1. Introduction

Peripheral nerve injury (PNI) is one of the most traumatic disorders for triggering a decrease or a complete loss of motor and sensory function in clinical practice [1]. It has been reported that an estimated annual incidence of 67,800 major PNIs occur in the United States alone, and the annual health-care dollars per individual were approximately $150 billion, causing an enormous socioeconomic burden [2, 3]. Despite the developing peripheral nerve has an intrinsic capability for regeneration, the outcomes of optimal structural and functional recovery are not always satisfactory [4]. Recent advances in nerve reconstruction and autologous nerve grafting remain the gold standard technique for the repair of acute nerve injury; however, these treatments exist some limitations, including the limited amount of autologous donor nerves, neuronal mismatch between the donor and the recipient site, even neuroma formation at the donor site [5, 6]. To overcome these limitations, current therapeutic strategies are focused on administration of exogenous growth

factors (GFs) as a therapeutic relevant agent to ameliorate axonal regrowth and remyelination following PNI [7].

GFs refer to a neurotrophic factor family of bioactive cytokines with the ability to regulate cellular proliferation, migration, and differentiation. Several preclinical trials have described that exogenous application of GFs to the lesion site of peripheral nerve is able to stimulate axonal sprouting, myelination, neurogenesis, and/or neovascularization [8–10]. These encouraging outcomes reveal that GFs may act as the potent therapeutic drugs for repairing PNI. As an intracrine protein of the GF subfamily, fibroblast growth factor 13 (FGF 13) is not only widely distributed in human adult and developing brain but also overexpressed in the mammalian heart. Initially, FGF13 is regarded as a candidate gene for diagnosing X-chromosome-linked mental retardation (XLMR) and negatively enhancing caveolae-mediated mechanoprotection [11, 12]. In the subsequent evaluation, FGF13 has been identified as a microtubule-stabilizing agent for guiding growth cone initiation, neuronal polarization, and axonal extension. For instance, lentivirus-mediated FGF13 overexpression could increase the level of microtubule stabilizing proteins to enhance axon regeneration and functional recovery after spinal cord injury (SCI) [13]. In early embryonic development, FGF13 also participated in neural differentiation via MEK5-ERK5 pathway [14]. Additionally, FGF13-deficient mice exhibited learning and memory impairment due to the imbalance of microtubule assembly in neocortex and hippocampus region [15]. Based on the above fact, we try to reveal whether FGF13 also plays an essential role on restoring PNI recovery.

As one component of cytoskeleton, microtubule provides an organizational framework to control neuronal extension, retraction, and steering through modifying growth cone dynamic growth and shrinkage. In living cells, microtubule stabilization is critical for neural polarization and axon formation, which can be reflected by detecting the content of microtubule-associated proteins (MAPs), such as acetylated- (Ace-) tubulin, tyrosinated- (Tyr-) tubulin, Tau, Kinesin-5, and Dynein. Increasingly, evidences have suggested that microtubule stability was closely associated with neuronal traumatic diseases [16]. Manipulation of microtubule stabilization with Taxol could reduce fibrotic scar formation and enable axonal regeneration after SCI via facilitating intrinsic axon growth capacity [17]. In line with this efficacy, systemic administration of epothilone B further induced microtubule polymerization into the neurite tips to restore axon elongation under an inhibitory environment after SCI [18]. Mechanistically, this positive feedback was modulated by a specific autophagy-inducing peptide, Tat-beclin1, suggesting a critical role of autophagy in maintaining microtubule stability [19]. Given that axon regeneration and scarring reduction appear to rely indirectly or directly on microtubule dynamics and stability, this mechanism may possibly play an instructive role in axon formation and remyelination following PNI.

In this work, we aim to identify whether FGF13 has a certain capability for improving the injured peripheral nerve regeneration in a rat model and reveal its underlying molecular mechanism via various comprehensive evaluations, including histological, morphological, and functional assessments. Our data proved that overexpression of FGF13 could maintain microtubule stabilization in Schwann cells (SCs) to promote their survival, axon regrowth, and remyelination, resulting in the improvement of locomotor recovery following PNI. These results suggest, for the first time, that supplement of FGF13 is an effective and feasible therapeutic strategy for rehabilitating PNI.

2. Materials and Methods

2.1. Animals and Ethics Statement. Forty male Sprague-Dawley rats, weighing from 200 to 220 g, were obtained from the Animal Center of the Chinese Academy of Science (Shanghai, China). The rats were individually housed in wire bottom cages under humidity (50-60%) and temperature (23-25°C) controlled conditions with a 12 h light/dark cycle. The animals had free access to water and food. All protocols involving animal care and experimental procedures were reviewed and approved by the Chinese National Institutes of Health.

2.2. Preparation of Nerve Transection Model and Drug Application. For the surgical procedure of sciatic nerve transection model, after anesthetizing with 4% pentobarbital sodium (30 mg/kg, i.p. injection), the rats were fixed on the operating table and shaved the hair on the right thigh. Then, the right sciatic nerve was isolated and exposed carefully by cutting skin and blunt splitting dorsolateral gluteal muscles. Next, the sciatic nerve was transected at approximately 0.5 cm distal to the sciatic notch using fresh scalpel blade. The proximal and distal ends of the cut nerves were sutured by 10/0 polypropylene sutures (Ethicon, Somerville, NY) under a microscope, followed by suturing the muscles and skin using 7/0 sutures.

After surgery, all the tested rats were randomly divided into three groups: a FGF13 lentiviral vector-treated group (FGF13), a blank lentiviral vector-treated group (vehicle), and a saline-treated group (PNI). Each group was consisted of 10 rats. For the FGF13 group, each animal was orthotopical injection of 10 μl (2×10^8 TU ml^{-1}) [13] lentivirus (LV) which expressed FGF13 into the sutured site via a Hamilton microsyringe at a rate of 500 nl min^{-1}. The LV-FGF13 were purchased from Shanghai GeneChem Co., Ltd. (Shanghai, China). The primer of lentiviral particles of FGF13 sequence was used forward: 5′-CCAACTTTGTGCCAACCGGTC GCCACCATGGCTTTGTTAAGGAAGTC-3′, reverse: 5′-AATGCCAACTCTGAGCTTCGTTGATTCATTGTGGCT CATG-3′. The vehicle group was administrated the same dosages of lentiviral vector. After injection, the needle was left in place for an additional 10 min and then slowly withdraw. Similarly, the rats in the PNI group received the same dose of saline. For the sham operation (control) group, the animals underwent only the surgical procedure without affecting the sciatic nerve.

2.3. Functional Recovery Analysis. The neurological recovery in all testing animals was evaluated through walking track analysis and von Frey hair test once a week for 6

weeks after surgery. The walking track analysis was quantified using the sciatic function index (SFI), which was calculated as the following formula proposed by de Medinaceli et al. [20]: $\mathrm{SFI} = (-38.3 \times (\mathrm{EPL} - \mathrm{NPL})/\mathrm{NPL}) + (109.5 \times (\mathrm{ETS} - \mathrm{NTS})/\mathrm{NTS}) + (13.3 \times (\mathrm{EIT} - \mathrm{NIT})/\mathrm{NIT}) - 8.8$. These indexes were taken both from the foot of the experimental foot print length (EPL), experimental foot toe spread (ETS), experimental foot intermediary toe (EIT), and nonoperated side (NPL, NTS, and NIT). The SFI value of about 0 represents normal recovery, while the SFI value close to -100 indicates total impairment.

The mechanical allodynia threshold was evaluated by von Frey hair test which described elsewhere [21]. Briefly, all the experimental rats were habituated in a glass cubicle on an elevated wire mesh platform for at least 1 hour. Then, the right hind paw in each animal was stimulated with a series of calibrated monofilaments (Stoelting, Wood Dale, IL). Monofilaments were applied with a constant increasing pressure until a perceptible bend of approximately 90° for lasting 2 seconds. At this moment, the monofilament of definitive ascending force was also recorded as the positive withdrawal force. The experimental process was repeated three times with an interval of 15 minutes by the same investigator who was blinded to the group design.

2.4. Tissue Preparation. At postoperative 6 weeks, all rats were anesthetized and sacrificed to harvest the regenerated sciatic nerves and gastrocnemius muscle. Meanwhile, the wet muscle weight in each rat was recorded. For histological staining, the nerve and muscle tissues were fixed with 4% paraformaldehyde at 4°C for 24 h. Subsequently, the samples were embedded in paraffin, cut into longitudinal or transverse sections of 5 μm thickness using a microtome (Thermo Fisher Scientific HM 315, Waltham, USA), and mounted on slides. For immunofluorescence staining, the 0.5 cm segment of regenerative nerve was embedded in optimal cutting temperature compound (OCT, Sakura Tokyo, Japan) and cut into 10 μm sections using a cryostat (Leica Microsystems Wetzlar GmbH, Hesse-Darmstadt, Germany). For immunoblotting and RT-PCR detection, the harvested sciatic nerve segment (0.5 cm length) taken from the lesion regions was immediately stored at -80°C.

2.5. Histological Staining and Morphometric Analysis. The serial paraffin sections were deparaffinized and rehydrated with xylene and a gradient ethanol solution. Thereafter, both of nerve and muscle sections were received Hematoxylin and Eosin (H&E) staining using H&E kit (Beyotime Institute of Biotechnology, China). For muscle sections, they were stained with H&E hematoxylin and eosin reagents for 5 min and 1 min, respectively. For nerve tissue sections, they were stained with these two dyes for 5 min and 8 min, respectively. The nerve sections also performed Masson's trichrome staining using Masson's trichrome staining kit (Solarbio, G1340) according to the instructions. Briefly, sections were first underwent deparaffinage and rehydration as describe by H&E staining, followed by staining with nucleus, fibrous, and collagen using hematoxylin, ponceau acid fuchsine solution, and aniline blue for 5 min, 5 min, and 20 s, respectively. After dehydrating, slides were mounted with neutral resin and covered by cove using rslips. In the end, all staining sections were observed and photographed using a Nikon microscope (Nikon, Tokyo, Japan).

The myelin sheath regeneration was also evaluated by transmission electromicroscope observation as previously described elsewhere [22]. Briefly, 2 mm regenerated nerve samples were fixed with 2.5% glutaraldehyde for 4 h, followed by postfixing with 1% osmium and 1% uranyl acetate for 1 h, respectively. After dehydrating in a graded acetone series, the samples were embedded in an Epon 812 resin and cut into semithin sections (thickness: 1.0 μm) for toluidine blue staining. The ultrathin cross sections with a thickness of 50–60 nm were also prepared and then were stained with lead citrate and uranyl acetate for the transmission electron microscope observation (TEM; HT7700, Hitachi, Ltd., Japan).

For the myelinated indexes including myelin counts, diameter of myelin sheath, thickness of myelin sheath, and G-ratio were calculated using the following two equations:

$$\text{Thickness of myelin sheath} = \frac{(\text{Myelin diameter} - \text{Axon diameter})}{2}, \tag{1}$$

$$\text{G} - \text{ratio} = \frac{\text{Axon diameter}}{\text{Myelin diameter}}, \tag{2}$$

where for individual myelin, the way for measuring axon diameter and myelin diameter per myelin was according to the bottom panel enlarged images in Figure 1(b). Quantification of myelin counts, axon diameter, and myelin diameter could be automatically obtained using the ImageJ software. The data of myelin counts were performed through measuring five randomly selected fields in each animal. For quantifying axon and myelin diameter, 70 myelin sheaths were randomly selected from at least 10 images per animal. Each group contained 5 animals. All counting were quantified by two blinded independent observers who were blind to the experimental procedures and samples.

2.6. Immunofluorescence. After blocking with 5% BSA for 30 min, frozen sections were colabeled with anti-NF-200 (1 : 100,000, ab4680, Abcam) and anti-MBP (1 : 1000, ab40390, Abcam) primary antibodies, overnight at 4°C. Then, FITC-conjugated anti-rabbit IgG (Abcam, ab150073) and TRITC-conjugated anti-mouse IgG (Abcam, ab7065) were diluted with PBS at the concentration of 0.67 μg/ml and dropped in the tissue samples, followed by incubating at 37°C for 1 h in dark condition. After staining nuclei with 0.1% of 4,6-diamidino-2-phenylindole (DAPI) for 5 min, the stained sections were observed and imaged using a confocal fluorescence microscope (Nikon, Japan).

With the observer blinded to the identity of the groups, approximately three-fourths sections of the regenerating bridge were photographed at high-power light microscopy (400x). Photographs were divided into several regions with 100 μm interval. Axon numbers, $\mathrm{NF200}^+$ and MBP^+ positive signals in each individual region of longitudinal section of the nerve cable, were analyzed using the ImageJ software as previously described [23]. The diagrammatic sketch of regional

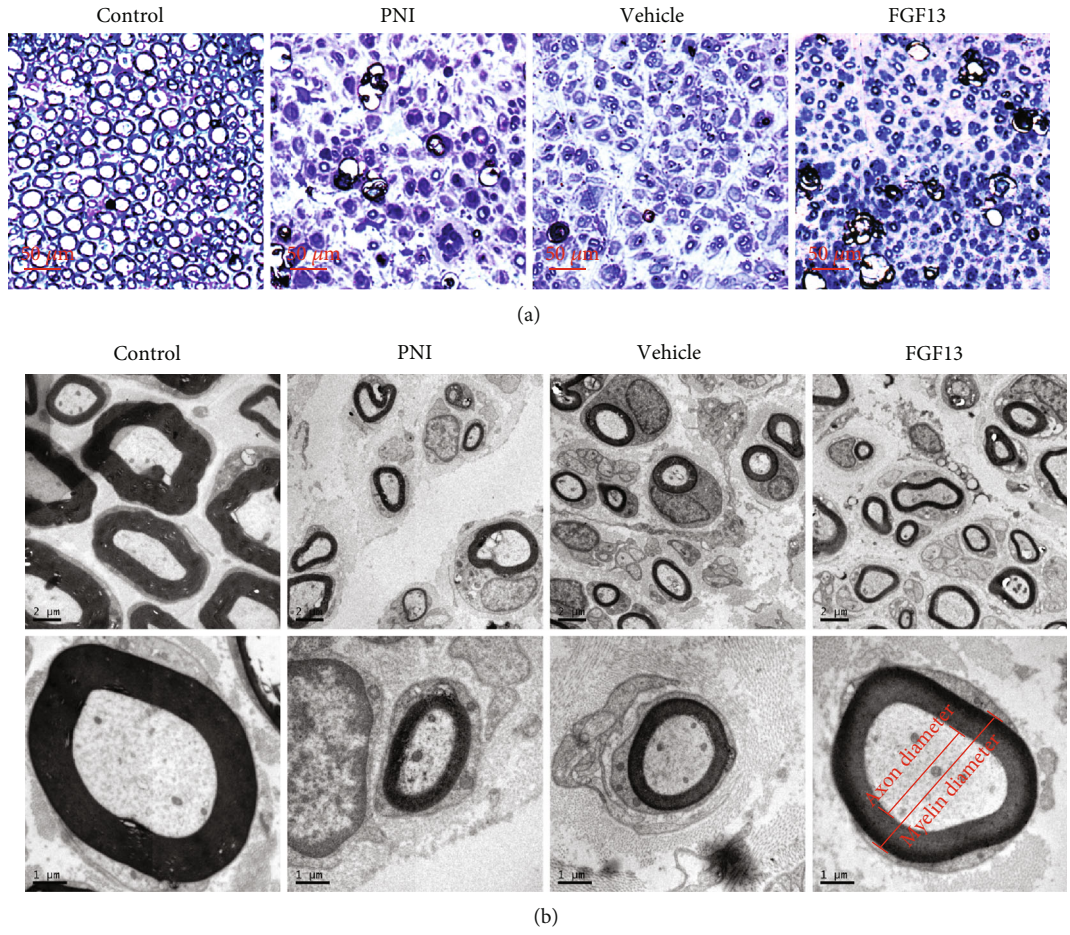

Figure 1: Analysis of regenerating cables at week 6 after injury. (a) Representative semithin transverse sections of regenerated nerves stained by toluidine blue in four groups; (b) TEM of ultrathin sectioned nerves of the four groups. The gross myelin distribution and regeneration were clearly seen via the lower magnification (2 μm) in the middle panel. The bottom panel enlarged images with the higher magnification of 1 μm were representative individual myelin in each group and not from the middle panel.

dividualing and identifying was shown in Figure 2(b). Three sections per animal and three animals per group were randomly selected for statistical analysis.

2.7. Immunoblotting. Total protein was extracted from regenerated sciatic nerve using RIPA lysis buffer containing 1% protease and phosphatase inhibitors. The protein concentration in different samples was measured using the BCA Assay Kit. A total of 80 μg of protein was separated by 12% (w/v) gels and then transferred to a PVDF membrane (Millipore), followed by blocking with 5% w/v nonfat milk for 1.5 h. After washing with TBST for three times, the PVDF membranes were incubated overnight at 4°C with primary antibodies targeting the following proteins: Ace-tubulin (1 : 1000, CST, Catalog No. #5335), Tyr-tubulin (1 : 500, Sigma, Catalog No. T9026), Tau (1 : 1000, Abcam, Catalog No. ab92676), Kinesin-5 (1 : 1000, Abcam, Catalog No. ab167429), Dynein (1 : 1000, Abcam, Catalog No. ab171964), Bax (1 : 500, CST, Catalog No. #14796), Bcl-2 (1 : 500, CST, Catalog No. #4223), and Cleaved caspase-3 (1 : 500, Abcam, Catalog No. ab2302). The next day, blots were washed in TBST and incubated with HRP-labeled secondary antibodies (1 : 2000 dilution) for 1 h at 25°C temperature. Immunobands were visualized by ChemiDocXRS + Imaging System, and band intensity was quantified by the ImageJ software.

2.8. Preparation of Myelin Extracts. Myelin debris were extracted from uncut sciatic nerve in adult rats as described in previous with modification [8]. Briefly, the collecting sciatic nerves were homogenized in 0.32 M sucrose using a homogenizer (PRO 200, USA), followed by centrifuging twice at 1,5000 g for 1 h. After removal of sucrose, myelin fractions were added PBS and filtered through 0.22 μm filters to sterilize and remove any particulate substance.

2.9. Cell Culture, Transfection, and Treatments. The RSC 96 cells (a rat Schwann cell line) were purchased from the cell bank of the Chinese Academy of Sciences (Shanghai, China). Before transfection, cells were maintained in Dulbecco's modified Eagle Medium (DMEM, Gibco) containing 10% foetal bovine serum (FBS, Thermo Fisher Scientific) and incubated in a humidified atmosphere containing 5% CO_2 at 37°C. At three passages, the cells were seeded on 6-well culture plates at an approximate density of $5 \times 10^4/cm^2$ and grown for 24 h to approximately 70% confluency. Afterwards, the old medium were replaced with fresh serum-free

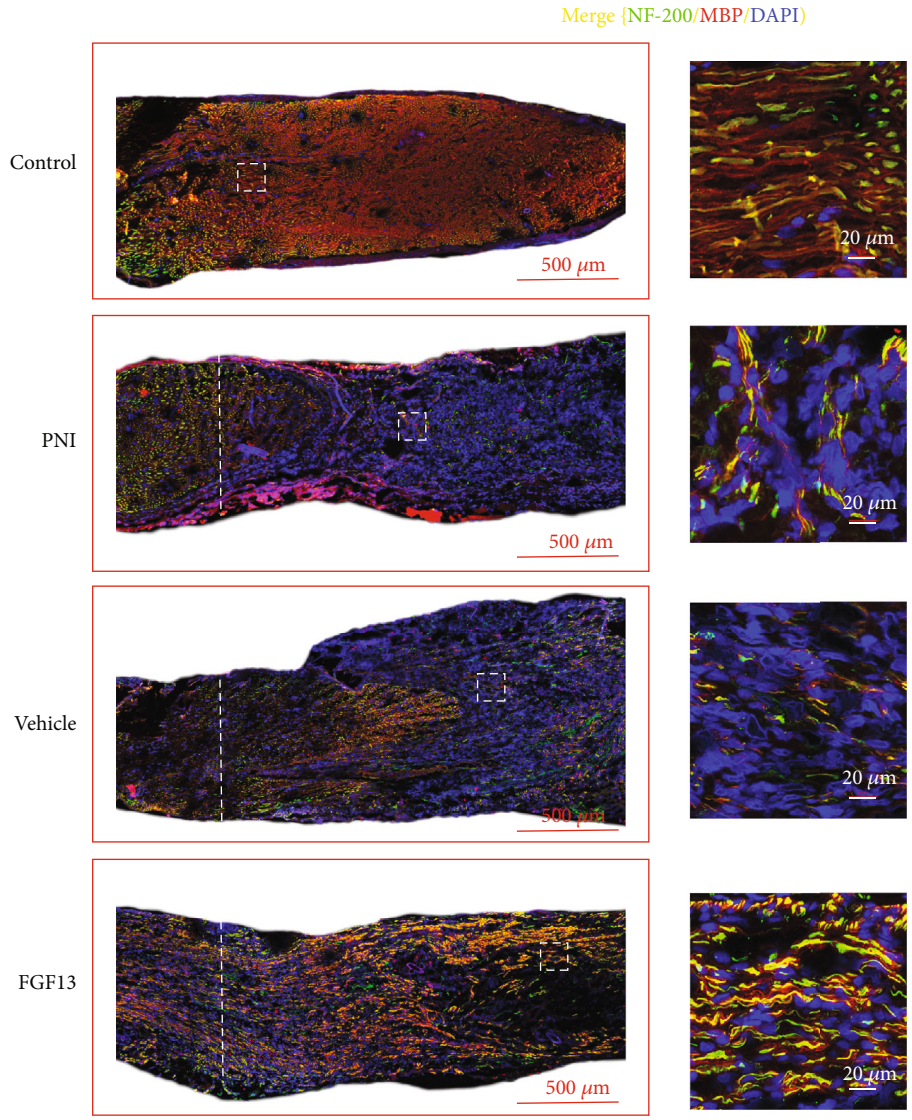

(a)

Figure 2: Continued.

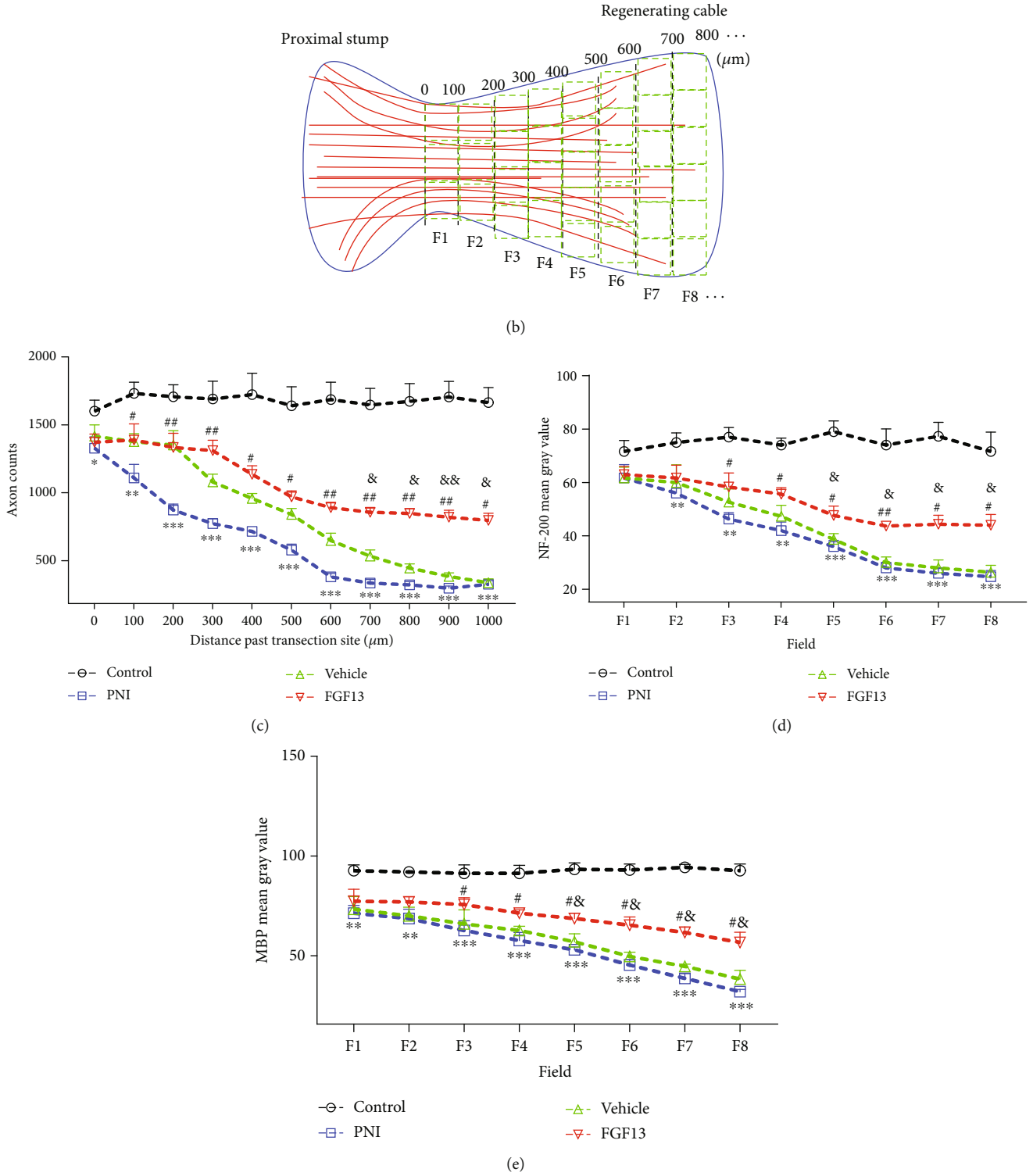

Figure 2: Histological analyses of the regenerated sciatic nerves in each group at 6 weeks after transection injury. (a) Representative costaining images for NF-200 and MBP of longitudinal sections in each experimental group. The scale bars in lower and higher magnifications were 500 μm and 20 μm, respectively. (b) Schema of nerve regeneration counting method proximal to the original transection through fields of the corresponding regenerating cable. (c) Quantification of total axon numbers in different fields of the indicated groups. (d, e) Quantitative analyses of average fluorescence intensity for NF-200 and MBP in indicated region of whole regenerated cable. Data are shown as means ± SEM, $n = 5$. PNI vs. control: $^{*}P < 0.05$, $^{**}P < 0.01$, and $^{***}P < 0.001$; FGF13 vs. vehicle: $^{\&}P < 0.05$ and $^{\&\&}P < 0.01$; FGF13 vs. PNI: $^{\#}P < 0.05$ and $^{\#\#}P < 0.01$.

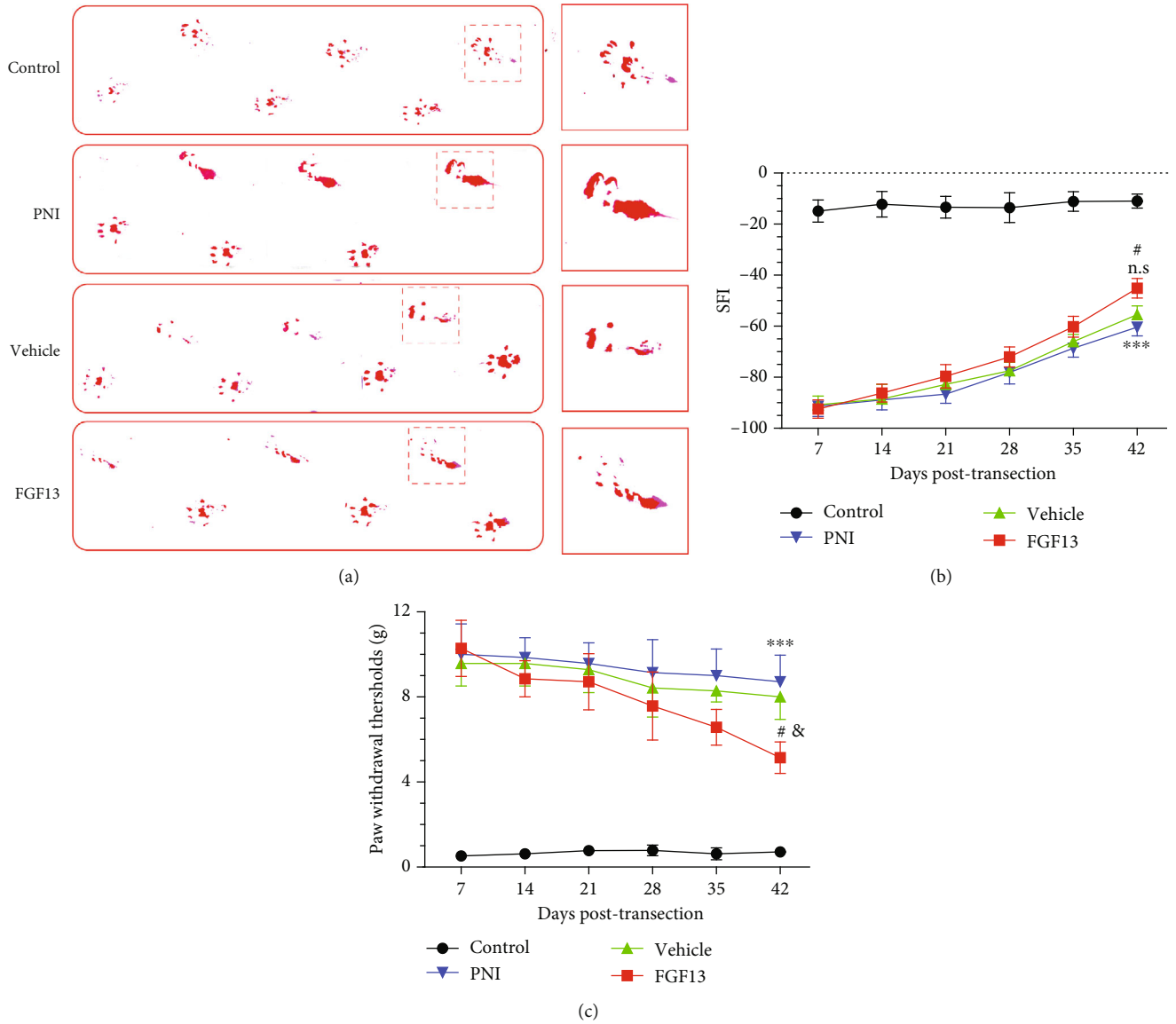

Figure 3: FGF13 promotes functional recovery after PNI: (a) representative images of the rats' footprints in the control, PNI, vehicle, and FGF13 groups at 6 weeks after treatment; (b) SFI analysis of the different groups at 1, 2, 3, 4, 5, and 6 weeks after operation; (c) withdrawal threshold was determined using von Frey hair test at indicated time points. Values are expressed as mean ± SEM, $n = 5$. PNI vs. sham: $^{***}P < 0.001$; FGF13 vs. vehicle: $^{\&}P < 0.05$, n.s representing not statistical significance; FGF13 vs. PNI: $^{\#}P < 0.05$.

medium; meanwhile, the cells were infected with recombinant lentiviral construct to overexpression FGF13 with the concentration of 1×10^8 TU/ml or empty lentiviral vectors (LV-vector) with the same concentration. After 24 h incubation, the cells were supplemented with normal growth medium containing 10 μg/ml myelin extracts for culturing another 2 days. The lentivirus expression vector (GV358) for overexpression FGF13 (LV-FGF13) was constructed by Genechem (Shanghai, China). We regarded the cell culturing in normal medium as the control group. The medium contains only myelin debris as the myelin group. The cells transfecting LV-FGF13 and myelin added were taken as the myelin+FGF13 group.

2.10. Live/Dead Staining Assay. Apoptotic cell death was quantified using the Live/Dead Viability Assay kit (L3224, Thermo Fisher) according the manufacturer's instructions. Briefly, after gently washing in PBS 3 times, the medium culturing RSC 96 cells were added 1 μM Calcein-AM and 2 μM propidium iodide for incubating 30 min at room temperature in the dark condition. Afterwards, the live cells were observed using a 490 nm excitation filter, whereas the dead cells were observed using a 545 nm excitation filter under a laser scanning confocal microcopy system (LSCM, Nikon, Z2). The live and dead cells were automatically calculated using the ImageJ software. The cell viability rate in each group was calculated as following equation: The cell viability rate (%) = the live cell numbers/total cell numbers × 100%. Five random fields were counted for each sample, and this experiment was performed in triplicate.

2.11. Statistical Analysis. All quantitative data are expressed as means ± SEM. Statistical comparisons were performed

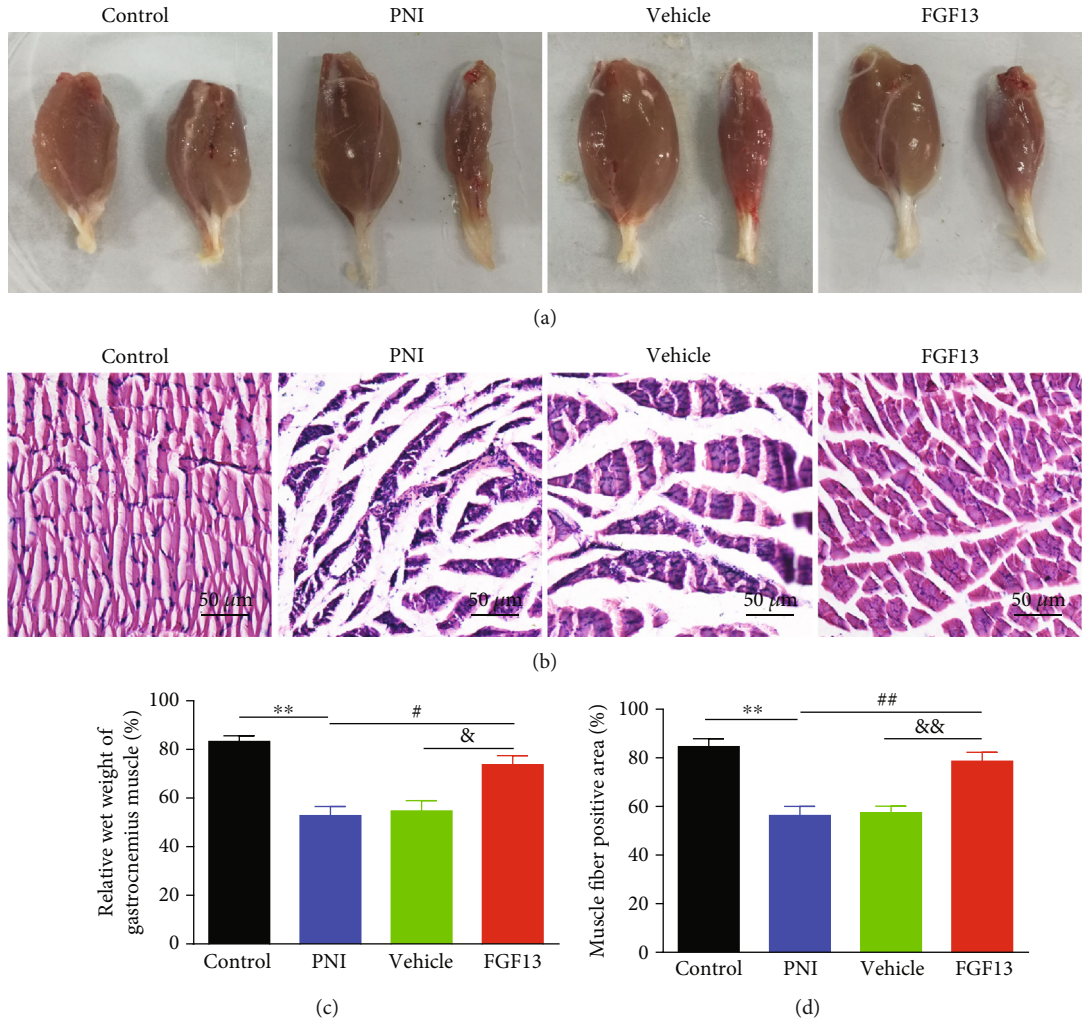

Figure 4: The morphological and microstructural analyses of gastrocnemius muscle. (a) The gross observation of the gastrocnemius muscles in the control, PNI, vehicle, and FGF13 groups at week 6 after the transection. (b) H&E staining of the cross-sections of the muscles in the four groups. Scale bar = 50 μm. (c) Quantification of the relative muscle weight from (a). (d) Quantification of the positive area of muscle fibers in the indicated groups from (b). Values are expressed as mean ± SEM, $n = 5$. $^{**}P < 0.01$ vs. the control group; $^{\&}P < 0.05$ and $^{\&\&}P < 0.01$ vs. the PNI group; $^{\#}P < 0.05$ and $^{\#\#}P < 0.01$ vs. the PNI group.

using the GraphPad Prism 7 Software (GraphPad Software Inc., La Jolla, CA, USA). For two-group comparison, statistical significance was analyzed by Student's t-test. For multiple group comparison, the statistical evaluation of the data was performed using one-way analysis of variance (ANOVA) followed by post hoc Tukey's test. In all the analyses, differences were considered significant at $P < 0.05$. Each experiment was performed at least three times to ensure accuracy.

3. Result

3.1. FGF13 Persistently Facilitates Neurologic Functional Recovery after PNI. To evaluate the motor function recovery in all groups, walking track analysis was performed at determine time postsurgery. Representative foot prints at 6 week postoperation from each group were shown in Figure 3(a). The result showed that the operative footprints in the FGF13 treating group had superior toe spread when compared with the PNI and vehicle groups. Meanwhile, the SFI values in all surgery groups were gradually became increased as time elapsed. It was worth noting that the SFI values in the FGF13 group were significantly higher than those in the PNI and vehicle groups at 6 weeks after surgery (Figure 3(b), $P < 0.05$). Additionally, recovery of sensory function was monitored weekly using the von Frey hair test. Consistent with the motor function evaluation, overexpression of FGF13 significantly accelerated sensory recovery following transection injury. At 6 weeks postsurgery, the paw withdrawal thresholds in FGF13-treated rats were approximately twofold than the only saline-treated PNI rats (Figure 3(c)).

3.2. FGF13 Attenuates Atrophy of the Gastrocnemius Muscle after PNI. Gastrocnemius muscle reinnervation, characterized by the increase of muscle weight and muscle fiber area, represents the functional recovery of the sciatic nerve [24]. We measured the isolated gastrocnemius muscle weights to evaluate the muscle atrophy and performed H&E staining to investigate the morphological changes in the

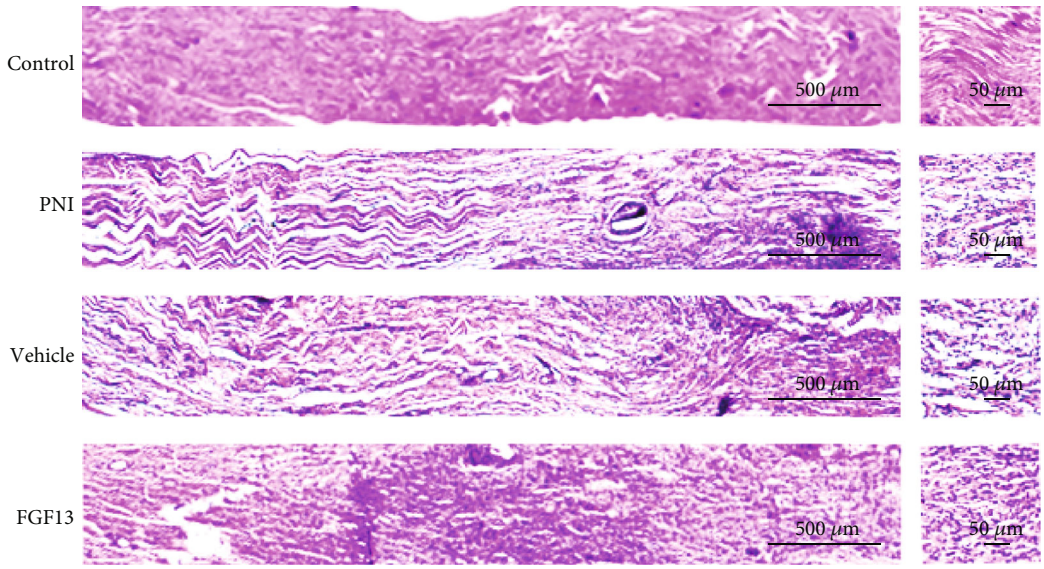

Figure 5: FGF13 promotes nerve regeneration after PNI. H&E staining was used to visualize the regenerated nerve fibers in the longitudinal sections of the regenerated segments in the control group, the PNI group, the vehicle group, and the FGF13 group at week 6 after the surgery. Scale bars, 500 μm (a); 50 μm (b).

gastrocnemius muscle. As illustrated in the gross images of the isolated gastrocnemius muscles (Figure 4(a)), the operative side in the PNI and vehicle groups rather than FGF13 group was obviously atrophic when compared with the corresponding normal side. Moreover, quantification of relative wet weight of gastrocnemius muscle results showed that there were little muscle fiber atrophy in the FGF13 group compared with the PNI and vehicle groups (Figure 4(c)). H&E staining revealed that the average percentage of muscle fiber positive area in the FGF13 group was significantly higher than those in the PNI and vehicle groups (Figures 4(b) and 4(d)), suggesting that FGF13 holds great promising to reverse muscle atrophy in rats with sciatic nerve transection.

3.3. FGF13 Improves Morphological Restoration of the Regenerated Sciatic Nerve after PNI. To investigate whether overexpressing FGF13 had a protective effect on enhancing nerve regeneration, the histological changes of the regenerated axon and fibrotic scar formation in each group were observed by H&E and Masson's trichrome staining. As shown in Figure 5, the control group had uniform and dense nerve fibers with structural integrity. Following 6 weeks after transection injury, the morphological observation of regenerated nerve fibers was exhibited, scattered, and disordered, while this abnormal nerve structure was significantly improved after injection of the recombinant FGF13 lentiviral vector solution.

Through Masson's trichrome staining, we could clearly observe that the amount of regenerative axons which were dyed in red showed similar pattern as H&E staining, namely, control group > FGF13 group > vehicle group > PNI group (Figure 6). However, the fibrotic scar which appeared blue showed the opposite trend, manifesting in the FGF13 group contained few fibrous formation than that of the PNI group and vehicle groups (Figure 6). All of these data suggested that FGF13 was contributed to support nerve regeneration and attenuate fibrotic matrix deposition.

3.4. FGF13 Enhances Remyelination following PNI. At 6 weeks after surgery, the myelin morphology at the distal portion of the transection site from four surgery groups was observed by toluidine blue staining and TEM. As shown in Figures 1(a) and 1(b), the control sciatic nerves displayed normal myelinated fibers with abundant fair arrangement and thick structure. In contrast, the PNI and vehicle groups exhibited scattered myelin sheaths with abnormal structure, manifesting in irregularity and thinning. This severe myelin abnormalities achieved greatly amelioration after receiving FGF13 lentivirus remedy. Additionally, statistical analysis of myelinated indexes, including myelin sheath counts, diameter, and thickness plus G-ratio in the FGF13 group, was significantly superior to in the PNI and vehicle groups and nearly reached to the control group (Table 1).

3.5. FGF13 Enhances Axonal Outgrowth following Nerve Transection. To address whether axonal regeneration after transection was enhanced by FGF13 treatment, double staining for NF-200 (green) and MBP (red) was performed. We found that the regenerated sciatic nerve in the lesion region and its distal stump without treatment showed few NF-200-positive axons and MBP-tagged myelins. Moreover, most of regenerated axons at the proximal site could not pass through the lesion region to reach the distal trunk, and the distribution of these sparse axons in the lesion core exhibited irregular (Figure 2(a)). Similarly, simple blank lentiviral vector treatment did not significantly increase the axon numbers, NF-200 and MBP immunoreactivity. In contrast, rats receiving FGF13 lentivirus were filled with NF-200 and MBP positive staining signals that extended from the proximal stump along a linear path through the whole lesion region toward the distal stump (Figure 2(a)). Additionally, analysis

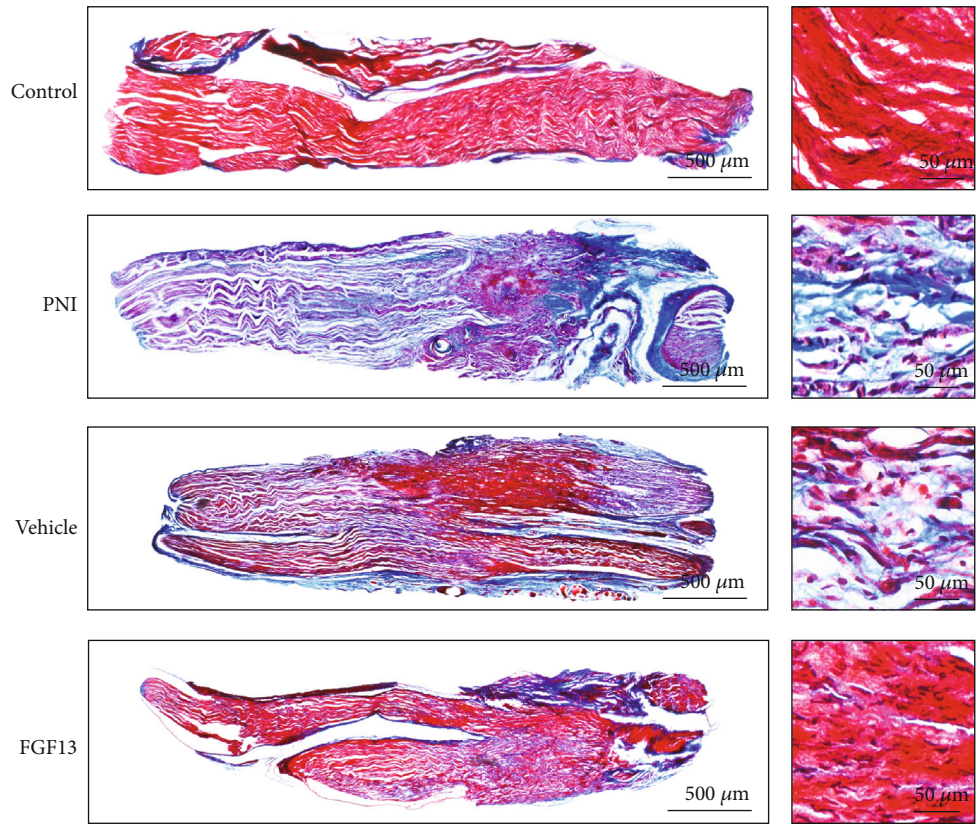

Figure 6: FGF13 attenuates fibrotic matrix deposition after PNI. (a) Masson's trichrome staining of the whole nerve stumps of longitudinal sections in the four groups of rats at 6 weeks after the injury. Scale bars, 500 μm (a); 50 μm (b).

Table 1: Morphometric evaluations of regenerated nerves in each group.

Group	Myelin counts (/mm^2)	Diameter of myelin sheath (μm)	Thickness of myelin sheath (μm)	G-ratio (axon to myelin diameter ratio)
Sham	33.950 ± 2773	5.11 ± 0.22	1.21 ± 0.09	0.63 ± 0.03
PNI	15.715 ± 1333***	3.41 ± 1.26***	0.56 ± 0.04***	0.84 ± 0.02***
Vehicle	16.557 ± 1381	2.56 ± 0.19	0.57 ± 0.07	0.82 ± 0.02
FGF13	23.293 ± 2197$^{\&,\#}$	3.62 ± 0.18$^{\&\&,\#\#}$	0.83 ± 0.06$^{\&,\#}$	0.68 ± 0.02$^{\&,\#\#}$

Statistical analysis of the nerve fiber density, diameters, thickness, and G-ratios in all groups using the ImageJ software. G-ratio was calculated by dividing the diameter of the axon by fiber diameter. The data are expressed as the mean ± SEM. PNI vs. control: $^{***}P < 0.001$; FGF13 vs. vehicle: $^{\&}P < 0.05$ and $^{\&\&}P < 0.01$; FGF13 vs. PNI: $^{\#}P < 0.05$ and $^{\#\#}P < 0.01$.

of axon numbers, NF-200, and MBP expression at 6 weeks postsurgery showed that the FGF13 treating group had the more axon regrowth and the higher protein expression than another two operative groups despite inferior to the sham operation group (Figures 2(c)–2(e)).

3.6. FGF13 Induces Microtubule Stability in SCs. SCs are integral components of peripheral nervous that play a pivotal role in myelin formation and axon regrowth [25]. Microtubule stability contributes to cytoskeletal remodeling to guide development and regeneration of the nervous system [26]. Microtubule stability needs to undergo frequent bouts of assembly and disassembly, which can be reflected by the relative ratio of acetylated and tyrosinated tubulins (A/T ratio) [27]. The higher its ratio, the better microtubule stabilization. Microtubule stability and dynamics are also regulated by other group of proteins, termed Tau, Dynein, and Kinesin-5. It is intuitive that tau has been proposed to regulate the assembly, growth, and bundling of microtubules in the growth cone [28]. Dynein is a complex cytoskeletal dynamic protein that drives long-range retrograde transport along microtubules [29]. Kinesin-5 is a motor protein that plays critical roles in shaping and organizing microtubules in both axons and dendrites [30]. To reveal the molecular mechanism of FGF13 promoting structural and functional recovery following PNI, we cultured SCs in myelin condition to imitate the local microenvironment of damaged sciatic nerve and detected the level of microtubule-related proteins

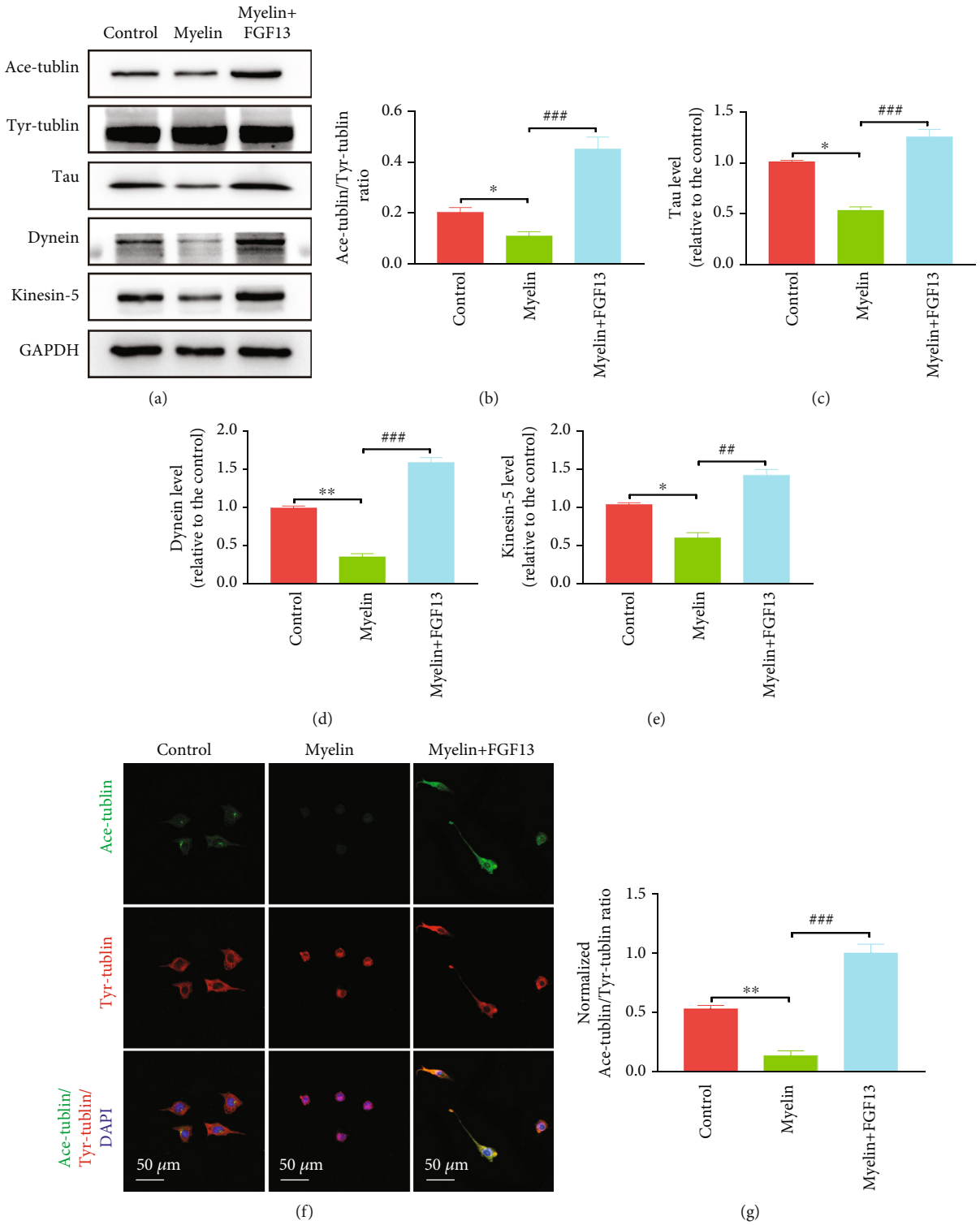

Figure 7: FGF13 induces microtubule stabilization in SCs. (a) Representative images of immunoblotting analysis of acetylated tubulin, tyrosinated tubulin, Tau, Kinesin-5, and Dynein in the control, myelin, and myelin+FGF13 groups. (b–e) Quantification results of the levels of the indicated proteins from (a). GAPDH was used as the loading control and for band density normalization. (f, g) Representative confocal images of Ace-tubulin and Tyr-tubulin fluorescence and quantitative results of A/T ratio in the different experimental groups. DAPI was used to label the nuclei. All these data represent the means ± SEM and sourced from three independent experiments. $^{*}P < 0.05$ and $^{**}P < 0.01$ vs. the control group; $^{\#\#}P < 0.01$ and $^{\#\#\#}P < 0.001$ vs. the myelin group.

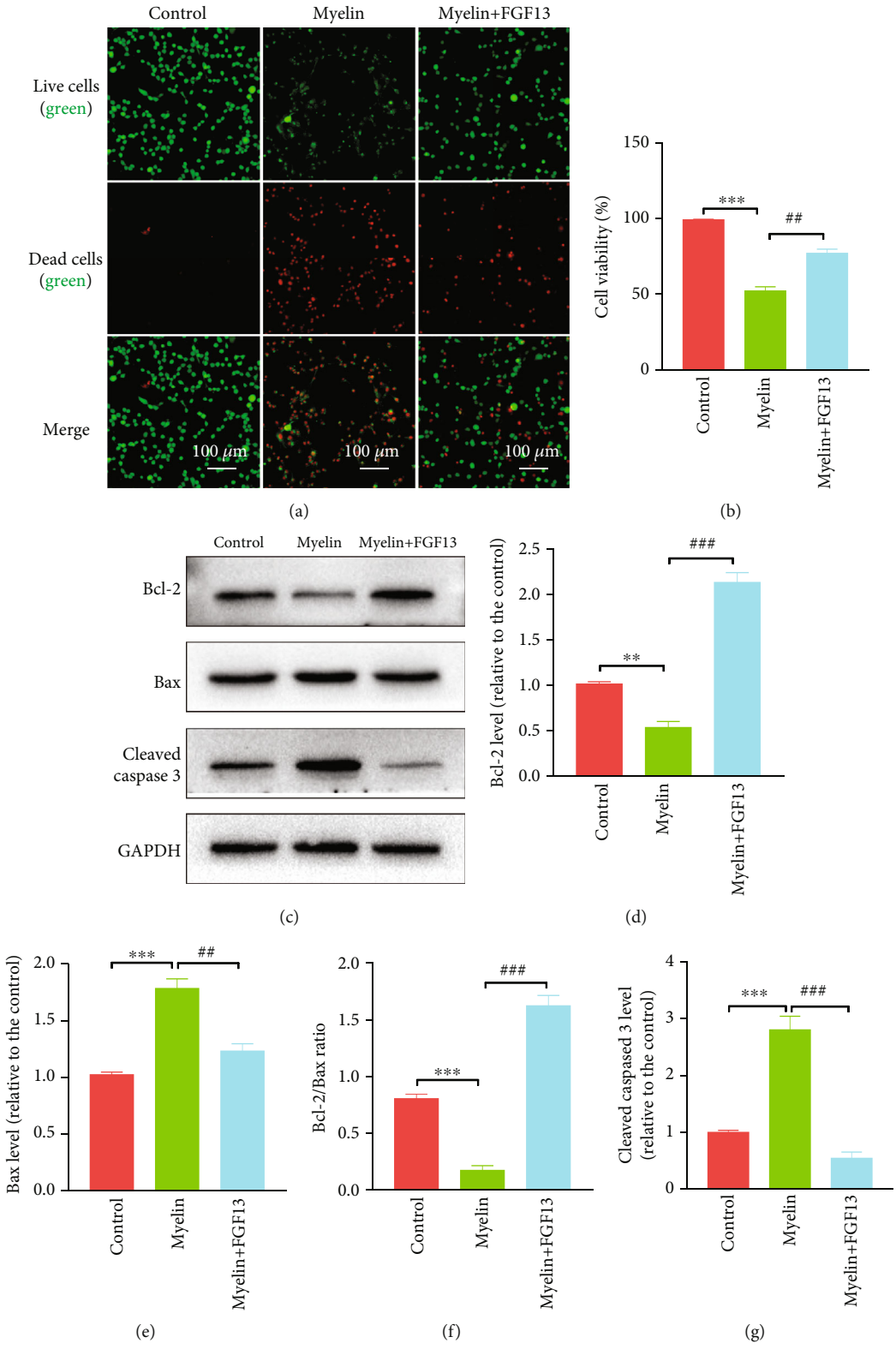

Figure 8: FGF13 alleviates cell death *in vitro*. (a) Live-dead staining was used to identify live (green) and dead (red) cells in the control, myelin, and myelin+FGF13 groups. (b) Quantification of cell viability from (a). (c) Representative immunoblotting images of Bcl-2, Bax, and Cleaved caspase-3 in the control, myelin, and myelin+FGF13 groups. GAPDH expression was used for normalization of protein loading. (d–g) Quantification of protein bands from (c) by densitometric analysis. The values represent the mean ± SEM and repeated in triplicate. $^{*}P < 0.05$ and $^{**}P < 0.01$ vs. the control group; $^{\#\#}P < 0.01$ and $^{\#\#\#}P < 0.001$ vs. the myelin group.

following transfection of LV-FGF13 via immunoblotting and immunofluorescence detection. As shown in Figure 7(a), Ace-tubulin protein was expressed normal in the control group but became very low when cultured in myelin condition. After infecting with LV-FGF13, the low level of Ace-tubulin was restored to the degree that was higher than the control group. Similarly, the trend of Tau, Dynein, and Kinesin-5 expression in control, myelin, and myelin+FGF13 groups was consisted with the change of Ace-tubulin expression (Figure 7(a)). Moreover, statistical analysis also revealed that the values of Tau, Dynein, and Kinesin-5 as well as A/T ratio in the myelin+FGF13 group were the highest in all testing groups and showed statistical significance when compared with the myelin group (Figures 7(b)–7(e)). Additionally, double immunostaining for Ace-tubulin and Tyr-tubulin also showed that treatment with LV-FGF13 caused a marked increase in the A/T ratio, accompanied by cellular outgrowth with a single polarized morphology, when compared with the myelin group (Figures 7(f) and 7(g)).

3.7. FGF13 Reverses Myelin-Induced SC Apoptosis. To examine whether FGF13 could alleviate SC apoptosis under damage condition, we transfected SC with lentivirus that overexpressed FGF13, followed by addition of myelin extracts. Using live/dead assay (Figures 8(a) and 8(b)), we found that there were nearly no dead cells in the normal condition, but this status became seriously terrible when SC exposed to myelin debris, manifesting in numerous cellular death or necrosis. Addition of LV-FGF13 remarkably decreased myelin-induced SC death, as evidenced by a dramatic increase in green signals (live cells) and decrease in red signals (dead cells). Similar changes were also observed for the apoptosis-related proteins in the three experimental groups (Figures 8(c)–8(g)). Specifically, compared with the normal condition, addition of myelin debris significantly upregulated the level of proapoptotic proteins, including Bax and Cleaved caspase-3, and downregulated the antiapoptotic protein Bcl-2 level, while pretreatment with LV-FGF13 effectively reversed this trend. These results suggest that LV-FGF13 is able to attenuate SC death and apoptosis at the condition of myelin-induced microenvironmental disorder.

4. Discussion

The results of present study support the role of FGF13 possess favorable biological property for exerting neuroprotection and neuroregeneration after transection of the sciatic nerve. Our results provide evidence that, following PNI, overexpressing FGF13 not only substantively ameliorated sensory and motor functional recovery but also remarkably promoted the morphological and pathological alterations, including axonal regrowth, myelin rehabilitation, and fibrotic scar reduction, as well as apoptotic decrease. Importantly, these benefit functions were closely associated with maintaining microtubule stabilization in SCs. Additionally, FGF13 was not participated in modulating nerve injury-induced inflammatory reaction (Figure S1 and Table. S1). In brief, these findings provide new insights into the beneficial effects of FGF13 in nerve reconstruction and functional restoration and open a possible investigation of applying FGF13 for treating PNI.

Microtubule network, contained in growth cone, guides axonal elongation and bending via interacting with microtubule-related proteins, including acetylated tubulin, tyrosinated tubulin, Tau, Kinesin-5, and Dynein [29]. During the process of cellular polarization and maturation, these proteins are gradually increased to stabilize microtubules that are contribute to cytoskeletal assembly [31]. Spatiotemporal regulation of cytoskeleton structures is beneficial for ameliorating intrinsic axon growth capacity [32, 33]. Conversely, destruction of microtubule stabilization using nocodazole impairs neuronal polarization, axon formation, and reconnection [34]. Thus, detecting the expression of microtubule-related proteins holds greatly promise for reflecting intrinsic growth capacity of damaged nerve system. In this study, we found SCs exposed to myelin debris significantly decreased the level of Tau, Kinesin-5, and Dynein expression, as well as reduced A/T ratio, but was strikingly reversed after receiving FGF13 treatment. These dates indicate FGF13-induced microtubule stabilization in SCs possibly become an intrinsic capacity for improving nerve structural and functional recovery following sciatic nerve transection injury.

After suffering from trauma and medical disorders, especially for transection of axons, adult nerve tissue regeneration is usually slow and incomplete due to the pathophysiologic disturbance-induced cell death, nerve demyelination, conduction defects, and/or muscle denervation. To achieve an effective nerve regeneration, therapeutic strategy should be possessed requirements as followings: first, stimulating microtubule protrude toward the growth cone leading edge to increase their intrinsic growth capacity [35, 36], and second, supplement of adequate biological molecules, such as GFs, in the lesion region to create a regenerative microenvironment for numerous axonal extension toward the target organ [37]. Finally, the proximal segment of axonal regrowth should be elongate at a right direction to match the corresponding injured target organs [38]. Our preliminary studies indicated that, compared with the model without treatment, FGF13 therapy shows great potential for regulating microtubule dynamic, enabling axon outgrowth and myelin regeneration, as well as promoting the locomotor recovery. To the best of our knowledge, this reason might be closely related to FGF13 as a microtubule-stabilizing protein that possess a capable for enhancing nerve intrinsic growth potential to achieve structural and functional recovery following PNI.

As an intracellular protein of the GF family, FGF13 can modulate initiation and propagation of action potentials via modulating Nav channel gating and trafficking in the developing nerve system [39]. Presently, the reasons for selection of FGF13 lentivirus for restoring severe sciatic nerve transection recovery are based on the following factors: (I) FGF13 has been regarded as a microtubule stabilizing protein that accelerates neural development and polarization and showed neuroprotective and neuroregenerative roles in promoting axonal growth and remyelination after SCI [13, 15]; (II) deficiency of FGF13 gene exhibits learning and memory decline, as well as synaptic excitatory–inhibitory imbalance [40]; and (III) in vivo transduction of wide variety of cells with

lentivirus that overexpress FGF13 resulting in continuously repairing PNI over several months. Thus, we speculate that overexpression of FGF13 is a potential strategy for improving morphological and functional recovery following PNI. To confirm this speculation, the adult rats with sciatic nerve of transection lesion were injected in situ FGF13 lentivirus. At determined time point, histological and functional recovery in the lesion region was evaluated via multiple comprehensive experiments. The result of our data demonstrated that application of FGF13 significantly ameliorated locomotor outcome and axonal and myelin regeneration, as well as fibrotic deposition, indicating FGF13 as a therapeutic agent not only supported neuroregeneration in central nervous system but also improved axonal generation and plasticity in peripheral nervous system.

In summary, our data provided the first direct evidence that FGF13 had the capacity for significantly promoting axonal regrowth, remyelination, and functional reinnervation after sciatic nerve transection injury. Moreover, the underlying molecular mechanism was probably through stabilizing microtubule in SCs to enhance their intrinsic growth capacity. The findings of this exploratory study suggest that FGF13 may serve as a novel therapeutic agent for repairing PNI or other PNS injury.

Data Availability

The datasets used and analyzed during the current study are available from the corresponding author on reasonable request.

Conflicts of Interest

The authors declare that they have no conflict of interest.

Authors' Contributions

J.Y., W.Y., and L.R. conceived and designed the research work. L.R., T.X., and H.M. performed the experiments. L.R., P.Y., and L.J. conducted statistical analysis and wrote the paper. All authors discussed the manuscript drafting. Rui Li, Xuetao Tao, and Minghong Huang contributed equally to this work.

Acknowledgments

This study was partially supported by a research grant from the National Natural Science Funding of China (81802238), the Medical and Health Science and Technology Project of Zhejiang Provincial (2019KY646, 2020KY908), and the Science and Technology Project of Zhejiang Health Committee (2021KY1075).

Supplementary Materials

Real-time quantitative PCR. According to the manufacturer's protocol, sciatic nerve tissues were collected and homogenized in TRIZOL (Invitrogen, California, CA, USA) to extract total RNA. Both reverse transcription and quantitative PCR (qPCR) were carried out using a two-step M-MLV Platinum SYBR Green qPCR SuperMix-UDG kit (Invitrogen, Carlsbad, CA). An Eppendorf Real plex 4 instrument (Eppendorf, Hamburg, Germany) was used to conduct real-time qPCR. The primers of target genes are listed in the Supplementary Table 1. The relative amount of mRNA was calculated by the comparative threshold cycle method with β-actin as control. Supplementary Figure S1: effect of LV-FGF13 on regulating inflammation response at 7d post-injury. (a) mRNA levels of the proinflammatory cytokines IL-6, IL-1β, and TNF-α in sciatic nerve tissue. (b) Gene expression of anti-inflammatory cytokines IL-4, IL-10, and IL-13 in sciatic nerve tissue from the control, PNI, vehicle, and FGF13 groups. Data are expressed as mean ± SEM for three independent experiments. ***Statistically significant difference ($P < 0.001$) versus the control group. No statistical significance (n.s) was observed between PNI and FGF13 groups, plus vehicle, and FGF13 groups. Supplementary Table 1: primer sequences for real-time qPCR. *(Supplementary Materials)*

References

[1] J. Noble, C. A. Munro, V. S. Prasad, and R. Midha, "Analysis of upper and lower extremity peripheral nerve injuries in a population of patients with multiple injuries," *The Journal of Trauma*, vol. 45, no. 1, pp. 116–122, 1998.

[2] C. A. Taylor, D. Braza, J. B. Rice, and T. Dillingham, "The incidence of peripheral nerve injury in extremity trauma," *American Journal of Physical Medicine & Rehabilitation*, vol. 87, no. 5, pp. 381–385, 2008.

[3] G. Lundborg and P. Richard, "Bunge memorial lecture. Nerve injury and repair–a challenge to the plastic brain," *Journal of the Peripheral Nervous System: JPNS*, vol. 8, no. 4, pp. 209–226, 2003.

[4] M. Schenker, R. Kraftsik, L. Glauser, T. Kuntzer, J. Bogousslavsky, and I. Barakat-Walter, "Thyroid hormone reduces the loss of axotomized sensory neurons in dorsal root ganglia after sciatic nerve transection in adult rat," *Experimental Neurology*, vol. 184, no. 1, pp. 225–236, 2003.

[5] S. Yi, L. Xu, and X. Gu, "Scaffolds for peripheral nerve repair and reconstruction," *Experimental Neurology*, vol. 319, article 112761, 2019.

[6] X. Gu, F. Ding, Y. Yang, and J. Liu, "Construction of tissue engineered nerve grafts and their application in peripheral nerve regeneration," *Progress in Neurobiology*, vol. 93, no. 2, pp. 204–230, 2011.

[7] R. Li, D. H. Li, H. Y. Zhang, J. Wang, X. K. Li, and J. Xiao, "Growth factors-based therapeutic strategies and their underlying signaling mechanisms for peripheral nerve regeneration," *Acta Pharmacologica Sinica*, vol. 41, no. 10, pp. 1289–1300, 2020.

[8] R. Li, D. Li, C. Wu et al., "Nerve growth factor activates autophagy in Schwann cells to enhance myelin debris clearance and to expedite nerve regeneration," *Theranostics*, vol. 10, no. 4, pp. 1649–1677, 2020.

[9] N. Z. Alsmadi, G. S. Bendale, A. Kanneganti et al., "Glial-derived growth factor and pleiotrophin synergistically promote axonal regeneration in critical nerve injuries," *Acta Biomaterialia*, vol. 78, pp. 165–177, 2018.

[10] D. S. Huo, M. Zhang, Z. P. Cai, C. X. Dong, H. Wang, and Z. J. Yang, "The role of nerve growth factor in ginsenoside Rg1-

induced regeneration of injured rat sciatic nerve," *Journal of Toxicology and Environmental Health. Part A*, vol. 78, no. 21-22, pp. 1328–1337, 2015.

[11] G. M. DeStefano, K. A. Fantauzzo, L. Petukhova et al., "Position effect on FGF13 associated with X-linked congenital generalized hypertrichosis," *Proceedings of the National Academy of Sciences of the United States of America*, vol. 110, no. 19, pp. 7790–7795, 2013.

[12] E. Q. Wei, D. S. Sinden, L. Mao, H. Zhang, C. Wang, and G. S. Pitt, "Inducible Fgf13 ablation enhances caveolae-mediated cardioprotection during cardiac pressure overload," *Proceedings of the National Academy of Sciences of the United States of America*, vol. 114, no. 20, pp. E4010–E4019, 2017.

[13] J. Li, Q. Wang, H. Wang et al., "Lentivirus mediating FGF13 enhances axon regeneration after spinal cord injury by stabilizing microtubule and improving mitochondrial function," *Journal of Neurotrauma*, vol. 35, no. 3, pp. 548–559, 2018.

[14] S. Nishimoto and E. Nishida, "Fibroblast growth factor 13 is essential for neural differentiation in Xenopus early embryonic development," *The Journal of Biological Chemistry*, vol. 282, no. 33, pp. 24255–24261, 2007.

[15] Q. F. Wu, L. Yang, S. Li et al., "Fibroblast growth factor 13 is a microtubule-stabilizing protein regulating neuronal polarization and migration," *Cell*, vol. 149, no. 7, pp. 1549–1564, 2012.

[16] S. Crunkhorn, "Microtubule stabilizer repairs spinal cord injury," *Nature Reviews. Drug Discovery*, vol. 14, no. 5, p. 310, 2015.

[17] F. Hellal, A. Hurtado, J. Ruschel et al., "Microtubule stabilization reduces scarring and causes axon regeneration after spinal cord injury," *Science*, vol. 331, no. 6019, pp. 928–931, 2011.

[18] J. Ruschel, F. Hellal, K. C. Flynn et al., "Axonal regeneration. Systemic administration of epothilone B promotes axon regeneration after spinal cord injury," *Science*, vol. 348, no. 6232, pp. 347–352, 2015.

[19] M. He, Y. Ding, C. Chu, J. Tang, Q. Xiao, and Z. G. Luo, "Autophagy induction stabilizes microtubules and promotes axon regeneration after spinal cord injury," *Proceedings of the National Academy of Sciences of the United States of America*, vol. 113, no. 40, pp. 11324–11329, 2016.

[20] L. De Medinaceli, W. J. Freed, and R. J. Wyatt, "An index of the functional condition of rat sciatic nerve based on measurements made from walking tracks," *Experimental Neurology*, vol. 77, no. 3, pp. 634–643, 1982.

[21] L. B. Bortalanza, J. Ferreira, S. C. Hess, F. Delle Monache, R. A. Yunes, and J. B. Calixto, "Anti-allodynic action of the tormentic acid, a triterpene isolated from plant, against neuropathic and inflammatory persistent pain in mice," *European Journal of Pharmacology*, vol. 453, no. 2-3, pp. 203–208, 2002.

[22] R. Li, J. Wu, Z. Lin et al., "Single injection of a novel nerve growth factor coacervate improves structural and functional regeneration after sciatic nerve injury in adult rats," *Experimental Neurology*, vol. 288, pp. 1–10, 2017.

[23] S. Walsh, J. Biernaskie, S. W. Kemp, and R. Midha, "Supplementation of acellular nerve grafts with skin derived precursor cells promotes peripheral nerve regeneration," *Neuroscience*, vol. 164, no. 3, pp. 1097–1107, 2009.

[24] M. Lavasani, S. D. Thompson, J. B. Pollett et al., "Human muscle-derived stem/progenitor cells promote functional murine peripheral nerve regeneration," *The Journal of Clinical Investigation*, vol. 124, no. 4, pp. 1745–1756, 2014.

[25] K. R. Jessen and P. Arthur-Farraj, "Repair Schwann cell update: adaptive reprogramming, EMT, and stemness in regenerating nerves," *Glia*, vol. 67, no. 3, pp. 421–437, 2019.

[26] P. W. Baas, A. N. Rao, A. J. Matamoros, and L. Leo, "Stability properties of neuronal microtubules," *Cytoskeleton*, vol. 73, no. 9, pp. 442–460, 2016.

[27] H. Witte, D. Neukirchen, and F. Bradke, "Microtubule stabilization specifies initial neuronal polarization," *The Journal of Cell Biology*, vol. 180, no. 3, pp. 619–632, 2008.

[28] R. Tan, A. J. Lam, T. Tan et al., "Microtubules gate tau condensation to spatially regulate microtubule functions," *Nature Cell Biology*, vol. 21, no. 9, pp. 1078–1085, 2019.

[29] M. Martin and A. Akhmanova, "Coming into focus: mechanisms of microtubule minus-end organization," *Trends in Cell Biology*, vol. 28, no. 7, pp. 574–588, 2018.

[30] B. J. Mann and P. Wadsworth, "Kinesin-5 regulation and function in mitosis," *Trends in Cell Biology*, vol. 29, no. 1, pp. 66–79, 2019.

[31] S. Chaaban and G. J. Brouhard, "A microtubule bestiary: structural diversity in tubulin polymers," *Molecular Biology of the Cell*, vol. 28, no. 22, pp. 2924–2931, 2017.

[32] M. T. Kelliher, H. A. Saunders, and J. Wildonger, "Microtubule control of functional architecture in neurons," *Current Opinion in Neurobiology*, vol. 57, pp. 39–45, 2019.

[33] O. F. Omotade, S. L. Pollitt, and J. Q. Zheng, "Actin-based growth cone motility and guidance," *Molecular and Cellular Neurosciences*, vol. 84, pp. 4–10, 2017.

[34] S. Dupraz, B. J. Hilton, A. Husch et al., "RhoA controls axon extension independent of specification in the developing brain," *Current Biology*, vol. 29, no. 22, pp. 3874–3886.e9, 2019.

[35] M. B. Steketee, C. Oboudiyat, R. Daneman et al., "Regulation of intrinsic axon growth ability at retinal ganglion cell growth cones," *Investigative Ophthalmology & Visual Science*, vol. 55, no. 7, pp. 4369–4377, 2014.

[36] P. W. Baas and F. J. Ahmad, "Beyond taxol: microtubule-based treatment of disease and injury of the nervous system," *Brain: A Journal of Neurology*, vol. 136, no. 10, pp. 2937–2951, 2013.

[37] A. C. Mitchell, P. S. Briquez, J. A. Hubbell, and J. R. Cochran, "Engineering growth factors for regenerative medicine applications," *Acta Biomaterialia*, vol. 30, pp. 1–12, 2016.

[38] T. P. Smith, P. K. Sahoo, A. N. Kar, and J. L. Twiss, "Intra-axonal mechanisms driving axon regeneration," *Brain Research*, vol. 1740, article 146864, 2020.

[39] J. C. Wong and A. Escayg, "Fgf13 identified as a novel cause of GEFS," *Epilepsy Currents*, vol. 16, no. 2, pp. 112-113, 2016.

[40] R. S. Puranam, X. P. He, L. Yao et al., "Disruption of Fgf13 causes synaptic excitatory-inhibitory imbalance and genetic epilepsy and febrile seizures plus," *The Journal of Neuroscience: The Official Journal of the Society for Neuroscience*, vol. 35, no. 23, pp. 8866–8881, 2015.